University of Newcastle upon Tyne
Department of Civil Engineering
Geotechnical Group

THE APPLICATION OF ELECTROKINETIC GEOSYNTHETIC MATERIALS TO USES IN THE CONSTRUCTION INDUSTRY

A Thesis Submitted In Partial Fulfilment For The Degree Of
Doctor Of Philosophy (Ph.D.)

by:

Eur Ing* Robert Colin Pugh *BEng MSc CEng MIMM FGS

May 2002

CONFIDENTIALITY STATEMENT

The information contained within this thesis is confidential. The Electrokinetic Geosynthetic (EKG) is covered under UK Patent GB 2301 311 A (Jones 1998), UK Patent application GB 2327686 A (Netlon 1998) and International Patent Application No. PCT/GB99/04263 (University of Newcastle 2000). Other applications are also covered by Sandanasamy (1998) European Patent Application No, 98103845.8.

The contents of this thesis must not be referred to in any publication or be used in any way without the written permission of the Geotechnical Group, Department of Civil Engineering, University of Newcastle upon Tyne.

ACKNOWLEDGEMENTS

I would like to dedicate this thesis to Ana: *El camino era muy largo, pero cada paso era más fácil contigo a mi lado. Te quiero con toda mi alma y corazón.*

I am indebted to my supervisors Prof. Colin Jones and Prof. Barry Clarke for all of their help, supervision and inspiration. I would also like to thank all the other member of staff, academic and support, of the Geotechnical Group at the University of Newcastle for their help during my happy time there. With a special mention for Mr David Hughes for his constant encouragement to complete this thesis and his priceless advice and help from my first day at the University until the last, thanks.

I would also like to thank my parents Idris and Lilian who have been constantly supportive of me throughout my career and without whom I would never have had the opportunity to begin this work.

I extend my gratitude to past and present employees of CAPITOL Waste Management, Kvaerner Cementation Foundations, Tensar International, WSP Environmental and 1NE. With special thanks to Dr Richard Austin, Dr Rab Fernie, Mr Yalcin Irfan, Mr John Lashmar, Mr Tim Oliver, Dr Martin Pedley, Mr Jim Penman, Mr Alan Taylor and Mr Nigel Wrigley.

Additionally, I must thank all at the "USAC" for allowing me the resources to produce this thesis and Isabel Tejero for her help in the typing of the manuscript of Chapters 1, 4, 5 and 7.

Thanks to you all, Muchas gracias a todos,

Diolch yn fawr iawn pawb.

PUBLICATIONS, PATENTS AND COURSES PRODUCED DURING RESEARCH

During this research the following have been produced as a direct result of the work carried out:

- *Geosynthetics in Reinforced structures: main applications, interaction with soil, design methods, related tests.* Short Course given at EuroGeo 2000, Bologna, Italy, October 15-18, 2000. Taken from Chapter 5 "Reinforced Soil" of this thesis, presented by Prof. C.J.F.P. Jones.

- Pugh, R.C. (2000) *A full-scale field trial of electrokinetically enhanced cohesive reinforced soil using electrokinetic geosynthetics.* Winning paper in IGS U.K. Chapter papers competition.

- Pugh, R.C., Clarke, B.G. & Jones, C.J.F.P. (2000) *An electro-osmosis consolidation trial using electrokinetic geosynthetics. Proceedings of the* 4th International Conference on Ground Improvement Geosystems, Helsinki, Finland, June 7-9. pp 533-540.

- University of Newcastle (2000) *An Electrokinetic Geosynthetic Structure.* International Patent Application No. PCT/GB99/04263.

- Jones, C.J.F.P. & Pugh, R.C. (2001) *A full-scale field trial of electrokinetically enhanced cohesive reinforced soil using electrically conductive geosynthetics.* In Ochiai *et al* (eds.) Landmarks in Earth Reinforcement IS-Kyushu 2001, Japan, Swets & Zeitlinger, pp 219-223.

ABSTRACT

Electro-osmosis is one of the five electrokinetic phenomena that may occur in soils, and the phenomenon of principal interest to this thesis. It may be defined as the movement of the pore fluid in a fine-grained soil caused by the application of a DC electrical potential difference across the soil mass. One of the main reasons that electro-osmosis has not received a more widespread application in the field of geotechnical engineering is due to the difficulty of successfully applying the electrical potential field to the soil mass. This thesis addresses the technique of using a carbon filled polymeric electrokinetic geosynthetics (EKG) to apply the electrical potential field and induce electro-osmosis in a soil mass.

The thesis reviews the historical development of geosynthetics and the different techniques available for making them electrically conductive are discussed. A new type of EKG band drain is introduced and its construction, durability and connection technology are presented.

The application of electro-osmosis, through the use of the EKG band drain, to the functions of soft soil consolidation, cohesive fill to reinforced soil structures and the volume control of shrinking and swelling susceptible soils are considered. Design methods are developed for these functions and are applied to two full-scale field trials in the application areas of electro-osmotically enhanced reinforced cohesive soil and electro-osmotic volume control of an embankment, and a smaller scale field trial of electro-osmotic consolidation of soft soil. The results of these field trials have been analysed with respect to the design methods developed and confirm their validity for future use.

Soil acceptability criterion have been developed to allow the applicability of electro-osmosis to a soil to be evaluated based upon conventional and electro-osmosis specific soil mechanics laboratory tests. Potential future applications for electro-osmosis and EKGs are suggested.

EXECUTIVE SUMMARY

The theory and background to electrokinetic phenomena in soils are introduced together with the influence that the soil structure, electrolyte and mineralogy has upon these phenomena. Subsequently a more detailed discussion of electro-osmosis, the phenomena of principal interest to this research, and its application to the field of geotechnical engineering through the removal of fluids from soil masses is given.

The concept of using electrically conductive geosynthetics (EKGs) for the application of electro-osmosis to soils is introduced and their physical properties and advantages over existing metallic electrodes discussed.

Electro-osmosis as applied to the consolidation of soft cohesive soil deposits is considered through a review of existing technologies that are alternatives to the problem of consolidation of soft cohesive ground. The mechanisms of soil consolidation by electro-osmosis are examined in detail and a field trial of electro-osmotic consolidation using electrokinetic geosynthetics presented. The design, installation, operation and monitoring stages are addressed together with the subsequent interpretation and conclusions of the trial.

The principles of reinforced soil are examined with particular reference being made to the use of cohesive fill in reinforced soil structures by means of a review of previous and current applications being given. The synergy between electrokinetic phenomena and reinforced cohesive soil is postulated. The first ever application of electrokinetically enhanced reinforced cohesive soil using EKGs by means of a full-scale field trial is then presented. All stages of design, construction, monitoring and subsequent interpretation are given.

The application of electrokinetics to the volume control of soils susceptible to shrinkage and swelling is introduced and the details of a field trial are given during which new installation and connection technologies for the use of EKGs were developed.

Finally, soil acceptability criterion are proposed to allow the applicability of electro-osmosis to a particular soil to be assessed, with their basis being upon using a combination of conventional soil mechanics laboratory tests to establish initial acceptability followed by more specific electrokinetic testing. The design methods and procedures for consolidation, reinforced cohesive soil and volume control by electrokinetics and EKGs are presented in a summarised form as a result of the field trials undertaken as part of the research. Potential future applications for electro-osmosis and EKGs are suggested.

LIST OF CONTENTS

LIST OF FIGURES

LIST OF TABLES

LIST OF PLATES

LIST OF SYMBOLS

Note: simple dimensions (*A* for cross-sectional area, *D* or *d* for depth or diameter, H for height etc.) are not included. Subscripts are not listed where their meaning is clear (e.g. *crit* for critical, *max* for maximum, *ult* for ultimate) Effective stress and effective stress parameters are denoted in the text by a prime (′).
Standard *Système International d'Unités* (SI) units have been used thought this thesis with decimal multiples and fractions denoted by prefixes before the unit symbol.

SYMBOL	EXPLANATION	SI UNIT
A	Activity	dimensionless
A_0	Surface charge density per unit pore volume	Cm^{-5}
B	Geogrid thickness	m
C_v	Coefficient of consolidation	m^2s^{-1}
C_{vr}	Coefficient of consolidation for radial flow	m^2s^{-1}
C_0	Concentration in external solution	ions m^{-3}
C_1, C_1	Constants of integration	variable
D	Dielectric constant	dimensionless
D_{10},D_{50}	Largest particle size in smallest 10% / 50% of particles by mass	m
E	Voltage difference Electrical energy	V Wh
E_D	Dilatometer modulus	Nm^{-2}
E_u	Undrained Young's modulus	Nm^{-2}
E^{θ}_{red}	Reduction voltage	V
E_o	Permittivity of vacuum	$C^2J^{-1}m^{-1}$
F_1, F_2	Scale / shape effect adjustment factors	dimensionless
G	Shear modulus	Nm^{-2}
G_s	Specific gravity	dimensionless
I	Electrical current	A
J_{ii}	Flux	variable
K	Boltzmann constant Double layer thickness	$J\ ^oK^{-1}$ m
K_a	Active earth pressure coefficient	dimensionless
K_p	Passive earth pressure coefficient	dimensionless
L_{ii}	Conductivity	variable
M	Slope of critical state line in p′, q space	dimensionless
N	Avogadro's number Number	molecules mol^{-1} dimensionless

P	Electrical power	W
P_R	Reinforcement load	N
P_s	Shear load	N
P_v	Vertical load	N
Q	Volume of fluid	m^3
R	Ratio anions / cations Resistance	dimensionless Ω
S	Surface area Geogrid aperture spacing Geosynthetic layer spacing	m^2 m m
T	Temperature Tension in reinforcement	°K N
T_r	Time factor for radial flow	dimensionless
T_v	Time factor	dimensionless
U	Average degree of consolidation	dimensionless
V	Valence Voltage	dimensionless V
X_{ii}	Driving gradient	variable
$\bar{a}_b$	Fraction of width for bearing	dimensionless
$\bar{a}_s$	Fraction solid surface area	dimensionless
c	Efficiency factor	dimensionless
c′	Effective cohesion	Nm^{-2}
c_u	Undrained shear strength	Nm^{-2}
e	Electronic charge Voids ratio	C dimensionless
i_e	Electrical potential gradient	Vm^{-1}
k	Hydraulic permeability	ms^{-1}
k_e	Electro-osmotic permeability	$m^2s^{-1}V^{-1}$
k_i	Electro-osmotic efficiency	$m^3s^{-1}A^{-1}$
m_v	Coefficient of volume compressibility	m^2N^{-1}
n	Porosity Number of electrode pairs	dimensionless dimensionless
n_0	Electrolyte concentration	ions m^{-3}
p′	Stress invariant (effective mean stress)	Nm^{-2}
q	Stress invariant (deviatoric stress) Unconfined compressive strength	Nm^{-2} Nm^{-2}
q_a	Flow through area “a”	m^3s^{-1}
t	Time	s
u	Porewater pressure	Nm^{-2}
v	Velocity in free pore fluid Specific volume	ms^{-1} dimensionless

v_e	Velocity of flow induced by electrical potential gradient	ms^{-1}
v_h	Velocity of flow induced by hydraulic gradient	ms^{-1}
w, w_c	Water content	dimensionless
w_k	Critical water content	dimensionless
z	Depth	m
α	Reinforcement adhesion factor	dimensionless
α_b	Bond coefficient	dimensionless
α_{ds}	Direct sliding coefficient	dimensionless
γ	Mean molar activity coefficient in external solution Bulk unit weight of soil/fluid	dimensionless Nm^{-3}
$\bar{\gamma}$	Mean activity coefficient in double layer	dimensionless
γ_w	Bulk unit weight of water	Nm^{-3}
δ	Double layer thickness Settlement Angle of friction soil/reinforcement	m m degrees (°)
ε_a	Axial strain	dimensionless
ζ	Zeta potential Potential across a condenser	V V
η	Viscosity	Nsm^{-2}
θ	Angle	degrees (°)
μ_g	Geological settlement correction factor	dimensionless
ν	Poisson's ratio	dimensionless
ξ	Electro-osmotic equation variable	kgm^{-2}
π	Pi	dimensionless
ρ	Resistivity	Ωm
ρ_c	Consolidation settlement	m
ρ_{oed}	Oedometric settlement	m
ρ_w	Density of water	kgm^{-3}
σ	Surface charge density Electrical conductivity	Cm^{-2} Sm^{-1}
σ'_b	Effective bearing stress	Nm^{-2}
σ'_n	Effective normal stress	Nm^{-2}
σ_1	Major principal stress	Nm^{-2}
σ_2	Intermediate principal stress	Nm^{-2}
σ_3	Minor principal stress	Nm^{-2}
τ	Shear stress	Nm^{-2}
ϕ	Angle of shearing resistance	degrees (°)
ψ_0	Surface potential	Volts
Ω	Resistance	Ω

CHAPTER 1

INTRODUCTION

1.1 GENERAL

This thesis is concerned with the application of Electrokinetic Geosynthetics (EKG) to uses in the construction industry. Principally, the application of electrokinetic phenomena, using electrically conductive geosynthetics, to the areas of soil consolidation, soil reinforcement and volume control.

The motivation behind the development of the EKG, as part of a research project, was to produce a new range of purpose designed geosynthetics to offer combinations of filtration, drainage and reinforcement, which would be enhanced by electrical conduction. Nettleton (1997) had observed that recent technological advances in materials science allowed the production of polymeric geosynthetic materials that were electrically conductive. This development was of interest as it meant that electro-osmosis could be combined with existing geosynthetic functions to increase the rate of removal of water from cohesive soils in comparison to conventional gravitational drainage. As remarked by Casagrande (1949) and Mitchell (1991), electro-osmosis has been noted as offering an efficient means of dewatering fine grained soils.

Additionally, research work undertaken at the University of Newcastle upon Tyne into composite drainage and reinforcement geosynthetics by Heshmati (1993) demonstrated that significant technological benefits could be achieved by combining these functions in a single geosynthetic. Thus allowing the use of fine grained (cohesive) soils for construction, a soil type that had previously been categorised as unacceptable. This research gave the inspiration of applying electro-osmosis through the use of EKG to the area of cohesive reinforced soil, as well as to the more apparent application of consolidation of soft cohesive soils.

The development of the EKG also has potential applications in the in situ remediation of contaminated land; electro-remediation (Lageman *et al* 1989). It has also been suggested that electro-remediation is the only means of remediation for contaminated fine grained soils in situ, due to their low hydraulic permeability (NATO/CCMS 1993). The sorption of heavy metals by the use of EKGs has also been demonstrated as being effective in recent research at the University of Newcastle upon Tyne (O'Dwyer 1994).

1.2 STATEMENT OF RESEARCH OBJECTIVES

The objectives of this research were to further develop the use of EKGs in the construction industry and to undertake their first ever use in the field for the applications of electro-osmotic consolidation and cohesive reinforced soil, as well as for any other opportune applications that arose during the period of the research.

Additionally, to gain experience and develop the associated technologies of installation and construction techniques in the use of EKGs and electro-osmosis in the field and to develop design methodologies for these techniques.

1.3 STRUCTURE OF THE THESIS

This thesis consists of eight chapters, the outlines of which are described in the following text.

- **Chapter 1 - Introduction**: The present chapter introduces the background to the research, states the objectives of the research and gives a brief summary of the contents of the thesis.

- **Chapter 2 – A review of electrokinetic phenomena in soils**: This chapter introduces from first principles the theory of electrokinetic phenomena in soils, beginning with a review of clay mineralogy, liquid and gas soil phases and then the fundamental concepts of how electrokinetic phenomena occur in soils. All the electrokinetic phenomena that occur in soils are then briefly discussed followed by a detailed discussion and derivation of the theory of electro-osmosis, which is the phenomenon of principal interest to the work presented in this thesis.

- **Chapter 3 - Electrokinetic geosynthetics**: This chapter begins with a review of existing geosynthetics, their forms, functions and materials. The concept of electrically conductive polymers is then introduced, followed by the introduction to the concept of an Electrokinetic Geosynthetic (EKG). The EKG produced by Netlon Ltd. is then introduced and discussed in detail, together with its limitations and suggestions for further improvement. The concepts of EKG connection technology are also discussed.

- **Chapter 4 – Ground improvement - electro-osmotic consolidation:** This chapter commences by introducing the concepts of ground improvement followed by a summary of ground improvement techniques. The techniques that are direct

competitors to electro-osmosis, i.e. those that are applicable to the same soil types, are discussed in some detail.
Electro-osmotic consolidation is then discussed by advancing the fundamental concepts introduced in Chapter 2 to the specific application of electro-osmosis to the consolidation of soils, together with a historical review of its past uses.
A small-scale consolidation trial at Newburn Haugh is then discussed. The geotechnical characteristics of the trial are introduced, together with the fundamental design of the trial, installation, anticipated performance, and monitoring. The results of the trial are then presented followed by their interpretation and comparison with the design values. Conclusions and recommendations for further work are then given.

- **Chapter 5 - EKG in soil reinforcement**: The chapter begins with a summary of the principles of soil reinforcement and considers aspects of soil-reinforcement interaction. This is followed by a brief overview of existing reinforced soil analysis methods. The concepts of the use of cohesive fill to reinforced soil structures is introduced by a review of previous experimentation and experience with cohesive fill, together with a review of current reinforced soil techniques that permit the use of cohesive fill. The Joint Stocks wall is then presented as the first ever field application of electro-osmosis to cohesive reinforced soil. Initially the laboratory testing on the cohesive fill material is given followed by the use of the results obtained to undertaken a long-term stability analysis of the wall. The short-term stability analyses are then discussed which establishes the improvement that electro-osmosis is required to achieve to maintain the short-term stability of the wall. The electro-osmosis design is then given using both approximate and more precise analysis methods.
  The field construction and monitoring of the wall is discussed and the results obtained from the trial are presented. Interpretations and conclusions are drawn from these results and finally recommendations for further work are given.

- **Chapter 6 - Volumetric control of soils:** This chapter addresses the application of electro-osmosis to the control of volume change of susceptible soils. The principle of changing a soil's volume change potential thought over-consolidation and electrochemical changes to the clay minerals is introduced.
  A discussion of a full-scale trial of electro-osmotic volume control of an embankment on London Underground's District Line between Wimbledon Park and Southfields Stations is then given. The design of the trial, its anticipated response, the installation and the connection methods are all discussed. The trial has not been powered up due to possible interference of the electrical field generated by the electro-osmosis trial on the signalling circuitry. This phenomenon is also discussed.

- **Chapter 7 - Electro-osmosis - philosophy and design**: This chapter draws together the information and experience acquired during the research to offer recommendations for the acceptability criteria for soils to be treated by electro-osmosis. Design recommendations and procedures are also given for electro-osmotic consolidation, electro-osmotically enhanced reinforced cohesive soil and electro-osmotic volume control. Other potential applications for EKGs and electro-osmosis are then given with the applications suggested ranging from tunnelling and pipe-jacking to slope stability.

- **Chapter 8 - Summary and main conclusions**: This chapter presents a summary of the research undertaken and gives a résumé of the main conclusions drawn in the areas of; EKGs, electro-osmotic consolidation, electro-osmotically enhanced cohesive reinforced soil, electro-osmotic volume control and philosophy. The fulfilment of the research objectives is then discussed together with recommendations for further research.

1.4 CHAPTER 1 REFERENCES

1. Casagrande, I.L. (1949) *Electro-osmosis in soils*, Géotechnique, Vol. 1(3), pp. 159-177.
2. Heshmati, S. (1993) *The action of geotextiles in providing combined drainage and reinforcement to cohesive soil.* Doctor of Philosophy Thesis, Geotechnical Group, University of Newcastle upon Tyne, U.K., p. 225
3. Lageman, R., Pool, W. and Seffinga, G.A. (1989) *Electro-reclamation: state-of-the-art*, In NATO/CCMS 3rd Int. Conf. on Demonstration of Remedial Action Technologies for Contaminated Land and Groundwater, Nov. 6-9, 1989, Montreal, Canada, pp. 115-136.
4. Mitchell, J.K. (1991) *Conduction phenomena: from theory to geotechnical practice.* Géotechnique, Vol. 41 No .3, pp. 299-340.
5. NATO/CCMS (1993) *Demonstration of Remedial Action Technologies for Contaminated Land and Groundwater*. (Final Report No. EPA/600/R-93/012a) North Atlantic Treaty Organisation, Committee on the Challenges to Modern Society.
6. Nettleton, I.M. (1997) *Research into new forms of geosynthetic materials.* Geotechnical Group, University of Newcastle upon Tyne, Internal Report. EPSRC Contract No. GR/K 20590.
7. O'Dwyer, S. (1994) *Adsorption Of Metals Using A Geosynthetic*. M.Sc. Dissertation, Geotechnical Group, University of Newcastle upon Tyne, U.K., p. 99.

CHAPTER 2

A REVIEW OF ELECTROKINETIC PHENOMENA IN SOILS

2.1 INTRODUCTION AND DEFINITION OF TERMS

This chapter reviews, from first principles, the mechanisms of electrokinetic phenomena in soils, beginning with a review of soil particle mineralogy, pore fluid chemistry and particle-fluid electrolyte systems. It then goes on to discuss the currently proposed theories for electrokinetic phenomena in soils, explaining how and why they occur.

Electrokinetics, for geotechnical applications, may be defined as the application or induction of, an electrical potential difference across a soil mass containing fluid, or a high fluid content slurry/suspension, causing or caused by the motion of electricity, charged soil and/or fluid particles (Pugh *et al* 2000).

Electrokinetic phenomena are the result of the coupling between hydraulic and electrical potential gradients in fine grained soils (Acar & Alshawabkeh 1993, Acar & Alshawabkeh 1994, Mitchell 1993, Yeung & Mitchell 1993, Yeung 1990). These phenomena occur due to the presence of the diffuse double layer around the fine grained soil particles and involve the movement of electricity, charged particles and fluids (Mitchell 1993). It is, therefore, necessary to have a thorough understanding of these components in order to fully understand the phenomena. The principles of hydraulic flow within a soil mass, as explained by Darcy's law, are met commonplace within geotechnical engineering and will not be elaborated upon further in this thesis. However, it is the Author's opinion that the subject areas of clay mineralogy, diffuse electrolyte double layers, soil structure and fabric are not commonly encountered by practicing geotechnical engineers and do require further explanation. This will be undertaken in the subsequent sections of this chapter, followed by detailed discussion on electrokinetics in soils.

Additionally, the field of electrokinetics within geotechnical engineering frequently uses terms that are not commonly encountered in other branches of geotechnical engineering. To assists the reader in their rapid understanding of the work presented in this thesis some of the more commonly encountered terms are defined below, with further explanation of other terms given later in this chapter.

Electro-osmosis: The net flow of water in a wet soil towards the cathode (-ve). It is caused by the viscous drag applied to the pore water by the water of hydration of ions induced to move by the application of an electrical potential (DC) across the soil mass.

Electrophoresis: The electrostatic attraction of discrete charged particles to one electrode and their repulsion from the other of opposite sign in a colloidal suspension as a result of the application of a DC electrical field.

Electrical potential: The work required to move an electric charge from a reference point to a specified point; measured in Volts.

Electrical potential difference: The difference in electrical potential (using the same reference point) between two points; measured in Volts.

Electrokinetic treatment of soil: The improvement of a soils engineering properties as a result of the application of a DC electrical potential difference.

2.2 INTRODUCTION TO ELECTROKINETICS

Reuss (1808) first observed electrokinetic phenomena when a direct current (DC) potential difference was applied to a clay water mixture. Water was observed to move through the capillary towards the cathode under the electrical field. When the electrical potential was removed, the flow of water immediately stopped. Napier (1846) distinguished electro-osmosis from electrolysis, and Quincke (1861) found that the electrical potential difference through a membrane resulted from streaming potential.

Helmholtz (1879) was the first to treat electro-osmosis analytically, providing a mathematical basis for its analysis; this was later modified by Smoluchowski (1914) to apply electrophoretic velocity. The Helmholtz-Smoluchowski theory thus contrived still forms the basis of electro-osmotic analysis today.

In 1939, Leo Casagrande demonstrated that applying electro-osmosis to soils with high water contents, resulted in an increase in the effective stress within the soil, increasing its shear strength to such a degree that even steep cuts remained stable. Two years later Casagrande again successfully utilised electro-osmosis in foundation engineering. It was indicated from Casagrande's practice, that small reductions in water content by electro-osmosis could produce significant increases in soil strength. From then on, electrokinetic treatment of soils has been investigated and used in many field projects, such as: improvement of excavation stability, electrochemical induration/hardening and the stabilisation, consolidation and densification of fine grained soil. In the late 1960's and early 1970's direct current was even applied successfully (Waxman & Smits 1967) to recover residual oil from deep seated geological formations (Enhanced Oil Recovery).

The soil types that are amenable to treatment by electrokinetic phenomena, and are applicable to the work undertaken in this thesis, are those which may be described as fine grained. These are defined as containing over 35% silt and clay sized fractions (BSI 1981), which typically exhibit low hydraulic permeabilities (10^{-7} to 10^{-10} ms^{-1}) and high porosities (35 to 50% for silts and 40 to 70% for clays (Freeze & Cherry 1979)). Soils coarser than this are usually unsuitable for treatment by electrokinetic phenomena as they are either lacking the surface chemistry and colloidal nature of silt/clay particles or their hydraulic permeabilities are excessively high for the electrokinetic phenomena to have any significant effect, this is discussed further in §2.3. In order to understand this important differentiation and the reasons for the occurrence of electrokinetic phenomena in soils it is necessary to examine the individual constituents of a fine grained soil mass, i.e. the solid, liquid and gas phases. A discussion of solid phase soil chemistry, and its effect on electrokinetic phenomena is presented in the following section, followed by a discussion of liquid and gas phase chemistry in §2.4. These three elements are then brought together in §2.5, with a discussion of particle-fluid electrolyte systems.

2.3 SOLID PHASE SOIL CHEMISTRY & COMPONENTS

The solid phase of a soil may contain various amounts of crystalline clay and non-clay minerals, non-crystalline clay material, organic matter, and precipitated salts. The crystalline minerals comprise the greatest proportion in most soils encountered in engineering practice, and the amount of non-clay material usually exceeds the amount of clay. Nonetheless, clay and organic matter in a soil usually influence properties in a manner far greater than their relative abundance (Mitchell 1993).

2.3.1 ORGANIC MATTER

The organic matter present in soils originates from the biomass that is characteristic for an active soil (Tan 1993). Organic matter in soil may be responsible for high plasticity, high shrinkage, high compressibility, low hydraulic conductivity and low strength. Soil organic matter is complex both chemically and physically, and a variety of reactions and interactions between the soil and the organic matter are possible (Oades 1989). Organic matter may be subdivided, for classification, into four categories:

- ***Plant Material:*** Plant materials are added to soils from living root systems, from dead roots, and as litter is added to the surface of the soil.
- ***Humic Material:*** The organic material in soil, not recognisable under a light microscope as possessing the cellular organisation of plant material.
- ***Nonhumic Substances:*** Carbohydrates, essential components of all living organisms and represents the major energy source for the soil biota.

- ***Microbial Mass:*** Living organisms apart from plants.

Living organic material that is present in soil also has an effect on the soil moisture content through evapotranspiration. The effects of organic matter in soils are discussed in §2.5.

2.3.2 MINERAL MATTER

Most inorganic soils contain 80% or more of rock derived material by weight (Simpson 1983). It is the clay fraction of this component of the soil's solid matter that predominantly governs its electrokinetic properties. Therefore, an understanding of the soil forming clay minerals and their chemistry enables an understanding of how electrokinetic phenomena occur in soils. Clay, as a mineral term refers to specific clay minerals that are distinguished by (Mitchell 1993):

(1) small particle size
(2) net negative electrical charge
(3) plasticity when mixed with water
(4) high weathering resistance

These minerals are primarily hydrous aluminium silicates, with magnesium or iron occupying all or part of the aluminium positions within the crystal lattice in some minerals, with alkalines or alkaline earths also present in some of them (Grim 1962, 1968).
Table 2.1 presents the main soil forming minerals and gives an indication to their resistance to weathering and an indication as to their contribution to a soil mass. It should also be appreciated that the parent rock from which the soil is derived is an essential factor in defining the soil mineralogy. For example, quartzose sandstone will not weather to yield a kaolinite rich soil.
The early stages of the formation of the mineral components of soils are dominated by the weathering of the parent rock material. Weathering takes place by physical, chemical or biological means, and usually by a combination of all three working together (Simpson 1983).

The minerals that occur in soils have been classified on the basis of both their composition and crystal structure. The first classification has subdivisions such as carbonates, phosphates, oxides and silicates. This classification is of limited use to the civil engineer since most of the abundant and important soil minerals are silicates. In fact, if all of the soil in the world were placed in one pile, over 90% of the weight of the pile would be silicate minerals (Lambe & Whitman 1969).

Table 2.1 Soil forming minerals (After Simpson 1983)

Mineral Group	Composition	Ease of Weathering	Contribution to soil
Quartz	Silica	Very resistant	Major parts of sands
Feldspars (Orthoclase, Plagioclase)	Alumino-silicates	Slow in arid soils, easily weathered elsewhere	**Clay minerals**, potassium, calcium
Micas: Muscovite - white Biotite - black	Alumino-silicates	Biotite weathers easily. Muscovite less so	**Clay minerals**, potassium, magnesium, iron
Carbonates: Dolomite, Calcite	Calcium and magnesium carbonates	Easily weathered and leached	Calcium, magnesium. Acidity control
Amphiboles and Pyroxenes	Alumino-silicates	Easily weathered	**Clay minerals**, iron, calcium, magnesium
Apatite	Calcium phosphate	Changes to other phosphates	Original source of phosphorus
Iron Compounds: Haematite, Limonite	Oxides of iron	Resistant	Colour, **clay minerals**, iron

Soils are usually the products of rock weathering and thus the most abundant soil minerals are common rock forming minerals which are resistant to weathering and the resistant weathered component of those that have weathered. The sheet and framework silicate minerals are therefore, the most abundant and common soil forming minerals.

Silicate minerals may be idealised by considering them to be made from basic structural units. However, it must be appreciated that this unit approach is a simplification of reality. The typical mineral has a complex structure, similar to the idealised arrangement but usually with irregular substitutions and interlayering. Figure 2.1 shows some basic silicate units.

The silicon-oxygen tetrahedron consists of four oxygen atoms positioned around a silicon atom to form the unit shown in Figure 2.1a&b. The atoms in this figure are drawn approximately to scale based on their atomic radii in units of angstroms (1Å = 0.1nm). The figures quoted to the right of each unit give the atomic valence distribution over the unit.

Figure 2.1c shows the aluminium-oxygen octahedron and Figure 2.1d the magnesium-oxygen octahedron. Combination of the silicon-oxygen tetrahedrons shown in Figure 2.1a&b gives the silica sheet shown in Figure 2.1e. Combination of the aluminium-oxygen octahedrons gives gibbsite (Figure 2.1f), and combining the magnesium-oxygen octahedron gives brucite (Figure 2.1g). A study of the valances given in Figure 2.1 shows that the tetrahedron and two octahedrons are ***not*** electrically neutral and therefore do not exist in nature as isolated units. Gibbsite and brucite are, however, electrically neutral and exist in nature as such (Lambe & Whitman 1969).

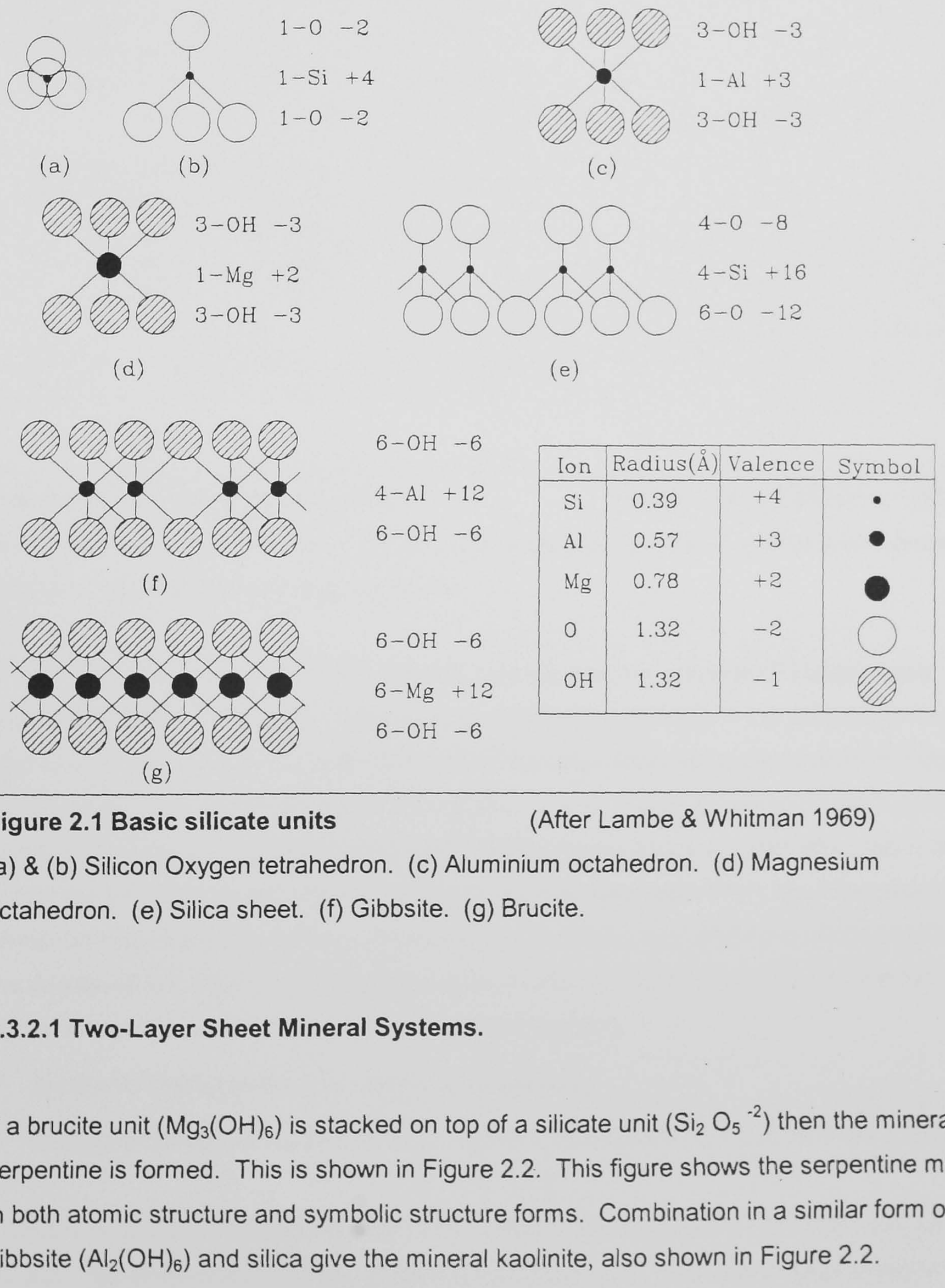

Figure 2.1 Basic silicate units (After Lambe & Whitman 1969)

(a) & (b) Silicon Oxygen tetrahedron. (c) Aluminium octahedron. (d) Magnesium octahedron. (e) Silica sheet. (f) Gibbsite. (g) Brucite.

2.3.2.1 Two-Layer Sheet Mineral Systems.

If a brucite unit ($Mg_3(OH)_6$) is stacked on top of a silicate unit ($Si_2 O_5^{-2}$) then the mineral serpentine is formed. This is shown in Figure 2.2. This figure shows the serpentine mineral in both atomic structure and symbolic structure forms. Combination in a similar form of gibbsite ($Al_2(OH)_6$) and silica give the mineral kaolinite, also shown in Figure 2.2.

The actual mineral particle does not usually consist of only a few basic layers as suggested by the symbolic structures in Figure 2.2. Instead, a number of minerals are stacked one on top of another to form an actual crystal. The linkage between the basic two-layer unit comprising of hydrogen bonding and secondary valence forces.

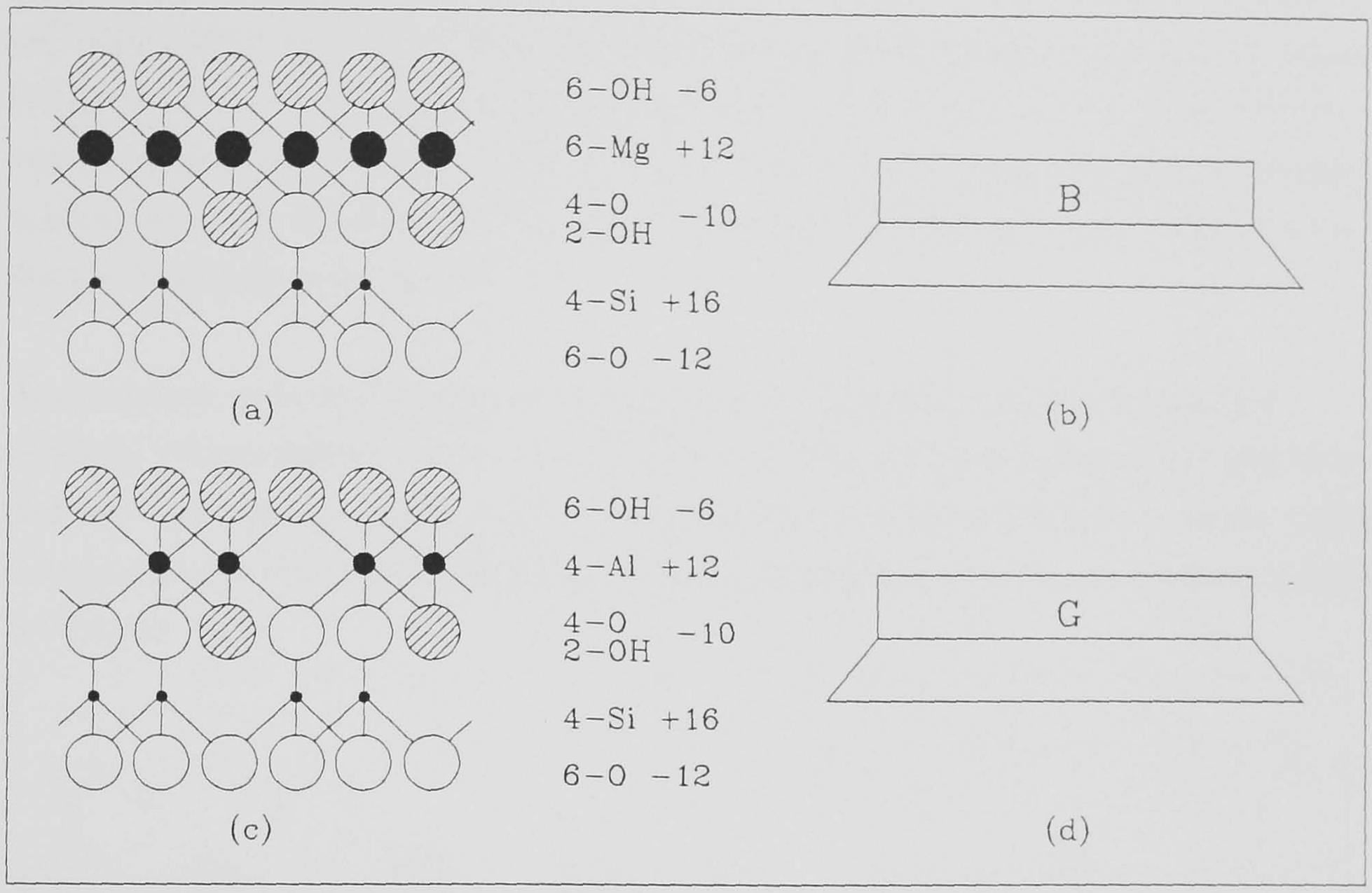

Figure 2.2 Two layer sheet systems (After Lambe & Whitman 1969)

(a) Serpentine atomic structure. (b) Serpentine symbolic structure. (c) Kaolinite atomic structure. (d) Kaolinite symbolic structure.

In the actual formation of the sheet silicate minerals the phenomenon of *isomorphous substitution* frequently occurs. Isomorphous substitution consists of the substitution of one kind of atom for another. For example, one of the sites filled with a silicon atom in Figure 2.2a&c could be occupied by an aluminium atom. Such a case of isomorphous substitution could occur if aluminium atoms were more readily in abundance at a site than silicon atoms during the formation of the mineral structure. Furthermore, aluminium has co-ordinating characteristics somewhat similar to those of silicon, thus it can fit into the silicon position in the crystal lattice, Figure 2.1. Substituting the aluminium atom with its +3 valence for the silicon atom with its +4 valence has two important effects:

- A net unit charge deficiency results per substitution.
- A slight distortion of the crystal lattice occurs since the ions are not identical in size.

Further discussion of the significance of the effect of the unit charge deficiency is given in §2.3.3. The associated distortion to the crystal lattice tends to restrict crystal growth and thus limits the size of the crystal.

2.3.2.2 Three-Layer Sheet Mineral Systems

The three layer sheet minerals are formed from either one gibbsite or one brucite unit sandwiched between two silica sheets. Pyrophyllite consists of a gibbsite unit sandwiched between two silica sheets as shown in Figure 2.3a&b, and talc of one brucite unit between two silica sheets. Isomorphous substitution also occurs in three layer sheet systems. Figure 2.3c&d show the mineral muscovite, which consists of the isomorphous substitution of one aluminium atom for one silicon atom. The net charge imbalance created by this substitution is balanced by the inclusion of potassium ions between the three layer units, these serve to link the three layer units together.

The two most common three layer structures in soils are montmorillonite and illite type minerals. Montmorillonite has a structure similar to pyrophyllite with the exception that there has been isomorphous substitution of magnesium for aluminium in the gibbsite sheet. Table 2.2 gives a summary of the sheet silicate minerals of importance to the civil engineer (Lambe & Whitman 1969).

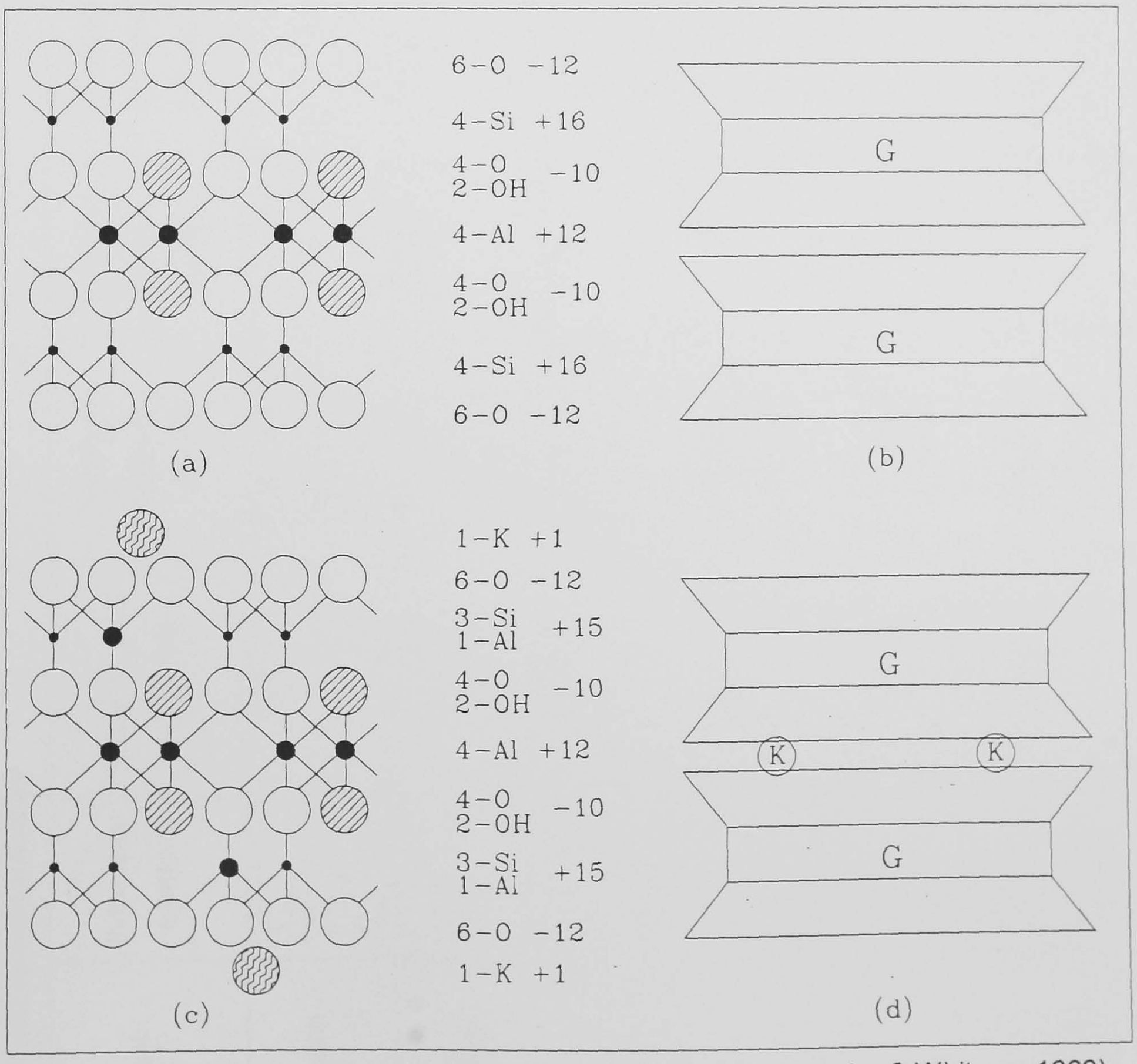

Figure 2.3 Three layer sheet systems (After Lambe & Whitman 1969)

(a) Pyrophyllite atomic structure. (b) Pyrophyllite symbolic structure. (c) Muscovite atomic structure. (d) Muscovite symbolic structure.

Table 2.2a Sheet silicate minerals (After Lambe & Whitman 1969)

Mineral	Structure symbol	Isomorphous substitution	Linkage between sheets	Specific surface (m^2/g)	1/Charge density ($Å^2$/ion)	Potential exchange capacity (me/100g)	Actual exchange capacity (me/100g)	Particle shape	Particle size
Serpentine	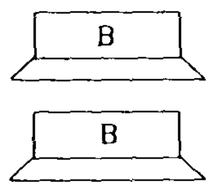	None	H-bonding+ Secondary Valence			1	1	Platy or fibrous	
Kaolinite	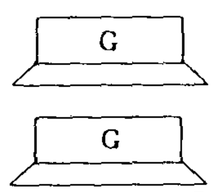	Al for Si 1 in 400	H-bonding+ Secondary Valence	10-20	83	3	3	Platy	d=0.3 to 3μm thickness =0.33 to 0.1d
Halloysite ($4H_2O$)	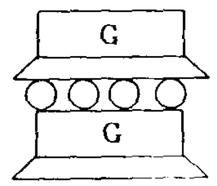	Al for Si 1 in 100	Secondary Valence	40	55	12	12	Hollow rod	OD = 0.07μm ID = 0.04μm L = 0.5μm
Halloysite ($2H_2O$)	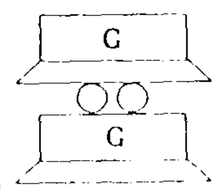	Al for Si 1 in 100	Secondary Valence	40	55	12	12	Hollow rod	OD = 0.07μm ID = 0.04μm L = 0.5μm
Talc	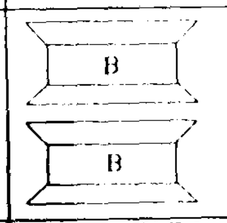	None	Secondary Valence			1	1	Platy	
Pyrophyllite	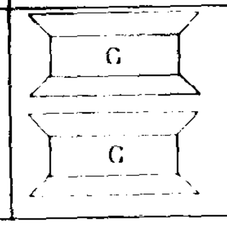	None	Secondary Valence			1	1	Platy	

Mineral	Structure symbol	Isomorphous substitution	Linkage between sheets	Specific surface (m^2/g)	1/Charge density ($Å^2$/ion)	Potential exchange capacity (me/100g)	Actual exchange capacity (me/100g)	Particle shape	Particle size
Muscovite	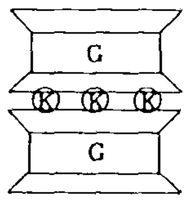	Al for Si 1 in 4	Secondary Valence + K linkage			250	5-20	Platy	
Vermiculite	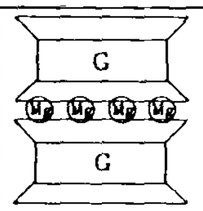	Al, Fe for Mg Al for Si	Secondary Valence + Mg linkage	5-400	45	150	150	Platy	t=0.1d to 0.03d
Illite	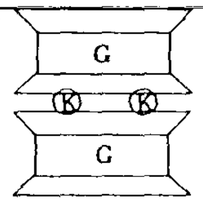	Al for Si, 1 in 7 Mg, Fe for Al Fe, Al for Mg	Secondary Valence + K linkage	80-100	67	150	25	Platy	d = 0.1to 2μm t =0.1d
Montmorillonite	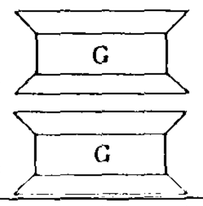	Mg for Al 1 in 6	2ndry Valence + exchangeable ion linkage	800	133	100	100	Platy	d = 0.1 to 1μm t = 0.01d
Nontronite	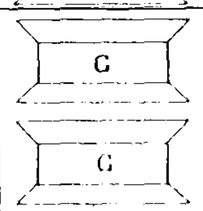	Al for Si 1 in 6	2ndry Valence + exchangeable ion linkage	800	133	100	100	Lath	l = 0.4 to 2μm t = 0.01 l
Chlorite	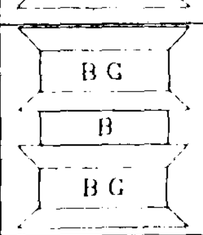	Al for Si, Fe, Al for Mg	2ndry Valence + brucite linkage	5-50	700	20	20	Platy	

Table 2.2b Sheet silicate minerals (After Lambe & Whitman 1969)

2.3.2.3 Mixed Layer Clays

More than one type of clay mineral is usually found in most soils. Due to the great similarity of the crystal structure amongst the different minerals, interstratification of two or more layer types often occurs within a single particle. Interstratification may be regular, with a definite repetition of the different layers in sequence, or it may be random. According to Weaver & Pollard (1973), randomly interstratified clay minerals are second only to illite in abundance.

The most abundant mixed layer material is composed of expanded water-bearing layers and contracted non-water-bearing layers. Montmorillonite-illite is most common, and chlorite-vermiculite and chlorite-montmorillonite are often found (Mitchell 1993).

2.3.3 SOLID PHASE ELECTRICAL CHARGE

Every soil particle carries an electrical charge. Although a soil particle can carry either a net negative or a net positive charge, most commonly negative charges have been measured (Lambe & Whitman 1969). This net negative electrical charge present on soil particles may arise from any one or a combination of the following factors:

- ***Isomorphous substitution*** of cations at their surfaces; this gives most clay particles a net negative surface charge. This process is a source of CEC (Cation Exchange Capacity, §2.5.1.2)
- ***Surface disassociation of hydroxyl ions***, replacement of hydrogen in exposed hydroxyl groups by other cations. Hydroxyls tend to disassociate in water

  $$SiOH \rightarrow SiO^{-} + H^{+}$$

  This process is catalysed by high pH conditions, leading to a greater net negative surface charge.
- ***Breaking of Bonds*** at particle edges which gives rise to unsatisfied negative charges, which may be balanced by sorption of cations. This is the major source of CEC in kaolinites. The importance of this process increases with decreasing particle size.
- ***Adsorption of anions.***
- ***Presence of organic matter.***

Whilst, in most cases clay surface charges are negative it is possible for positive surface charges to form. Aluminium, which is amphoteric may become ionised positively at low pH values and negatively at high pH values. Hence, a positive edge charge may form in acidic environments e.g. kaolinite at low pH values (Mitchell 1993). Of these charge affecting

factors isomorphous substitution is the most important (Lambe & Whitman 1969). In addition to a net charge, a soil particle can carry a distribution charge because the seat of the negative charge and positive charge do not coincide, this can be seen in the atomic structure diagrams given in Figures 2.1, 2.2 and 2.3.

Since the magnitude of the electrical charge is directly related to the surface area of the soil particle, it follows that the larger the surface area per unit mass of dry soil the greater the relative influence of the electrical forces on the behaviour of the soil particle over mass derived forces. The adjective for particles whose behaviour is controlled by surface derived forces, rather than mass derived forces is "colloidal". The size range of colloids has been set at between 1nm to 1μm. Smaller than 1nm lies the diameter of atoms and molecules, larger than 1μm and the particles are predominantly influenced by forces of mass, a lower limit of a specific surface of $25m^2/g$ has also been suggested as the lower limit for colloidal behaviour (Lambe & Whitman 1969). Table 2.3 presents typical soil particle properties for the range of particle sizes usually encountered in soils, and Tables 2.2a&b gives values of specific surface for commonly encountered clay minerals.

However, the distinction between silts and clays has been based partially upon laboratory settlement times calculated using Stokes' Law (Stokes 1891), which assumes spherical particles. True "clay" particles are however found with particle sizes up to 20μm, whereas "non-clay" particles are found with sizes as low as 1μm (Lee *et al* 1983). Hence, some silt particles demonstrate colloidal properties.

Table 2.3 Characteristics of soil particles (After Foth 1984)

Particle	Diameter (mm)	Number of particles per gram	Surface area per gram (cm^2)
Very Coarse Sand	-	90	11
Coarse sand	2.00 - 0.02	720	23
Medium sand	-	5,700	45
Fine sand	0.20 - 0.02	46,000	91
Very fine sand		722,000	227
Silt	0.02-0.002	5,776,000	454
Clay	Below 0.002	90,260,853,000	8,000,000

2.3.4 SOLID PHASE FABRIC AND STRUCTURE

The soil *fabric* is defined as the size, shape and arrangement of the solid particles, organic inclusions and the associated voids within a soil mass. The term *structure* is the element of fabric that deals with the arrangement of a particular size range. Thus clay particle

arrangements constitute structure whereas the arrangement of particle groups for example in layers having different particle sizes comes under fabric (Rowe 1972). There are four principle structural arrangements of clay particles that are described by van Olphen (1977); these are shown in Figure 2.4:

- **Dispersed**. No face-to-face (FF) association of clay particles.
- **Aggregated.** Face-to-face (FF) association of several clay particles.
- **Flocculated.** Edge-to-edge (EE) or edge to face (EF) association of aggregates.
- **Deflocculated.** No association between aggregates.

Stable suspensions or dispersions of clay particles require the particles to be deflocculated, and this is of great importance in drilling mud engineering. The arrangement of clay particles can be altered by controlling the pH and ion concentrations of clay particle suspensions.

For example, Na^+ clays tend to deflocculate, whereas Ca^{2+} clays tend to flocculate. This is due to Na^+ ions being smaller and having water of hydration attached to them; thus separating the clay particles more (Bitton & Gerba 1984).

In addition, the addition of NaCl to a clay suspension will cause the particles to flocculate due to suppression of the diffuse double layer thickness, see § 2.5.1.

If the salt is then leached out of the clay thus formed it will tend to deflocculate and disperse on remoulding, thus forming a "quick" clay (Bjerrum & Rosenqvist 1956).

The soil fabric and especially the *macrofabric*, i.e. those features and their spatial arrangement that are apparent to the unaided eye or low powered magnification, (McGown *et al* 1980) can have a significant effect upon the way in which a soil will behave in terms of its shear strength, compressibility, consolidation and permeability characteristics.

2.4 LIQUID AND GAS PHASE SOIL CHEMISTRY

A saturated soil with a void ratio of greater than 1.0 has a greater volume of water than of solids, and void ratios in excess of 1.0 are the norm in the case of fine grained soils (Mitchell 1993). Historically, the study of soil has concentrated on the study of structure and mineralogy of the solid phase, with little emphasis placed upon the role of the liquid and gas phases. Mitchell (1993) suggests two possible reasons for this:

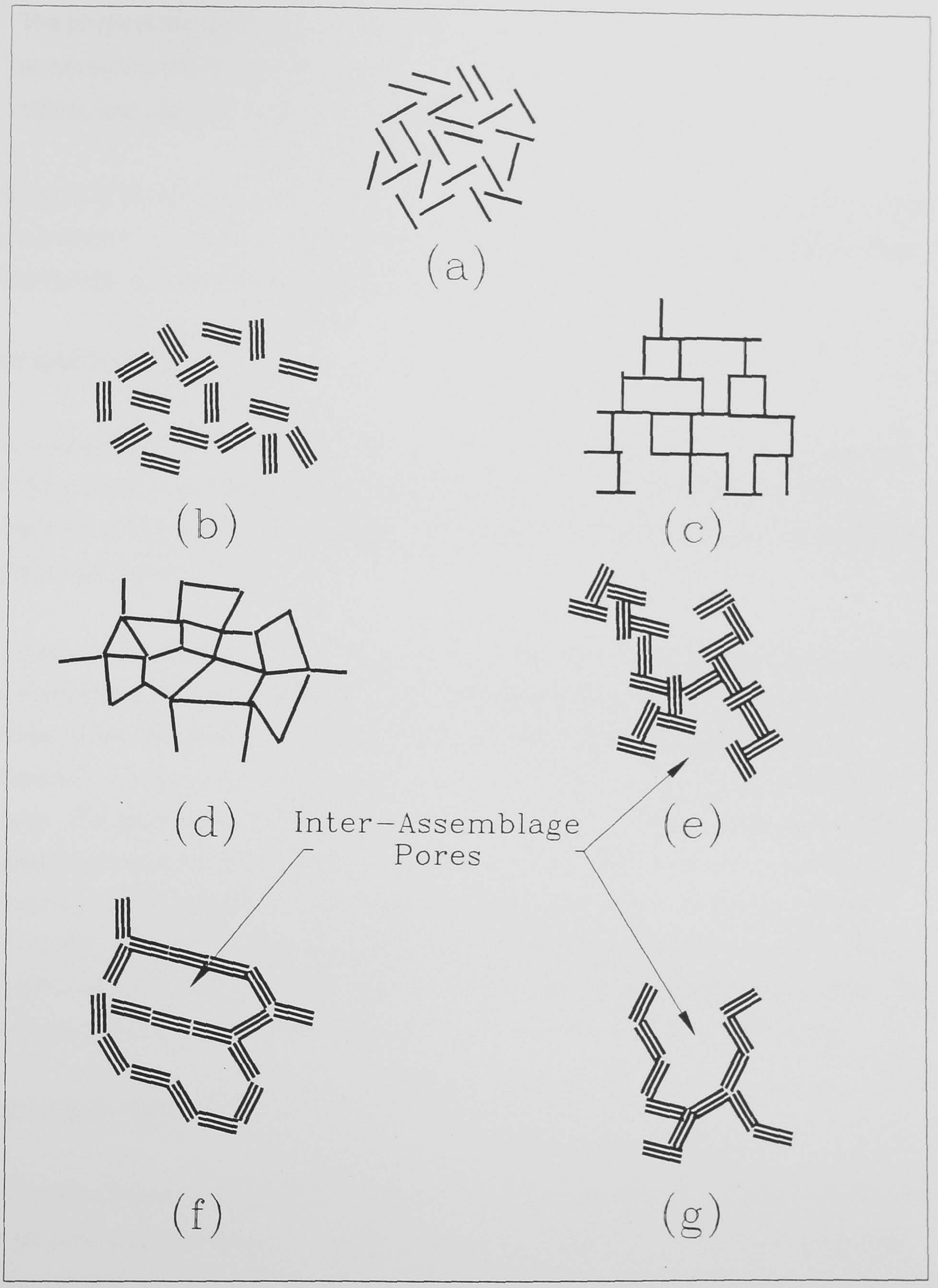

Figure 2.4 Modes of particle association in clay suspensions (After van Olphen 1977)
(a) Dispersed and deflocculated. (b) Aggregated and deflocculated. (c) Dispersed and flocculated. (d) Dispersed and flocculated. (e) Aggregated and flocculated. (f) Aggregated and flocculated. (g) Aggregated and flocculated

- Classical soil mechanics is founded on the concept of effective stress, which postulates that volume change and strength behaviour depend on the stress carried by the soil grain structure and that the fluid phase is neutral.

- The physical properties of water are well known - a clear, colourless, odourless, tasteless liquid that has a density very nearly equal to unity, freezes at 0°C, boils at 100°C, and has quite well defined viscosity and thermal properties.

The reality of the situation is not, however, so simple because neither water nor the surfaces of the soil minerals are inert. They, therefore, interact with each other, with water molecules being strongly attracted to and adsorbed on soil particle surfaces.

2.4.1 GAS PHASE

Most sedimentary clay deposits are fully saturated or very nearly so, and it is in these soils that the process of consolidation is most significant. The presence of air in the voids is discounted; to allow for partial saturation would make the analysis much too complicated for practical use (Head 1994).

The gaseous constituents of a soil are derived largely from the atmosphere, the respiration and metabolism of soil organisms, and from the evaporation of soil moisture. Soil air is continuous with the atmosphere provided that the soil surface is not sealed due to compaction or crusting, and such continuity ensures the free movement and exchange of gasses. The gases move along gradients of partial pressure, so that oxygen will tend to migrate from the atmosphere where its partial pressure is high into the soil where it is low. Conversely, carbon dioxide and water vapour will tend to migrate from the soil into the atmosphere. Movement of gases may occur by diffusion, mass flow or in dissolved form, with diffusion being by far the most significant of these processes (Ellis & Mellor 1995). The role of the gas phase present in soils will not be discussed any further in this thesis.

2.4.2 LIQUID PHASE

A pure water molecule (H_2O) is composed of a V-shaped arrangement of atomic nuclei that has an average H-O-H angle of slightly less than 105°, as shown in Figure 2.5. The outer shell electronic charges, six from the oxygen and one from each of the hydrogen atoms, are distributed in the form of electron pairs. The resulting configuration is a tetrahedron with two positive corners that are the sites of the hydrogen protons and two negative corners that are located above and below the plane of the atomic nuclei. This arrangement causes an imbalance of charges, with the centre of the positive charge at one end and the centre of the negative charge at the other end (Tan 1993). Bond energy considerations have shown that the H-O-H bond is about 40% ionic and 60% covalent, thereby accounting for both the directionality of the bond and for producing a permanent dipole (Pauling 1960).

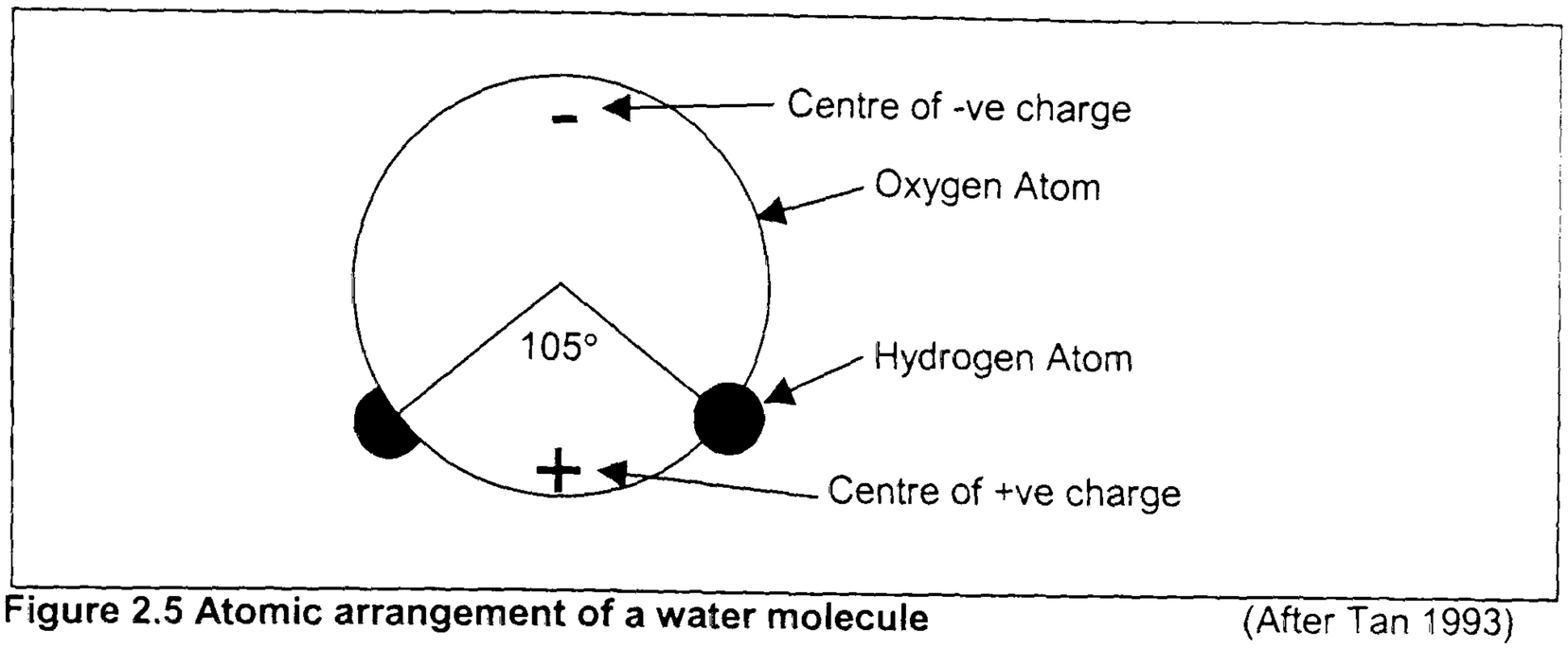

Figure 2.5 Atomic arrangement of a water molecule (After Tan 1993)

In water and ice, the positive corner of one molecule attracts the negative corner of another. The proton (hydrogen nucleus) is shared by the two oxygens, which results in hydrogen bonding and a tendency for each molecule to bond to four neighbouring molecules that surround it tetrehedrally (Frank 1958).

The structure of liquid water is not definitively known, except that some hydrogen bonding and ice structure remains. Stillinger (1980) provides a good description of the structure of liquid water:

"Liquid water consists of macroscopically connected, random networks of hydrogen bonds, with frequent strained and broken bonds, that is continually undergoing topological reformation. The properties of water arise from the competition between relatively bulky ways of connecting molecules into local patterns characterised by strong bonds and nearly tetrahedral angles and more compact arrangements characterised by more strain and bond breakage."

2.5 LIQUID/SOLID PHASE INTERACTION

Interactions between small soil particles, dissolved ions, and water are caused by unbalanced force fields at the interface between soil and water. When two particles are in close proximity, their respective (electrical) force fields overlap and influence the behaviour of the system, if these forces are large relative to the weight of the particles themselves, i.e. a colloidal system. Clay particles are especially influenced by these forces due to their very small size and platy shape (Mitchell 1993). These forces are the governing factors in the flocculation-deflocculation behaviour of clays in suspension and volume change and strength behaviour at naturally occurring voids ratios.

Clay-water electrolyte systems may be classified as hydrophobic colloids as they consist of liquid dispersions of small solid particles that have the following characteristics (Mitchell 1993 & van Olphen 1977):

- Two phase systems with a large interfacial surface area.
- Have behaviour dominated by surface forces.
- Can flocculate in the presence of small amounts of salt.

2.5.1 ION DISTRIBUTIONS IN CLAY-WATER SYSTEMS

In a dry clay, adsorbed cations are tightly held by the negatively charged clay particles. Cations in excess of those required to neutralise the negative charge of the clay particles and any anions, are present as salt precipitates.

When the clay is inundated by water the precipitated salts go into solution. This is the state in which most natural soils are encountered, with the salts and anions in solution.
Due to the negative surface charge of the soil particles the adsorbed cations are in much higher concentration near the surface of the clay particle. However, they are also subject to diffusion forces to try and equalise the concentration of cations throughout the liquid phase. Their freedom to migrate is restricted by the negative electrical field that originates from the clay particle surface. The repulsive force due to diffusion and the attractive force due to electrostatic attraction lead to the traditionally accepted *diffuse double layer* model for ion concentrations adjacent to a clay particle surface. This phenomenon is key to understanding the electrokinetic phenomena in soils.

Several theories have been proposed for the quantitative description of the ion distribution adjacent to a charged surface. The Gouy-Chapman diffuse double layer is the generally accepted model within the field of soil mechanics (Gouy 1910, Chapman 1913). Although this theory has only been shown to accurately describe the actual distribution of ions for smectite particles suspended in a monovalent electrolyte solution at low (<100 mole/m^3) concentration (Sposito 1989). Figure 2.6 schematically shows the distribution of anions and cations adjacent to a soil particle based upon the Gouy-Chapman theory after Stern (1924).

The theory developed independently by Gouy (1910) and Chapman (1913) was originally developed for flat plates but has been shown by Verwey and Overbeek (1948) to be applicable to round or spherical particles. Stern (1924) and Carnie & Torrie (1984) later improved the model by taking into account the ionic dimensions themselves.

The mathematical derivation of charge and potential distributions adjacent to a charged surface is complex and will not be derived here. The reader is referred to Mitchell (1993)

and Tan (1993) for a more detailed discussion. The equation for the thickness of the double layer (K) is given as Equation 2.1 in order to make the reader aware of the system variables that govern its magnitude.

$$\frac{1}{K} = \left(\frac{E_0 D k T}{2 n_0 e^2 v^2} \right)^{1/2} \qquad \text{Eqn. 2.1}$$

Where:

E_0 = Permittivity of vacuum ($8.8542*10^{-12}$ $C^2 J^{-1} m^{-1}$)

D = Dielectric constant of fluid medium (Water =80 at 20°C)

k = Boltzmann Constant ($1.38 *10^{-23}$ $J°K^{-1}$)

T = Temperature (°K)

n_0 = Electrolyte concentration

e = electronic charge ($1.602 *10^{-19}$ C)

v = Cation valence

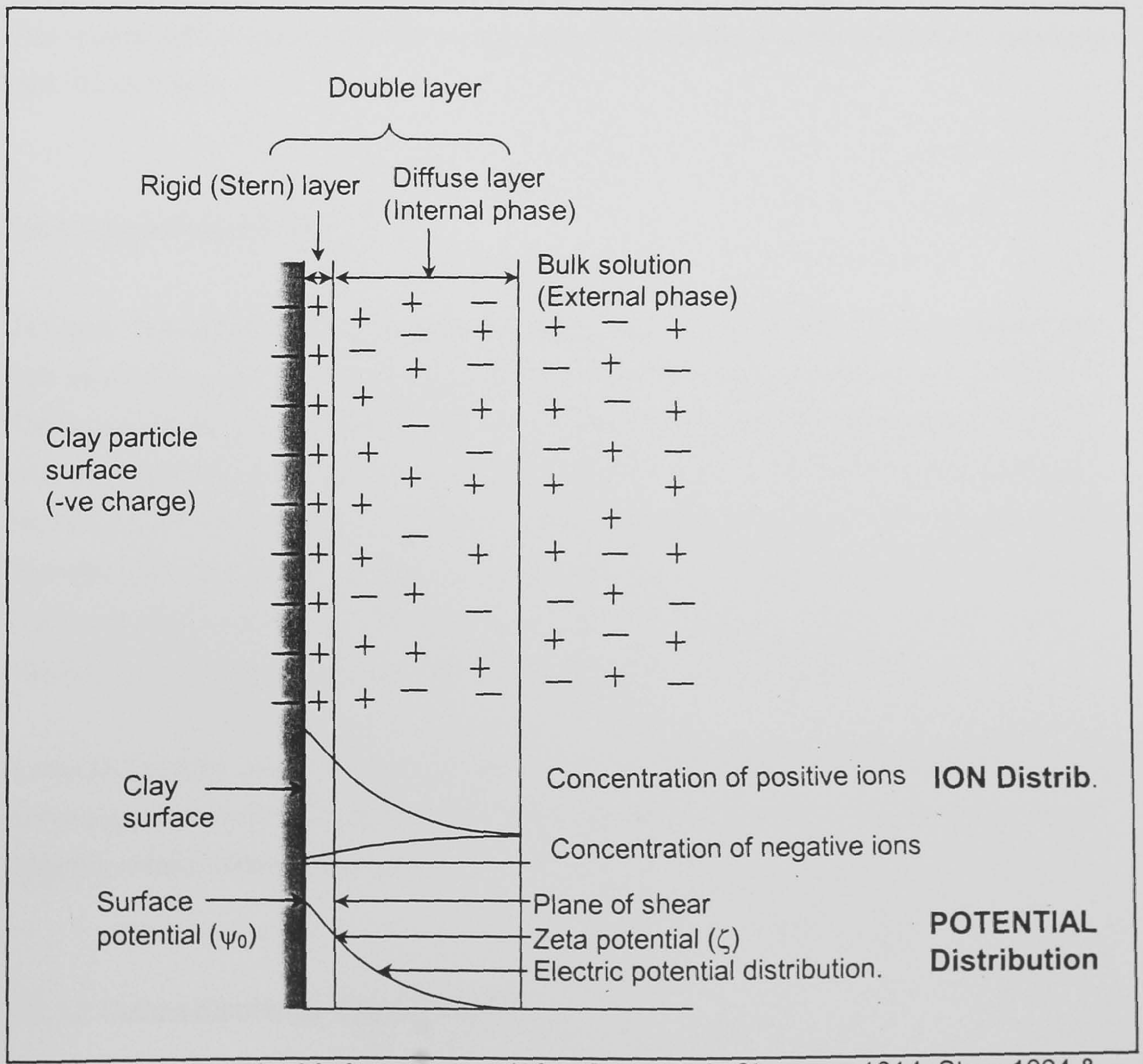

Figure 2.6 Diffuse double layer (After Gouy 1910, Chapman 1914, Stern 1924 & Mitchell 1993)

It is useful to summarise the implications of Equation 2.1 as given in Figure 2.7.

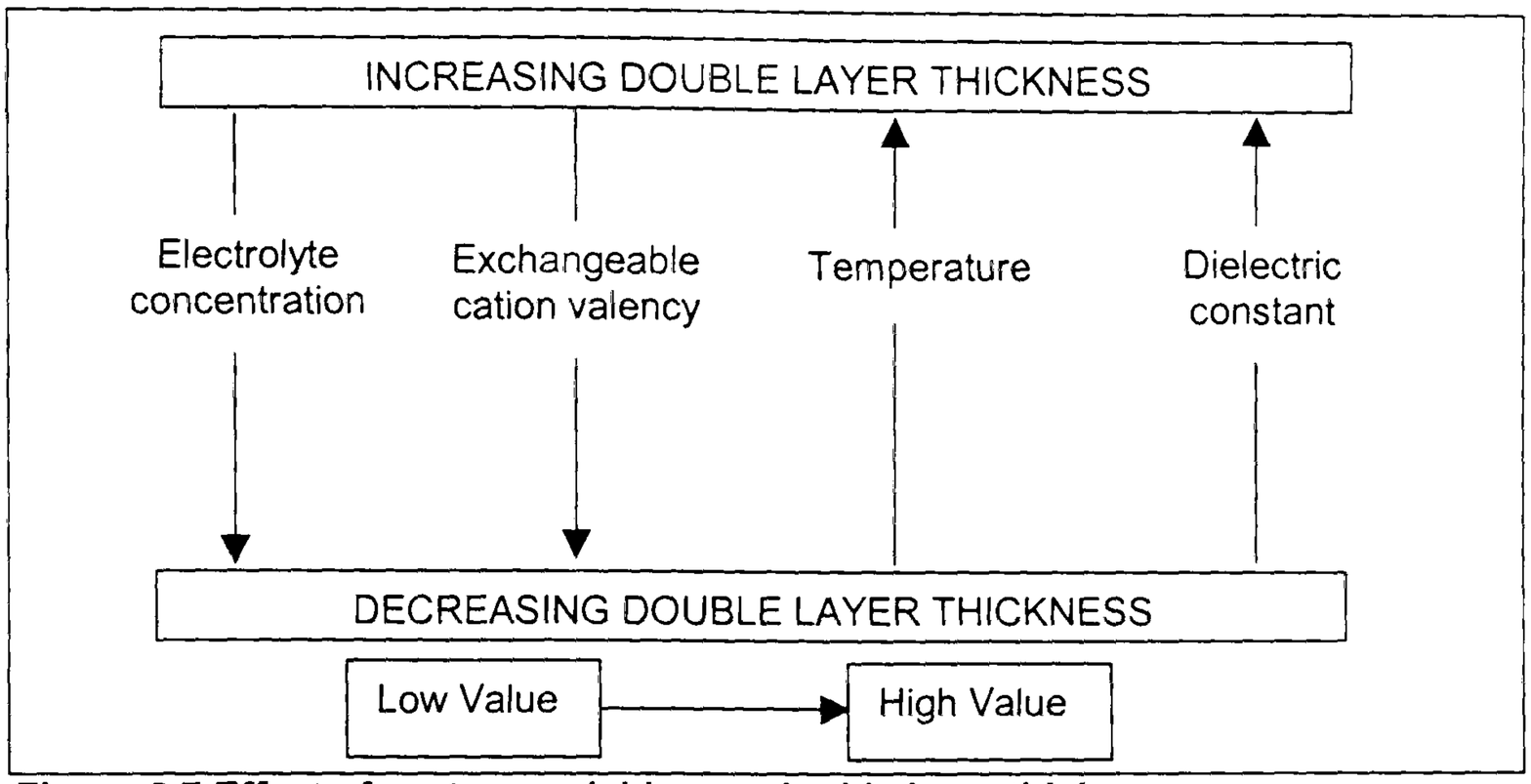

Figure 2.7 Effect of system variables on double layer thickness

The implications of the double layer in terms of electrokinetic phenomena will be discussed later in this thesis.

2.5.1.1 Zeta Potential (ζ)

The zeta potential is the electrical potential developed at the surface of shear between the bulk liquid and an envelope of water retained by the soil particle, as shown in Figure 2.6. The exact position of the shearing plane is unknown, and in reality it is a region of rapidly changing viscosity rather than a mathematical plane (Shaw 1969), and the zeta potential represents the electrical potential at an unknown distance from the colloidal particle surface. The zeta potential is, however, less than the surface potential (ψ_0) which exists at the solid liquid interface (van Olphen 1977). Perhaps it is comparable to the Stern potential (Tan 1993). Typical values of ψ_0 are in the range of 0mV to -50mV (Mitchell 1993).

It should again be noted that positive surface charges can also occur with certain soil mineralogy, however, in the remainder of this thesis all soil surface charges are assumed negative unless stated otherwise.

2.5.1.2 Cation Exchange Capacity (CEC)

Cation exchange is the interchange between a cation in a solution and another cation on the surface of any surface-active material (Foth 1984). Cation Exchange Capacity (CEC) is defined as the sum total of exchangeable cations absorbed, expressed in milliequivalents

per 100g of oven dry soil. An equivalent weight is the quantity that is chemically equal to 1g of hydrogen. The number of hydrogen atoms in an equivalent weight is Avogadro's number ($N=6.02*10^{23}$/g mol). A milliequivalent is equal to 0.001g of hydrogen. For example, 1g of soil with a CEC of 100me/100g would contain $6.02*10^{20}$ per milliequivalent adsorbed monovalent cations. Clays have a highly variable CEC ranging from less than 10 to more than 100, as shown in Table 2.2a&b (Foth 1984). The type of clay minerals present is the principal factor governing the CEC of a clay soil.

The sand and silt fractions of a soil also have unsatisfied negative charges as was discussed in §2.3.3, however, because of their low specific surface (Table 2.3) they contribute little to the CEC of most soils (Foth 1984). They, therefore, have little effect on the electrokinetic properties of a soil. The CEC of silicate clays is partially dependent upon pH, increasing gradually above a pH of about 6 for kaolinite and montmorillonite, as also shown in Figure 2.8. However, the CEC of organics present in soils is highly pH dependent as also shown in Figure 2.8.

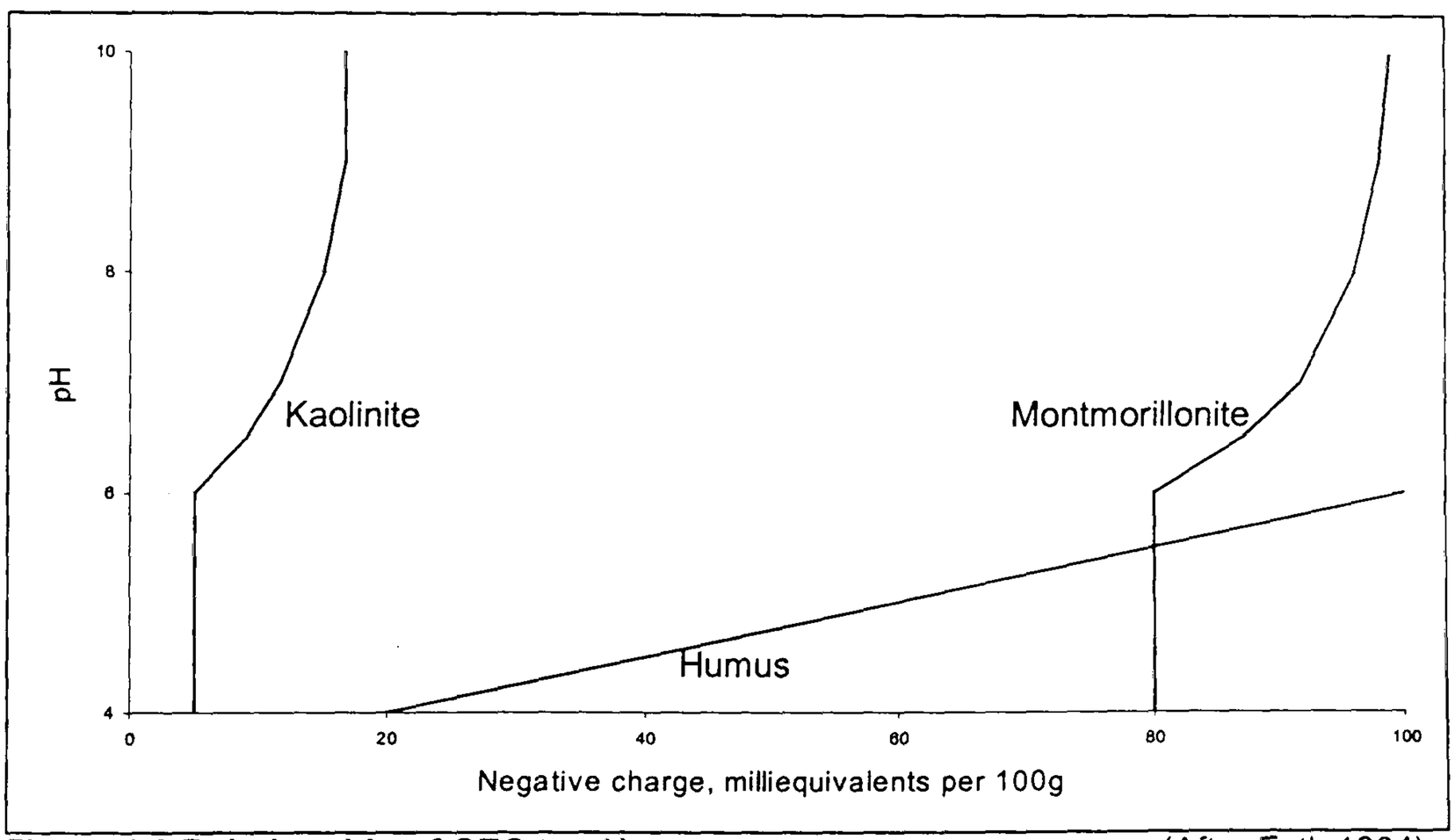

Figure 2.8 Relationship of CEC to pH (After Foth 1984)

The types of cations present in a soil are usually derived from mineral weathering. The greater the supply of a given cation from weathering the greater the likelihood that the cation will be adsorbed according to the law of mass action. The amount and type of cations actually absorbed is significantly affected by the cations valence and hydrated atomic radius. Cations with a greater valence are adsorbed more strongly or efficiently than cations of a lower valence. For a given valence, the cation with the smallest hydrated radius will be more strongly adsorbed. The dehydrated and hydrated radii of commonly occurring monovalent ions is given in Table 2.4.

From the data presented in Table 2.4 it is possible to produce a replaceability series for commonly found monovalent cation in soil; Al>Ca>Mg>K>Na. This gives an indication to the order of abundance of the cations in a natural soil.

Table 2.4 Atomic properties of some monovalent ions (After Foth 1984)

Ion	Radii of Ions, Angstroms (Å)(10^{-8}cm)		Order of Cation Exchange Efficiency
	Dehydrated	Hydrated	
Li	0.78	10.03	4th
Na	0.98	7.90	3rd
K	1.33	5.32	2nd
Rb	1.49	5.09	1st

2.6 CONDUCTION PHENOMENA IN SOILS

Several types of flows may exist within soil systems, the flows may occur independently of each other or may be coupled, i.e. one type of flow causes flow of another type to occur. The four types of flow which occur in soils may be categorised into four groups; fluid, electrical, chemical and thermal. It has been established that provided the state of the soil remains unchanged each flow rate, or flux, (J) is linearly related to its corresponding driving gradient (X) by Equation 2.2 (Mitchell 1991, 1993):

$$J_{ii} = L_{ii} X_i \qquad \text{Eqn. 2.2}$$

Where L_{ii} is the soil conductivity for the flow in question. When Equation 2.2 is written in the terms commonly adopted for each of the flow phenomena one of the four classical flow equations given in Table 2.5 are obtained.

Table 2.5 Governing flow equations (After Mitchell 1991, 1993)

LAW	Equation	Flow Type
Darcy's	$q_h = k_h i_h$	Hydraulic
Fourier's	$q_t = k_t i_t$	Thermal
Ohm's	$I = \sigma_e i_e$	Electrical
Fick's	$J_D = D i_c$	Chemical

Comparison of the equations presented in Table 2.5 with Equation 2.2 demonstrates that q_h, q_t, I and J_D are the hydraulic, thermal, electrical and chemical fluxes (flow rates). The coefficients k_h, k_t, σ_e and D are the hydraulic, thermal, electrical and diffusion coefficients respectively. The coefficients i_h, i_t, i_e and i_c are the hydraulic, thermal, electrical and chemical gradients inducing the flows to take place.

2.6.1 COUPLED FLOWS

In most cases, a single flow type does not occur independently, although only a single driving force may exist (Mitchell 1991, 1993). A clear example of this is the movement of water containing chemicals under a conventional hydraulic gradient, there is an associated flow of chemicals with the hydraulic flow.

It has been observed that a gradient of one type can cause a flow of another type to take place conforming to the equation below, Equation 2.3 (Mitchell 1991, 1993):

$$J_{ii} = L_{ij} X_i \qquad \text{Eqn. 2.3}$$

Where L_{ij} is a coupling coefficient. The types of coupled flows that can occur are given in Table 2.6.

The coupled flow phenomena of interest to this thesis are the electrokinetic phenomena that occur in soils under an applied electrical gradient or which can generate an electrical potential. These are discussed in the ensuing section. The reader is referred to Mitchell (1991, 1993) for further discussion of the other coupled and direct flow phenomena.

Table 2.6 Direct and coupled flow phenomena (After Mitchell 1991, 1993)

Flux (J)	Gradient (X)			
	Hydraulic head	Thermal	Electrical	Chemical concentration
Fluid	Hydraulic conduction *Darcy's Law*	Thermo-osmosis	Electro-osmosis	Chemical osmosis
Heat	Isothermal heat transfer	Thermal conduction *Fourier's Law*	Peltier effect	Dufour effect
Current	Streaming current/potential	Thermoelectricity *Seebeck effect*	Electrical conduction *Ohm's Law*	Diffusion and membrane potentials
Ion	Streaming current/potential	Thermal diffusion of electrolyte *Soret effect*	Electrophoresis/ Ion migration	Diffusion *Fick's Law*

Key: Text = *Electrokinetic phenomena of relevance to this thesis*

Text = *Other phenomena of relevance to this thesis*

2.7 ELECTROKINETIC PHENOMENA IN SOILS

Electrokinetic phenomena, as they occur within soils, may be defined in terms of five categories. Each of which is either related to the movement of charged particles in a fluid medium under the action of an applied potential difference, or inducing a potential difference, or the movement of fluid within a matrix of charged particles which induces a potential difference within the system. The five categories are defined below:

- ***Streaming Potential*** - Electrical potential difference induced by fluid flow in a charged soil particle matrix.
- ***Migration / Sedimentation Potential*** - Electrical potential difference induced by movement of charged soil particles in a fluid medium.
- ***Electromigration/Ion migration*** - Applied electrical potential difference induces ion migration within the fluid phase of a charged soil particle matrix.
- ***Electrophoresis*** - Applied electrical potential difference induces movement of charged soil particles within a fluid medium.
- ***Electro-osmosis*** - Applied electrical potential difference induces fluid flow in a charged soil particle matrix.

Streaming potential, migration potential, electromigration / ion migration and electrophoresis will be discussed briefly in the subsequent sections followed by a more detailed discussion of electro-osmosis, which is the phenomenon of principal interest in this thesis.

2.7.1 STREAMING POTENTIAL

When a hydraulic flow is caused through a soil mass by the application of a hydraulic gradient, Figure 2.9, the double layer charges (see § 2.5.1) are displaced in the direction of flow. This displacement results in a deficit of positive charges in the region where the water flow enters the soil element and an increasing excess of positive charges as the soil element is passed through. The overall effect of this charge displacement is the generation of an electrical potential difference over the soil element, which is proportional to the hydraulic flow rate. Streaming potentials of several tens of millivolts have been measured in clays (Mitchell 1991, 1993).

2.7.2 MIGRATION / SEDIMENTATION POTENTIAL

The movement of charged particles, such as clay particles, relative to a solution, as during sedimentation of clay particles in a water suspension generates an electrical potential difference, Figure 2.9. This is caused by the viscous drag of the solution that retards the movement of the diffuse double layer cations relative to the charged particles themselves.

2.7.3 ELECTROMIGRATION / ION MIGRATION

The movement of anions and cations within the fluid phase of a soil mass induced by the application of an electrical potential difference. Ions are attracted to the electrode of opposite sign and repelled from the electrode of like sign. The principal difference between ion migration and electrophoresis is that ion migration can take place within the pore fluid of a fixed soil matrix, whereas electrophoresis is the passage of discrete (usually clay) particles within a fluid / particle suspension.

Lageman *et al* (1989) reports the average mobility of ions in soils as $5*10^{-8}$ m^2/Vs, an order of magnitude greater than the average electro-osmotic permeability of $5*10^{-9}$ m^2/Vs (Casagrande 1952). Hence, anions can usually overcome the electro-osmotic flow and migrate towards the anode (Hellawell 1994).

2.7.4 ELECTROPHORESIS

If a DC electrical field is applied across a colloidal suspension, charged particles are attracted electrostatically to one of the electrodes and repelled from the other. Negatively charged clay particles move towards the anode as shown in Figure 2.9.

Electrophoretic mobilities reported by Lageman *et al* (1989) and by van Olphen (1977) are in the ranges $1*10^{-10}$ to $3*10^{-10}$ m^2/Vs and $1*10^{-8}$ to $3*10^{-8}$ m^2/Vs respectively. The migration of these charged particles affects the soil conductivity and the electro-osmotic mobility (Hellawell 1994).

Electrophoresis has found applications in the densification and dewatering of sludges and mine tailings. (Lo *et al* 1991b, Shang & Lo 1997, Lo & Shang 1995, Colin 1986, Wakeman 1982, Sauer & Davis 1994).

Esrig (1968) reports that the process is inconsequential for most naturally occurring soils.

2.7.5 ELECTRO-OSMOSIS

When a DC electrical potential difference is applied across a wet soil mass ion migration (see § 2.7.3) takes place. As the ions migrate they drag with them their water of hydration and they also exert a viscous drag on the water around them. Since there are more cations than anions in a soil composed of negatively charged clay particles there is a net flow towards the cathode (Pamukcu 1996). The flow is initiated in the diffuse double layer, where there are significantly more cations than anions due to the proximity of the negatively charged clay surface. Figure 2.10 shows the development of the electro-osmotic flow with time induced in the double layer. It is possible that due to the electro-osmotic flow the

double-layer charges are displaced in the direction of flow, producing a potential difference between the ends of the soil mass. This streaming potential may decrease the effect of electro-osmosis by reversing the polarity (Pamukcu 1996).

ELECTRO-OSMOSIS

The potential difference (electrical gradient) induces water flow.

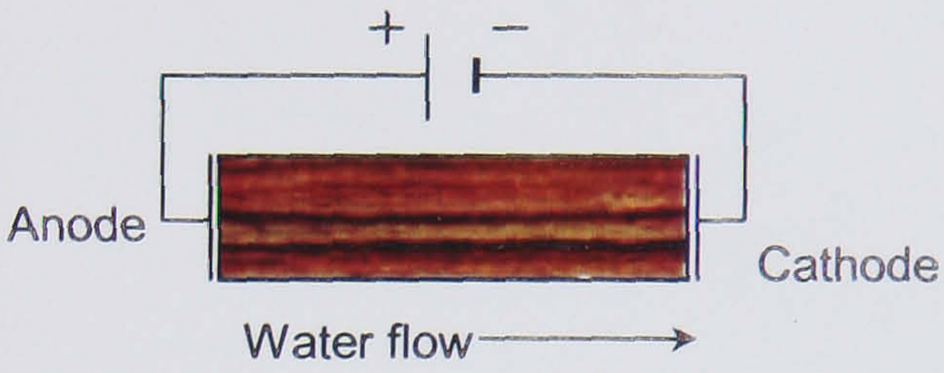

ELECTROPHORESIS

The potential difference (electrical gradient) induces particle movement.

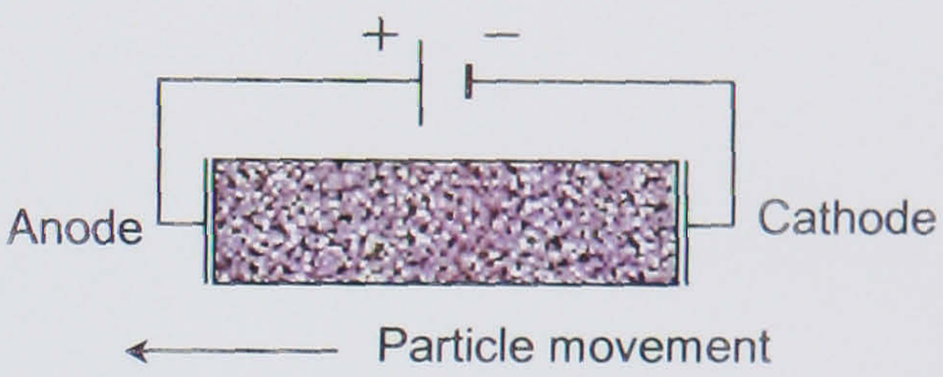

ELECTROMIGRATION

The potential difference (electrical gradient) induces anion and cation migration.

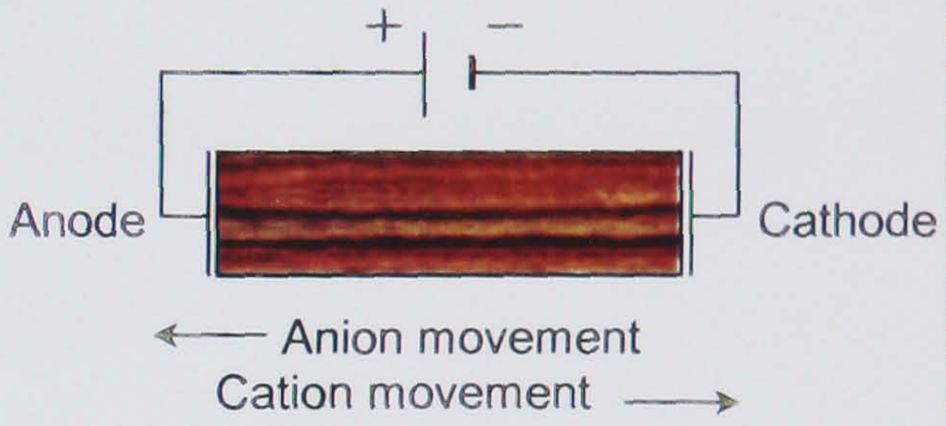

ELECTROKINETIC (STREAMING) POTENTIAL

The movement of the water induces a small electrical potential.

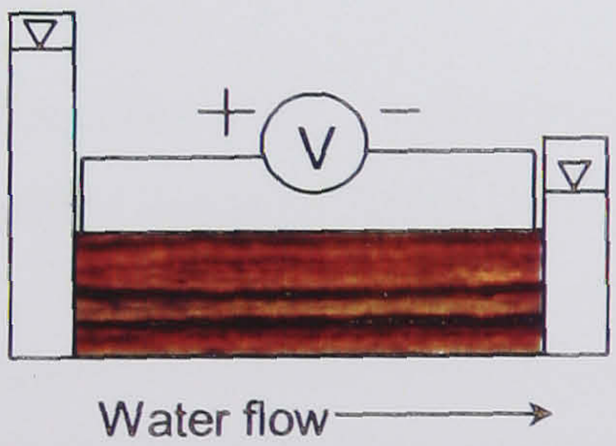

MIGRATION (SEDIMENTATION) POTENTIAL

The movement of the soil particles induces a small electrical potential.

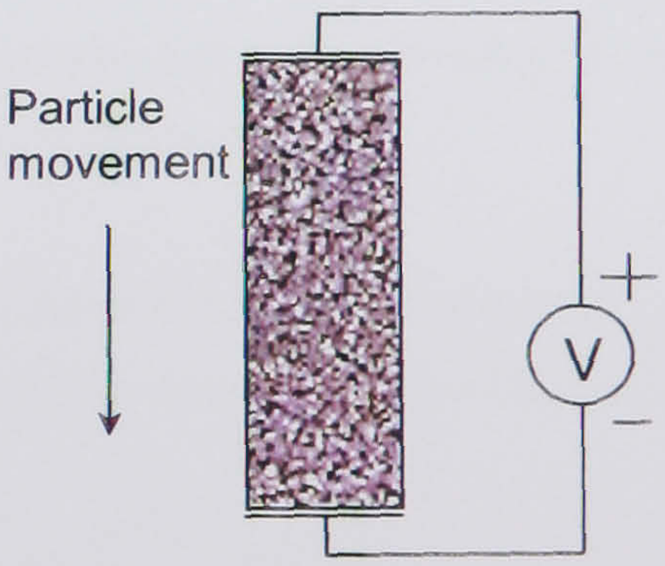

KEY

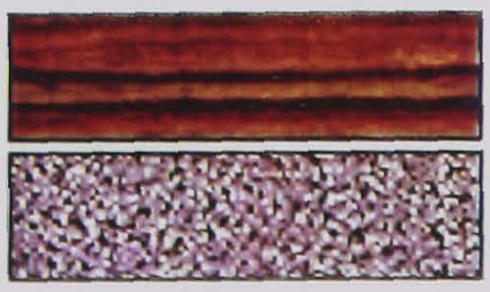

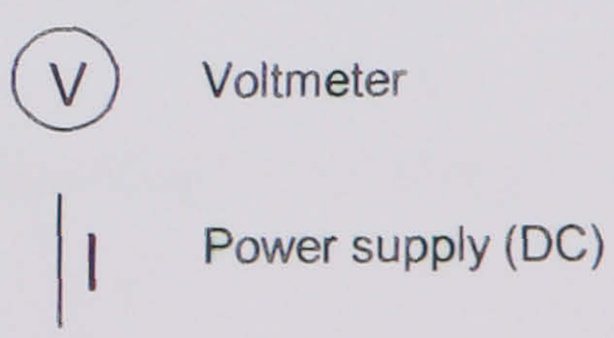

Figure 2.9 Electrokinetic phenomena (After Mitchell 1991, 1993)

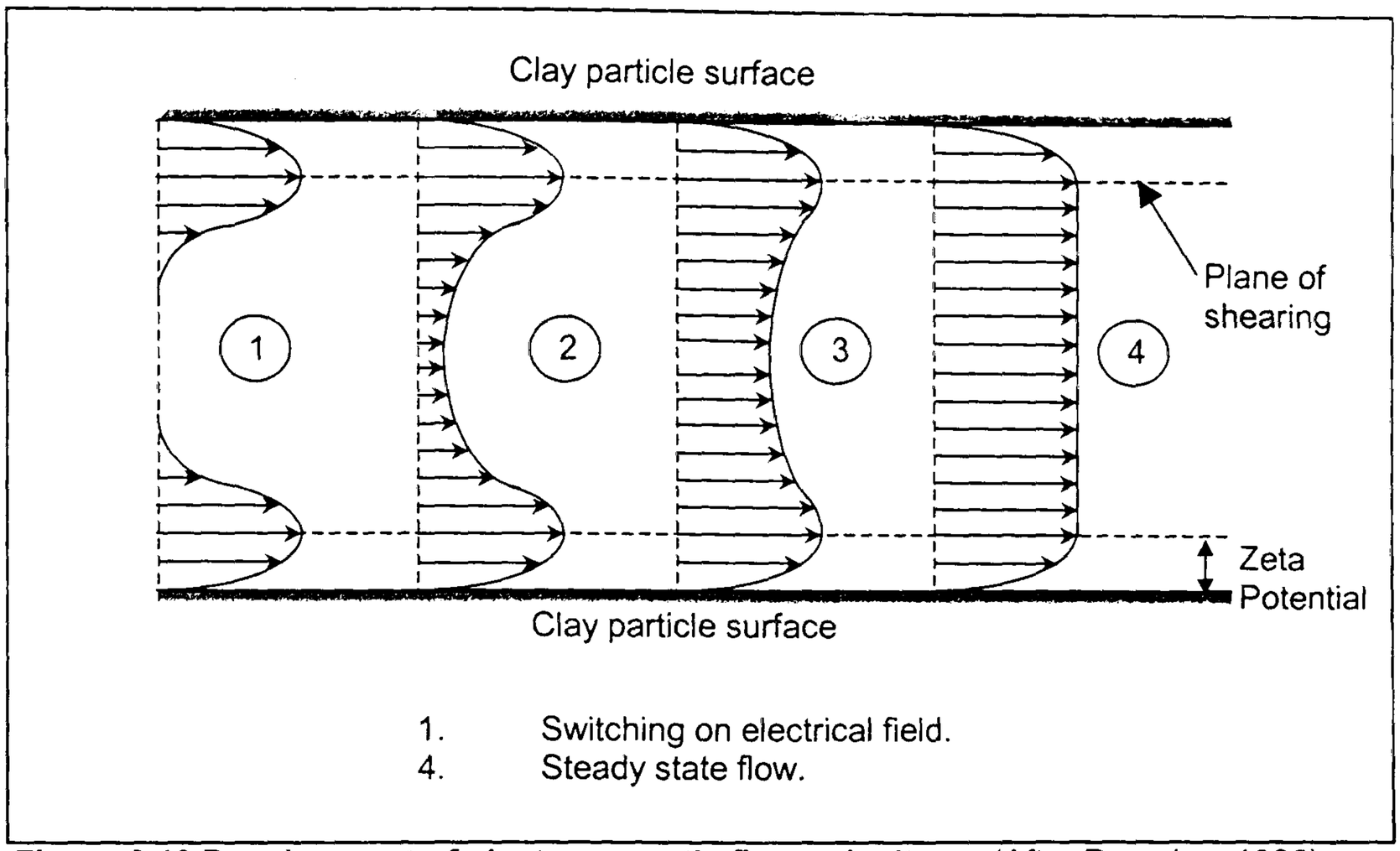

Figure 2.10 Development of electro-osmotic flow velocity (After Pamukcu 1996)

There are three theories in general use for electro-osmosis:

- Schmidt (1950, 1951): A small pore theory, allowing for the extension of the counterion (ions of opposite sign to the charged surface) layer into the pore space.
- Spiegler (1958): Takes into account the interactions of the mobile components (water and ions) on each other and of the frictional interactions of these components with the pore walls.
- Helmholtz (1879) - Smoluchowski (1914): A large pore theory treating the liquid filled capillary between the soil particles as an electrical condenser.

Although the Helmholtz-Smoluchowski theory is one of the earliest it is one of the most widely used (Mitchell 1993), and will be developed fully here as it forms the basis for later work in this thesis.

The electrical condenser analogy assumes that the soil capillaries have charges of one sign on or near the surface of the wall and countercharges concentrated in a layer in the liquid a small distance from the wall, as shown in Figure 2.11. It will be seen from the previous discussions on soil particle charges and liquid/solid phase interactions that these assumptions are valid.

The mobile shell of counterions is assumed to drag water through the capillary by plug flow, resulting in a high velocity gradient between the two plates of the condenser. The rate of

water flow is controlled by the balance between the electrical force causing water movement and friction between the liquid and the wall.

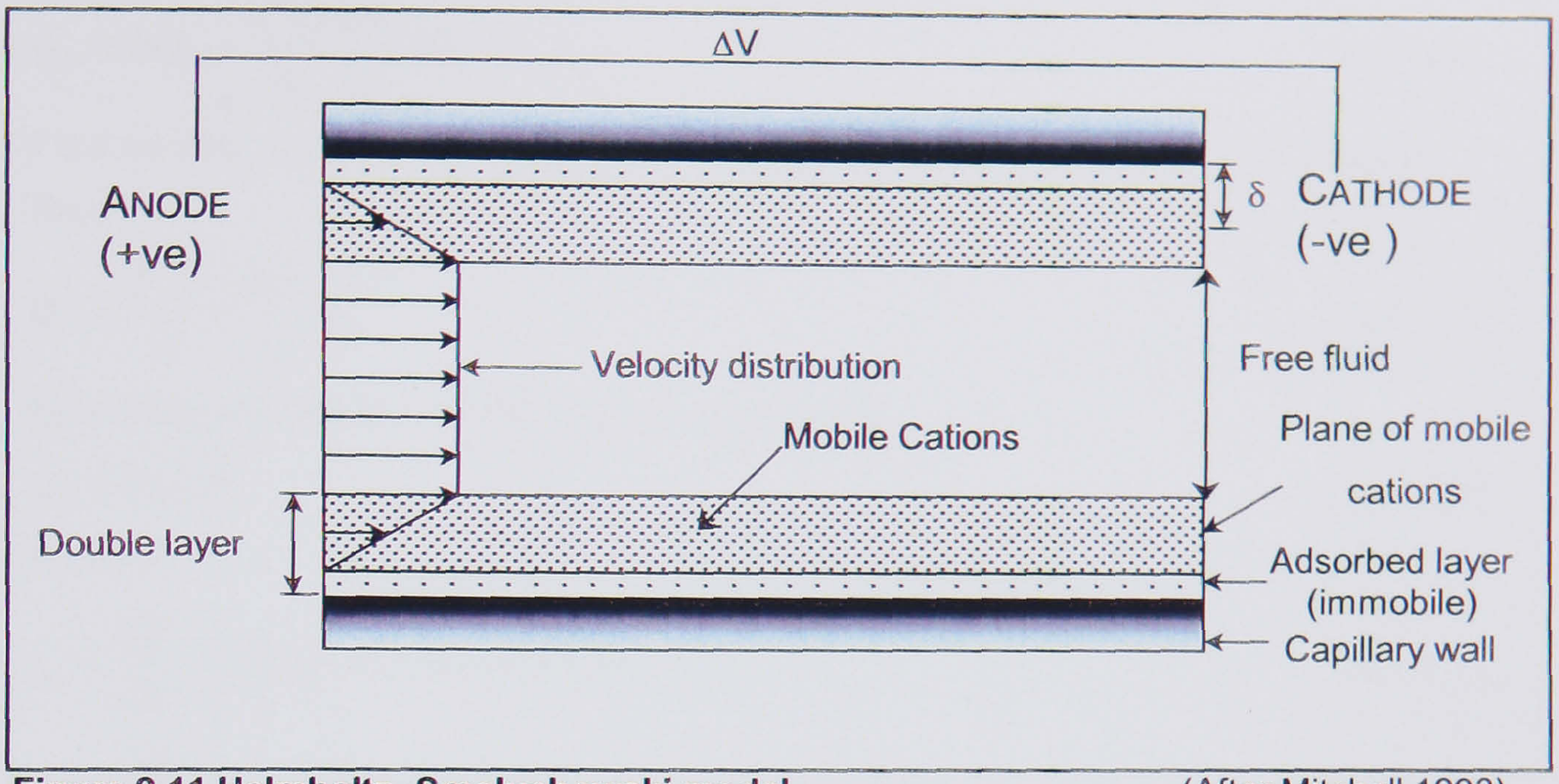

Figure 2.11 Helmholtz -Smoluchowski model (After Mitchell 1993)

If v is the flow velocity and δ is the distance between the wall and the centre of the plane of mobile charges, then the velocity gradient between the wall and the centre of the positive charges is v/δ; thus, the drag force per unit area is $\eta dv/dx = \eta v/\delta$ where η is the viscosity. The force per unit area from the electrical field is $\sigma \Delta E/\Delta L$, where σ is the surface charge density and $\Delta E/\Delta L$ is the electrical potential gradient. At equilibrium:

$$\eta \frac{v}{\delta} = \sigma \frac{\Delta E}{\Delta L} \qquad \text{Eqn. 2.4}$$

or

$$\sigma\delta = \eta\, v \frac{\Delta L}{\Delta E} \qquad \text{Eqn. 2.5}$$

From electrostatics, the potential gradient ζ across a condenser is given by:

$$\zeta = \frac{\sigma\delta}{D} \qquad \text{Eqn. 2.6}$$

Where D is the relative permittivity, or dielectric constant of the pore fluid. Substitution of σ and δ into Equation 2.4 gives:

$$v = \left(\frac{\zeta D}{\eta}\right)\frac{\Delta E}{\Delta L} \qquad \text{Eqn. 2.7}$$

The potential ζ is the zeta potential, which is not equal to the surface potential of the double layer §2.5.1.1. For a single capillary of area a the flow rate is:

$$q_a = va = \frac{\zeta D}{\eta}\frac{\Delta E}{\Delta L}a \qquad \text{Eqn. 2.8}$$

And for a group of *N* capillaries within total cross-sectional area *A* normal to the flow direction:

$$q_A = Nq_a = \frac{\zeta D}{\eta}\frac{\Delta E}{\Delta L}Na \qquad \text{Eqn. 2.9}$$

If the porosity is *n*, then the cross-sectional area of the voids is *nA*, which must equal *Na*. Thus,

$$q_A = \frac{\zeta D}{\eta} n \frac{\Delta E}{\Delta L} A \qquad \text{Eqn. 2.10}$$

By analogy with Darcy's law this may be re-written as:

$$q_A = k_e i_e A \qquad \text{Eqn. 2.11}$$

In which,

$$i_e = \frac{\Delta V}{\Delta L} = \text{Electrical potential gradient (V/m)} \qquad \text{Eqn. 2.12}$$

$$k_e = \frac{\zeta D}{\eta} n = \text{Coefficient of electro-osmotic permeability} \qquad \text{Eqn. 2.13}$$

k_e is, according to the Helmholtz-Smoluchowski theory, relatively independent of pore size (Casagrande 1949, Mitchell 1993) as shown in Table 2.7

Casagrande (1952) suggested that for most practical applications a value for $k_e = 5*10^{-5}$ cm^2/sec-V can be accepted. It can be seen that electro-osmosis can be effective for water movement in fine grained soils compared to water flow under hydraulic gradients (Mitchell 1993). This can be demonstrated by Figure 2.12 that shows the hydraulic permeabilities of a range of typically encountered soils.

<table>
<tr><td>Coefficient of hydraulic permeability (m/s)</td><td colspan="12">1 10^{-1} 10^{-2} 10^{-3} 10^{-4} 10^{-5} 10^{-6} 10^{-7} 10^{-8} 10^{-9} 10^{-10} 10^{-11} 10^{-12}</td></tr>
<tr><td rowspan="2">Typical soil types</td><td rowspan="2">Clean gravels</td><td colspan="2">Clean sands & sand-gravel mixtures</td><td colspan="2">Very fine sands, silts and clay-silt laminate</td><td colspan="6" rowspan="2">Unfissured clays and clay-silts (>20% clay)</td></tr>
<tr><td colspan="4">Dessicated and fissured clays</td></tr>
<tr><td>Drainage characteristics</td><td colspan="6">GOOD</td><td colspan="2">POOR</td><td colspan="4">PRACTICALLY IMPERVIOUS</td></tr>
<tr><td>Permeablity classification</td><td colspan="3">HIGH</td><td colspan="2">MEDIUM</td><td colspan="2">LOW</td><td colspan="2">VERY LOW</td><td colspan="2">PRACTICALLY IMPERMEABLE</td></tr>
</table>

Figure 2.12 Coefficients of hydraulic permeability (After BSI 1986 & Head 1994)

Table 2.7 Coefficients of electro-osmotic permeability and associated parameters (After Mitchell 1993, Wrigley 1999)

No.	Material	Water Content (%)	K_e in 10^{-5} (cm^2/sec-V)	Conductivity σ (Siemens/m)	Approximate k_h (cm/sec)	K_i water per unit charge (m^3/sec/Amp)	Reference
1	London clay	52.3	5.8	N/A	10^{-8}	N/A	Casagrande (1952)
2	Boston blue clay	50.8	5.1	N/A	10^{-8}	N/A	Casagrande (1952)
3	Kaolin	67.7	5.7	N/A	10^{-7}	N/A	Casagrande (1952)
4	Clayey silt	31.7	5.0	N/A	10^{-6}	N/A	Casagrande (1952)
5	Rock flour	27.2	4.5	N/A	10^{-7}	N/A	Casagrande (1952)
6	Na-Montmorillonite	170	2.0	N/A	10^{-9}	N/A	Casagrande (1952)
7	Na-Montmorillonite	2000	12.0	N/A	10^{-8}	N/A	Casagrande (1952)
8	Mica powder	49.7	6.9	N/A	10^{-5}	N/A	Casagrande (1952)
9	Fine sand	26.0	4.1	N/A	10^{-4}	N/A	Casagrande (1952)
10	Quartz powder	23.5	4.3	N/A	10^{-4}	N/A	Casagrande (1952)
11	Ås quick clay	31.0	2.0	N/A	$2.0*10^{-8}$	N/A	Bjerrum *et al* (1967)
12	Bootlegger Cove clay	30.0	2.4-5.0	0.02	$2.0*10^{-8}$	$1*10^{-7}$	Long & George (1967)
13	Silty clay, West Branch Dam	32.0	3.0-6.0	0.25	$1.2*10^{-8}$ - $6.5*10^{-8}$	$9.6*10^{-9}$ - $2*10^{-8}$	Fetzer (1967)
14	Clayey silt, Little Pic River, Ontario	26.0	1.5		$2*10^{-5}$		Casagrande *et al* (1961)
15	Decomposed Granite, Silty CLAY	N/A	30	0.17	10^{-4} - 10^{-5}	$1.8*10^{-7}$	Chappell & Burton (1975)
16a	Silty CLAY	23	5.0	0.08 - 0.12	0.5 - $8*10^{-5}$	6.3 - $4.2*10^{-9}$	Chen & Murdoch (1997)
16b	Silty CLAY	10	9.0	0.02	$1*10^{-5}$	$4.5*10^{-8}$	Chen & Murdoch (1997)
17	Marine Silty CLAY	37	6 -9	0.024 - 0.033	10^{-7}	1.8-$3.8*10^{-7}$	Eggestad & Føyn (1983)

This statement does, however, require qualification by stating that electro-osmosis is not always an efficient means to transfer water within fine-grained soils because power requirements may make it uneconomical or the rate of consolidation may be too slow. This is discussed in the following sections.

2.7.5.1 Electro-Osmosis Efficiency

The efficiency and economics, and hence the commercial viability, of electro-osmosis depends upon the quantity of water moved per unit charged passed (Grey & Mitchell 1967). According to Mitchell (1993), this factor may vary by several orders of magnitude depending upon the soil type, water content and electrolyte concentration. A method for evaluating the electro-osmotic efficiency has been presented by Grey (1966), Grey & Mitchell (1967) and Mitchell (1993) and is described below.

The method is based upon the fact that electro-osmotic water flow occurs due to the *net* frictional drag exerted on the water molecules by the movement of excess hydrated ions of one polarity (§2.7.5). Thus, the greater the excess of ions of one polarity the greater the net drag and the greater the electro-osmotic flow.

Due to the electro-negativity of clay particles, the concentration of cations in the double layer is higher, and the concentration of anions is lower than in the free external solution, Figure 2.6, as described in § 2.5.1. The distribution of anions and cations in the pore fluid may also be obtained using the Donnan theory (Donnan 1924).

The Donnan theory is based upon the fact that at equilibrium the potentials of the internal and external phases (Figure 2.6) are equal and the electro-neutrality must be preserved. In the case of electronegative clay particles anions will tend to be excluded from the internal solution due to the charge on the particles themselves. This is known as Donnan exclusion. Thus, it can be seen that the efficiency of electro-osmosis depends upon the relative concentration of ions within the internal phase. It has been shown (Grey 1966, Grey & Mitchell 1967) that the ratio R of cations to anions in the internal phase, for a symmetrical electrolyte ($Z^+ = Z^-$), is given by Equation 2.14.

$$R = \frac{C^+}{C^-} = \frac{1 + (1 + y^2)^{1/2}}{-1 + (1 + y^2)^{1/2}} \qquad \text{Eqn. 2.14}$$

Where:

$$y = \frac{2C_0 \gamma \pm}{A_0 \bar{\gamma} \pm} \qquad \text{Eqn. 2.15}$$

Where C_0 is the concentration in the external phase, γ is the mean molar activity coefficient in the external solution, $\bar{\gamma}$ is the mean activity coefficient in the double layer, and A_0 is the surface charge density per unit pore volume. A_0 is given by:

$$A_0 = \frac{(cec)\rho_w}{w} \qquad \text{Eqn. 2.16}$$

Where ρ_w is the density of water, w is the water content and *cec* is the cation exchange capacity (§ 2.5.1.2). The theoretical results of the effect of different activity (A) clay minerals on electro-osmotic efficiency are presented schematically in Figure 2.13.

This shows that inactive clays with a low *cec* are more electro-osmotically efficient (i.e. transport more water per amp passed) than high activity clays with a high *cec*. This theoretical derivation was confirmed by Grey (1966) who presented a plot of the electro-osmotic efficiency of sodium kaolinite (inactive clay) and sodium illite (more active clay) as shown in Figure 2.14.

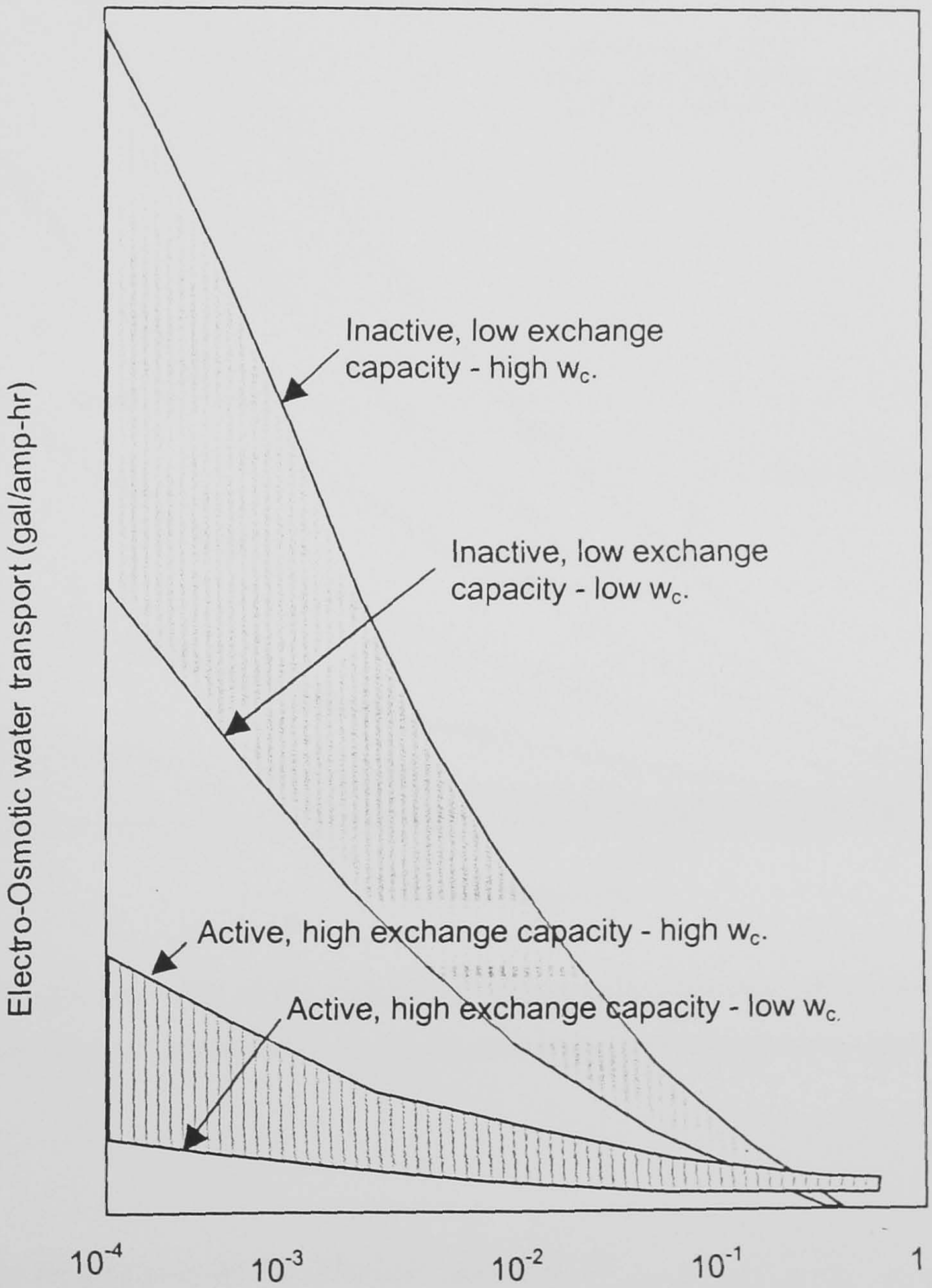

Figure 2.13 Schematic prediction of water transport by electro-osmosis in different clay types according to the Donnan concept (After Grey 1966)

Thus, in conclusion, the efficiency of electro-osmosis depends upon the electrical conductivity of the soil mass. The electrical conductivity is in turn controlled by the water content, the *cec*, and the free electrolyte concentration of the pore fluid, as indicated by Grey

& Mitchell (1967) and validated by Lockheart (1983) (Acar & Hamed 1991 and Mitchell 1993). The mineralogy of the soil itself also has a major implication upon the soil conductivity. These factors are discussed further in Chapter 7 when acceptability criteria for soils for electro-osmotic treatment are developed.

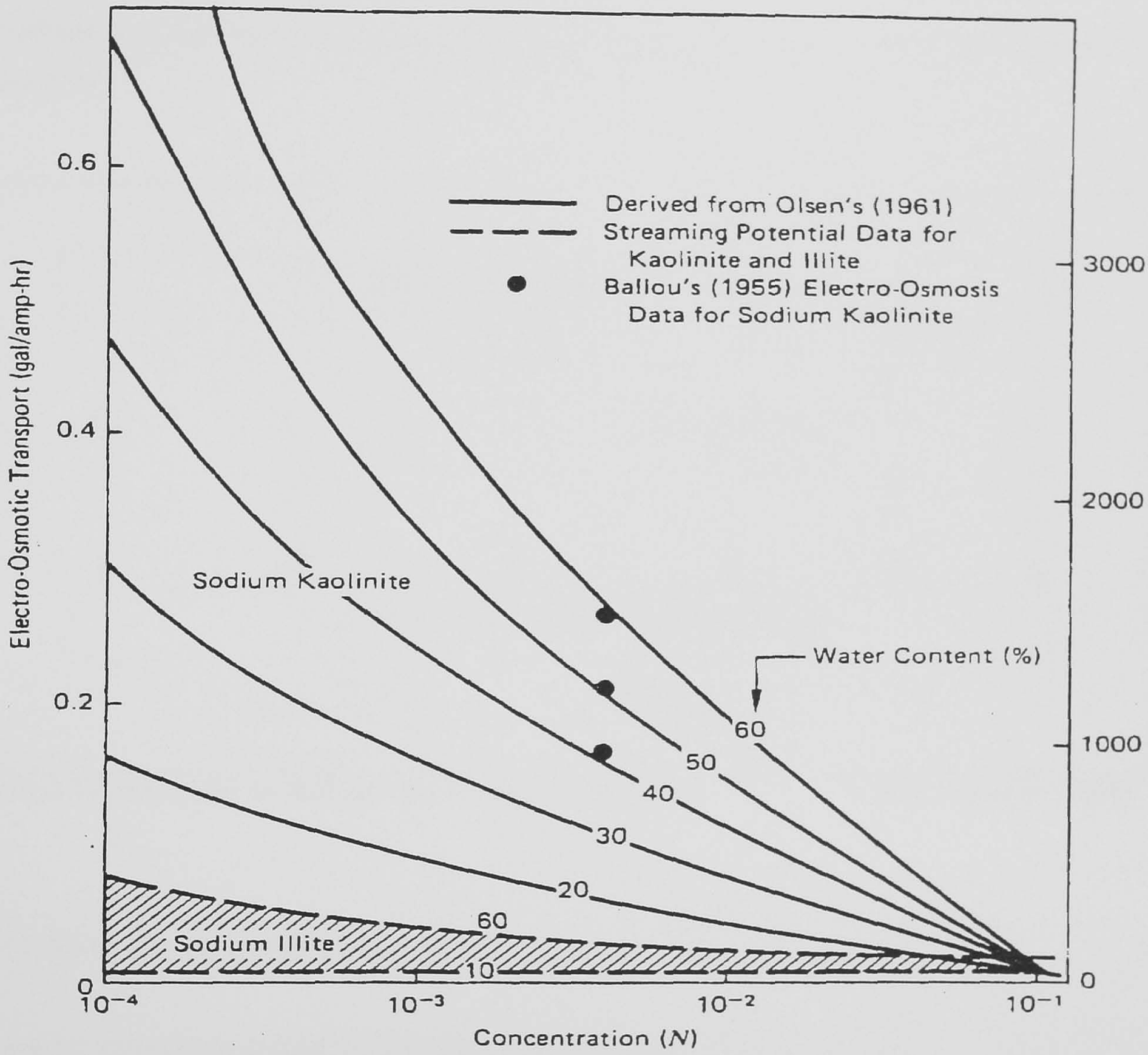

Figure 2.14 Electro-osmotic water transport versus concentration of external electrolyte solution for homoionic kaolinite and illite at various water contents (Grey 1966)

2.7.5.2 Energy Requirements For Electro-Osmosis

As has been seen, the quantity of water moved per unit charge passed (Gal/h/Amp or mole/faraday) is extremely useful in assessing the viability of using electro-osmosis on a particular site. If this quantity is expressed as k_i then:

$$q = k_i I \qquad \text{Eqn. 2.17}$$

Where k_i can vary over a wide range, unlike k_e. The power consumption is defined by:

$$P = \Delta E I = \frac{\Delta E q h}{k_i} \qquad \text{Eqn. 2.18}$$

for ΔE in Volts and I in Amps. The power consumption per unit volume of flow is thus:

$$\frac{P}{qh} = \frac{\Delta E}{k_i} * 10^{-3} \ kWh \qquad \text{Eqn. 2.19}$$

The influence of the various soil parameters on the efficiency of electro-osmosis is shown in Figure 2.15

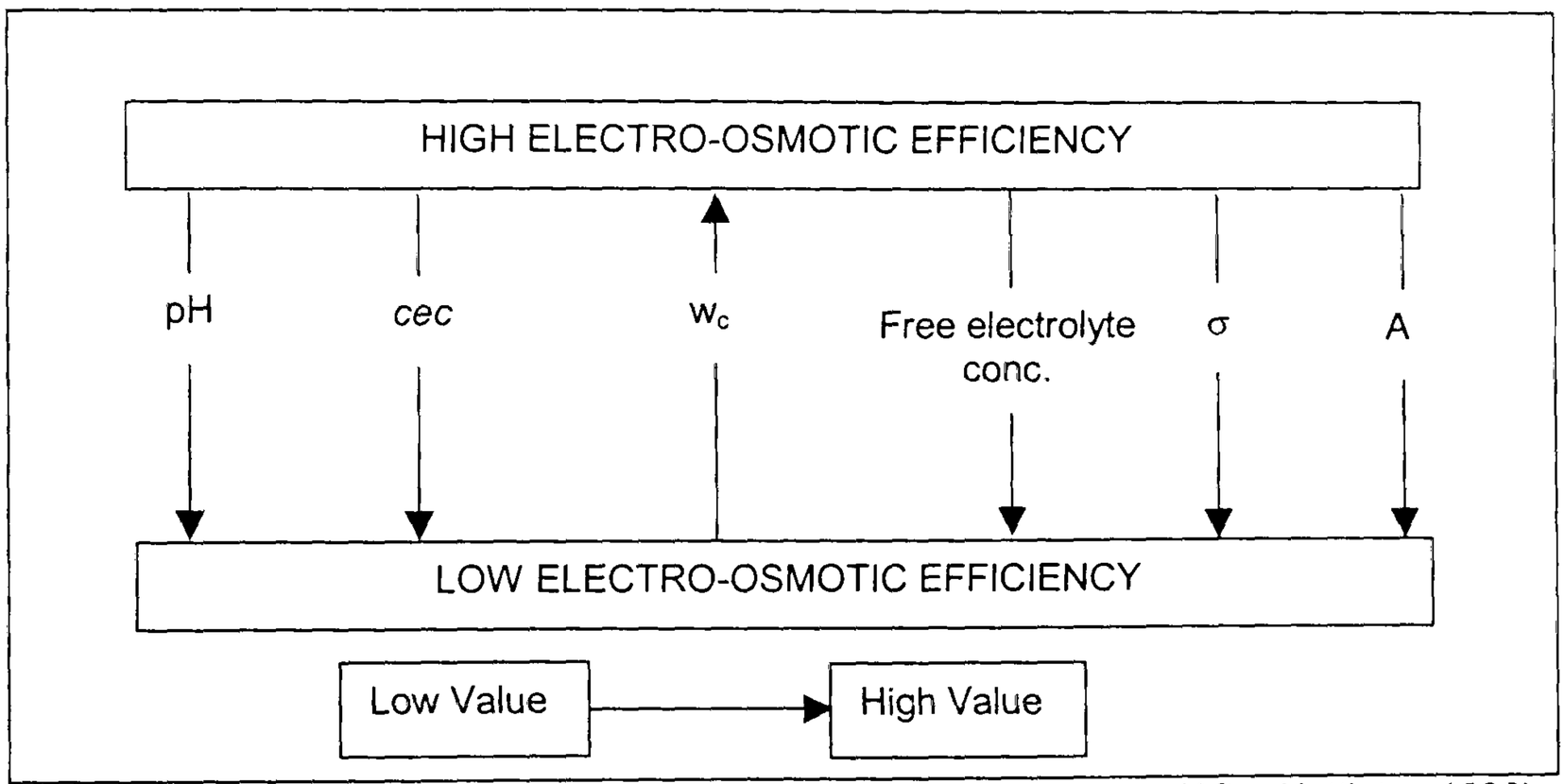

Figure 2.15 Influence of soil variables on e-o efficiency (After Nettleton 1996)

2.7.5.3 Relationship Between k_e And k_i

The electro-osmotic flow rate is given by:

$$q_h = k_i I = k_e \frac{\Delta E}{\Delta L} A \qquad \text{Eqn. 2.20}$$

However, ΔE/I is resistance and (ΔL/resistance *A) is specific conductivity (σ), hence the above equation becomes (Grey 1966, Grey & Mitchell 1967):

$$k_i = \frac{c k_e}{\sigma} \qquad \text{Eqn. 2.21}$$

Where:

k_e = Electro-osmotic permeability (cm/s/v/cm)

k_I = Electro-osmotic efficiency (gallons/amp/hour)

σ = Specific conductivity (Siemens/m)

c= Constant (1.0 using stated units)

This equation is useful in that k_e varies within narrow limits as shown in Table 2.7. Hence, the electro-osmotic efficiency measured by k_I is dependant upon the electrical specific conductivity of the soil (σ). This association will be utilised and advanced in Chapter 7 to assist in defining acceptability criteria for soils to be treated by electro-osmosis based upon standard laboratory tests.

2.7.5.4 Constant Current And Constant Voltage Tests

Electro-osmosis may be carried out by applying constant current or constant voltage. During treatment the resistivity of the soil changes due to electro-chemical changes (§2.7.5.5) and desiccation of the soil. When constant voltage is applied, the magnitude of the current decreases corresponding to the increase in the resistance of the soil mass being treated. Likewise, if constant current is applied, the corresponding applied voltage would increase.

Hamir (1997) carried out a series of basic tests to assess the difference between constant voltage and constant current tests. The findings of his investigation were that in terms of the properties of the treated soil no distinction between the two methods could be found.

However, it should be remembered that the generation of negative pore water pressure is proportional to the applied voltage, see § 2.7.5.6.

2.7.5.5 Electrolysis Effects Associated With Electro-Osmosis

During electro-osmotic treatment of a soil mass the whole system acts like an electro-chemical cell in which cations migrate to the cathode and anions migrate to the anode. Reduction reactions take place at the cathode, with the principal reaction being the reduction of water into hydrogen gas. At the anode there is the possibility of two distinct oxidation reactions; the oxidation of the anode material itself into its oxide or the oxidation of H_2O to yield O_2 (Eastwood 1997). Hence, the anode will degrade, with the rate of degradation being dependent upon the material from which the anode is manufactured. A schematic of the movement of current and the electrolytic reactions that may occur during electro-osmotic treatment are given in Figure 2.16 The durability of alternative anode materials is discussed in the chapter on the development of the EKG, Chapter 3.

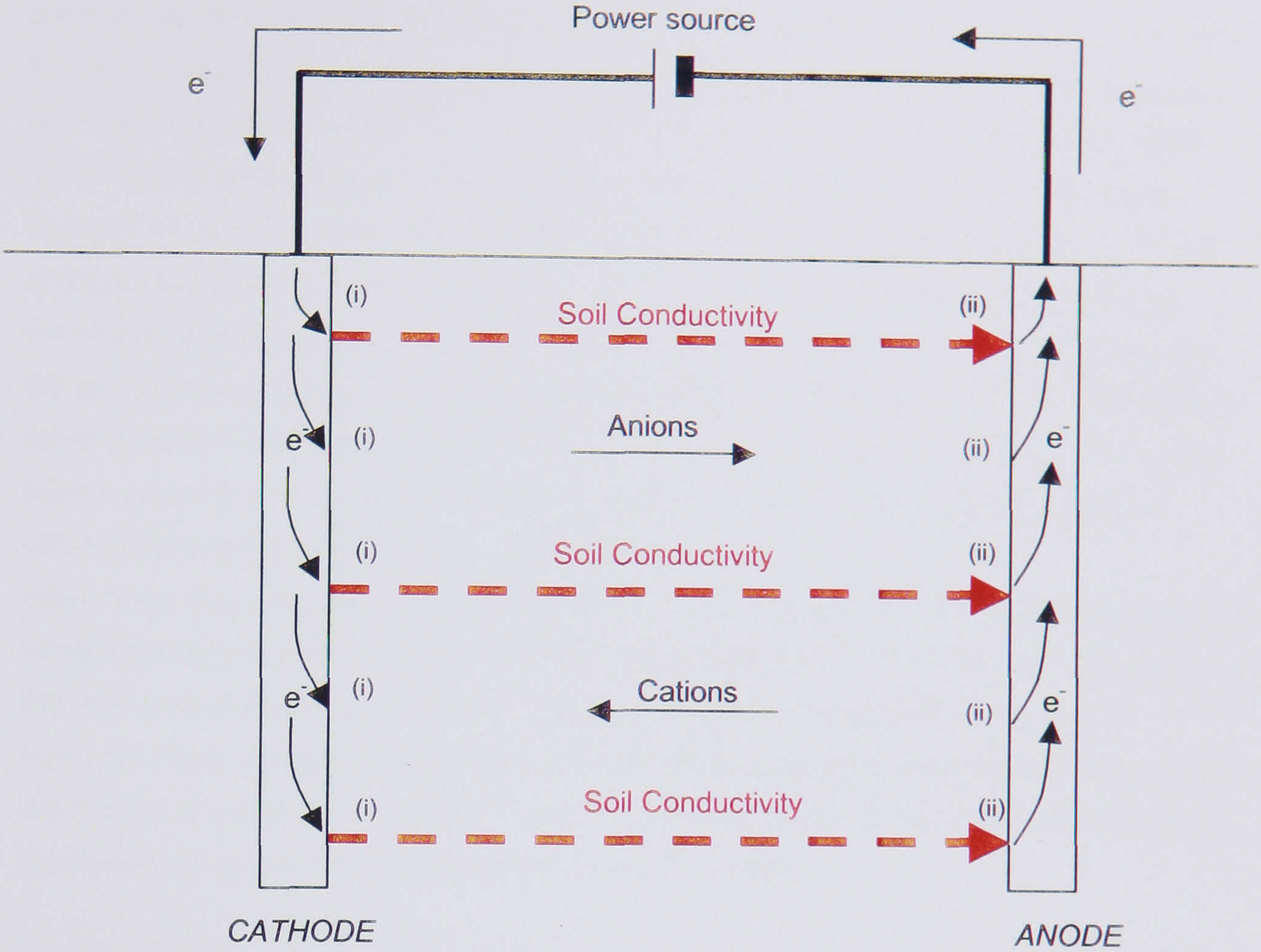

Figure 2.16 Schematic illustrating the movement of current through the electrochemical cell set up by electrokinetic phenomena imposed upon a soil mass (After Eastwood 1997)

(i) $2H_2O + O_2 + 4e^- \rightarrow 4OH^-$ or $2H^+ + 2e \rightarrow H_2$

(ii)

Iron anode:	$Fe + H_2O \rightarrow FeO + 2H^+ + 2e^-$	or	$2H_2O \rightarrow O_2 + 4H^+ + 4e^-$
Copper anode	$Cu + H_2O \rightarrow CuO + 2H^+ + 2e^-$	or	$2H_2O \rightarrow O_2 + 4H^+ + 4e^-$
Carbon anode	$C + 2H_2O \rightarrow CO_2 + 4H^+ + 4e^-$		

The liberation of hydrogen ions at the anode causes a decrease in the pH (more acidic) whereas the increase in hydroxide ions at the cathode causes an increase in pH (more alkaline) (Eykholt & Daniel 1994 and Alshawabkeh & Acar 1996). If these ions are not removed or neutralised from the anode and cathode electromigration/ion migration will take place (§ 2.7), with hydrogen ions moving towards the cathode (acid front) and hydroxide ions moving towards the anode (base front). The advance of acid and base fronts is governed by ion migration as well as electro-osmotic flow, diffusion, and the buffering capacity of the soil medium (Hicks & Tondorf 1994 and Acar *et al* 1993). Owing to a higher ratio of charge to ionic size H^+ ions move more rapidly than OH^- ions during electromigration. Additionally, electro-osmotic flow occurs in the same direction as H^+ migration, but it opposes the

direction of OH^- migration. As a consequence, the acid front from the anode moves faster than the base front from the cathode, so that acidic conditions prevail throughout most of the soil mass (Acar *et al* 1993, Jacobs *et al* 1994, Eykholt & Daniel 1994, Hicks & Tondorf 1994). The electrical conductivity of the soil is affected by the distribution of H^+ and OH^- as well as other ions in the pore fluid, in turn the electrical conductivity of the soil affects the potential gradients that drive electro-osmosis (Chen *et al* 1999). Where the acid and base fronts intersect, H^+ and OH^- react to form water and create a zone where the pH is almost neutral and the ionic strength of the pore fluid is minimal. As a result, the electrical conductivity within this zone decreases causing the electrical gradient to steepen. Away from this zone the electrical conductivity generally increases because of an increase in the concentration of either H^+ or OH^- (Alshawabkeh & Acar 1996 and Chen *et al* 1999). The result of this is that electro-osmosis becomes inefficient due to a large proportion of the electrical potential difference being dropped over the "neutral" zone.

Interactions may also occur between the soil minerals and pore fluid during electro-osmosis. Many laboratory studies of electro-osmosis have utilised kaolinite as their soil medium, as this is a relatively pure monomineralic clay these interactions may well be minimised. However, many real soils contain minerals that interact and retard ion transport. As a result the rates of migration of H^+ and OH^- may be significantly slower in real soils in the field than in laboratory experiments using kaolinite (Chen *et al* 1999).

2.7.5.6 Pore Water Pressures Induced By Application Of An Electrical Potential Field

Esrig (1968) has presented solutions for the development of pore water pressures under an applied electrical potential field. The solution derived by Esrig hinges upon some basic assumptions that are simplifications of the real situation, but without these simplifications the analysis of electro-osmotic treatment would be greatly complicated. These assumptions may be summarised as (after Esrig (1968) and Casagrande (1983)).

- The soil is homogenous and in a fully saturated state.
- The physical and physiochemical properties of the soil are uniform throughout and are constant with time.
- Electrophoresis of fine grained soil particles does not occur.
- There is a proportionality between the electrically induced velocity of water flow (v) through the soil and the voltage gradient (V). The proportionality factor being the coefficient of electro-osmotic permeability i.e. the Helmholtz- Smoluchowski equation is applicable:

$$v = k_e \frac{\partial V}{\partial x}$$

- All applied voltage is effective in moving water.
- The electrical field produced throughout the soil mass is constant with time.
- No reactions occur at the electrodes (e.g. electrolysis).

- Fluid flows due to an electrical field and due to a hydraulic gradient may be superimposed to find the total fluid flow.

Some of these assumptions are inherantly incorrect:

- A natural material is very rarely, if ever, homogenous.
- The resistivity of the soil undergoing electro-osmosis has been shown to vary, with both position and time (Wade 1976 and Adali 1999), both due to desiccation and electrochemical changes. Separation of the electrodes from the soil may also occur due to gas formation caused by electrolysis. Hence, the physical and physiochemical properties of the soil vary with time as does the electrical field.
- Electrolysis does occur during all electro-osmotic treatments.

However, the assumption that fluid flow caused by an electrical field may be superimposed on the flow caused by a hydraulic gradient is particularly important for the theory developed by Grey (1966). The validity of the assumption has been confirmed both prior to and since the publication of Grey's theory. Grey & Mitchell (1967) demonstrated the validity of the theory indirectly through the measurement of streaming potentials resulting from hydraulic flows and Wan & Mitchell (1976) for the superposition of porewater pressures generated by surcharge loading and electro-osmosis. The acceptance of this assumption is key in that it signifies that it is irrelevant if hydraulic flows have been induced by the application of load or in response to the application of an electrical field.

Accepting the validity of superposition of electrical and hydraulically driven flows through an incompressible soil mass and limiting consideration to 1-D flow gives, by conservation of mass:

$$\frac{\partial v}{\partial x} + \frac{\partial V_h}{\partial x} = 0 \qquad \text{Eqn. 2.22}$$

Where v is the velocity of flow due to the electrical potential gradient ($\partial V/\partial x$) (i.e. Helmholtz - Smoluchowski equation) and V_h is the velocity of flow due to the hydraulic gradient (i.e. Darcy's equation).

Differentiation of Equation 2.22 with respect to *x* and inserting Helmholtz - Smoluchowski's and Darcy's equations give:

$$k_e \frac{\partial^2 V}{\partial x^2} + \frac{k}{\gamma_w} \frac{\partial^2 u}{\partial x^2} = 0 \qquad \text{Eqn. 2.23}$$

rearranging gives:

$$\frac{\partial^2 u}{\partial x^2} + \frac{k_e \gamma_w}{k} \frac{\partial^2 V}{\partial x^2} = 0 \qquad \text{Eqn. 2.24}$$

and substitution of the variable ξ, where:

$$\xi = \frac{k_e \gamma_w}{k} V + u \qquad \text{Eqn. 2.25}$$

gives:

$$\frac{\partial^2 \xi}{\partial x^2} = 0 \qquad \text{Eqn. 2.26}$$

which is Laplace's equation in a 1-D system. Integrating once gives:

$$\frac{\partial \xi}{\partial x} = C_1 \qquad \text{Eqn. 2.27}$$

and integrating again gives:

$$\xi = xC_1 + C_2 \qquad \text{Eqn. 2.28}$$

Where C_1 and C_2 are constants of integration, which are dependant upon the boundary conditions. The possible drainage conditions that may exist at the electrodes that govern these boundary conditions are discussed in the following section.

2.7.5.7 Electrode Drainage Conditions And Pore Water Pressures

The drainage conditions, which may apply to either the anode or the cathode, may be defined as one of the following two conditions:

- ***Open:*** This condition exists when the electrode is open to the atmosphere and contains atmospheric or hydrostatic pressure, such that no excess pore pressure can exist at the electrode i.e. u_e=0. This condition will occur where an EKG is utilised with an external filter in place, or where a more conventional metallic type electrode is used together with an associated drainage path, e.g. sand drain or hollow perforated electrode. An open electrode may also be pumped, recharged or simply allowed to overflow.
- ***Closed:*** This condition exists when the electrode is essentially sealed such that no passage of gas or fluid can take place along the length of the electrode and excess pore pressures may develop. An example of a closed electrode would be a reinforcing bar or a length of railway track.

Anode and cathode open with recharge

The boundary conditions for the solution of Equation 2.28 in this situation are:

Cathode: x = 0, V = 0, u = 0 and hence $\xi = 0$

Anode: x = L, V = V_{max}, u = 0 and hence $\xi = \frac{k_e \gamma_w}{k} V_{max}$

Where V_{max} is the maximum voltage applied to the system at the anode. Substitution of the cathode boundary conditions into Equation 2.28 gives C_2 = 0 and substitution of the anode boundary condition gives the constant of integration C_1 as being equal to:

$$C_1 = \frac{k_e \gamma_w}{k} \frac{V_{max}}{L}$$ Eqn. 2.29

and substitution of this into Equation 2.28 to give ξ and then into Equation 2.25 to give u yields:

$$u = \frac{k_e}{k} \gamma_w \left(V_{max} \frac{x}{L} - V \right)$$ Eqn. 2.30

However, in a linear electrical potential field the term in parenthesis in Equation 2.30 is equal to zero. Hence, u=0 at all points between the anode and the cathode, i.e. zero excess pore water pressure is generated, hence no consolidation occurs. This pore water pressure distribution is shown schematically in Figure 2.17.

Anode closed and cathode open with free access to water

In this instance the boundary conditions for the solution of Equation 2.28 are:

Cathode: x = 0, V = 0, u = 0 and hence $\xi = 0$

Anode: x = L, V = V_{max}, flow velocity is zero $\frac{\partial \xi}{\partial x} = 0$

Once again due to the cathode boundary condition the constant of integration C_2=0. Substitution of the anode boundary condition into Equation 2.27 also gives C_1=0, hence, from Equation 2.28 ξ=0. Substitution of this into Equation 2.25 gives the solution for u:

$$u = -\frac{k_e \gamma_w V}{k}$$ Eqn. 2.31

Hence, u varies in direct proportion to the voltage at any point, going from zero at the cathode to a minimum at the anode. This pore water pressure distribution is shown schematically in Figure 2.17.

However, from a practical point of view Johnston (1978) has demonstrated that due to the occurrence of cavitation in the pore water the minimum negative pore water pressure that can be generated is limited to approximately -100kPa.

Anode open and cathode closed

The boundary conditions for this arrangement for the solution of Equation 2.28 are:

Cathode: x = 0, V = 0, and flow velocity is zero $\frac{\partial \xi}{\partial x} = 0$

Anode: x = L, V = V_{max}, u = 0 and hence $\xi = \frac{k_e \gamma_w}{k} V_{max}$

Where V_{max} is the maximum voltage applied to the system. Substitution of the cathode boundary conditions into Equation 2.28 gives:

$$C_2 = \frac{k_e \gamma_w}{k} V_{max}$$ Eqn. 2.32

and the substitution of this into Equation 2.28 to give ξ and then into Equation 2.25 to give u yields:

$$u = \frac{k_e}{k}\gamma_w (V_{max} - V) \qquad \text{Eqn. 2.33}$$

Indicating that positive pore water pressures will develop at the cathode and tend to zero at the anode. This pore water pressure distribution is shown schematically in Figure 2.17.

Drainage Regime	Boundary Conditions	Pore Water Pressure Distribution
open / open 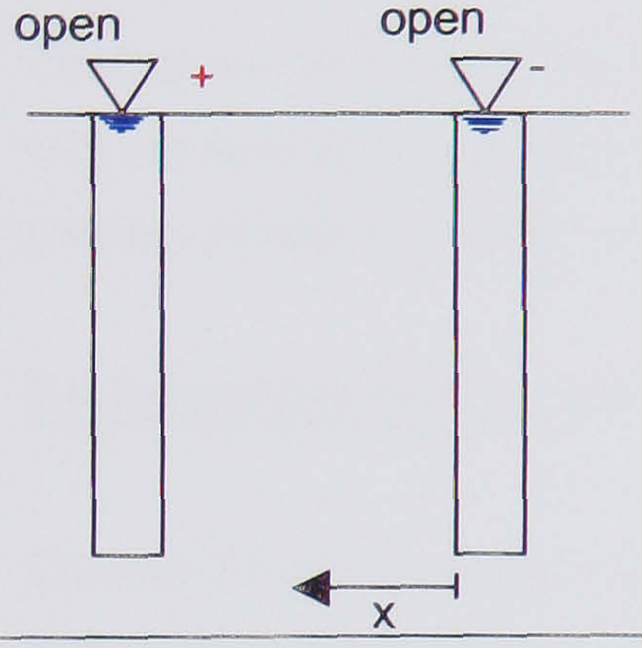	Cathode: x = 0, V = 0, u = 0 Anode: x = L, V = V_{max}, u = 0	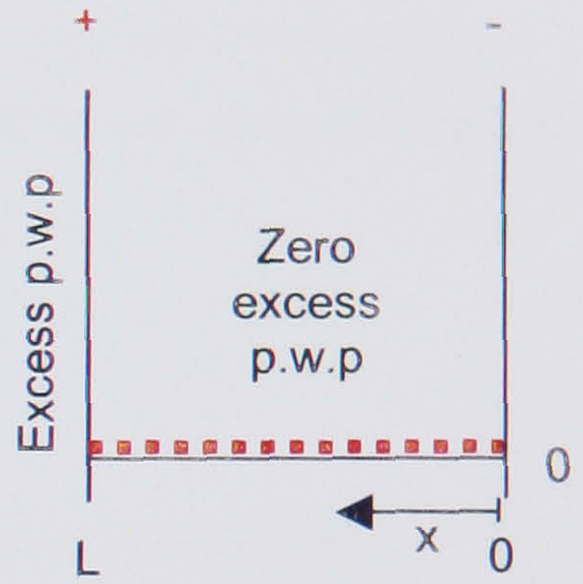
closed / open 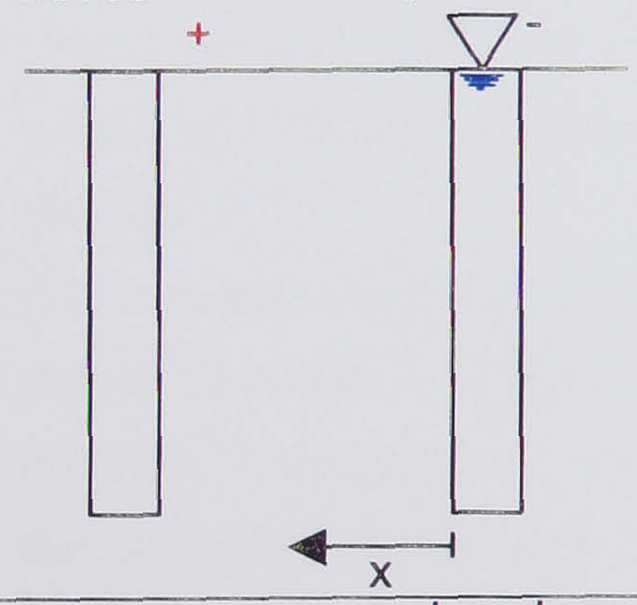	Cathode: x = 0, V = 0, u = 0 Anode: x = L, V = V_{max}, $\frac{\partial \xi}{\partial x} = 0$	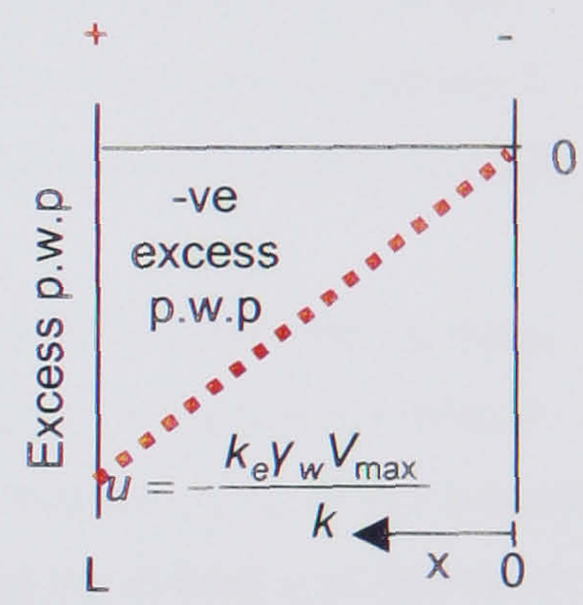
open / closed 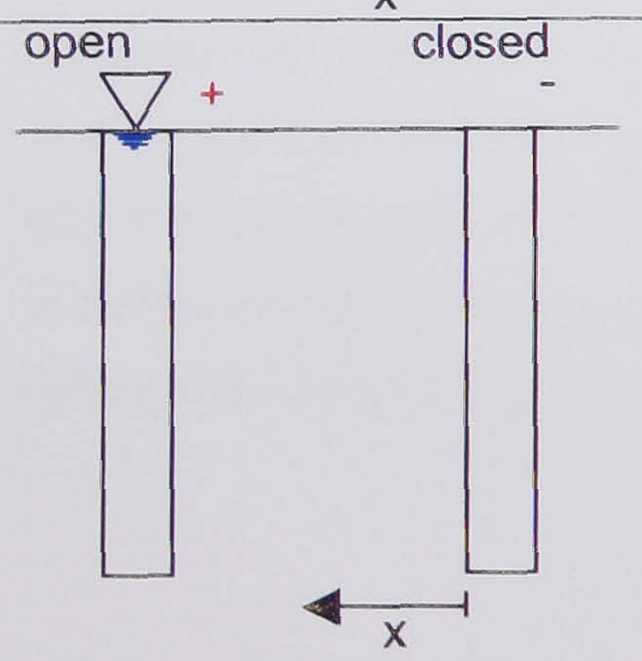	Cathode: x = 0, V = 0, $\frac{\partial \xi}{\partial x} = 0$ Anode: x = L, V = V_{max}, u = 0	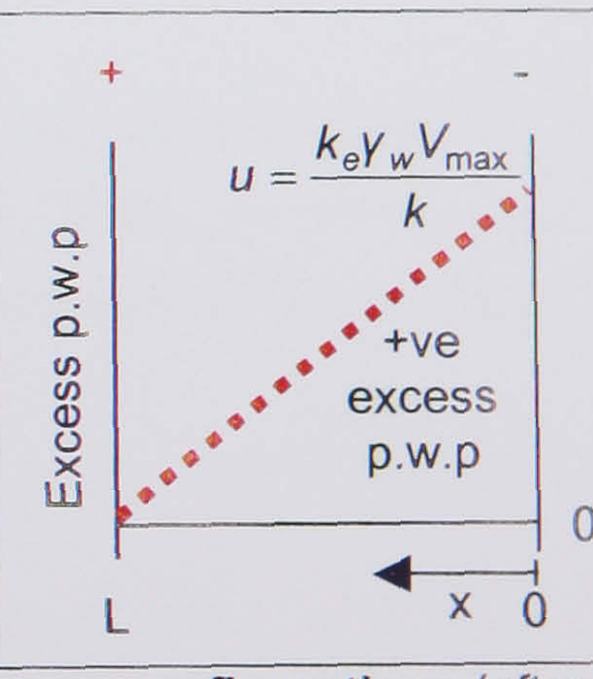

Figure 2.17 Pore water pressures for different electrode drainage configurations (after Esrig 1968)

2.7.5.8 Uses Of Different Electrode Configurations

The proposed use of the electro-osmosis installation governs how the open and closed electrodes are located within the electro-osmosis system. Table 2.8 summarises applications for the different permutations of electrode configurations that have been used in the field and laboratory.

From Table 2.8 it will be seen that the configurations used for consolidation / dewatering in practice and in laboratory studies are:

- *Open* Anode not recharged - *Open* Cathode with overflow
- *Closed* Anode - *Open* Cathode with overflow
- *Closed* Anode - *Open* Cathode pumped
- *Closed* Anode - *Closed* Cathode

Comparison of Table 2.8 with Figure 2.17 shows that these configurations are associated with the formation of zero or negative excess pore water pressures at the anode and zero or positive excess porewater pressures at the cathode.

2.8 SYNOPSIS OF CHAPTER 2

Chapter 2 has introduced the fundamental constituents of soils that are amenable to treatment by electrokinetic phenomena. The solid, liquid and gaseous phases of soil have been discussed to introduce the background as to why the electrokinetic phenomena occur in soils and how the different parameters may influence the efficiency of the electro-osmosis process.

The concepts of coupled flows and electrokinetics have been discussed briefly with a more detailed discussion and derivation of the theory behind electro-osmosis, the phenomena of principal interest to the work undertaken in this thesis. The chemical reactions of electrolysis that take place during electrokinetic treatment were discussed and the inherent problems of durability that these reactions cause introduced.

The idea of electrokinetic efficiency was then developed and the influence of the soils electrical conductivity as an acceptability criterion was introduced. Finally, the development of pore water pressures associated with electro-osmosis were discussed and the concepts of different drainage regimes at the electrode positions introduced.

CATHODE Drainage condition	***ANODE*** *Drainage Condition*		
	Open not recharged	*Open with recharge*	*Closed*
Open not recharged (overflow)	**EXPERIMENTAL:** Casagrande (1949) Hamir (1997) **CONSOLIDATION:** Lo *et al* (1991a)	**EXPERIMENTAL** Casagrande (1949) Hamed *et al* (1991) Reed *et al* (1995)	**CONSOLIDATION** Chappell & Burton (1975) **EXPERIMENTAL:** Hamir (1997)
Open with recharge	**EXPERIMENTAL:** Abiera *et al* (1999) **EXPERIMENTAL:** Bacteria transport DeFlaun & Condee (1997)	**EXPERIMENTAL** Abiera *et al* (1999) Esrig (1968) Grey (1970) **DE-CONTAMINATION BY FLUSHING** Schultz (1997)	**EXPERIMENTAL** Casagrande (1949) Esrig (1968)
Open and pumped	N/A	**DE-CONTAMINATION BY FLUSHING** Schultz (1997)	**SLOPE STABILITY** Casagrande *et al* (1961) **PILE FRICTION IMPROVEMENT** Milligan (1994) **CONSOLIDATION** Casagrande *et al* (1981) Fetzer (1967)
Closed	N/A	**EXPERIMENTAL** Abiera *et al* (1999) Esrig (1968)	**CONSOLIDATION** Eggestat & Føyn (1983) Bjerrum *et al* (1967) Chappell & Burton (1975)

Table 2.8 Electrode drainage regime permutations and uses

2.9 CHAPTER 2 REFERENCES

1. Abiera, H.O., Miura, N., Bergado, D.T. & Nomura, T. (1999) *Effects of using electro-conductive PVD in the consolidation of reconstituted Ariake clay.* Geotechnical Engineering Journal of Southeast Asian Geotechnical Society, Vol. 30, No. 2, August, pp 67-83.
2. Acar, Y.B., & Hamed, J. (1991) *Electrokinetic soil processing in waste remediation/treatment,* (Paper No. 910106) Transport Research Board, National research Council: Washington D.C., USA.
3. Acar, Y.B., & Alshawabkeh, A.K. (1993) *Principles of electrokinetic remediation.* Environmental Science and Technology, Vol. 37 (13), pp 2638-2647.
4. Acar, Y.B., Alshawabkeh, A.K. & Gale, R.J. (1993) *Fundamentals of extracting species from soils by electrokinetics.* Waste Management, Vol. 13, pp 141-151.
5. Acar, Y.B., & Alshawabkeh, A.K. (1994) *Modelling conduction phenomena in soils under an electric current.* In Proc. 13th Int. Conf. on Soil Mech. and Found. Eng., January 5-10, 1994, Vol. 2, New Deli, India. Publ. by Balkema, Rotterdam, The Netherlands. pp 669-672.
6. Adali, E. (1999) *Study of electro-osmosis in multi-layered soils.* MSc. dissertation, Geotechnical Group, University of Newcastle upon Tyne, U.K.
7. Alshawabkeh, A.N. & Acar Y.B. (1996) *Electrokinetic remediation: I theoretical model.* Journal of Geotechnical Engineering Division, ASCE, Vol. 122 (GT3), pp 186-196.
8. Bjerrum, L., Moum, J., & Eide, O. (1967) *Application of electro-osmosis to a foundation problem in a Norwegian quick clay.* Géotechnique, Vol. 17, pp 214-235.
9. Bjerrum, L. & Rosenqvist, I.Th. (1956) *Some experiments with artificially sedimented clays.* Géotechnique, Vol. 6, pp 124-136.
10. Bitton, G. & Gerba, C.P. (1984) *Groundwater Pollution Microbiology.* Wiley, New York, USA, p 377.
11. British Standards Institution (1981) *BS 5930: Code of Practice for Site Investigation*, BSI, Hemel Hempstead, U.K.
12. British Standards Institution (1986) *BS 8004: Code of Practice for Foundations*, BSI, Hemel Hempstead, U.K.
13. Carnie, S.L., & Torrie, G.M. (1984) *The statistical mechanics of the electrical double layer.* Advances in Chemical Physics, Vol. 56, pp 141-253.
14. Casagrande, L. (1949) *Electro-osmosis in soils.* Géotechnique, Vol. 1(3), pp 159-177.
15. Casagrande, L. (1952) *Electro-osmotic stabilisation of soils,* Jour. of the Boston Soc. of Civil Engineers section, ASCE, Vol. 39, pp 51-83.
16. Casagrande, L. (1983) *Stabilization of soils by means of electro-osmosis.* Jour. of the Boston Soc. of Civil Engineers section, ASCE, Vol. 69, No. 2, pp 255-302.
17. Casagrande, L., Loughney, R. & Matich, M.A.J. (1961) *Electro-osmotic stabilization of a high slope in loose saturated silt.* Proceedings of the 5th International Conference on Soil Mechanics and Foundation Engineering, Paris, Vol. 2, pp 555-561.

18. Casagrande,L., Wade, N., Wakely, M. & Loughney, R. (1981) *Electro-osmosis projects. British Columbia, Canada.* Proceedings of the 10th European Conference on Soil Mechanics and Foundation Engineering, Rotterdam, pp 607-610.
19. Chapman, D.L. (1913) *A contribution to the theory of the electrocapillarity.* Philosophical Magazine, Vol. 25, No. 6, pp 475-481.
20. Chappell, B.A., & Burton, P.L. (1975) *Electro-Osmosis Applied To Unstable Embankment.* Journal of Geotechnical Engineering, ASCE, Vol. 101 (GT8), pp 733-740.
21. Chen, J.L. & Murdoch, L. (1997) *Field demonstration of in situ electroosmosis between horizontal electrodes.* Proceedings of the ASCE annual fall national convention, Minneapolis, Geotechnical Special Publication No. 71, pp 545-559
22. Chen, J.L., Al-Abed, S.R., Bryndzia, L.T. & Murdoch, L. (1999) *Cation transport and partitioning during a field test of electroosmosis.* Water Resources Research, Vol. 35, No. 12, December, pp 3841-3851.
23. Colin, F. (1986) *Application of electrical fields to thicken and dewater sewage sludges.* In New Developments in Processing of Sludges and Slurries (Eds. Bruce, A.M., L'Hemite, P. and Newman, P.J.), Elsevier, London. pp 3-13.
24. DeFlaun, M.F. & Condee, C.W. (1997) *Electrokinetic transport of bacteria.* Journal of Hazardous Materials, Vol. 55, Elsevier Science, pp 263-277.
25. Donnan, F.G. (1924) *The theory of membrane equilibrium,* Chemical Review, Vol. 1, pp 73-90.
26. Eastwood, B.J. (1997) *A fundamental study of the electrochemical failure mechanism of a novel impressed current cathodic protection system.* PhD Thesis, Department of Chemistry, University of Newcastle upon Tyne, U.K.
27. Eggestad, Å. & Føyn, T. (1983) *Electro-osmotic improvement of a soft sensitive clay.* Proceedings of the 8th European Conference on Soil Mechanics and Foundation Engineering, Helsinki, Vol. 2, pp 597-602.
28. Ellis, S. & Mellor, A. (1995) *Soils and environment.* 1st Ed., Routledge Physical Environment series, London. p 364.
29. Esrig, M.I. (1968) *Pore Pressures, Consolidation And Electrokinetics.* Journal of the Soil Mechanics And Foundation Division, ASCE, Vol. 94 (SM4), pp 899-921.
30. Eykholt, G.R. & Daniel, D.E. (1994) *Impact of system chemistry on electro-osmosis in contaminated soils.* Journal of Geotechnical Engineering, ASCE, Vol. 120 (GT5), pp 797-815.
31. Fetzer, C.A. (1967) *Electro-Osmotic Stabilization Of West Branch Dam.* Journal of the Soil Mechanics And Foundation Division, ASCE, Vol. 93 (SM4), pp 85-106.
32. Foth, H.D. (1984) *Fundamental of soil science.* 7th Ed, John Wiley & Sons, New York. p 436.
33. Frank, H.S. (1958) *Covalency in the hydrogen bond and the properties of water and ice.* Proceedings of the Royal Society, A247, pp. 481-492.

34. Freeze, R.A. & Cherry, J.A. (1979) *Groundwater.* Prentice - Hall: Englewood Cliffs, N.J. USA. p 604.
35. Gouy, G. (1910) *Sur la constitution de la charge électrique a la surface d'un électrolyte.* Anniue Physique, Paris, Série 4, Vol. 9, pp 457-468.
36. Grey, D.H. (1966) *Coupled flow phenomena in clay-water systems,* PhD Thesis, University of California, Berkley, USA.
37. Grey, D.H. (1970) *Electrochemical Hardening Of Clay Soils.* Géotechnique, Vol. 20 (1), pp 81-93.
38. Grey, D.H. (1976) *Electro-osmosis applied to unstable embankment - discussion,* Journal of Geotechnical Engineering, ASCE, Vol. 102, GT1, pp 119-121.
39. Grey, D.H. & Mitchell, J.K. (1967) *Fundamental aspects of electro-osmosis in soils,* Journal of the Soil Mechanics And Foundation Division, ASCE, Vol. 93 (SM6), pp 209-136. Closure discussion in Vol. 95, (SM3), 1969. pp 875-879.
40. Grim, R.E. (1962) *Applied Clay Mineralogy,* McGraw-Hill, New York. p 422.
41. Grim, R.E. (1968) *Clay Mineralogy,* 2nd Ed. McGraw-Hill, New York. p 384.
42. Hamed, J., Acar, Y.B. & Gale, R.J. (1991) *Pb (II) removal form kaolinite by electrokinetics.* Journal of Geotechnical Engineering, ASCE, Vol. 117, No. 2, pp 241-271.
43. Hamir, R. (1997) *Some aspects and applications of electrically conductive geosynthetic materials.* Doctor of Philosophy Thesis, University of Newcastle upon Tyne, U.K., p 225.
44. Head, K.H. (1992) *Manual Of Soil Laboratory Testing, Vol. 1: Soil classification and compaction tests,* 2nd Ed., Pentech Press, London. p 339.
45. Head, K.H. (1994) *Manual Of Soil Laboratory Testing, Vol. 2: Permeability, Shear Strength and Compressibility Tests,* 2nd Ed., Pentech Press, London. p 440.
46. Hellawell, E. (1994) *Modelling transport processes in soil due to hydraulic, density and electrical gradients.* Doctor of Philosophy Thesis, Cambridge University, U.K.
47. Helmholtz, H. (1879) *Wiedemanns Annalen d.* Physik, Vol. 7, p 137.
48. Hicks, R.E. & Tandorf, S. (1994) *Electrorestoration of metal contaminated soils.* Environmental Science Technology, Vol. 28, No. 12, pp 2203-2210.
49. Jacobs, R.A, Sengun, M.Z., Hicks, R.E. & Probstein, R.F (1994) *Model and experiments on soil remediation by electric fields.* Journal of Environmental Science and Health, Part A, Vol. 29, No. 9, pp 1933-1955.
50. Johnston, I.W. (1978) *Electro-osmosis and its application to soil and foundation stabilisation.* In: Symposium on Soil Reinforcing and Stabilising Techniques. Sydney, Australia, pp 459-476.
51. Jones, C.J.F.P. (1998) *Improvements relating to geosynthetics.* U.K. Patent No. GB2301311B.
52. Lageman, R., Pool, W. & Seffinga, G.A.(1989) *Electro-Reclamation: State of the Art* in NATO/CCMS Third International Conference on Demonstration of Remedial Action

Technologies for Contaminated Land and Groundwater, November 6-9, Montreal, Canada, pp 115-136.

53. Lambe, T.W. & Whitman, R.V. (1969) *Soil Mechanics.* John Wiley & Sons, Inc. New York. p 565.
54. Lee, I.K., White, W., & Ingles, O.G. (1983) *Geotechnical Engineering.* Pitman, London. p 508.
55. Lo, K.Y., Ho, K.S., & Inculet, I.I. (1991a) *Field test of electroosmotic strengthening of soft sensitive clay.* Canadian Geotechnical Journal, Vol. 28, pp 74-83.
56. Lo, K.Y., Ho, K.S., & Inculet, I.I. (1991b) *A novel technique of electrical strengthening od soft sensitive clay by dielectrophoresis.* Canadian Geotechnical Journal, Vol. 29, pp 599-608.
57. Lo, K.Y. & Shang, J.Q. (1995) Applications *of electrokinetics in mining reclamation.* In Proceedings of the 1st SCH-CORE workshop, Bejing, China.
58. Lockheart, N.C. (1983) *Electro-osmotic dewatering of clays: II Influence of salt, acid and flocculants.* Colloids and Surfaces, Vol. 6, pp 239-251.
59. Long, E. & George, W. (1967) *Turnagain slide stabilization, Anchorage, Alaska.* Journal of the Soil Mechanics and Foundation Division, ASCE, Vol. 93 (SM4), pp 611-627.
60. McGown, A., Marsland, A., Radwan, A.M. & Garb, A.W.A. (1980) *Recording and interpreting soil macrofabric data.* Géotechnique, Vol. 30, No. 4, pp 417-447.
61. Milligan, V. (1994) *First application Of Electro-Osmosis To improve Friction Pile Capacity-Three Decades Later.* Proc. of the 13th Int. Conf. on Soil Mech. and Found. Eng., Jan. 5-10, Vol. 5. New Delhi, India, Pub. Balkema. pp 1-5.
62. Mitchell, J.K. (1991) *Conduction Phenomena: from theory to geotechnical practice.* Géotechnique, Vol. 41, No. 3, pp 299-340.
63. Mitchell, J.K. (1993) *Fundamentals of Soil Behaviour.* 2nd Ed., Pub. John Wiley & Sons Inc. New York, USA. p 437.
64. Morley, A. & Hughes, E. (1994) *Principles of Electricity.* 5th Ed. Longman Scientific & Technical, Harlow. p 384.
65. Napier, J. (1846), Phil. Mag., Vol. 29, No.10.
66. Netlon Ltd (1998) *Electrically-Conducting Element.* British Patent Application No. 9813432.3.
67. Nettleton, I.M. (1996) *Electro-Bioremediation.* Internal Report, Geotechnical Group, University of Newcastle upon Tyne, U.K., p 70.
68. Oades, J.M. (1989) *An introduction to organic matter in mineral soils.* Chapter 3 in; Dixon ,J.B. & Weed, S.B. (Eds.) *Minerals in soil environments.*, 2nd Ed, Soil Science Soc. of America Book Series 1, Madison, WI, pp 89-159.
69. Pamukcu, S. (1996) *Electro-Chemical Technologies for in-situ restoration of contaminated subsurface soils.* The Electronic Journal of Geotechnical Engineering, available at http://139.78.66.61/ejge/.

70. Pauling, L. (1960) *The nature of the chemical bond.* Cornell University Press, Ithaca, NY. p 644.
71. Pugh, R.C., Clarke, B.G., & Jones, C.J.F.P. (2000) *An electro-osmosis consolidation trial using electrokinetic geosynthetics* Proc. 4th International Conference on Ground Improvement Geosystems, Helsinki, June 7-9, Vol. 2, pp 533-540.
72. Quincke, G. (1861) Pogg. Ann. Physik, Vol. 113. 513.
73. Reed, B.E., Berg, M.T., Thompson, J.C. & Hatfield, J.H. (1995) *Chemical conditioning of electrode reservoirs during electrokinetic soil flushing of Pb -contaminated silt loam.* Journal of Environmental Engineering, ASCE, Vol.121, No.11, pp 805-815.
74. Reuss, F.F. (1808) *Sur un nouvel effet de l'électricité glavanique.* Mémoires de la Societé Impériale des Naturalistes de Moscou, Vol. 2, pp 327-337.
75. Rowe, P.W. (1972) *The relevance of soil fabric to site investigation practice - The 12th Rankine Lecture.* Géotechnique, Vol. 22, No. 2, pp 195-300.
76. Sandanasamy, R.D. (1998) *A Vertical Drain.* European Patent Application No, 98103845.8.
77. Sauer, J.E. & Davis E.J. (1994) *Electrokinetically enhanced sedimentation of colloidal contaminants.* Environmental science and technology, Vol. 28, No. 4, pp 737-745.
78. Schmidt, G. (1950) *Zur Elecktrochemie Feinporiger Kapillarsystems.* Zhurnal fur Elektrochemie, Vol. 54, pp 425.
79. Schmidt, G. (1951) *Zur Elecktrochemie Feinporiger Kapillarsystems.* Zhuranl fur Elektrochemie, Vol. 55, pp 684.
80. Schultz, D.S. (1997) *Electroosmosis technology for soil remediation: laboratory results, field trial, and economic modelling.* Journal of Hazardous Materials, Vol. 55, Elsevier Science, pp 81-91.
81. Shang, J.Q. & Lo, K.Y. (1997) *Electrokinetic dewatering of a phosphate clay.* Journal of Hazardous materials, Vol. 55, pp 117-133.
82. Shaw, D.J. (1969) *Electrophoresis.* Academic Press, London & New York. p 152.
83. Simpson, K. (1983) *Soil.* Longman handbooks in agriculture, Longman, New York. p 283.
84. Smoluchowski, M. (1914) In Graetz, L. (Ed) *Handbuch der Elektrizitat und Magnetisums.* Vol. 2, J.A.Barth, Leipzig, Germany.
85. Spiegler, K.S. (1958) *Transport processes in ionic membranes.* Transactions of the Farady Society, Vol. 54, pp 1408-1428.
86. Sposito,G. (1989) *The Chemistry of Soils.* Oxford University Press, New York, USA, p 277.
87. Stillinger, F.H. (1980) *Water revisited.* Science, Vol. 209, p 451.
88. Stern, O. (1924) *Zur Theorie der Elektrolytischen Doppelschriht.* Zeitschrift Electrochem, Vol. 30, pp 508-516.
89. Stokes, Sir G.G. (1891) *Mathematical and Physical Paper III.* Cambridge University Press

90. Tan, K.H. (1993) *Principles of Soil Chemistry.* 2nd Ed., Marcel Dekker Inc., USA. p 521.
91. van Olphen, H. (1977) *An Introduction to Clay Colloid Chemistry,* 2nd Ed., Wiley Interscience, New York, p 318.
92. Van Vlack, L.H. (1982) *Materials for engineering: Concepts and applications,* Addison-Wesley Series in Metallurgy and Materials. p 604.
93. Verwey, E.J.W., & Overbeek, J.T.G. (1948) *Theory of the stability of Lyophobic colloids,* Elsevier, New York. p 205.
94. Wade, N.H. (1976) *Slope stability by electro-osmosis.* Proceedings of the 29th Canadian Geotechnical Conference, Vancouver, Section X, pp 44-46.
95. Wakeman, R.J. (1982) *Effects of solids concentration and pH on electrofiltration.* Filtration and separation, Vol. 19, Part 4, pp 316-319.
96. Wan, T.Y. & Mitchell, J.K. (1976) *Electro-osmotic consolidation of soils.* Journal of the Geotechnical Engineering Division, ASCE, Vol. 102 (GT5), pp 473-491.
97. Waxman, M.H. & Smits, L.J.M. (1967) *Electrical conductivities in oil bearing shaly sands.* Soc. of Petroleum Engineers, Proc. of 42nd Annual Fall meeting, Houston, Texas, SPE-1863-A, pp V-145 - V-160.
98. Weaver, C.E. & Pollard, L.D. (1973) *The Chemistry of Clay Minerals.* Developments in Sedimentology 15, Elsevier, Amsterdam, p 213.
99. Wrigley, N.E. (1999) *The practical use of Electro-osmosis.* Personal communication, July.
100. Yeung, A.T. (1990) *Electrokinetic barrier to contaminant transport through compacted clay.* Doctor of Philosophy Thesis, University of California, Berkeley, USA.
101. Yeung, A.T., & Mitchell, J.K. (1993) *Coupled fluid, electrical and chemical flows in soil.* Géotechnique, Vol. 43 (1), pp 121-134.

CHAPTER 3

ELECTROKINETIC GEOSYNTHETICS

3.1 INTRODUCTION

The purpose of the development of Electrokinetic Geosynthetics (EKGs) is to combine the existing functions of geosynthetics (filtration, drainage, reinforcement, separation and barriers) with electrical conductivity so that electrokinetic phenomena can be used to enhance their performance. These electrokinetic geosynthetics can provide an alternative and often more cost-effective solution to complex environmental and ground engineering problems than traditional methods.

3.2 EXISTING GEOSYNTHETIC MATERIALS

Modern geosynthetics were first developed for the Dutch "Delta Project" during the 1950's following the catastrophic floods which occurred in the Netherlands in February 1953 (Van Santvoort 1994). The sudden demand for construction materials outstripped the available supply and new innovative solutions were developed, with woven geotextiles replacing granular filter materials and woven willow branch scour protection (John 1987).
During the 1960's and 70's the use of geosynthetics in filtration, separation and drainage applications increased. Rhone-Poulenc produced their needle punched "Bidim" range of geosynthetics, and ICI produced their heat bonded "Terram" range (John 1987).
Geosynthetic materials used for reinforcement in the form of strips, tapes, sheets and grids were introduced in the 1970's.
The behaviour of a geosynthetic material is governed by either its structural configuration, i.e. how its filaments are aligned, or the properties of the materials from which it is composed. The most common polymers used in geosynthetics are discussed in the following sections followed by a discussion of manufacturing processes to illustrate the diversity of types and applications of these materials.

3.2.1 GEOSYNTHETIC RAW MATERIALS

Geosynthetics are generally produced from *thermoplastics* that are polymers that can be refashioned by heating as opposed to *thermosetting* plastics, which cannot be remoulded by reheating, and *elastomers,* which are materials that undergo very large elastic strains under minimal stress (Van Vlack 1982). Thermoplastics are further subdivided into two types:

Amorphous: Which have a non-crystalline structure, due to their large molecular size.
Partially -Crystalline: These polymers contain partially crystallinity in their structure, beyond which they pass into an amorphous structure. Degrees of crystallinity are usually between 30% and 75%.

The majority of geosynthetics are produced from partially-crystalline polymers (Koerner 1990). The most common polymers used in geosynthetics and their approximate usages are given below, and their properties defined in Table 3.1 (Koerner 1990):

- Polypropylene (65%)
- Polyester (32%)
- Polyamide (2%)
- Polyethylene (1%)

The manufacture of geosynthetics from these raw materials normally consists of two steps. The first step consists of making linear elements such as fibres and yarns. The second step consists of combining these linear elements to make a planar structure in the form of a fabric or grid. An alternative manufacturing process uses extrusion to form grids or impervious sheets. Grids can be formed from the latter (FHWA 1985).

Table 3.1 Relative properties of geosynthetics (After John 1987 & Nettleton 1996)

PROPERTY	POLYESTER	POLYAMIDE	POLYPROPYLENE	POLYETHYLENE
Strength	High	Intermediate	Low	Low
Elastic Modulus	High	Intermediate	Low	Low
Strain @ Failure	Intermediate	Intermediate	High	High
Creep	Low	Intermediate	High	High
Unit Weight	High	Intermediate	Low	Low
Cost	High	Intermediate	Low	Low
RESISTANCE TO:				
UV Stabilised	High	Intermediate	High	High
UV Unstabilised	High	Intermediate	Intermediate	Low
Alkalis	Low	High	High	High
Fungus / Vermin	Intermediate	Intermediate	Intermediate	High
Fuel	Intermediate	Intermediate	Low	Low
Detergents	High	High	High	High

3.2.1.1 Polymer Additives

The chemical nature of the polymer from which the geosynthetic is manufactured is also significant in governing the durability of the geosynthetic (Van Santvoort 1994). One characteristic of synthetics over traditional construction materials is their relative insensitivity to a great number of chemical and environmental effects. Many synthetic polymers are, however, sensitive to oxidation; either at high temperatures associated with processing (thermo-oxidation) and/or due to sunlight (photo-oxidation). The effect of oxidation on a polymer is that mechanical properties such as strength, elasticity and strain absorption capacity deteriorate and the geotextile eventually becomes brittle and cracks (Van Santvoort 1994). Specific additives have been developed to counteract these processes:

- **Anti-Oxidants:** These are chemical compounds added to the polymer to reduce the oxidative break-down of the polymer which occurs at higher processing temperatures (processing anti-oxidant). They also minimise long-term oxidation when the product is in use ("end use" anti-oxidation).
- **UV-Stabiliser:** These are chemical compounds added to the polymer, together with anti-oxidants in the processing stage to prevent degradation due to UV light. This is particularly important for plastic products that are exposed for part or the whole of their working life to sunlight.

3.2.2 GEOSYNTHETIC PRODUCTS

The polymers used in the manufacture of geosynthetics permit a large range of production techniques to be employed. The polymers are typically extruded to form (FHWA 1995):

- Sheets of extruded polymer, typically up to 5m wide.
- Slitfilm, 1 to 3mm wide tape like fibres produced by slitting and extruding film.
- Fibrillated yarns.
- Strips 20 - 40mm wide.
- Coarse filaments.
- Filaments.

The filaments may be further processed to produce base materials such as:

- Staple fibres formed from short lengths (20 to 100mm) of filaments.
- Monofilament yarn formed from a single filament.
- Multifilament yarn formed from fine filaments.

- Spun yarn formed from interlaced and twisted together staple fibres.

Many geosynthetics are produced from an individual type of base material, but some are created from a combination of these materials. Geosynthetics generally fall into one of the groups outlined in the following section.

3.2.3 GEOSYNTHETIC TYPES

Geosynthetic types can be subdivided into groups as follows:

Wovens: These are produced by having longitudinal warp yarns through which transverse weft yarn are interlaced. The intersection is usually at 90°, but some weaving looms weave at a skew angle (FHWA 1985). Monofilament, multifilament, spun, slit film or fibrillated yarns can be used for the production of woven geosynthetics. Monofilament and slit film wovens are typically thin (0.5mm), while multifilament, spun and fibrillated wovens are typically thicker (3 to 10mm). Woven geotextiles have been used for filtration, drainage, erosion prevention, reinforcement and separation.

Non Wovens: These are formed from staple fibres or filaments arranged in an orientated or random pattern to form a planar structure (FHWA 1985). The fibres are then bonded together by one of the following methods:

1. *Chemical bonding*: the fibrous material is laid out and sprayed, or impregnated with a chemical bonding agent, such as acrylic resin. The material is then commonly air dried to re-establish the open pore structure.
2. *Thermal bonding*: the fibrous material passes between heated rollers, forcing the fibres into contact with each other and causing partial melting. This leads to the formation of thermal bonds at the crossover points. Heat bonded non wovens are usually made from single polymer type fibres, as fibres of the same type form the best thermal bonds (John 1987). Thermally bonded geotextiles tend to be thin (0.5 to 1mm) and light, for example Terram from Exxon. These geotextiles are commonly used for filtration and separation materials.
3. *Mechanical bonding:* the fibrous material passes through a device that punches an array of thousands of finely barbed needles through it, and then withdraws the needles, leaving the fibres entangled. This creates a mechanically entangled non woven structure typically 1 to 5mm thick.

Weft Insert Warp Knit (WIWK)/ Stitch Bonded: These geotextile production techniques offer an extremely large variety of possibilities of producing materials and composites with particular functions. WIWK technology utilises a combination of weaving and knitting: the weft fibres are inserted across the width of the machine, behind the needles. The needles

then knit along the machine direction (warp) by forming and stitching loops. This technique allows a wide range of geometries to be created; load bearing fibres to be introduced without tight radius curves; and brittle or difficult to handle fibres to be utilised (Andersson *et al* 1994). These techniques can be used with brittle fibres such as glass and carbon fibres. The weft inserts can be introduced in two different ways:

1. Impaled structures with stitches piercing the insert yarns.
2. Non impaled structures with stitches around the insert yarns.

Geogrids: These are grid like structures with large apertures (typically 20 to 100mm). They are generally produced by:

- Punching a regular array of holes in an extruded polymeric sheet, these are then stretched either uniaxially or biaxially, depending upon the characteristics required.
- Stitch bonding a rectangular mesh of fibre ropes, which are coated in PVC or other polymers to form a protective coating.
- Laser welding of solid polymer bars (typically polyester).
- Weaving or knitting from yarns.

These materials are most commonly used for reinforcement and separation.

Geowebs: These may be formed from a very coarse weave fabric made of strips (20 to 40mm wide), or from fibres encased in a tough durable sheath. These materials are typically used for reinforcement, erosion control, bank protection and anchorages.

Geomats: These are produced from extrusion of coarse filaments with a tortuous shape, which are bonded at their contact points. These mats are used for erosion prevention and as drainage materials.

Geonets: These are also known as meshes, but the industry has standardised on "Geonets" as the name (Koerner 1990). These are formed on extrusion of coarse filaments though a die with a set of counter-rotating segments. The molten polymer flows at angles (typically 60° to 90°) forming discrete ribs in two planes. The ribs are typically 1 to 5 mm in diameter, and the openings are typically 10 to 100mm. Nets are generally used for reinforcement and drainage.

Geomembranes: These are typically 5m wide extruded sheets of polyethylene or PVC. They are relatively impermeable and are use as barriers to flow.

Geocomposites: Geocomposites are essentially made up from the other geosynthetic types. For example, a geonet structure sandwiched between two filter materials to provide a

filtration and drainage composite. Other examples include the incorporation of reinforcement materials into a non-woven separation material.

Geosoils: Theses are soils that have geosynthetic materials mixed with them before they are deposited (John 1987).

3.3 ELECTRICALLY CONDUCTIVE MATERIALS

Geosynthetic materials can be made electrically conductive in a number of ways as discussed below.

3.3.1 INTRINSICALLY DOPED POLYMERS

Doped polymers can be produced by electrical or chemical deposition, examples are polybithiophene, which can be n(+) reduction or p(-) oxidation doped. However, these organic conducting polymers are not particularly stable, and are quickly attacked by oxygen and water, a process in which the double bonds are attacked and the compound hydrolysed (Nettleton 1996).

Spun polypyrrole is a relatively cheap material that has an electrical conductivity of 100 S/cm. However, this material is very brittle and would require supporting on some other material such as PET or Polymethylmethacrylate (Campbell 1994).

3.3.2 CARBON FILLED POLYMERS

Carbon filled polymers are produced by the addition of conductive carbon black powder to conventional polymers. Conductive carbon black powder is a high structure (long carbon chains) very fine particulate powder formed from the controlled burning of hydrocarbons. Virtually all thermoplastics can be compounded with carbon black powder (Wright & Woodham 1989). As the concentration of carbon black powder added to the polymer base increases so the electrical conductivity increases until the polymer becomes conductive, as show schematically in Figure 3.1.

When carbon black is added to a polymer the physical strength properties are generally reduced with the degree of loss being proportional to the concentration of carbon black added, the higher the concentration of carbon black the lower the strength. In these composites it is the carbon filler that conducts electricity and not the polymer. If carbon black is used as the filler then a loading of between 20% - 30% by weight will be required to produces a suitable conductive polymer (Jones *et al* 1996).

3.3.3 CARBON FIBRES

Pure carbon fibres are more conductive than carbon filled polymers, but are more difficult to process. For example, carbon fibre rolled crystals are good stable conductors, but are stiff and brittle (Nettleton 1996).

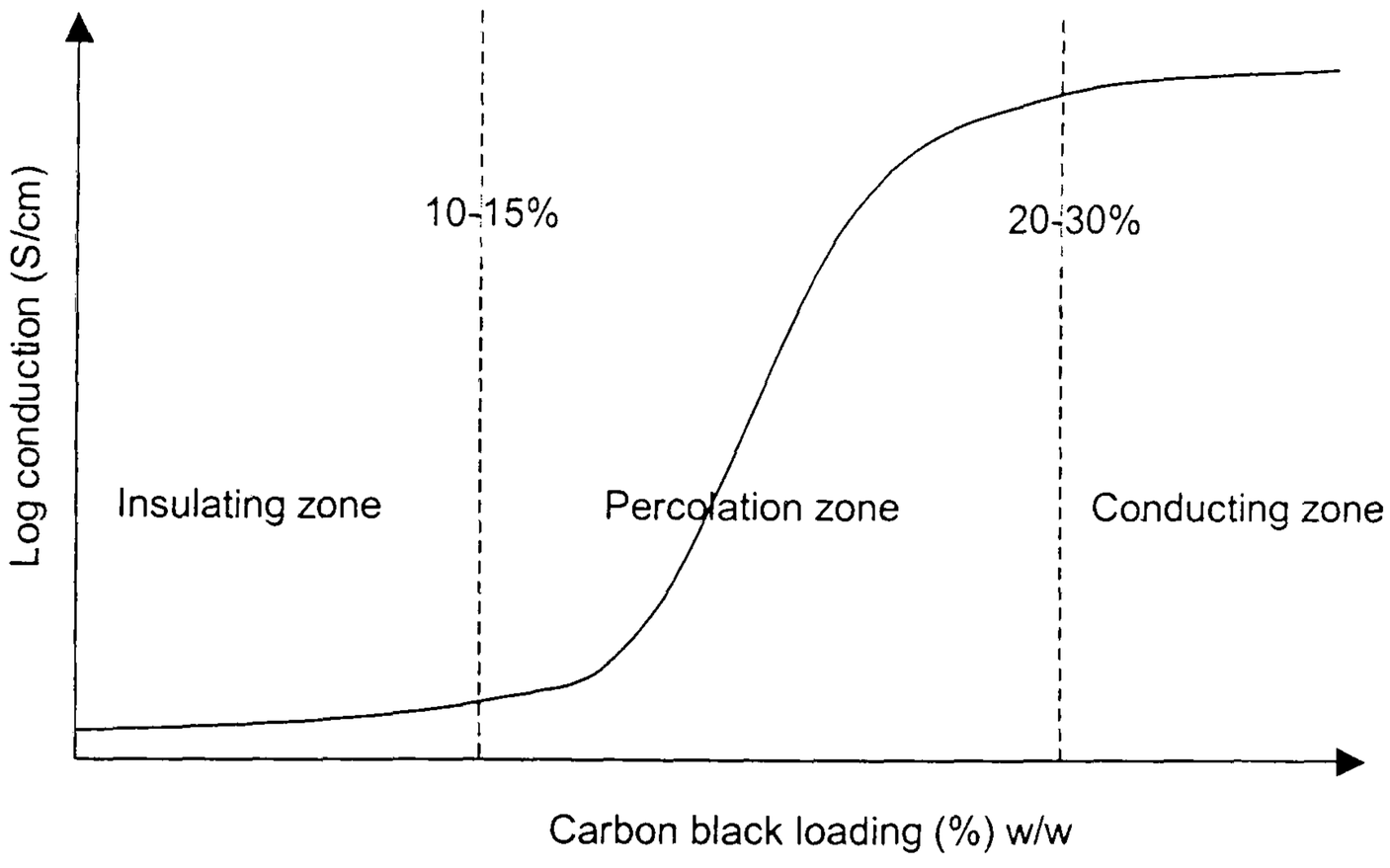

Figure 3.1 Schematic of conductivity against carbon black loading for thermoplastic

An additional possible problem with materials that use carbon as the conductive medium is that at large voltages carbon oxidises to liberate carbon monoxide and dioxide at the anode, Equations 3.1 and 3.2 (Eastwood 1997):

$$C + 2H_2O \rightarrow CO_2 + 4H^+ + 4e^- \qquad E^{\theta}_{red} = 0.207V \qquad \text{Eqn. 3.1}$$

$$C + H_2O \rightarrow CO + 2H^+ + 2e^- \qquad E^{\theta}_{red} = 0.518V \qquad \text{Eqn. 3.2}$$

However, the addition of salt (NaCl) at the anode can prevent this. An additional problem is that in low pH (<4) environments carbon is oxidised, and if there is sufficient loss of carbon (40% percolation) gaps may from in the structure and electrons can no longer pass through the material and conductivity is lost (Nettleton 1996). These problems would also exist with a carbon filled polymer. However, at the voltages used for electro-osmosis this problem is unlikely to be significant.

3.3.4 METALLIC FIBRES

Fibres, metallized fibres or metal-coated fibres can be incorporated into the manufacturing process particularly if the material is formed by needle punching or weaving. Metal-coated fibres have a low electrical conductivity (10^{-6} - 10^{-1} S/cm) and are unsuitable for use in EKGs.

However, the metal and metallized fibres are considered suitable, although their durability under anodic conditions is likely to be poor, unless they are noble metals, see §3.5.2.

3.4 THE EVOLUTION OF ELECTROKINETIC GEOSYNTHETICS

An electrokinetic geosynthetic (EKG) may be defined as "A composite material which may provide filtration, drainage, reinforcement in addition to electrical conduction" (IGS 1996).

The development of new and advanced forms of geosynthetic reinforcement has been brought about by a number of factors including market forces, technical challenges, innovation and better understanding of the fundamental mechanisms of reinforced soil applications (Jones *et al* 1996).

The origins of the EKG began with groundbreaking research undertaken at the University of Newcastle upon Tyne during the early 1990's. The early work began by looking into the effects of combined drainage and reinforcement followed by the concept of making geosynthetics electrically conductive.

Jones *et al* (1996) have reported a series of tests to study the effects of combining a drainage material with grid reinforcement in a clay soil (Heshmati 1993). The results of this investigation demonstrated that the inclusion of a combined drainage / reinforcement geotextile reduced the effective angle of internal friction (ϕ') of the soil but caused a major increase in the effective cohesion (c'). Interestingly, Heshmati (1993) found that the materials providing drainage and reinforcement used separately produced greater improvement that the same materials providing combined drainage and reinforcement. The explanation for this unexpected result being the development of a plane of weakness at the interface of the two materials. The implication of this being that it is an essential requirement when combining the functions of drainage and reinforcement for the materials to be made integral. This finding has also been confirmed by Cunningham (1995).

Jones *et al* (1996) introduced the concept of an electrically conductive geosynthetic material (EKG) and defined them as a range of geosynthetics, which, in addition to providing filtration, drainage and reinforcement can be enhanced by electrokinetic techniques for the transport of water and chemical species within fine grained low permeability soils, which are otherwise difficult or impossible to deal with. In addition transivity, sorption, wicking and hydrophobic tendencies may also be incorporated in the geosynthetic to enhance other properties. It is suggested that the EKG can take the form of a single material which is electrically conductive, or a composite material, in which at least one element is electrically conductive. They can be of the same basic form as present day filter, drainage, separator and reinforcement materials, but offer sufficient electrical conduction to allow the application of electrokinetic techniques. Jones *et al* (1996) undertook a series of laboratory studies to evaluate the use of conductive geotextiles as electrodes in electro-osmotic consolidation and

reinforced soil. The types of geosynthetics used included needle punched geotextiles with a 1mm diameter copper wire inserted into the geotextile to make it electrically conductive, conductive fibre (carbon) needle punched material and modified polyester reinforcing tape (Paraweb®). The latter was made electrically conductive by the addition of a metal stringer aligned parallel to the polyester reinforcing elements. The results of the tests were favourable and indicated that the EKG behaved as well as a conventional copper electrode.

In the reinforced soil tests the EKG electrode was used as an anode, with the cathode formed from a needle punched EKG. The results of pullout tests showed an increase in reinforcement bond of up to 211% and increases in shear strength of up to 200% compared to the values obtained when the geosynthetics were not electrically conductive. Hamir (1997) presents the results of the laboratory tests quoted by Jones *et al* (1996) in their entirety.

The laboratory experiments showed that the EKG electrodes were as good as or better that the copper disk control in the generation of negative porewater pressures. It was also found that the electrical interface resistance for the EKGs was higher than for the copper disk electrode, this was to be expected, as the conducting element of the EKG did not make direct contact with the soil, only indirectly through the pore fluid. EKG electrodes were also found to function as well as copper electrodes in laboratory consolidation trials but with better durability in both normal and reverse polarity electro-osmotic consolidation.

The concepts of the research presented by Heshmati (1993), Hamir (1997), O'Dwyer (1994) and Nettleton (1996) were protected under patent by Jones (1998). This patent was also augmented to covering the additional findings and applications presented in this thesis, as well as additional interim work undertaken at the University of Newcastle upon Tyne by the patent filed by the University of Newcastle (2000).

Nettleton *et al* (1998) continued the work presented by Jones *et al* (1996) and Hamir (1997) and suggested that a band drain type electrode would be the most suitable configuration to fulfil all of the electrode requirements associated with consolidation, bioremediation and moisture control in embankments. They suggested that a band drain can be made to act as a local distributor of electrical current by incorporation of carbon black fillers into the base polymer (see §3.3.2) for either the geotextile filter or the drainage component of the band drain. Due to the electrical current requirements for electrokinetic treatment in commonly encountered soils a stringer was also required to conduct and distribute the bulk of the current through the band drain. The stringer could take the form of a metallic wire coated with a conductive polymer to prevent corrosion due to electrolysis (Nettleton 1996). This statement by Nettleton (1996) is perhaps somewhat misleading in that the coating of the

metallic wire with a conductive polymer will not prevent corrosion (§3.5.2) but will significantly reduce the rate of corrosion of the electrode.

Sandanasamy (1998) published an European Patent relating to a vertical drain for draining fluid from a soil, where the drain comprises an elongate core having one or more channels extending along the length of the core to receive fluid and additionally being electrically conductive along a substantial length of the core. This is essentially an electrically conductive band drain as suggested by Nettleton *et al* (1998) and Nettelton (1996).

Netlon Ltd (1998) have filed a patent relating to an electrically conductive band drain which was produced in collaboration with the University of Newcastle upon Tyne and is the EKG type that has been employed in all field trials related to this thesis. This type of EKG is discussed in §3.5.

Abiera *et al* (1999a & b) produced an electro-conductive PVD (Prefabricated Vertical Drain) through the insertion of 2mm diameter copper rods into a conventional prefabricated geosynthetic drain. The PVD itself consisted of a porous geotextile filter wrapped around a plastic drainage core. Other electrode types produced during their research were:

- 12 copper rods inserted into a conventional PVD
- 4 copper rods inserted into a conventional PVD
- Conventional PVD coated with electro-conductive paste
- Conventional PVD wrapped with carbon fibres

These electro-conductive PVDs were then used in consolidation experiments and it was found that for the same overburden load a faster rate of settlement was achieved using electro-conductive drains than when using a non-electro conductive drain with the same properties (Abiera *et al* 1999b).

In terms of electrode performance it was found that the PVD wrapped in carbon fibres produced more settlement at a faster rate. It is also suggested by Abiera *et al* (1999a) that as carbon was inert to electrolytic reactions, it prevented introduction of additional chemical species that would have complicated the electro-chemistry of the process, and that the copper electrodes were oxidised which caused corrosion of the electrode especially at the anode.

The Author's interpretation of these findings is that as the PVD was wrapped with carbon fibre, and there would be intimate contact between the carbon fibres and the soil, the interface resistance was less for this electrode type than any other thus giving a greater voltage drop over the soil itself. This would result in a more rapid removal of water from the soil giving a greater overall settlement and at a greater rate, as observed by Abiera *et al* (1999a). Again, the statements regarding the degradation of carbon are erroneous as discussed in §3.5.2 although it is correct that copper wire would degrade at a greater rate.

The field application of EKGs has been reported by Pugh *et al* (2000), Pugh (2000) and Jones & Pugh (2001) and in this thesis. The results presented demonstrate that EKG can

lead to improvements beyond those that can be achieved by conventional geosynthetics alone. The EKG used in these field applications is the one that is protected by the now Tensar International Ltd. patent (Netlon Ltd 1998) based upon the original Nettleton (1996) concept.

3.5 THE NETLON ELECTROKINETIC GEOSYNTHETIC

This electrically conductive band drain was originally developed under EPSRC Contract No. GR/K20590 (Nettleton 1996). The form of the band drain developed consisted of an electrically conductive geonet core surrounded by a thermally bonded non-woven filter fabric. The specific design has been patented by Netlon Limited under Patent application GB 2327686 A (Netlon Ltd 1998).

3.5.1 THE NETLON EKG CONSTRUCTION

The core of the EKG consists of a geonet construction manufactured using the counter-rotating die method as shown in Figure 3.2, utilising a stationary outer die (Mercer 1987).

The geonet was extruded from Cabot Cabelec® 3892 polymer, which is a specifically formulated conductive compound based upon conductive carbon black dispersed in a modified high density polyethylene resin (CABOT 1997) i.e. a carbon filled polymer (see §3.3.2). The polymer is specifically designed for extrusion applications, and was originally developed for the minimisation of electrostatic discharge hazards in electrostatic sensitive environments. The material properties for Cabelec® 3892 are given in Table 3.2. The extrusion process consisted of keeping the outer die-head stationary and rotating the inner die-head, such that the geomesh produced consisted of horizontal ribs intersected by diagonal ribs. At the centre of alternate horizontal ribs were located monofilament wires to act as current distribution stringers. The reason for these stringers is that the electrical conductivity of wire is significantly higher than that of the conductive polymer and as such gives more efficient distribution of current through the length of the EKG. If the stringer were not included then the electrical current would take the path of least resistance and the majority of the current would be passed where the EKG enters the conductive medium to be treated, resulting in high localised current densities, causing accelerated degradation in this region. A schematic of the drain is presented in Figure 3.3.

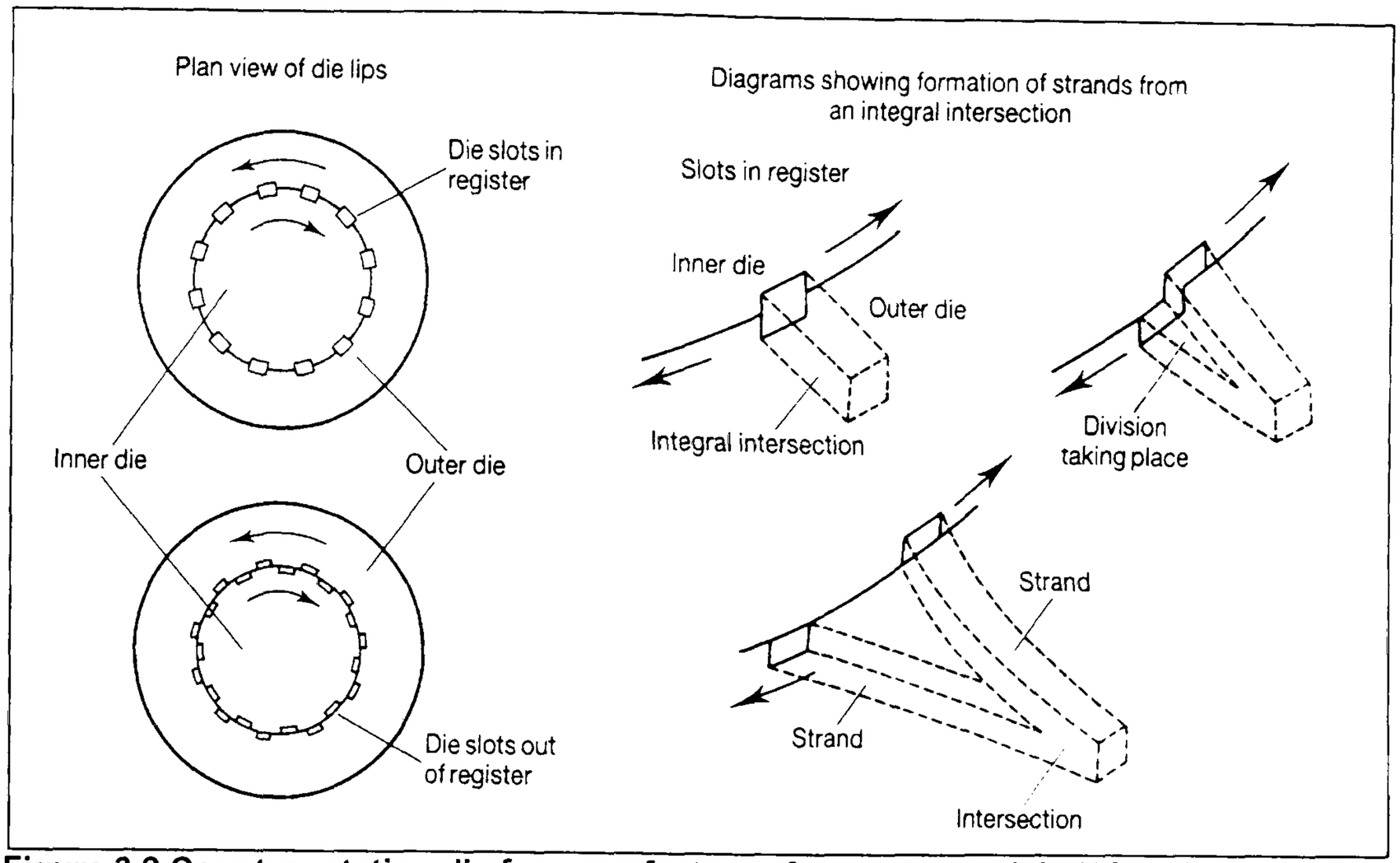

Figure 3.2 Counter-rotating die for manufacture of geonet materials (After Mercer 1987)

The core of the drain may, if required, be wrapped with a non-woven filtration fabric as shown in Figure 3.3; Terram 1000 was used for commercial reasons. The use of this filter effectively makes the electrode an open electrode, see §2.7.5.6 and as such negative porewater pressures cannot be generated. However, in this configuration the electrode is suited for the flushing or purging of porewater if no recharge occurs at the anode.

Table 3.2 Physical properties of Cabelec® 3892 (After CABOT 1997)

PROPERTY	TEST METHOD	UNITS	VALUE
Density @ 23°C	ISO R1183	kg/m^3	1063
Volume resistivity	CABOT - D007B	Ω cm	$4*10^2$
Surface resistivity	CABOT - D042C	Ω/sq	10^3
Tensile strength at break	ISO 527	MPa	18
Tensile strength at yield	ISO 527	MPa	25
Elongation at break	ISO 527	%	160
Surface resistivity *	CABOT -D042D	Ω/sq	$5x10^2$

*Note: * Typical value for CABELEC® 3892 obtained on 0.4mm- thick extruded tape.*

3.5.2 ELECTRODE DURABILITY

As discussed in §2.7.5.5 electrochemical reactions take place during electrokinetic treatment of soil which result in chemical reactions taking place at the anode and cathode. The anodic reactions result in the consumption of the anode material giving the anode a finite life. The durability / service life of the anode is dependant upon the material that is used for its

manufacture. Table 3.3 presents typical corrosion rates for three commonly used anodic materials. The apparently low consumption rate of carbon quoted appears to be as a result of its low molecular mass and the requirement of $4e^-$ for the oxidation of each carbon atom (Eastwood 1997), i.e. more electric current is passed per degradation of each atom.

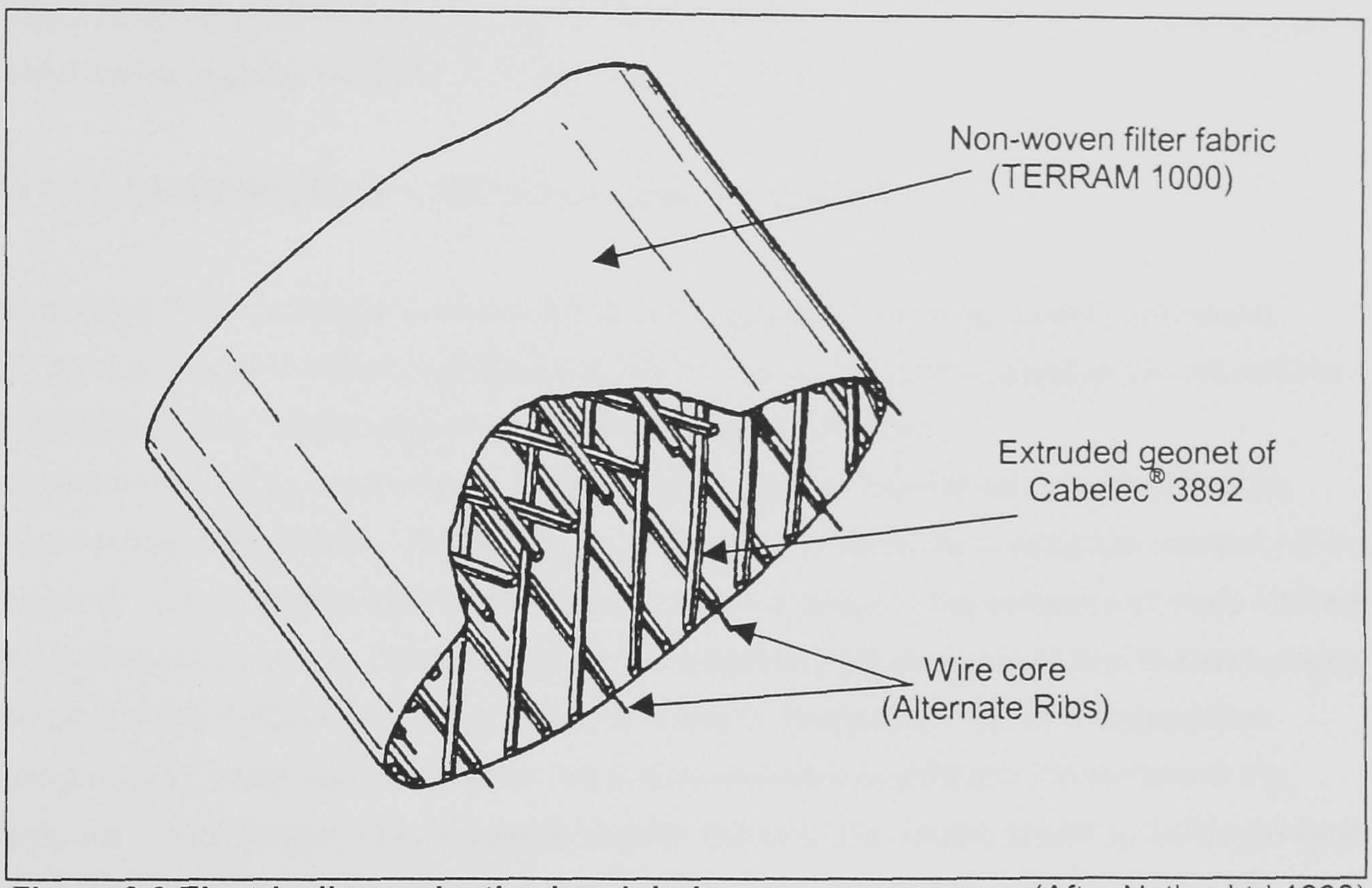

Figure 3.3 Electrically conductive band drain (After Netlon Ltd 1998)

Table 3.3 Corrosion rates for common anodic materials (Eastwood 1997)

Anode Material	Atomic Mass	Degradation reaction	No. Of Electrons	Stoichiometric predicted consumption (kg A^{-1} $year^{-1}$)	Typical corrosion rate (kg A^{-1} $year^{-1}$)
Fe	55.85	$Fe \rightarrow Fe^{2+} + 2e^-$	2	9.1	9.0
Al	26.98	$Al \rightarrow Al^{3+} + 3e^-$	3	2.9	4.5
C (graphite)	12.01	$C + 2H_2O \rightarrow CO_2 + 4H^+ + 4e^-$	4	1.0	0.5 - 2.0

The typical corrosion rate of 0.5 kg A^{-1} $year^{-1}$, for the consumption of graphite, is believed to be representative of the degree of corrosion for graphite block electrodes operating at current densities of up to $10Am^{-2}$.

Materials that are more exotic have also found use or have been specifically developed for anode materials. These include the naturally occurring noble metal platinum (Pt), gold (Au), magnetite (iron oxide Fe_3O_4), other metal oxides and the conductive ceramic Ebonex (Atravee 2001). These materials are able to withstand significantly higher current densities with only a negligible, if any, consumption rate. However, these materials are prohibitively

expensive for use in civil engineering applications unless the electrodes are extracted and reused.

Geokinetics of the Netherlands (Geokinetics 2001) have successfully used Ebonex anodes in the commercial application of electroremediation, however, they extracted the electrodes upon completion of treatment for reuse. Extreme care must be taken during the extraction of the Ebonex electrodes due to its brittle, unmaleable nature.

3.5.3 DEGRADATION OF CARBON LOADED POLYMERS

Eastwood (1997) undertook research into the degradation of the Anodeflex impressed current protection system (Reychem Ltd 2001), and as part of this research looked into the degradation of a copper wire coated with a conductive polymer.
When employed as an anode the carbon loaded polymer experiences dissolution of the carbon from the polymer. This results in an increase in the surface electrical resistivity of the polymer due to the decrease in the carbon content and due to the presence of voids forming on a microscopic scale. The dissolution of the carbon from the surface also exposes carbon located more deeply within the polymer structure to dissolution. As such, degradation progresses deeper into the polymer this is demonstrated by pitting in the surface of the polymer. The research also suggests that the failure of the system would occur before even half of the carbon black content was consumed. Once a path has been established to the metallic core of the element degradation takes place within a few hours with the polymeric coating to the core being forced open due to the increase in volume of the core metal as it is oxidised under electrochemical attack. Plate 3.1 shows the cracking of the polymer coating of the EKG in laboratory tests, showing the bursting out of the copper oxide from the core.

3.5.4 DURABILITY OF EKG

During the development of the prototype EKG in the current research the question was posed; how can the EKG be made more durable and what is the best combination of polymer and metallic core for durability? As a result of this four prototype electrodes were produced by Netlon Ltd. with the following characteristics, all to the same configuration as that shown in Figure 3.3.

- Alternate copper wire cores with Cabelec 3892 coating and alternate ribs.
- Alternate copper wire cores with Cabelec 3892 with antioxidant IRGANOX (CIBA 2001) coating and alternate ribs.
- Alternate stainless steel wire cores with Cabelec 3892 coating and alternate ribs.
- Alternate stainless steel wire cores with Cabelec 3892 with antioxidant IRGANOX (CIBA 2001) coating and alternate ribs.

3.5.4.1 Durability Test - Apparatus

In order to determine the durability of each electrode type all were tested simultaneously as shown in Figure 3.4.

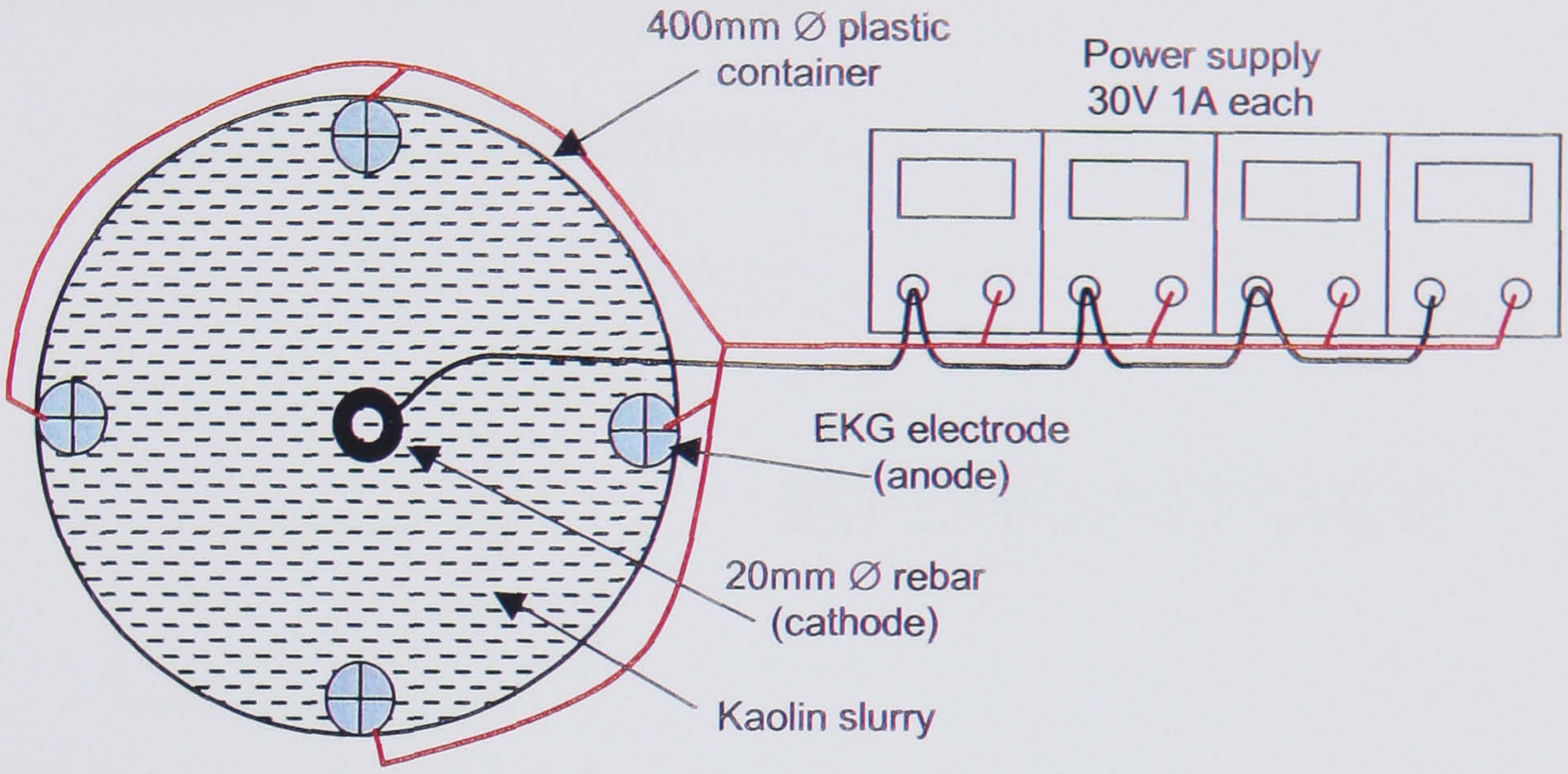

Figure 3.4 Schematic plan of durability test

The test consisted of a 400mm diameter plastic container filled to a depth of approximately 300mm with a high conductivity kaolin slurry. Into the centre of the container and supported with an insulated clamp was placed a 20mm diameter mild steel reinforcing bar. This was made into the cathode. At positions of 90° relative to the central cathode were located the 4 prototype electrodes, as shown in Figure 3.4. These electrodes were cable tied to the plastic container and the holes sealed with silicon sealant. Each electrode was then connected to the positive terminal of a 30V 1A power supply i.e. a total possible output of 30V - 4A. Each power supply was then set to a constant current of 0.5Amps with the voltage control set at maximum such that the voltage would increase up to a maximum of 30V to maintain the constant current. In this way each electrode passed the same amount of current during the test period and hence direct comparison of the durability of the different electrode types could be made. As discussed in §3.5.2 the anodic consumption is dependent upon the quantity of current passed.

3.5.4.2 Durability Test - Results

The power against time curves for each of the electrodes was similar indicating that a similar quantity of current had been passed by each electrode, denoting that the comparison of the results for each electrode was valid. The stainless steel electrodes used slightly more power due to the lower volume conductivity of stainless steel in comparison with copper. The

assessment of the degradation of each of the electrodes was carried out in two ways; a visual inspection of the condition of the electrode and a quantitative measurement of the surface resistivity of the conductive polymer both before and after use.

The surface resistivity of the polymer was assessed using a digital multimeter to measure the resistance between two fixed points as show in Figure 3.5. To avoid errors a total of 10 randomly positioned measurements of the resistivity were taken for each of the four electrodes, with five reading each being taken on solid polymer and metallic cored elements.

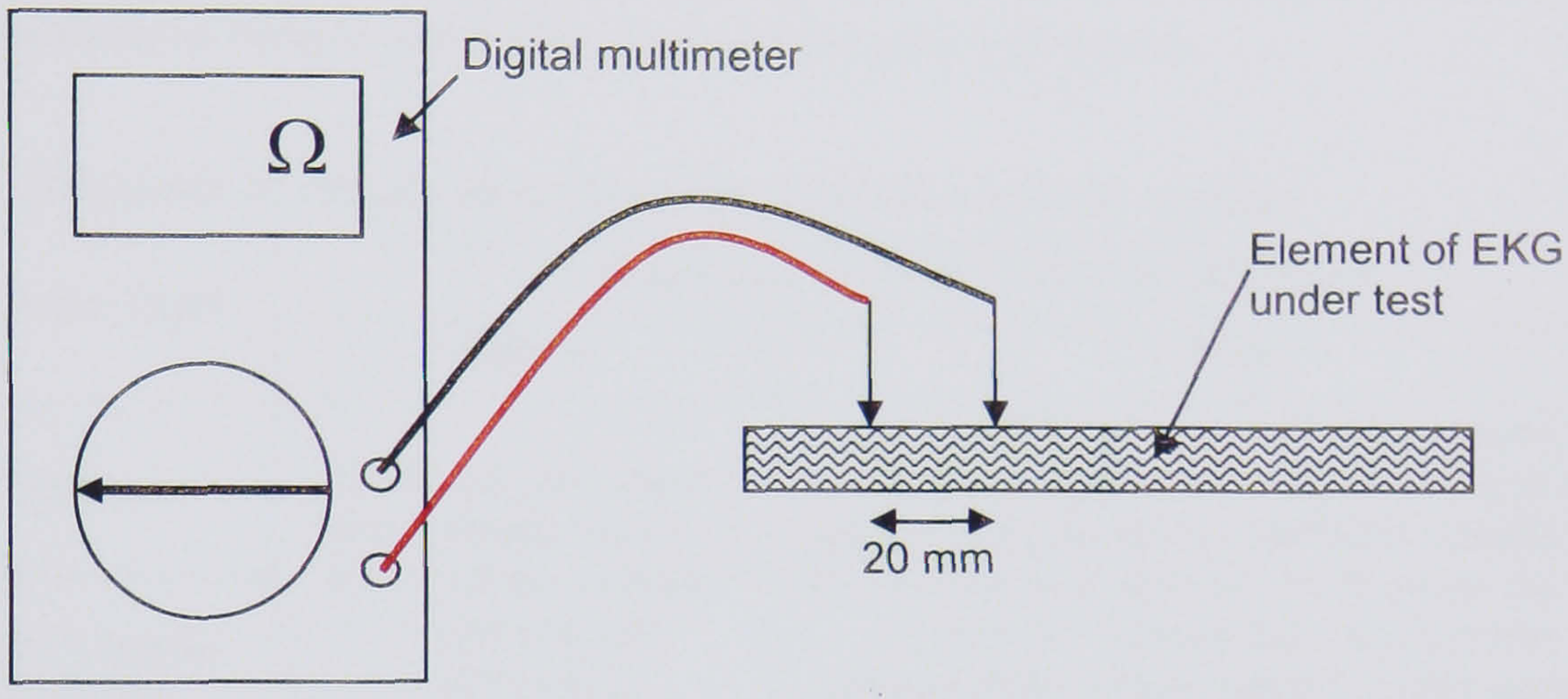

Figure 3.5 Schematic of apparatus used to measure surface resistance

The results of the resistance tests are presented in Table 3.4.

Table 3.4 Results of surface resistance measurements

Electrode Type	Measured surface resistance (Ohms)	
	Before	After
Copper	1.56kΩ	>2MΩ*
Copper + metal deactivator	1.62kΩ	>2MΩ*
Stainless steel	1.49kΩ	>2MΩ*
Stainless steel + metal deactivator	1.53kΩ	>2MΩ*

Maximum resistance measurable by the laboratory multimeter.

The visual inspection of each of the electrodes was carried out under well-illuminated conditions in the laboratory with the aid of a 10X-magnification hand lens. The results of the visual inspection are given in Table 3.5.

3.5.4.3 Durability Test - Conclusions

The results show that the surface resistances of all of the electrode types had increased in agreement with the carbon dissolution mechanism proposed by Eastwood (1997) for the degradation of carbon loaded polymers discussed in §3.5.3. Additionally, the visual

inspection demonstrated that the polymer experiences cracking with the end result that electrochemical degradation of the metallic core takes place and due to oxidation of the metallic core, and associated increase in volume, the crack width is increased and the rate of degradation also increases. The use of stainless steel as opposed to copper appears to make little difference once the polymer coating is breached, although it may give an extra couple of hours of life. The addition of the metal deactivator gave slightly better performance than the polymer with no metal deactivator. The practicality of using a metal deactivator or not would have to be assessed on a commercial basis. The EKG is a major improvement over conventional metallic electrodes, for the same geometry section.

Table 3.5 Results of visual inspection with hand lens of EKG anodes

Electrode Type	Visual description of Anode condition	
	Before	After
Copper	Good condition with bright plastic surface. Some of the metallic cores are not centralised	Dull plastic surface with some hairline cracking and green staining (CuO) and some open cracks revealing corroded metallic core sometimes corroded so much so as not to be present. Cracks tend to be more concentrated where metallic cores were not centralised
Copper + metal deactivator		
Stainless steel	Good condition with bright plastic surface. Some of the metallic cores are not centralised	Dull plastic surface with some hairline cracking and brown staining (FeO) and some open cracks revealing corroded metallic core sometimes corroded so much so as not to be present. Cracks tend to be more concentrated where metallic cores were not centralised
Stainless steel + metal deactivator		

As a result of the durability testing undertaken and the review of degradation mechanisms the Author developed a calculation method for predicting the anticipated serviceability life of EKG in service. The calculation method is presented in Annex A and may be utilised for the approximation of EKG electrode life in any application.

3.5.5 SUGGESTIONS FOR IMPROVEMENT

Based upon the tests carried out at the University of Newcastle and upon the literature review carried out on the durability of conductive polymers the following recommendation are made for the improvement of the Netlon EKG:

- The metallic core should be centralised within the polymer shroud to prevent localised hot spots of high current density that lead to accelerated corrosion and eventual failure of the EKG.
- The thickness of the polymer coating to the metallic core should be increased as much as is practical for the manufacturing process, however, increasing the thickness will

increase the service life of the electrodes but will increase the overall resistance of the system.

- The non-woven filter fabric, when required, would be better situated within the central core of the EKG. In this way the conductive elements of the EKG make direct contact with the soil and decrease the soil/electrode interface resistance. An additional improvement would be to replace the filter fabric with a drainage composite that has in plane flow capabilities.

3.5.6 EKG CONNECTION TECHNOLOGY

The connection of the power distribution cables to the Netlon EKG has been investigated both at the University of Newcastle and at Netlon Ltd. From this research, it has been established that the ideal connection would have the following characteristics:

- Quick and easy to undertake both on site and in the laboratory.
- Achieves a good electrical connection to all of the metallic cores.
- Cheap to manufacture.
- Insulated so that it does not corrode at an accelerated rate compared to the degradation of the EKG.

As a result of these criteria the following connection types were investigated.

Large crimp

A single large crimp connection was tested at Netlon Ltd, Blackburn, which consisted of a large galvanised connector that accepted all of the elements of the EKG, both polymeric and metallic. The connector was attached to the EKG using a hydraulic crimping tool. This connection method was found to be unsatisfactory as the crimp did not always penetrate the conductive polymer coating to the metallic cores and as such did not achieve a good contact with the copper core. This resulted in different resistances in the connection and in practice caused a non-uniform potential difference field and possible accelerated degradation of the elements of the EKG (Lashmar 1999).

Double crimp

The use of two crimps in place of one large one was also tested but was also found to experience the same problem with non-uniformity of connection to the metallic cores of the EKG (Lashmar 1999). The finished connection is shown in Plate 3.2.

Double crimped - stripped EKG

This method was found to be the most efficient in achieving a good, reproducible, connection to the EKG. The method is shown in Figure 3.6. Although this connection method was more time consuming than either of the other methods this additional time cost was outweighed by the quality and reliability of the connection achieved. A completed connection is shown in Plate 3.3.

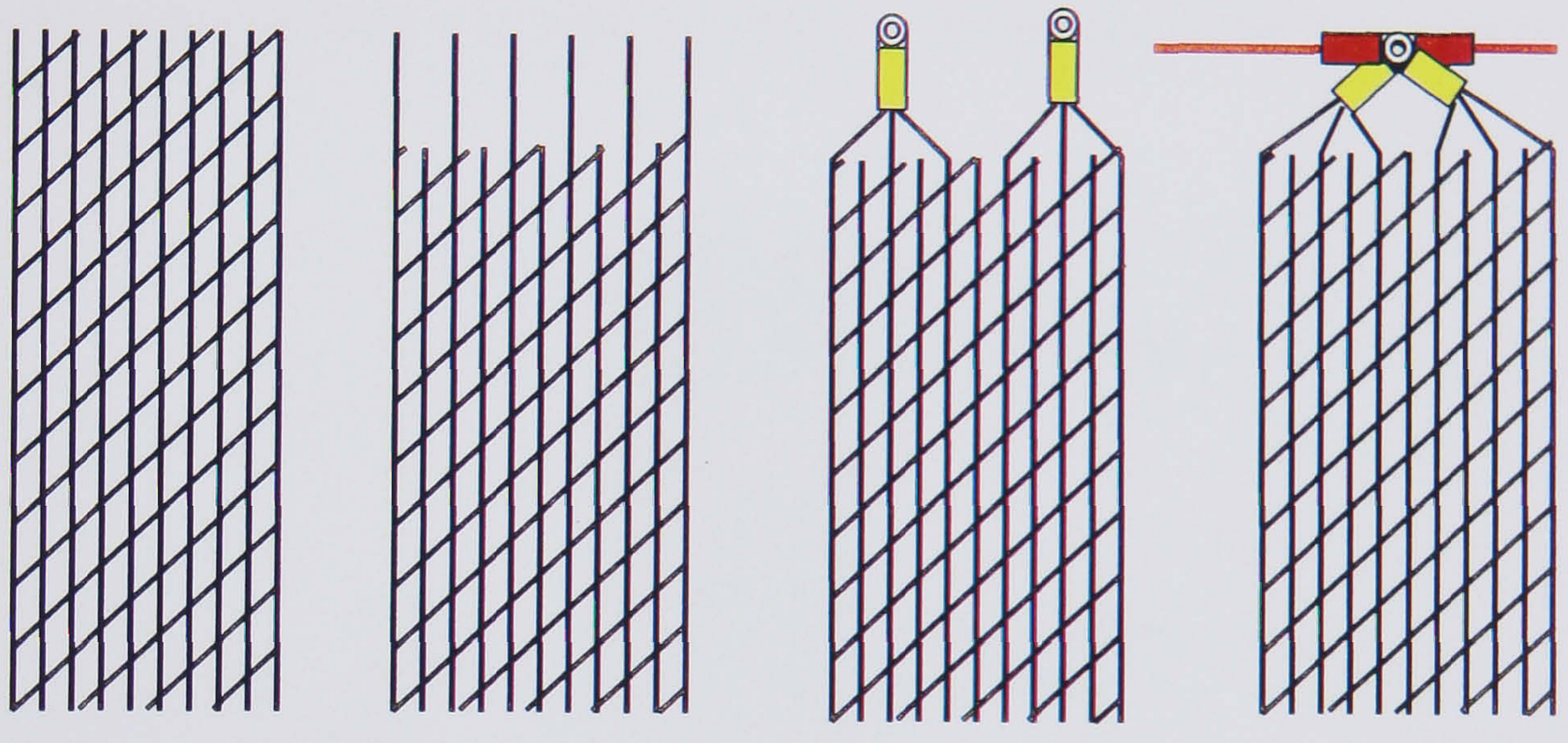

Figure 3.6 Double crimped electrode connection details

A modification to this connection, but based upon the same principle was developed to allow for the use of armoured cable with earth return. The details of this connection are given in Figure 3.7, and shown in Plate 3.4.

3.5.7 THE FUTURE OF EKGs

Science, engineering and technology are constantly in a state of flux and as such it is difficult to predict what the future will have in store for EKG development.

However, it is apparent that one of the next major steps would be the development of a combined drainage, reinforcement and electrically conductive element, possibly along the lines of an electrically conductive Paradrain (Terram Ltd 2000) (see §5.6.2.2) as discussed later on in this thesis, with a sacrificial electrically conductive element.

One aspect of EKG that needs to be addressed is durability. As has been discussed, the EKG in its current form has a finite life due to the degradation of the carbon black in the polymer matrix. However, as materials and knowledge develop it may be possible to develop more electrochemically stable materials at a lower cost that may be used in future EKGs.

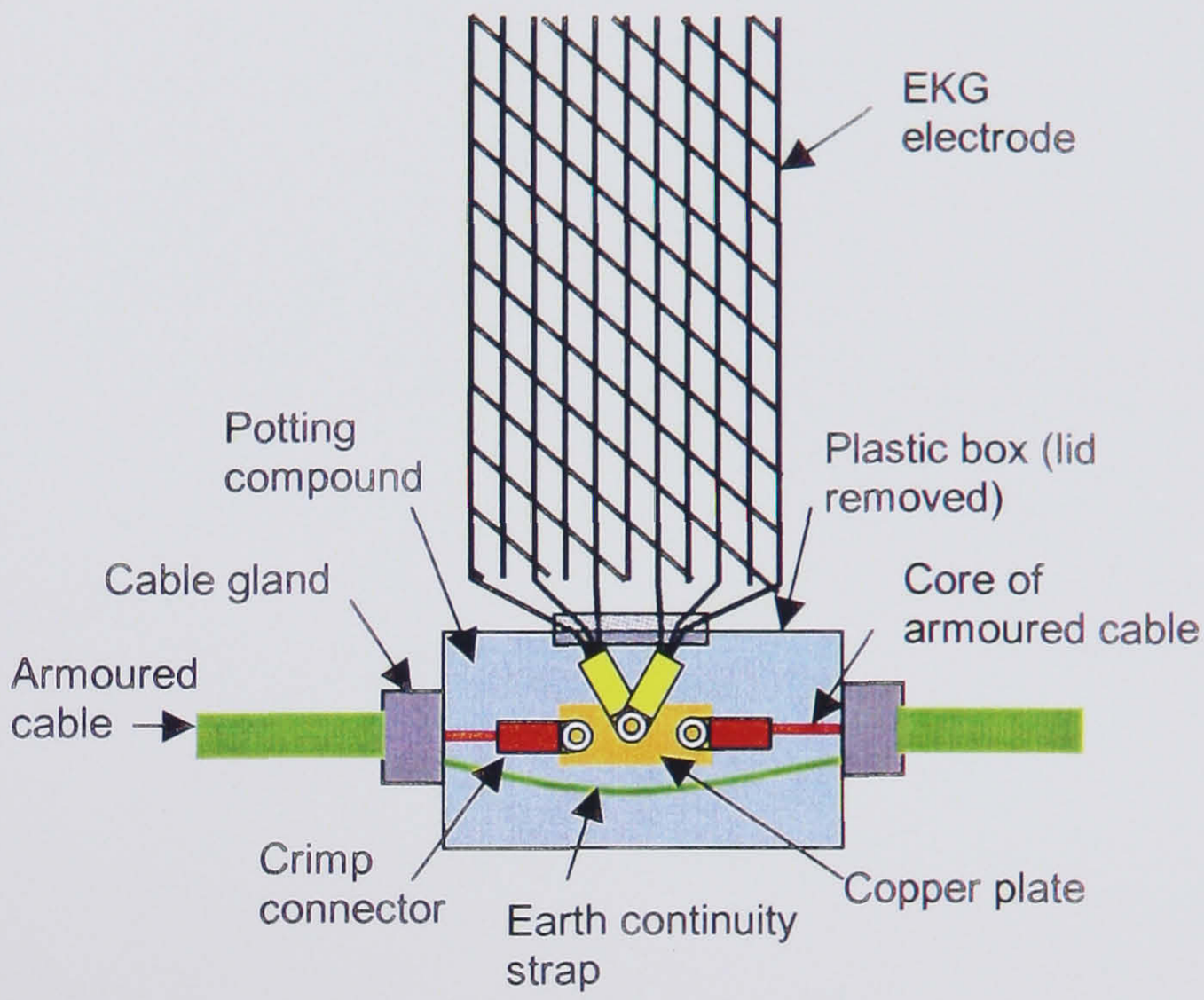

Figure 3.7 Waterproof double crimped electrode connection details with armoured cable (lid removed)

3.6 SYNOPSIS OF CHAPTER 3

This chapter has briefly addressed the history behind the development of modern geosynthetics and has outlined the types of materials that are used for the manufacture of geosynthetics and the products that are produced from these raw materials.

The theme of making geosynthetics electrically conductive has then been introduced through a review of electrically conductive materials that could be used to form geosynthetics. The historical development of Electrokinetic Geosynthetics (EKG) has then been discussed from fundamental studies carried out by Heshmati (1993), O'Dwyer (1994), Cunningham (1995) and Hamir (1997) to the filing of patents in this field by Jones (1998), Netlon Ltd (1998) and University of Newcastle (2000) through to full scale field trials reported by Pugh *et al* (2000), Pugh (2000) and Jones & Pugh (2001). The Netlon EKG has been introduced (Netlon Ltd

1998) and its construction, durability and use in the field discussed. The chapter then concluded with a brief look at the future development of EKG technology.

3.7 CHAPTER 3 REFERENCES

1. Abiera, H.O., Miura, N., Bergado, D.T., & Nomura, T. (1999a) *Effects of using electro-conductive PVD in the consolidation of reconstituted Ariake clay.* Geotechnical Engineering Journal, Vol. 30, No. 2, August, Southeast Asian Geotechnical Society. pp 67-83.
2. Abiera, H.O., Miura, N. & Bergado, D.T. (1999b) *Electro-osmotic consolidation of soft Ariake clay using electro-conductive PVD.* In Eds. Miura, N. & Bergado, D.T. Improvement of Soft Ground; Design, Analysis and Current Research. Balkema, pp 59-73.
3. Andersson, C.H., Eng, K., Zah, W. & Stahl, J.E. (1994) *Warp - Knitted Direct Orientates Structures for Pre-shaped Composites.* In Techtextil - composites, 6th International Techtextil Symposium, Paper 314, June 15-17, Frankfurt, Germany.
4. Atravee (2001) Atravee web site at http://www.members.aol.com/atravee
5. CABOT (1997) *Product Information Sheet - CABELEC 3892.* Cabot Plastics International, Interleuvenlaan 5, 3001 Leuven, Belgium
6. Campbell, I.M. (1994) *Introduction to Synthetic Polymers.* Oxford Science Publication, London, UK. p 213.
7. CIBA (2001) *IRGANOX Antioxidant*, Ciba Speciality Chemicals available at www.cibasc.com
8. Cunningham, J. (1995) *The effects of bonding geosynthetic reinforcement used for drainage and strength in cohesive soil.* Master of Engineering Dissertation, University of Newcastle upon Tyne, U.K.
9. Eastwood, B.J. (1997) *A Fundamental Study of the Electrochemical Failure Mechanisms of a Novel Impressed Current Cathodic Protection System.* Doctor of Philosophy Thesis, Department of Chemistry, University of Newcastle upon Tyne, U.K. p 182.
10. FHWA (1985) *Geotextiles Engineering Manual.* US Department of Transport, Federal Highway Administration, National Highways Institute, Washington D.C. Contract No. DTFH61-83-C-00150.
11. Geokinetics (2001) Geokinetics web site at http://www.geokinetics.com/
12. Hamir, R. (1997) *Some aspects and applications of electrically conductive geosynthetic materials.* Doctor of Philosophy Thesis, Geotechnical Group, University of Newcastle upon Tyne, U.K. p 225.
13. Hamir, R., Jones C.J.F.P., & Clarke, B.G. (2001) *Electrically conductive geosynthetics for consolidation and reinforced soil.* Geotextiles and Geomembranes, Vol. 19, No. 8, Elsevier, pp. 455-483.
14. Heshmati, S. (1993) *The action of geotextiles in providing combined drainage and reinforcement to cohesive soils.* Doctor of Philosophy Thesis, Geotechnical Group, University of Newcastle upon Tyne, U.K. p 225.

15. IGS (1996) *Recommended descriptions of geosynthetics, functions, geosynthetics terminology, mathematical and graphical symbols.* 3rd Edition, International Geosynthetic Society (IGS) Secretariat, 226 Sitton Road, Easley, South Carolina 29642, USA.
16. John, N.W.M. (1987) *Geotextiles.* Blackie, Glasgow, U.K. p 347.
17. Jones, C.J.F.P., Fakher, A., Hamir, R. & Nettleton, I.M. (1996) *Geosynthetic materials with improved reinforcement capabilities.* Proceedings of the International Symposium on Earth Reinforcement, Fukuoka Kyushu, Japan, 12-14 November, Vol. 2, pp 865-883.
18. Jones, C.J.F.P. (1998) *Improvements relating to geosynthetics.* U.K. Patent GB 2301311B.
19. Jones, C.J.F.P. & Pugh, R.C. (2001) *A full-scale field trial of electrokinetically enhanced cohesive reinforced soil using electrically conductive geosynthetics.* In Ochiai *et al* (eds) Landmarks in earth reinforcement, IS-Kyushu, Japan, Swets & Zeitlingr, pp. 219- 223.
20. Koerner, R.M. (1990) *Designing with Geosynthetics.* Prentice Hall, Englewood Cliffs, New Jersey, USA. p 424.
21. Lashmar, J. (1999) *Personal communication.*
22. Mercer, F.W. (1987) *Lecture to Royal Society*, London.
23. Netlon Ltd (1998) *Electrically - Conducting Element,* U.K. Patent Application GB 2327686A.
24. Nettleton, I.M. (1996) *Electro-Bioremediation.* 1st year interim report for EPSRC Contract No. GR/K20590. Geotechnical Group, University of Newcastle upon Tyne, U.K. p 70.
25. Nettleton, I.M., Jones, C.J.F.P., Clarke, B.G., & Hamir, R. (1998) *Electrokinetic geosynthetics and their applications.* Proceedings of the 6th International Conference on Geosynthetics, 25 - 29 March, Atlanta, Georgia, USA, Vol. 2, pp 871-876.
26. O'Dwyer, S. (1994) *Adsorption of metals using a geosynthetic.* Master of Science Dissertation, Geotechnical Group, University of Newcastle upon Tyne, U.K., p 99.
27. Pugh, R.C. (2000) *A full scale field trial of electrokinetically enhanced cohesive reinforced soil using electrokinetic geosynthetics.* Winning paper in the IGS-U.K. Chapter Student Paper competition, September.
28. Pugh, R.C., Clarke, B.G., & Jones, C.J.F.P. (2000) *An electro-osmotic consolidation trial using electrokinetic geosynthetics.* Proceedings of the 4th International Conference on Ground Improvement Geosystems, Helsinki, Finland, June 7-9, Vol. 2, pp. 533-540.
29. Reychem Ltd (2001) *Anodeflex current impressed cathodic protection system.* Available at www.reychem.com
30. Sandanasamy, R.D. (1998) *A Vertical Drain.* European Patent Application EP - 0870875A2, Application No. 981038458, Filed 4-3-98, Published 14-10-98.
31. Terram Ltd (2000) Paradrain website: www.paradrain.com
32. University of Newcastle (2000) *An electrokinetic geosynthetic structure.* International Patent Application PCT/GB99/04263.

33. Van Santvoort, G.P.T.M. (1994) *Geotextiles and Geomembranes in Civil Engineering.* Revised edition, A.A. Balkema, Rotterdam. p 595.
34. Van Vlack, L.H. (1982) *Materials for Engineering: Concepts and Applications.* Addison-Wesley Publishing Group, p 604.
35. Wright, W.M. & Woodham, G.W. (1989) *Conductive Plastics.* In 3rd Ed. Margolis, J.M. (ed.) Conductive polymers and plastics. Chapman & Hall, London, U.K., pp 119-170.

3.8 CHAPTER 3 PLATES

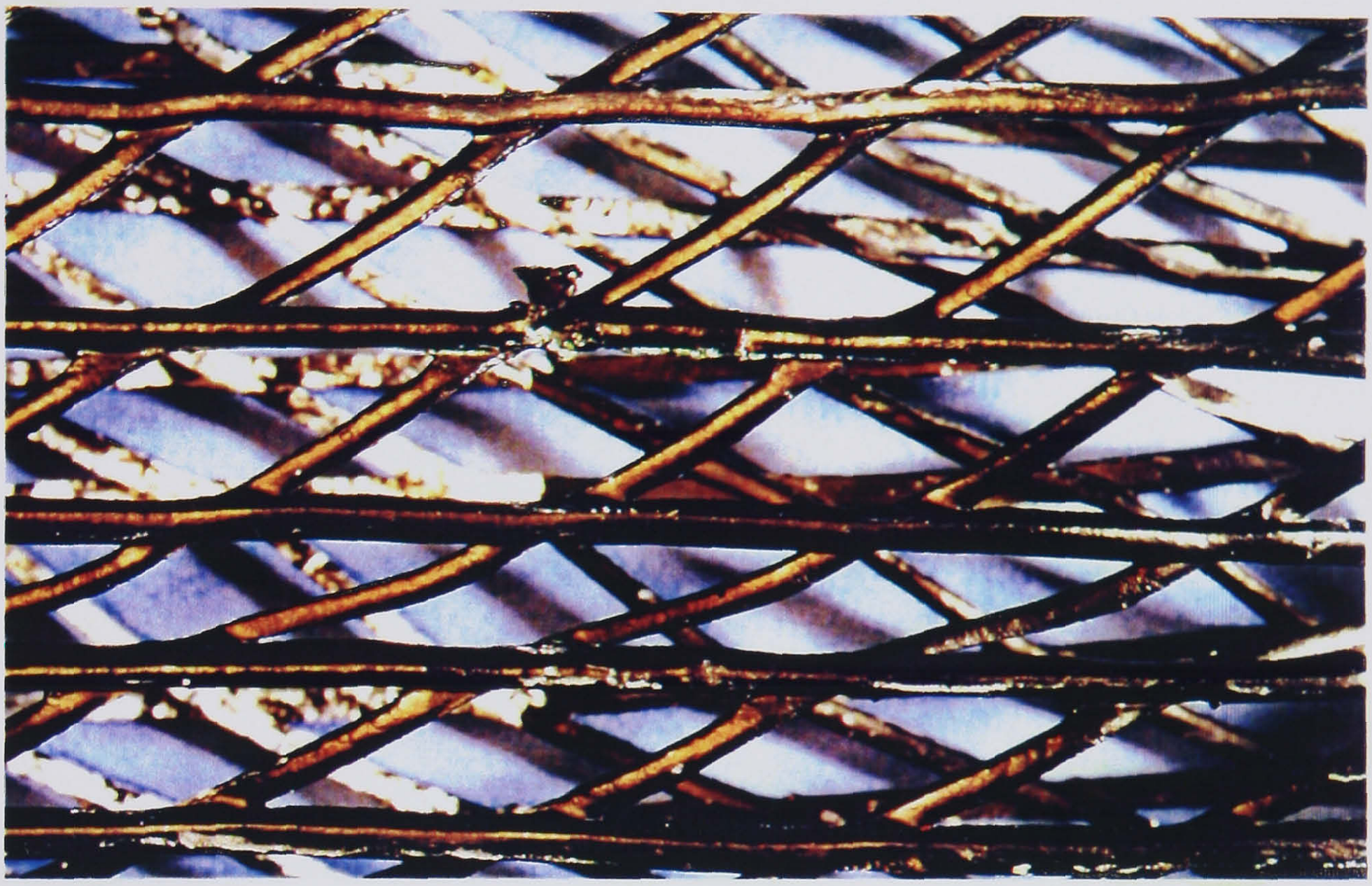

Plate 3.1 Electro-chemical cracking of polymeric coating on EKG

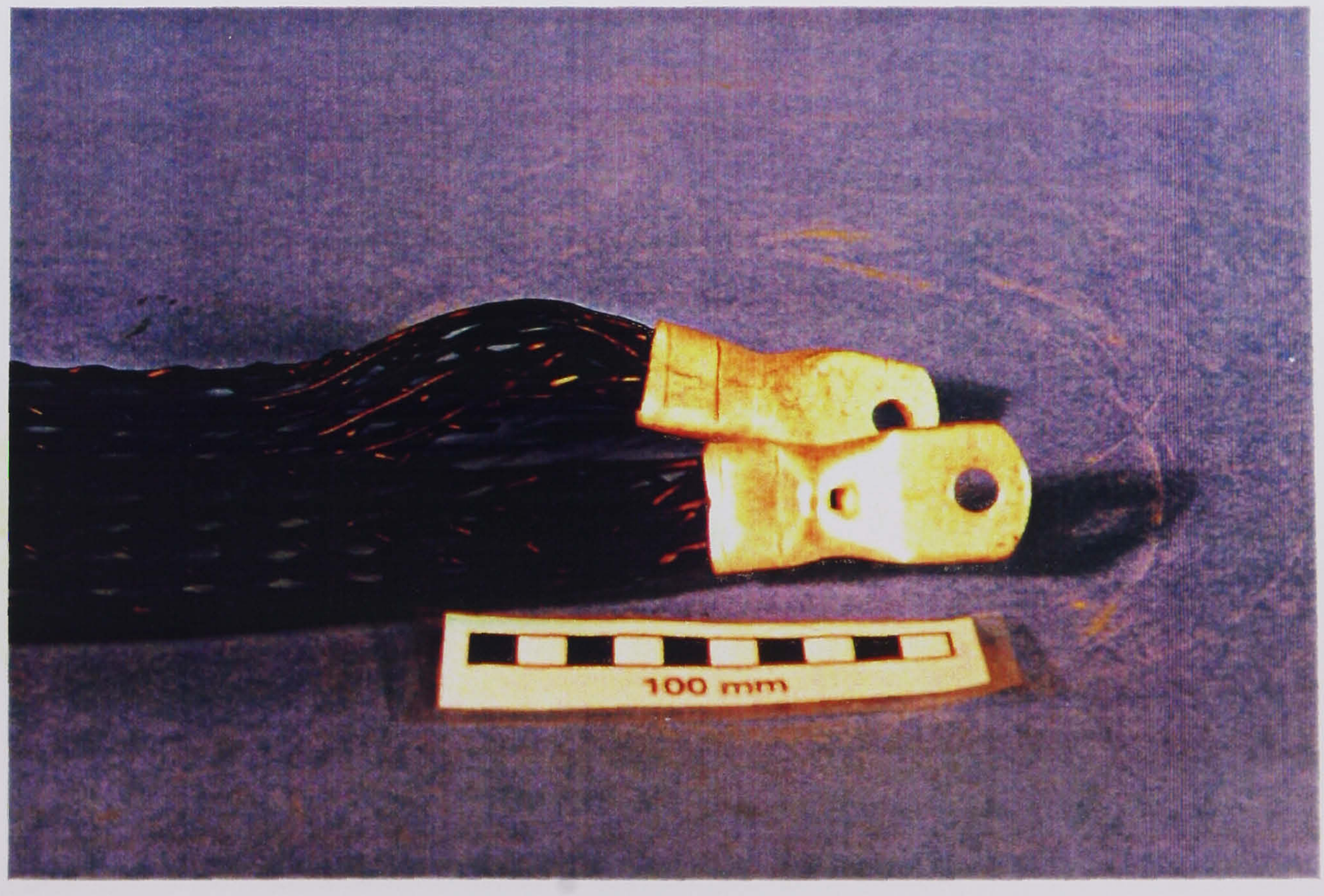

Plate 3.2 Large double crimp connector

Plate 3.3 Double crimped stripped connection

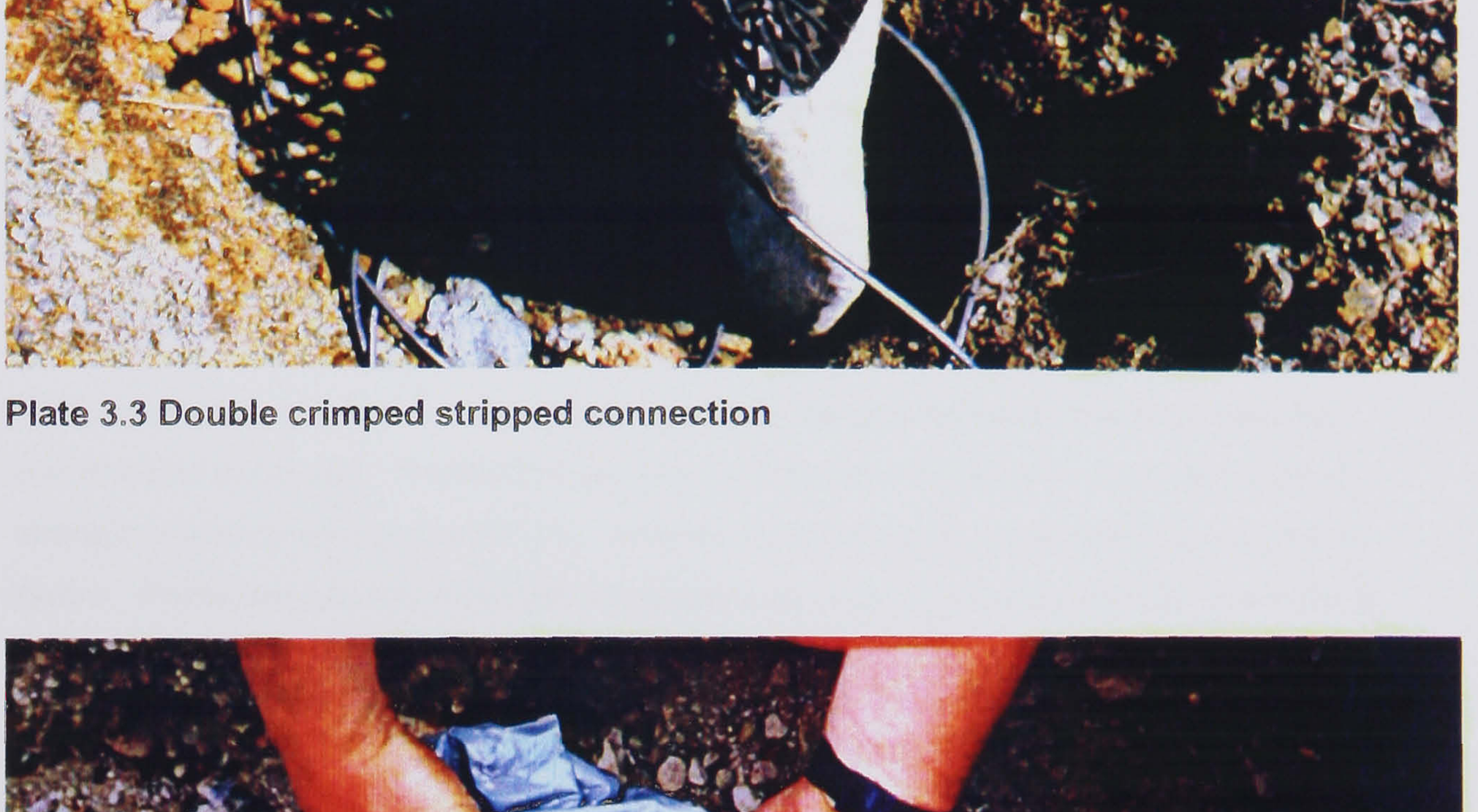

Plate 3.4 Armoured cable double crimped stripped connection

CHAPTER 4

GROUND IMPROVEMENT - ELECTRO-OSMOTIC CONSOLIDATION

4.1 GROUND IMPROVEMENT - INTRODUCTION

The definition of what ground improvement is and why it has come about as a technique is perhaps summed up best by the following two quotations:

"*Due to the shortage of developable land and the ever-increasing size of the world population we, as engineers, are often forced to develop on land which is initially inadequate for the loads that are proposed to be placed upon it, without resorting to elaborate deep foundations. Ground improvement techniques are the methods which engineers have to make originally unacceptable ground fit for its purpose.*" (Mitchell 1970).

"*Ground improvement of a soil involves improving the geotechnical characteristics for construction purposes. Problems relating to construction in soil arise from their lack of strength which manifests itself in their deformation or in some exceptional cases ground failure. Problems are also associated with water in soils. Hence ground improvement is primarily concerned with enhancing a soils strength or reducing or excluding the water content.*" (Bell 1993b).

4.1.1 GROUND IMPROVEMENT TECHNIQUES - A REVIEW

Ground Improvement techniques can essentially be divided into two groups dependant upon soil type (Mitchell 1970). Those acceptable primarily for treatment of cohesionless soils and those used for treatment of fine grained, cohesive soils.

Loose cohesionless soils generally do not prove serious problems in terms of strength under static loading, but may be hazardous from the standpoint of liquefaction under seismic or other types of dynamic loading (Mitchell 1970). In contrast, inadequate strength is more often the main problem encountered when dealing with soft clay.

A further subdivision may also be made depending upon whether the treatment method is applied in situ or ex situ. As it is envisaged that electro-osmosis, for consolidation purposes, would be applied in-situ only in situ ground improvement techniques are reviewed in this chapter.

Cohesionless soils may be treated in situ by (after Mitchell 1970):

- Blasting - Explosive compaction
- Cement stabilization
- Compaction piles
- Dynamic compaction
- Grouting and compaction grouting
- Vibrocompaction
- Vibroreplacement

Cohesive soils may be treated in situ by:

- Additives
- Compaction
- Compaction grouting
- Concrete columns
- Dynamic compaction
- Electro-osmosis
- Jet grouting
- Lime and lime/cement columns
- Lime piles
- Precompression with or without wick/sand/band drains
- Thermal treatment
- Vacuum preloading with drains
- Vibroreplacement - stone columns

The applicability of these methods is best demonstrated by relating them to the usual range of soil particle size to which they are applied, as shown in Figure 4.1.

No further discussion will be given relating to ground improvement techniques for granular soils, to which electro-osmosis is not applicable. The reader is referred to Bell (1993b), Bergado *et al* (1994) and Moseley (1993) for further information and discussion on these techniques.

4.1.2 GROUND IMPROVEMENT TECHNIQUES FOR COHESIVE SOILS

The ground improvement techniques that are applicable to cohesive soils have been outlined in §4.1.1 and are given in Figure 4.1. These are direct alternatives to electro-osmotic consolidation and will now be discussed based upon the classification of the type of treatment method.

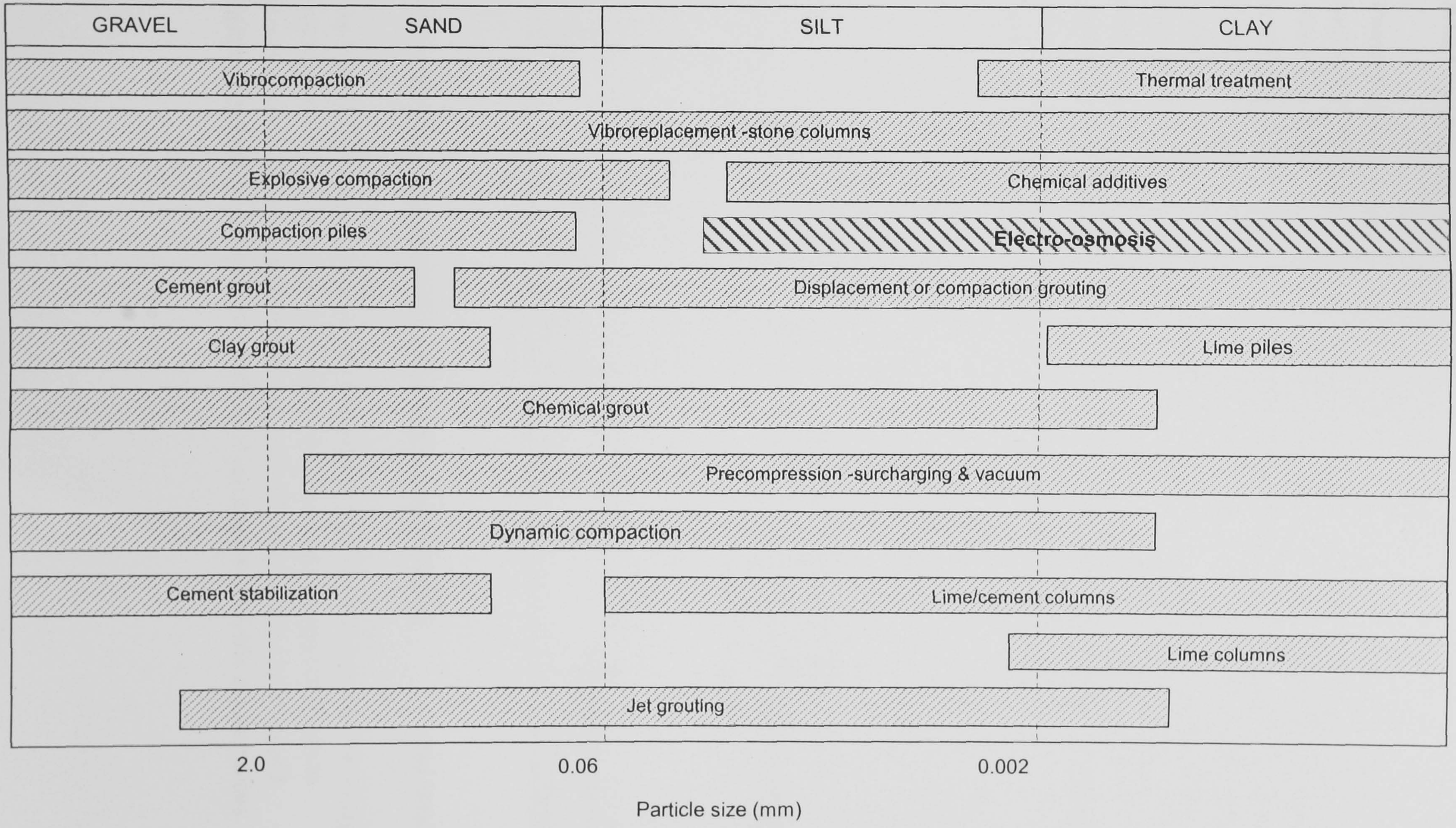

Figure 4.1 Applicability of different in situ ground improvement techniques related to soil particle size (After Mitchell 1970, Bell 1993b & Moseley 1993)

4.1.2.1 Precompression

Precompression involves compressing the soil under an applied pressure prior to placing a load (Aldrich 1965). As such it has proved an effective means of enhancing the support afforded to shallow foundations and is commonly used for controlling the magnitude of post construction settlements. The soils that are best suited to improvement by precompression include compressible silts, saturated soft clays, organic clays and peats. Precompression is normally brought about by preloading, which involves the placement and removal of a dead load (Johnson 1970). This compresses the foundation soils inducing settlement prior to construction. If the load intensity from the preload exceeds the pressure from the final structural load then the process is called surcharging. Figure 4.2 demonstrates the concept of precompression and the influence of a surcharge load upon the rate at which consolidation occurs.

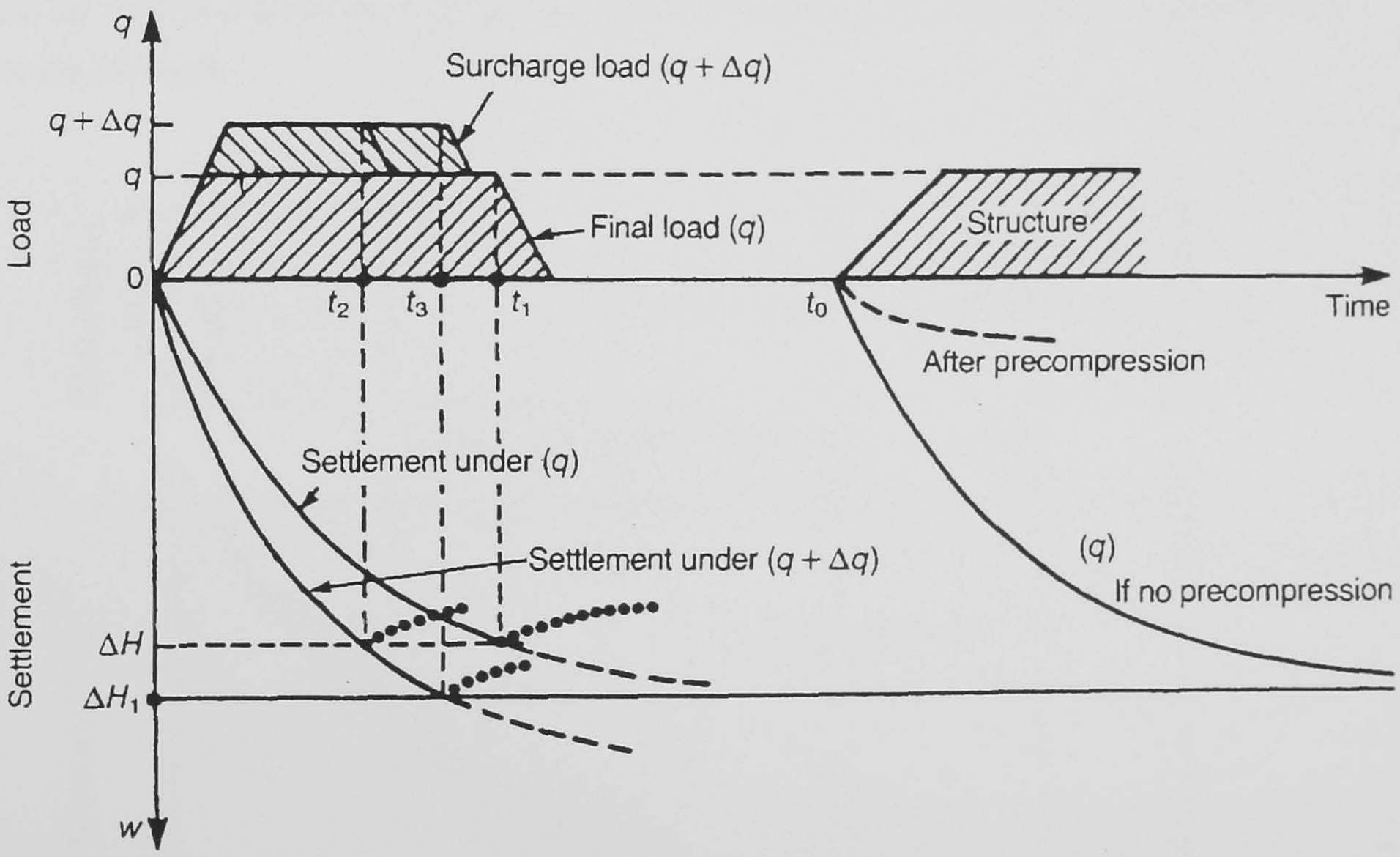

Figure 4.2 Principle of precompression using surcharge loading (Bell 1993b)

The installation of vertical drains beneath the precompression load reduces the time required to bring about primary consolidation through a reduction in the drainage path length as shown in Figure 4.3 and by the results of a full-scale field trial presented by Eriksson & Ekström (1983) where an overburden of 37kN/m^2 was applied with drains at 1.4m centres.

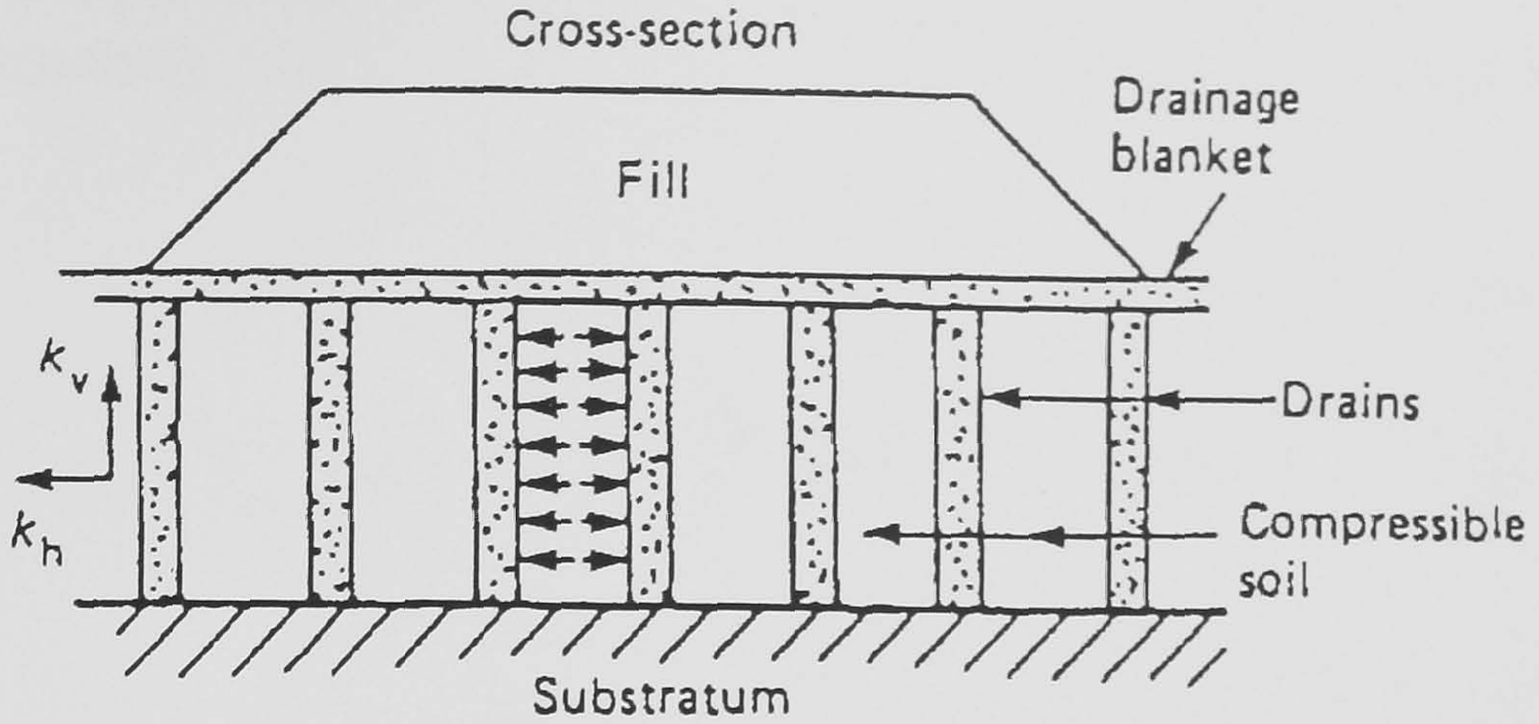

Figure 4.3 Vertical drains beneath surcharging (Bell 1993b)

The results are presented in Figure 4.4, which demonstrate that the consolidation in the areas with vertical drains was complete after approximately 27 months, whereas the areas with no vertical drains would experience the same amount of settlement in approximately double this time.

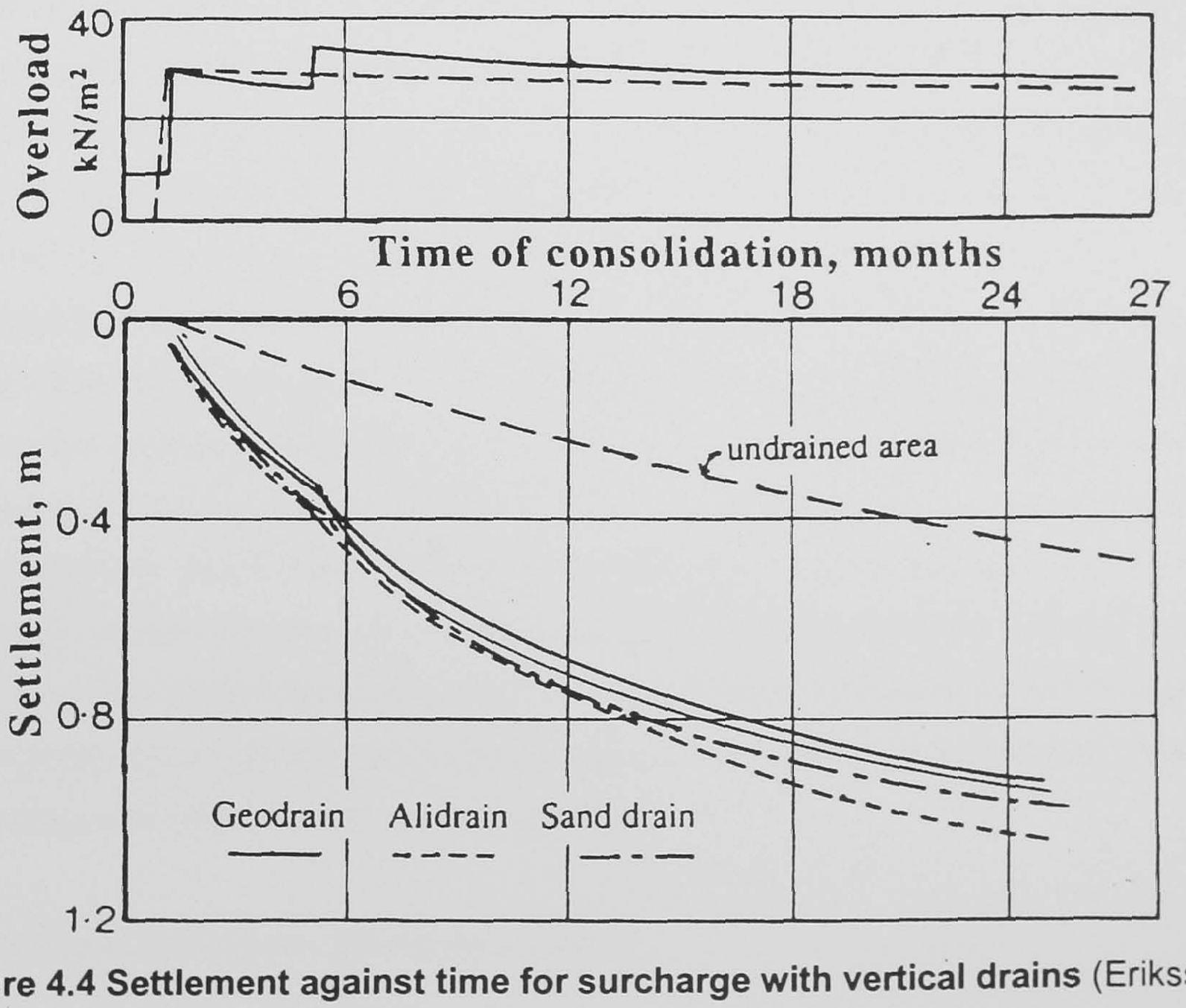

Figure 4.4 Settlement against time for surcharge with vertical drains (Eriksson & Ekström 1983)

4.1.2.2 Vacuum Preloading

The application of a preload to a soil may also be brought about through the application of a vacuum to the soil mass by pumping air from beneath an airtight impervious membrane

placed over the ground surface and sealed along its edges. The method was first successfully applied in a full-scale field trial undertaken by the Swedish Geotechnical Institute (SGI 1949). A schematic of a vacuum preloading installation is presented in Figure 4.5.

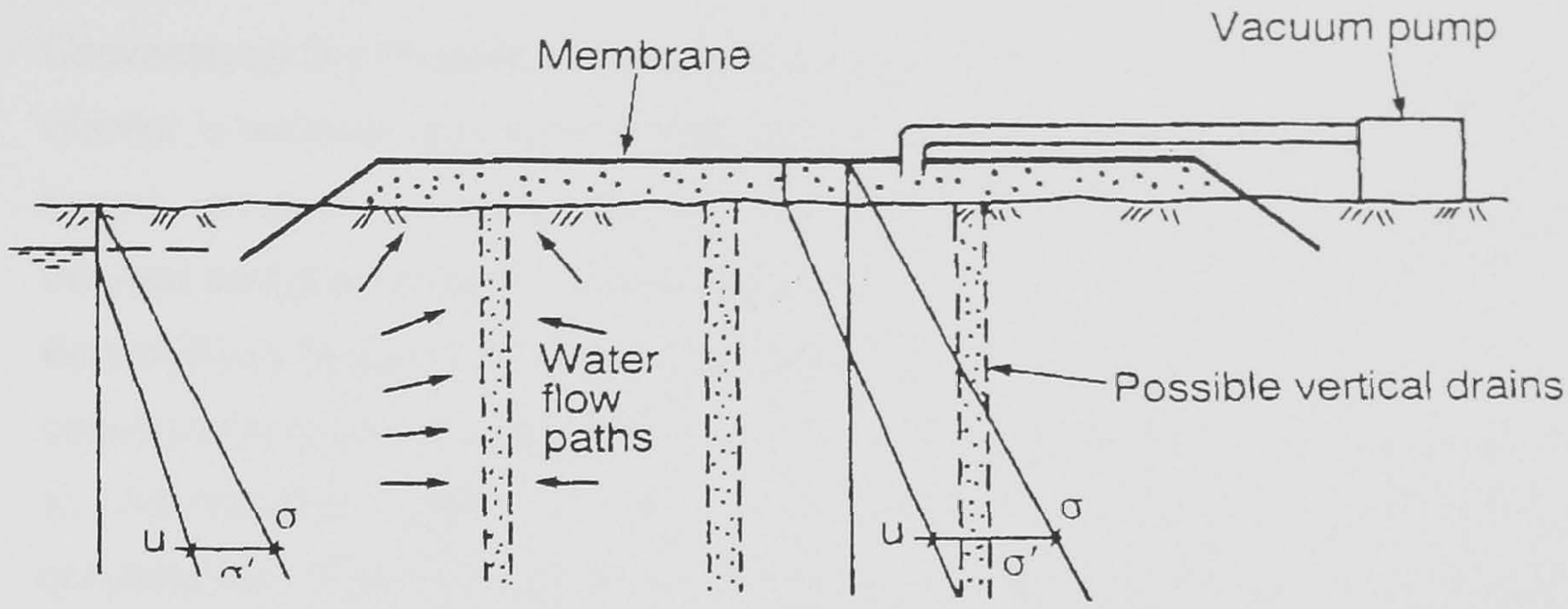

Figure 4.5 Vacuum preloading (Bell 1993b)

The "negative" pressure created by the application of the vacuum causes the water in the pores of the soil to move towards the surface due to the hydraulic gradient set up (Bell 1993b). The degree of vacuum that can be obtained is dependant upon the soil type, the vacuum pump capacity and the airtightness of the seals, generally values of 60 - 70% vacuum can be obtained (-60 to -70kPa). Due to the low pressures imposed upon the soil the air bubbles present in the soil voids increase in size and may reduce the hydraulic permeability. The method may be improved by the installation of vertical drains. Additionally, vacuum preloading may be used in conjunction with surcharge loading with the vacuum load being applied first to enhance the behaviour of the soil so that it is competent to support the surcharge load that is subsequently placed (Tang & Goa 1989). Vacuum preloading is also particularly suited to use on very soft soils as there is no risk of bearing capacity failure. Additionally, if the soft soil is located under water then the equivalent surcharge imposed on the soil is equivalent to the vacuum pressure imposed plus the water pressure at the seabed (Hansbo 1993). A case study of vacuum preloading is presented by Choa (1989) which compares test areas with conventional surcharging and vacuum preloading with different vertical drain spacings.

4.1.2.3 Stone Columns - Vibroreplacement

Clay soils are largely unaffected by induced vibrations due to any induced stresses being taken up as porewater pressure. Nevertheless, vibroflotation may be used to treat clay soils by the introduction of densely compacted columns of coarse backfill. These stone columns utilise the passive resistance of the soil to absorb the vertically applied load through radial expansion of the columns, thereby increasing its bearing capacity and reducing settlements.

The stabilisation process is also aided by the reduced drainage path lengths provided by the stone columns and the associated use of the horizontal permeability of the soil.
There are three construction methods employed for the construction of stone columns (Keller 1992):

- Conventional Dry Process - The hole is formed by a crane suspended vibrator, the vibrator is removed and stone backfill added to the hole and compacted by the vibrator in stages, assisted by compressed air. The hole must be self-supporting for this process to be used and groundwater must be absent.
- Bottom Feed System - A specially designed vibrator remains in the ground during construction of the stone column, the stone infill being supplied internally to the vibrator tip. Applicable to a wide variety of soil types and not inhibited by the presence of groundwater. The construction sequence for the bottom feed system is given in Figure 4.6.
- Wet Process - Uses a crane suspended vibrator and jetting water to remove soft material, stabilise the hole and allow stone backfill to reach the bottom of the hole where it is compacted. The system has a water requirement of in excess of 2500 gallons/rig/hour and the effluent produced also requires removal and possibly treatment.

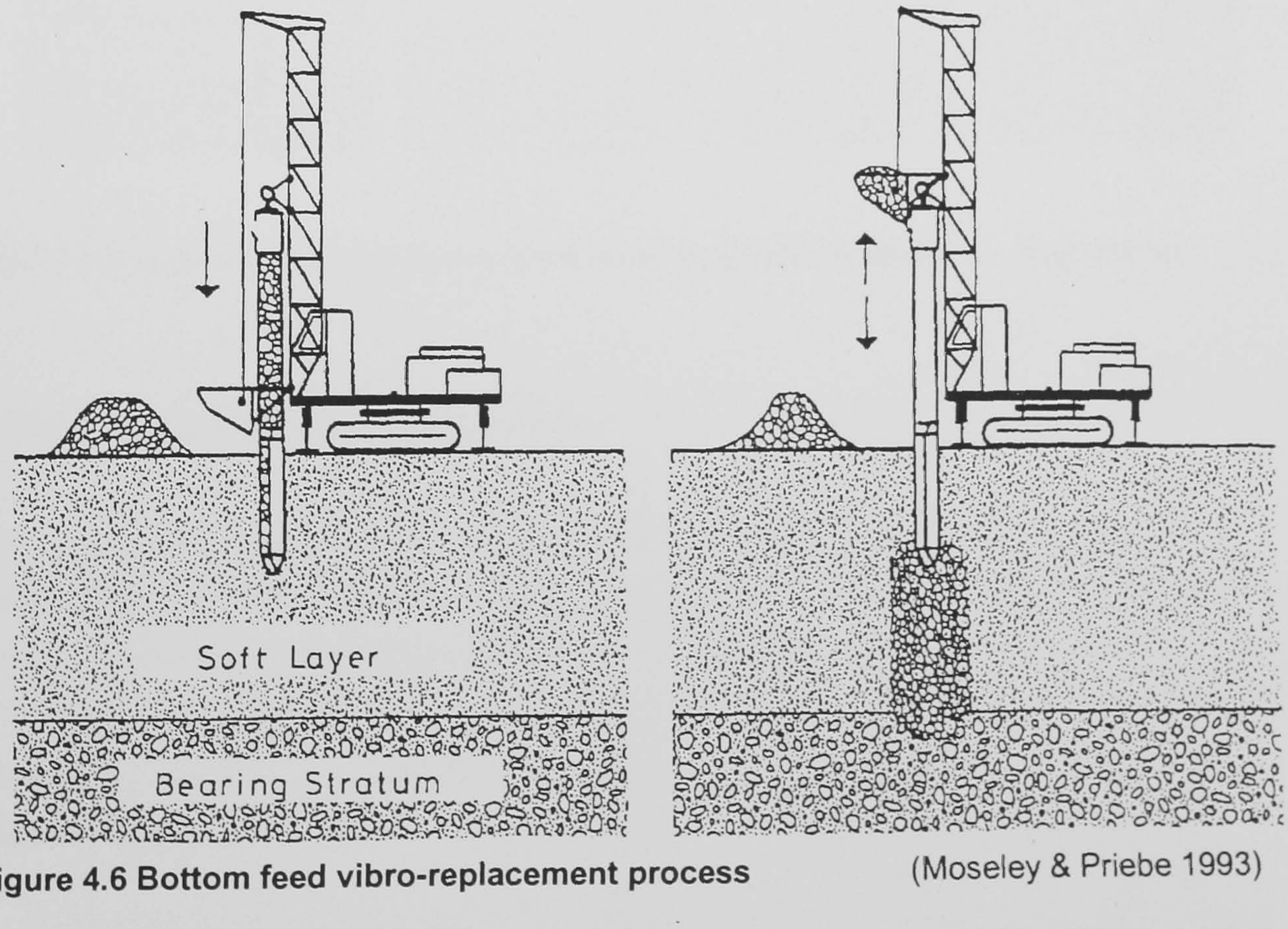

Figure 4.6 Bottom feed vibro-replacement process (Moseley & Priebe 1993)

4.1.2.4 Concrete Columns

The construction of vibro concrete columns is similar to that of the bottom feed system stone column installation process, except that concrete is used instead of a stone infill. The columns may be reinforced with conventional steel reinforcement because they are constructed from concrete. Due to the construction process enlarged bases and heads are possible and because of this they are more efficient than a conventional piling solution. They do not rely upon passive resistance or horizontal drainage as stone columns do. The construction process is given in Figure 4.7.

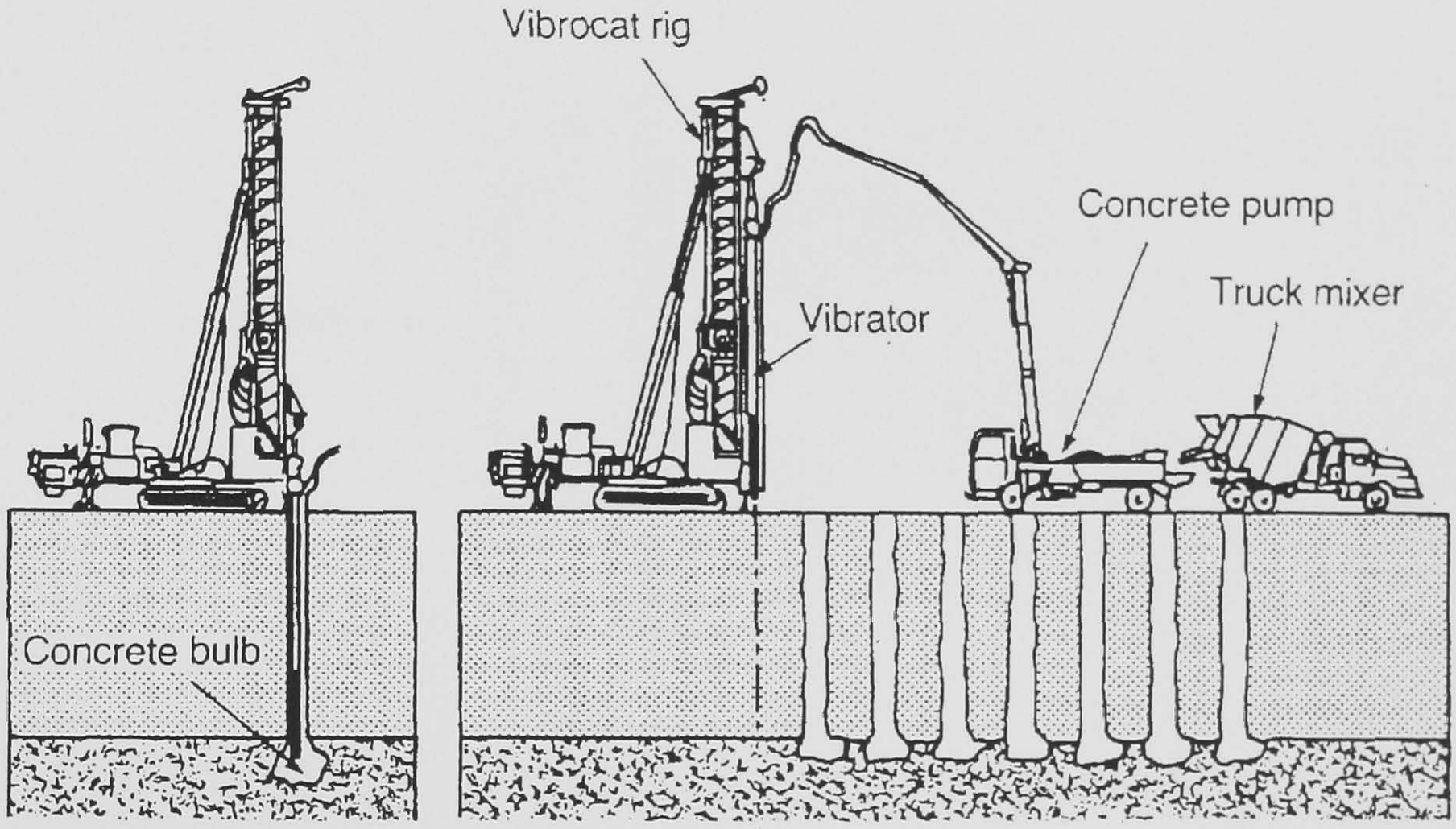

Figure 4.7 Construction sequence of vibrated concrete columns (Bell 1993b)

4.1.2.5 Lime And Lime/Cement Columns

Lime columns can be used to increase the bearing capacity of soft clay and silt and to reduce settlements. In this method the soft soil is mixed in situ with unslaked lime (CaO) or a mixture of lime and cement by a tool shaped like a giant dough mixer (Broms 1993). The mixing tool is rotated down into the soil to the required depth and then slowly withdrawn (≤25 mm/rev) as unslaked lime or lime/cement is forced down into the soil by compressed air, as shown in Figure 4.8.

The immediate increase in the shear strength of the soft clay or silt when mixed with lime is caused by flocculation of the clay particle and by a reduction in the water content (Broms 1993).

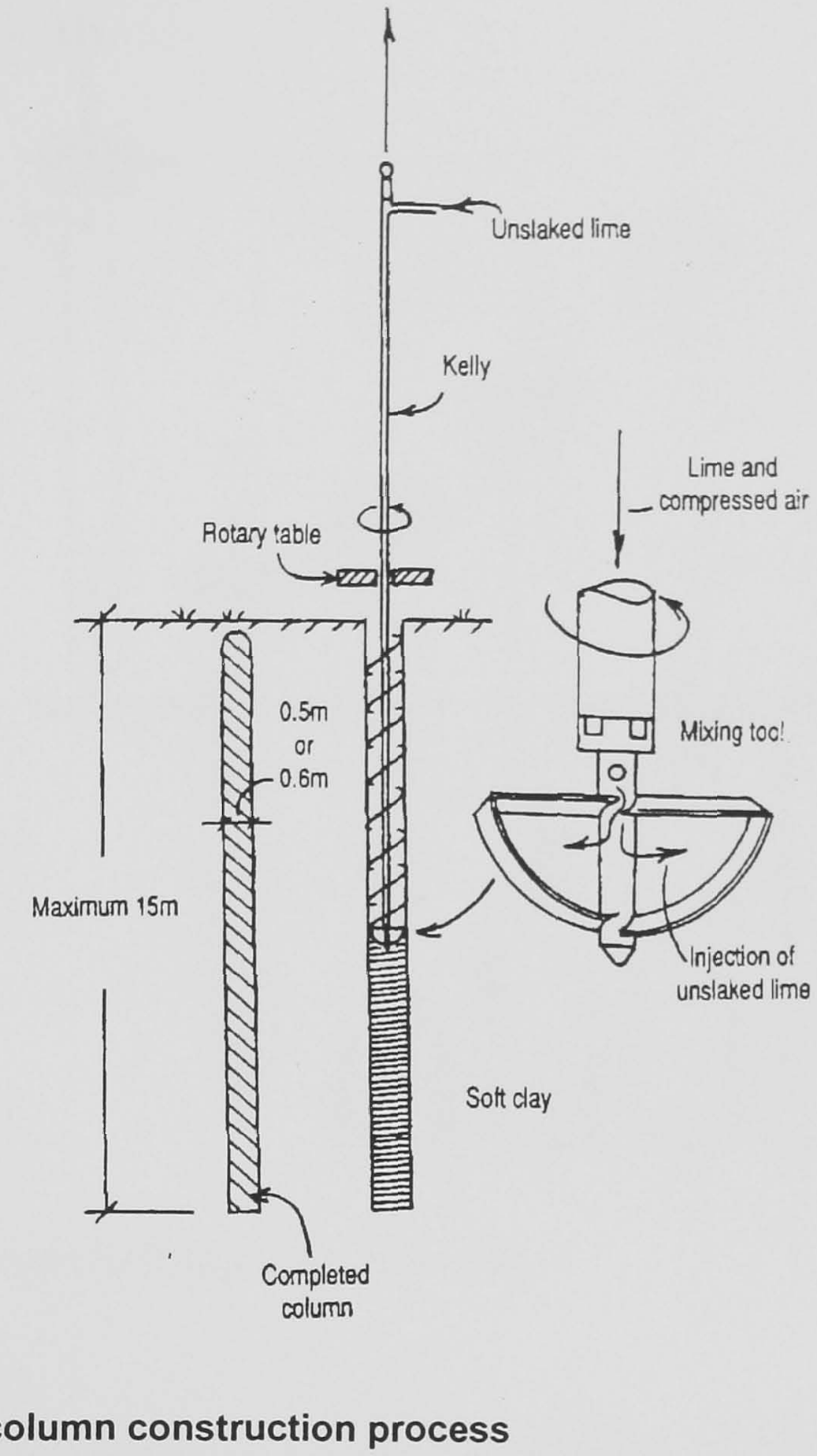

Figure 4.8 Lime column construction process (Broms 1993)

4.1.2.6 Lime Piles

Lime piles may be installed in saturated clayey soils by means of a special metal tube with a closed tip (200mm - 500mm∅). The tube is vibrated and forced into the soil and then withdrawn from the soil and the hole filled with lumps of quicklime, as shown in Figure 4.9.

The quicklime is then compacted by tamping. On contact with groundwater the quicklime gradually slakes causing an expansion of the pile diameter of 30% to 70% of its original diameter (Bell 1993b) consolidating the surrounding soil. A large amount of heat is released by the slaking process causing evaporation of some of the porewater in the surrounding soil. Lime also penetrates the soil, thereby effecting its stabilisation.

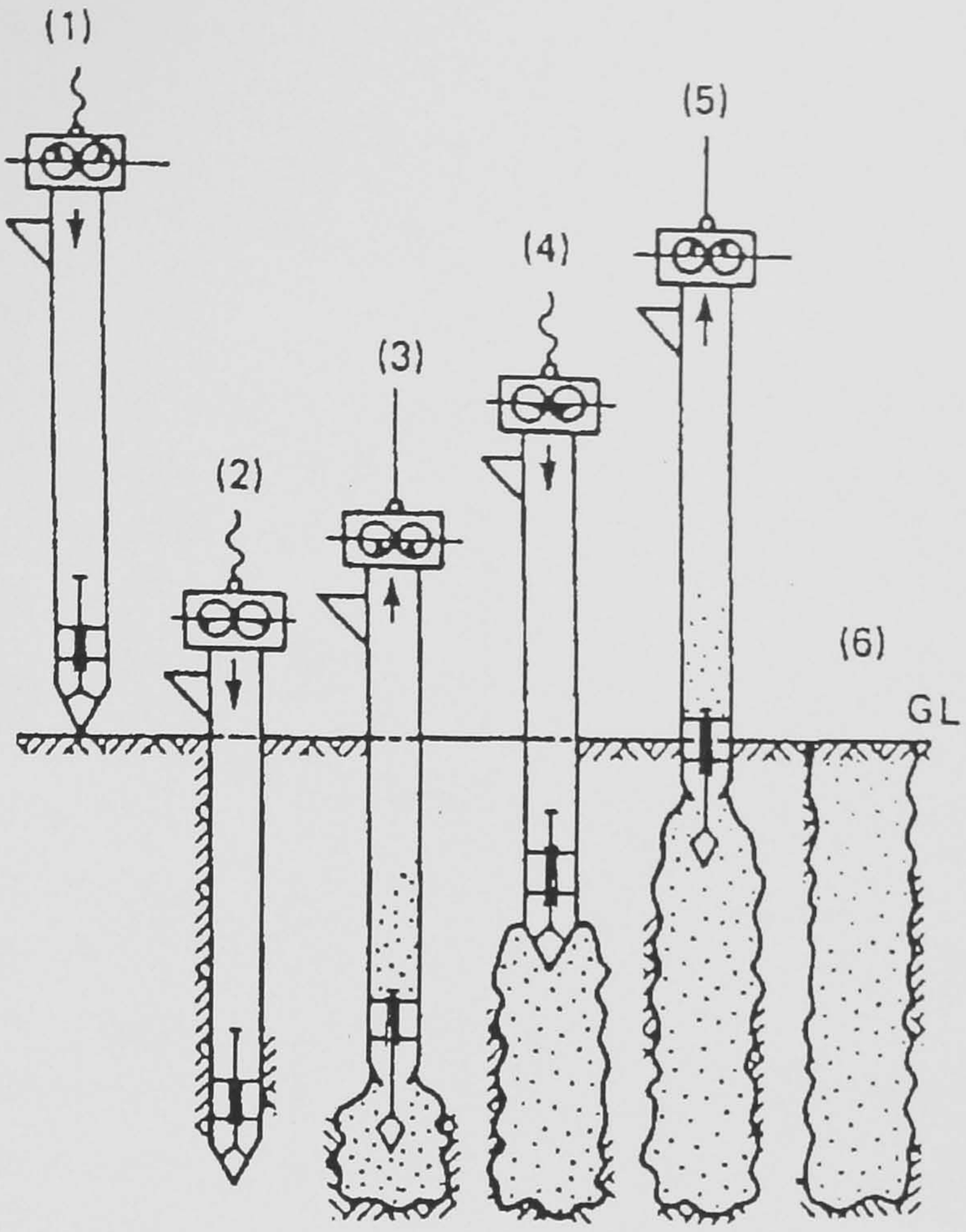

Figure 4.9 Construction sequence for lime piles (Bell 1993b)

4.1.2.7 Thermal Stabilisation

Clay soils if heated to a sufficiently high temperature, in excess of 400°C, undergo changes in their crystalline structure, notably the loss of the (OH) group. These changes are irreversible and result in the clay being permanently hardened.

The procedure consists of driving extremely hot exhaust gases from burning fuel into holes in the ground. The distribution of temperature with depth produced from the hot gases depends upon the soil porosity, moisture content, excess porewater pressure and the temperature of the gases injected. Until the free water enclosed in the pore spaces of the soil is completely evaporated the temperature does not exceed 100°C. Thermal stabilisation cannot be applied to soils that are saturated since the latent heat of evaporation of the water makes the process prohibitively expensive. Electrical heat sources have also been used down the hole instead of hot exhaust gases (Bell 1993b).

4.1.2.8 Dynamic Compaction

Dynamic compaction is carried out by repeatedly impacting the ground surface by dropping a weight from a given height using a heavy-duty crane. Substantial compaction results,

thereby reducing the total and differential settlements that may occur after the erection of structures and permitting the use of spread footings (Gambin 1987). Dynamic compaction has been used to densify a wide range of soils from organic and silty clays to loosely packed coarse grained soils and fills (Menard & Broise 1975).

- **Granular soils**

In dry granular soil i.e. sand, gravel, ash, brick, rock, slag etc. dynamic compaction improves the soil characteristics through the displacement of the soil particles and, to a lesser extent, low frequency excitation will reduce the void ratio and increase the relative density (Slocombe 1993).

Where the granular material extends below the water table, a high proportion of the dynamic impulse is transferred to the porewater that may eventually rise to a sufficient level to induce liquefaction. Low frequency vibrations caused by further stress impulses will then reorganise the particles into a denser state. The dissipation of porewater pressure, in conjunction with the surcharge of the overlying layers, results in a further increase in the relative density over a relatively short period of time (Slocombe 1993).

In the U.K., the practice is to try to avoid liquefaction by designing the treatment to provide compaction by displacement without dilation or high excess porewater pressures. This is achieved through a smaller number of impacts from a lower drop height. This method requires substantially lower energy input than the liquefaction approach, with consequent economies.

- **Cohesive soils**

Due to the dynamic nature of the preloading imposed by dynamic compaction it applies a virtually instantaneous surcharge that is transferred to the porewater on a localised basis. This creates a zone of positive water pressure gradients that induce water to drain rapidly from the soil matrix. This effect is further accelerated by the formation of additional drainage paths along shear zones and by hydraulic fracture. Consolidation therefore occurs much more rapidly than would be the case with static loading.

In clays located below the water table, a much larger reduction in moisture content is generally required in the presence of a smaller available pore-pressure gradient and a longer drainage path. Only nominal degrees of improvement have been achieved in thick layers of relatively weak alluvial clays and silts, even with additional measures such as drainage trenches filled with sand or wick drains (Slocombe 1993).

4.1.2.9 Jet Grouting

Jet grouting employs erosion caused by jets of high pressure grout, grout with air shroud or water with air shroud to break down the soil structure removing varying proportions of the resulting soil particles and replacing them with cement based grouts placed during the

erosive process (Bell 1993b). Soil particles not removed become mixed with the grout in situ to form the treated mass. Due to the erosive nature of jet grouting the procedure may be applied to a wide range of soil types from gravels to clays.

The procedure for jet grouting is to drill a borehole (100 to 150mm∅) to the required treatment depth. This may be done with either the jetting pipes "monitor" or a separate drill string, depending upon the soil conditions. The stability of the borehole is important to allow the eroded material to be brought to the surface during jetting. The stability of pre-drilled holes is usually maintained, prior to monitor insertion, by the use of a bentonite suspension. With self-boring monitors the circulation of the flushing medium maintains the stability. After drilling the next stage is jetting to erode the ground locally, thus enabling the placement of the grout slurry. Three types of grouting system are currently in use, single (S), double (D) and triple (T) (Keller 1990) these are shown in Figure 4.10.

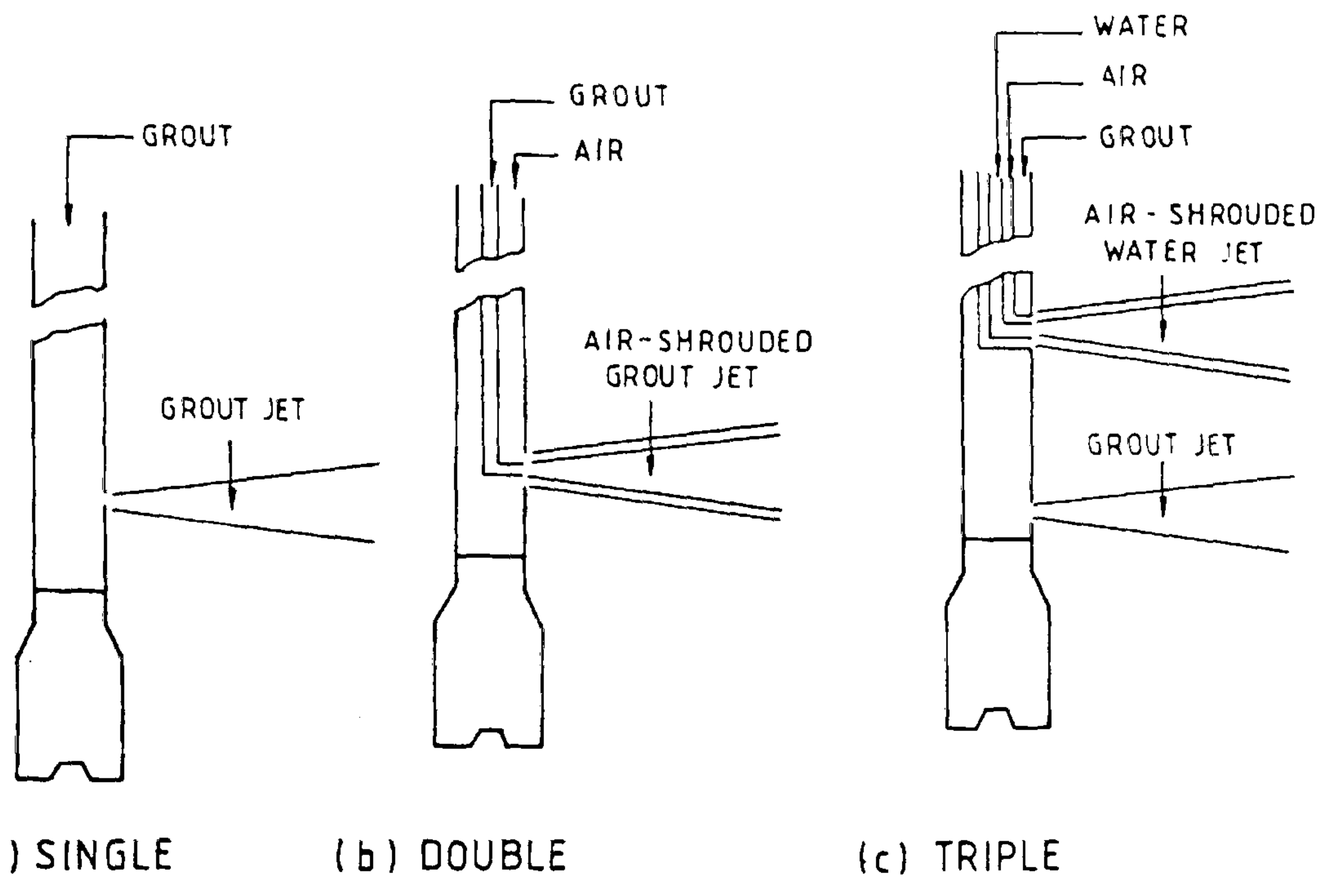

Figure 4.10 Jet grouting systems (Keller 1990 & Bell 1993a)

The single system (S) uses grout to simultaneously erode the soil and place grout. The double system (D) uses a shroud of compressed air over the grout jet to enable a greater treated volume during jetting compared to the single system. The triple system (T) uses an air shrouded water jet for soil erosion and a separate injection nozzle for placement of grout. Figure 4.11 gives typical expected column diameters in three different soil types for both the single (S) and triple systems (T).

Expected compressive strengths for soils treated by jet grouting are given in Table 4.1

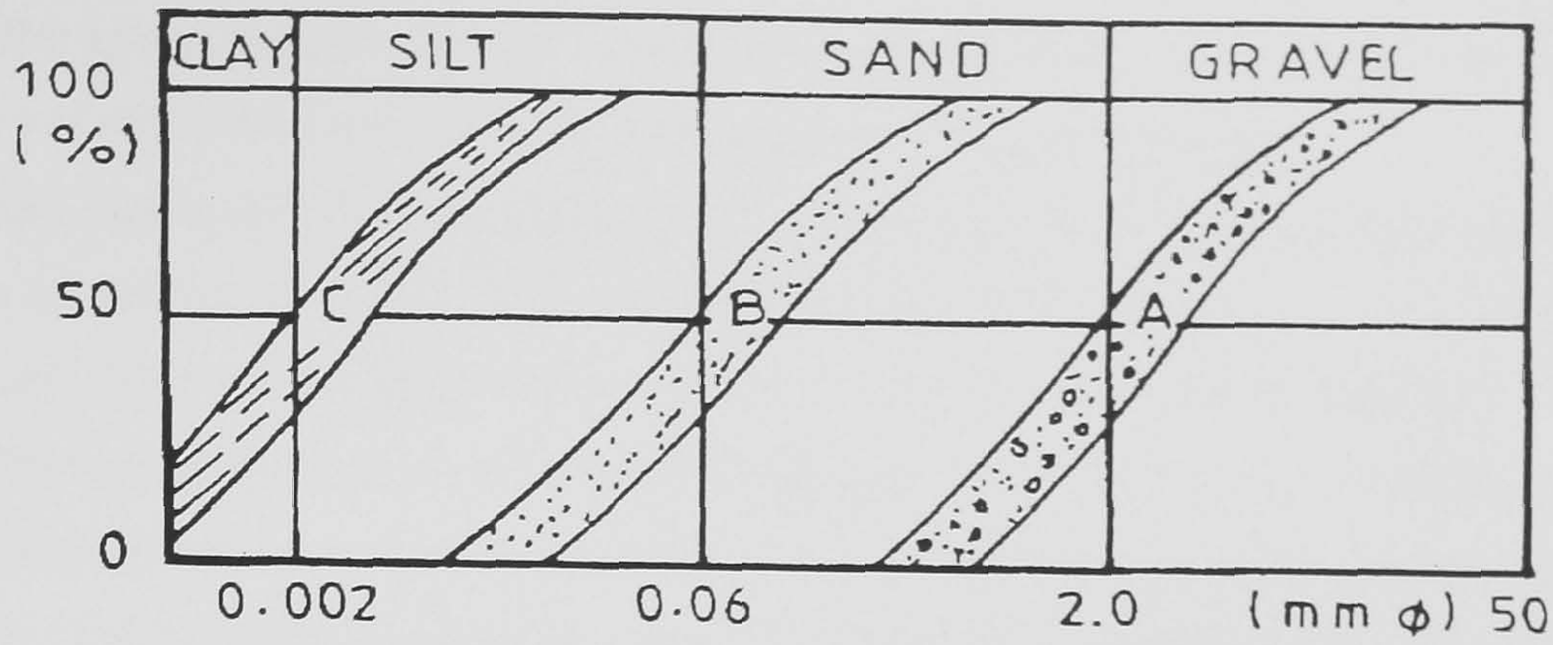

SOIL DESCRIPTION	JET GROUT DIA S (m)	JET GROUT DIA T (m)
C CLAYEY SILT	0.4 – 0.5	0.8 – 1.0
B SILTY SAND	0.8 – 0.9	1.4 – 1.6
A SANDY GRAVEL	0.9 – 1.0	2.0 – 2.4

Figure 4.11 Jet grouting column diameters in different soil types (Bell 1993a)

Table 4.1 Expected compressive strength of jet grouted soil (Bell 1993a)

Soil type	**Compressive strength (N/mm^2)**	**Coefficient of permeability, k, (m/s)**
Gravels including sandy gravels	5 to >30	10^{-7} to 10^{-9}
Sands including silty or gravelly sands	5 to > 25	10^{-7} to 10^{-10}
Silts including clayey silts	4 to 18	10^{-7} to 10^{-10}
Clays including silty and peaty clays	0.5 > 8	10^{-7} to 10^{-10}

4.1.2.10 Compaction Grouting

Compaction grouting uses a highly viscous grout of cement, soil, clay and/or PFA and water (less than 25mm slump) to compress the surrounding soil (Warner & Brown 1974). The hardened grout forms a bulb or column of strong, relatively incompressible material. Although compaction grouting may be used in any soil type the soil conditions which lend themselves to effective compaction grouting fall into five general categories (Rubright & Welsh 1993).

- Loose, granular soils above or below the groundwater table. The soil is mostly sand and/or gravel but can contain substantial amounts of silt and some clay provided that the soil still drains and behaves mechanically like a granular soil.
- Loose, non-saturated fine-grained soils. Soils composed primarily of silt and/or clays can usually be improved by compaction grouting if they are not saturated. Poorly placed cohesive fills are the most common occurrence under this category. Treatment of thick saturated silt or clay should not be performed. On several projects compaction grouting is believed to have squeezed the saturated soil causing a dramatic increase in pore pressure which cannot dissipate. This elevated porewater pressure leads to a direct and sudden loss of shear strength that causes dramatic settlement of the structure.
- Collapsible soils. Collapsible soils can be defined or artificially collapsed by compaction grouting, thus avoiding the risk of water related collapse.
- Voids. Voids in soil or rock at depth may be filled by compaction grouting rather than fluid grouts. Compaction grout is more controllable under these circumstances as it is more viscous and will not travel far beyond the intended treatment area.
- Thin, unimprovable soil strata contained by adequate surcharge. The soil can be a dry of saturated silt, clay or organic provided that it is not more than 2m in thickness and is under at least 2m of competent or improvable soils. The compaction grout does not improve this soil but rather bridges through it by creating pedestals on which to support some load.

4.1.2.11 Compaction

Compaction may be a suitable method for ground improvement where the cohesive soil may be excavated, dried or wetted to within agreed tolerances of the optimum moisture content and compacted by means of standard compaction plant in predetermined lift heights as presented in Table 4.2.

Where the soil is required to be treated in situ, conventional compaction is not a feasible treatment method due to the applied compactive stress being taken by the porewater and not being dissipated rapidly enough to allow an increase in effective stress due to the relatively low permeability of fine grained soils. Additionally, due to stress distribution with depth the deeper down the soil is the lower the compactive stress and less compaction will occur. Table 4.3 illustrates this hypothetically assuming a 45° stress distribution. Dynamic compaction may be used on fine grained soils and this is discussed in §4.1.2.8.

Major division	Subgroup	Suitable type of compaction plant	Minimum number of passes for satisfactory compaction	Maximum thickness of compacted layer (mm)	Remarks
Soils having low plasticity	Silts (inorganic) and very fine sands, silty of clayey fine sands with slight plasticity Clayey silts (inorganic) Organic silts of low plasticity	Sheepsfoot roller Smooth - wheeled roller Pneumatic - tyred roller Vibratory roller over 70kg per 100mm of roll Vibratory plate compactor over 1400 kg/m^2 of baseplate Vibro-tamper Power rammer	4 - 8 depending on type of plant	100 - 450 depending on type of plant	If moisture content is low it may be preferable to use a vibratory roller. Sheepsfoot rollers are best suited to soils at a moisture content below their plastic limit
Soils having medium plasticity	Silty and sandy clays (inorganic) of medium plasticity Clays (inorganic) of medium plasticity				
	Organic clays of medium plasticity				Generally unsuitable for earthworks
Soils having high plasticity	Fine sandy and silty soils, plastic silts Clay (inorganic) of high plasticity, fat clays				Should only be used when circumstances are favourable
	Organic clays of high plasticity				Should not be used for earthworks

Table 4.2 Typical compaction characteristics for fine soils (After BSI 1981)

Table 4.3 Hypothetical stress distribution due to surface compaction

Depth below surface (m)	Stressed area	Stress (kPa)
0m	1m*1m	1000 kPa
1m	3m*3m	111 kPa
2m	5m*5m	40 kPa
3m	7m*7m	20 kPa

4.2 ELECTRO-OSMOTIC CONSOLIDATION

4.2.1 CRITICAL REVIEW OF ELECTRO-OSMOTIC CONSOLIDATION

Casagrande introduced electro-osmosis into civil engineering in the late 1930's for the stabilisation of a railway cutting in Salzgitter, Germany (Casagrande 1941a, 1941b, 1947 and 1952). The principal engineering, non-environmental, use of electro-osmosis has tended to be as a means to temporarily stabilise soils to facilitate construction, for example during excavation, with the general desired effect being an increase in the shear strength of the soil caused primarily by the increase in effective stress.

Casagrande *et al* (1961) describes the application of electro-osmosis to a slope in loose saturated silt to facilitate the construction of a bridge pier. In this instance it was the increase in the undrained shear strength through the reduction of water content, and the lowering of the phreatic surface that was facilitated by electro-osmosis.

An unsuccessful application reported by Caron (1971a, 1971b) indicates that the presence of continuous sand and silt layers in the subsoil to be treated are undesirable because of the relatively high conductivity of such layers, causing possible "short circuiting" of the system. This indicates the importance of correctly identifying the soil's macrofabric, see §2.3.4.

Casagrande *et al* (1981) again describes two applications of electro-osmosis to the stabilisation of silts to allow the excavation of steep slopes in soft silty clay. Electro-osmosis was used to increase the undrained shear strength such that the excavation remained stable.

Bjerrum *et al* (1967) discusses the use of electro-osmosis to stabilise a quick clay to allow the construction of a sewage treatment plant to proceed. Without an increase in the undrained shear strength of the quick clay bottom heave of the excavation would have occurred and the overall stability of the slope within which the work was to be undertaken would have been jeopardised.

Lo *et al* (1991a) describes a field investigation of a true consolidation application of electro-osmosis. The electrodes chosen for use were perforated copper pipes to allow the passage of expelled water and gas without the requirement for pumping, and additionally to minimise localised resistance at the electrode/soil interface due to corrosion products as the corrosion products of copper, copper oxide and hydroxide, are highly conductive. This electrode was

used for both anode and cathode. During treatment surface settlement, vane shear strength and voltage distribution with time were measured, polarity reversal was also employed, Figure 4.15. The results of the trial showed surface settlements of up to 62mm were achieved with average increases in the undrained shear strength of the soil of approximately 62%. It was also found that the reversal of polarity caused a more uniform treatment of the trial area. After a period of 10 months at the end of the trial it was found that the shear strength was unchanged, indicating the treatment effects are permanent, Figure 4.15. Although this application was only a trial, the results obtained demonstrate the practicality of electro-osmosis for the consolidation of soft clay deposits.

Morris *et al* (1985) reports on the treatment of a sensitive silty clay by electro-osmosis in the laboratory. The results are worthy of mention because after treatment by electro-osmosis cyclic triaxial testing was carried out on the soil samples. The results obtained indicate that the electro-osmotically treated clay required a significant increase in the number of stress applications to reach an accumulated strain of 5%, for equivalent values of stress ratio. This is significant to seismic design using electro-osmotically treated soils.

Fetzer (1967) presents a large dam project, West Branch Dam, in which electro-osmosis was used to strengthen a soft clay founding stratum under the dam that was approaching failure during construction and was preventing any further construction on the dam due to the high porewater pressures present within the clay layer. Electro-osmosis was used successfully and the excess porewater pressures in the founding stratum were dissipated and the undrained shear strength improved.

Soderman & Milligan (1961) and Milligan (1994) report on the use of electro-osmosis to improve the friction pile bearing capacity of steel H piles. The piles were used as anodes and cathodes were installed on the periphery of the pile group. The site geology consisted of varved clay and stratified silts. The load capacity of the piles was more than doubled and load testing carried out thirty years after treatment had been completed indicated that the pile bearing capacity had not decreased.

Eggestad & Føyn (1983) report on the application of electro-osmosis to increase the shear strength and stability of an excavation in soft marine silty clay in Oslo. The electrodes used were 20mm diameter iron rods at a spacing of 1-1.5m with the treatment being carried out for a period of approximately 90 days with reverse polarity being used to obtain a more uniform increase in the strength within the soil mass. The increase in undrained shear strength obtained was more than double.

Wilkins & Chandler (1989) present the results of an unsuccessful full-scale field trial that was undertaken on a Malaysian marine clay. The reason for the trial was to demonstrate the

applicability of electro-osmosis as a treatment technique for reducing the settlement of road embankments in Malaysia. The trial is stated as being unsuccessful due to the lack of funding and an inadequate power supply. However, it is interesting to note that the electrically conductivity of the soil (0.26S/m) was very high and well outside the acceptable range suggested by the Author in Chapter 7 of this thesis on soil acceptability criteria (0.05S/m - 0.005S/m).

Chappell & Burton (1975) describe the application of electro-osmosis to an unstable embankment constructed on a silty clay in Singapore. Electro-osmosis was used to increase the shear strength of the embankment fill material and to act as a dewatering technique to maintain the stability of the embankment. Chappell & Burton (1975) state that one surprising thing about this application was the high hydraulic permeability of the soil treated (10^{-6}-10^{-7} m/s). However, the Author's review of acceptability criteria for electro-osmosis indicate that the soil's particle size distribution signifies that the soil may be amenable to treatment by electro-osmosis, due to over 70% of the particles being within the silt-clay particle size range (see §7.2.1.4).

4.2.2 ADVANCED THEORY OF ELECTRO-OSMOTIC CONSOLIDATION

The application of an electrical potential difference to an impermeable soil with the appropriate drainage conditions (usually anode closed and cathode open or closed) generates negative pore water pressures within the soil mass as given by Equation 4.1 (see also Equation 2.29).

$$u = -\frac{k_e}{k}\gamma_w V \qquad \text{Eqn. 4.1}$$

As the porewater pressures generated are negative it is apparent from the classic effective stress equation presented by Terzaghi (1936) that the generation of negative porewater pressures (u) causes an increase in the effective stress (σ') within the clay with no change in total stress (σ):

$$\sigma' = \sigma - u \qquad \text{Eqn. 4.2}$$

As there is an increase in effective stress the soil particles pack together more tightly and as such the soil surface settles. Due to the form of the negative porewater pressure distribution described by Equation 4.1 (shown in Figure 2.17) the maximum theoretical settlement occurs at the anode and zero settlement occurs at the cathode.

For the 1-D case, it is possible to equate the increase in effective stress to an equivalent surface loading which would generate the same increase in effective stress and hence the same surface settlement, Figure 4.12.

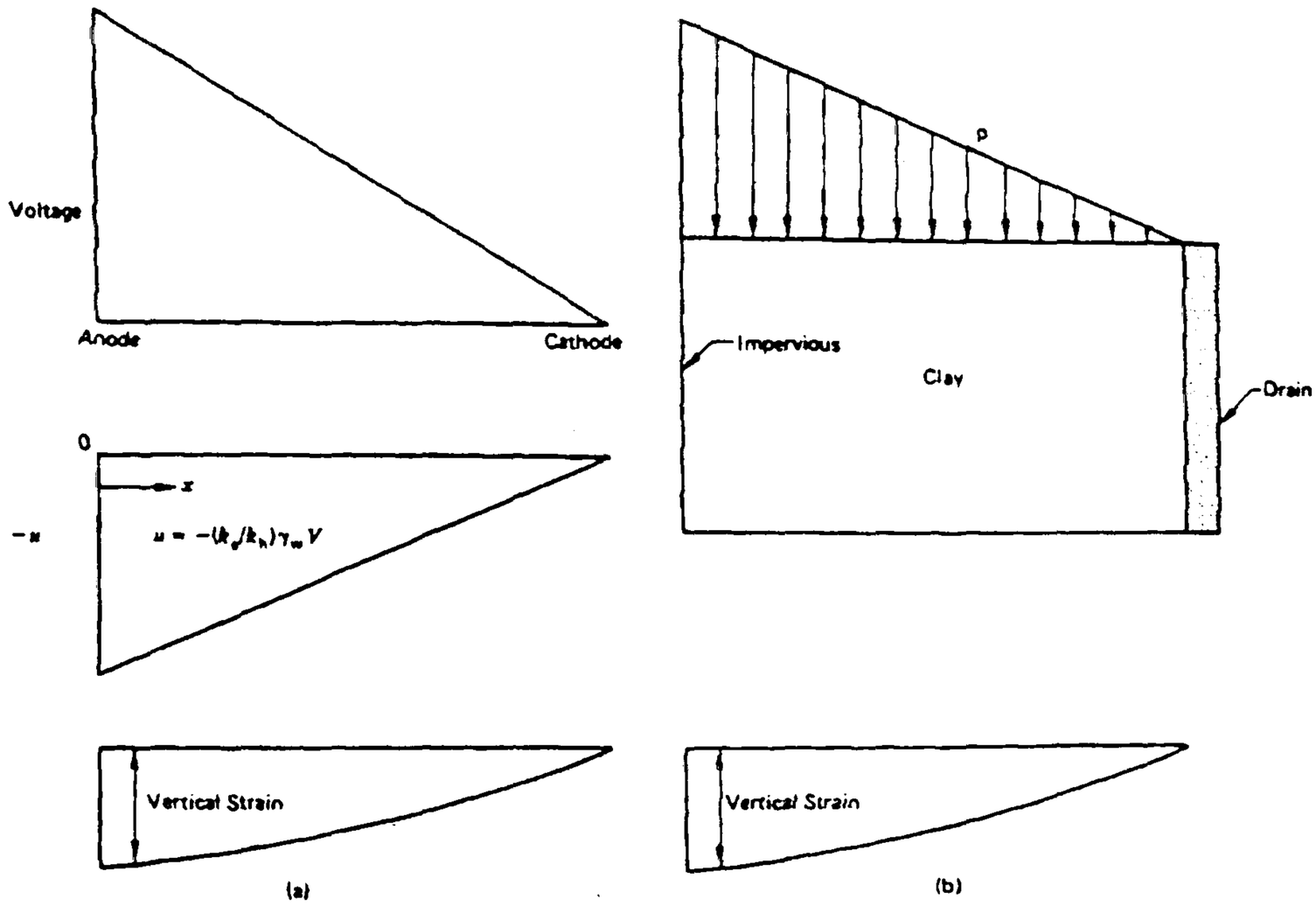

Figure 4.12 Electro-osmotic and direct loading, one-dimensional (Mitchell 1993)

The consolidation settlement caused by electro-osmosis is assumed to continue until the hydraulic force that drives water back towards the anode exactly balances the electro-osmotic force driving water towards the cathode (Mitchell 1993).

The two factors that are required to be known with regard to electro-osmotic consolidation are:

- How much consolidation will take place?
- How long will it take?

The answers to these questions may be obtained by using the coupled flow equation (see §2.6.1) in place of Darcy's Law in conventional consolidation theory.

$$k_e \frac{\partial V}{\partial x} + \frac{k}{\gamma_w} \frac{\partial u}{\partial x} = 0 \qquad \text{Eqn. 4.3}$$

In a real soil, which is compressible, the effect of the combined hydraulic and electrical potential gradients is to generate hydraulic flow (q_h):

$$q_h = -\frac{k}{\gamma_w} \frac{\partial u}{\partial x} - k_e \frac{\partial V}{\partial x} \qquad \text{Eqn. 4.4}$$

However, by conservation of mass the rate of outflow must be equal to the rate of volume change. Hence, introducing Equation 4.4 in place of Darcy's Law into the derivation of the diffusion equation governing consolidation in one dimension leads to Equations 4.5 and 4.6:

$$\frac{\partial^2 u}{\partial x^2} + \frac{k_e \gamma_w}{k} \frac{\partial^2 V}{\partial x^2} = \frac{1}{C_v} \frac{\partial u}{\partial t} \qquad \text{Eqn. 4.5}$$

$$\frac{k}{\gamma_w} \frac{\partial^2 u}{\partial x^2} + k_e \frac{\partial^2 V}{\partial x^2} = m_v \frac{\partial u}{\partial t} \qquad \text{Eqn. 4.6}$$

where m_v is the coefficient of volume compressibility and c_v is the coefficient of consolidation.

4.2.2.1 Amount Of Consolidation

Equation 4.1 indicates that electro-osmotic consolidation continues at a specific location until a negative porewater pressure, relative to the initial value, has been developed that depends upon the ratio k_e/k. As k_e only varies within a certain range (see Table 2.7) the amount of consolidation that can be achieved depends largely upon k. Thus, the potential for consolidation by electro-osmosis increases as the soil grain size decreases, because the finer grained the soil, the lower the value of k (see Figure 2.12). However, the amount of consolidation that will take place depends upon the soil compressibility as well as the change in effective stress. It follows that electro-osmosis will be of little use in an overconsolidated clay unless the increase in effective stress is large enough to bring the soil back onto the virgin compression line (see §7.2.3.1 on soil acceptability) (Mitchell 1993).
It has been shown, however, that in the field the minimum negative porewater pressure generated by electro-osmosis is limited to approximately -100kPa (Johnston 1978), and the magnitude and distribution of settlement can be obtained based upon conventional consolidation theory (see § 4.3.3.1 for full design).

4.2.2.2 Rate Of Consolidation

The solution to Equation 4.5 has been obtained for several electrode configurations (Esrig 1968, 1971). For the 1-D case and assuming a freely drained cathode (open) and a closed anode (no flow), the porewater pressure at any time is given by Equation 4.7:

$$u = \frac{k_e}{k}\gamma_w V(x) + \frac{2k_e\gamma_w V_m}{k\pi^2} \bullet \sum_{n=0}^{\infty} \frac{(-1)^n}{\left(n+\frac{1}{2}\right)^2} \sin\left[\frac{\left(n+\frac{1}{2}\right)\pi x}{L}\right] \bullet \exp\left[-\left(n+\frac{1}{2}\right)^2 \pi^2 T_v\right]$$

Eqn. 4.7

where $V(x)$ is the voltage at x, V_m is the maximum applied voltage and T_v is the time factor, defined in terms of the distance between electrodes L and the real time t as:

$$T_v = \frac{C_v t}{L^2}$$

Eqn. 4.8

where C_v is the coefficient of consolidation as defined by Equation 4.9. Additionally from Equation 4.7 when $t \to \infty$, $T_v \to \infty$ and the porewater pressure is given by the first term in Equation 4.7; i.e. the final negative porewater pressure at any point is dependant upon the ratio k_e/k and the voltage at that point. The higher the ratio k_e/k and the voltage $V(x)$ the greater will be the consolidation pressure. The average degree of consolidation U as a factor of time is given in Equation 4.10.

$$C_v = \frac{k}{m_v \gamma_w}$$ Eqn. 4.9

$$U = 1 - \frac{4}{\pi^3} \sum_{n=0}^{\infty} \frac{(-1)^n}{\left(n + \frac{1}{2}\right)^3} exp\left[-\left(n + \frac{1}{2}\right)^2 \pi^2 T_v\right]$$ Eqn. 4.10

The solution to Equations 4.7 and 4.10 are given in Figures 4.13 and 4.14 respectively:

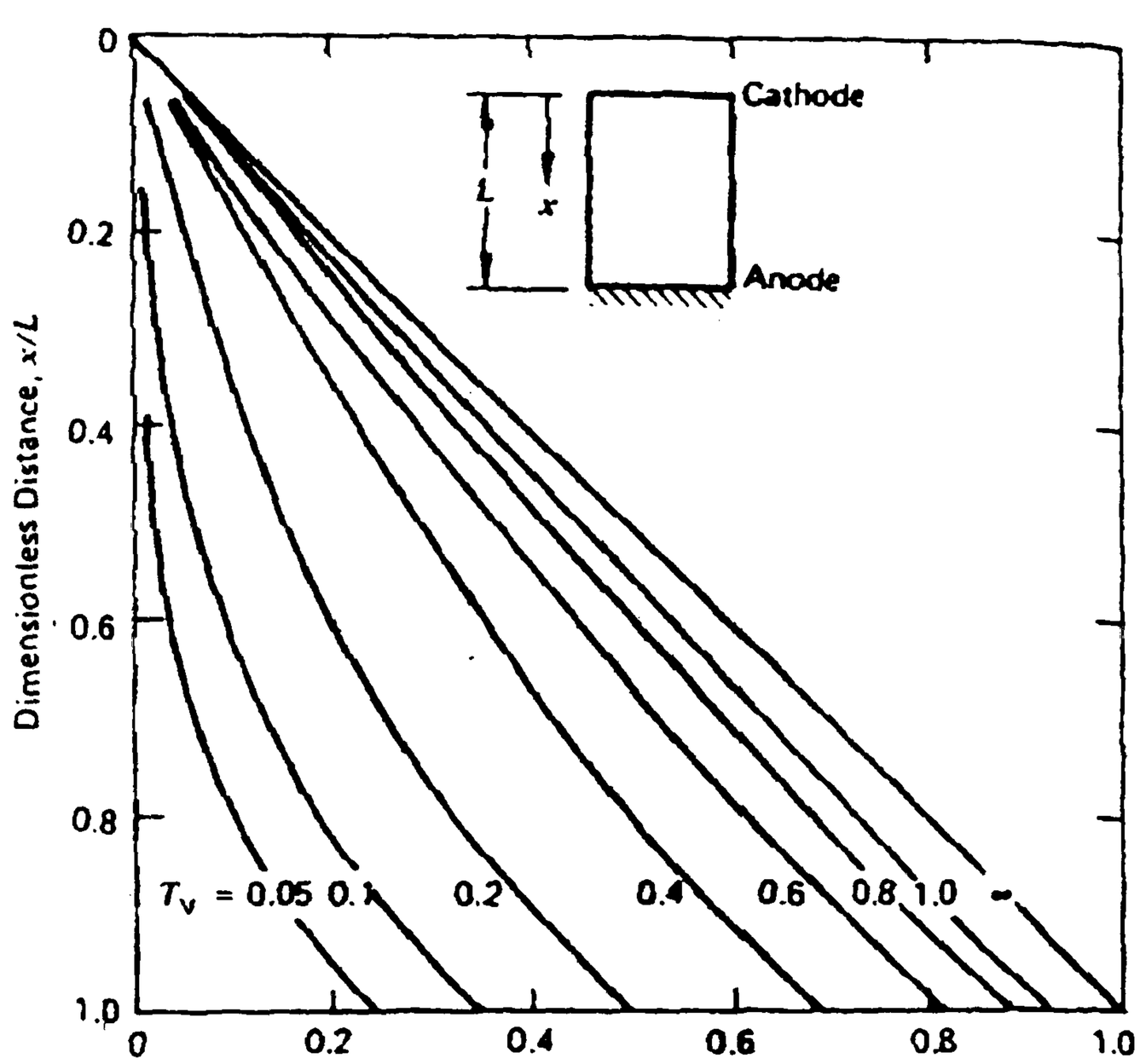

Figure 4.13 Dimensionless pore pressure as a factor of dimensionless time (Mitchell 1993)

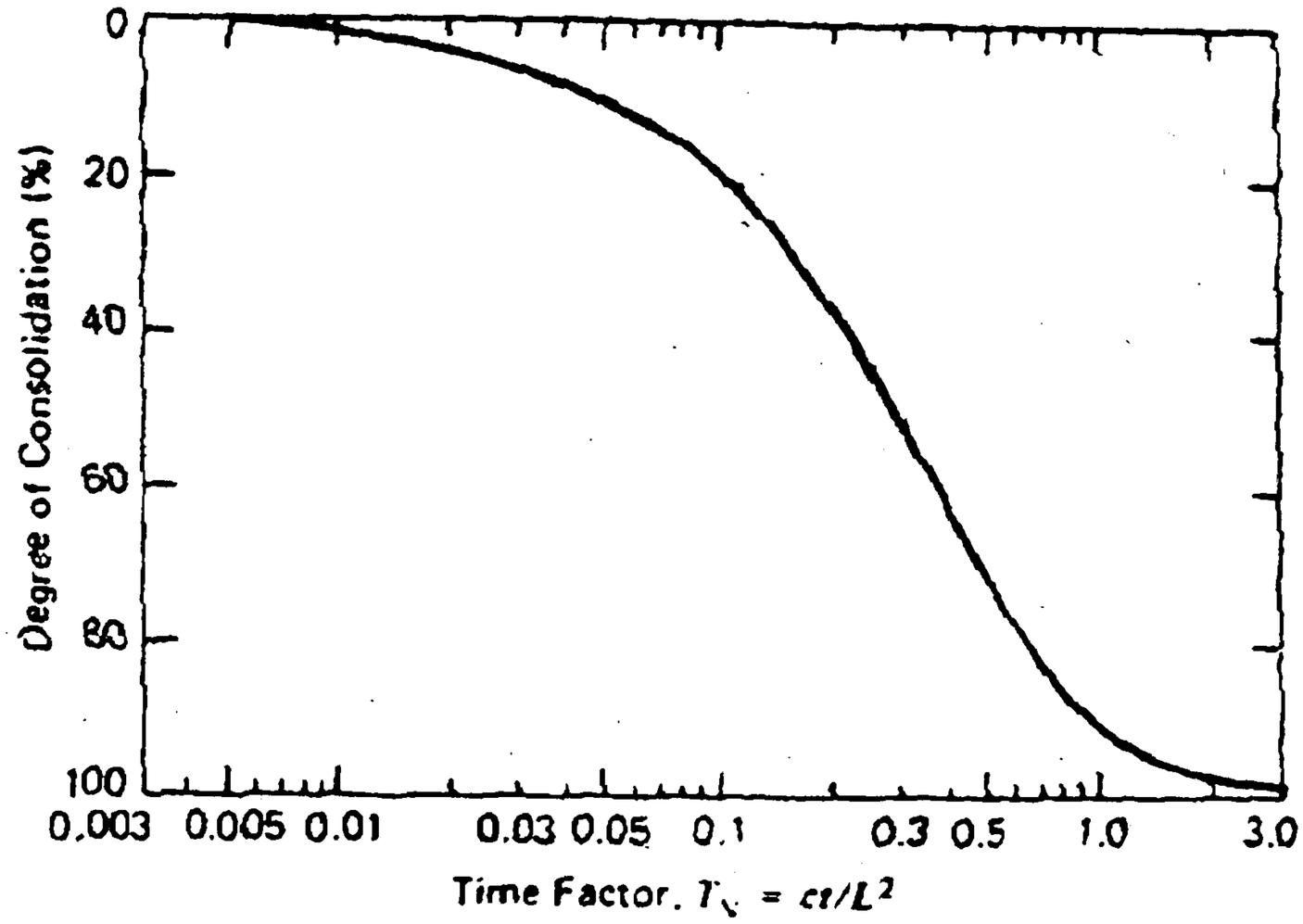

Figure 4.14 Average degree of consolidation (Mitchell 1993)

Both Figures 4.13 and 4.14 are used in the same way as the theoretical solutions for classical consolidation theory (Mitchell 1993). It is important to note from these solutions that the rate of consolidation depends completely on the coefficient of consolidation, which varies directly with k but is completely independent of k_e. Thus, low values of k, as in the case of highly plastic clays, mean long consolidation times. Whereas, a low value of k means a high value of k_e/k and the potential for a high effective consolidation pressure, it also means a longer required consolidation time for a given electrode spacing. The optimum situation is one where k_e/k is high enough to generate a very low negative porewater pressure at a reasonable electrode spacing and a safe voltage, but when k is high enough to enable consolidation in a reasonable time. Additionally, as noted in §2.7.5.1 and §2.7.5.2 the electrical conductivity of the soil is also critical, if it is too high electro-osmosis is unlikely to be economically viable. Acceptable limits for soil parameters with regard to electro-osmosis are considered in Chapter 7.

4.2.2.3 Radial Flow

The equation governing radial flow electro-osmosis, i.e. when electrodes act as single point electrodes and not as an equivalent plate electrode, are similar to those governing electro-osmosis consolidation for the one-dimensional case except that Equation 4.4 is modified to take into account the cylindrical geometry of the system. This obviously has repercussions upon the subsequent derivation of the diffusion equation presented in Equations 4.5 & 4.6. Additionally, the voltage distribution for radial flow is described by a logarithmic curve and

not a linear one, as is the case of one-dimensional flow (see Figure 4.12). The solution to radial flow electro-osmosis has been presented by Esrig (1968 & 1971) and is summarised by Mitchell (1993); discussion on radial flow in general is presented by Barron (1948). The reader is referred to these references for further information on this topic.

4.2.3 PERMANENCE OF TREATMENT

Electro-osmotic treatment may be considered as permanent in terms of the strength gains achieved, although historically it has sometimes been employed as a temporary measure to facilitate construction, see §4.2.1. Milligan (1994) demonstrated this in the field through the load testing of piles in electro-osmotically enhanced clay. It was found that even after a period of 30 years the piles were behaving in the desired manner with no apparent loss of strength being observed in the clay. Lo *et al* (1991a) also undertook tests to assess the permanence of the strength improvements brought about by electro-osmosis. After a period of 10 months after the end of treatment it was observed that there was no decrease in the measured values of shear strength, indicating the permanence of treatment, Figure 4.15.
The permanence of electro-osmotic treatment may be though of as consisting of two elements, electro-chemical changes and consolidation.
The permanence of the treatment occurs through chemical changes that take place in the clay mineral structure that alters the plasticity indices of the soil as observed by Bjerrum (1967).

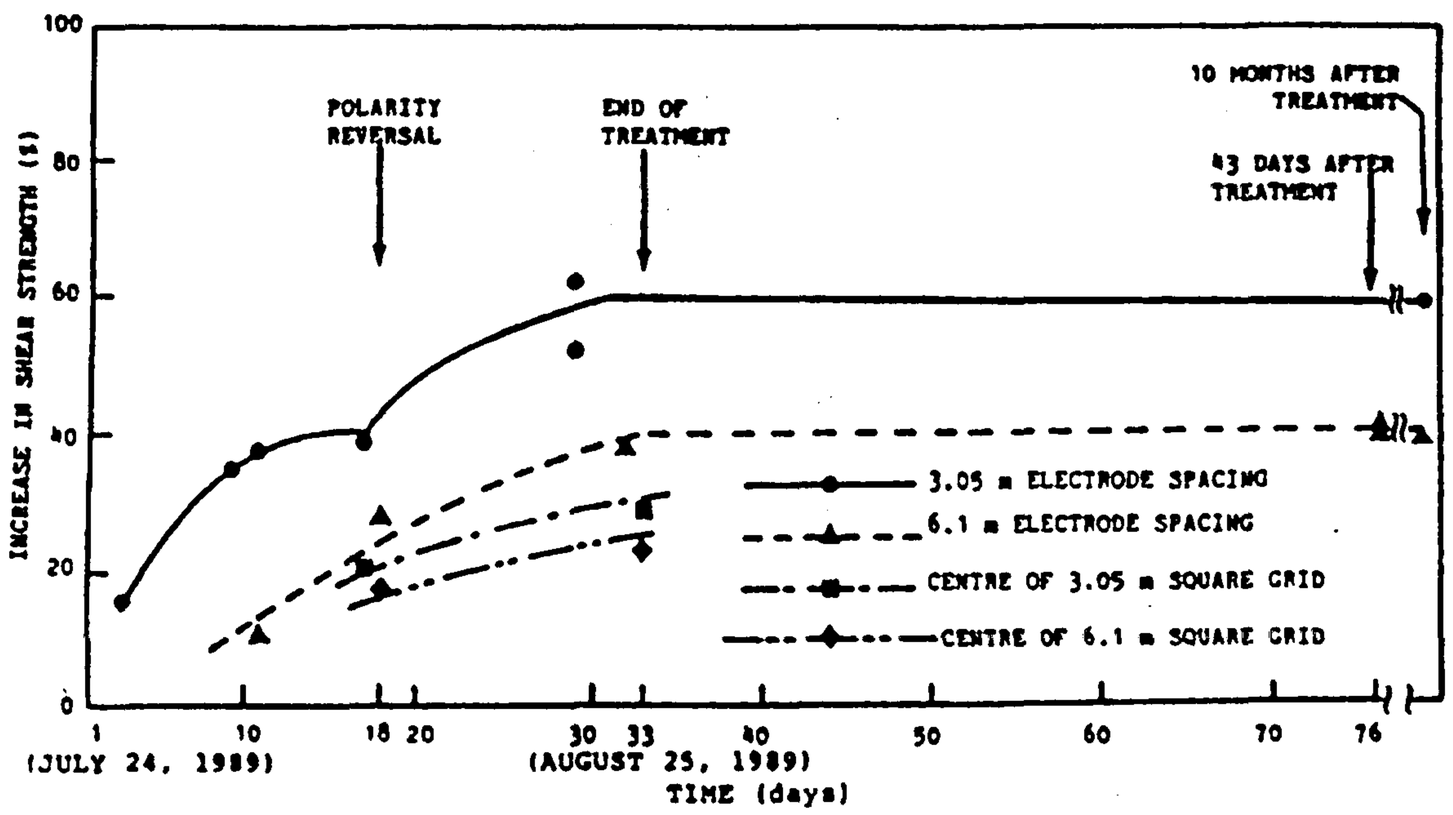

Figure 4.15 Demonstration of permanence of treatment (Lo *et al* 1991a)

Additionally, considering the process of electro-osmosis on a normally consolidated clay in terms of the voids ratio (e) versus the logarithm of the effective consolidation pressure (log σ') plot it is apparent that even if no chemical changes were to take place within the soil it would not return to its original state as it now overconsolidated as shown in Figure 4.16.

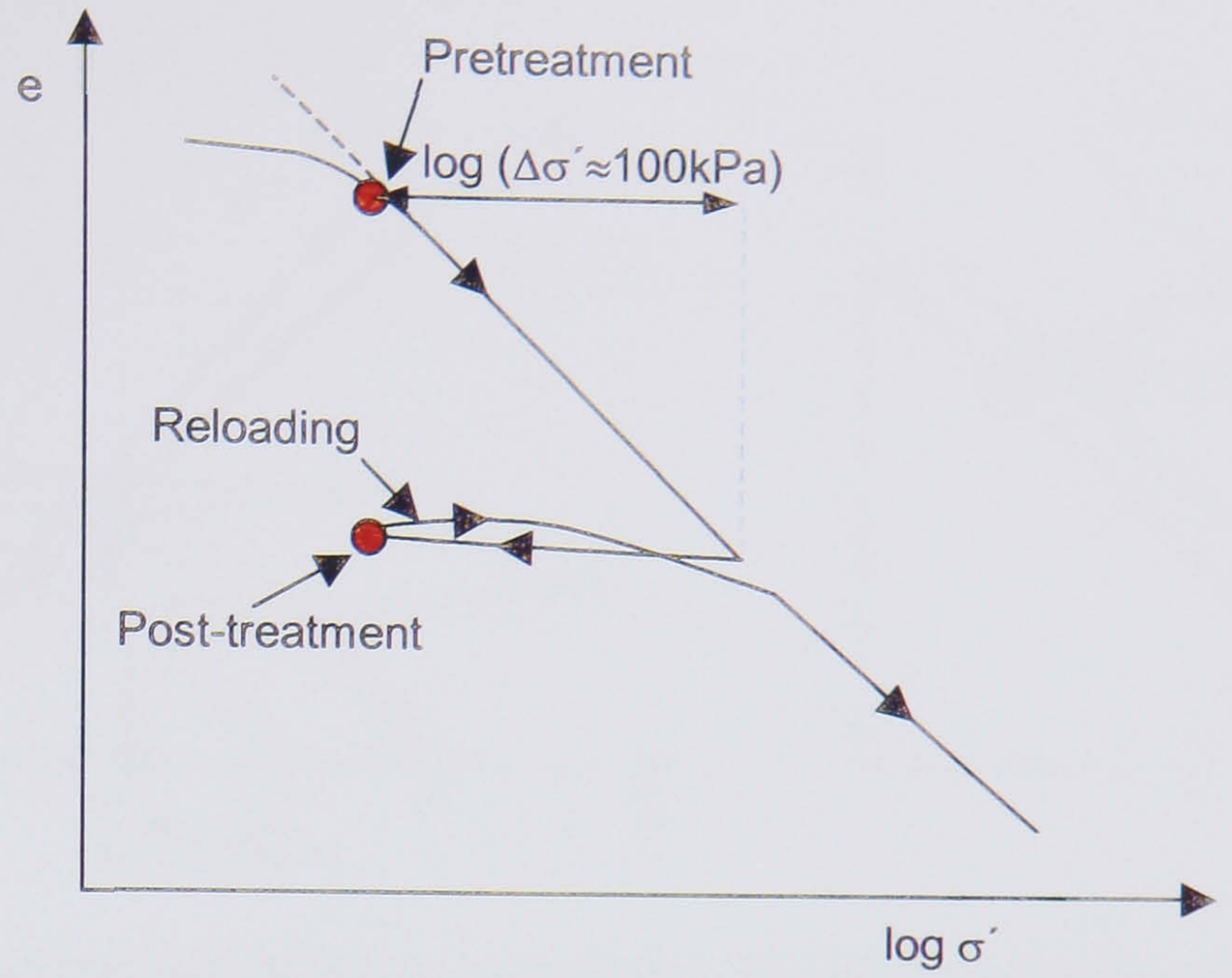

Figure 4.16 Void ratio versus effective stress for electro-osmotic consolidation

The same conclusion is evident when plotting in deviatoric stress ($q=\sigma_1-\sigma_3$) versus average mean effective stress ($p'=((\sigma_1+2\sigma_3)/3)-u$) and $ln\ p'$ versus specific volume ($v=1+e$) space as shown in Figure 4.17 for drained reloading and Figure 4.18 for undrained reloading and assuming isotropic hardening. Figures 4.17 and 4.18 also demonstrate the effect any chemical cementing of the clay particles, causing an increase in ϕ', would have upon the Critical State Line (CSL) by increasing its gradient M (Bishop 1971), indicating that the soil could withstand a greater deviator stress before failure. Casagrande (1983) presents experimental data for the change in grain size for quartz sand caused by electro-osmosis and evidence presented by Pugh (1999) shows a slight shift in the grain size distribution of kaolin subject to electro-osmosis.

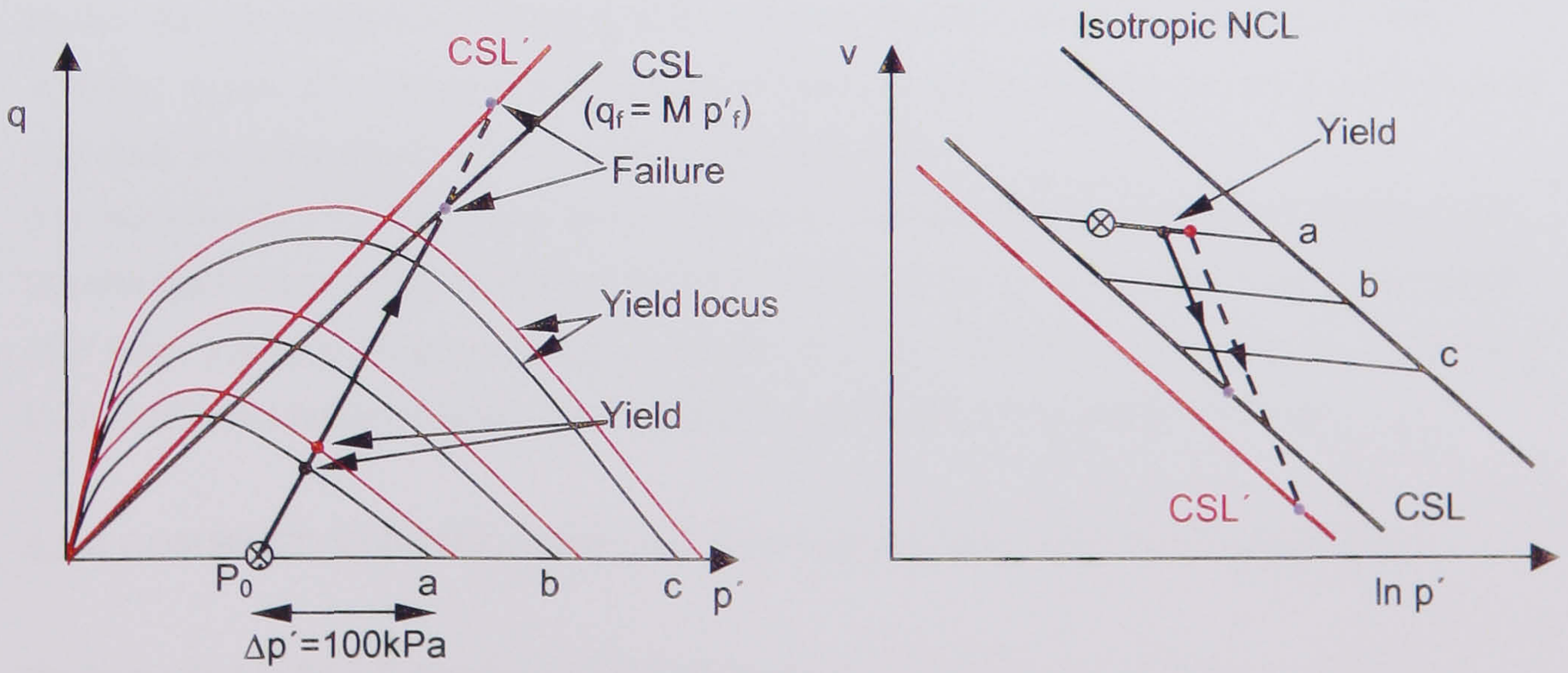

Figure 4.17 Drained reloading critical state model after electro-osmosis (After Powrie 1997, Roscoe & Burland 1968)

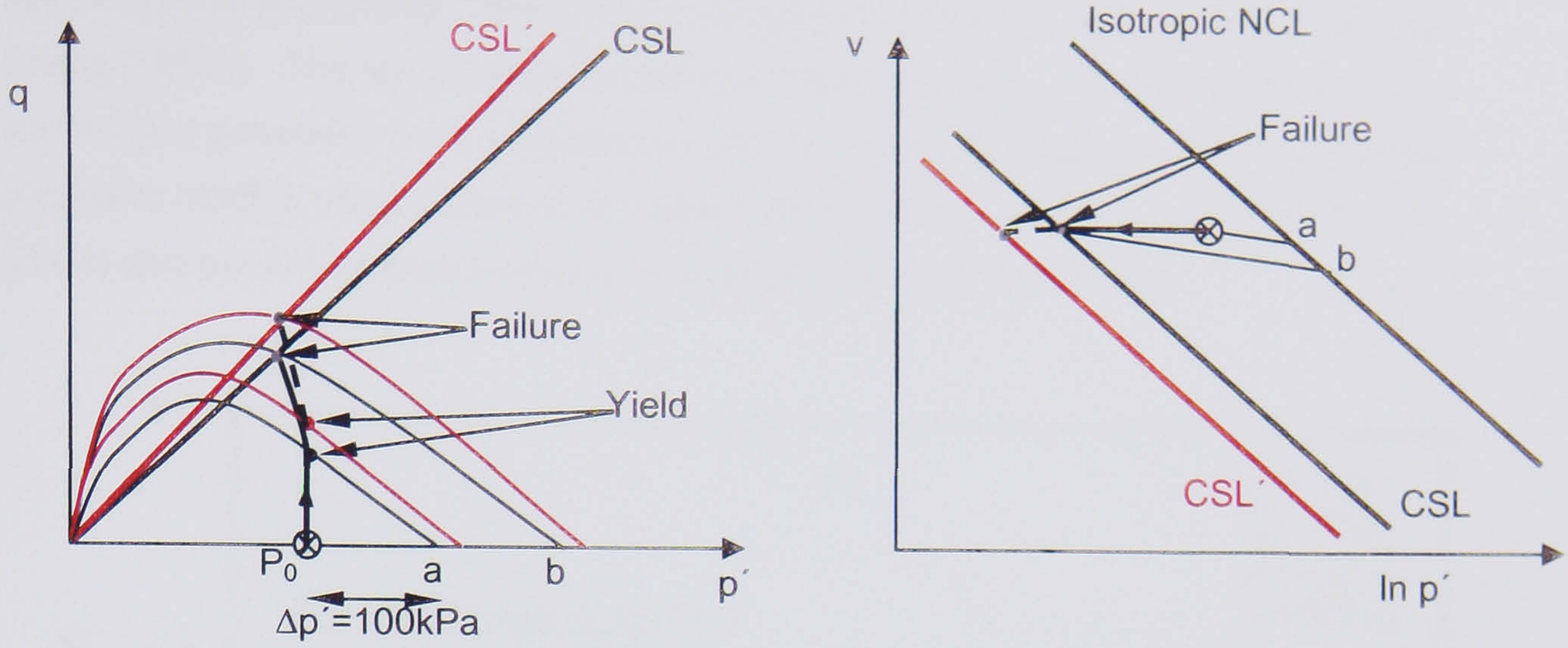

Figure 4.18 Undrained reloading critical state model after electro-osmosis (After Powrie 1997, Roscoe & Burland 1968)

From Figure 4.17 it is apparent that the electro-osmotically treated soil yields at a point on the yield locus defined by the additional effective stress imposed upon the soil by the application of electro-osmosis, point "a". Upon reaching the yield locus defined by "a" the rate of change of specific volume "v" in relation to the increase in p' dramatically increases until failure is reached on the critical state line (CSL). If a change in the grain size of the soil particles does take place during electro-osmosis, with an associated increase in the ϕ' of the soil then the yield loci and critical state line will be redefined as shown in red and by "CSL´" in Figure 4.17. The effect of this will be to cause yield at a higher load of p´ and failure on CSL´ at a higher deviator stress.

Figure 4.18 demonstrates the critical state model for undrained reloading. Again, because of the effective overconsolidation produced by electro-osmosis, the soil yields at a point defined by the yield locus applicable to an effective preconsolidation pressure of approximately 100kPa. Again, if a change in the value of ϕ' occurs in the soil the shape of the yield locus is changed, as is the position of the critical state line (CSL´)

It is important to note that in the design methods developed by the Author in Chapter 7 that the changes brought about by electrochemical cementing etc. (i.e. an increase in the value of ϕ' and c′) are not relied upon due to the difficulty in predicting their magnitude. This leads to an additional factor of safety in the designs undertaken using electro-osmosis.

4.2.4 COMBINED ELECTRO-OSMOTIC CONSOLIDATION AND SURCHARGING

As discussed in §4.2.2 electro-osmotic consolidation may be considered as an effective surcharge load for analytical purposes, however, electro-osmosis may be combined with conventional surcharging where electro-osmosis is used to induce an additional effective consolidation pressure to accelerate the dissipation of positive pressures.

Theories combining the two methods of consolidation have been presented by Wan and Mitchell (1976) and Shang (1998a) and a comparison of the two methods separately by Shang (1998b). The results obtained demonstrate that electro-osmosis combined with surcharging generates lower excess porewater pressures and that the excess porewater pressures reach a value of zero at an earlier time as shown in Figure 4.19. Hamir *et al* (2001) also presented experimental evidence confirming these findings.

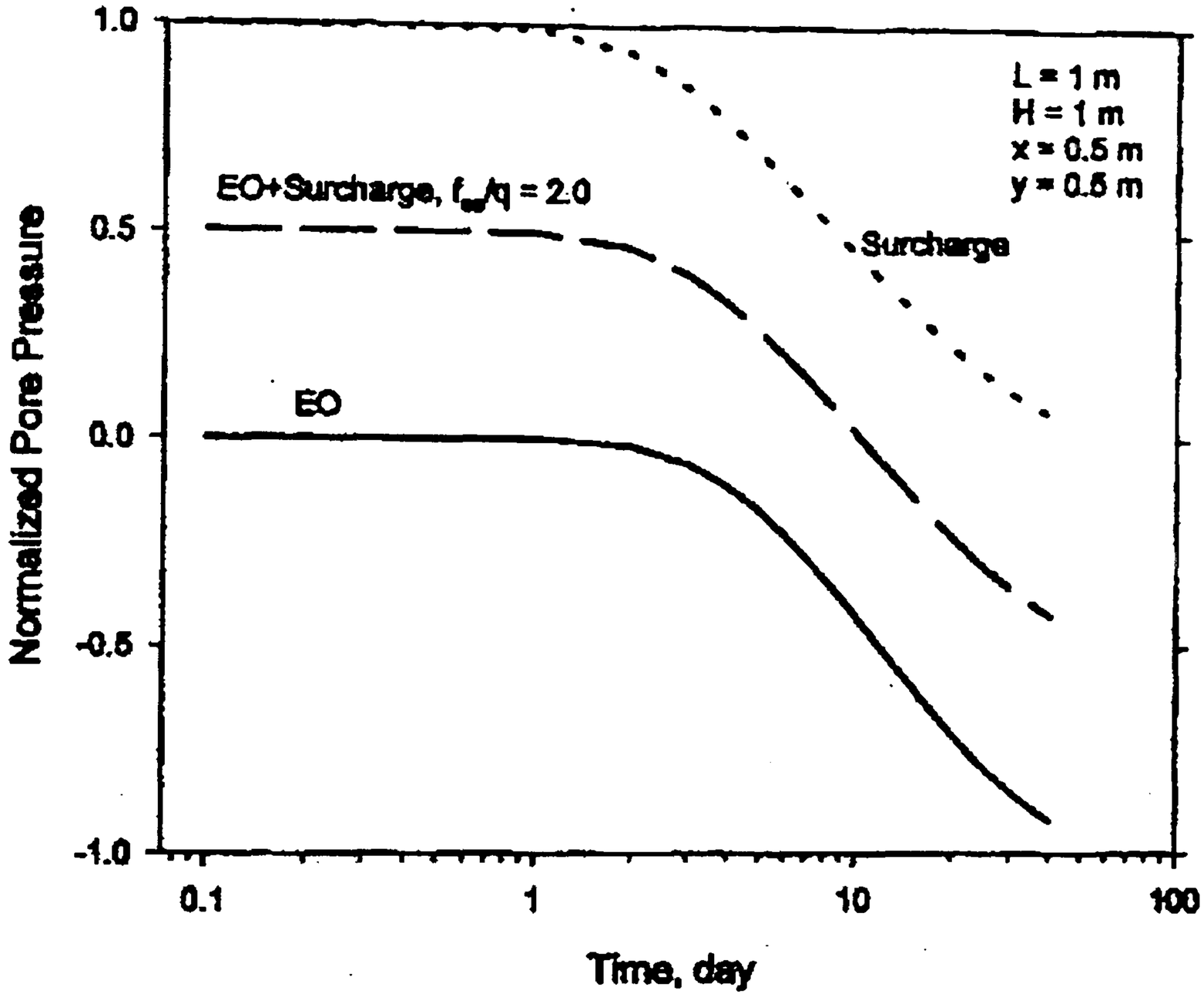

Figure 4.19 Development of excess porewater pressure against time (Shang 1998a)

The significance of this is that the factor of safety against bearing capacity failure is improved. It is also apparent from Figure 4.19 that after the positive porewater pressures induced by the surcharge loading have been dissipated, electro-osmosis continues to produce negative porewater pressures, causing further consolidation.

4.2.5 POLARITY REVERSAL

As demonstrated by Equation 4.1 the negative porewater pressures produced during electro-osmotic consolidation vary from a minimum at the anode, where the voltage is at a maximum, to zero at the cathode, where the voltage is zero. This non-uniformity of negative porewater pressure inevitably produces a variation in the amount of consolidation across the soil mass with an inherent variation in the undrained shear strength and stiffness parameters of the soil between the electrodes. In engineering practice this variation of the soil

parameters over such a small distance is seldom acceptable, as it is likely to cause differential settlement of any structure constructed on ground of this nature. A method of partially overcoming this variability is to reverse the polarity and drainage conditions of the electrodes. In doing so the soil near the cathode (new anode) is consolidated producing a more uniform consolidation of the soil between the electrodes. Figure 4.20 gives the results of moisture content reductions produced across a soil treated by electro-osmosis, with and without reverse polarity. It can be seen from this figure that polarity reversal produces a more uniform distribution of w_c and hence undrained shear strength, similar results for water content distribution after polarity reversal were also achieved by Jones & Shim (2001).

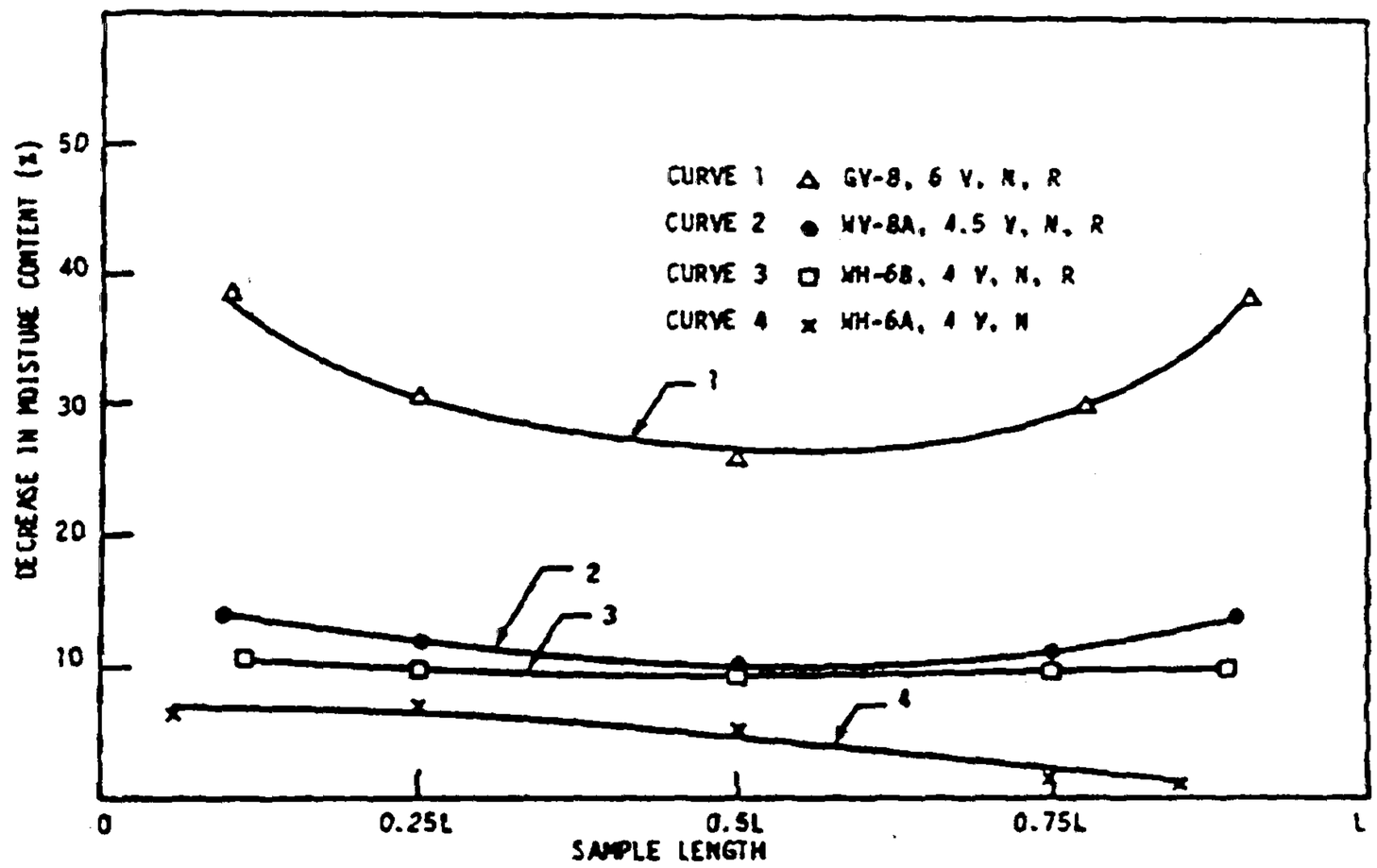

Figure 4.20 Variation in moisture content with and without reverse polarity (Lo *et al* 1991) (R= polarity reversal, N= normal polarity)

The negative porewater pressure produced by polarity reversal are independent of the first-stage consolidation undertaken (Wan and Mitchell 1976) and may be analysed using Equation 4.1 as shown in Figure 4.21.

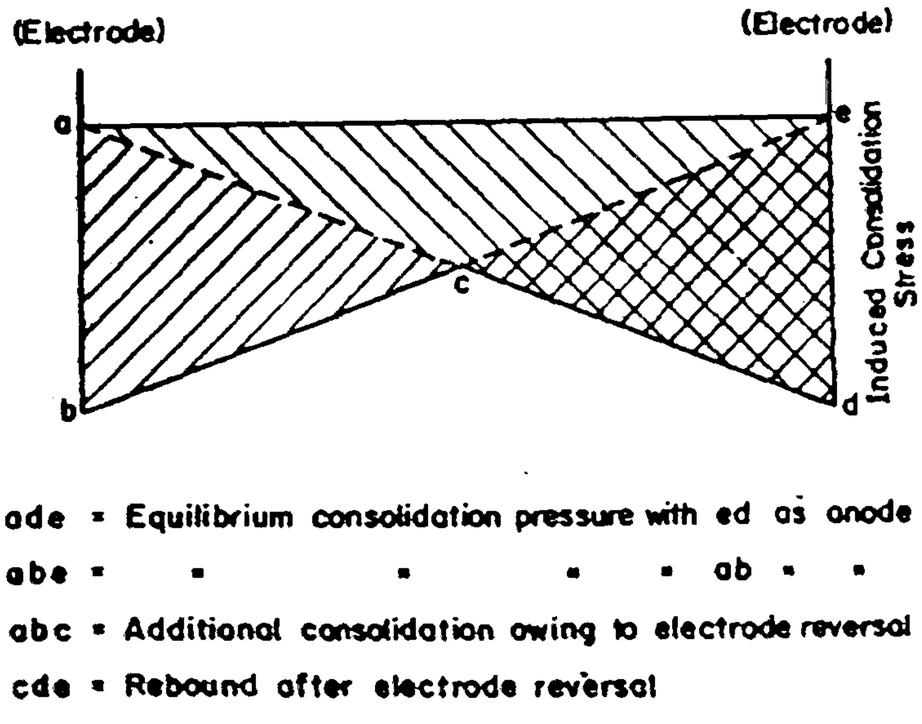

Figure 4.21 Stress distributions before and after polarity reversal (Wan and Mitchell 1976)

Theoretical studies carried out by Wan and Mitchell (1976) indicated that a large gain in effective stress might be achieved in a relatively short time by the doubling of the applied voltage after polarity reversal as shown in Figure 4.22. However, for practical field applications the doubling of the applied potential difference is unlikely to be feasible for safety reasons.

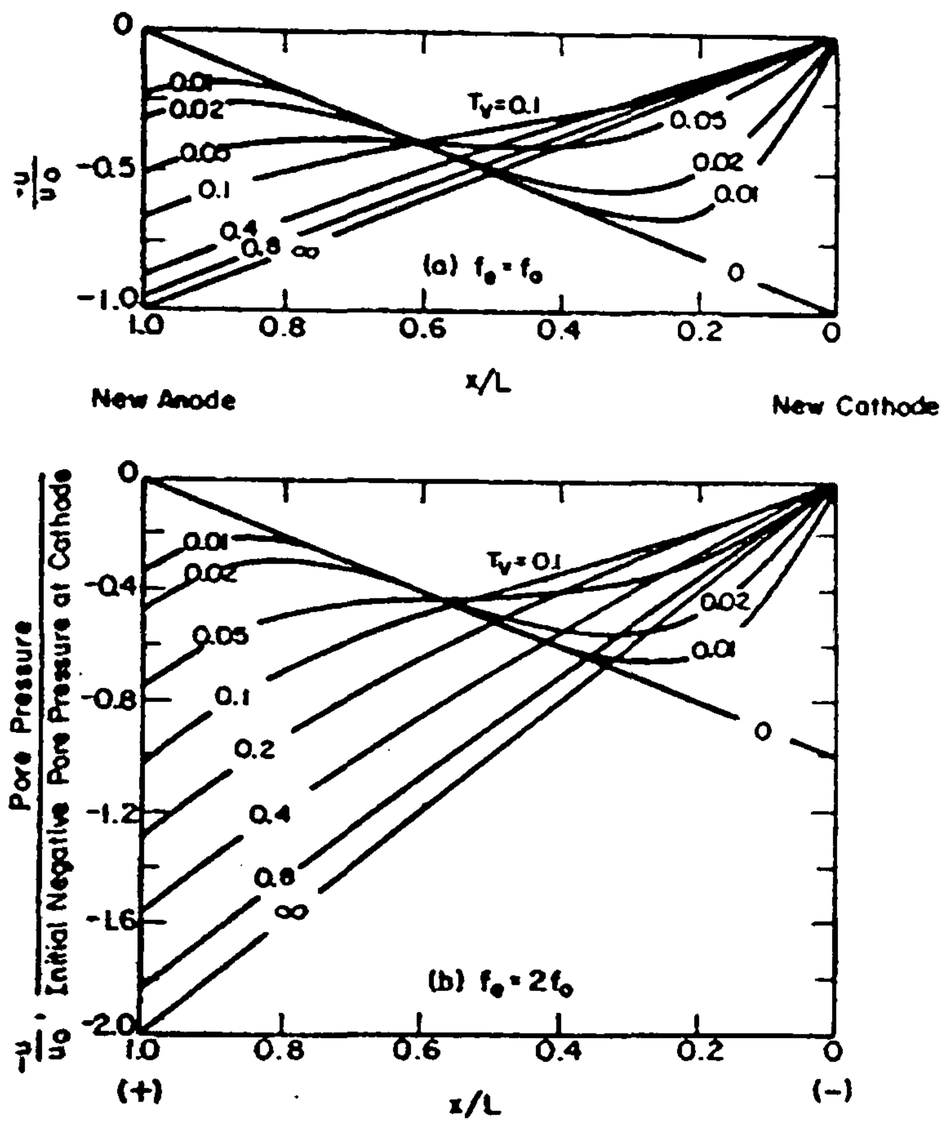

Figure 4.22 Pore pressure distributions during consolidation after electrode reversal for equal and double applied voltage (Wan and Mitchell 1976)

From examination of Figure 4.22 it will be seen that at time T_v=0.1, after polarity reversal with double the initial voltage, the negative porewater pressure generated is already equal to the minimum negative porewater pressure generated at the first equilibrium state. On reversal of polarity it can take some time for the water flow to be discernible at the new cathode and for observed settlement to continue, particularly if the water content of the soil at the original anode (new cathode) has been reduced to a very low level (Wrigley 1999).

The effect of polarity reversal on the efficiency of electro-osmotic treatment was also studied by Shang *et al* (1995). They concluded that the technique is viable for increasing the efficiency of the process, with the increase in efficiency being attributed to the reduction in the adverse electro-chemical reactions that can occur during electro-osmosis, as discussed in §2.7.5.5. This result was also found by Broš *et al* (1983) who temporarily interrupted the power supply to an electro-osmosis installation to allow for the redistribution of chemical species produced by the adverse electro-chemical reactions.

4.3 NEWBURN HAUGH CONSOLIDATION TRIAL - INTRODUCTION

Newburn Haugh is located on the northern bank of the River Tyne approximately 5km to the west of Newcastle upon Tyne, United Kingdom. The site is currently being developed by One North East (1NE), previously called English Partnerships, into a business park with the assistance of European Commission funding. The development principally consists of factory units to encourage new businesses into the area that, due to the closure of several industries in the area, has a high level of unemployment. The site was previously occupied by the coal fired Stella North Power Station, and the location where the field trial was carried out was an area of previous railway sidings and coal stockpiles. The purpose of the trial was to investigate the validity of the design methods developed by the Author presented in this chapter. The trial is documented in the paper by Pugh *et al* (2000).

4.3.1 SITE GEOLOGY AND GEOTECHNICAL CHARACTERISTICS

The general ground conditions for the site consist of recent made ground deposits generally associated with the now demolished power station, and interbedded sequences of cohesive and granular alluvium associated with the horizontal migration and development of the River Tyne. Quaternary fluvioglacial, lacustrine and glacial till underlie the alluvium deposits and overly the Carboniferous Middle Coal Measures, which have been previously worked by shallow mining techniques. The superficial layers that are pertinent to the electro-osmotic trial are given in Figure 4.23.

4.3.1.1 Laboratory Testing

From the previous site investigations that had taken place on the site several complete and partially used U100 samples of the cohesive alluvium were made available by WSP Environmental. Laboratory testing was undertaken on these samples in the form of, electrical conductivity studies, undrained triaxial tests and the determination of Atterberg Limits. Insufficient sample material was available to permit testing in the electro-osmosis cell. The results of the tests are presented in Table 4.4. The results presented in Table 4.4 fall within the soil acceptability criteria which were established during the research and are presented later in this thesis in § 7.2.

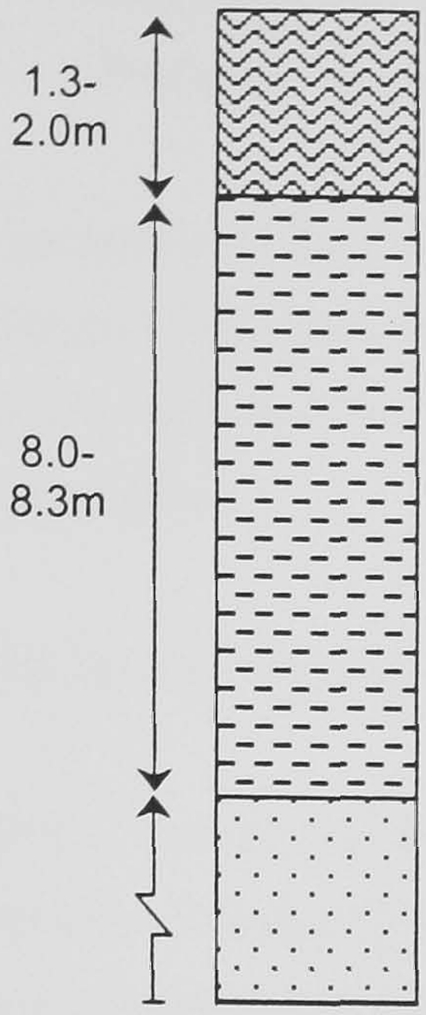

MADE GROUND - Grey black sandy gravely CLAY, gravel is fine to coarse angular to subangular and consists of brick, sandstone, concrete, slag and glass.

COHESIVE ALLUVIUM - Very soft to soft grey brown mottled slightly sandy occasionally organic CLAY of low to intermediate plasticity with occasional peaty bands and wood fragments.

GRANULAR ALLUVIUM - Medium dense grey brown speckled black slightly gravely SAND. Gravel is fine to medium subrounded and consists of siltstone and quartzite.

* Water table fluctuates between 0.2m and 1.6m BGL

Figure 4.23 Summary of stratigraphy within test influence zone

Table 4.4 Result of testing on Newburn Haugh U100 samples

Test	B.S. reference	Result
Atterberg Limits	BS 1377: 1990, Part 2	LL ≈ 48% PL = 15 %
Undrained shear strength (UUTXL)	BS 1377: 1990, Part 7	c_u =13 & 17 kPa
Electrical conductivity (Disk electrodes)	BS 1377: 1990, Part 3	0.025 S/m
Coefficient of volume compressibility (m_v)	BS 1377: 1990, Part 5	0.94 m^2/MN

4.3.1.2 In Situ Testing

The in situ characterisation of the trial area was undertaken to quantify the geotechnical parameters. The characterisation was carried out before the electro-osmosis trial to establish base line parameters and also assess the suitability of the site for treatment by electro-osmosis. Additionally, previous site investigations had been undertaken on the site for the purpose of geotechnical design for the proposed redevelopment of the power station site, and these reports were made available to the Author.

To quantify the soil parameters for the cohesive alluvium, the stratum to be treated by electro-osmosis, the following in-situ tests were undertaken:

- Dynamic Probe Heavy (DPH)
- Marchetti Dilatometer (MDMT)
- Full displacement Pressuremeter (FDPM)

The details of each can be found in Pennine (1988), Briaud & Miran (1992) and Houlsby & Withers (1988) respectively. Additionally, the Author was also given access to undisturbed (U100) samples that were surplus to the geotechnical testing from a previous site-wide site investigation.

The purpose of the three investigation methods employed was the following:

DPH:- To ascertain the depth of the made ground and additionally the depth at which the transition between the cohesive and granular alluvium took place. The DPH was also undertaken at each electrode location, initially to locate the exact depth of the cohesive/granular transition and secondly to produce a pilot hole to facilitate the subsequent installation of the EKG into the ground by means of driving with the DPH apparatus and a modified driving shoe. Additionally, although the DPH is a far from ideal test method for establishing stiffness and strength parameters it was possible to convert the DPH blow count into an equivalent Standard Penetration Test (SPT) N-value using the correlations proposed by Chan & Chin (1972) and Leach & Row (1995). From these equivalent SPT N-values an estimation of the undrained shear strength (c_u) could be made using the correlations suggested by Stroud (1975) and the plasticity index. Subsequent transformation of c_u into E_u using the relationships suggested by Bowles (1988) could not be justified due to the crudity of the test method.

MDMT:- Using the correlations suggested by Briaud & Miran (1992) and Schmertmann (1986) the values of undrained shear strength (c_u) and dilatometer modulus (E_D) were obtained and hence the undrained elastic modulus (E_u), assuming an undrained Poisson's ratio (ν) of 0.5 (Bowles 1988).

FDPM:- Using the correlations proposed by Houlsby & Wither (1988) and assuming an undrained Poisson's ratio (ν) of 0.5 the values of c_u and shear modulus (G) were calculated and hence E_u for an unload-reload cycle.

The results in terms of undrained shear strength (c_u) for the DPH, based upon a clay of low-intermediate plasticity, for the MDMT and the FDPM are presented in Figure 4.24.

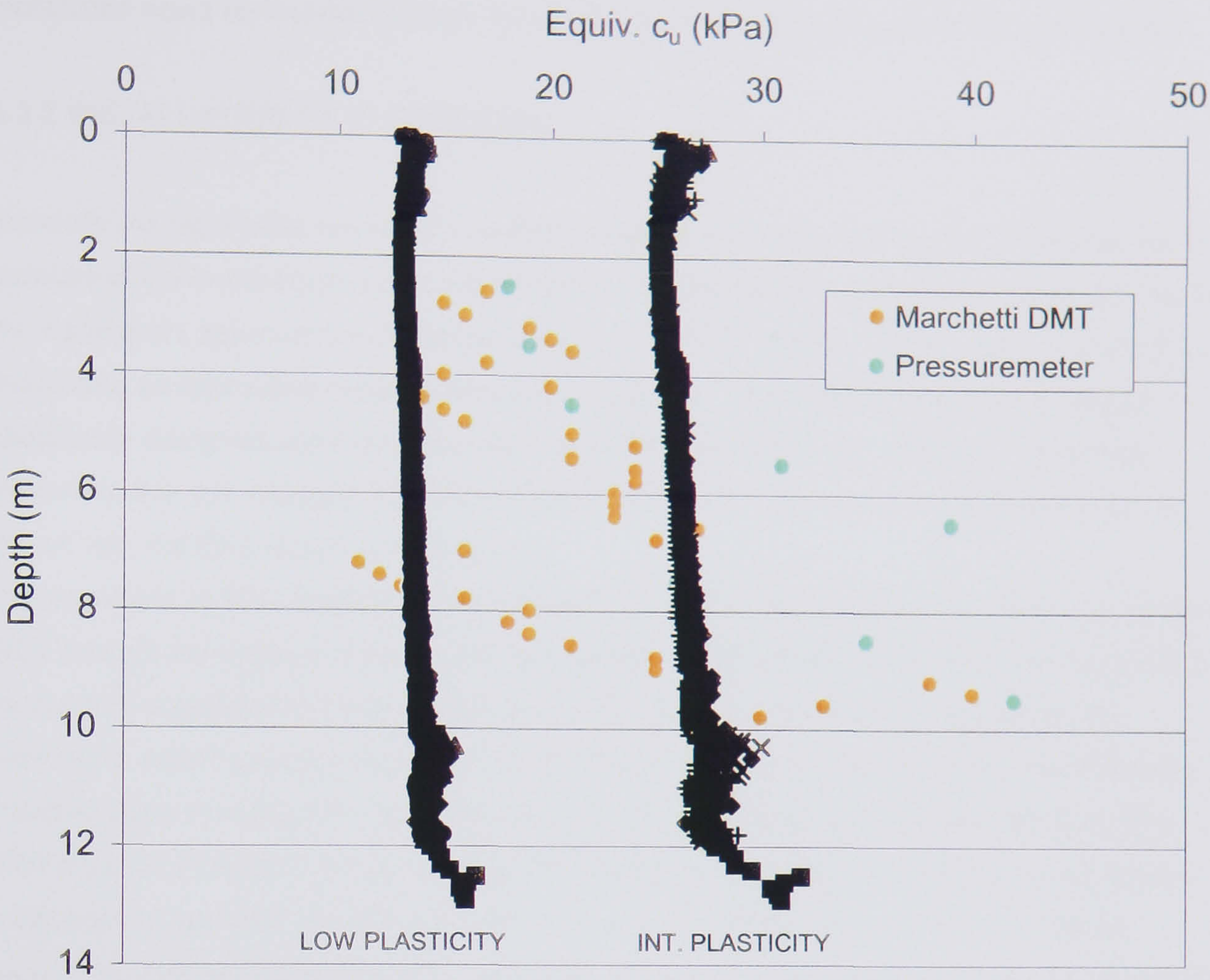

Figure 4.24 Variation of c_u measured in situ by MDMT, FDPM and DPH

As will be seen from Figure 4.24, the undrained shear strength of the cohesive alluvium generally lies in the range of 10-25 kPa from a depth of ≈ 2 - 10 m b.g.l.

4.3.1.3 Conclusions Of Pre-Trial Testing

The pre-trial laboratory testing indicated that the cohesive alluvium should be amenable to treatment by electro-osmosis as the results fell within the acceptability criteria established, presented later in § 7.2. Additionally, the in-situ testing undertaken on the site also gives results for the value of c_u that appear to be in the range of acceptable values given in Table 7.11.

The unknown variables in the testing regime are the parameters of the made ground, due to a lack of availability of samples for testing in the laboratory, and due to the presence of brick and concrete it was not possible to test in situ with the MDMT or the FDPM. Ideally, this material would be isolated from the alluvial clay by insulating the electrode through the made ground and sealing it so that water cannot enter the electrodes sideways or from above and possibly re-circulate. Additionally, there is the risk of short-circuiting through the made ground if its macrofabric comprises continuous courser grained layers and an electrolyte of

higher conductivity than the conductivity of the clay (0.025 S/m) (Caron 1971a & b). The electrodes could be isolated through the made ground by encasing them in plastic piping.

4.3.2 INSTALLATION OF ELECTRODES

Normally the electrodes would be installed by means of a wick drain lance. However, for the purpose of the small-scale trial it was not economically viable to mobilize this item of plant for the installation, approximate mobilization cost of £10,000 (Pedley 1999). Hence, the Author developed an alternative cheaper installation method. The method consisted of using a specifically designed and manufactured oversized dynamic probe cone that, while been driven into the soil, dragged the EKG electrode behind it. The specially designed cone is shown with the EKG attached in Plate 4.1.

The drawback of this installation method was that it was not possible to insulate / isolate the EKG through the made ground as the hole formed by the driving of the cone quickly closed up due to the presence of water and due to the vibrations produced. Thus, it was not possible to install a plastic tubing around the EKG. The driving records obtained using the modified cone showed little correlation with the driving records produced by the pilot hole DPH drive. Additionally, it was found to be necessary to prebore through the made ground using a large diameter window sampler to allow the modified driving cone to be driven. Installation depths of between 5.5m and 9.3m were achieved. The EKGs were installed with the Terram filters in place, as due to the open structure of the polymeric grid it was likely to snag during driving, (Plate 4.2). The electrode length was marked on the filter to allow its progress during driving to be monitored.

4.3.3 DESIGN OF ELECTRODE LAYOUT

The electrode layout was designed to ensure that if electro-osmosis was to be suitable to the site then the electrode layout would demonstrate this using a minimal number of electrodes to reduce installation/manufacturing costs. The electrode layout adopted consisted of two centrally located anodes surrounded by six cathodes. Additionally, with the central anodes being surrounded by cathodes the drainage paths were reduced such that the installation should demonstrate improvement results within a short period of time. The electrode layout is shown in Figure 4.25.

Each EKG was individually connected to a power supply cable using a double crimped stripped connection, see §3.5.6 for details of the connection method, as shown in Plate 4.3.

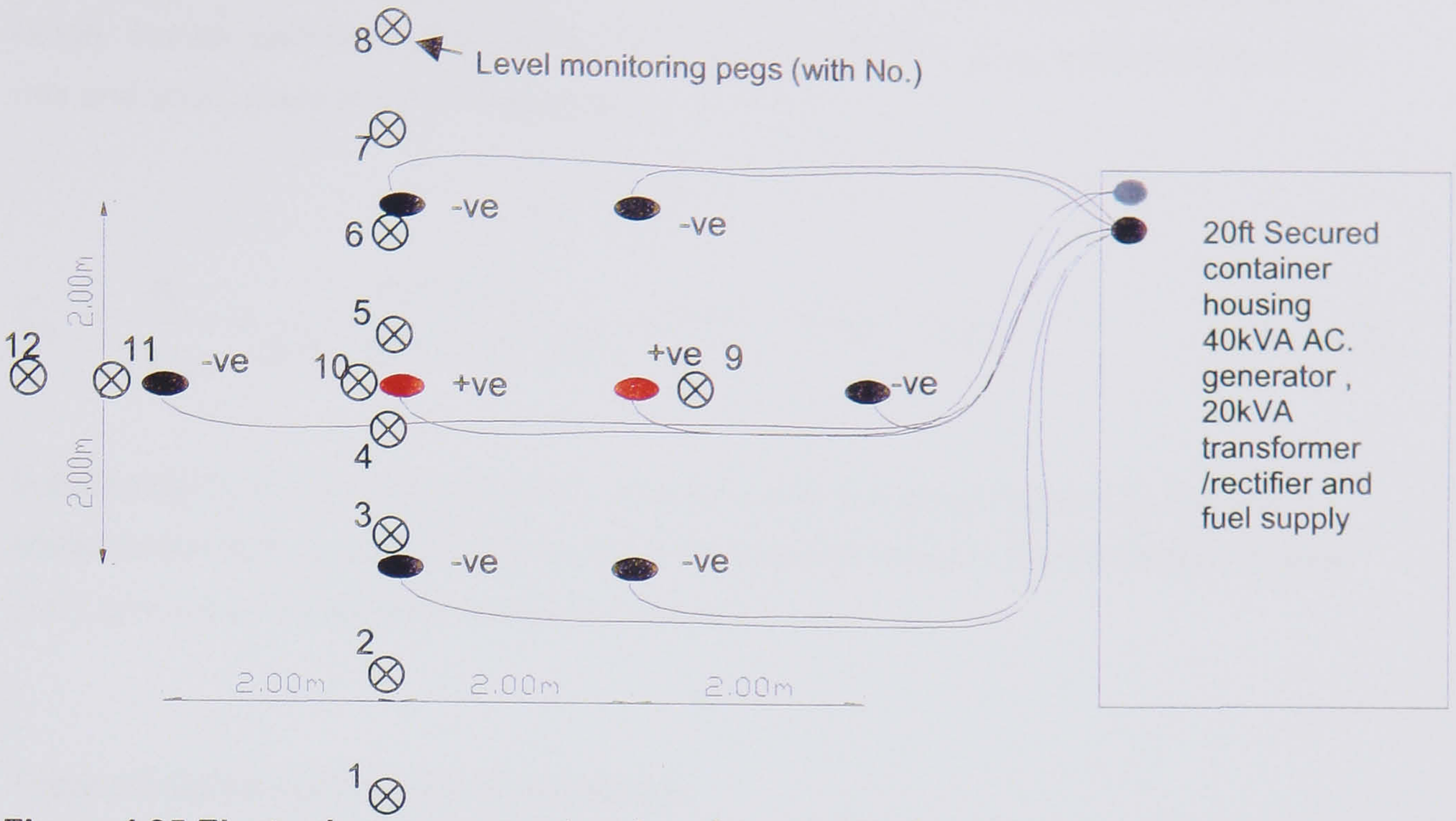

Figure 4.25 Electrode arrangement and surface monitoring peg layout

4.3.3.1 Anticipated Settlement

Based upon the value of volume compressibility (m_v) obtained from laboratory testing and correlating the undrained shear strength (c_u) with the coefficient of volume compressibility using the relationship suggested by Carter (1983). The anticipated range of values for m_v for the cohesive alluvium was 0.8-2.0 m^2 / MN. Based upon these values and the theory developed in §4.2.2 assuming a closed anode and open cathode the minimum pore water pressure developed at the anode positions is -100kPa which varies to 0kPa at the cathode positions.

At anode $\left(u = -100\ \text{kPa} \therefore \Delta\sigma' = 100\ \text{kPa}\right)$

Assuming clay thickness = 8.0 m and lower bound $m_v = 0.8\ m^2/MN$

$$\delta_{max} = m_v \Delta\sigma' h = 0.8 * 10^{-6} * 100 * 10^3 * 8.0 = 0.64m \qquad \text{Eqn. 4.11}$$

Hence, the settlement profile should vary from approximately 640 mm at the anode positions to 0mm at the cathode positions. The made ground is assumed to be incompressible and not susceptible to treatment by electro-osmosis.

The rate of settlement can be calculated in accordance with the theory given in §4.2.2.2 assuming a 1 - Dimensional field and closed anode and open cathode. Initially calculating the time factor (T_v) by assuming the hydraulic permeability (k) for the clay is in the range of 10^{-11} - 10^{-9} m/s (Carter & Bentley 1991) which due to the soft nature of the clay and its

slightly sandy particle size distribution it is probably at the higher end of this permeability range. Hence, calculating the coefficient of consolidation (C_v) using a permeability of 10^{-9} m/s and an m_v value of 0.8 m^2/MN gives:

$$C_v = \frac{K}{m_v \gamma_w} = \frac{10^{-9}\,m/s}{0.8 * 10^{-6} * 10 * 10^{-3}} = 1.25 * 10^{-6}\,m^2/sec \qquad \text{Eqn. 4.12}$$

Substituting C_v into the equation for T_v (Equation 4.8) and using Figure 4.14 the rate of consolidation may be calculated where *d* is the distance between the anode and cathode (2m), giving the results summarised in Table 4.5.

Table 4.5 Estimation of rate of settlement

T_v	% Consol.	δ surface (mm)	t (days) k =10^{-9}m/s, m_v =0.8 m^2 /MN	t (days) k = 10^{-10}m/s, m_v =0.8m^2/MN
0.045	10	64 mm	2	16
0.3	50	320 mm	11	111
1.0	90	576 mm	37	370

Using the results presented in Table 4.5 it is obvious that, for a treatment time of 2 weeks, a settlement at the ground surface should be recorded regardless of the hydraulic permeability of the soil, due to the soft nature of the clay and its large coefficient of volume compressibility.

4.3.3.2 Estimation Of Current Demand

Due to the lack of available soil samples, it was not possible to undertake laboratory electro-osmosis cell tests on the alluvial clay. As such, an estimation of current demand is difficult to undertake. Recourse may, however, be made to the equation presented by Casagrande (1983), presented here as Equation 4.13.

$$I_t = ncs\,\sigma\frac{E}{L} \qquad \text{Eqn. 4.13.}$$

Where:

I_t = Total current required for installation

n = No. of electrode pairs energized

c = Efficiency factor (2 Anode/cathode ≈ 0.8-0.9,)

s = Embedded surface area of electrode (cm^2)

σ = Electrical conductivity of soil being treated S/cm

E = Voltage applied in field (Volts)

L = Distance from anodes to cathodes (cm)

Assuming:

(i) That the number of electrode pairs is 4 (6 cathodes / 2 anodes) and that the efficiency factor is 0.8.

(ii) That all of the surface area of the electrode in effective, i.e. both vertical and diagonal elements carries current.

(iii) The electrical conductivity obtained from the laboratory sample is applicable.

(iv) The applied voltage is 40V with an anode-cathode spacing of 2 m.

$$I_t = 4 * 0.8 * 170066 * 0.2527 * 10^{-3} * \frac{40}{200} = 2.76 Amps$$

This value was thought to be an under estimation of the current that would be drawn by the installation as the value of the electrical conductivity was obtained from a partially unsealed U100 sample that was several months old and as such had undergone some degree of desiccation and would thus give a lower value for the electrical conductivity. The drop in current with treatment time would be anticipated to be of the order of 66% (Casagrande 1983 & Wrigley 1999). Although work undertaken by the Author would suggest a reduction of the order of 95%, see § 5.7.4.4 and § 5.7.8.2.

A more sophisticated analysis of the installation could have been undertaken using the finite difference technique discussed in § 7.6.2. However, due to the lack of soils data it was not considered worthwhile to use a more sophisticated power estimation, due to the increased calculation time required and the lack of additional accuracy. It is also noteworthy that the resistance path analysis method discussed in § 7.6.1 is not capable of analysing the installation accurately without significant modifications, due to the non-square installation pattern of the electrodes and unequal number of anodes and cathodes.

4.3.3.3 Monitoring

The installation was monitored before, during and after the powered treatment phase for several variables.

- Fuel consumption - monitored by means of registering the quantity of fuel added and the generator time at which it was added.
- Surface settlement - measured by means of a digital level (Wild NA2000) referred to a Temporary Bench Mark (TBM) located on a concrete retaining wall to an accuracy of 0.1 mm using 0.5 m long re-bars hammered into the ground at the positions shown in Figure 4.25.
- Electrical Voltage & Current - measured by means of analogue dials in the power supply container.

4.3.4 RESULTS OF MONITORING

4.3.4.1 Fuel Consumption

The fuel consumption of the generator is shown in Figure 4.26 against the generator running time. This graphic was calculated based upon the cumulative quantity of gas oil added to the generator fuel tank during the trial. The average fuel consumption for the trial was approximately 1.4 litres/hour

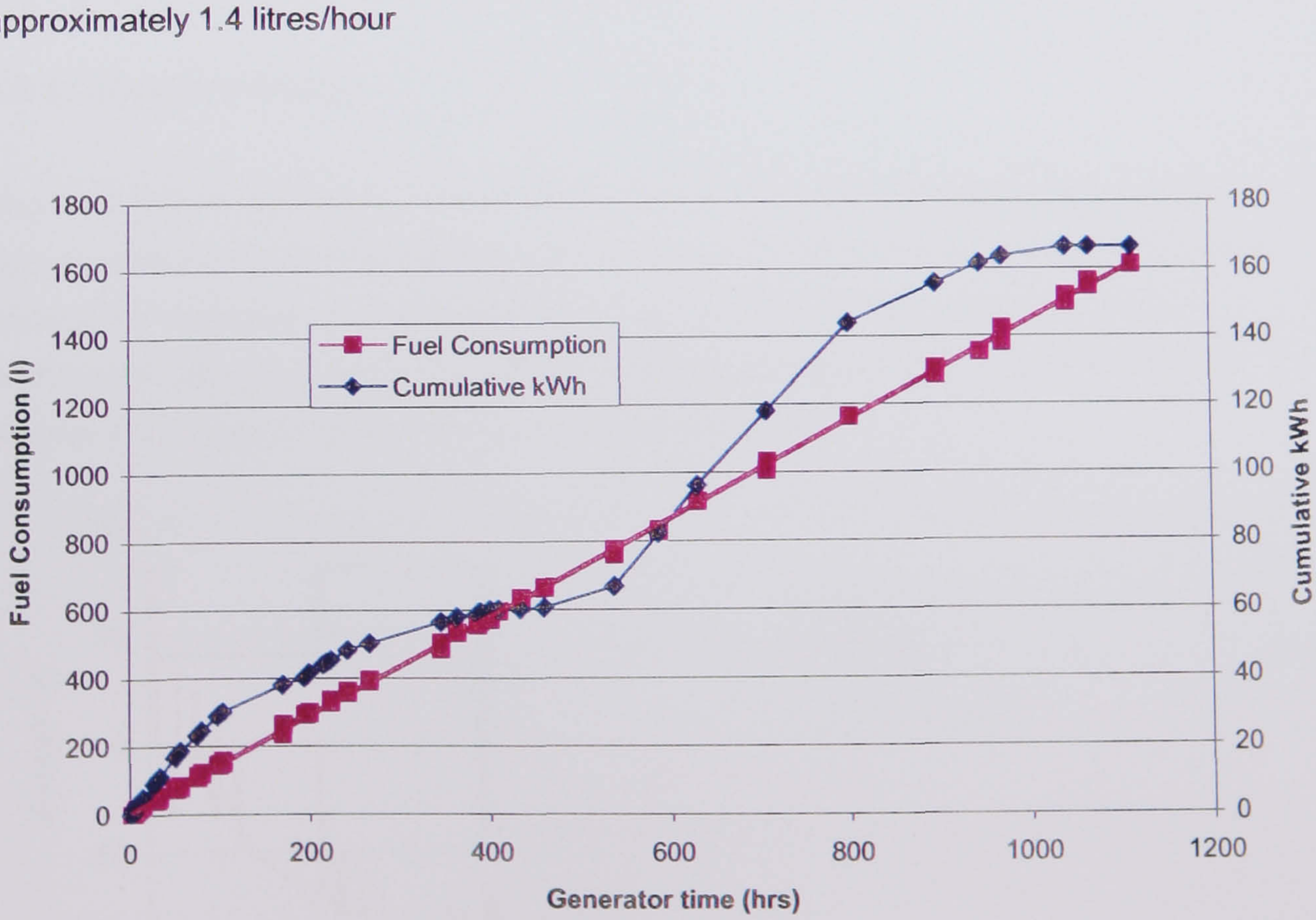

Figure 4.26 Cumulative fuel consumption against time

4.3.4.2 Surface Settlement

The results of the levelling of the surface settlement pegs is presented in Figure 4.27 using the peg numbering system given in Figure 4.25. The level of the peg is presented against generator run time. Plate 4.4 shows the measurement of the pegs in the field.

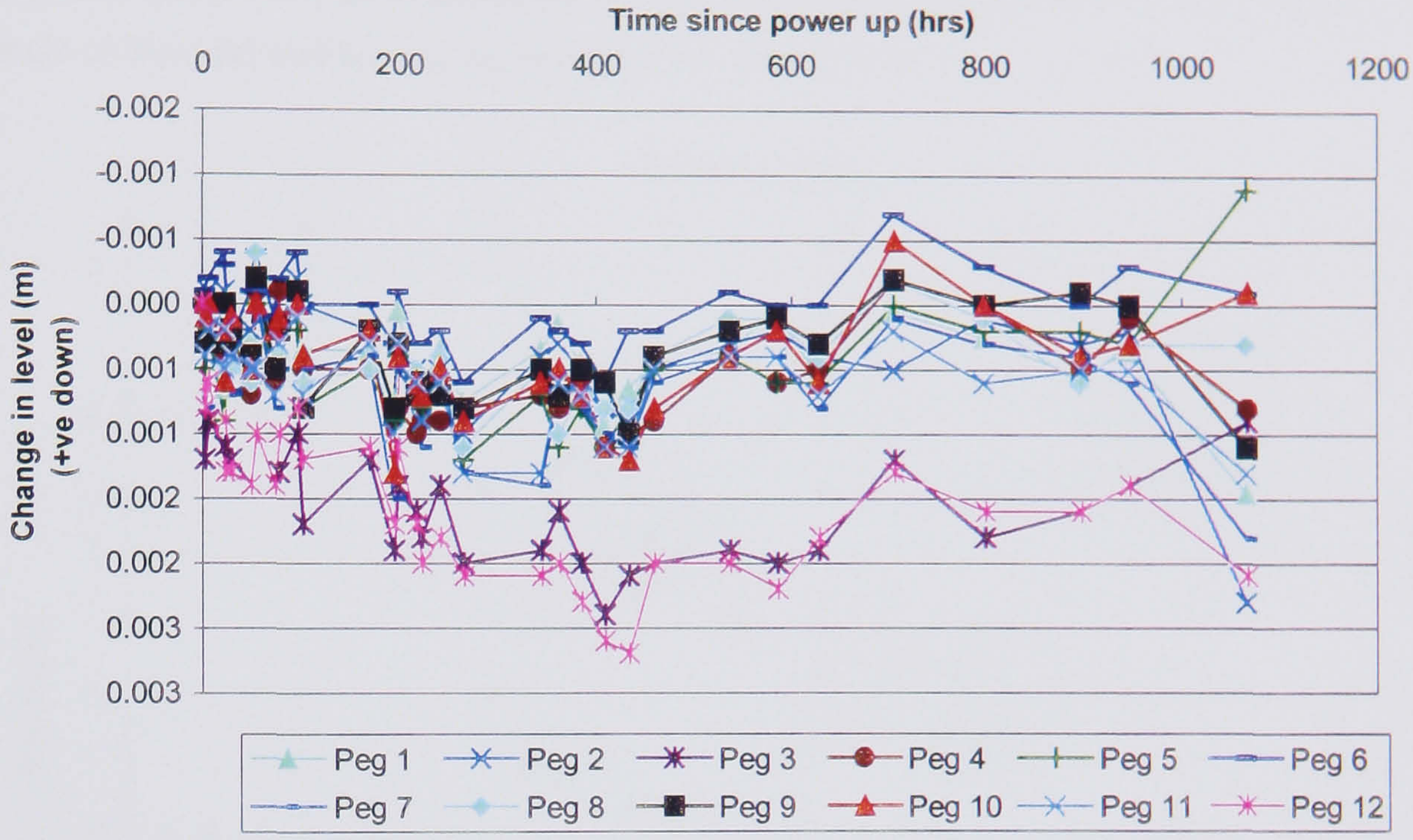

Figure 4.27 Results of surface monitoring pegs

4.3.4.3 Electrical Energy

The electrical voltage and current drawn by the installation is presented in Figure 4.28. It was decided during the trial that the applied voltage should be increased to 80 V after the current had decreased to approximately 80% of its initial value to assess the effect. Additionally, after the current had declined to zero amps the polarity was reversed in an attempt to produce a more uniform treatment of the area.

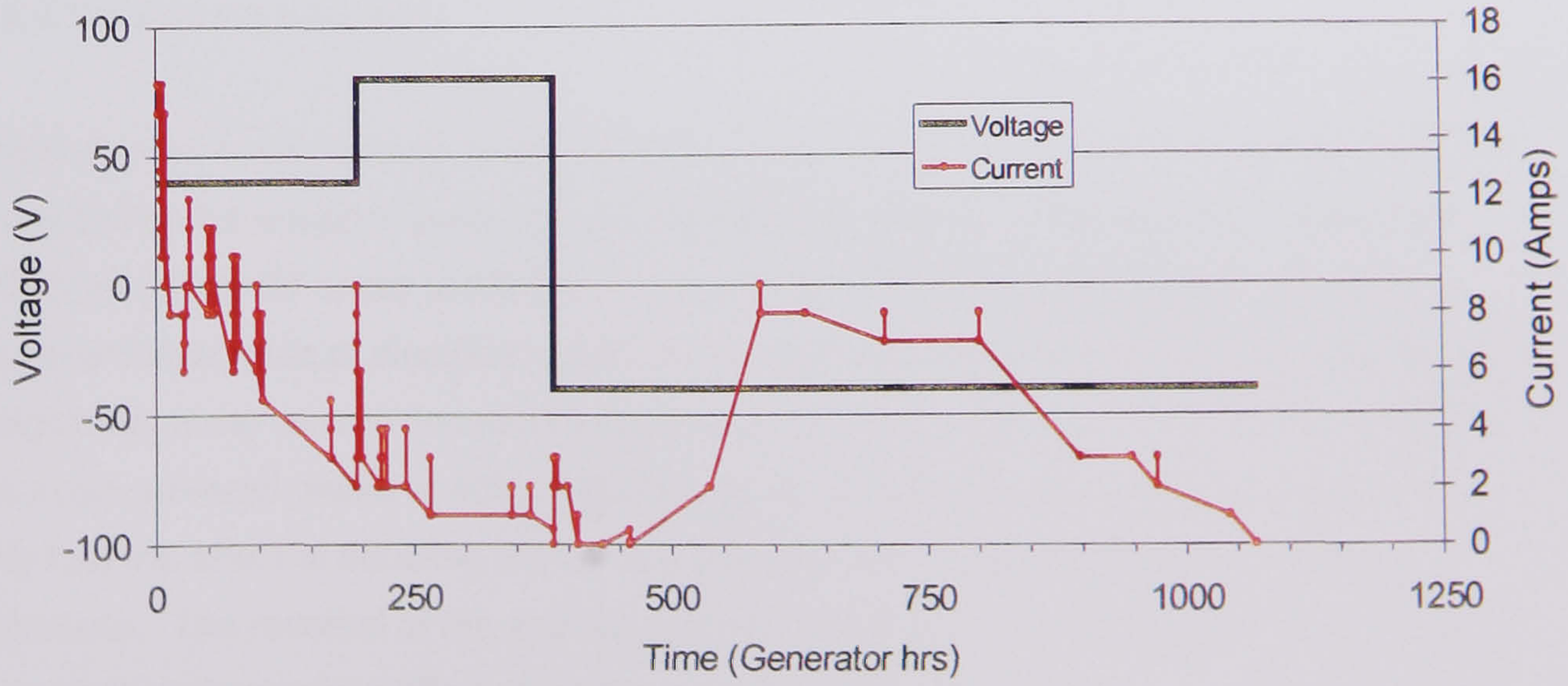

Figure 4.28 Electrical current & voltage against generator time

4.3.4.4 Post Trial In Situ Testing

To confirm if the electro-osmotic treatment had been effective, or not, a second phase of in situ testing was undertaken to assess if any change in the measured values of c_u and E_u could be ascertained. The test methods (MDMT) and apparatus used were identical to those utilised for the pre-trial testing to minimise any errors in the interpretation of the results. The results of the post-trial testing are presented in Figure 4.29.

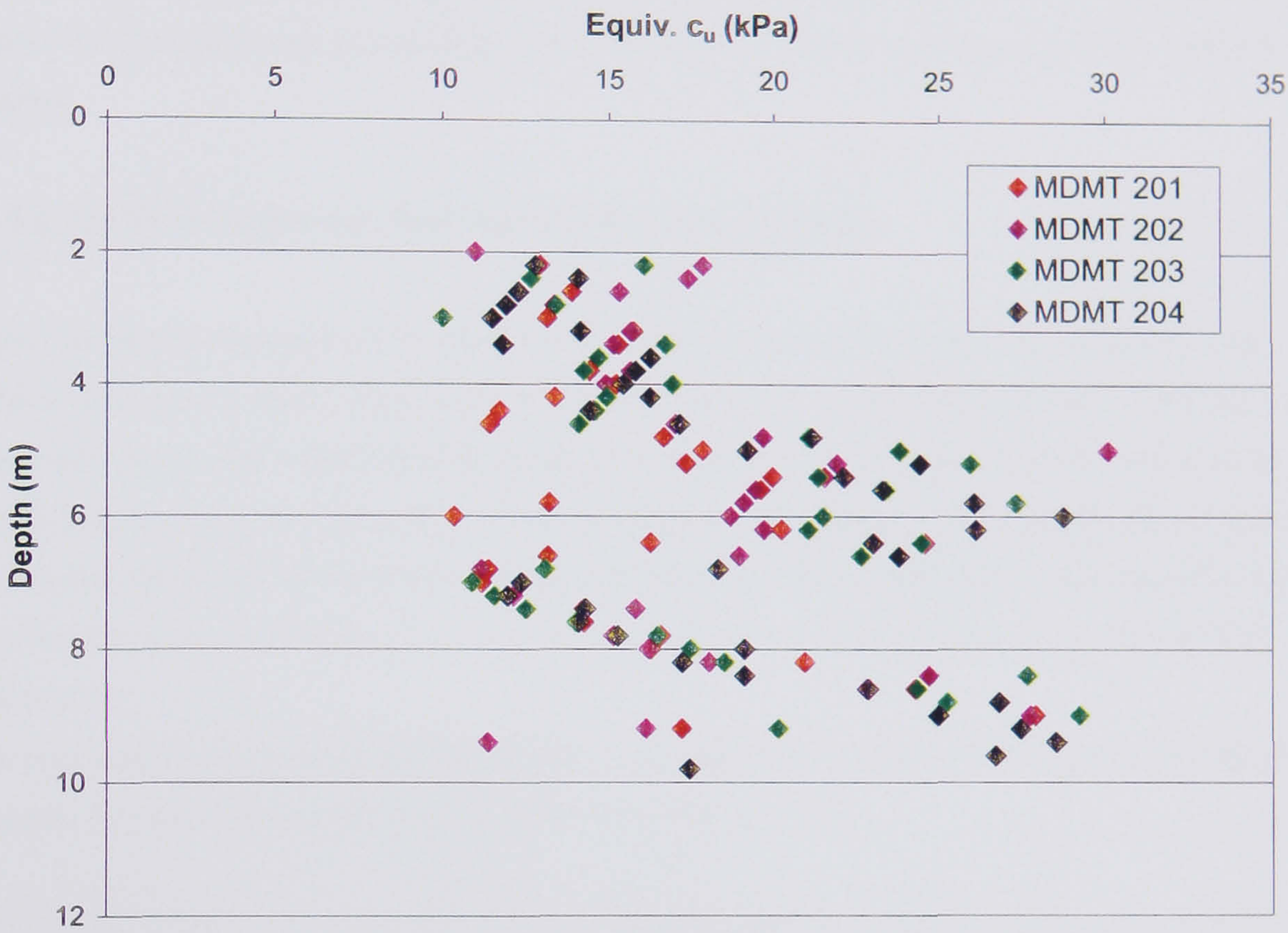

Figure 4.29 Results of post trial in situ testing

4.3.5 INTERPRETATION OF RESULTS OF THE NEWBURN HAUGH TRIAL

4.3.5.1 Electrical Energy

The electrical energy drawn by the installation was of the same order of magnitude as that predicted by the equation presented by Casagrande (1983). However, the Casagrande (1983) equation did under predict the current drawn, probably as a result of the non-representative value of electrical conductivity obtained from the U100 sample. The order of magnitude of the current decrease with time of the installation was of the order of 85% for the initial powered phase at 40V. The subsequent doubling of the applied voltage to 80V only had the effect of doubling the current drawn in accordance with typical Ohmic behaviour. The reversal of the applied potential difference after a treatment time of 382 hours had no immediate effect upon the current drawn. The effect of the voltage reversal was noted by an increase in the current drawn approximately 150 hours after the reversal of

voltage had taken place with the current showing an initial decrease from 2 Amps to 0 Amps, followed by an increase up to 8 Amps and then a subsequent decrease to 0 Amps again at which time the trial was powered off. The delay in the power drawn by the installation has been observed by several researchers, Lo *et al* (1991a) and Eggestad & Føyn (1983). The reasons suggested for the delay are the wetting up of the desiccated soil in the region of the new cathode before full electrical flow is re-established. Additionally, the Author suggests that the redistribution of the chemical species that have been differentiated by the electro-osmosis process as observed by Acar *et al* (1990), Grey & Somogyi (1977) and Sprute & Kelsh (1975) contributes to the delay demonstrated by the electrical current after polarity reversal.

4.3.5.2 Surface Settlement And Undrained Shear Strength

From the results presented in Figure 4.27 it is apparent that the response of the ground surface was not as anticipated, with the monitoring pegs demonstrating both settlement and expansion of the soil mass over the treatment time with no discernable trend towards an overall settlement of the ground surface as would be anticipated. Additionally, the maximum movement recorded over the test period was less than 3 mm settlement, significantly less than the 64 mm calculated in § 4.3.3.1 and presented in Table 4.5 for a low permeability assumption.

The post trial in situ testing demonstrated no discernable increase in the undrained shear strength of the cohesive alluvium, as shown in Figure 4.30.

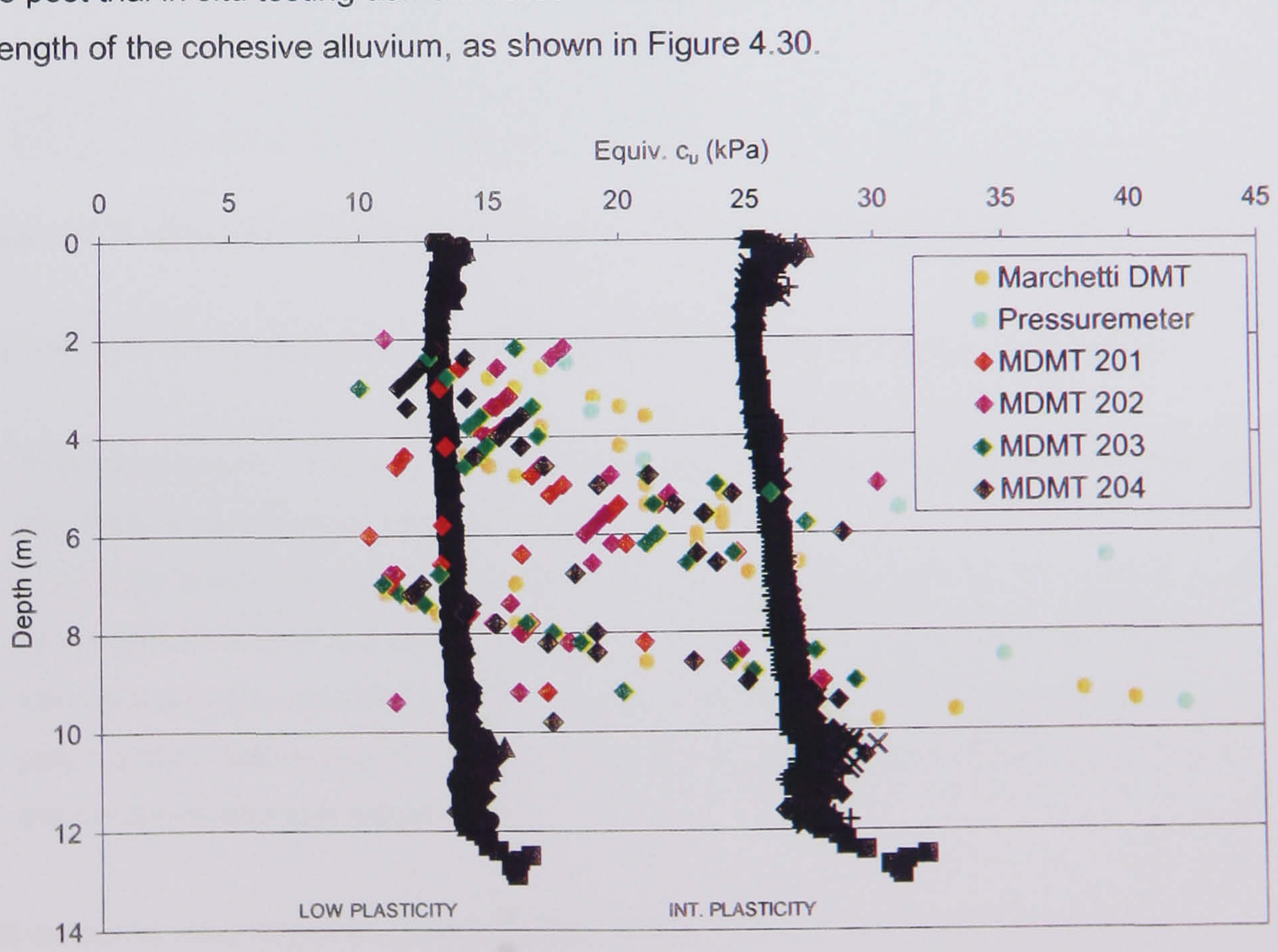

Figure 4.30 Interpretation of in situ testing

The only rational supposition that may be drawn from these results is that the electro-osmotic treatment did not have the desired effect on the cohesive alluvium, in terms of increasing the undrained shear strength and causing a settlement of the ground surface, although the results of the electrical energy consumption, Figure 4.28, demonstrates a trend commensurate with a successful treatment process. These findings may be explained if the macrofabric of the made ground overlying the cohesive alluvium is considered to contain granular layers that permit the passage of water between the anode and cathode positions at a greater velocity than through the cohesive alluvium, i.e. essentially short-circuiting the electro-osmosis treatment process. As demonstrated in Figure 4.31.

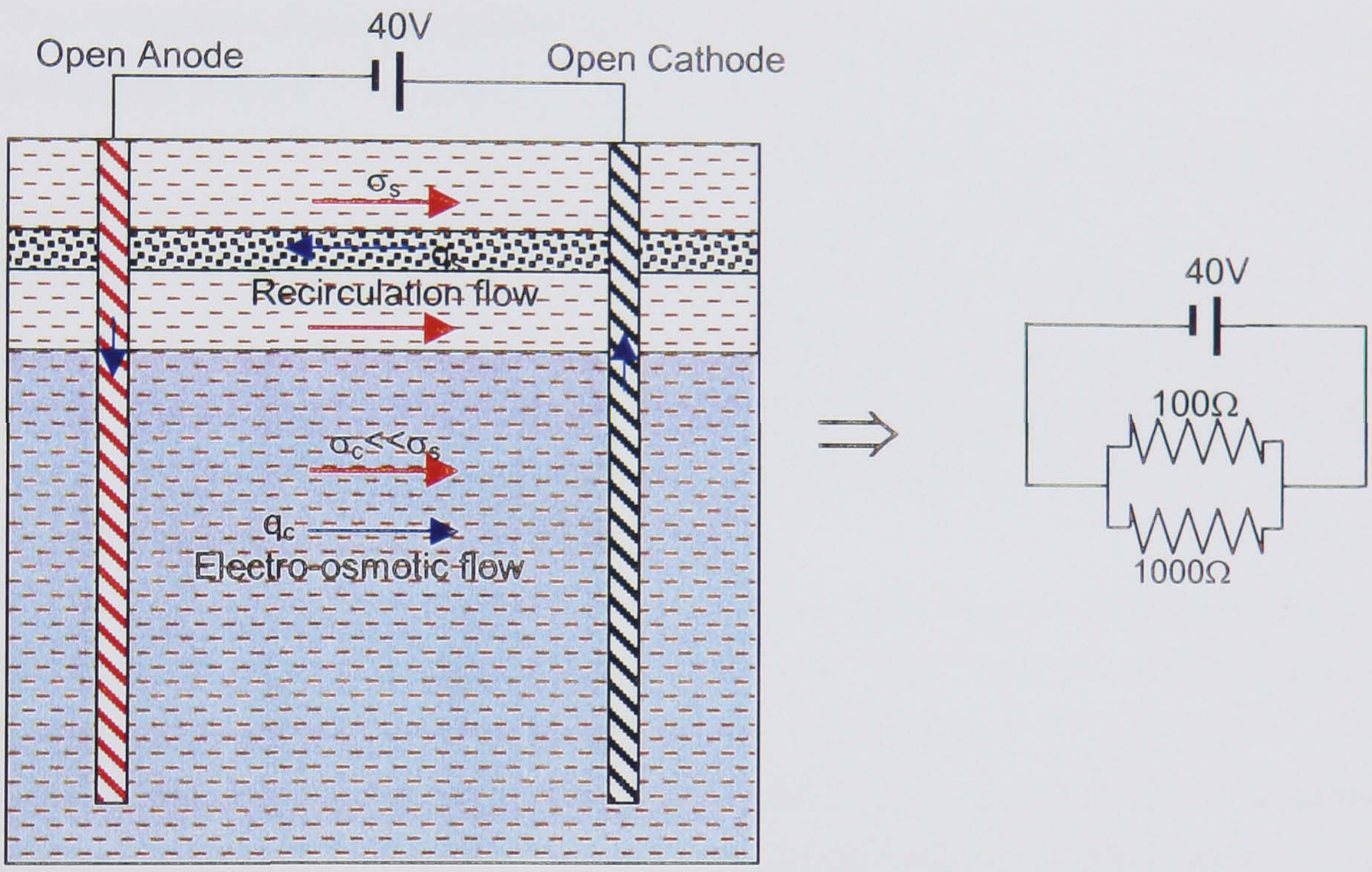

Figure 4.31 Short-circuiting of e-o treatment through made ground

The interpretation presented in Figure 4.31 would have the following consequences.

- The current drawn by the installation would be higher than anticipated due to the greater electrical conductivity of the made ground.
- The water moved through the cohesive alluvium from the anode to the cathode could recirculate through the granular layers in the macrofabric of the made ground; thus counteracting the electro-osmosis process. Hence, no net water movement would take place and no settlement of the ground surface or significant change in shear strength of the cohesive alluvium would occur.

This outcome was, however, unforeseeable at the design stage due to the lack of undisturbed soil samples in the made ground and the inability of the site investigation methods to detect the composition and macrofabric of the made ground. As was mentioned in § 4.3.1.3 the installation of a sleeve to seal the EKG from the made ground could have

prevented the occurrence of the short-circuiting through the made ground. However, due to the installation method used, for economic reasons, it was not possible to sleeve or insulate the EKG through the made ground, thus both anode and cathode remained "open" and susceptible to recharge. A similar outcome was encountered by Caron (1971 a & b) caused by lack of information on the soil macrofabric which would have shown the existence of laminations of higher permeability soils located within a soil of lower permeability.

4.3.6 CONCLUSIONS

The following conclusions may be drawn from the trial:

- The installation method developed by the Author using a modified DPH cone for the installation of the EKG was found to be successful.
- The electrical power drawn by the installation was commensurate with that predicted by calculation using the equation suggested by Casagrande (1983).
- The surface monitoring pegs and in situ testing did not show any evidence of improvement in the cohesive alluvium as a result of the electro-osmotic treatment. It is thought that short-circuiting of the installation occurred through the made ground and allowed recirculation of the water between cathode and anode, thus negating any dewatering caused by electro-osmosis.
- The establishment of representative soil parameters and accurate recording and interpretation of the macrofabric of all of the soils through which the electrodes pass is essential to avoid unforeseen occurrences and possible failure of the process.
- The short-circuiting through the made ground could have been prevented by sealing the EKGs through the made ground, by means of encasing them in a plastic tube.

The site is currently been developed and the area were the trial was located has been drilled on a grid pattern to grout up the shallow mine workings located beneath. Thus, further work in the area is not possible. Before the area was grouted steel reinforcement bars were driven into the ground to act as a second phase trial to establish if closed electrodes would prevent the recirculation of the ground water through the made ground. However, the power supply generator was stolen from the site and it was not possible to undertake the second phase trial before the grouting operations were underway.

In view of the practical difficulties experienced with the initial field trial a decision was taken to undertake full-scale EKG consolidation trials in a specially designed test facility that could guarantee known conditions and where the experiment could be instrumented. These tests were undertaken as a follow up to the research presented in this thesis (Jones & Shim 2001).

4.4 SYNOPSIS OF CHAPTER 4

The chapter began by introducing the currently available techniques for ground improvement for use in both cohesionless and cohesive soils. The techniques for use in cohesive soils were then discussed in some detail, as they are direct competitors to the consolidation of the ground using electro-osmosis. The alternative techniques discussed were; precompression, vacuum preloading, vibroreplacement, concrete columns, lime & lime/cement columns, lime piles, thermal stabilisation, dynamic compaction, grouting techniques and conventional compaction.

The process of electro-osmotic consolidation was then introduced beginning with a historical review of its application to the field of civil engineering. This was then followed by a review of the advanced theory of electro-osmotic consolidation, detailing calculation methods for the amount and rate of consolidation that may be anticipated. The permanence of the electro-osmotic treatment was then discussed by reference to the experience of other researchers and by reference to e-log σ' and critical state models. The concepts of combined surcharging and electro-osmotic consolidation were discussed as well as the technique of polarity reversal to achieve a more uniform treatment of the ground.

The Newburn Haugh consolidation trial was introduced with a discussion of the site geology and the laboratory testing undertaken by the Author to establish the geotechnical parameters used for design. The in situ testing of the site was then discussed with the purpose of obtaining the undrained shear strength (c_u) of the cohesive alluvium and, additionally, the undrained deformation modulus (E_u) could also be calculated.

The installation method developed by the Author for the installation of the EKGs using a standard DPH rig with a modified driving cone was then described, together with the installation pattern used.

Design calculations for the installation were presented, giving the estimation of the quantity of settlement and the rate at which it should occur, together with an estimate of the current drawn. The monitoring regime adopted for the trial was described, together with the results obtained from the trial.

The post-trial in situ testing was presented and the results of the MDMT testing given. This was followed by the interpretation of all of the results obtained during the trial, i.e. electrical energy, surface settlement and undrained shear strength.
Conclusions were then drawn indicating that the likely explanation for the lack of surface settlement was the short-circuiting of the system through the made ground both electrically and hydraulically due to a lack of information on the soil's macrofabric. Recommendations

for further work were then given; it was recommended that no further work should be undertaken on the Newburn Haugh site due to the grouting operations that subsequently took place in the trial area. The development of a large-scale test facility at the University of Newcastle was suggested to allow consolidation trials to be undertaken without disruption.

4.5 CHAPTER 4 REFERENCES

1. Acar, Y.B., Gale R.J., Hamed, J. & Putnam, G. (1990) *Acid/Base distributions in electrokinetic soil processing.* Transportation Research Record 288, Transportation Research Board, National Research Council, Washington D.C., pp 23-24.
2. Aldrich, H.P. (1965) *Precompression for support of shallow foundations.* Journal of the Soil Mechanics And Foundation Division, ASCE, Vol. 91, SM2, pp 5-20.
3. Barron, R.A. (1948) *Consolidation of fine grained soil by drain wells.* Transactions of the ASCE, Vol. 113, pp 718-742.
4. Bell, A.L. (1993a) *Jet Grouting.* In Moseley, M.P (ed.) Ground Improvement. Blackie Academic & Professional, Glasgow, UK. pp 149-172.
5. Bell, F.G. (1993b) *Engineering treatment of Soils.* E & F.N. Spon, London. p 302.
6. Bergado, D.T., Chai, J.C., Alfaro, M.C. & Balasubramaniam, A.S. (1994) *Improvement techniques of soft ground in subsiding lowland.* A.A.Balkema, Rotterdam, Netherlands. p 222.
7. Bishop, A.W. (1971) *Shear strength parameters in undisturbed and remoulded soil specimens.* In stress-strain behaviour of soils; Proceedings of the Roscoe Memorial Symposium, Cambridge, (Ed. Parry, R.H.G.) Foulis, Yeovil, pp 3-8.
8. Bjerrum, L., Moum, J. & Eide, O. (1967) *Application of electro-osmosis to a foundation problem in a Norwegian quick clay.* Géotechnique, Vol. 17, pp 214-235.
9. Bowles, J.E. (1988) *Foundation Analysis & Design.* McGraw Hill International Editions. p 1004.
10. Briaud, J.L. & Miran, J. (1992) *The flat dilatometer test.* US Dept of Transport, Federal Highway Administration, Publication No. FHWA-SA-91-044, pp 102 Washington D.C.
11. Broms, B. (1993) *Lime Stabilization.* In Moseley, M.P (Ed.) Ground Improvement. Blackie Academic & Professional, Glasgow, U.K., pp 65-97.
12. Broš, B., Dzidowska, K. & Koszela, J. (1983) *Influence of flocculants on the process and efficiency of electro-osmosis in fine-grained soils.* Proceedings of the 8th International Conference on Soil Mechanics and Foundation Engineering, Helsinki, Vol. 2, pp 587-590.
13. BSI (1981) *Code of practice for Earthworks, BS 6031.* British Standards institution, 2 Park Street, London, U.K.
14. Caron, C. (1971a) *Consolidation électrochimique du sol de la culée rive droite du Pont de la Basse chaîne à Angers.* Annales de l'Institut Technique du Bâtiment et des Travaux Publics, Paris, France, No. 66, pp 11-13.
15. Caron, C. (1971b) *Consolidation des terrains argileux por électro-osmose.* Annales de l'Institut Technique du Bâtiment et des Travaux Publics, Paris, France, No. 82, pp 75-92.
16. Carter, M. (1983) *Geotechnical Engineering Handbook.* Pentech Press, London, p 226.
17. Carter, M. & Bentley, S.P. (1991) *Correlations of soil properties.* Pentech Press, London, p 130.

18. Casagrande, L. (1941a) *Die entwässerung feinkörniger böden.* Die Strasse, N° 19-20.
19. Casagrande, L. (1941b) *Zur frage der entwässerung feinkörniger böden.* Deutche Wasserwirtschaft, N° 11.
20. Casagrande, L. (1947) *The application of electro-osmosis to practical problems in foundations and earthworks.* Technical Paper N° 30, Building Research Station, England, U.K.
21. Casagrande, L. (1952) *Electro-osmotic stabilisation of soils.* Journal of the Boston Society of Civil Engineers Section, ASCE, winter, Vol. 39, No. 1, pp 51-83.
22. Casagrande, L. (1983) *Stabilization of soils by means of electro-osmosis state-of-the-art.* Journal of the Boston Society of Civil Engineers Section, ASCE, winter, Vol. 69, No. 2, pp 255-302.
23. Casagrande, L., Loughney, R.W. & Matich, M.A.J. (1961) *Electro-osmotic stabilisation of a high slope in loose saturated silt.* Proceedings of the 5th International Conference on Soil Mechanics and Foundation Engineering, Paris, France, Vol. 2, pp 555-561.
24. Casagrande, L., Wade, N., Wakely, M. & Loughney, R. (1981) *Electro-osmotic projects, British Columbia, Canada.* Proceedings of the 10th International Conference on Soil Mechanics and Foundation Engineering, Rotterdam, pp 607-610.
25. Chan, S.F. & Chin, F.K. (1972) *Engineering characteristics of the soils along the federal highways in Kuala Lumpur.* Proc. 3rd S.E. Asian Conf. on soil Engineering, pp 41-45.
26. Chappell, B.A. & Burton, P.L. (1975) *Electro-osmosis applied to unstable embankment.* Journal of the Geotechnical Engineering Division, ASCE, Vol. 101, GT8, August, pp 733-740.
27. Choa, V. (1989) *Drains and vacuum preloading pilot test.* Proceedings of the 12th International Conference on Soil Mechanics and Foundation Engineering, Rio de Janeiro, Vol. 2, Balkema, pp 1347-1350.
28. Eggestad, Å. & Føyn, T. (1983) *Electro-osmotic improvement of a soft sensitive silty clay.* Proceedings of the 8th European Conference on Soil Mechanics and Foundation Engineering, Helsinki, Finland, May 23-26, Vol. 2, Balkema, pp 597-602.
29. Eriksson, L. & Ekström, A. (1983) *The efficiency of three different types of vertical drain - results from full-scale tests.* Proceedings of the 8th European conference on Soil Mechanics and Foundation Engineering, Helsinki, Finland, May 23-26, Vol. 2, Balkema.
30. Esrig, M.I. (1968) *Pore pressures, consolidation and electrokinetics.* Journal of the Soil Mechanics Division, ASCE, Vol. 94, SM4, pp 899-921.
31. Esrig, M.I. (1971) *Electrokinetics in soil mechanics and foundation engineering.* Transactions of the New York Academy of Science, Series II, Vol. 33, No. 2, pp 234-245.
32. Fetzer, C.A. (1967) *Electro-osmotic stabilisation of West Branch Dam.* Journal of the Soil Mechanics And Foundation Division, ASCE, Vol. 93, SM4, pp 85-106.
33. Gambin, M.P. (1987) *Dynamic consolidation of volcanic ash in Sumatra.* Proceeding of the 9th South East Asian Geotechnical Conference, Bangkok, pp 8/145 - 8/158.

34. Grey, D.H. & Somogyi, F. (1977) *Electro-osmotic dewatering with polarity reversals.* Journal of the Geotechnical Engineering Division, ASCE, Vol. 103, No. GT1, January, pp 51-54.
35. Hamir, R., Jones, C.J.F.P. & Clarke, B.G. (2001) *Electrically conductive geosynthetics for consolidation and reinforced soil.* Geotextiles and Geomembranes, Vol. 19, No. 8, Elsevier, pp 455-483.
36. Hansbo, S. (1993) *Band Drains.* In Moseley, M.P. (Ed.) Ground Improvement. Blackie Academic & Professional, Glasgow, U.K., pp 40-62.
37. Houlsby, G.T. & Withers, N.J. (1988) *Analysis of the cone pressuremeter test in clay.* Géotechnique, Vol. 38, No. 4, pp 575-587.
38. Johnson, S.J. (1970) *Precompression for improving foundation soils.* Journal of the Soil Mechanics And Foundation Division, ASCE, Vol. 96, SM1, pp 145-175.
39. Johnston, I.W. (1978) *Electro-osmosis and its application to soil and foundation stabilisation.* Proceedings of the Symposium on Soil Reinforcing and Stabilising Techniques, Sydney, Australia, pp 459-476.
40. Jones, C.J.F.P. & Shim, G.C.S. (2001) *Consolidation trial using electrokinetic geosynthetic electrodes.* Research Report No. 010/01, University of Newcastle upon Tyne, U.K.
41. Keller (1990) *Soilcrete - Jet grouting.* Keller Colcrete Brochure, Wetherby, England, U.K.
42. Keller (1992) *Vibro-replacement, vibro-compaction.* Keller Foundations Brochure, Coventry, England, U.K.
43. Leach & Row (1995) *The role of dynamic probing in geotechnical investigations on pipelines.* In probing and penetration testing, meeting of East Midlands Geotechnical Group and Engineering Group of the Geological Society 10th May, Loughborough.
44. Lo, K.Y., Ho, K.S. & Inculet, I.I. (1991a) *Field test of electro-osmotic strengthening of soft sensitive clays.* Canadian Geotechnical Journal, Vol. 28, pp 74-83.
45. Lo, K.Y., Ho, K.S. & Inculet, I.I. (1991b) *Electro-osmotic strengthening of soft sensitive clays.* Canadian Geotechnical Journal, Vol. 28, pp 62-73.
46. Menard, L. & Broise, Y. (1975) *Theoretical and practical aspects of dynamic consolidation.* Géotechnique, Vol. 15, pp 3-18.
47. Milligan, V. (1994) *First application of electro-osmosis to improve friction pile capacity - three decades later.* Proceedings of the 13th International Conference on Soil Mechanics and Foundation Engineering, New Delhi, India, Vol. 5, Balkema, pp 1-5.
48. Mitchell, J.K. (1970) *In-Place Treatment Of Foundation Soils.* Journal of the Soil Mechanics And Foundation Division, ASCE, Vol. 96, SM1, pp 73-110.
49. Mitchell, J.K. (1993) *Fundamentals of Soil Behaviour.* 2nd Ed. Published by John Wiley & Sons Inc. New York, USA. p 437.
50. Moseley, M.P. (Ed.) (1993) *Ground Improvement.* Blackie Academic & Professional, Glasgow, U.K., p 217.

51. Moseley, M.P. & Priebe, H.J. (1993) *Vibro techniques.* In Moseley, M.P. (Ed.) Ground Improvement. Blackie Academic & Professional, Glasgow, U.K., pp 1-20.
52. Morris, D.V., Hillis, S.F. & Caldwell, J.A. (1985) *Improvement of sensitive silty clay by electroosmosis,* Canadian Geotechnical Journal, Vol. 22, pp 17-24.
53. Pedley, M.J. (1990) *Personal communication.* Kvaerner Cementation Foundations, Maple Cross House, Rickmansworth, United Kingdom.
54. Pennine (1988) *An introduction to the dynamic probe.* Pennine Ground Engineering Ltd, unit 8, New Line Industrial Estate, New Line, Bacup, Lancashire, OL13 9RW, U.K.
55. Powrie, W. (1997) *Soil mechanics - concepts and applications.* E&FN Spon, London, U.K., p 420.
56. Pugh, R.C. (1999) *Mid-term review report.* EPSRC Research Report, University of Newcastle upon Tyne, U.K.
57. Pugh, R.C., Clarke, B.G. & Jones, C.J.F.P. (2000) *An electro-osmotic consolidation trial using electrokinetic geosynthetics.* 4th International Conference on Ground Improvement Geosystems, Helsinki, 7-9 June. Finish Geotechnical Society, pp 533-540.
58. Roscoe, K.H. & Burland, J.B. (1968) *On the generalised stress-strain behaviour of "wet" clay.* In Engineering Plasticity (Eds. Heyman, J. & Leckie, F.A.) Cambridge University Press, Cambridge, U.K., pp 535-609.
59. Rubright, R. & Welsh, J. (1993) *Compaction Grouting.* In Moseley, M.P (Ed.) *Ground Improvement.* Blackie Academic & Professional, Glasgow, U.K., pp 131-148.
60. Schmertmann, J.H. (1986) *Dilatometer to compute foundation settlement.* 14th PSC, ASCE, pp. 303-321.
61. SGI (1949) *Redogörelse för atatens geotekniska institutus verksamhet under åren 1944-1948. (Report on activities of the Swedish Geotechnical Institute in the years 1944-1949).* Statens Geotekniska Institut, Meddelande, No. 2.
62. Shang, J.Q. (1998a) *Electroosmosis - enhanced preconsolidation via vertical drains.* Canadian Geotechnical Journal, Vol. 35, pp 491 - 499.
63. Shang, J.Q. (1998b) *Two dimensional electro-osmotic consolidation.* Ground Improvement, Vol. 2, Part 1, pp 17-25.
64. Shang, J.Q., Lo, K.Y., & Inculet, I.I. (1995) *Polarisation and conduction of clay - water electrolyte systems.* Journal of the Geotechnical Engineering Division, ASCE, Vol. 121, GT3, pp 243 - 248.
65. Slocombe, B.C. (1993) *Dynamic Compaction.* In Moseley, M.P (Ed.) *Ground Improvement.* Blackie Academic & Professional, Glasgow, U.K., pp 20-39.
66. Soderman, L.G. & Milligan, V. (1961) *Capacity of friction piles in varved clay increased by electro-osmosis.* Proceedings of the 5th International Conference on Soil Mechanics and Foundation Engineering, Paris, France, Vol. 2, Balkema, pp 143-148.
67. Sprute, R.H. & Kelsh, D.J. (1975) *Limited Field Tests in electrokinetic densification of mine tailings.* R1 8034, U.S. Bureau of Mines.

68. Stroud, M.A. (1975) *The standard penetration test in insensitive clays and soft rocks* Proceedings of the European Symposium on penetration testing, Vol. 2, pp 367-375.
69. Tang, Y. & Goa, Z. (1989) *Experimental study and application of vacuum preloading for consolidating soft soil foundations* . Proceedings of the 12th International Conference on Soil Mechanics and Foundation Engineering, Rio de Janeiro, Vol. 2, Balkema, pp 1423-1426.
70. Terzaghi, K. (1936) *The shearing resistance of saturated soils.* Proceedings of the First International Conference on Soil Mechanics, Vol. 1, Balkema, pp 54-56.
71. Wan, T.Y. & Mitchell, J.K. (1976) *Electro-osmotic consolidation of soils.* Journal of the Geotechnical Engineering Division, ASCE, Vol. 102, GT5, pp 473-491.
72. Warner, J. & Brown, D.R. (1974) *Planning and performing compaction grouting.* Journal of the Geotechnical Engineering Division, ASCE, Vol. 100, No. GT6, pp 653-666.
73. Wilkins, E.A. & Chandler, B.C. (1989) *Electro-osmosis trial section 6/3 Muar Flat.* Proceedings of the International Symposium on Trial Embankments on Malaysian Marine Clay, November 6 - 8, Kuala Lumpur, Malaysia, Vol. 2, pp 48-52.
74. Wrigley, N.E. (1999) *The practical use of electro-osmosis. Personal communication*, October.

4.6 CHAPTER 4 PLATES

Plate 4.1 - Specially designed DPH cone for the installation of the EKG (EKG attached)

Plate 4.2 - Installation of EKG using DPH rig

Plate 4.3 - Detail of stripped double crimped connection

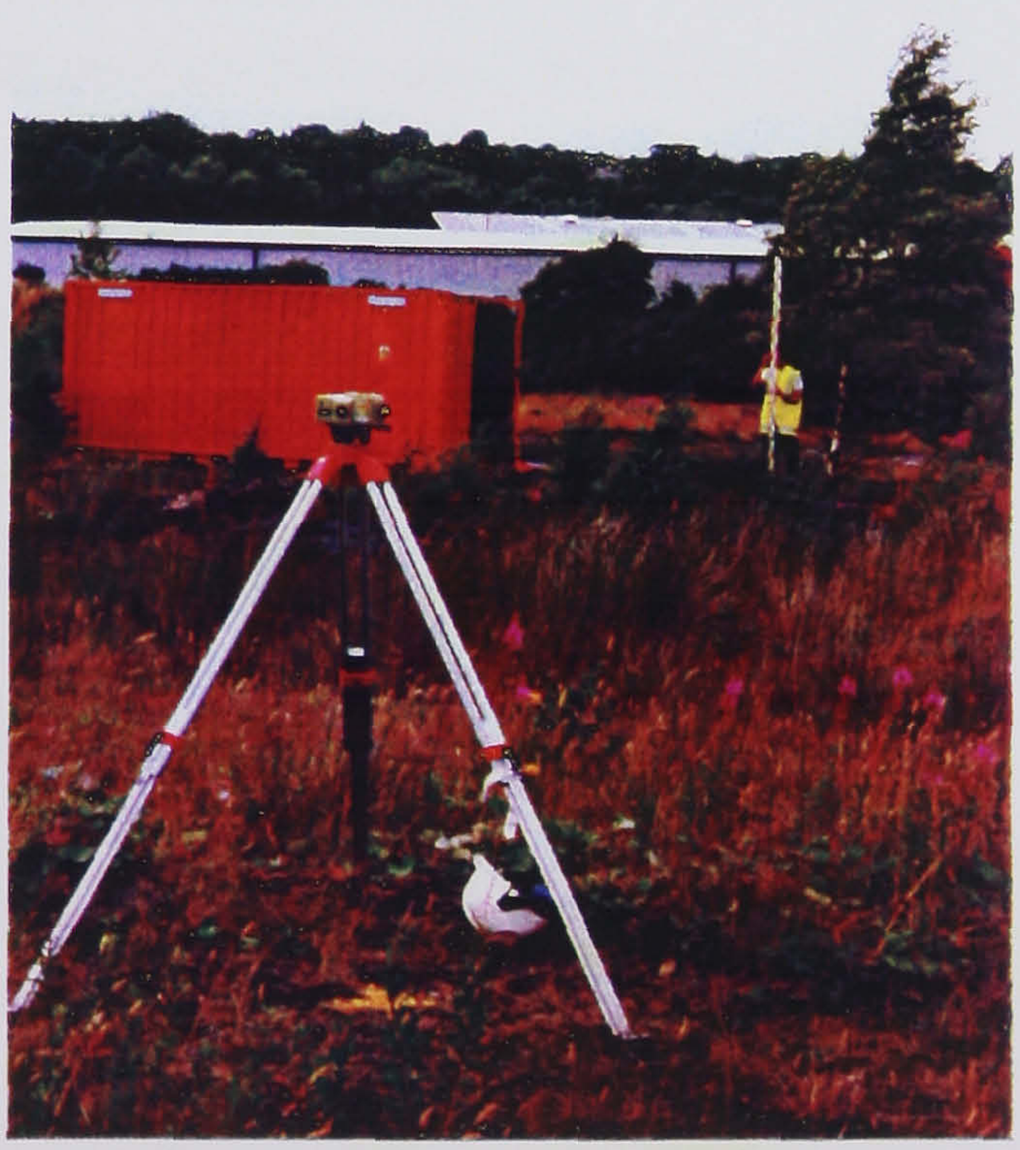

Plate 4.4 - Levelling of settlement monitoring pegs with digital level
(power supply container also visible)

CHAPTER 5

EKG IN SOIL REINFORCEMENT

5.1 INTRODUCTION

The concept of soil reinforcement is not new. The Ziggurat of Agar-Quf, 5 km north of Baghdad, is believed to be some 3000 years old and is constructed of clay bricks reinforced with woven mats of reeds. The Great Wall of China is also constructed of a mixture of clay and gravel reinforced with tamarisk branches (Jones 1996).

The modern concept of earth reinforcement and soil structures was postulated by Casagrande, who idealised the problem in the form of a weak soil reinforced by high strength membranes laid horizontally in layers (Westergaard 1938). The reinforced soil systems of today are, however, derived from the invention of *Reinforced Earth* by Henri Vidal in 1963 (Vidal 1963, 1966, 1969a, 1969b). He was the first to formalise a rational design of a modern reinforced soil system (Bergado *et al* 1994).

The reinforced earth system patented by Vidal consisted of metal strip reinforcement, usually made of galvanised steel, located in high quality, but expensive, clean dry sand and gravel backfill to be able to generate the required frictional resistance between backfill soil and reinforcement.

However, rapid development in polymer technology has produced a wide variety of geosynthetic materials resulting in the growth of many different reinforcing systems. The advent of grid type polymer reinforcements, which have high pull out resistance, has enabled the use of cheaper low quality cohesive frictional soil as backfill (Jones 1990).

5.2 MECHANISMS OF SOIL REINFORCEMENT

Reinforced soils are fundamentally different from conventional earth retaining systems, which are externally stabilised, in that they utilise a different mechanism for support and are internally stabilised.

An externally stabilised system uses an external structural wall against which stabilising forces are mobilised. An internally stabilised system involves reinforcements installed within and extending beyond the potential failure mass. Within this system, shear transfer to mobilise the tensile capacity of closely spaced reinforcing elements has removed the need for a structural wall and has substituted a composite system of reinforcing elements and soil as the primary structural entity (Jones 1996).

The action of reinforced soil is best considered by visualising two steep slopes one of which is reinforced and the other not, as shown in Figure 5.1.

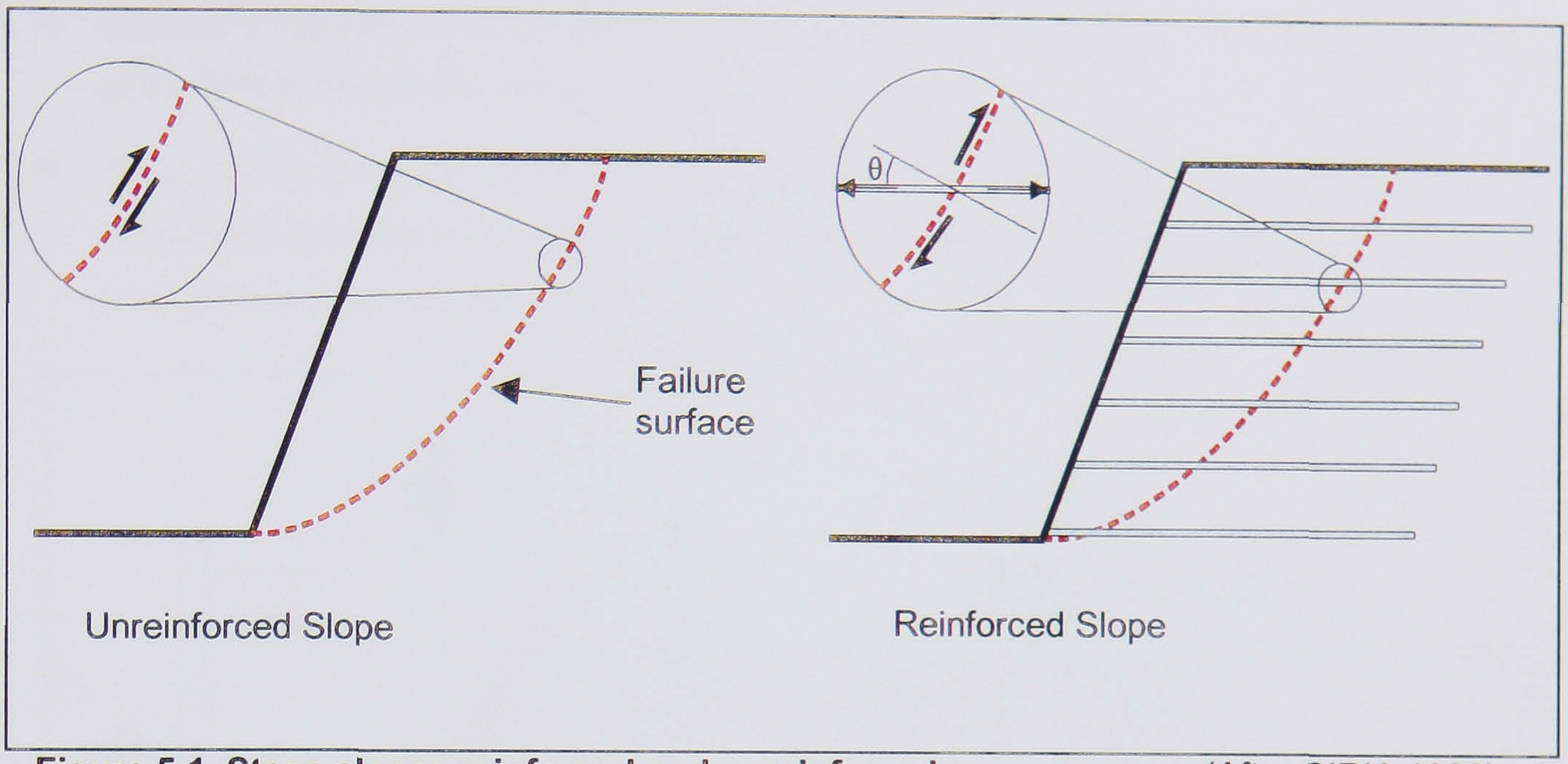

Figure 5.1 Steep slopes reinforced and unreinforced (After CIRIA 1996)

If the unreinforced element of soil shown in Figure 5.1 is rotated by approximately 90° then it may be idealised as a shear box test as show in Figure 5.2.

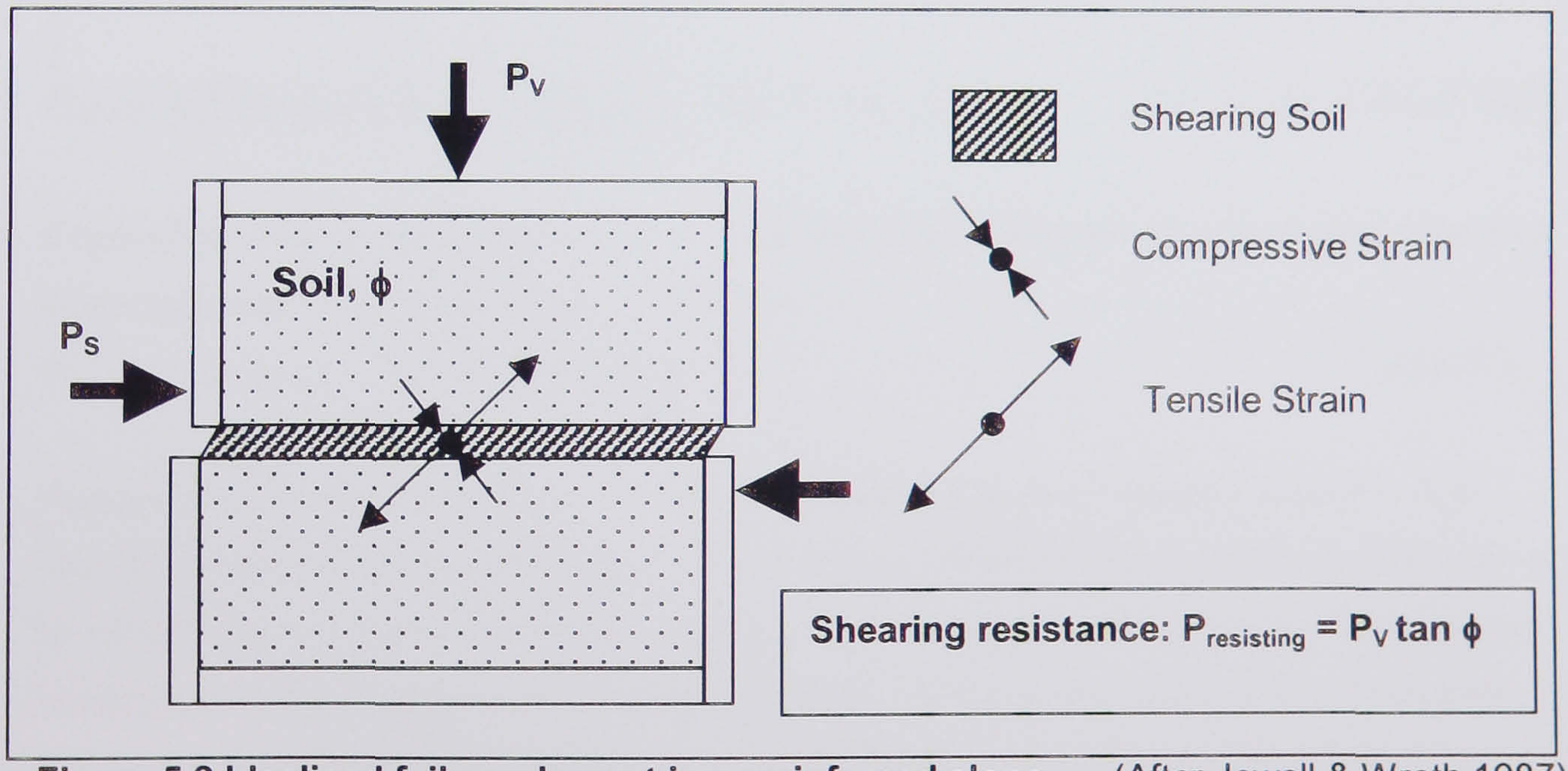

Figure 5.2 Idealised failure element in unreinforced slope (After Jewell & Wroth 1987)

From the figure, it is apparent that the shear resistance that can develop on a failure surface is given by Equation 5.1:

$$P_{resisting} = P_V \tan \phi \qquad \text{Eqn. 5.1}$$

Where P_V is the vertical load in the shear box or the normal load on the failure surface in an unreinforced slope. If a reinforced soil element as shown in Figure 5.1 is now considered in

a similar manner, the shear box analogy is as given in Figure 5.3. From the resolution of forces within the reinforcement and shearing soil element, it can be seen that the reinforcement has two beneficial effects on the shear resistance of the reinforced soil mass:

- There is a reduction in the shear force inducing failure through the horizontal component of the tensile force in the reinforcement.
- There is an increase in the normal force applied to the shear surface, and hence an associated increase in the shear resistance derived from the vertical component of the tensile force in the reinforcement.

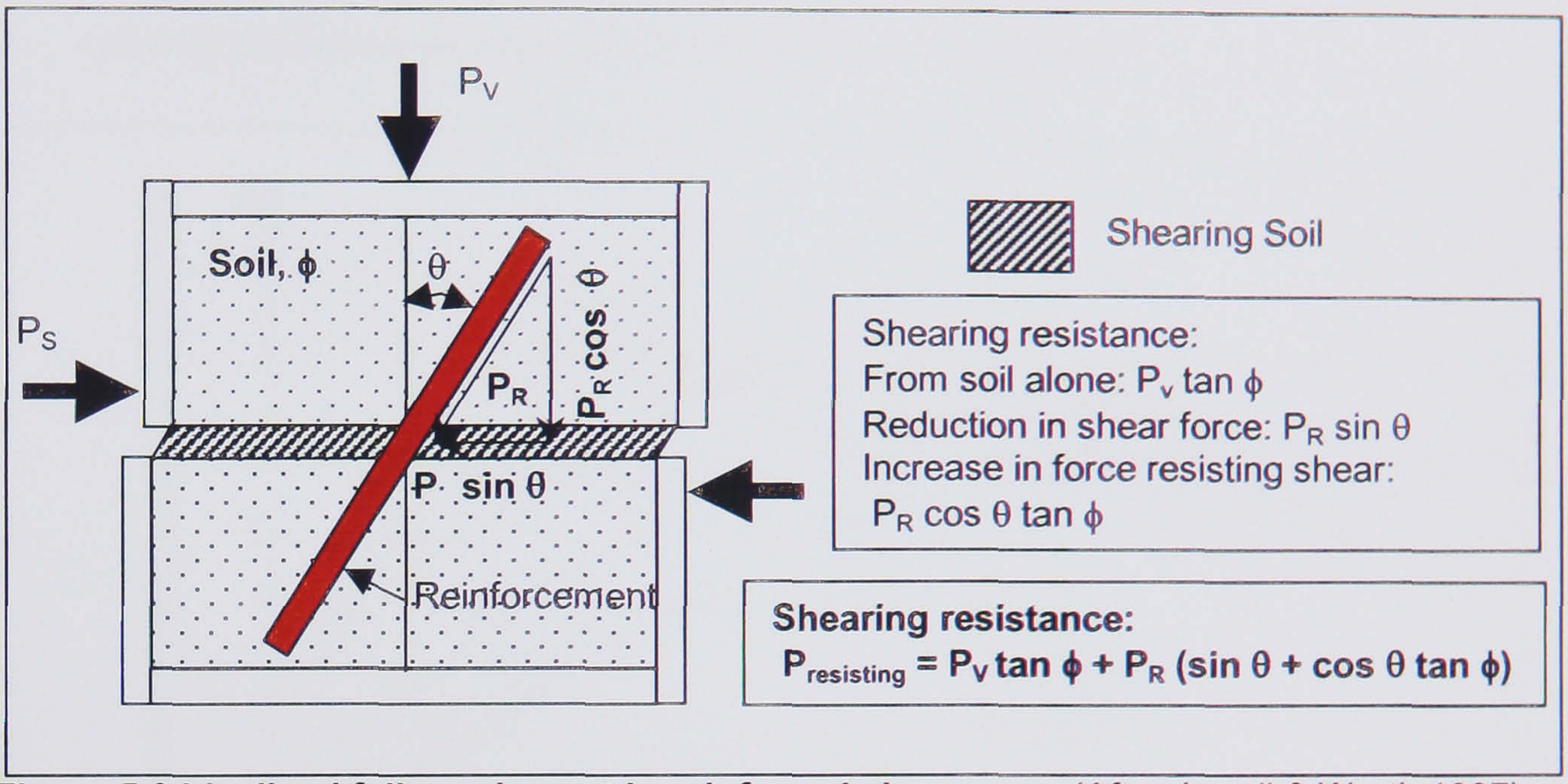

Figure 5.3 Idealised failure element in reinforced slope (After Jewell & Wroth 1987)

It follows that the shearing resistance of the element of reinforced soil is increased from that given in Equation 5.1 to that given in Equation 5.2:

$$P_{resisting} = P_V \tan \phi + P_R (\sin \theta + \cos \theta \tan \phi) \qquad \text{Eqn. 5.2}$$

Fundamental studies have shown that the reinforcement is most effective aligned in the direction of tensile strain in the soil, so that tensile reinforcement force develops (McGown *et al* 1978). The orientation (θ in Figure 5.3) of the reinforcement with respect to the potential shear plane is the only geometry variable in Equation 5.2 and hence it is apparent that the inclination of the reinforcement is the governing factor in how much additional shear resistance is generated by the inclusion of the reinforcement. Figure 5.4 demonstrates the variation of the function given in Equation 5.2 with respect to different θ and ϕ angles.

It can be seen from Figure 5.4 that the optimum orientation for the reinforcement is given by $\theta_{OPT} = 90° - \phi$ (CIRIA 1996). In practice, the degree of improvement is critically dependent upon the magnitude of the mobilised reinforcement force (P_R). Two physical factors require consideration in the evaluation of P_R:

- The maximum force that a piece of "strong" reinforcement can carry is ultimately governed by the bond between the soil and reinforcement. The bond being at a maximum when the maximum compressive stress in the soil acts perpendicular to the plane of the reinforcement.

- The stiffness of the reinforcement influences the soil shear deformation required to mobilise the reinforcement force. The maximum possible tensile strain in the reinforcement is equal to the tensile strain in the adjacent soil in the direction of the reinforcement. Thus, reinforcement orientated in the direction of maximum tensile strain will experience the greatest elongation for any given shear deformation in the soil. This optimum reinforcement angle (θ_ε), is also shown in Figure 5.4.

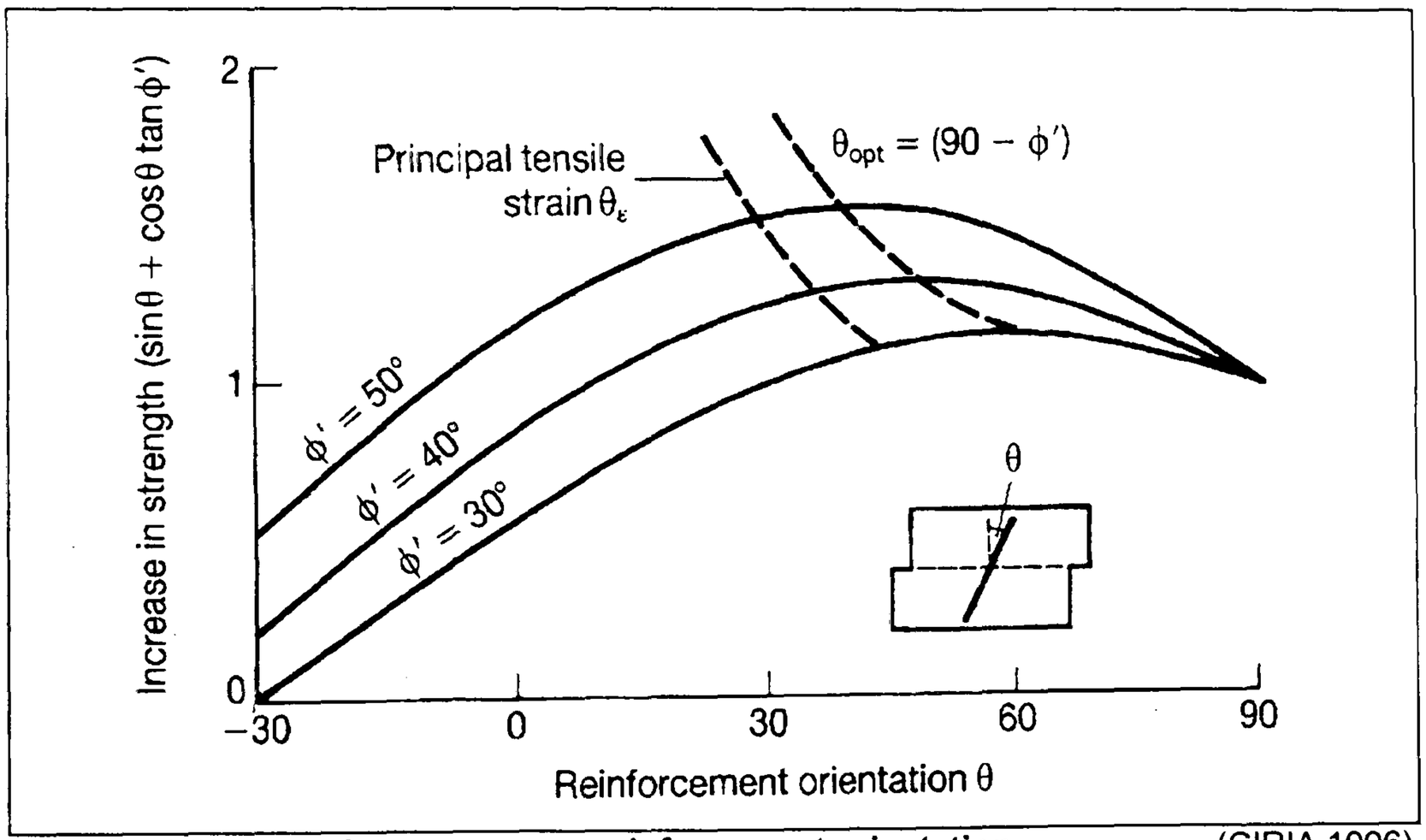

Figure 5.4 Shear resistance versus reinforcement orientation (CIRIA 1996)

The orientation of the principal axis of stress and incremental strain are closely aligned in shearing soil such that the two optimum orientations described above are approximately equal. This leads to the rule of thumb that geotextile reinforcement should be placed in a soil at an orientation within the range $45° \geq \theta \geq 0°$ with respect to the critical slip surface (Figures 5.3, 5.4). This is roughly horizontal in the main reinforced soil applications (CIRIA 1996). The reader is referred to Jewell and Wroth (1987) for a more detailed discussion.

5.3 CORNER STONES OF ANALYSIS AND STRAIN COMPATIBILITY

The cornerstones for the analysis of reinforced soil structures are that of the soil strains, soil stresses, soil reinforcement interaction and gravity, reinforcement and boundary forces are all interconnected (Jones 1996). This has been illustrated by Bolton (1991) and is presented in Figure 5.5.

From §5.2 it is apparent that equilibrium in a reinforced soil structure is obtained when the tensile strain in the reinforcement and that in the surrounding soil is equal.

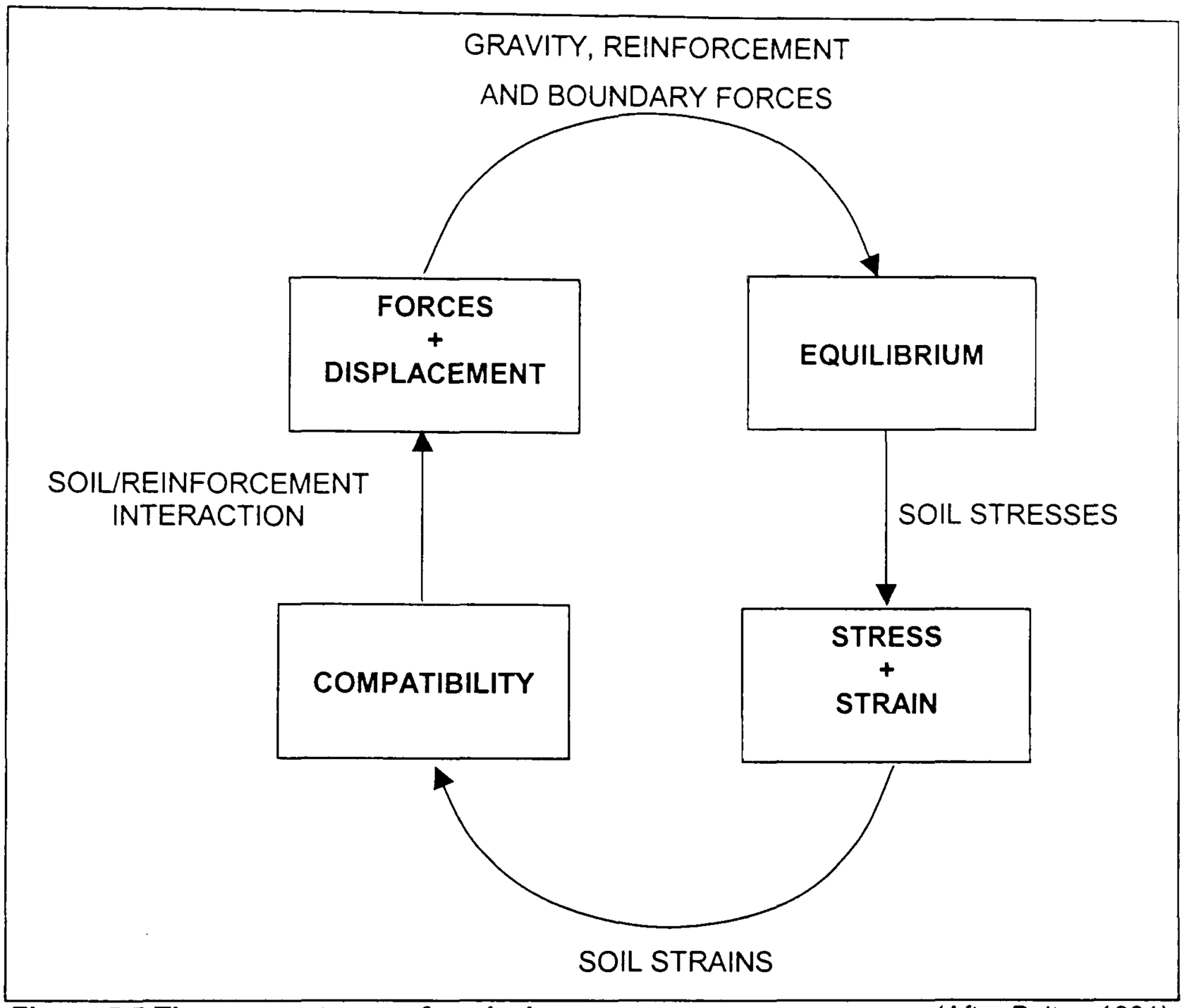

Figure 5.5 The cornerstones of analysis (After Bolton 1991)

From a practical point of view, the magnitude of the tensile strain possible within a reinforced soil structure is governed by two criteria:

- At the tensile strain at which equilibrium occurs the magnitude of the reinforcement tensile force and the shearing resistance of the soil can be realistically mobilised.
- The tensile strain at equilibrium can be achieved with acceptable deformations in the structure.

Hence, it is necessary to consider the stress strain response of both the soil and the reinforcement individually and in a combined state. The stress-strain response of a typical granular material and a normally consolidated clay under drained and undrained loading is demonstrated in Figure 5.6 under the stress system found within reinforced soil applications. The stress-strain curves for typical reinforcing geotextiles are given in Figure 5.7a.

The tensile strain at equilibrium and the force in the reinforcing elements in a reinforced soil structure can thus be obtained theoretically from these two curves by combining them as shown in Figure 5.7b. This figure demonstrates the stress generated in the reinforcement by

plotting the stress available in the reinforcement, from the conventional stress-strain curve (Figure 5.7) for the geotextile in question, and the stress required from the soil, from the soil's stress-strain curve.

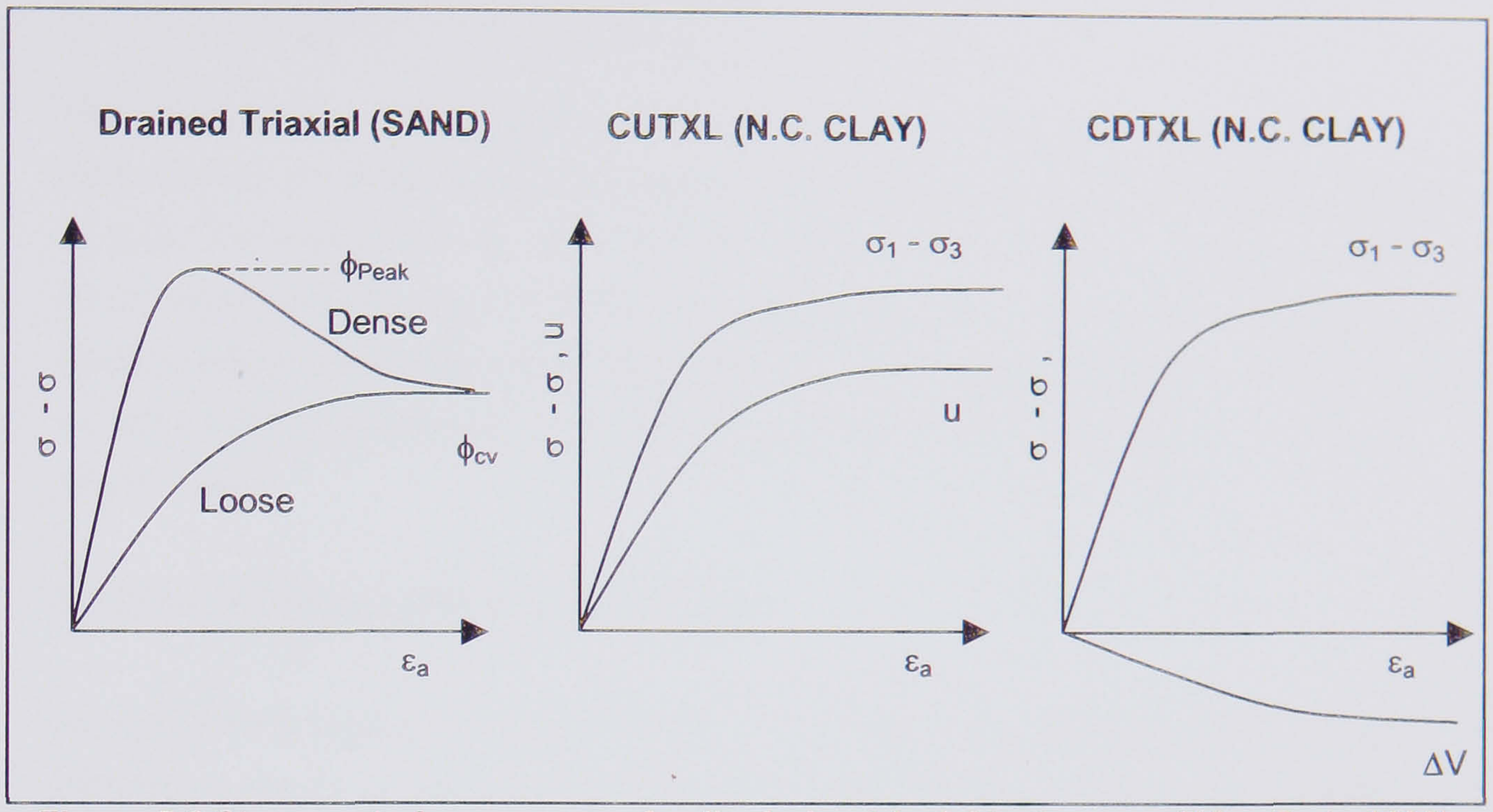

Figure 5.6 Stress - strain response of soils during triaxial test (After Craig 1992)

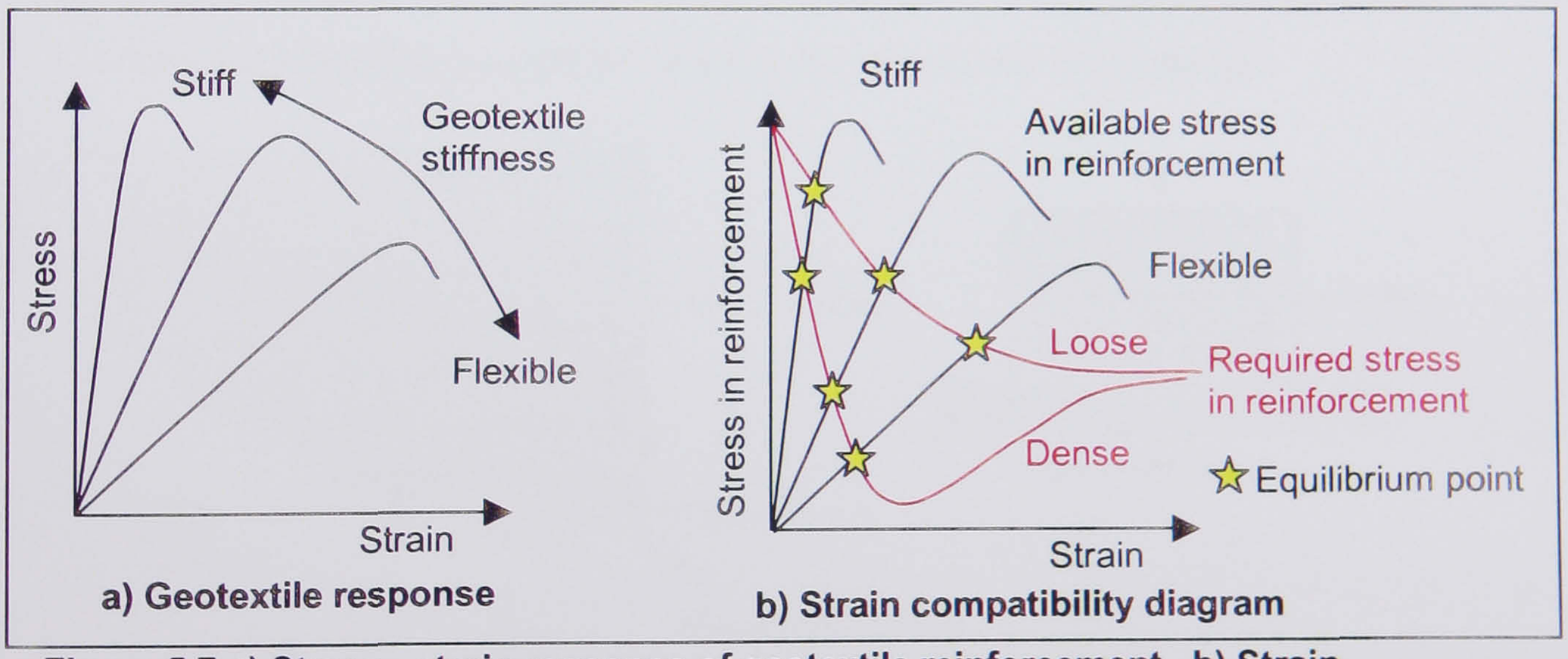

Figure 5.7 a) Stress - strain response of geotextile reinforcement. b) Strain compatibility diagram for equilibrium in reinforced soil (After Jewell 1985, CIRIA 1996, Jones 1996)

This compatibility curve is essentially a plot of a) the maximum *required* force for equilibrium in the soil, which depends on the mobilised shearing resistance and b) the associated maximum available force from the reinforcement. From Figure 5.7 it is apparent that (after Jones 1996):

a) Stress in different materials (soil/reinforcement) is based upon strain level.

b) Stiff reinforcing materials will attract stress and flexible reinforcing materials will shed stress.
c) Reinforcing materials prone to creep will loose stress.
d) Compacted fill will strain less than loose fill to achieve equilibrium.

The stiffness of the reinforcement has a fundamental effect upon the behaviour of a reinforced soil structure. Axially stiff reinforcement will experience little strain before taking up load. The stress in the reinforcement can accumulate rapidly and may occur at lower strains than those required to mobilise peak soil shear strength. Flexible reinforcement requires greater deformation before taking up the stress imposed by the soil. This may lead to higher strains and the peak shear strength of the soil may be approached or exceeded (Jones 1996).

5.4 SOIL / REINFORCEMENT INTERACTION

As well as the intrinsic properties of the soil and the reinforcement, the properties of their interactions are also an essential consideration for reinforced soil. There are two limiting modes of interaction as shown in Figure 5.8:

1. Direct Sliding - Where a failure surface slides over a layer of reinforcement.
2. Pullout - When a layer of reinforcement pulls out from the soil having mobilised the maximum available bond stress between the reinforcement and the soil.

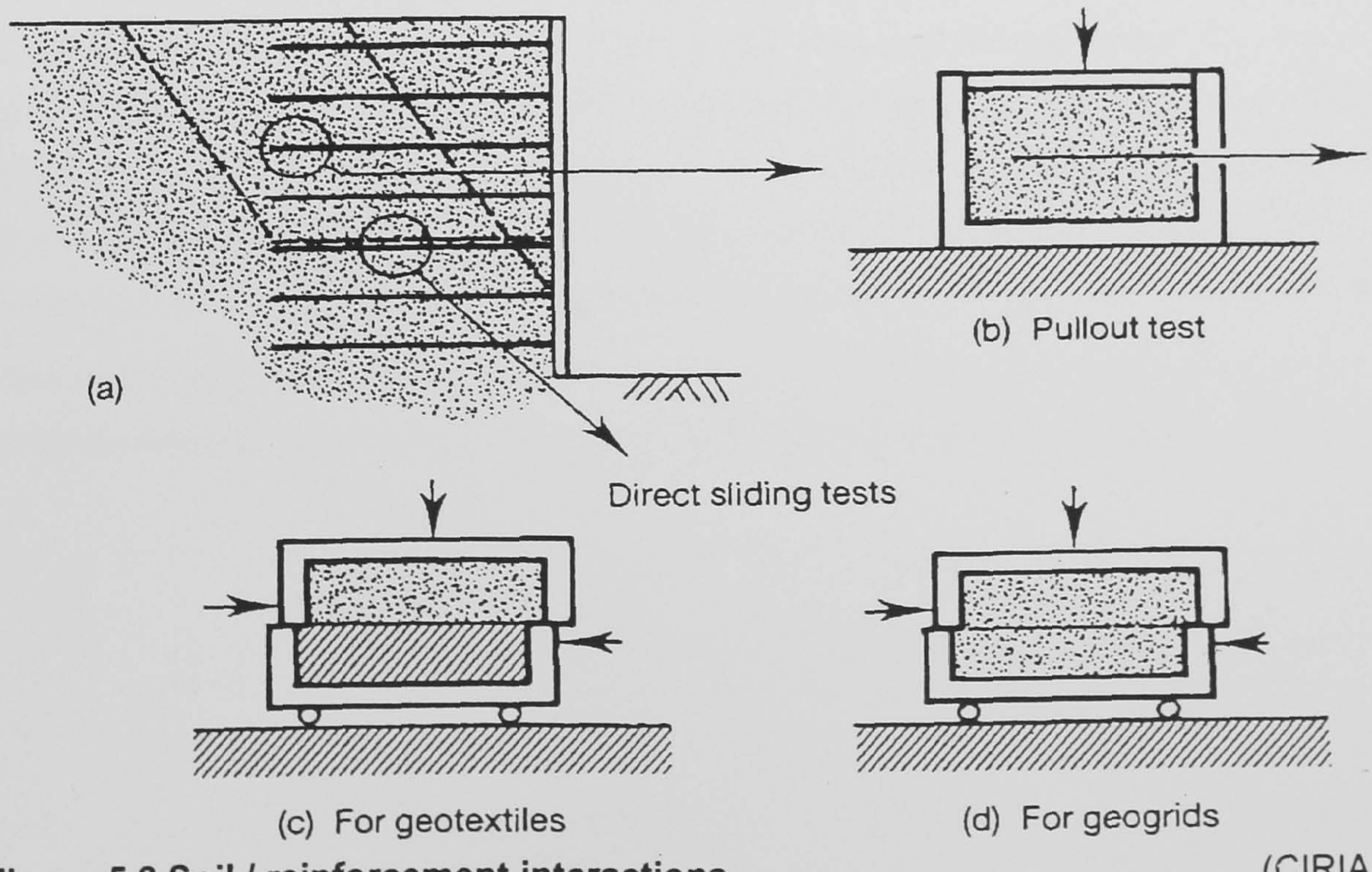

Figure 5.8 Soil / reinforcement interactions (CIRIA 1996)

5.4.1 DIRECT SLIDING

The coefficient of direct sliding between the soil and the reinforcement can be measured in the laboratory using a modified shear box apparatus. For woven or non-woven sheet type

geotextiles direct sliding occurs between the soil and the geotextile over the full plan contact area. As such the geotextile may be supported on a solid block or soil in the lower half of the shear box apparatus, Figure 5.8c (CIRIA 1996).

The direct sliding resistance of geogrids is more complex than that of sheet type geotextiles and consists of soil sliding over soil in the apertures of the grid, as well as soil sliding over the polymeric material of the geogrid itself. As a result geogrids have to be tested in the shear box with both upper and lower halves of the box filled with soil, Figure 5.8d. Modified direct shear tests for granular backfills are described in BS 6909 (BSI 1991).

5.4.2 PULLOUT

Pullout tests can be conducted in a special pullout box. However, the results are greatly influenced by the conditions that exist within the test apparatus (Palmeira & Milligan 1989). For sheet type woven and non-woven geotextiles the bond mechanism on both sides of the geotextile is very similar to that in direct sliding. The bond coefficient obtained from pullout tests on these sheet geotextiles has been found to agree closely with the direct sliding coefficient measured in the modified direct shear apparatus (CIRIA 1996). Hence, it is usually unnecessary to conduct pullout tests on sheet geotextiles when direct shear tests can be carried out much more easily.

For geogrid reinforcement the mode of interaction between the geotextile and the soil during pullout is distinctly different from that during direct shear, as demonstrated by Dyer (1985). This study indicated that geogrids develop bond partly through concentrations of bearing stress against the transverse members of the grid, and partially by shear of soil over the geogrid surface area. Hence, the bond coefficients for geogrids can only be measured by pullout tests. Jewell (1990) has suggested that for design purposes the bond coefficient may be calculated based upon the grid dimensions and the soil properties. The analysis suggested is for a general case of reinforcement as shown in Figure 5.9. Using this general case when the fraction of the grid surface area that is solid is set to unity ($\bar{a}_s = 1$) the proposed relationships reduce to those for sheet type woven and non-woven geotextiles.

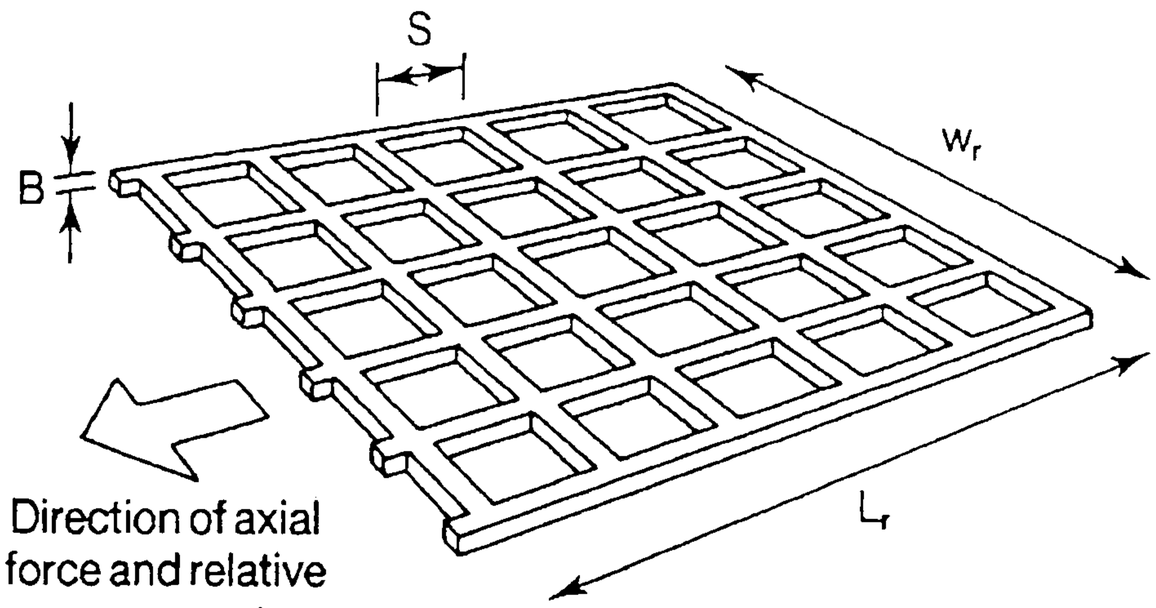

$\bar{a}_s$ Fraction of grid surface area that is solid
$\bar{a}_b$ Fraction of grid width w_r available for bearing

Figure 5.9 Geometrical definitions for geotextiles (CIRIA 1996)

5.4.3 COEFFICIENT OF DIRECT SLIDING

The shear resistance to direct sliding of a soil-reinforcement system is dependent upon:

a) Shear between the soil and the planar surface of the reinforcement.

b) Soil - soil shear through the apertures of the reinforcement.

The overall direct sliding coefficient is defined by the coefficient α_{ds}. The theoretical expression for direct sliding resistance recommended for design is given in Equation 5.3:

$$\alpha_{ds} \tan\phi' = \bar{a}_s \tan\delta + (1 - \bar{a}_s)\tan\phi' \qquad \text{Eqn. 5.3}$$

Where tan δ is the skin friction for soil shearing over the planar surface of the reinforcement, and the other terms are defined in Figure 5.9 (Jewell *et al* 1984). This may be rearranged to give the coefficient of direct sliding (α_{ds}):

$$\alpha_{ds} = \bar{a}_s \frac{\tan\delta}{\tan\phi'} + (1 - \bar{a}_s) \qquad \text{Eqn. 5.4}$$

For a sheet type woven or non-woven geotextile with no apertures $\bar{a}_s = 1$ and the coefficient of direct sliding is analogous to the skin friction between a construction material and soil:

$$\alpha_{ds} = \frac{\tan\delta}{\tan\phi'} \qquad \text{Eqn. 5.5}$$

The coefficient of direct sliding is typically in the range $1.00 \geq \alpha_{ds} \geq 0.60$ for a wide spectrum of woven and non-woven geotextiles and soils (Williams & Houlihan 1987). The lower values generally apply to geotextiles with smooth, even surfaces. The minimum possible direct sliding resistance would be of the order of $\alpha_{ds} = 0.4$ which applies for soil shearing over a smooth metal sheet (Potyondy 1961, Kishida & Uesugi 1987). Woven geotextiles with significant surface roughness mobilise greater direct sliding resistance in the

range $\alpha_{ds} = 0.8$ *to* 1.0. The skin friction between granular soil and a solid sheet of polymer is of the order $tan\delta = 0.6 tan\phi'$. Many available geogrids have an area ratio of the order $\bar{a}_s = 0.5$, which when substituted into Equation 5.4 gives a typical coefficient of direct sliding resistance for geogrids of $\alpha_{ds} = 0.8$.

5.4.4 COEFFICIENT OF BOND

The two main mechanisms of load transfer, which provide bond between soil and reinforcement, are skin friction and bearing stress as shown in Figure 5.10. Bond may be defined in terms of a bond coefficient, α_b. The contribution to bond from skin friction depends upon the planar surface area of the reinforcement, $\bar{a}_b B / 2S$, and on the ratio of the bearing stress to the stress acting normal to the reinforcement σ'_b / σ'_n, Figures 5.9 and 5.10.

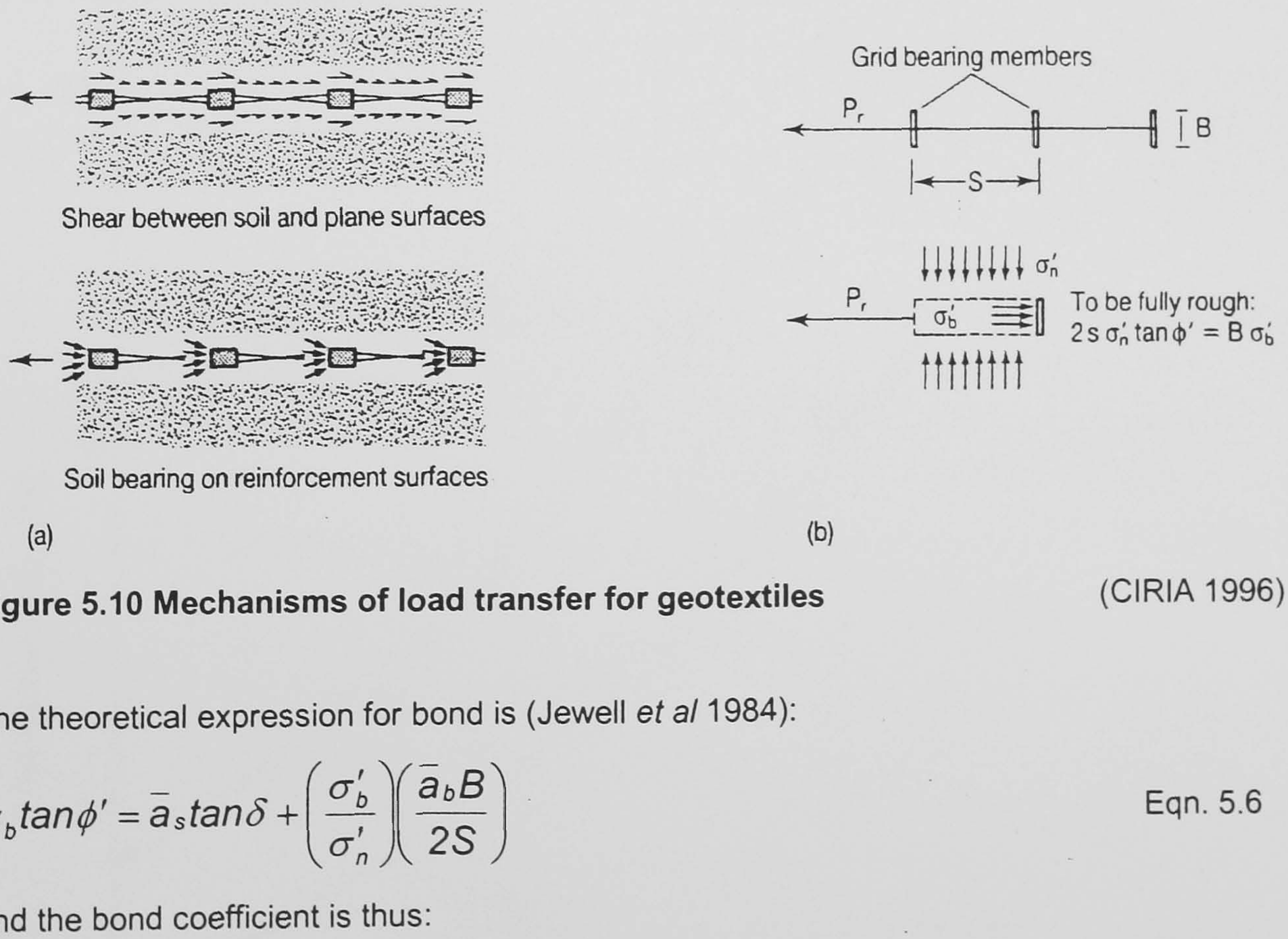

Figure 5.10 Mechanisms of load transfer for geotextiles (CIRIA 1996)

The theoretical expression for bond is (Jewell *et al* 1984):

$$\alpha_b tan\phi' = \bar{a}_s tan\delta + \left(\frac{\sigma'_b}{\sigma'_n}\right)\left(\frac{\bar{a}_b B}{2S}\right) \qquad \text{Eqn. 5.6}$$

and the bond coefficient is thus:

$$\alpha_b = \bar{a}_s \frac{tan\delta}{tan\phi'} + \left(\frac{\sigma'_b}{\sigma'_n}\right)\left(\frac{\bar{a}_b B}{2S}\right)\frac{1}{tan\phi'} \qquad \text{Eqn. 5.7}$$

The result for woven and non-woven sheet type geotextiles may be found by setting the term $\bar{a}_s = 1.0$ and $\bar{a}_b = 0.0$, thus:

$$\alpha_b = \frac{tan\delta}{tan\phi'} = \alpha_{ds} \qquad \text{Eqn. 5.8}$$

Confirming that the bond and direct sliding coefficients for these materials are equivalent. The parameters for use in Equation 5.7 are well defined except for the bearing stress ratio σ'_b / σ'_n , Figure 5.10. Relations giving theoretical upper and lower bounds to the bearing stress ratio have been found to bound the data on bearing stress recorded in pullout testing, Figure 5.11. The lower bound curve in Figure 5.10 is defined by Equation 5.9 and is recommended for design (CIRIA 1996).

$$\left(\frac{\sigma'_b}{\sigma'_n}\right)_\infty = tan\left(\frac{\pi}{4}+\frac{\phi'}{2}\right)e^{\left(\frac{\pi}{2}+\phi'\right)tan\phi'} \qquad \text{Eqn. 5.9}$$

If typical parameters for geogrid reinforcement are substituted into Equation 5.9 then it is demonstrated that the maximum possible bond in compact granular fill, $\alpha_b \approx 1.0$ (equivalent to a rough sheet), can be achieved by geogrids with geometry of the order $S / \bar{a}_b B < 20$.

The two separate components that contribute to the bond of grid reinforcement are summarised in Table 5.1 for a range of grid geometries and angles of soil friction assuming $tan\delta = 0.6tan\phi'$.

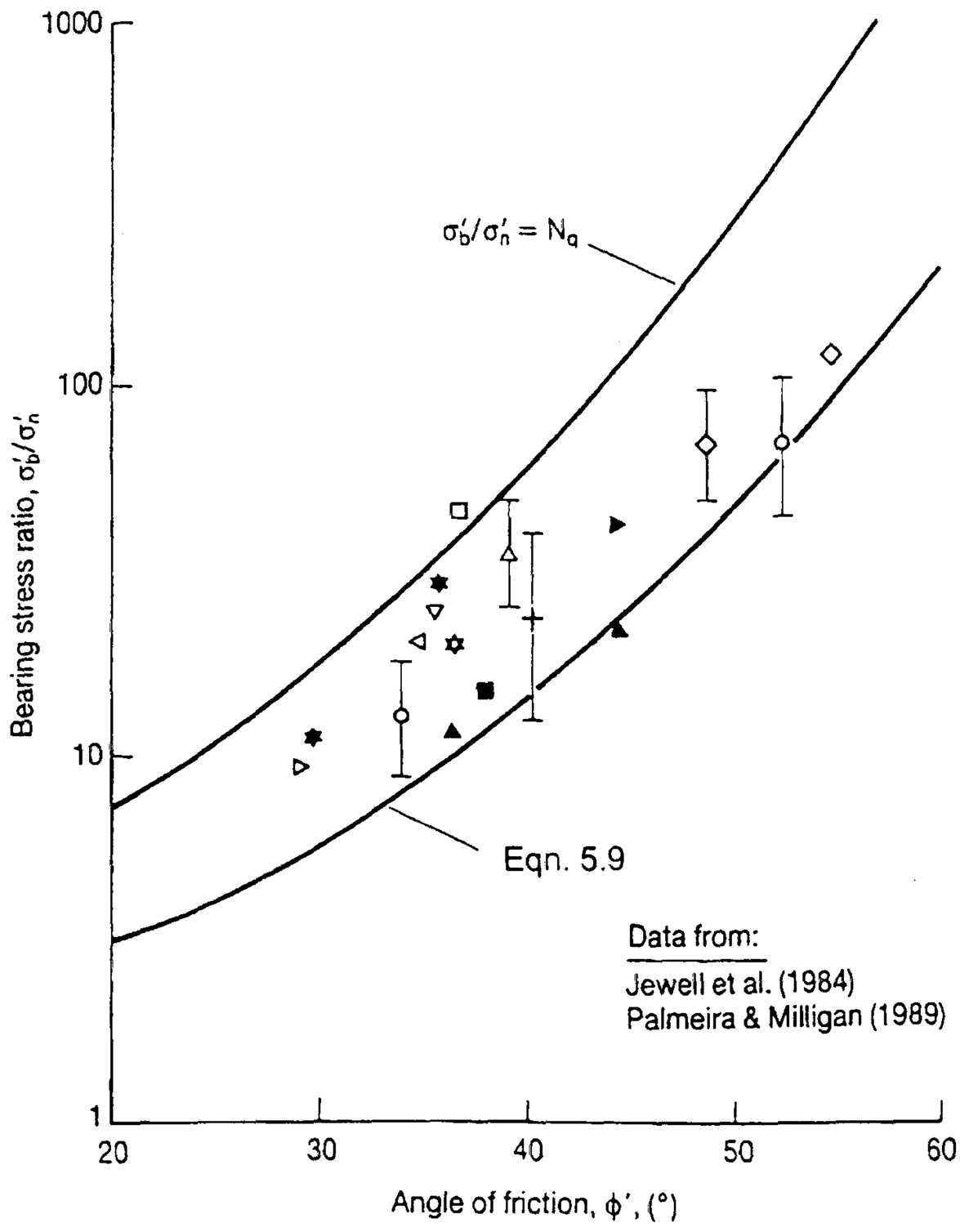

Figure 5.11 Bearing stresses on reinforcement (after CIRIA 1996)

Table 5.1 Bond coefficients for grid reinforcement (Eqn. 5.7) (after CIRIA 1996)

$\bar{a}_s$	ϕ' 25°	ϕ' 30°	ϕ' 35°	ϕ' 40°	ϕ' 45°
0.10	0.06	0.06	0.06	0.06	0.06
0.25	0.15	0.15	0.15	0.15	0.15
0.50	0.30	0.30	0.30	0.30	0.30
0.75	0.75	0.75	0.75	0.75	0.75

Component of α_b from surface shear (First term in Eqn. 5.7)†

$S/\bar{a}_b B$	ϕ' 25°	ϕ' 30°	ϕ' 35°	ϕ' 40°	ϕ' 45°
10	0.43	0.50	0.63	0.86	1.00
25	0.17	0.20	0.25	0.34	0.51
50	0.09	0.10	0.13	0.17	0.25
100	0.04	0.05	0.06	0.09	0.13

Component of α_b from bearing stress (Second term in Eqn. 5.7)‡

† $tan\delta = 0.6 tan\phi'$

‡ Subject to a maximum doubling from particle size effects

The bond coefficient for any devised combination of these is found by adding the two components together, subject to a limit of $\alpha_b \leq 1.0$.

Palmeira & Milligan (1989) have shown that there is an important scale effect due to the mean particle size (D_{50}) which increases the bearing load transfer once $B/D_{50}<10$, Figure 5.12.

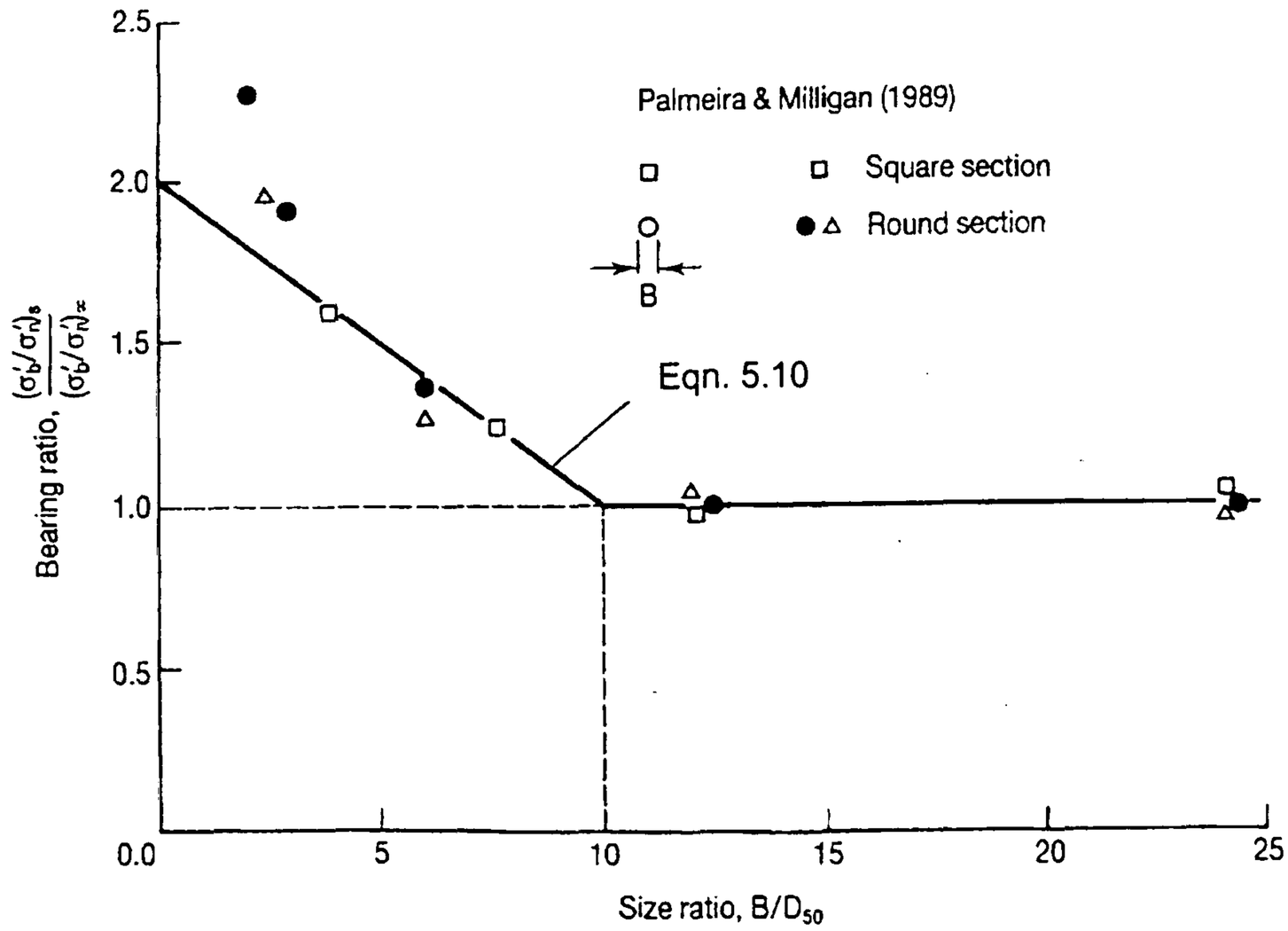

Figure 5.12 Influence of particle size on soil bearing stress (CIRIA 1996)

This is consistent with the scale effects observed in other bearing capacity problems (Kerisel 1972). The empirical relation shown in Figure 5.12 is recommended to allow these scale effects to be taken into account and is given by Equation 5.10:

$$\left(\frac{\sigma'_b}{\sigma'_n}\right) = \left(\frac{20 - \frac{B}{D_{50}}}{10}\right)\left(\frac{\sigma'_b}{\sigma'_n}\right) = F_1\left(\frac{\sigma'_b}{\sigma'_n}\right)_\infty \qquad \text{Eqn. 5.10}$$

and applies when $B/D_{50}<10$. The bearing stress ratio $\left(\sigma'_b / \sigma'_n\right)_\infty$ for a continuum (no particle size effects) is defined in equation 5.9 for bearing on transverse members of circular cross-section. For rectangular cross-sections an increase by a factor of 1.2 is appropriate (CIRIA 1996). Hence, both scale effects and the shape factor can increase the load transfer in bearing by up to a factor of two or more, explaining the scatter in Figure 5.11. Adopting these refinements the expression given in Equation 5.7 may be re-written as:

$$\alpha_b = \bar{a}_s \frac{\tan\delta}{\tan\phi'} + F_1 F_2 \left(\frac{\sigma'_b}{\sigma'_n}\right)_\infty \left(\frac{\bar{a}_b B}{2S}\right)\frac{1}{\tan\phi'} \qquad \text{Eqn. 5.11}$$

Where the factor F_1 allows for scale effects and is defined by Equation 5.10 when $B/D_{50}<10$ otherwise $F_1=1.00$. The shape factor $F_2=1.0$ for circular bar and $F_2=1.2$ for rectangular bar.

5.5 ANALYSIS OF CONVENTIONAL GEOGRID REINFORCED WALLS

The design of the EKG/reinforced cohesive wall was based upon modified conventional design practice and, therefore, it is necessary to briefly review the analysis methods for conventional reinforced soil walls. The discussion is limited to the use of geogrids for reinforcement, as this type of reinforcement was utilised in the field trials. The discussion and theories developed may, however, be adopted for different reinforcement types.

5.5.1 DESIGN METHODOLOGY

Walls and abutment structures are conventionally constructed using horizontally placed reinforcement. The vertical spacing of the reinforcement may remain constant throughout the full height of the wall, but the density or strength of the reinforcement is likely to be greater towards the base of the wall, where the horizontal thrusts are at a maximum.
The simplest layout of reinforcement is a uniform distribution of identical reinforcing elements throughout the entire length and height of the structure (Jones 1996). This layout is usually uneconomical except on small-scale works. A more economical design may be achieved by using reinforcement of different properties or by dividing the structure into different zones. Currently there are two design methods that encompass design methodologies in the United

Kingdom, USA and parts of Europe. These are the *coherent gravity* hypothesis and the *tieback wedge* hypothesis.

5.5.1.1 Coherent Gravity

The coherent gravity method is an empirical technique that has been described by Mitchell and Villett (1987) and the Ministères des Transports (1979). It was developed to provide for structures with reinforced steel strip (inextensible) reinforcement. The method contains four basic assumptions for the internal stability of reinforced soil structures (Netlon Ltd 1986 and Jones 1996):

1) The reinforced soil mass is divided into two fundamental zones, an active zone and a resisting zone, delineated by the line of maximum tension in the reinforcement as shown in Figure 5.13. This failure mode is analogous to that formed in a mass of cohesionless soil supported by a rigid wall rotating about the top; see Figure 5.14.
2) The state of stress within the reinforced mass varies from an "at rest" (K_o) condition at the top of the structure to an active (K_a) stress state at a critical depth, the calculation of lateral earth pressure is based upon this assumption. Cohesionless fill only is used.
3) An apparent coefficient of adherence between the reinforcing elements and the fill based upon the results of pullout tests is assumed.
4) A Mayerhoff pressure distribution is assumed to exist both beneath and within the reinforced fill.

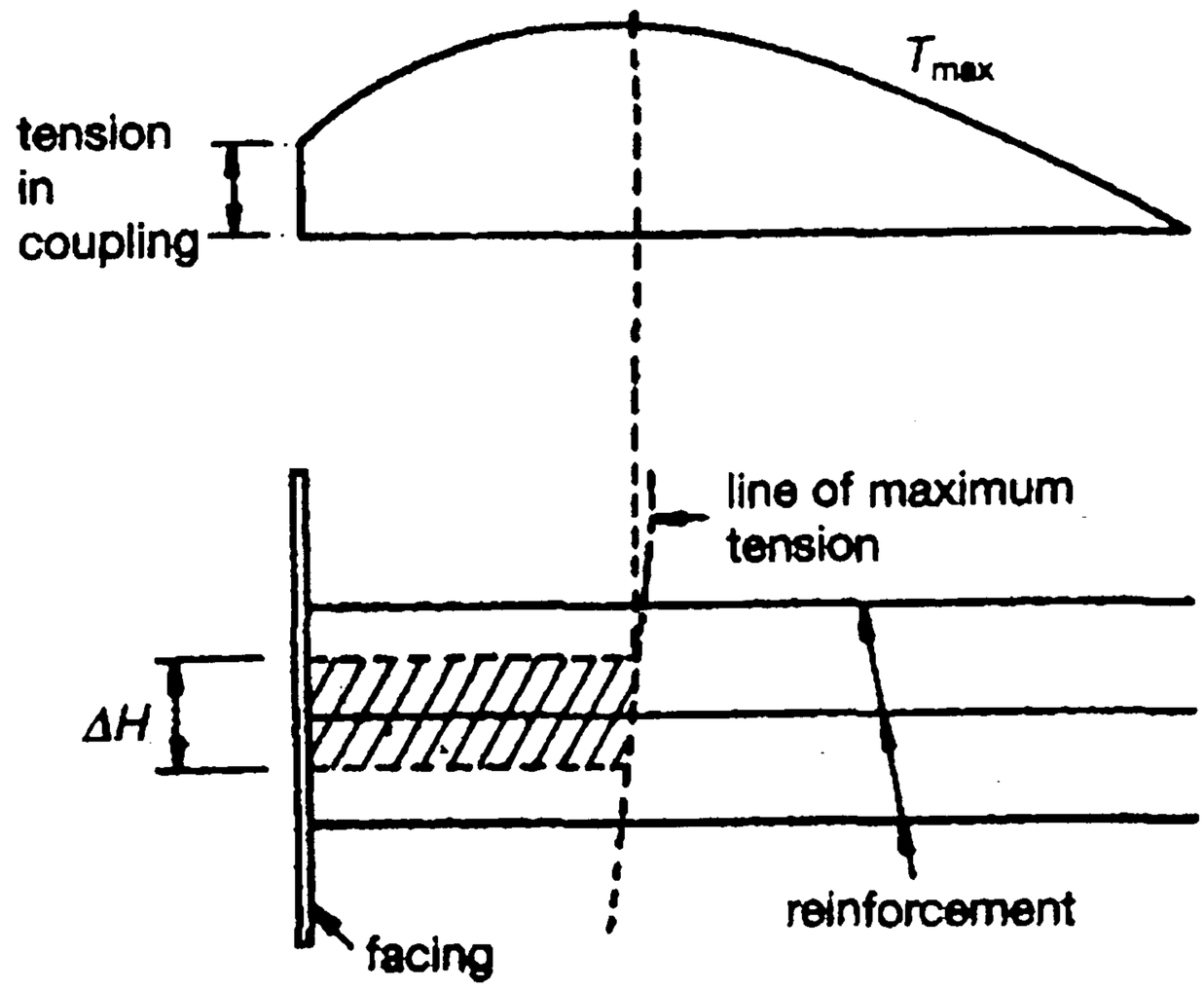

Figure 5.13 Tension distribution in coherent gravity analysis (Jones 1996)

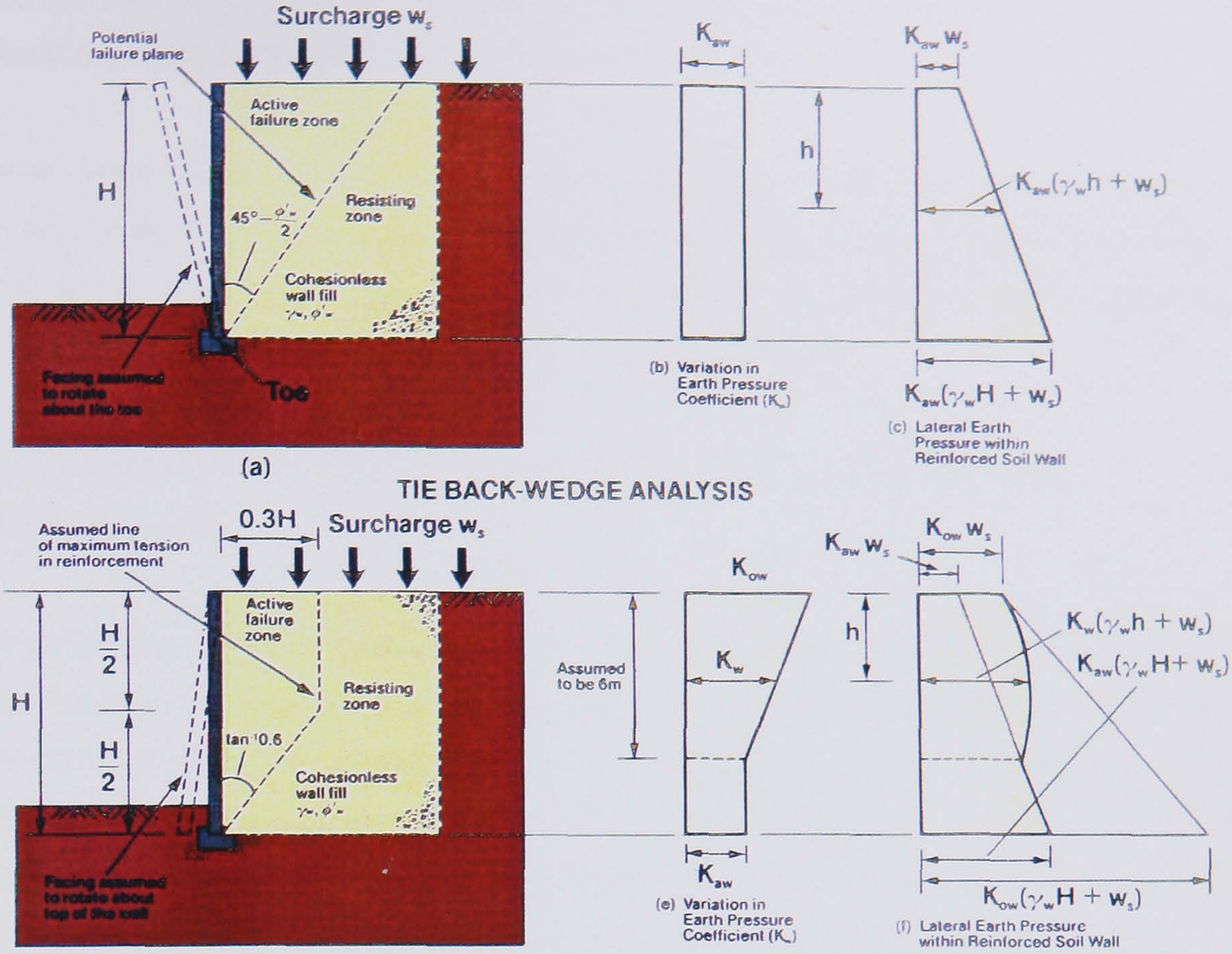

Figure 5.14 Earth pressure distributions in different analysis methods (Netlon Ltd 1986)

5.5.1.2 Tie-Back Wedge

The tie-back wedge method was developed by the UK Department of Transport (1978) and is based upon limit equilibrium methods. It is independent of the reinforcement material type, and is used with both inextensible and extensible reinforcement and anchors. The tie back wedge analysis assumes that the lateral earth pressures within the structure are all due to the active earth pressure coefficient (K_a), thereby neglecting any additional earth pressure that may have been produced by heavy compaction plant on the wall fill as shown in Figure 5.14. Details of the tie-back wedge analysis used for the design of the full-scale trial wall are given in Annex B.

5.6 COHESIVE FILL TO REINFORCED SOIL

The development of polymeric reinforcements has allowed the possibility of using indigenous soils and waste fills (Jones *et al* 1996) in reinforced soil structures, thus providing the possibility of realising significant savings in construction costs.

The acute lack of conventional frictional fill in some countries, such as Japan, has lead to the use of cohesive soils in major reinforced soil structures in theses countries. It has also been shown (Tatsuoka *et al* 1992 and Tatsuoka 1992) that geosynthetic reinforced soil structures formed using cohesive or cohesive frictional fill are potentially more stable than structures

formed from purely frictional fill. It is notable that this type of cohesive soil structure withstood the Kobe earthquake (Tatsuoka *et al* 1995).

However, many codes of practice, including BS 8006 (BSI 1995) do not permit the use of purely cohesive soil in the construction of reinforced soil structures for permanent works, with the reasons for its exclusion stated as; low strength, high moisture content, high creep and low bond strength between the soil and the reinforcement.

5.6.1 HISTORICAL EXPERIMENTATION AND EXPERIENCE IN COHESIVE REINFORCED SOIL

Schlosser and Long (1974) conducted early research into the effect of the proportion of fine grained material in reinforced soil backfill using powdered clay mixed with glass balls. Their results demonstrated that for undrained saturated conditions as the percentage of clay in the soil increased so the undrained angle of shearing resistance (ϕ_u) tended towards zero and the undrained shear strength (c_u) tended towards that of the pure clay.
Further experiments into the coefficient of friction between the fill and reinforcement indicated that the ratio between the coefficient of friction between the soil and metallic reinforcement (Tan δ) and Tan ϕ_u was in the range of 1.0 - 0.5, for soils with up to 30% of the particles less that 80μm.

Murray & Boden (1979) conducted a full-scale, 6m high, composite trial of reinforced cohesive fill and reinforced granular fill after an earlier (Boden *et al* 1978) small-scale wall had proved satisfactory. The variation in construction height of the wall with time, and its composition, is shown in Figure 5.15.

The lower cohesive fill was placed as wet as possible consistent with the limits of trafficability. The upper cohesive fill was placed at a moisture content consistent with that considered suitable for the construction of a cohesive fill embankment in the U.K. (Murray & Boden 1979); see Table 5.2. The central layer of granular fill was used to provide a direct comparison between the performance of conventional granular and cohesive fills. It did, however, also act as a drainage layer for any excess pore water pressures generated in the cohesive layers.

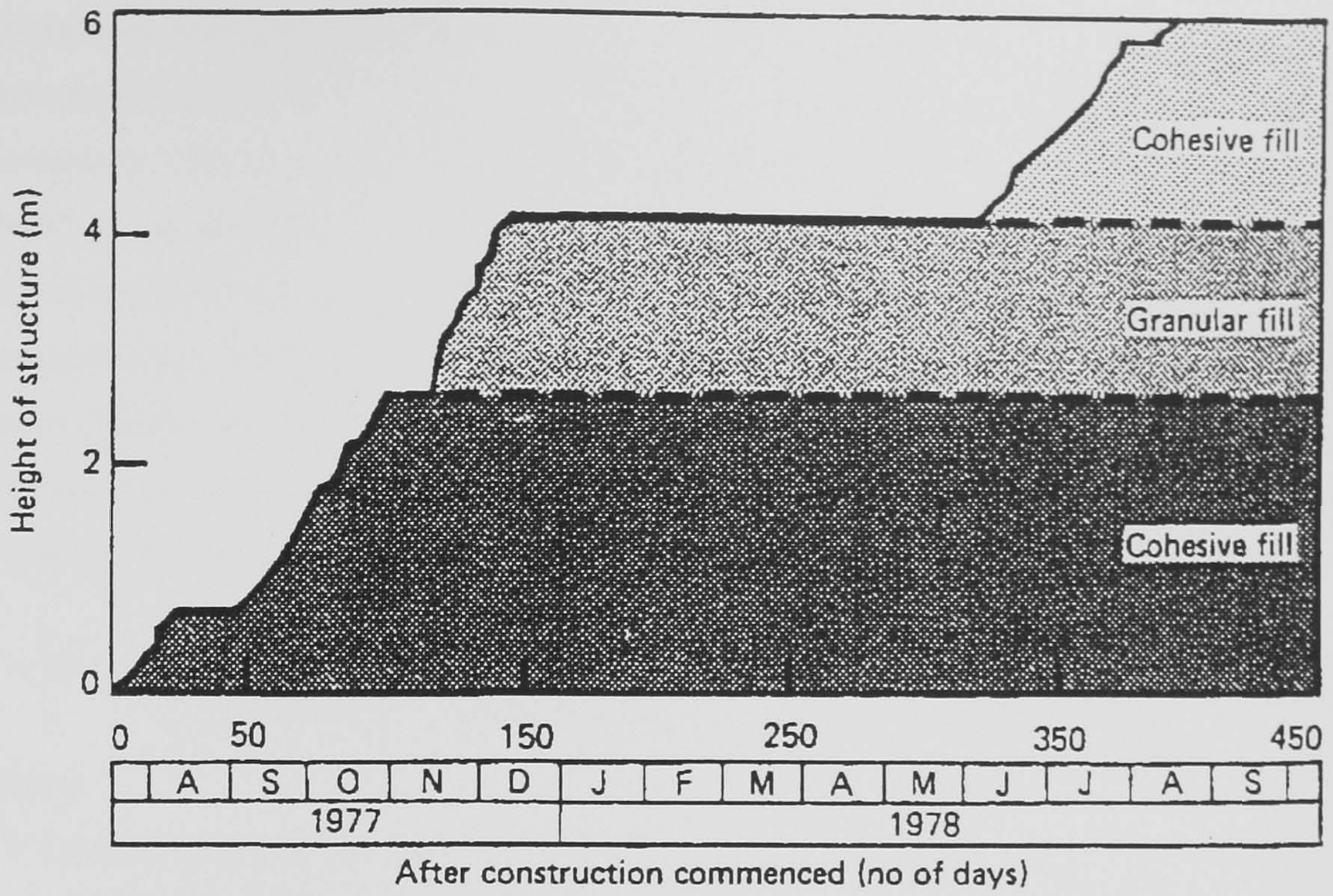

Figure 5.15 Height of construction against time (Murray & Boden 1979)

The reinforcements types used in the structure were; stainless steel, mild steel (galvanised, aluminium and plastic coated), prestressed concrete planks, fibre reinforced plastic (FRP) and non-woven fabric.

Table 5.2 Summary of soil properties in Murray & Boden (1979) wall

Position	Liquid Limit	Plastic Limit	% Sand	% Silt	% Clay	Average w (%)	c_u (kPa)	k (m/s $*10^{-10}$)
Lower Cohesive	30	17	51	39	10	17	45	6.0
Upper Cohesive	42	21	7	65	28	18	90	0.4

The following observation was made during the construction of the wall (Murray & Boden 1979):

"The porewater pressure was seen to rise with increasing depth from the face of the wall"

This was probably due to the increasing distance from a drainage path, this interpretation is corroborated by the fact that very small or zero pore water pressures were recorded at all times for locations less than 1m distant from the wall facing. The maximum pore water pressures were observed immediately after the lower cohesive zone had been built up to full height, before the delay in construction. The dissipation of pore water pressure was in agreement with that calculated from consolidation parameters measured in the laboratory.

The tensile force in the reinforcement was also measured using eight pairs of strain gauges mounted at intervals on opposite sides of selected reinforcements. The results obtained demonstrated that the change in tensile force in the reinforcement was related to the increase in effective stress due to the dissipation of excess pore water pressure. This is shown in Figure 5.16.

This is of significance in the design of reinforced structures using cohesive fill as it demonstrates that tensile resistance is mobilised through effective stress rather than total stress (Murray & Boden 1979). It was noted that at locations where the excess pore water pressures were small or zero the tensions in the reinforcement agreed well with those predicted by the theoretical equation presented in Equation 5.12.

$$T = \left[K_a \gamma Z \left(1 + K_a \left(\frac{Z}{L} \right)^2 \right) \right] S_V S_h \qquad \text{Eqn. 5.12}$$

Where:

T = Tension in reinforcement

K_a = Coefficient of active earth pressure

γ = Unit weight of fill

Z = Depth to reinforcement in fill

L = Length of reinforcement

S_V, S_h = Spacing of reinforcement in vertical and horizontal directions

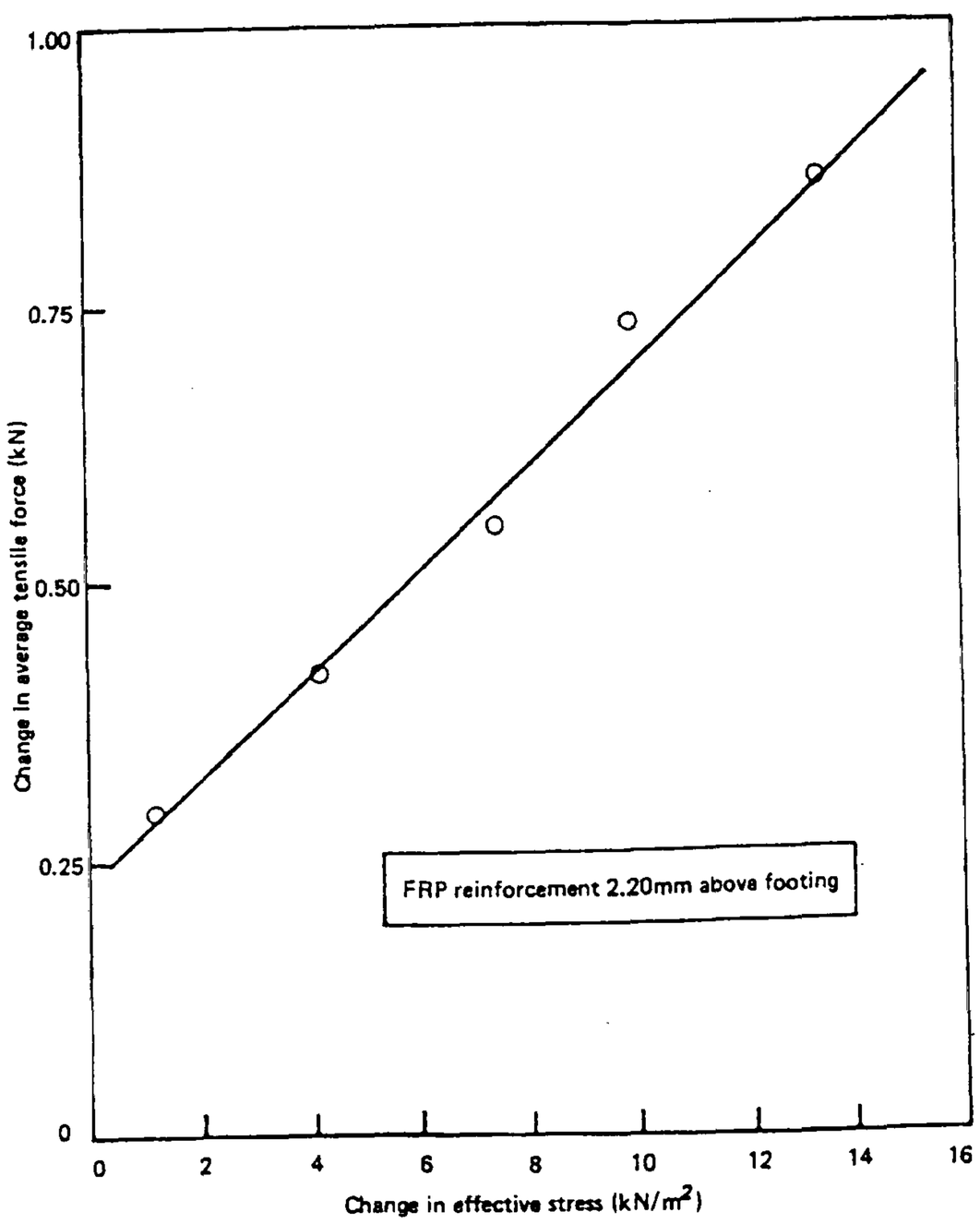

Figure 5.16 Effective stress against force generated in reinforcement (Murray & Boden 1979)

The following conclusions were also drawn from the results:

- Horizontal pressures - with soils close to saturation high pore water pressures are generated (due to compaction and overburden) which act on the wall but subsequently decay as dissipation takes place.
- Tension in reinforcement - excess pore water pressures inhibit the development of effective stress and reduce the bond between soil and reinforcement.
- Distribution of tension in reinforcement - due to the presence of a drainage boundary at the wall face, the full effective stresses are quickly mobilised in this region whereas at other locations the effective stresses are much smaller. In the short-term much of the support for the wall may develop over a relatively small proportion of the length of the reinforcement. As consolidation takes place more available resistance develops and some redistribution of tension may take place.

Jewell & Jones (1981) discussed the experimental and full-scale field application of a 2.0m - 6.0m high reinforced soil structures built from cohesive mine waste. The laboratory work was undertaken on lightly overconsolidated kaolin reinforced with polymeric grid type reinforcement. The reinforced samples were then tested in the direct shear apparatus in both drained ($0.28x10^{-3}$mm/s) and undrained (0.12 mm/s) states.
The load displacement graphs for both types of test are presented in Figure 5.17.

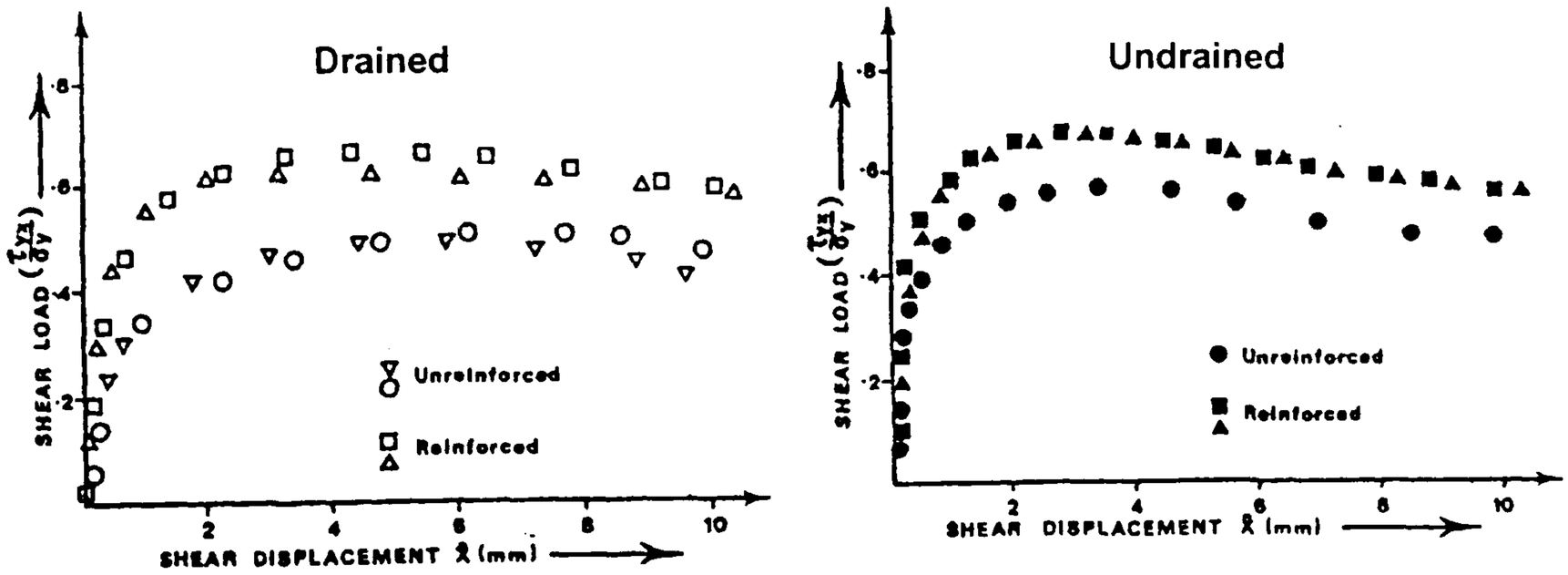

Figure 5.17 Load displacement curves for direct shear tests (Jewell & Jones 1981)

The drained tests demonstrate that the inclusion of grid type reinforcement improves both the strength and the stiffness of the kaolin compared to the unreinforced case. The undrained tests also show a similar improvement in both strength and stiffness. The paper also states that in tests carried out by Jewell (1980) grid type reinforcements were found to be the most effective type of reinforcement for both cohesionless and cohesive soils.

Ingold (1981) presents the results of a series of simulated reinforced soil walls reinforced with a polyethylene mesh. The walls were brought to failure by the application of a vertical surcharge. The results were then analysed using total stress analysis methods for short-

term stability. Ingold (1981) presented two analytical methods for the reinforced clay wall; a discrete theory and a composite theory. The discrete theory considers the restoring forces in the wall to be the sum of two discrete forces, those due to the clay fill and those developed by the reinforcement. The composite theory considers the undrained shear strength of the clay - reinforcement composite system.

Initially the investigations carried out a systematic study of soil-reinforcement adhesion coefficients (α) using three different test methods, shear box with inclined reinforcement, shear box with horizontal reinforcement and pullout tests. The adhesion factors obtained from each of these tests are presented in Table 5.3.

Table 5.3 Results of interaction tests undertaken on "geogrid" in clay by Ingold (1981)

Test Type	Adhesion coefficient (α)
Inclined reinforcement shear box	1.03
Horizontal reinforcement shear box	0.89
Pullout	0.18

Although there is a large variation in the α values obtained from these tests some of the apparent discrepancies may be explained:

- Inclined shear box - The grid is surrounded by soil and is subject to flexure by the test method as well as pullout/direct sliding along the grid/soil interface.
- Horizontal shear box - Only the upper half of the shear box apparatus was filled with soil material, the lower half being filled with a solid aluminium blank. As discussed in §5.4 this test method is inappropriate for grid type geosynthetics and both halves of the shear box should contain soil. Hence, the horizontal shear box tests conducted by Ingold (1981) are likely to give an underestimation of the interaction coefficient due to the soil/aluminium and polymer/aluminium interfaces being smoother than the soil/soil or soil/polymer interactions.
- Pullout - The reason proposed by Ingold (1981) for the low values obtained in the pullout tests are the relatively high extensibility of the polyethylene mesh resulting in a non-uniform distribution of relative strain and mobilised adhesion. McGown (1979) indicates that, for an extensible non-woven fabric, strains are high at the loaded "pullout" end dropping rapidly to zero or near zero values towards the free end of the sample. As a result, the equation proposed by Ingold (1981) for the calculation of the adhesion coefficient, which is based upon the overall dimension of the geotextile under test, under predicts the adhesion coefficient. However, for stiff reinforcement the strain distribution is more uniform and the equation proposed by Ingold (1981) gives consistent results.

Sridharan *et al* (1991) presented a novel technique for the use of fine grained soil in reinforced earth which comprises of using relatively thin layers of a frictional type material (e.g. sand) around the reinforcement to allow mobilisation of the full interface shearing resistance of the sand and using cohesive fill as the bulk fill. The concept is demonstrated in Figure 5.18.

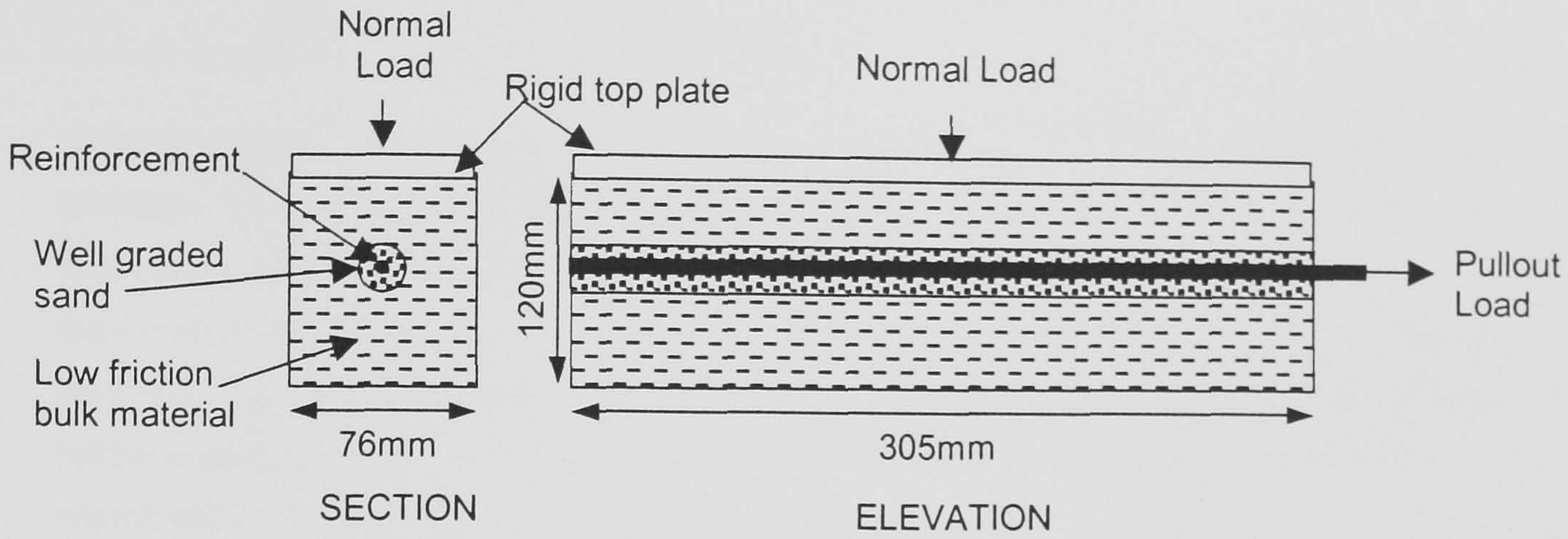

Figure 5.18 Cross-section through pullout apparatus utilised by Sridharan *et al* (1991)

However, the study only covered laboratory investigations utilising pullout tests and no full-scale trials were conducted to investigate the practicality of building the composite system. The results demonstrated, as would be anticipated, that as the thickness of the sand layer increased so the overall pullout resistance increased, tending towards that for the pullout apparatus full of sand. However, if flat reinforcement (3mm thick), as opposed to bar reinforcement was used the thickness of the sand layer required to mobilise the maximum amount of pullout resistance was found to be of the order of 10mm either side of the reinforcement.

The inclusion of sand layers in reinforced soil would appear to be a technique worthy of further research as the technique combines drainage layers with zones of increased anchorage resistance for the reinforcement. One possible drawback of the technique is that to drain very fine grained soils it may be necessary to utilise a variety of grain sizes to establish a filter to prevent the loss of fines from the cohesive bulk fill. The technique is also likely to be difficult to construct.

Jones *et al* (1996) and Nettleton *et al* (1998) introduced the concept of developing a range of geosynthetics that in addition to providing filtration, drainage and reinforcement can be enhanced by electrokinetic techniques for the transport of water and chemical species within fine grained low permeability soils.

The papers suggest the use of electrokinetic geosynthetics (EKG) for reinforced soil and present the results of pullout tests as evidence that there is a synergy between electro-osmosis and reinforced soil, the results are presented in Table 5.4. The full test details and results may be found in Hamir (1997).

Table 5.4 Increases in shear strength and soil/reinforcement bond when using EKGs at different overburden pressures Jones *et al* (1996) Nettleton *et al* (1998)

Consolidation pressure (kPa)	Increase in c_u (%)	Increase in bond strength (%)
110	150	211
140	200	113
356	70	54

Hamir *et al* (2001) continues upon the work presented in Jones *et al* (1996) and Nettleton *et al* (1998). Stating that the development of permeable, non-metallic reinforcing elements which are not susceptible to corrosion would allow the dissipation of excess pore water pressures generated in reinforced cohesive soil and lead to improved bond between soil and reinforcement. The paper goes on to state that the performance of the reinforcement can be further enhanced by making it electrically conductive thereby introducing electro-osmotic consolidation to reinforced soil technology. The potential benefits are stated as:

- Increasing the rate of dissipation of positive pore pressure in the cohesive fill in excess of that which can be achieved using permeable reinforcement alone.
- Inducing additional consolidation (and associated increase in shear strength) to that obtained by the self-weight of the fill material above.
- Dissipating positive pore pressure at the soil/reinforcement interface to a greater degree than with impermeable reinforcement, thereby increasing reinforcement/soil bond.

5.6.2 EXISTING REINFORCED COHESIVE SOIL SYSTEMS - STATE OF PRACTICE

Two systems are currently available which attempt to overcome the problems associated with the use of cohesive fill in reinforced soil and the generation of high excess pore water pressures.

5.6.2.1 Textomur System

The Swiss Textomur (Keller Comtec 2000) system is a system developed for the use of cohesive fill, which utilises a non-woven geotextile to provide drainage and a geogrid reinforcement to provide reinforcement (Jones *et al* 1996). The system may, however, be criticised in that the reinforcement is placed where the maximum excess pore water pressures and slowest dissipation occurs, hence, bond will be drastically reduced between the soil and reinforcement in this zone. Ideally, the system would provide combined drainage and reinforcement at the same location. The system is shown schematically in Figure 5.19

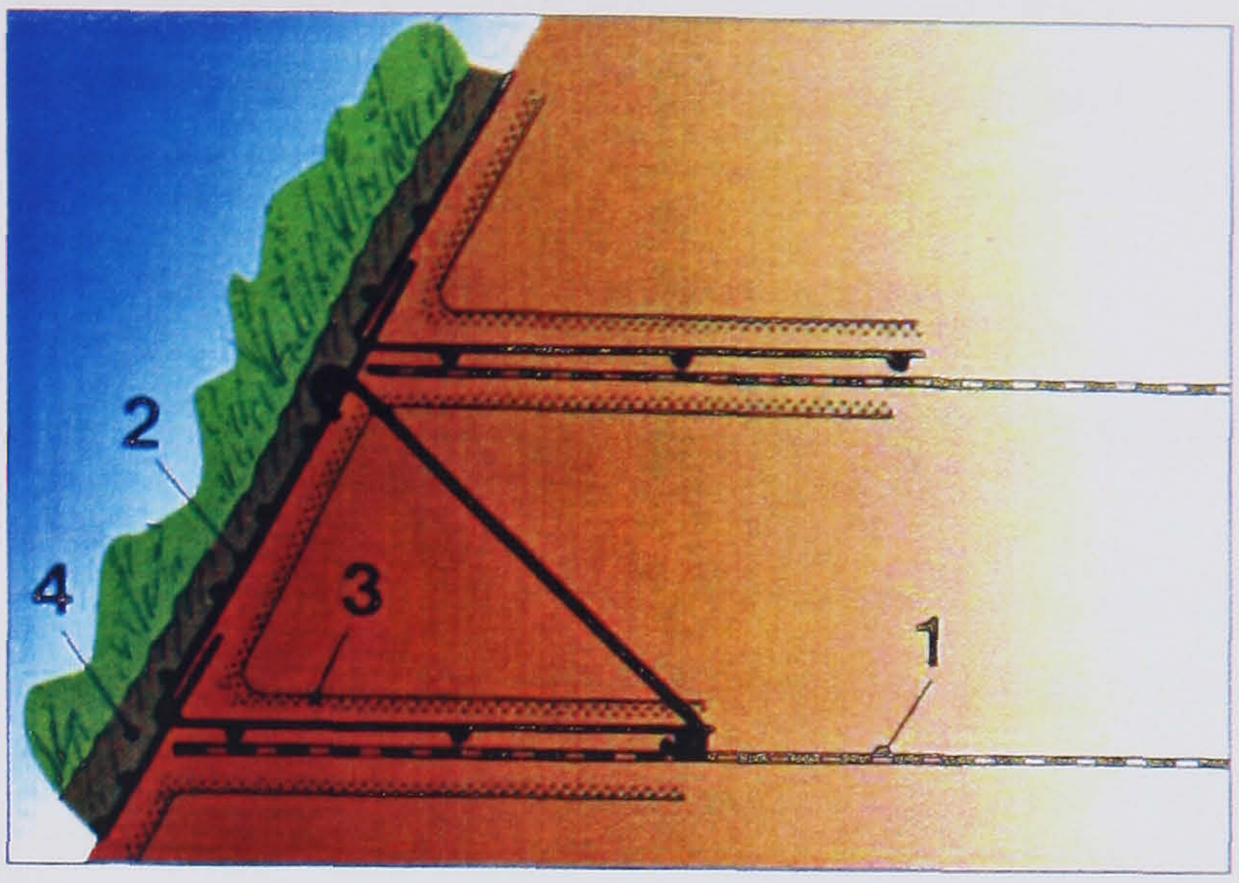

Figure 5.19 Cross-section through Textomur system (Keller Comtec 2000)

5.6.2.2 Paradrain System

The Paradrain system is relatively modern system that combines both drainage and reinforcement (Terram Ltd. 2000, Kempton *et al* 2000). The idea originally behind this concept was investigated at the University of Newcastle by Heshmati (1993), who combined drainage material and grid reinforcement in clay soil with the objective of identifying the separate and combined actions of the materials in improving the overall shear strength characteristics of a clay. Details of the Paradrain system are shown in Figure 5.20.

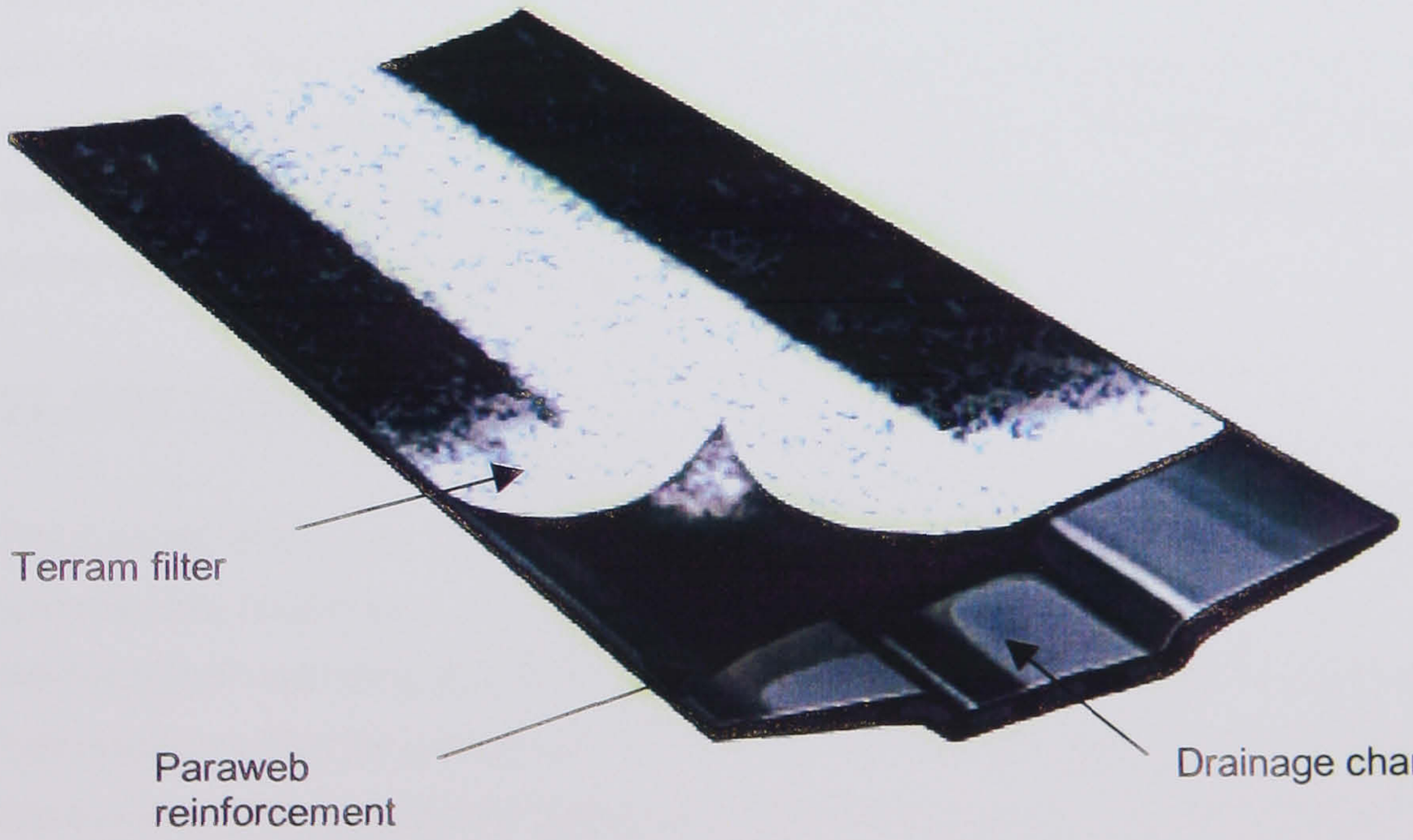

Figure 5.20 Details of Paradrain combined reinforcement/drain (Terram Ltd 2000)

Dissipation tests undertaken using the Paradrain indicated that excess porewater pressures of 50 and 100kPa could be dissipated to 20% of their initial value in 36 to 42 hours. Additionally, pullout tests conducted in English China Clay showed that the Paradrain could

improve the soil reinforcement bond after only partial dissipation of the excess porewater pressure. After full dissipation the pullout resistance at small displacements can increase by as much as 500% when compared to geogrids of similar construction but with no drainage channel.

5.6.3 CONCLUSIONS OF STATE OF PRACTICE AND HISTORICAL REVIEW

From the review of previous experimentation and experience in reinforced cohesive soil it is apparent that if the porewater pressures generated within a reinforced cohesive mass can be controlled such that the effective stress within the structure increases an effective bond between the soil and reinforcement may be achieved (Murray & Boden 1979). The dissipation of the porewater pressure may be achieved by the inclusion of drainage layers (Sridharan *et al* 1991), non-woven geosynthetics that act as drains (Keller Comtec 2000) or drainage elements that are combined with reinforcement (Terram 2000). Reinforced cohesive soil structures have also been demonstrated to be more stable than conventional cohesionless soil structures under seismic loading (Tatsuoka *et al* 1992 and Tatsuoka 1992). The inclusion of reinforcement has also been shown to increase both the strength and stiffness of cohesive soils in both drained and undrained conditions (Jewell & Jones 1981). Jewell (1980) has also demonstrated that grid type reinforcement may be effectively employed for the reinforcement of cohesive soils.

Jones *et al* (1996), Nettleton *et al* (1998), Hamir (1997) and Hamir *et al* (2001) have demonstrated that a synergy exists between reinforced cohesive soil and electrokinetic phenomena. They have also suggested the use of electrically conductive geosynthetics as a means to achieving this synergy in practice. The remainder of this chapter presents the realisation of these suggestions through the construction of a full-scale electrokinetically enhanced cohesive reinforced wall, the Joint Stocks wall.

5.7 JOINT STOCKS WALL

The purpose of the Joint Stocks wall was to demonstrate, by means of a full-scale trial, that electrokinetic phenomena could be applied through the use of EKGs to construct a reinforced soil wall using an extremely wet cohesive fill, which without undergoing significant improvement would be unable to be built. Thus demonstrating the synergy between electrokinetic phenomena and reinforced cohesive soil through the use of EKGs in the field at full-scale.

The site for the construction of the wall was made available to the University of Newcastle upon Tyne for the purpose of this research by CAPITOL Waste Management. The site is located within the Joint Stocks waste disposal and recycling centre approximately 1km north-east of Coxhoe and 500m north-west of Kelloe, County Durham, United Kingdom (Grid Ref:

NZ 329364). The site is currently a domestic landfill and recycling centre located within the old Joint Stocks Magnesian Limestone quarry. The location of the trial itself is in the centre of the site adjacent to a small lake on a slope of westerly aspect composed of 20 year old capped landfill.

5.7.1 SELECTION OF FILL MATERIAL

The fill material to construct the wall had to fall outside the limits of the acceptable soil types outlined in the British Standard on reinforced soil BS 8006 (BSI 1995) and also be amenable to improvement by electrokinetic phenomena. The soil type that satisfies these two criteria is a wet *cohesive fill* as defined by the Specification for Highway Works (DoT 1993).
Two distinct soil types were tested in the laboratory to assess their suitability for use in the wall, a pink silt sized material and a laminated clay. The pink silt material was investigated as a possible source of fill for use in the reinforced trial wall as a large quantity of the material was available at the Joint Stocks complex, and as such would negate the need to transport fill to the site. The pink/grey silt was originally derived from a Magnesium limestone waste product from limekilns and large stockpiles of it were available on site. The laminated clay was obtained from Bracken Hill Business Park, Peterlee, County Durham, United Kingdom. The clay was a waste product excavated by Greenfield Excavations during the groundworks for the construction of portal frame factory units and was to be sent to landfill for disposal.

5.7.2 LABORATORY TESTING

Laboratory tests were undertaken to assess the suitability of the fill materials that were available. The suite of testing consisted of:

- Establishing the undrained shear strength (c_u) and its variation with moisture content undertaken using quick shear box tests to BS 1377: Part 7 (BSI 1990c) on remoulded samples formed in the consolidometer.
- Establishing the effective stress shear strength parameters (c',ϕ') for both peak and residual states using shear box tests to BS 1377: Part 8 (BSI 1990d) on remoulded samples formed in the consolidometer.
- Establish electrical parameters (σ) using the disk electrode method to BS 1377: Part 3 (BSI 1990b)
- Establish general index properties (LL, PL, PSD) to BS 1377: Part 2 (BSI 1990a)

The parameters obtained for both of the soil types tested are presented in Table 5.5.

Table 5.5 Soil parameters for possible fill materials for the Joint Stocks wall

Parameter	Pink Silt	Laminated Clay
LL (%)	18	60
PL (%)	N/A	35
PSD (D_{10},D_{50}) (mm)	0.008, 0.063	<0.002, 0.03
Gs	2.65	2.61
c_u (kPa) @ w_c	*Not undertaken due to unacceptability*	89 @32%, 49 @35% 24 @41%
Peak ϕ', c' (Remoulded)		21° & 7.6kPa, 23° & 7.3kPa. 22° & 6.6kPa
Peak ϕ', c' (Undisturbed)		23° & 10.5kPa
Residual ϕ', c' (Remoulded)		20° & 5.5kPa, 18° & 7.6kPa, 19° & 6.3kPa
Residual ϕ', c' (Undisturbed)		12° & 7.8kPa
σ (Siemens/m)	$1.79*10^{-3}$	0.6¥
E-O Cell (%) improvement	0%	61%

¥ *This value was obtained using the water available on site*

Based upon the results of these tests the pink silt material was rejected for use in the wall and the laminated clay was accepted, although its electrical conductivity was on the high side. The E-O cell improvement presented in Table 5.5 was undertaken using the electro-osmotic cell developed by Hamir (1997) and further used by Laidler (1999), see § 7.2.7.1. The percentage improvement was taken as the increase in the volume of water removed from the sample in the E-O cell above that removed in the control cell (no voltage), as such it is a measure of the improvement induced by electro-osmosis.

5.7.3 DESIGN OF THE WALL

Initially the wall was designed for long-term stability using the effective stress parameters for the laminated clay established from the laboratory testing using Tensar International's design package Winwall 6.14 (Netlon Ltd 1998). The long-term design was then checked for short-term stability based upon a minimum required undrained shear strength for the clay utilising four different analysis methods, critical height, Coulomb, discrete theory and composite theory. It was necessary to carry out the design in this order as Winwall 6.14 (Netlon Ltd 1998) was unable to analyse the structure for stability in the short-term as it is not possible to model cohesive fill due to its unacceptability in BS 8006 (BSI 1995). Therefore, cohesive reinforced soil design methods have been developed. These do, however, rely upon the geometry of the reinforcement layout been known before the analysis can be undertaken. Hence, the recommended chronology for design is long-term design followed by short-term design to confirm the required value of c_u which electrokinetics are required to attain to achieve stability.

5.7.3.1 Tie-back Wedge Analysis - Long-term Stability

The analysis method consists of a tie-back wedge method of analysis as discussed in §5.5.1.2 and the details of the code used by the programme are given in Annex B of this thesis.

A parametric study was undertaken to assess what variation took place in the reinforcement layout with changes in the effective stress parameters. The parametric study was conducted for a 4.8m high, vertically faced wall. The results of the study are presented in Table 5.6.

Table 5.6 Results of parametric study for long-term stability using Winwall 6.14

Soil Parameters		Reinforcement Layout			Total No. grids
ϕ'_{cv}	c´				
12.5°	0kPa	80RE * 6	40RE * 3	SS20 * 8	17
12.5°	5kPa	80RE * 4	40RE * 4	SS20 * 8	16
15°	0kPa	80RE * 4	40RE * 4	SS20 * 8	16
20°	0kPa	80RE * 3	40RE * 5	SS20 * 8	16

Notes: 4.8m high wall with vertical face, $\alpha_{pullout}$=1.0. $\alpha_{sliding}$=0.8. Retained fill ϕ'_{cv}=42.5°

From the parametric study it was found that the reinforcement layout for the soil parameters ϕ'=12.5°, c´=5kPa and for ϕ'=15°, c´=0kPa were the same for the given wall geometry. Based upon the soil parameters which had been obtained from the laboratory testing on the laminated clay given in Table 5.5, conservative, but realistic soil parameters were assumed (ϕ'_{cv}=15°, c´=0kPa) for the long-term analysis of the wall. The residual values of ϕ' were assumed to be applicable for the analysis as it requires that ϕ'_{cv} is used to ensure strain compatibility, see §5.3. Additionally, as the reinforced fill would be cohesive in nature it would be required to strain more to achieve equilibrium and it was considered that it would achieve equilibrium at a post-peak strain, tending towards a ϕ'_r, value of ϕ', see §5.3. The average of all residual ϕ'_r obtained from the laboratory testing was 17° with a minimum value of 12° for the undisturbed sample. Hence, it was felt by the Author that the value of ϕ'=15° was a realistic, slightly conservative design value for ϕ'. Additionally, the parametric study had demonstrated that even if ϕ' was assumed as a value of 20° it would make little difference to the final reinforcement design. Cohesion was assumed to be zero for long-term design as is the norm in long-term cohesive slope design. The designs produced by Winwall 6.14 (Netlon Ltd 1998) are given in Figure 5.21. The retaining end blocks of the wall which were constructed using acceptable granular fill were also deigned using Winwall 6.14 (Netlon Ltd 1998) and were only designed for the long-term due to the granular nature of the fill used. The output from the Winwall 6.14 parametric study is given in Annex C.

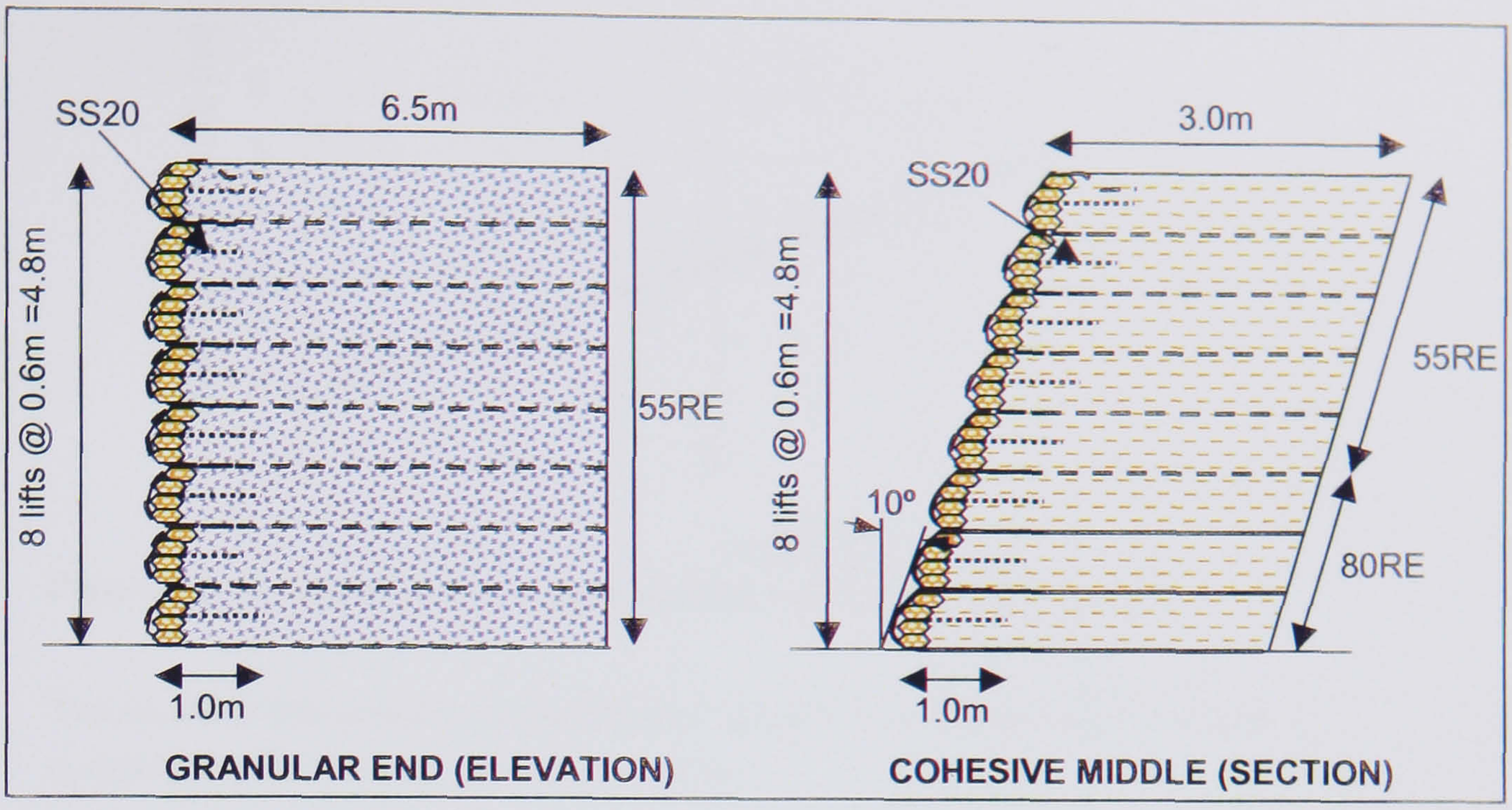

Figure 5.21 Long-term designs produced by Winwall 6.14 for the Joint Stocks wall

5.7.3.2 Critical Height Analysis - Short-term Stability

Short-term stability of the wall was considered in several ways based upon undrained soil parameters, i.e. c_u & ϕ_u. To simplify the analysis the 80° inclination of the front face was ignored and it was considered as vertical, this assumption is conservative. Initially a crude assumption was made based upon the analysis method proposed by Terzaghi & Peck (1967) for calculating critical vertical cut heights (H_c) in cohesive soil of bulk unit weight (γ) and undrained shear strength (c_u). The equation used in the calculation is presented as Equation 5.13:

$$H_c = \frac{4\,c_u}{\gamma} \qquad \text{Eqn. 5.13}$$

Based upon the required design height of the wall of 4.8m it was possible to calculate the necessary value of c_u that the cohesive fill was required to have to be stable at the design height. A graph presenting the variation of critical height against undrained shear strength is presented in Figure 5.22.

It was appreciated that this analysis method is a specific case of the Coulomb analysis, 45° failure plane (see §5.7.3.3), and was an unsophisticated simplification of the reality in that no account was taken of the presence of the reinforcement or sandbag facing. However, for obtaining an initial consideration of the increase in the strength of the cohesive fill required during construction, until full height was achieved, it was deemed satisfactory.

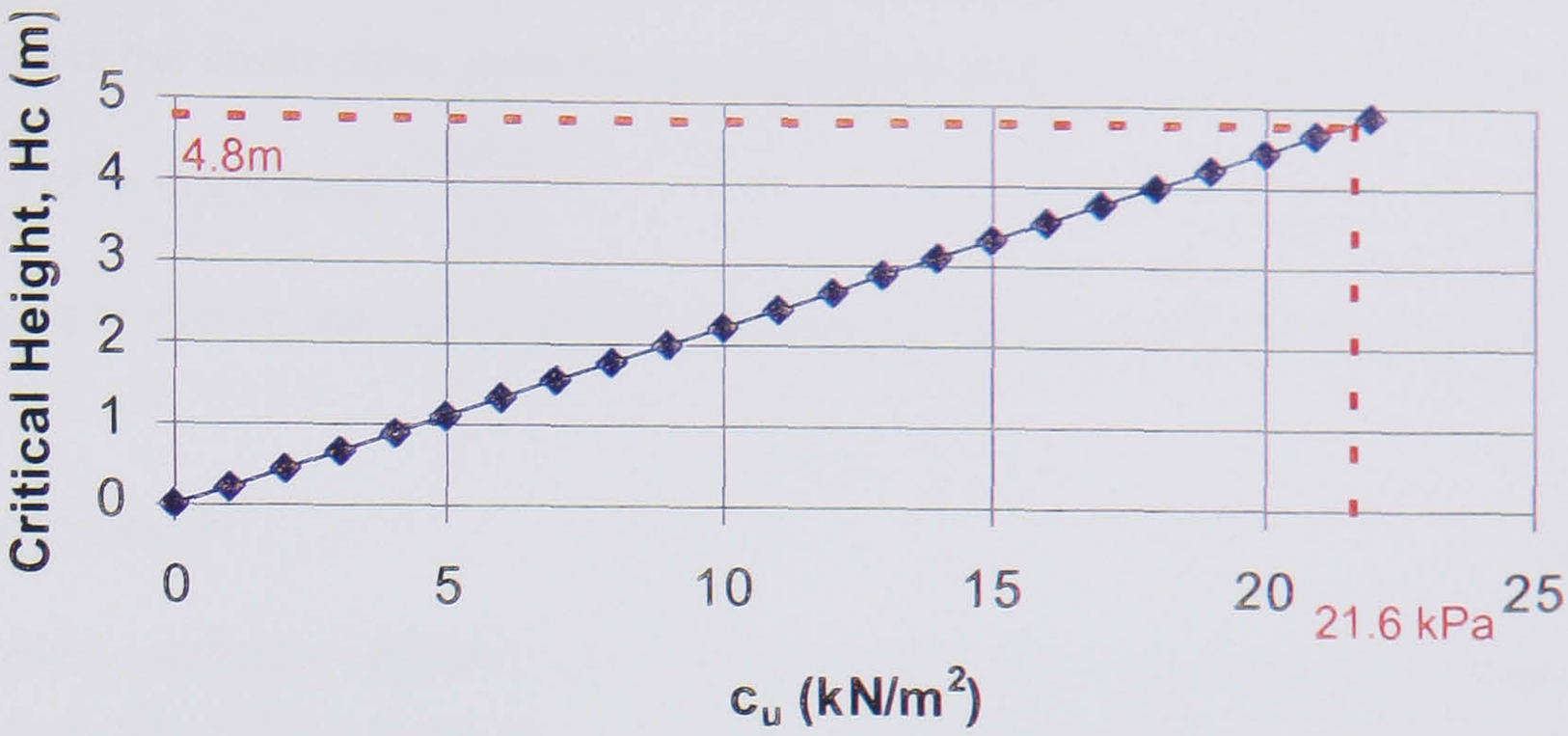

Figure 5.22 Graph of critical height against undrained shear strength

The results of this analysis indicated that a clay with an undrained shear strength of c_u=22kPa would be stable at a height of 4.8m.

5.7.3.3 Coulomb Analysis - Short-term Stability

A more sophisticated undrained analysis was undertaken continuing upon the work presented by Ingold (1981) on the total stress analysis of reinforced clay walls based upon Coulomb (1776) (Heyman 1972) total stress analysis. Initially a failure plane was assumed through the reinforced slope at an inclination of $45^o + \phi'/2$ as it has been shown that even under conditions of undrained loading failure is controlled by effective stress whence the true failure plane is inclined at $45^o + \phi'/2$ to the horizontal (Terzaghi 1936, Skempton 1948, Bishop & Bjerrum 1960). For comparison a failure plane inclined at 45° (i.e. $\phi' = 0 = \phi_u$) was also analysed. Figure 5.23 shows a schematic of the geometry of the analysed problem.

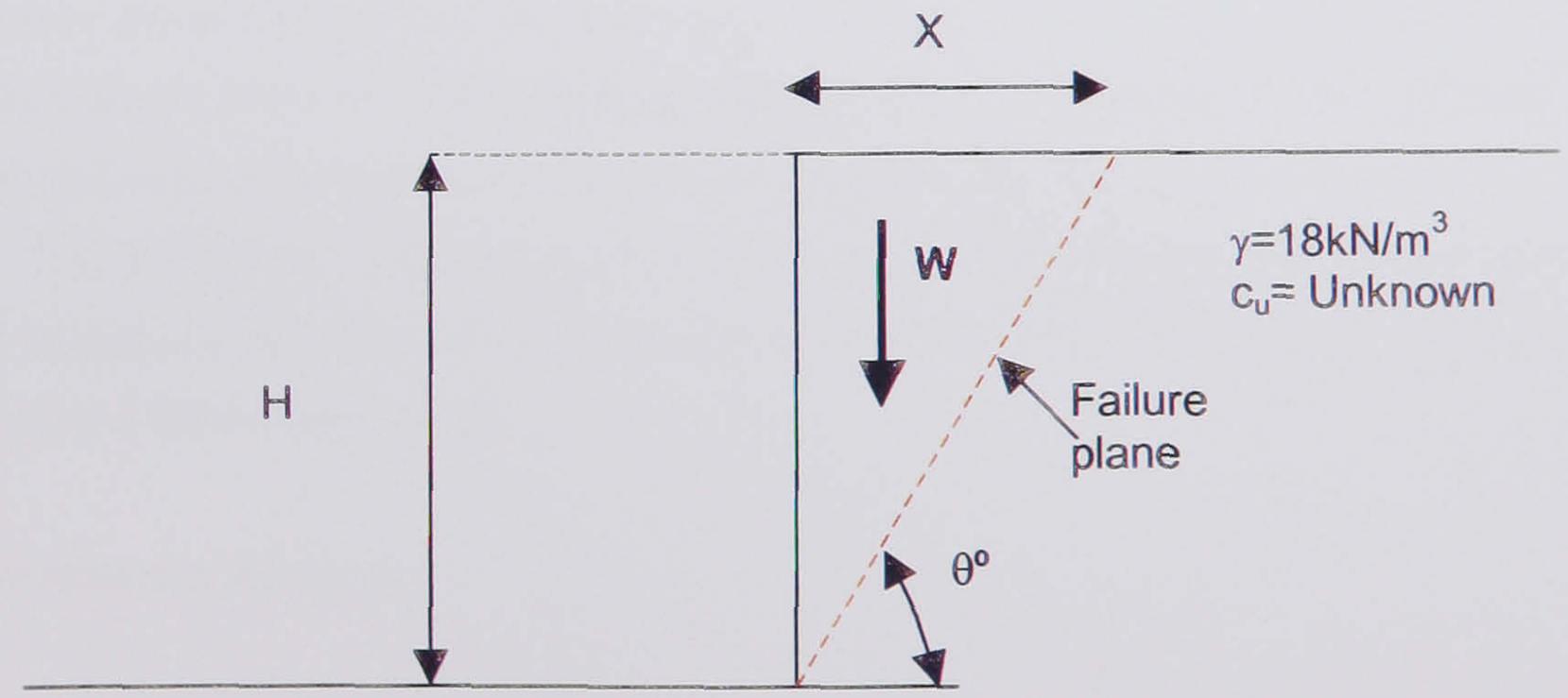

Figure 5.23 Schematic geometry of analysis case for short-term stability

The weight of the wedge of soil (W) related to quantities that are known or assumed gives:

$$W = \frac{1}{2} H^2 \gamma \cot\theta \qquad \text{Eqn. 5.14}$$

Taking the component of *W* that acts parallel to the theoretical shear surface and dividing by the length of the shear plane gives the average shear stress (τ) acting on the failure surface:

$$\tau = \frac{1}{2} H^2 \gamma \cot\theta \sin\theta * \frac{\sin\theta}{H} \qquad \text{Eqn. 5.15}$$

Simplifying and using the trigonometric double angle identity $\sin 2\theta = 2 \sin\theta \cos\theta$ gives:

$$\tau = \frac{1}{4} H\gamma \sin 2\theta \qquad \text{Eqn. 5.16}$$

Inserting the values of γ=18kN/m^3 and H=4.8m the variation in the value of the average shear stress (τ) acting on the failure plane can be ascertained for a range of different failure plane inclinations (θ) as shown in Figure 5.24.

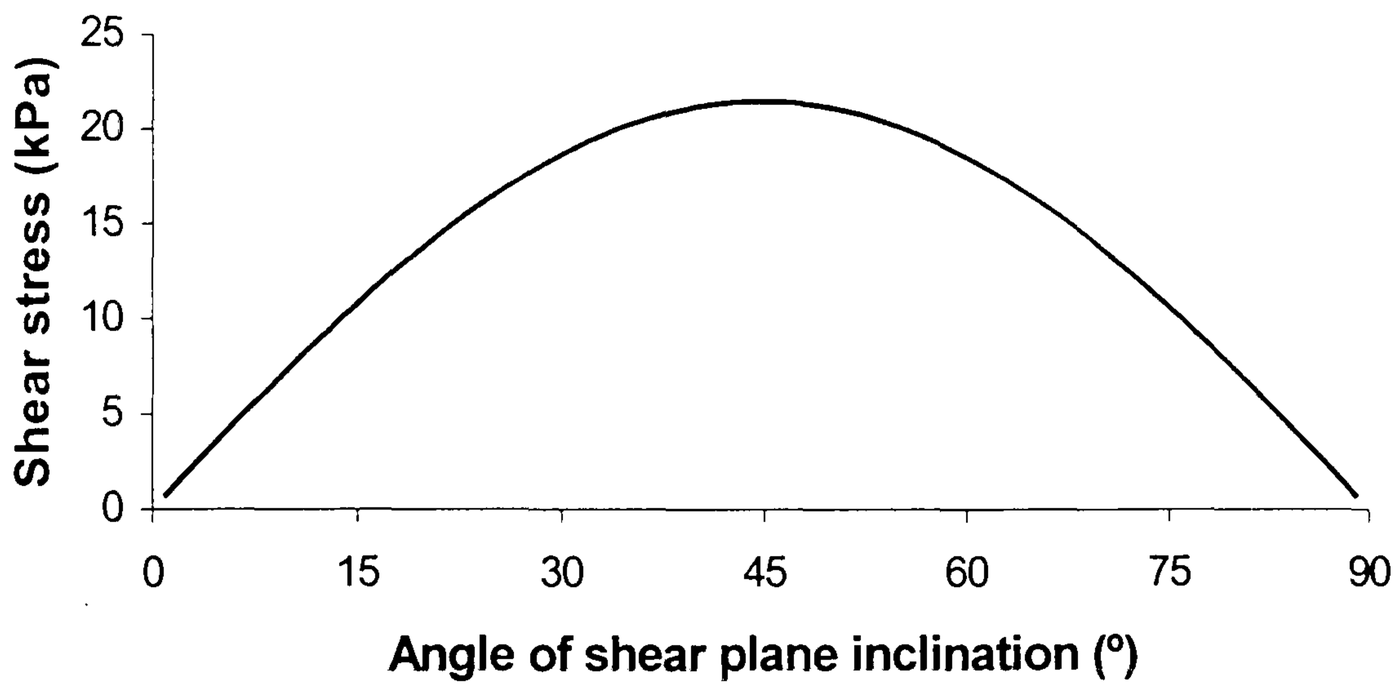

Figure 5.24 Average shear stress against variation in inclination of shear plane

For failure along a plane inclined at an angle of 45° and 45°+ϕ'/2 (ϕ'=15°) the average shear stresses are 21.6kPa and 20.9kPa respectively which corresponds to the minimum undrained shear strength that is required of the fill for the slope to remain stable in the short-term. The difference in the required value of c_u for the two failure surfaces is less than 5%, which is typically less than the measurable variation in the undrained shear strength in the field using a hand shear vane.

Reinforcement Aspects

The tensile force in the reinforcement is given by Equation 5.17 (Ingold 1981):

$$T = 2\alpha c_u L b \qquad \text{Eqn. 5.17}$$

Where *L* is the embedded length α the reinforcement adhesion factor and *b* is the breadth of the reinforcement, the *2* is to take account of both sides of the reinforcement in contact with the soil.

It is implicit that the maximum value of T is governed by the lesser of two values, the ultimate tensile strength of the grid or the pullout load of the reinforcement from the restraining zone. The long-term strength of a geosynthetic is governed by several variables that apply reduction factors to the index properties measured on virgin material in the laboratory these factors are (CIRIA 1996):

- Mechanical damage due to construction (f_d)
- Environmental factors (f_{env})
- Material factors (f_m)

However, for short-term design it is considered by the Author that not all of these factors have to be considered due to the relatively short time the geosynthetic will spend in the ground and under the application of these loading conditions. It is considered that the index properties should, however, be reduced by a factor to allow for mechanical damage during installation and construction (f_d). Mechanical damage factors for geogrids have been suggested by Bush (1988) and Netlon Ltd. (1990) and a typical value for the type and strength of geogrids used in the Joint Stocks wall is $f_d = 1.1$.

For design it is assumed that the undrained shear strength (c_u) of the cohesive fill is uniform and that the failure modes that may occur are either pullout of the grids or tensile failure of the grids. Due to the soft nature of the clay, the most likely failure mechanism is considered to be pullout.

5.7.3.4 Pullout Analysis By Discrete Theory - Short-term Stability

Due to the wraparound facing of the wall, the presence of the sandbags at the front face of the wall and the full-strength bodkin joint, which interconnects consecutive layers of geogrid it, is not considered feasible that pullout from Zone I will occur. It is far more probable that pullout from Zone II will be the mode of failure, see Figure 5.25.

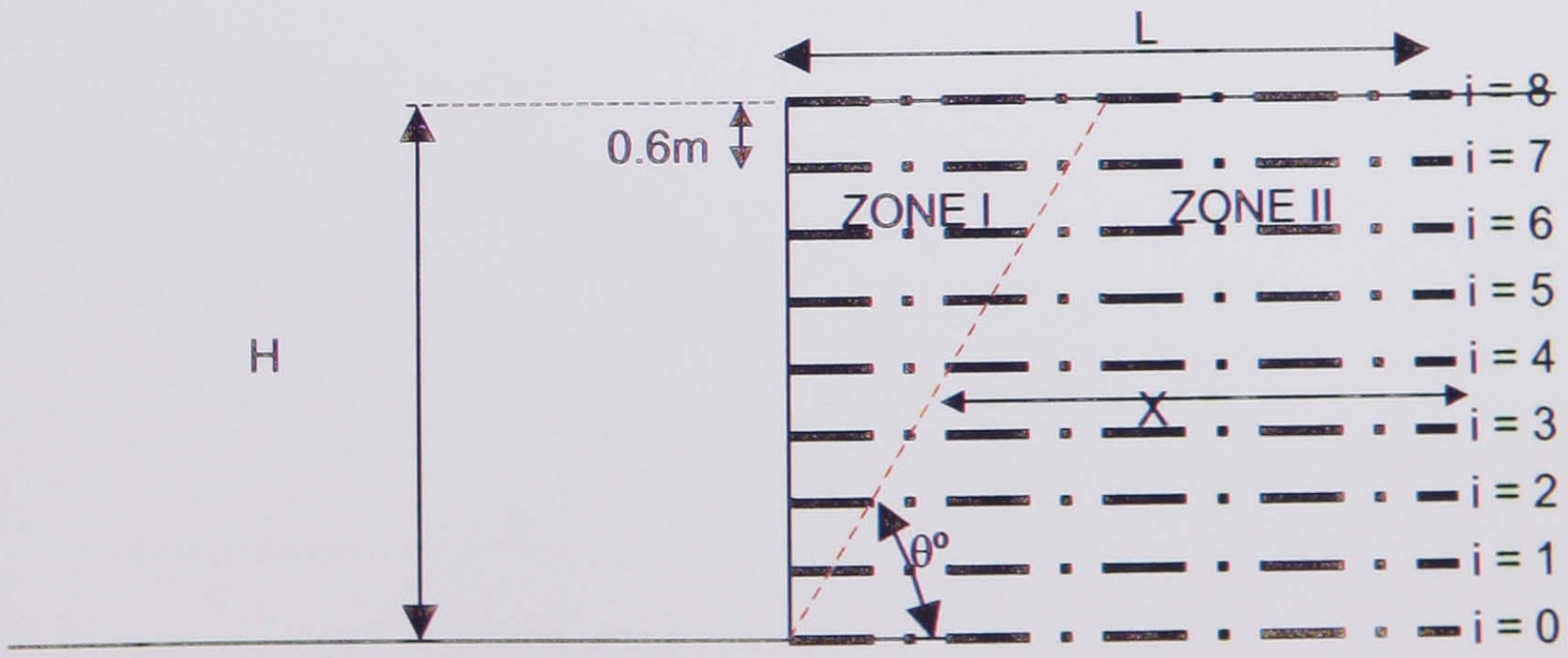

Figure 5.25 Schematic of reinforced wall with failure plane

It is assumed for analysis purposes that the uppermost and lowest grids offer no pullout resistance due to lack of overburden stress and position respectively. Equation 5.18 gives the pullout resistance ($R_{pullout}$) for any grid, per metre breadth:

$$R_{pullout} = 2\alpha\, c_u x$$ Eqn. 5.18

Where x is the length of the grid embedded in Zone II, as shown in Figure 5.25. The value of x may be expressed in terms of θ as given in Equation 5.19:

$$x = L - 0.6\cot\theta(grid\ No.(i))$$ Eqn. 5.19

The total pullout resistance of all of the geogrids (No. 1→7) may be evaluated using Equation 5.20:

$$Rt_{pullout} = 2\alpha\, c_u \sum_{i=1}^{7}(L - 0.6\, i\cot\theta)$$ Eqn. 5.20

Inserting the values of L=3.0m and evaluating Equation 5.20 for i=1→7 and ignoring the pullout resistance of any grids were x>L gives, for the two failure planes being considered:

- $Rt_{pullout}=12\alpha c_u$ *for* $\theta=45°$ *(grids 1→4)*
- $Rt_{pullout}=16.66\alpha c_u$ *for* $\theta=45° + \phi'/2$ *(grids 1→6)*

As given in Equation 5.15, the shear stress induced on any failure plane by the self-weight of the unstable mass is given by:

$$\tau = \frac{1}{2}H^2\gamma\cot\theta\sin\theta * \frac{\sin\theta}{H}$$ Eqn. 5.15

However, if the presence of reinforcement is considered then this shear force is reduced due to the tensile force induced in the reinforcement as discussed in §5.2 of this thesis and given in Equation 5.2. However, in the undrained case as $\phi_u=0°$ the increase in shear resistance caused by the increase in the normal load perpendicular to the failure plane is neglected and the shear stress is only reduced by the component of the reinforcement tensile force perpendicular to the failure plane. A schematic of the analysis case is presented in Figure 5.26.

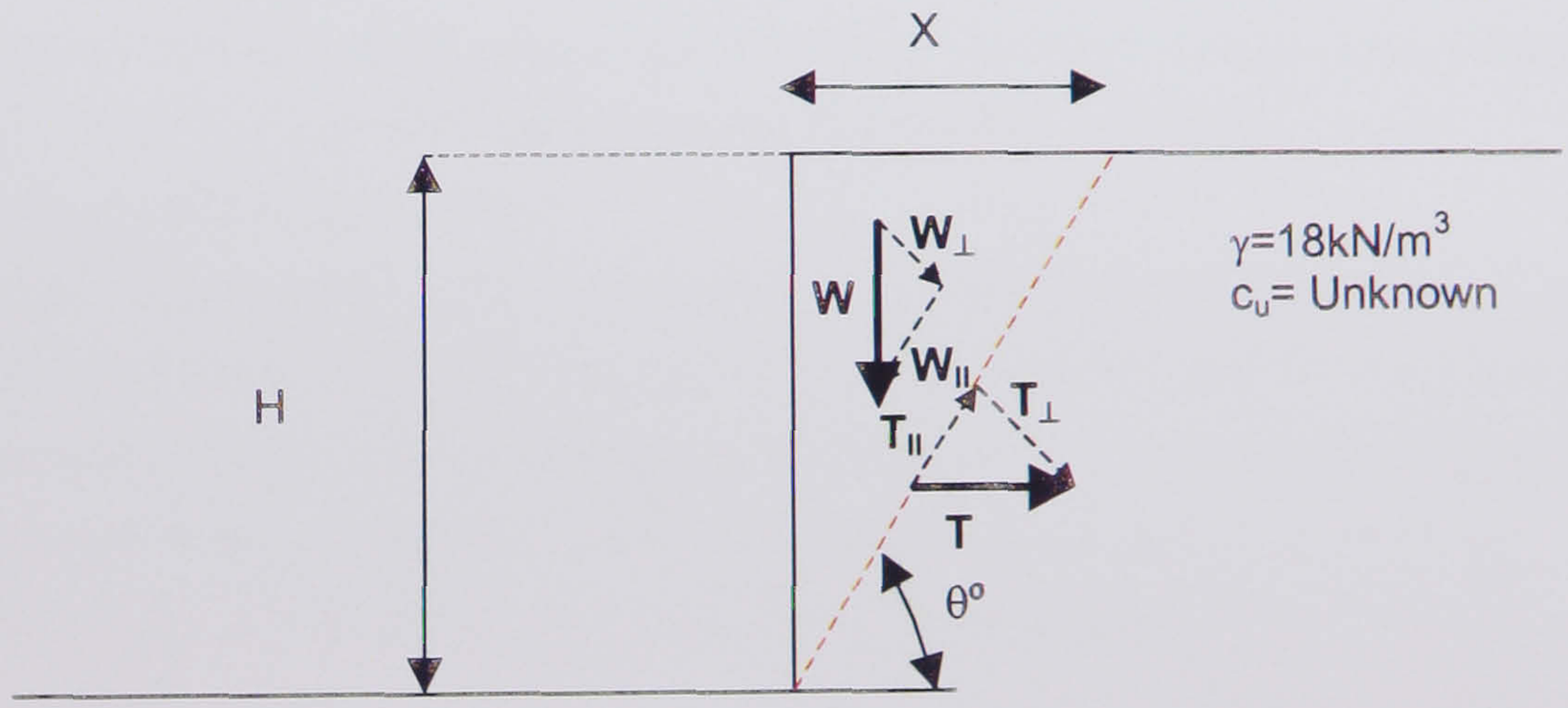

Figure 5.26 Schematic geometry of analysis case for short-term stability with reinforcement

The component of T acting parallel ($T_{//}$) to the failure plane and divided by the length of the failure plane to give the resultant reduction in shear stress is given by Equation 5.21:

$$T_{//} = \frac{T\sin\theta\ \sin\theta}{H} = \frac{T\sin^2\theta}{H}$$ Eqn. 5.21

Hence, resolving parallel to the failure plane the disturbing force is caused by the self-weight and the restoring forces are generated by the undrained shear strength of the soil and the component of the reinforcement tension, Equation 5.22.

$$\frac{1}{4}H\gamma\ \sin 2\theta = \frac{T\sin^2\theta}{H} + c_u$$ Eqn. 5.22

Inserting the values of $Rt_{pullout}$ =T (Equation 5.20) and rearranging to solve for the values of c_u gives the following equations:

$$c_u = \frac{1}{4}H\gamma\ \sin 2\theta - \frac{12\alpha\ c_u\sin^2\theta}{H}$$ For θ=45° Eqn. 5.23

$$c_u = \frac{1}{4}H\gamma\ \sin 2\theta - \frac{16.66\alpha\ c_u\sin^2\theta}{H}$$ For θ=45°+ϕ′/2 Eqn. 5.24

Inserting the values of H=4.8m, γ=18kN/m^3, $\alpha_{pullout}$=1.0 ($\alpha_{pullout}=\alpha_b$ see §5.4.4) and solving for c_u gives c_u=9.6kPa (θ=45°) and c_u=8.1kPa (θ=45°+ϕ′/2).

5.7.3.5 Pullout Analysis By Composite Theory - Short-term Stability

An alternative approach to the discreet theory elaborated in §5.7.3.4 is to consider the undrained shear strength of the clay-reinforcement composite system. In normal laboratory practice the unconfined compressive strength (q) of a clay is assumed to be equal to twice the undrained shear strength (c_u), Equation 5.25:

$$q = 2c_u$$ Eqn. 5.25

However, this assumption applies to samples with an aspect ratio of 2 and therefore not subject to platen friction. As the aspect ratio decreases the effect of platen friction becomes very significant and as such this system may be considered as analogous to soil - reinforcement friction (Ingold 1981).

To investigate this possibility further, consideration should be made of the equilibrium of an element of clay of length *dx* and thickness *S* undergoing plane strain compression between two rigid adhesive platens of width *b* subject to a vertical stress σ_z as shown in Figure 5.27. If the clay is everywhere at yield then, $\tau = \alpha c_u$, and since c_u is constant, then $d\sigma_x = d\sigma_z$. In this case the equilibrium of the soil element is defined by Equation 5.26:

$$2\alpha\ c_u dx + Sd\sigma_z = 0$$ Eqn. 5.26

Integrating Equation 5.26 and applying the boundary conditions $x=b$, $\sigma_z=2c_u$ to evaluate the constants of integration results in Equation 5.27:

$$2\alpha\ c_u x - 2\alpha\ c_u b + S\sigma_z - S2c_u = 0$$ Eqn. 5.27

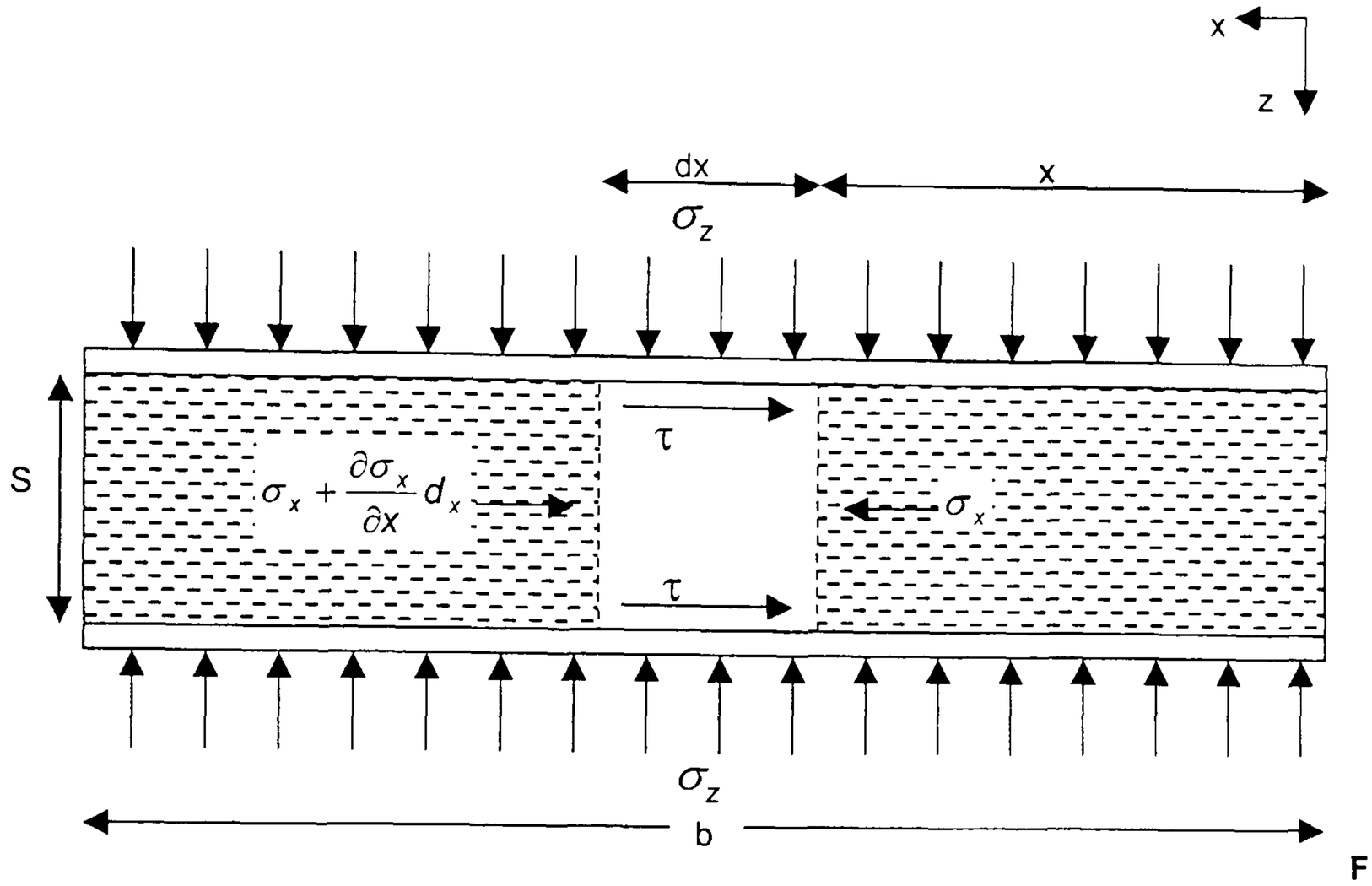

igure 5.27 Compression between adhesive platens (Ingold 1981)

Simplifying Equation 5.27 and solving for σ_z gives Equation 5.28:

$$\sigma_z = 2c_u\left[1+\frac{\alpha(b-x)}{S}\right] \qquad \text{Eqn. 5.28}$$

The mean vertical stress intensity occurs when x=b/2 leading to Equation 5.29:

$$\sigma_z = 2c_u\left[1+\frac{\alpha b}{2S}\right] \qquad \text{Eqn. 5.29}$$

However, σ_z is equal to the unconfined compressive strength of $2c_u$ thus giving an equivalent value of c_u of c_u' that takes into account the presence of the reinforcement.

$$c_u' = c_u\left[1+\frac{\alpha b}{2S}\right] \qquad \text{Eqn. 5.30}$$

Inserting the equivalent value of c_u' into Equation 5.16 and assuming that S=0.6m (reinforcement spacing) and that b=3.0m (length of reinforcement) gives Equation 5.31:

$$c_u\left[1+\frac{3.0\alpha}{2*0.6}\right] = \frac{1}{4}H\gamma\, sin2\theta \qquad \text{Eqn. 5.31}$$

Solving Equation 5.31 for θ=45° and θ=45° + $\phi'/2$ and α= 1.0 gives c_u=6.2kPa and c_u=6.0kPa respectively.

5.7.3.6 Summary Of Short-term Analysis Methods

Four different theories have been developed for the short-term undrained analysis of the reinforced clay wall; critical height, Coulomb, discrete and composite, the results of which are presented in Table 5.7.

Table 5.7 Results of short-term analysis using different analysis methods

	Analysis method	Inclination of failure plane	
		θ=45°	θ=45° + ϕ′/2
Reinforcement not considered	Critical Height	c_u= 21.6kPa	
	Coulomb	c_u= 21.6kPa	c_u= 20.9kPa
Reinforcement considered	Discrete	c_u= 9.6kPa	c_u= 8.1kPa
	Composite	c_u= 6.2kPa	c_u= 6.0kPa

Note: A factor of safety of 1.0 has been applied to these values.

The results presented in Table 5.7 appear to be reasonable in that the analysis methods that do not consider the presence of the reinforcement require a higher value for c_u for stability. Whereas, the analysis methods that do consider the presence of the reinforcement give lower values of c_u due to a proportion of the destabilising force being carried by the reinforcement. The results are also consistent in demonstrating that a failure plane inclined at an inclination of 45° gives a more onerous shear strength requirement.

The significance of these results to the actual Joint Stocks wall may be postulated as:

- An undrained shear strength of the cohesive fill of the order of 6kPa may be stable but the strains required to achieve equilibrium are likely to be on the high side.
- An undrained shear strength of the cohesive fill in excess of 10kPa should be stable as a composite system with both the reinforcement and shear strength of the clay being utilised to maintain the stability of the system.
- An undrained shear strength of the cohesive fill in excess of approximately 22kPa should be sufficiently high such that the system will be stable with little if any load being taken by the reinforcement.

In conclusion, it is considered that if the undrained shear strength of the cohesive fill could be increases to within the range of 10-20kPa then the wall will remain stable in the short-term and allow construction to be completed to the design height.

5.7.4 ELECTRO-OSMOTIC DESIGN

The long and short-term designs of the wall were now completed giving the reinforcement layouts given in Figure 5.21 and from the short-term design methods it had been established that an undrained shear strength (c_u) of approximately 20kPa was required from the clay to ensure the stability of the wall.

The purpose of the electro-osmotic design was to establish the following variables:

- The voltage and current to be drawn.
- The length of treatment time required to improve the shear strength of the clay to 20kPa.

In order to assess these variables a design method based upon that suggested by Bjerrum *et al* (1967) was developed based upon the quantity of water that it was necessary to remove from the soil to achieve the desired increase in undrained shear strength.

5.7.4.1 Preliminary Electro-Osmotic Design

From the laboratory testing discussed in §5.7.2, and given in Table 5.5, the relationship presented in Figure 5.28 was established relating the undrained shear strength of the clay to the water content for remoulded samples of the clay to be used in the Joint Stocks wall. The use of remoulded samples is justified because the clay for the wall will be remoulded before it is placed in the wall on site.

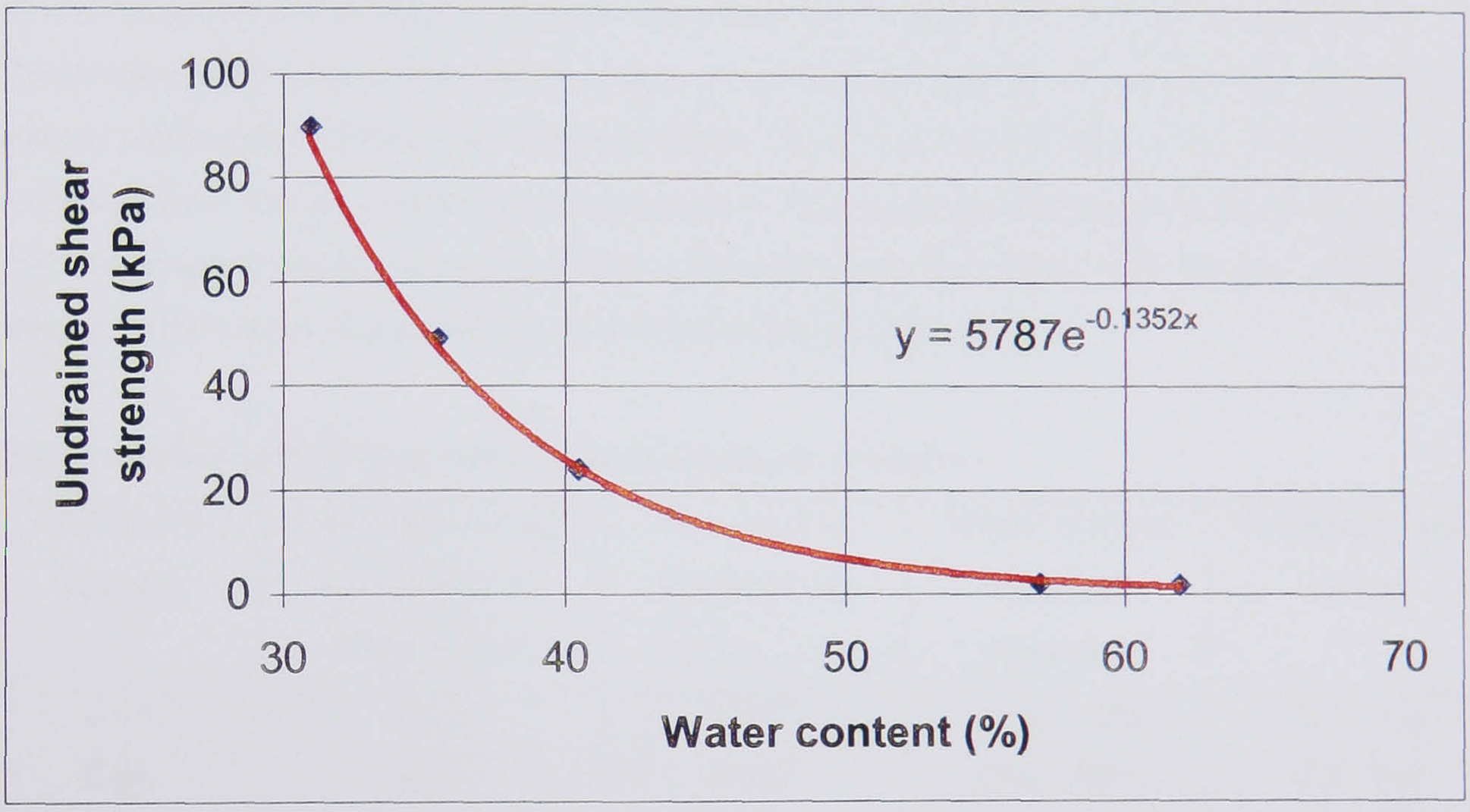

Figure 5.28 Relationship between c_u and water content for remoulded Joint Stocks fill

Assuming that the clay was placed in a very fluid state with an undrained shear strength of approximately 1-1.5kPa with an associated water content of the order of 75-65%, as shown in Figure 5.28. Additionally, knowing that the required shear strength of 20kPa is associated with a water content of 42% then it was possible to establish the required reduction in water content that electro-osmosis was required to achieve, i.e. approximately 33-23%.

This final desired water content of 42% was checked using the critical water content graph suggested by Piaskowski (1957) for the clay fraction contained in the proposed Joint Stocks fill, a critical water content of 14% was obtained (20% clay particles) which is significantly less than the 42% required for an undrained shear strength of 20kPa, see § 7.2.1.2.

From Bjerrum *et al* (1967) and Casagrande (1952) the flow rate for electro-osmosis is given by Equation 5.32, as derived in §2.7.5 and given as Equation 2.11.

$$q_A = k_e i_e A \quad or \quad \frac{Q}{t} = k_e \frac{V}{L} A \qquad \text{Eqn. 5.32}$$

Where Q is the quantity of water in cm^3 transported through an area A (cm^2) under an applied voltage gradient V/L (volts/cm) in time t (sec) in a soil with an electro-osmotic permeability of k_e (cm/s per V/cm). For the volume of soil to be treated, per lift, in the Joint Stocks wall (0.6*3.0*24.0) 43.2m^3, and for a 23% & 33% reduction in water content from 65% to 42% and 75% to 42% the volume of water that needs to be removed is 9.7m^3 and 12.7 m^3 respectively. If the value of k_e is assumed to be that suggested by Casagrande (1952), k_e=5*10^{-5}cm/sec per V/cm, and V/L is established by simply dividing the applied voltage by the distance between the anode and cathode, assuming point electrodes, and the plan area is calculated from geometry (72m^2), then a preliminary treatment time of between 3.7 and 9.0 days is obtained for each 600mm lift of clay. The calculations for the estimation of the reduction of the volume of water are presented in Annex D. Hence, summarising these results for each of the three sections of the trial wall and for the whole wall gives the values presented in Table 5.8. It is also worth noting that if 9.7m^3 and 12.7m^3 of water are removed from the soil mass then the change in volume associated with the removal of this volume of water would cause a surface settlement of approximately 130-175mm over the whole surface area, if manifested as vertical settlement alone.

Table 5.8 Results of simplistic electro-osmosis analysis

Electrode spacing	Assumed voltage gradient at 30 Volts (V/cm)	Assumed k_e (cm^2/sec-V)	Water content reduction required	Treatment time (days)
0.4m	0.83	5*10^{-5}	23% - 33%	3.7 - 4.9
0.8m	0.60	5*10^{-5}	23% - 33%	5.2 - 6.8
1.2m	0.45	5*10^{-5}	23% - 33%	6.9 - 9.0
Whole wall	0.63	5*10^{-5}	23% - 33%	4.9 - 6.5

From Table 5.8 it is apparent that by varying the electrode spacing and, hence the voltage gradient, as well as the initial water content the theoretical treatment time can be greatly altered. It is noteworthy that the treatment times calculated in this manner are simplifications as they do not take into account the desiccation of the soil with time nor do they take into account electrochemical changes that take place within the soil mass during electro-osmosis treatment. As a result the times calculated in this way may be considered as lower bound values for the treatment time.

5.7.4.2 Advanced Electro-Osmotic Design

The preliminary design presented in §5.7.4.1 may be enhanced by refining the input parameters that are used in Equation 5.32. The parameters that may be refined are:

- Electro-osmotic permeability (k_e) - The value of k_e applicable to the soil in question at the relevant voltage gradient may be established from laboratory testing and additionally its variation with time may be taken into account.
- The voltage gradient (V/L) - May be established more realistically, taking into account the geometry of the electrode layout, using Laplace's equation and a finite difference or resistance path analysis.

The remaining parameters; Q, t and A may not be refined in any significant way to make the analysis more realistic.

Refinement of the electro-osmotic permeability (k_e)

Mitchell (1993) states that the value of the parameter k_e is generally in the range of $1x10^{-9}$ to $1x10^{-8}$ m^2/s-Volt (m/s per V/m) and Casagrande (1983) states the range as being $2x10^{-9}$ to $5x10^{-9}$ m^2/s-Volt, which is in agreement with the values presented in Table 2.7 and §2.7.5. However, as treatment progresses and electro-chemical reactions take place (see §2.7.5.5) desiccation of the soil occurs due to the removal of water by the electro-osmosis process. As a result, the quantity of water moved per unit of voltage decreases.

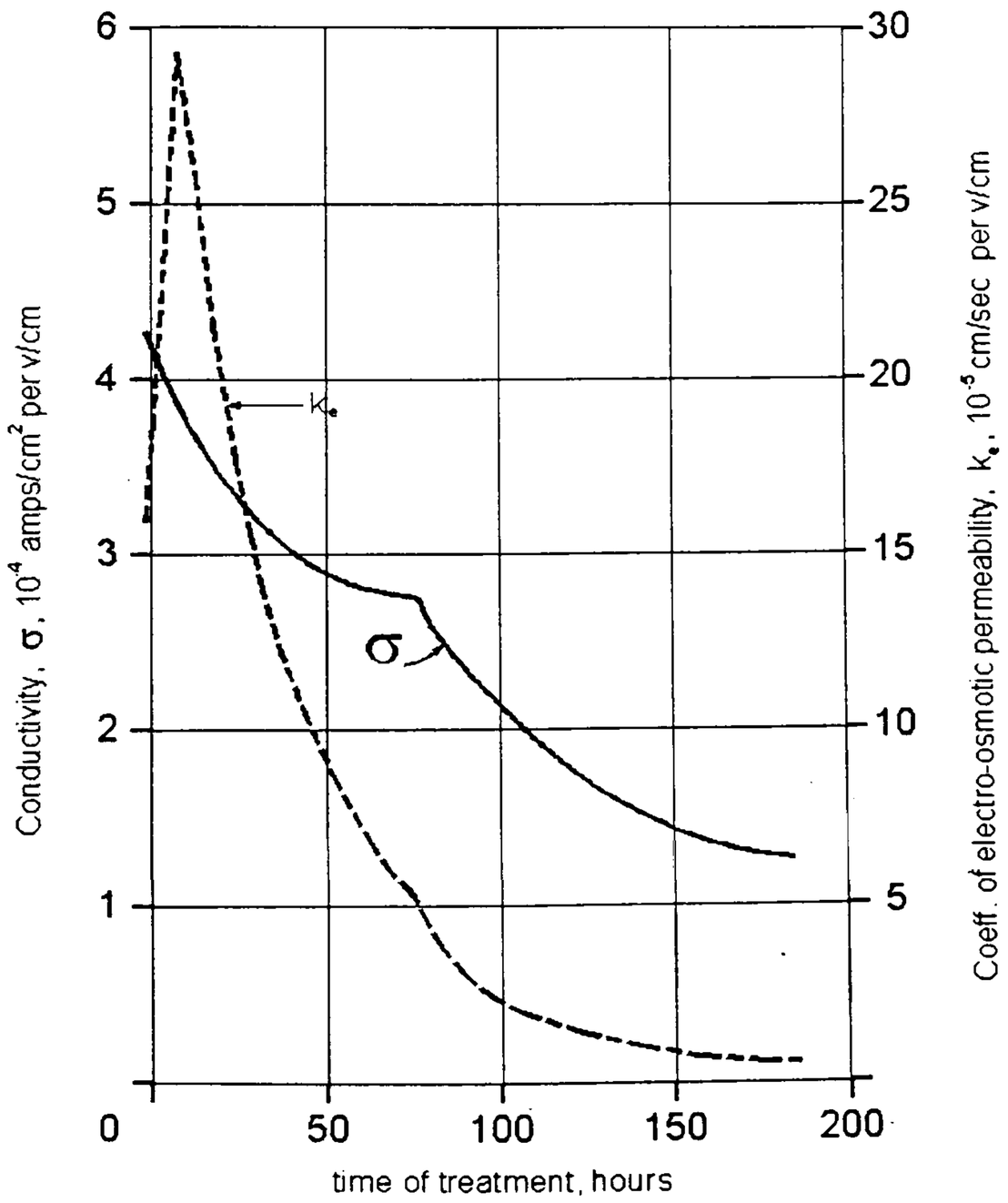

Figure 5.29 Variation in k_e and σ with time averaged over 15 tests (Casagrande 1983)

This is equivalent to a decrease in the value of k_e as observed by Casagrande (1983) and presented here as Figure 5.29. The significance of this variation in k_e is that initially the flow of water achieved by electro-osmosis increases to a maximum within the first 12 hours, or so, of treatment followed by a rapid decrease in the volume of water moved per unit time, followed by a lower steady state flow with time. To model this phenomena for practical applications there are two possible alternatives:

- The assumption that that treatment time for the project is large and that a global reduction factor should be applied to the measured initial laboratory value of k_e. Wrigley (1999) has adopted this approach and suggests a reduction factor of 3 based upon the graph presented by Casagrande (1983), reproduced here as Figure 5.29. Although this method is simple to use in practice it is a gross simplification of the true time-dependant behaviour of the reduction of k_e with time.
- A more accurate constitutive model for the variation of k_e with time may be achieved by undertaking laboratory experiments to establish the true time variation of k_e for the soil that will be used in the field application and at the appropriate voltage gradients as shown in Figure 5.30.

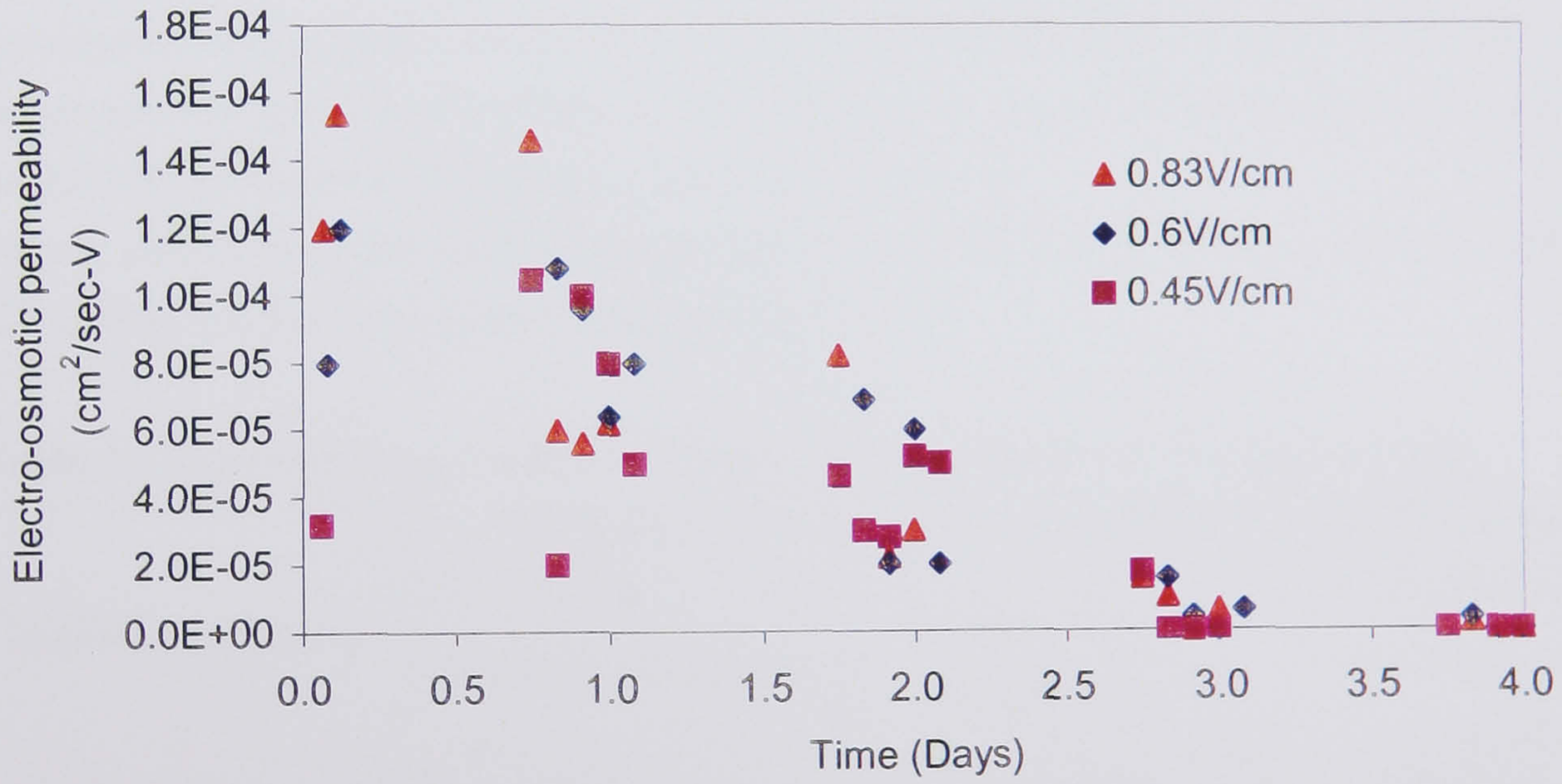

Figure 5.30 Results of k_e against time for different voltage gradients

From the results presented by Casagrande (1983) and the results obtained by the Author from laboratory testing it would appear that the best representation of the variation in k_e with time is given by a graphical interpretation of the laboratory results obtained as shown in Figure 5.31.

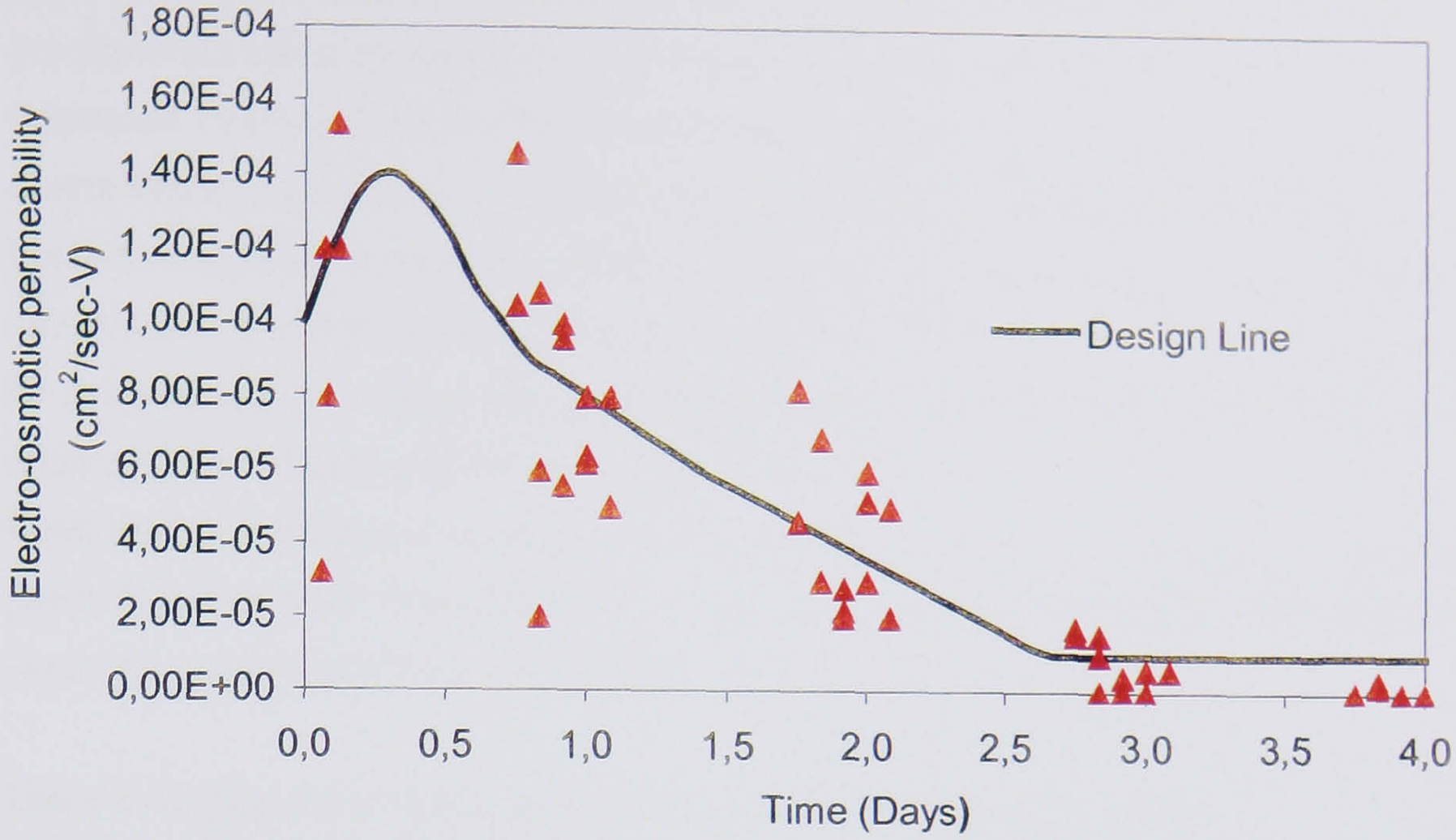

Figure 5.31 Graphical interpretation of k_e against time for design purposes

The calculation of treatment times based upon the graphical interpretation presented in Figure 5.31 has been undertaken by digitising the curve and using a spreadsheet to calculate the volume of water that flows in a time increment of 0.1days. In this way when the cumulative flow volume is equal to the volume of water that is required to be removed the corresponding cumulative treatment time is established. A copy of the spreadsheet is given on the CD accompanying this thesis (D:\Analysis\t & cu.xls).

Hence, summarising the results of the simplified and refined k_e analyses as given in Table 5.9 utilising the simplistic linear voltage variation.

Table 5.9 Summary of estimated treatment times using linear voltage variation

Electrode spacing	Treatment time @ 30V for 23% & 33% w_c reduction (Days)		
	Simplistic analysis	k_e reduced by a factor of 3	k_e variation obtained from laboratory testing
0.4m	3.7 - 4.9	11.1 -14.8	3.1 - 9.0
0.8m	5.2 - 6.8	15.5 - 20.4	9.5 - 17.5
1.2m	6.9 - 9.0	20.8 - 27.1	18.2 - 28.8

Refinement of the voltage gradient parameter (V/L)

In §5.7.4.1 it was assumed for the simplistic design that the voltage gradient could be obtained by simply dividing the applied voltage by the spacing between anodes and cathodes. This is a simplification of what occurs in reality in that the true voltage distribution obtained by the application of a potential difference by point electrodes is given by Laplace's

equation (Stroud 1990 and Young & Freedman 1996). Laplace's equation may be programmed into a conventional spreadsheet program, such as Microsoft Excel 97 (Microsoft 1997) and the distribution of the potential field more realistically modelled, as demonstrated by Williams *et al* (1993) for the modelling of potential heads governed by Laplace's equation for flownets. The modelling of the voltage field produced by point electrodes in a uniformly conducting soil is discussed further in § 7.6. An alternative method for ascertaining the voltage distribution is the resistance path concept as suggested for this application by Wrigley (1999), also discussed in § 7.6.1.

From the finite difference model a more representative value of (V/L) may be obtained for use in Equation 5.32. The results of the finite difference and resistance path models of the electrode layout used in the Joint Stocks wall are presented in Table 5.10.

Table 5.10 Results of finite difference and resistance path models

Anode - cathode spacing zone (m)	Simplistic linear calculation (V/m)	Finite difference model (V/m)	Resistance path model (V/m)
0.4	83	48	56
0.8	60	33	28
1.2	45	25	18

It is appreciated that in reality the voltage distribution will change with time because of the variation of the resistance of different zones of the soil due to desiccation and electro-chemical changes within the soil mass. This has been observed both in the field and in the laboratory by several researchers (Wan & Mitchell 1977, Bjerrum *et al* 1967, Lo *et al* 1991a, Lo *et al* 1991b). However, to model the complexity that this continual variation of resistance with time would introduce is not considered viable for design purposes and is thus beyond the scope of this thesis.

Summarising the treatment times predicted by the simplistic and refined analyses gives the results presented in Table 5.11.

Table 5.11 Summary of estimated treatment times using different voltage & k_e variations for 23% and 33% reductions in water content

Electrode spacing	Treatment time @ 30V for 23% & 33% w_c reduction (Days)								
	Simplistic linear voltage variation			Finite difference voltage variation			Resistance path voltage variation *		
	k_e	$k_e/3$	Lab	k_e	$k_e/3$	Lab	k_e	$k_e/3$	Lab
0.4m	3.7-4.9	11.1-14.8	3.1-9.0	6.5-8.5	19.5-25.4	16.0-26.0	5.6-7.3	16.8-21.9	11.4-19.9
0.8m	5.2-6.8	15.5-20.4	9.5-17.5	9.4-12.3	28.3-34.0	30.7-45.2	11.1-14.5	33.3-43.5	39.2-50+
1.2m	6.9-9.0	20.8-27.1	18.2-28.8	12.4-16.3	37.3-48.8	45.8-50+	17.3-22.6	50+-50+	50+-50+

**These values have not been calculated using the Kvaerner (1999) spreadsheet as it contains errors in the calculation of the treatment times.*

Additionally, using the relationship presented in Figure 5.28 between the water content and the undrained shear strength (c_u), and utilising the variation of electro-osmotic permeability (k_e) obtained from the laboratory testing, presented in Figure 5.31, it is possible to predict the variation of the undrained shear strength as treatment time progresses. This is demonstrated in Figure 5.32 for the voltage gradients established from the finite difference analysis and for the two different initial water contents that have been considered.

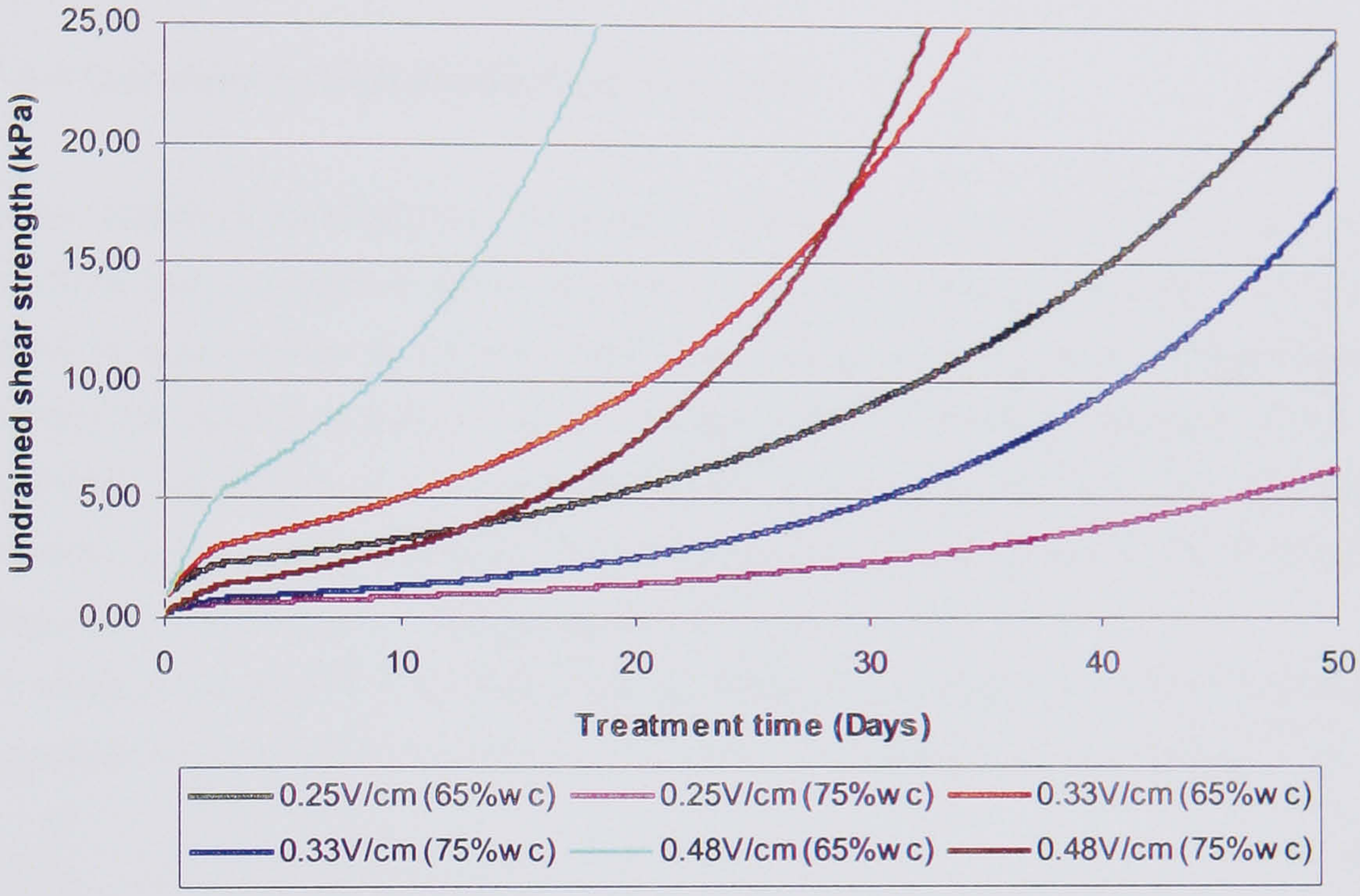

Figure 5.32 Variation of c_u against time at different voltage gradients and initial w_c

It will be observed in Figure 5.32 that the curves predicting the undrained shear strength contain a kink at a treatment time of approximately 2.7 days. This kink is explained by the change in the electro-osmotic permeability to a constant value, as shown in Figure 5.31. The prediction of the variation of c_u with treatment time is particularly useful as it is a parameter that can be measured rapidly in the field by means of a hand shear vane to confirm that the electro-osmotic treatment is progressing as anticipated.

5.7.4.3 Discussion Of The Predicted Treatment Times

Inspection of Table 5.11 reveals that the treatment times predicted using the linear voltage variation are the shortest due to the higher voltage gradient associated with the simplifications used to obtain the voltage gradient. They may thus be considered as a lower bound solution for the treatment time.

The treatment times predicted by the finite difference and resistance path models are noteworthy in that the finite difference model gives a less pronounced variation of the voltage gradient as a function of the electrode spacing, due to the fact that the model takes into account the voltage distribution over the full distance between the electrodes. Whereas, the resistance path model utilises the voltage gradient across a series of elongated central

elements, as shown in Figure 7.22 and discussed in § 7.6.1. Additionally, the resistance path model does not take into account the effect of the difference in voltage gradient in the plane of the same polarity electrodes, whereas the finite difference model does this inherently based upon the theory used in its derivation.

It is also important to note that scale effects have not been considered in the extrapolation of the laboratory results to the field prediction.

5.7.4.4 Calculation Of Electrical Power Demand

The calculation of the electrical power that will be drawn by a particular electrode installation is a critical factor in assessing the economic viability of a project and is dependant upon the applied voltage and the resistance of the electrode/soil system and its variation with time. Normally the applied voltage, or current, is controlled by the design engineer of the installation, depending upon whether the installation is being used as a constant voltage, constant current or hybrid system. The operation of systems as constant current or constant voltage or hybrid systems is discussed in § 2.7.5.4.

The variable that enables the calculation of voltage from current, or current from voltage is the resistance of the system based upon Ohm's Law, given here as Equation 5.33:

$$R = \frac{V}{I} \qquad \text{Eqn. 5.33}$$

With the resistance (R) of the system being influenced by the electrode arrangement geometry and the electrical conductivity of the soil. The effect of the electrode distribution geometry may be estimated from the finite difference analysis or the resistance path analysis as discussed in § 7.6. As the voltage gradient is different, so the rate of change of resistance is different, as shown in Figure 5.33.

The variation of the electrical conductivity (σ) of the soil needs, however, to be modelled as due to desiccation and electro-chemical changes it varies with time, as observed by Casagrande (1983), see Figure 5.29. This variation of σ may be modelled by one of two methods:

- Wrigley (1999) assumes that *regardless of the treatment time* of the installation there is a reduction in the electrical conductivity of the soil by a factor of three, which is taken into account by assuming a constant current level and the gradual increase of the applied voltage from a third of its maximum value at the beginning of the treatment process. This value of a reduction by a factor of three has been established based upon the results presented by Casagrande (1983) presented here in Figure 5.29.
- A more accurate prediction of the variation of σ with time may be obtained by undertaking laboratory testing on a soil sample at the appropriate voltage gradient and establishing a graphical representation of the variation obtained. For the soil used in the

Joint Stocks field trial the variation of σ versus time at different voltage gradients is presented in Figure 5.33.

Additionally, the variation of the electrical resistivity (ρ), equal to the reciprocal of the electrical conductivity (σ), is related to the overall resistance of the system (R) by the Ohm's law:

$$R = \rho \frac{L}{A} \qquad \text{or} \qquad R = \frac{1}{\sigma} \frac{L}{A} \qquad \text{Eqn. 5.34}$$

Where:

L = length of the sample (distance between the electrodes)

A = cross- sectional area (plan area of the trail {24*3=72m^2})

Hence, based upon Equation 5.34 and the graph of the variation of electrical conductivity with time obtained from laboratory testing, Figure 5.33, an estimation of the overall resistance of the system can be made, and of its variation with time. Additionally, as the voltage gradient is a constant set by the engineer, the variation of current and hence power and energy (E) may be calculated using Equation 5.35:

$$E = VIt \text{ (Watt-hours)} \qquad \text{Eqn. 5.35}$$

Where:

V = Voltage (Volts)

I = Current (Amps)

t = Time (Hours)

Using the different times (t) presented in Table 5.11 for different k_e variations and the set voltage (V) of 30V the energy consumptions have been calculated as presented in Table 5.12 and Table 5.13 for both the laboratory variation of conductivity (σ) and the variation suggested by Wrigley (1999) of a global reduction to a third of the initial electrical conductivity. The laboratory variation of conductivity used in the prediction of the energy demand is that associated with a voltage gradient of 0.45V/cm, which is the average of all of the voltage gradients calculated by the different methods summarised in Table 5.10 (V_{ave}=44V/m), Figure 5.33. The electrical conductivity beyond a period of 12 days has been assumed constant at a value of 0.025S/m; see Figure 5.33. In undertaking the energy consumption calculations, if the predicted current is larger than 200A (the maximum generator current), then 200A has been assumed as the current drawn.

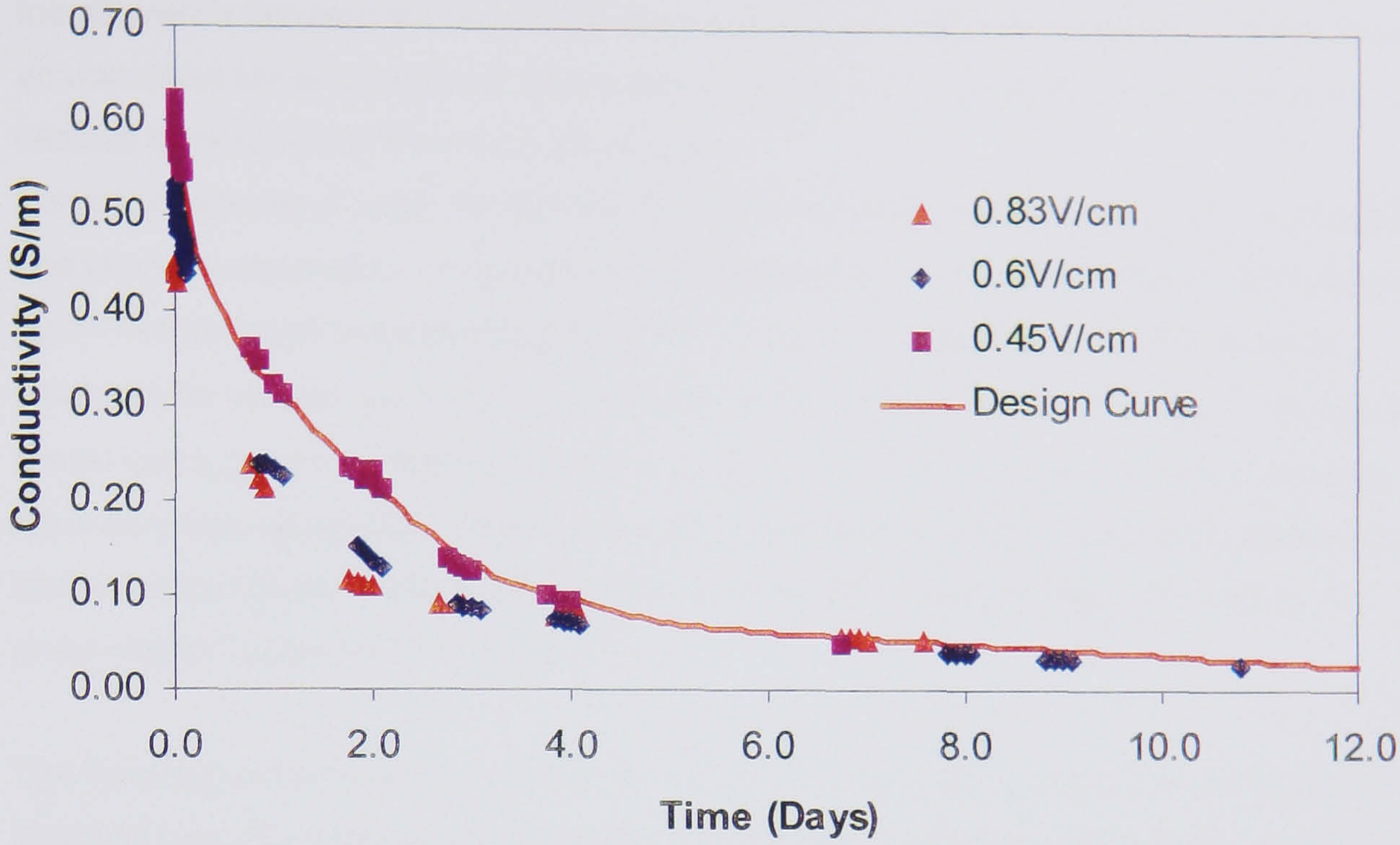

Figure 5.33 Variation of σ against time at different voltage gradients

Figure 5.33 demonstrates that the actual reduction in electrical conductivity is of the order of 95% over a period of approximately 12 days, significantly more than the 66% reduction proposed by Wrigley (1999) based upon the data presented by Casagrande (1983). This result being reflected in the greater energy consumptions predicted by the resistance path method.

5.7.5 CONCLUSIONS OF THE THEORETICAL ANALYSES

The stability analysis of the wall has been carried out in the long-term to ascertain the reinforcement layout using the soil's critical state shear strength parameters. The calculated reinforcement layout is given in Figure 5.21. The short-term stability of the wall was analysed using several different analysis methods:

- Critical height
- Coulomb
- Discrete
- Composite

As a result of these analyses the minimum undrained shear strength of the clay fill, to achieve short-term stability was calculated and the results are given in Table 5.7. Based on these calculations it was considered that an undrained shear strength of 20kPa was required from the cohesive fill to achieve stability. The electro-osmosis design was then undertaken. The electro-osmosis design was based upon the water content - undrained shear strength

curve for the fill material ascertained from laboratory testing, Figure 5.28. Using this curve the difference between the as placed water content and the water content corresponding to an undrained shear strength of 20kPa was calculated, giving the volume of water that needed to be removed from each lift of clay.

Using this volume of water the electro-osmosis calculations were undertaken. A simplistic analysis was undertaken using a linear voltage gradient and fixed soil parameters, followed by a more complex analysis using finite difference and resistance path techniques to establish the voltage gradient, and variations in the values of k_e and σ using an empirical model and a graphical interpretation of the actual variations of k_e and σ measured in the laboratory was considered. The results of these analyses yielded estimated treatment times and estimated power demands drawn by the installation. A summary of the results is presented in Tables 5.11, 5.12 and 5.13.

The following sections of this chapter discuss the construction, monitoring and the results obtained from the construction of the Joint Stocks wall based upon the design calculations. This is then followed by a detailed comparison of the predicted and actual field results for the wall. The completed design layout to which the wall was constructed is presented in Figure 5.21.

Table 5.12 Predicted energy consumptions (kWh) using laboratory variation of conductivity (max 200Amp supply)

Electrode spacing	Predicted energy consumption @ 30V for 23% & 33% w_c reduction (kWh)								
	Simplistic linear voltage variation			Finite difference voltage variation			Resistance path voltage variation ¥		
	k_e	$k_e/3$	Lab	k_e	$k_e/3$	Lab	k_e	$k_e/3$	Lab
0.4m	540-713	1605-2094	454-1303	943-1231	2716-3468	2249-3545	814-1058	2353-3014	1648-2755
0.8m	756-986	2184-2820	1375-2444	1361-1770	3843-4582	4155-6034	1606-2055	4491-5813	5256-6655+
1.2m	1001-1303	2871-3688	2535-3908	1783-2288	5010-6513	6112-6655+	2418-3105	6655+-6655+	6655+-6655+

¥ *These values have not been calculated using the Kvaerner Spreadsheet as it contains errors.*

Table 5.13 Predicted energy consumptions (kWh) using resistance path model of conductivity (max 200Amp supply)

Electrode spacing	Predicted energy consumption @ 30V for 23% & 33% w_c reduction (kWh)								
	Simplistic linear voltage variation			Finite difference voltage variation			Resistance path voltage variation ¥		
	k_e	$k_e/3$	Lab	k_e	$k_e/3$	Lab	k_e	$k_e/3$	Lab
0.4m	540-713	1605-2131	454-1303	943-1231	2808-3658	2304-3744	814-1058	2419-3154	1648-2866
0.8m	756-986	2232-2938	1375-2520	1361-1771	4075-4896	4421-6509	1606-2088	4795-6264	5645-7200+
1.2m	1001-1303	2995-3902	2621-4147	1786-2347	5371-7027	6595-7200+	2491-3254	7200+-7200+	7200+-7200+

¥ *These values have not been calculated using the Kvaerner Spreadsheet as it contains errors.*

5.7.6 CONSTRUCTION OF THE WALL

The preparation of the wall construction site began in January of 1999 after permission to proceed with the works had been granted by Capitol Waste Management the owners of the site. Initially the laminated clay fill for use in the cohesive zone of the wall was brought onto site from its source locality and left to soak in the lake adjacent to the construction area until the beginning of construction proper in March 2000, as shown in Figure 5.34. The first lift of clay was in place and the power turned on for the first time on the 5th April 2000. April 2000 was the wettest April since Meteorological Office records began in 1766, with 219% of the average April precipitation falling (Met Office 2000). This had an adverse effect on the trial in that construction activities were delayed, and due to the large quantities of water on the site the current drawn by the installation was maintained at a high level for a longer time. Construction of the wall continued until the end of January 2001 at which time the wall had reached a height of between 4.2 and 2.1m. Several delays were also experienced during this period due to the theft of the generator before the beginning of the trial, from another site, and additionally due to the fuel shortage that took place towards the end of the year 2000.

5.7.6.1 Preparation Of Trial Area

Initially the heavy vegetation from the trial area was cleared using a Komatsu PC240LC 360° excavator and a Caterpillar D5H bulldozer to establish a level platform adjacent to the lakeshore in preparation for the establishment of working and construction platforms. The back slope was then cleared of vegetation and was steepened to provide a back to the trial wall. Additionally, for safety reasons a rock bund was constructed at the top of the back slope to prevent vehicles from approaching the top of the slope and potentially falling into the construction area, the steepened slope and construction of the rock bund are shown schematically in Figure 5.34.

A reinforced construction platform was then established for the wall itself. This consisted of two rolls of Tensar SS40 biaxial geogrid laid over the natural ground and then a 500 mm thick construction platform being constructed over it in a single lift. The fill for the construction platform comprised of crushed building rubble complying with the requirements of Class 6B Selected Granular Fill (DoT 1993). Compaction of the construction platform was carried out using a Caterpillar D5H Bulldozer towing a Stothert & Pitt T182B vibrating roller. Five passes or the roller was used in accordance with the Specification for Highway Works (DoT 1993) method compaction specification for Method 5 compaction using 6B fill and a 3400kg/m-vibrating roller.

The working platform in front of the wall itself was then capped with a thin granular layer and compacted to allow ease of movement of plant and personnel in this area during adverse weather conditions.

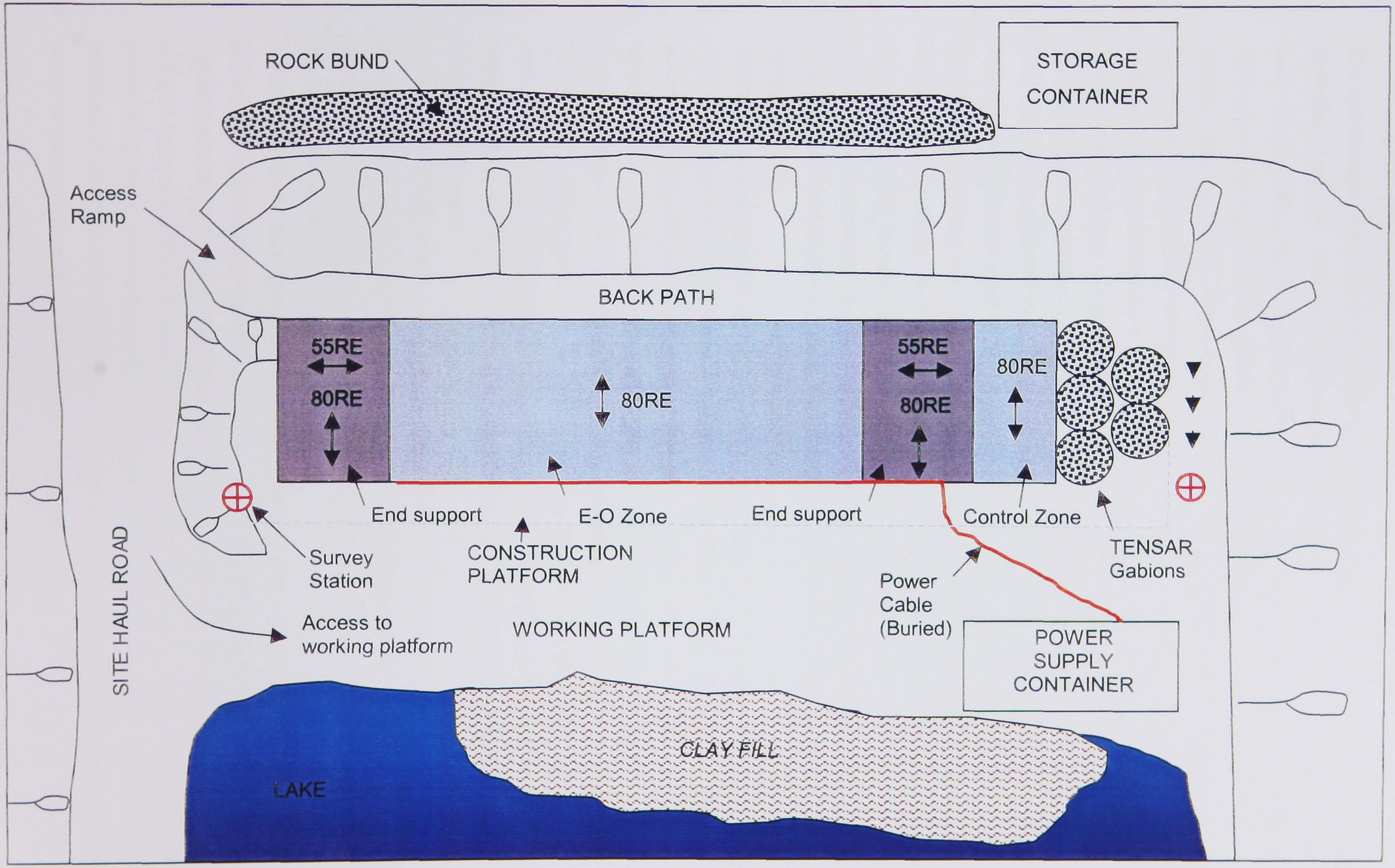

Figure 5.34 Schematic plan of construction area

5.7.6.2 First Lift Construction

The construction of the first lift consisted of establishing a string line to set out the toe of the front face of the wall. This was located approximately 3.5m in front of the back slope of the wall. Tensar 80RE uniaxial geogrids were then cut to the required length of 4.1m for the 80° inclined front face and 7.1m long 55RE uniaxial geogrids were cut for the vertically faced granular retaining blocks. These lengths included a 0.6m allowance for coverage of the face itself and 0.5m for a bodkin connection length. The locations and orientations of the different grids are shown schematically in the plan of the construction area in Figure 5.34.

The cut grids were then laid out on the construction platform as shown in Figure 5.35, which summarises the construction sequence for a single granular lift. Hessian sandbags were filled using medium sand sized crushed building rubble by hand using a specially designed hopper to assist in their rapid filling. Initially the sandbags were closed using the string ties provided with the bags themselves, however, it was found that these often broke and slowed down the filling process. An alternative method was found using plastic cable ties to seal the sandbags, this was found to be much quicker and gave a better standard of closure to the bags. The filled sandbags were then placed along the string line to form the toe of the front face of the wall and perpendicular to the string line to form the foot of the vertical granular retaining blocks.

Crushed brick and concrete complying with the Specification for Highway Works (DoT 1993) Type 6I selected well graded granular fill to reinforced earth and anchored earth was then placed in an approximately 100mm thick layer in the granular ends of the structure. This was compacted to a final thickness of 75mm using 12 passes of a Bomag BW75E single drum pedestrian roller complying with method 2 Compaction for a 567kg/m vibratory roller (DoT 1993). Later in the project a twin drum Bomag BW60S pedestrian roller (1395kg/m) was used. This roller again used 12 passes to compact the 6I fill to a 75mm thick layer, however, the operation was found to be a lot safer and easier to use, especially when the structure was several lifts high.

A second lift of Type 6I fill was then compacted on top of the first to bring the granular ends up to a height of 150mm, level with the height of the first sandbag. The next layer of sandbags was then placed around the granular ends of the structure and a further 2 lifts of Type 6I fill placed and compacted.

A wooden template was manufactured by the University of Newcastle to assist in the placing of the sandbags on the front face of the wall in order to achieve the required 80° inclination. Secondary reinforcement, Tensar SS20, was then placed in a 1m wide strip around the front and side faces of the granular ends of the wall. The next layer of sandbags was then placed around the granular ends and two lifts of Type 6I fill placed and compacted. The fourth and final layer of sandbags was then placed along with two lifts of compacted type 6I fill. The wrapover was then done in both directions, i.e. front and side.

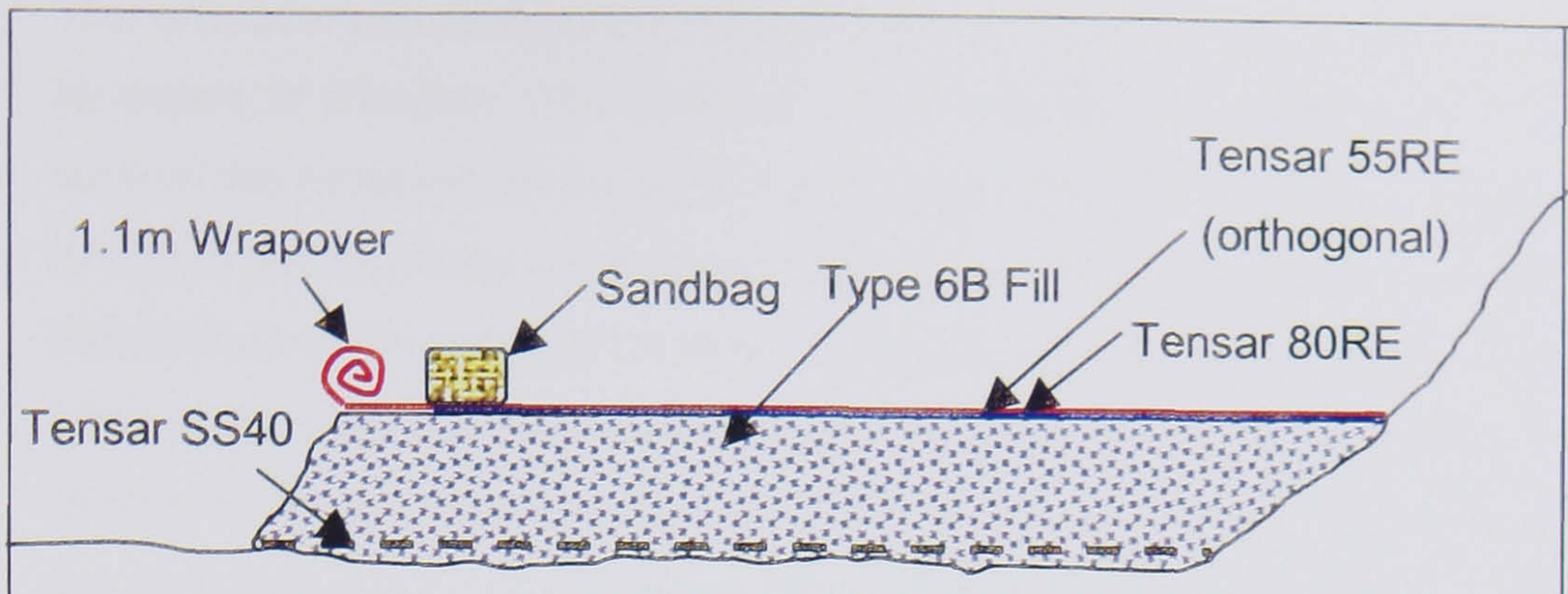

STAGE 1

Place Tensar 55RE and Tensar 80RE geogrid and place sandbag on string-line to establish toe of wall.

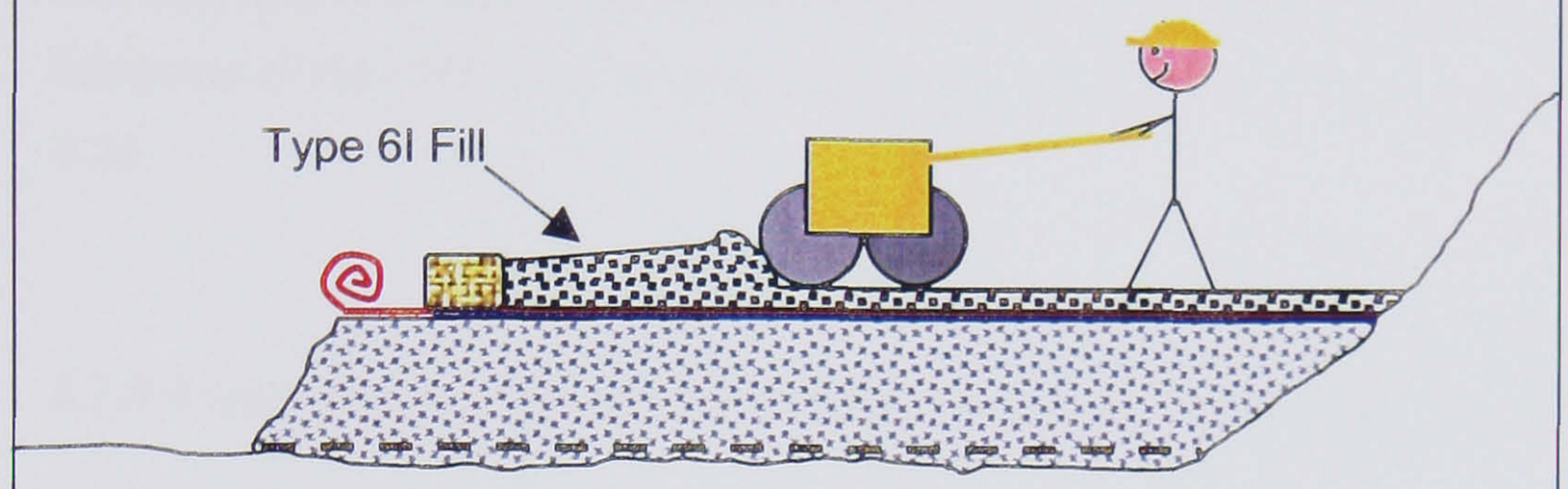

STAGE 2

Place approx 100mm of Type 6I fill and compact using 12 passes of pedestrian roller to 75mm thickness.

STAGE 3

Repeat stage 2 until lift height is 300mm high. Place bags at 80° inclination using template. Place 1m wide Tensar SS20 secondary reinforcement.

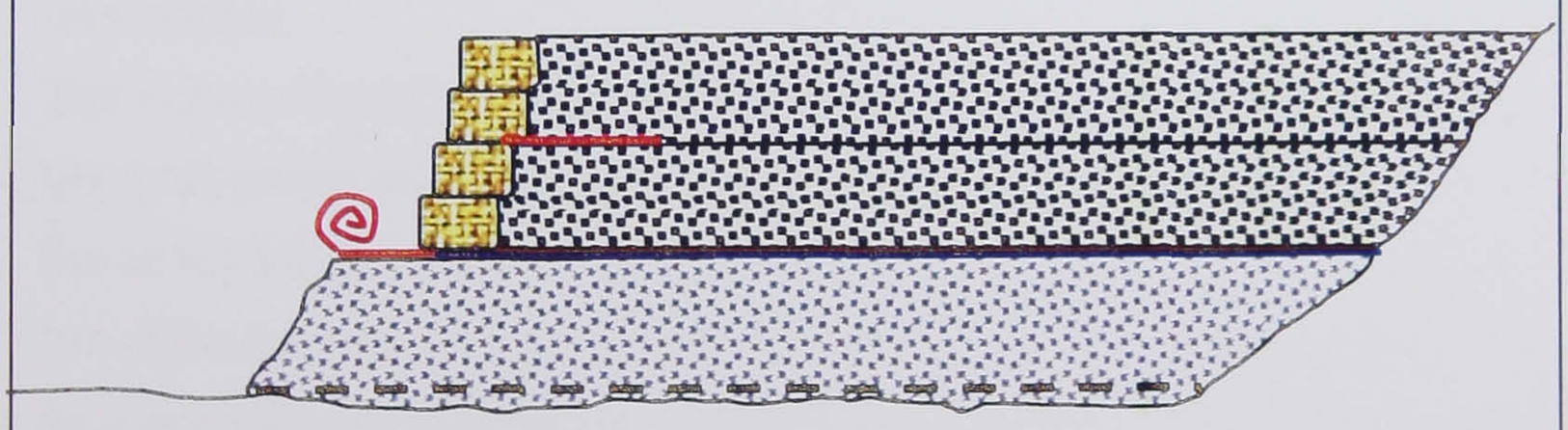

STAGE 4

Repeat stage 2 until lift is 4 bags (600mm), 8 compacted layers high.

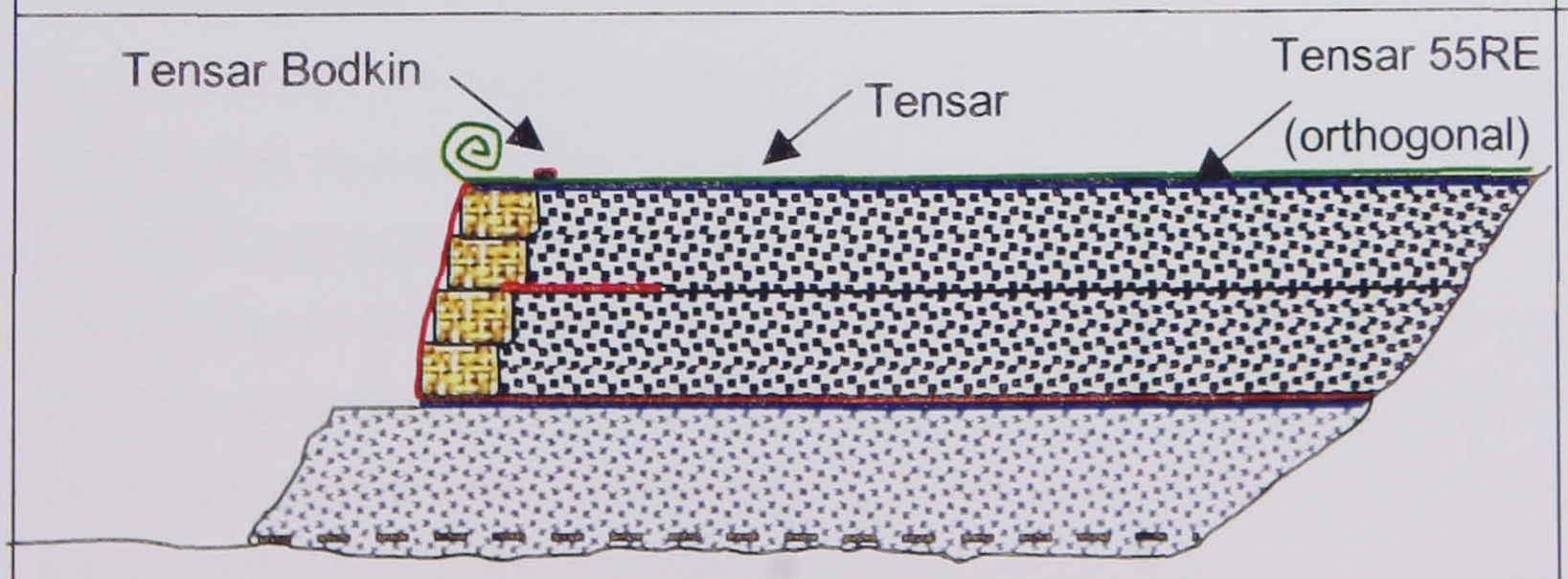

STAGE 5

Place 55RE and wrapover over front face and bodkin in next layer of reinforcement. Repeat stages 1-5.

Figure 5.35 Construction sequence for granular end blocks (Front face)

The wrapover consisted of connecting the next layer of reinforcement onto the layer below by means of a bodkin. The new grid was then pulled towards the back of the structure to tension the wrapover on the lift of 4 sandbags. Whilst the tension was being maintained in the grids the sandbags were tapped into shape using the back of a spade, this ensured a better finish to the faces of the wall. The grids, whilst still tensioned, were pegged at the back of the structure to maintain the tension in them. The grids in the side faces were tensioned, the sandbags tapped into place and pegged. Sandbags were then placed along the front and side faces of the wall, Type 6I fill placed and the whole process repeated until the next lift of four sandbags was complete. The construction sequence for a single wrapover of the front face in the granular region of the wall is shown schematically in Figure 5.35.

5.7.6.3 Construction Of Cohesive Electro-Osmosis Zone And Control Zone

The construction sequences for the two cohesive zones of the wall were identical and contemporaneous. The only difference that existed between the E-O and control zones was that no electricity was applied, although electrodes were incorporated during construction, to the control zone. This was to demonstrate that any differences that existed between the two zones must be as a direct result of the applied electrical potential difference and the associated electrokinetic phenomena. The construction process is shown schematically in Figure 5.36.

The construction sequence for the cohesive zones closely followed that for the granular end blocks, except that electrodes and filters were incorporated into the lift and that electricity was applied.

The construction of the first lift consisted of placing the 4.1m long Tensar 80RE uniaxial geogrids perpendicular to the string-line and then placing the first layer of sandbags along the string-line to form the toe of the wall. A path was formed at the back of the grids, at the toe of the back-slope, using Type 6I fill. The purpose of this path was two fold, firstly it acted as a drain for any water drawn out of the clay fill by electro-osmosis and/or gravity and secondly it allowed both personnel and plant to traverse from one end of the wall to the other at wall construction height. The back-path was constructed in a single lift of 600mm, the same height as a single lift. Occasionally the back-path was reinforced with Tensar SS40 biaxial geogrid to increase its stability and trafficability.

Electrodes and filters were placed on top of the first layer of sandbags at predetermined positions to correspond with electrode spacings of 1.2m, 0.8m and 0.4m in the electro-osmosis zone and 0.6m in the control zone. The second layer of sandbags was placed on top of the first to hold the electrodes and filters in place, shown in Plate 5.1.

The electrodes and filters were then placed back over the front face of the wall to allow placement of the slurrified clay. The clay was slurrified using a 360° excavator, either a

Komatsu Pc240LC or a CAT 235D, within the lake located at the front of the trial area. The clay was slurrified by excavating a hole within the clay in the lake and adding water to the clay, shown in Plate 5.2. The mixture was worked with the bucket of the excavator for approximately one hour or so until its consistency was that of a fluid slurry, such that when placed within the wall structure it would be self-levelling. Laboratory water content tests on the slurry gave a water content of approximately 75% (approximately liquid limit + 20%) which corresponded to a c_u of approximately 1-1.5kPa, see Figure 5.28. During the construction of the very first lift the moisture content during placing was slightly lower at approximately 50% with a corresponding c_u of the order of 5kPa, this was due to a lack of mixing and inexperience of the construction technique.

The clay was placed to a depth of 150mm, corresponding to the height of the lower sandbag. The final levelling of the clay slurry was undertaken by hand as shown in Plates 5.3 and 5.4. The electrodes and filters were placed on top of the fluid clay and pressed slightly into the clay to prevent their movement, shown in Plate 5.1. The remainder of the wall was then filled with slurrified clay to a total depth of 300mm (2 sandbags). The 1m wide secondary reinforcement SS20 was then placed on top of the sandbags. The third layer of sandbags was placed on top of the secondary reinforcement to hold it in place. EKG electrodes and filters were placed on top of the third layer of sandbags in a staggered fashion such that the electrodes were located above filters and filters above electrodes. The final layer of sandbags was placed to bring the total height of the lift to 600mm. The electrodes and filters were then placed over the front of the wall and 150mm of slurrified clay was placed in the wall bringing the depth of clay to 450mm. The electrodes and filters were then placed on the clay and pushed slightly into the surface to prevent their movement. The final 150mm of slurrified clay was then placed over the electrodes, bringing the total depth of clay to 600mm. The electrodes and filters were then passed through the corresponding aperture in the geogrid, in preparation for the wrapover of the grids for the construction of the next lift. The electrodes were stripped and each one connected to an individual power supply cable using a double-crimped stripped connection (see §3.5.6), shown in Plate 5.5. The colour coding initially adopted was red cables for the anodes and black cables used for the cathodes. These cables were then connected in groups of five using crimp connectors to the transformer/rectifier in the power supply container. The numbering adopted for the cables is as shown in Figure 5.37.

When the lift was ready, the installation was powered up to the prescribed voltage of 30V, and the trial monitored until treatment of the layer was complete (see §5.7.7 for detailed monitoring). Once the layer had reached the required undrained shear strength (≅20kPa) the power was turned off and construction of the clay zone continued. During the electro-osmotic treatment of the clay work progressed on the granular zones.

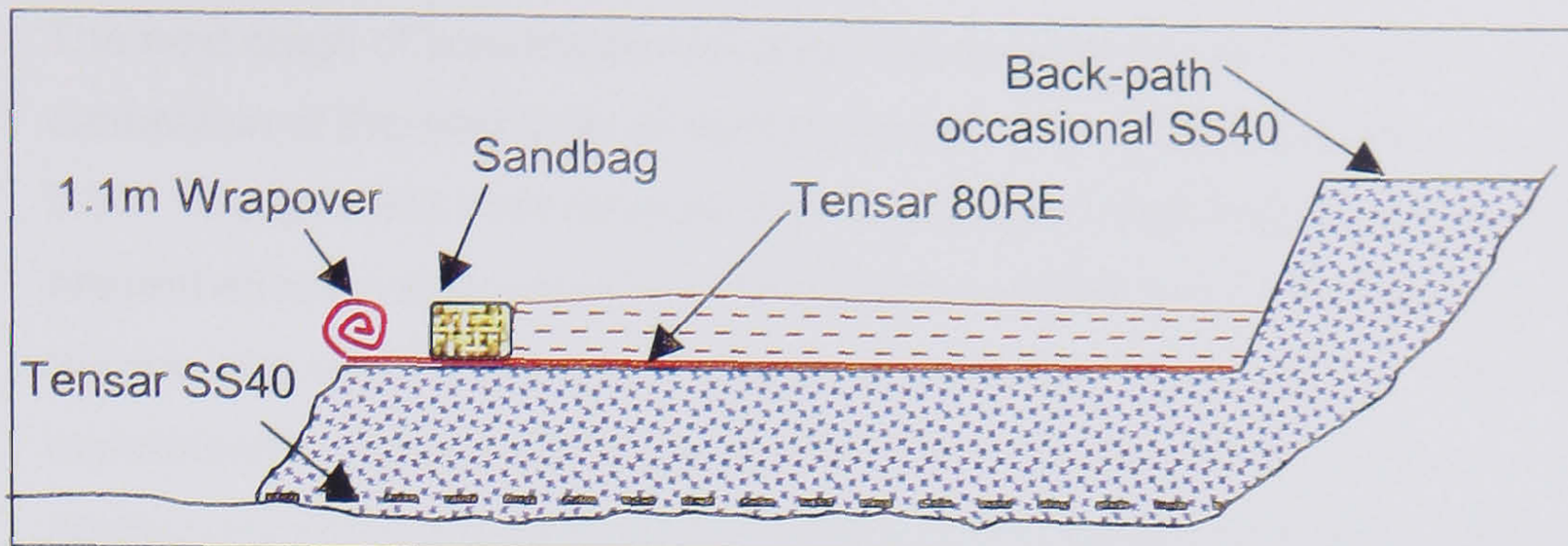

STAGE 1

Place Tensar 80RE geogrid and sandbag, construct back-path, fill with clay slurry to 150mm

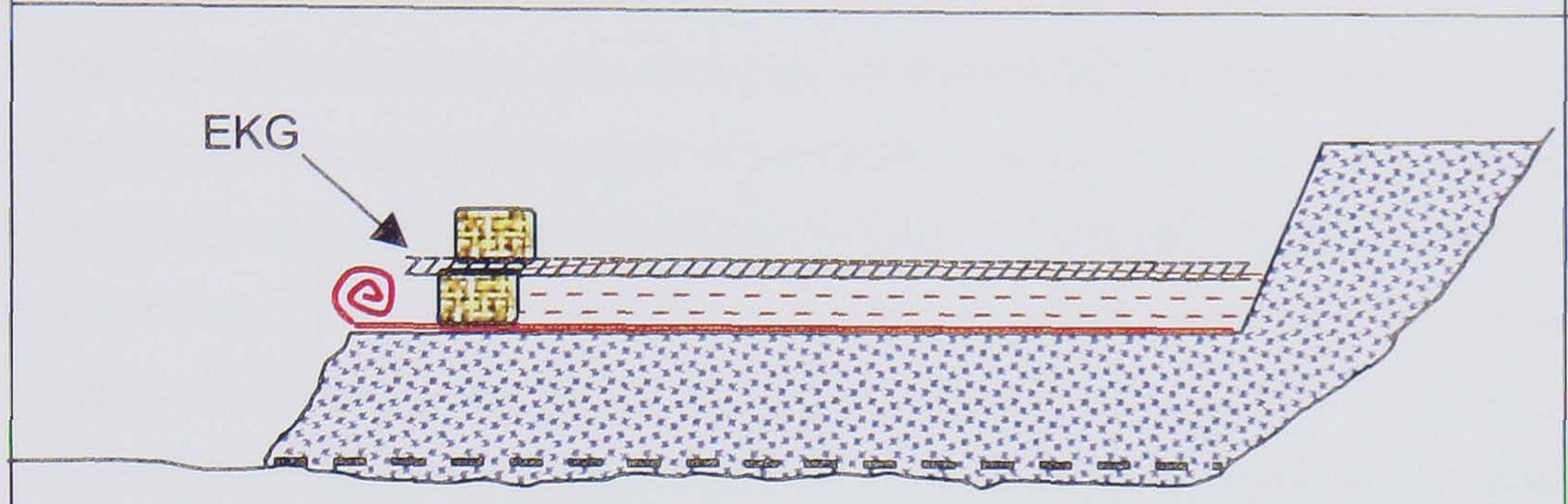

STAGE 2

Place EKG in position and place another layer of sandbags. Press EKG into clay to stop movement

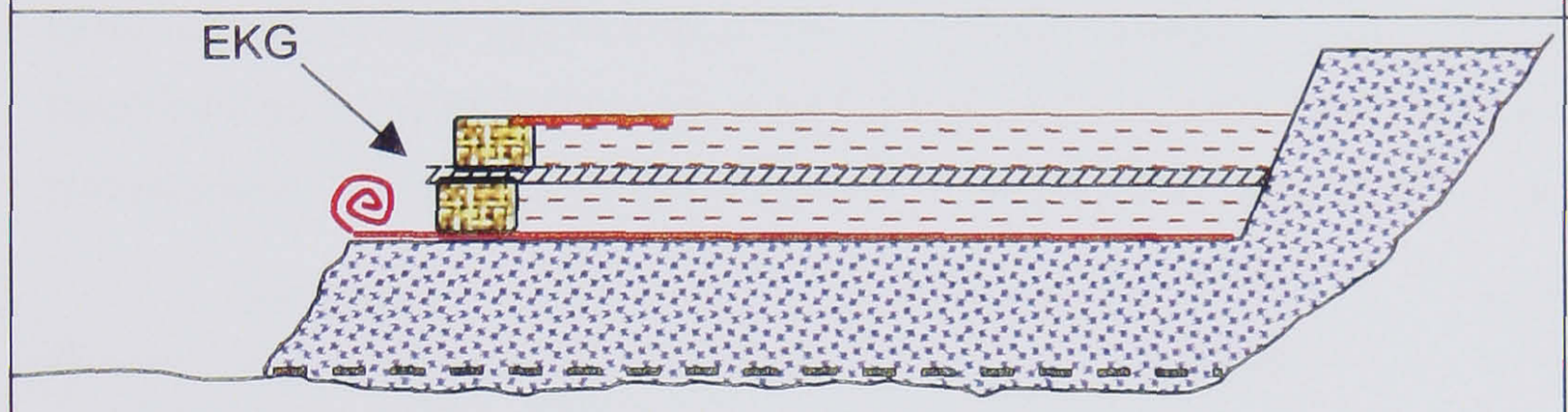

STAGE 3

Place another 150mm of clay slurry and secondary reinforcement

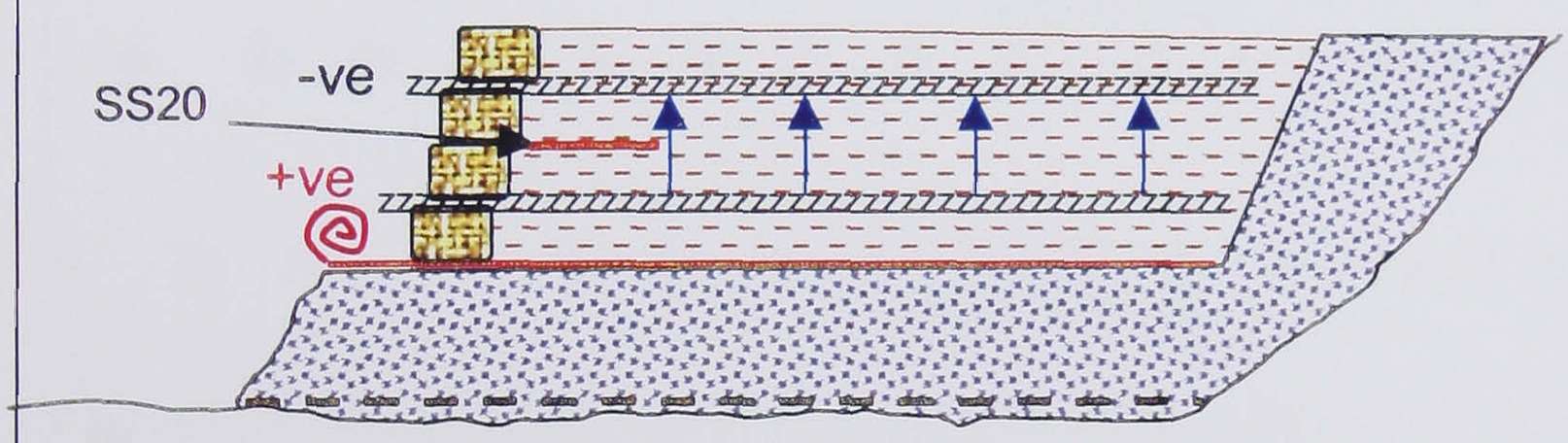

STAGE 4

Repeat stage 3 until 4 bags high. Connect EKG to power supply, cathodes uppermost

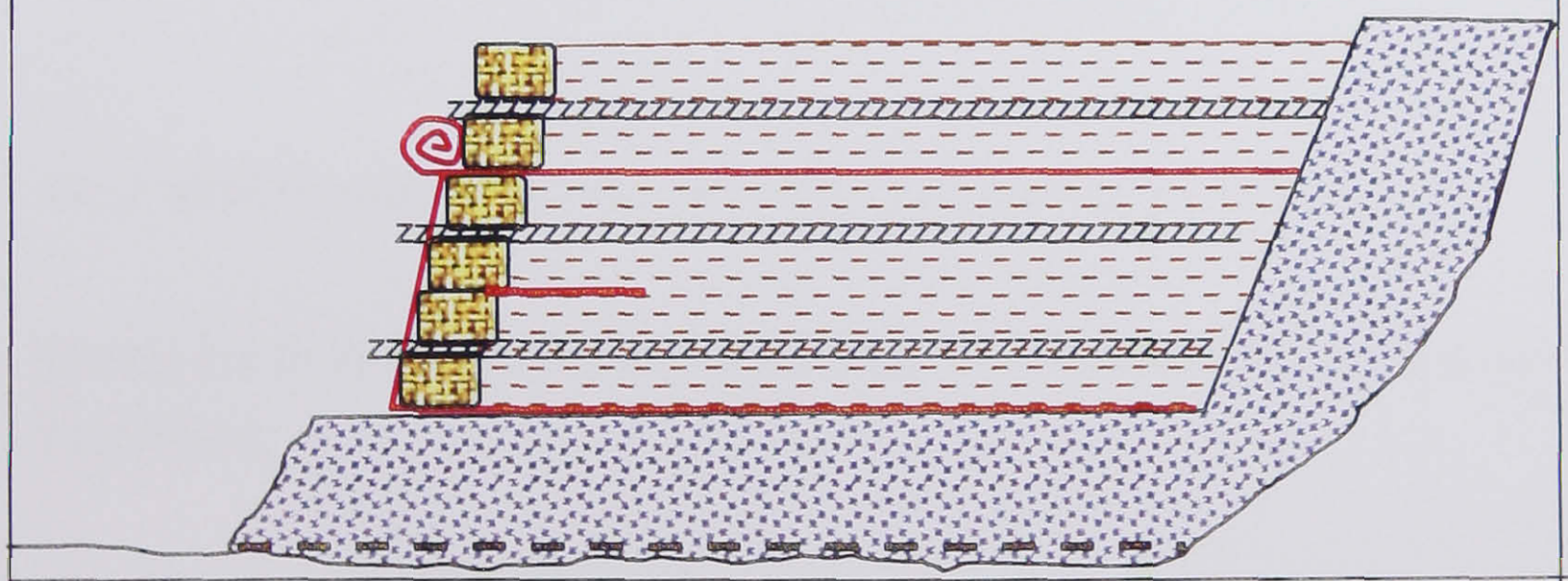

STAGE 5

When treatment is complete bodkin next layer of reinforcement. Repeat stages 1 to 3 until wall is 6 bags high

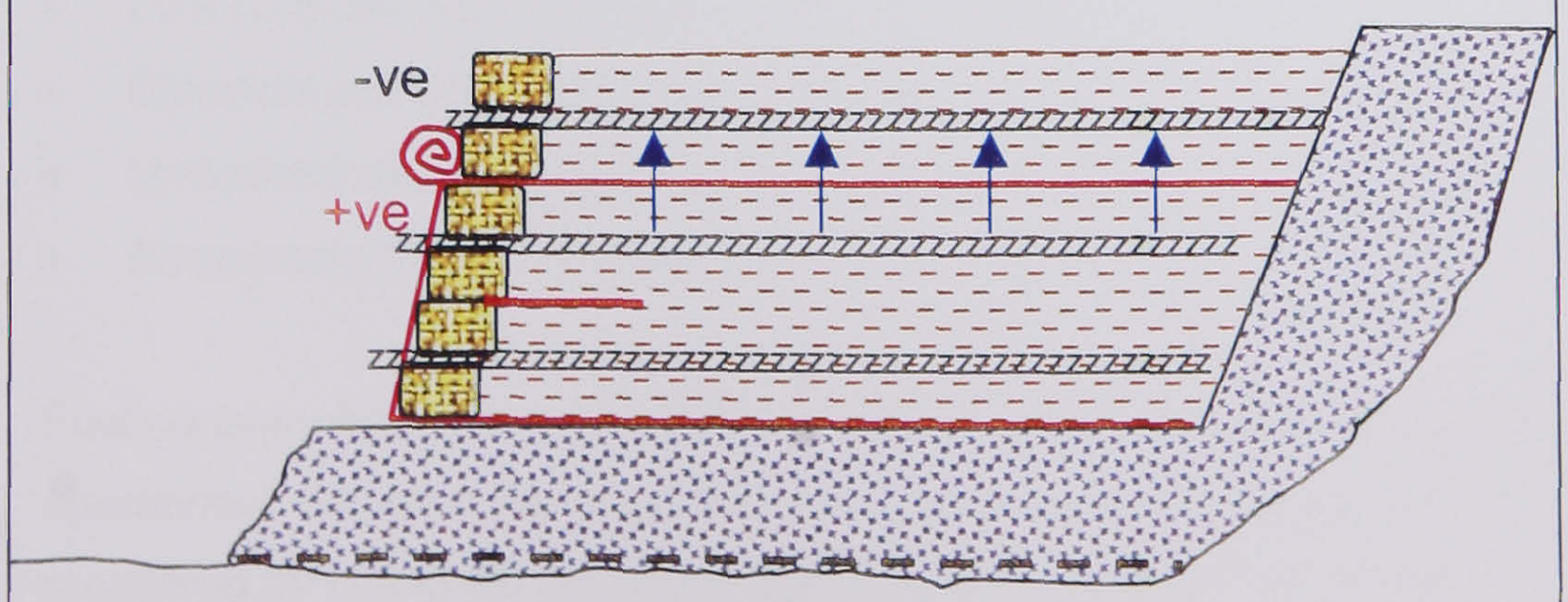

STAGE 6

Change the polarity of the electrodes, as shown, cathodes uppermost. When treatment is complete repeat stages until wall is complete

Figure 5.36 Construction sequence for cohesive wall

The next stage of construction involved the construction of the bodkin joint to achieve the connection of the next layer of reinforcement to the underlying layer, as shown in Figure 5.36. The grid was then tensioned to remove any slack from the front face of the wall and prevent excessive movement of the front face of the wall as construction proceeded. The tension was applied to the grid using a standard tensioning beam. The tension was maintained in the grid and it was trodden into the clay surface to lock the tension in the grid, additionally sandbags were placed on the grid to prevent slackening of the front face of the wall. Construction then proceeded as for the first lift to a total height of 900mm, i.e. ready for the placement of the next layer of secondary reinforcement. The cables from the lower electrodes were then removed from the lowest electrodes and connected to the new upper electrodes. The connection to the transformer/rectifier was then swapped over to make the upper electrode the cathode (-ve) and the lower electrode the anode (+ve), i.e. always driving the water in an upward direction. The installation was then powered up and the treatment monitored until the layer was sufficiently treated. Construction then proceeded as described earlier until the design height of the wall was achieved. This process is summarised in Figures 5.36 and Figure 5.38 presents a cutaway of the entire wall.

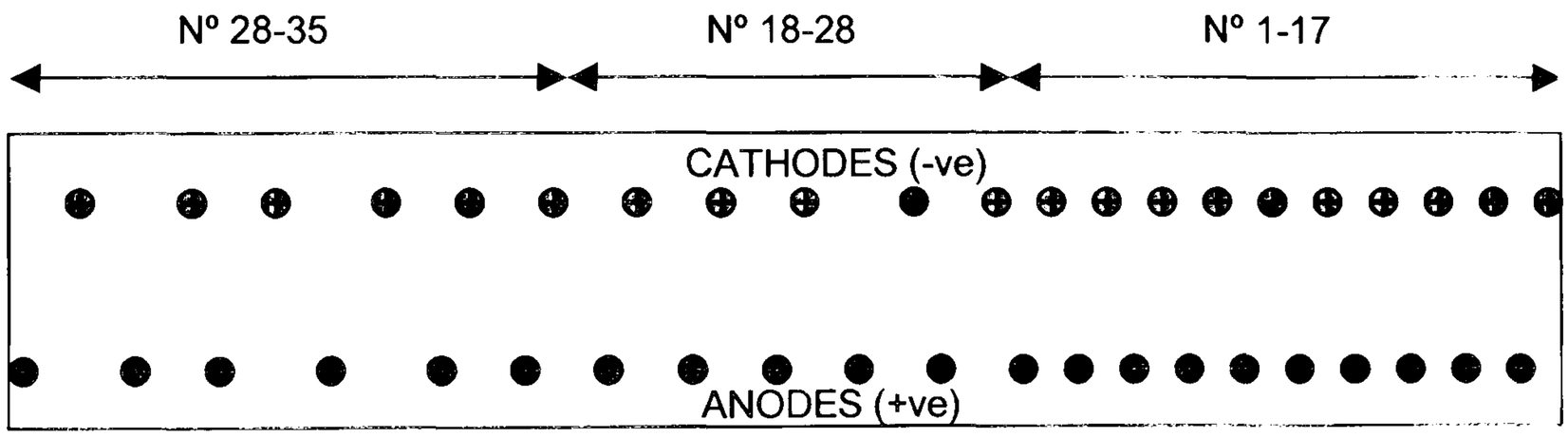

Figure 5.37 Electrode numbering and polarity for first lift

5.7.7 MONITORING REGIME OF THE JOINT STOCKS WALL

During the construction of the Joint Stocks wall several aspects of the construction were monitored:

- Fuel consumption (Gas Oil).
- Electrical power (Voltage and Current).
- Undrained shear strength (c_u) of the cohesive fill.
- Movement of the front face.

Fuel consumption was monitored on a regular basis during the time that the generator was operational, i.e. when the electro-osmosis process was underway. Fuel consumption was monitored by noting the quantity of fuel that was added to the generator fuel tank and the

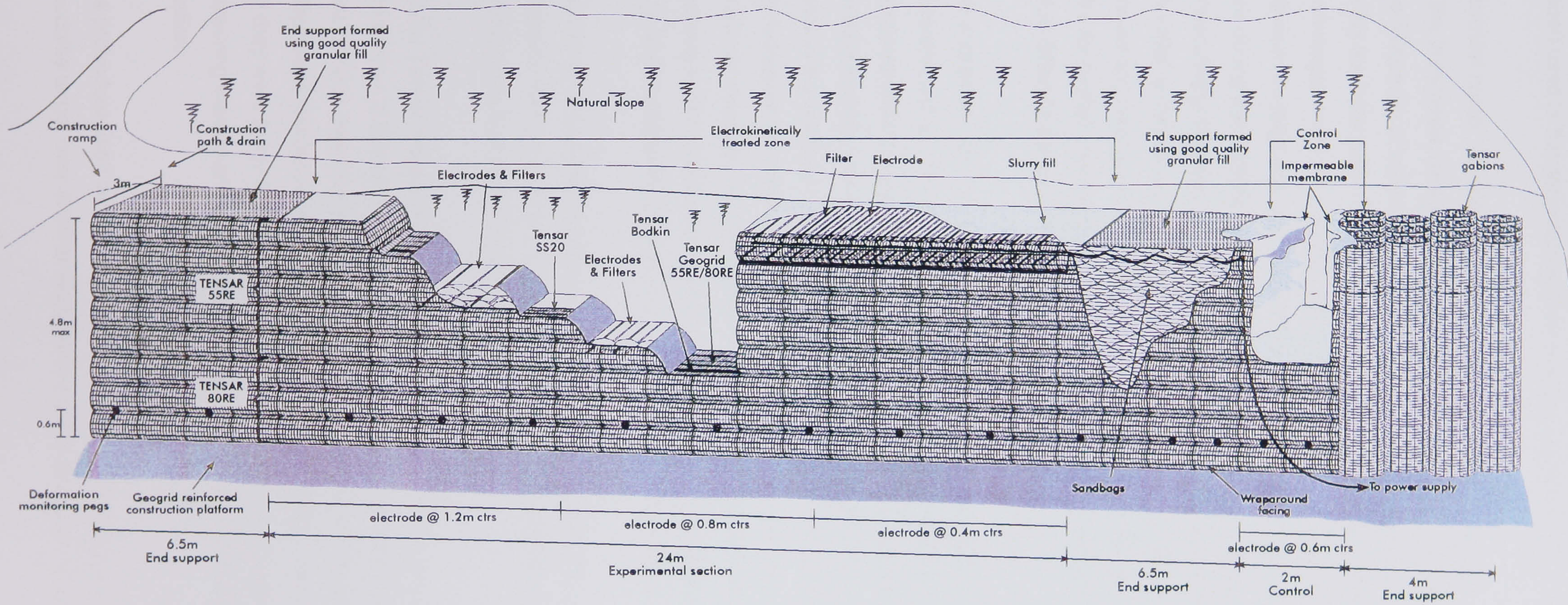

Figure 5.38 Schematic cutaway of the Joint Stocks wall

time indicated on the generator clock when the fuel was added. The cost of the gas oil (red diesel) used in the generator was on average 46 pence/litre during the duration of the trial.

Electrical power variation with time was measured by recording the quantity of current drawn at the prescribed voltage (30V) using the analogue dials located on the transformer/rectifier. The frequency of readings was varied to reflect the rate of change of current drawn i.e. during the initial powering up of a lift for treatment by electro-osmosis readings were taken, on average, every 15 minutes. As the rate of change of current declined the time interval between readings was gradually increased until one reading was taken approximately every hour during the working shift. During initial powering up the electrodes were connected consecutively in groups of 5, i.e. 5 anodes and 5 cathodes, in this way it was possible to get the initial current drawn by the different electrode spacing configurations and this also allowed any discrepancies in electrical resistance to be identified to a set of five electrode pairs for further investigation. It also enabled a quantification of the difference in resistance of the different electrode spacings used in the trial.

The undrained shear strength of the cohesive fill undergoing electro-osmotic treatment was measured using a Pilcon hand shear vane with a 1¼" (31mm) vane. The measurements of undrained shear strength were taken at two depths, 0.25m and 0.5m to try to distinguish the variation in shear strength in the clay between the anode and cathode positions. To reduce errors in the readings 5 readings were taken at each location and averaged at each depth, at approximately the same locations along the wall. The undrained shear strength was measured every 2m along the full 24m length of the electro-osmosis zone and at 3 different locations in the control zone. Additionally, samples were taken of the soil from the shear vane test locations for laboratory testing to establish their water content.

The movement of the front face of the wall was also measured using offsets from a Wild T2 theodolite, with an accuracy of ½". The configuration used to measure the deformation of the front face is shown in Figure 5.39.

Initially, Tensar Pegs were hammered into the sandbag facing at the location where the deformation of the wall was to be monitored. The pegs were then painted with yellow marker paint to aid in their location. Figures 5.38 and 5.39 show the approximate location of the deformation monitoring pegs on the front face of the wall. The pegs were checked to ensure that they were firmly seated into the wall and that they were orientated such that the measuring tape could be fixed to the pegs and could be observed from the theodolite location.

The procedure used consisted of setting up the theodolite over a fixed survey point and a theodolite target over another fixed survey point, the points are shown schematically in

Figure 5.34. Thus, establishing a line of sight between the two survey points, as shown in Figure 5.39. The theodolite was then locked on the horizontal circle so that the line of sight could not be displaced in the horizontal but was free to rotate in the vertical plane. A measuring tape was then attached to the monitoring peg to be measured and pulled taught. The minimum reading was then taken by observing the tape through the theodolite and reading the intersection of the tape with the theodolite cross hairs. The process was repeated for all of the monitoring points along the front face of the wall. In this way the movement of the front face of the wall was recorded. The deformation monitoring pegs also allowed a levelling staff to be placed on each peg to give the vertical movement of each peg. As a result, the deformation vector of the front face could be established from the vertical and horizontal components measured in this way. It was also possible to level the clay fill surface using the level and the staff, although due to the very fluid nature of the clay this was found to be impractical.

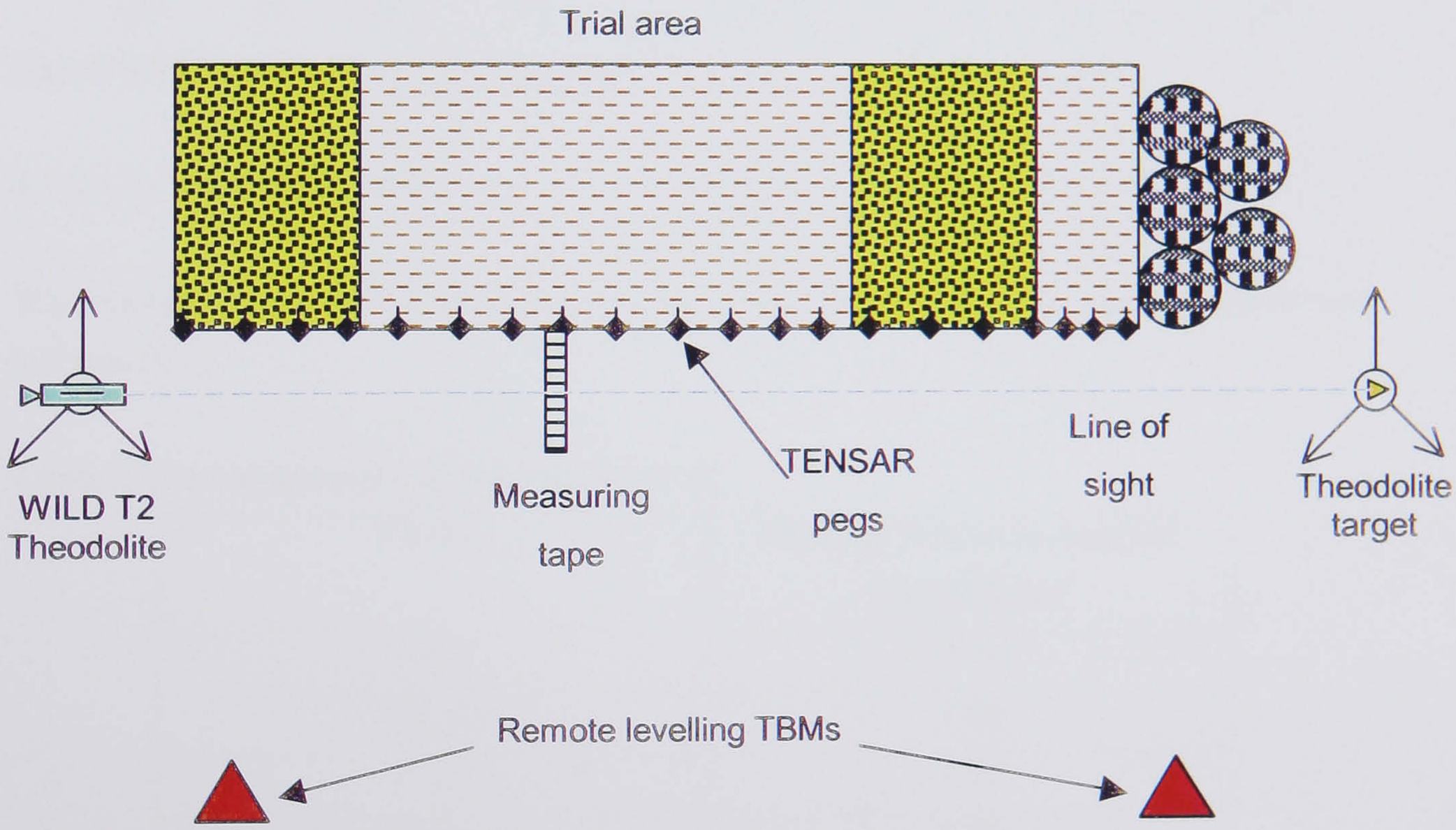

Figure 5. 39 Survey configuration used to measure deformation of the wall

5.7.8 RESULTS OF THE JOINT STOCKS TRIAL

The results obtained from the Joint Stocks trial are presented in the following sections for lifts up to a maximum height of 2.1m in the electro-osmosis and control zones and up to a height of 4.2m in the granular end walls. This is followed by a detailed interpretation/analysis of the results and their comparison with the design values. The overall construction height against time for the wall is presented in Figure 5.40.

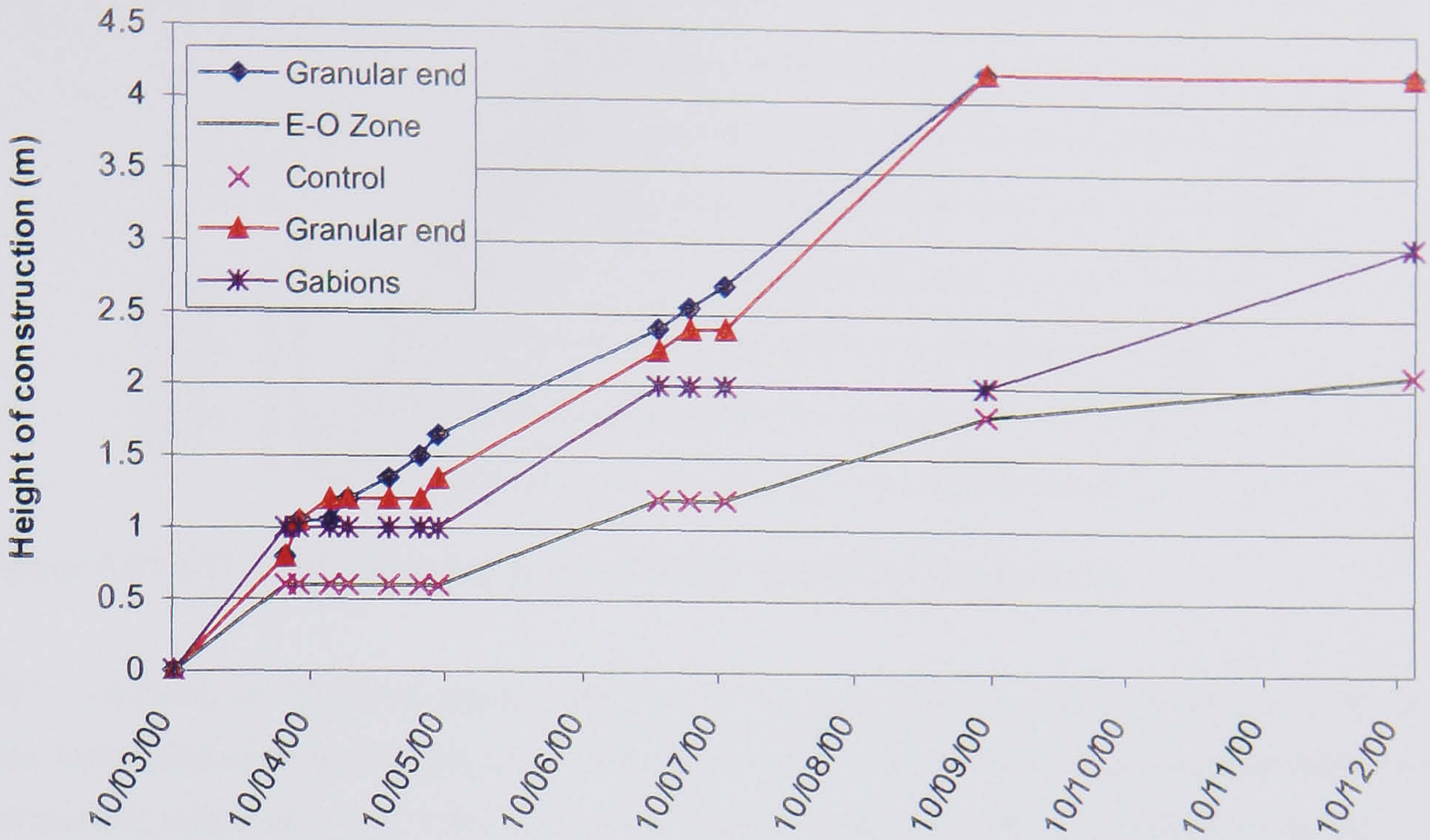

Figure 5.40 Construction height against time for the Joint Stocks Wall

5.7.8.1 Fuel Consumption

The results obtained for the average fuel consumption for the lifts undertaken are presented in Table 5.14.

Table 5.14 Average fuel consumption per lift

Lift No.	Average fuel consumption (litres/hour)
Lift 1	2.11
Lift 1a	1.62
Lift 2	2.00
Lift 2a	1.90
Lift 3	2.39

These results give an average fuel consumption for the whole trial of 2.00 litres/hour. The definition of the lift numbering system that is used in Table 5.14 is defined in Figure 5.41. This nomenclature is also used for the other results presented in this section.

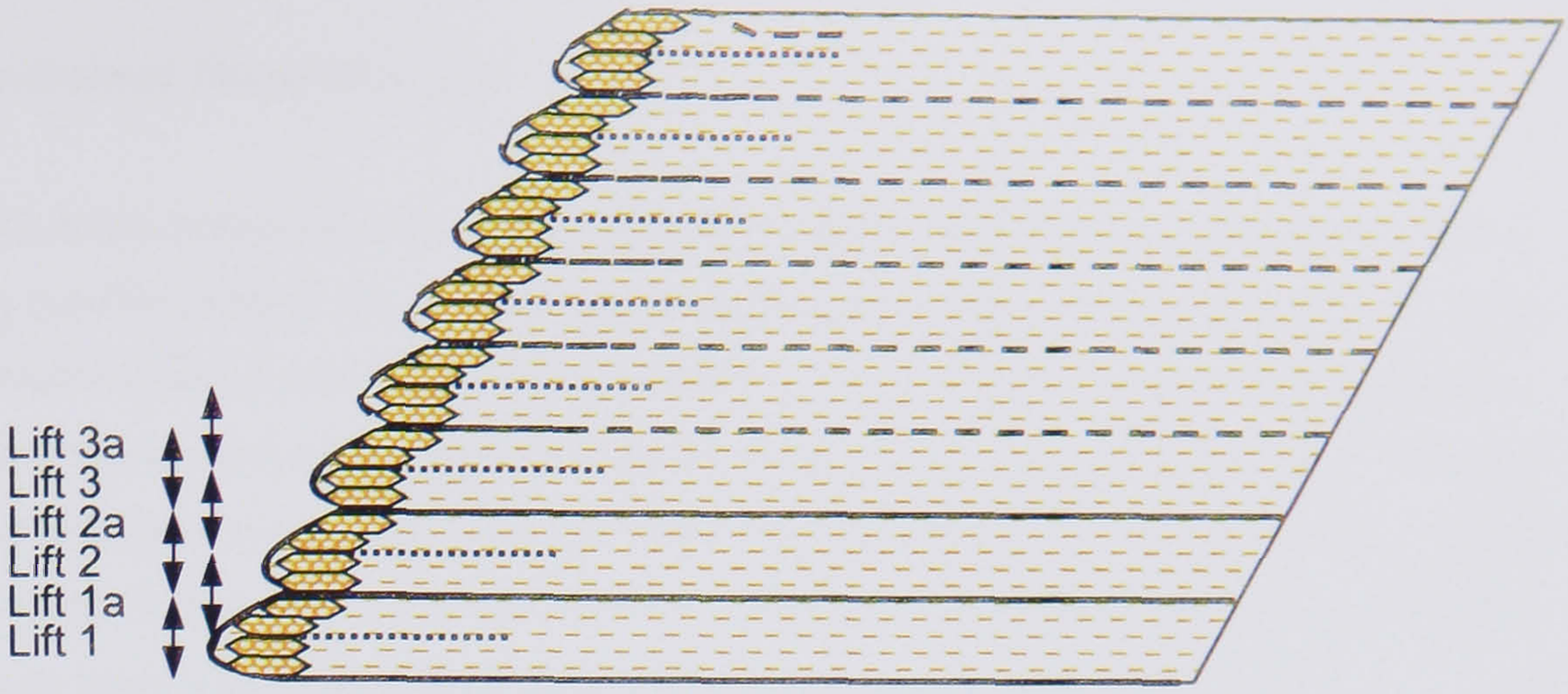

Figure 5.41 Lift numbering nomenclature for electro-osmosis zone

Lift 1 is defined as the lift for the first 600mm of the wall using the lowest electrodes, lift 1a then brings the wall up to a height of 900mm (i.e. level with the secondary reinforcement of the second wrapover). Lift 2 brings the wall up to a height of 1.2m and is geometrically identical to lift 1.

5.7.8.2 Electrical Energy

The current drawn by each lift is presented in Figure 5.42, as current against cumulative generator time, with the voltage being fixed at 30V. The nomenclature used for each lift is as presented previously in Figure 5.41.

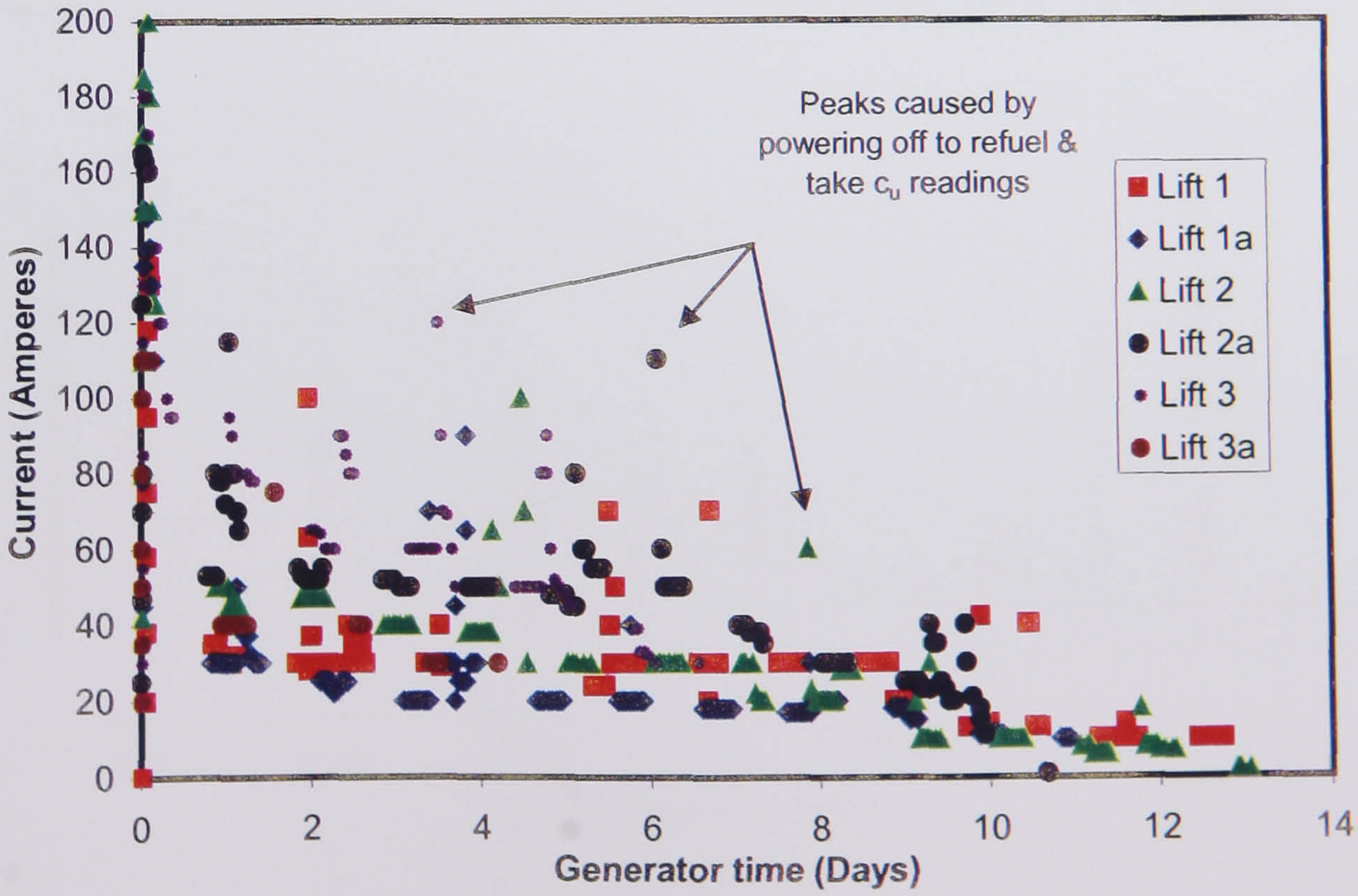

Figure 5.42 Electrical current drawn by each lift

5.7.8.3 Undrained Shear Strength

The results of the measurements of the undrained shear strength (c_u) as measured in the field using the Pilcon hand shear vane are presented in Figure 5.43 and Figure 5.44, for the two test depths used, 0.25m and 0.5m respectively. The results have been differentiated according to the electrode spacing in the zone in which they were obtained, i.e. 0.4m, 0.8m, 1.2m and the control zone. The have not been differentiated by the lift from which they were obtained. A correction factor of 1.0 for the conversion of vane shear strength to field shear strength has been used based upon a plasticity index of 25%, presented in Table 5.5, and the correlation suggested by Bjerrum (1972) and Carter & Bentley (1991).

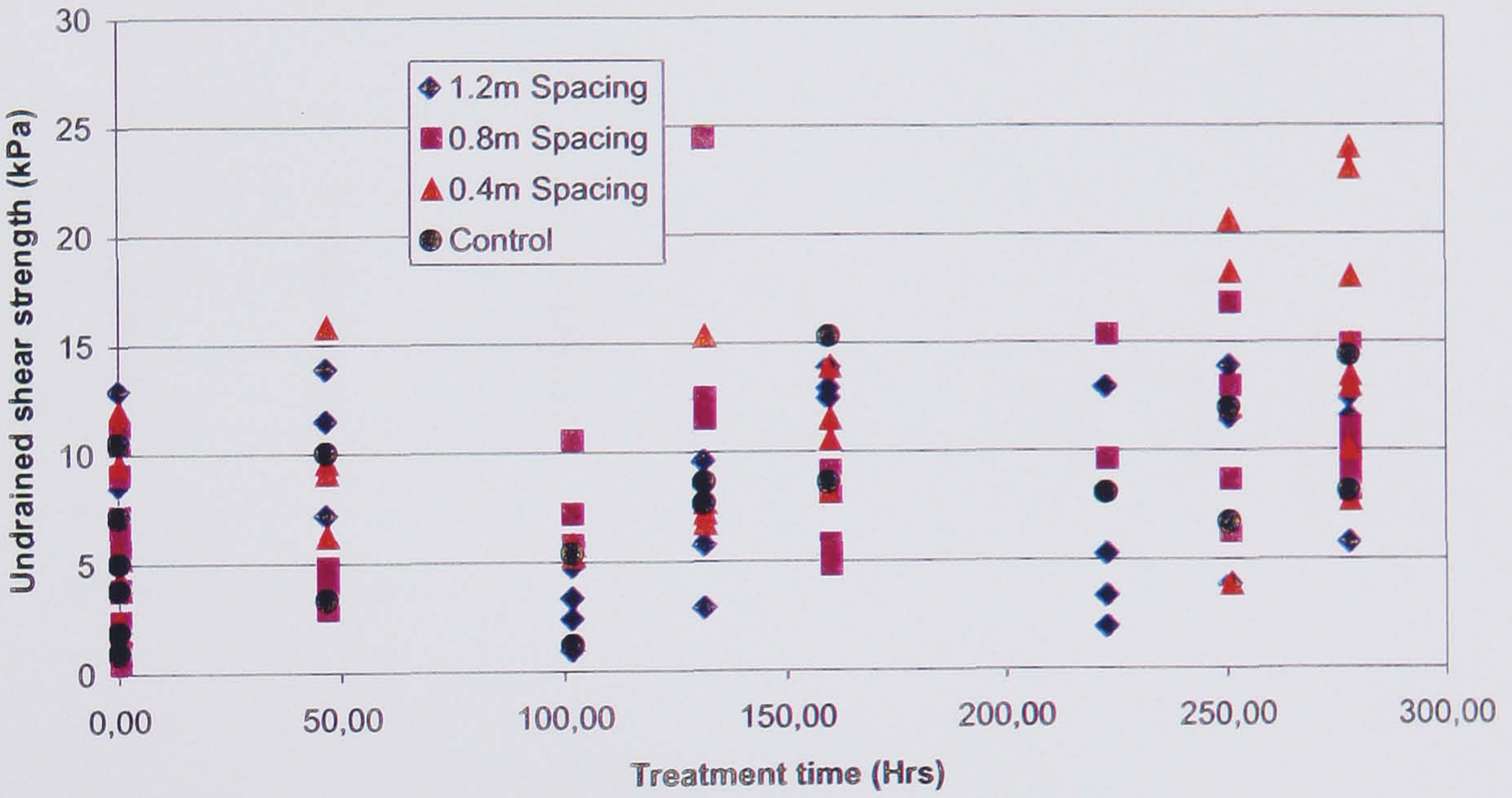

Figure 5.43 Undrained shear strength (c_u) against treatment time (0.25m depth)

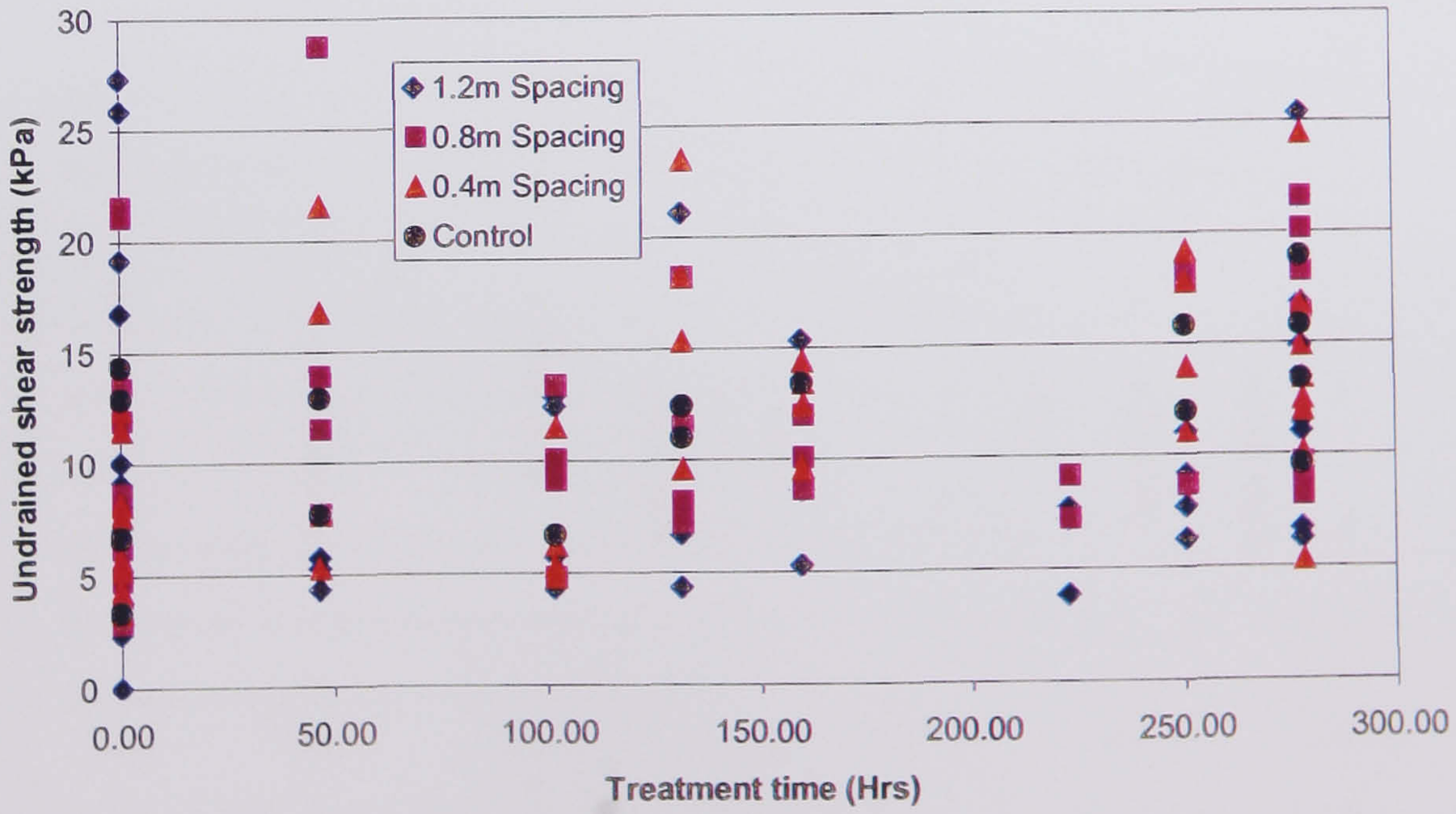

Figure 5.44 Undrained shear strength (c_u) against treatment time (0.5m depth)

5.7.8.4 Water Content

The results of the laboratory measurements of the water content (w_c) are presented in Figure 5.45 and Figure 5.46, for the two test depths used, 0.25m and 0.5m. The results have been differentiated according to the electrode spacing in the zone in which they were obtained, i.e. 0.4m, 0.8m, 1.2m or the control zone. During treatment water was seen to migrate to the surface and pond at the cathode positions, Plate 5.5, this was also associated with the movement of fines to the surface with the water, Plate 5.6, and the formation of hydrogen gas bubbles, Plate 5.7.

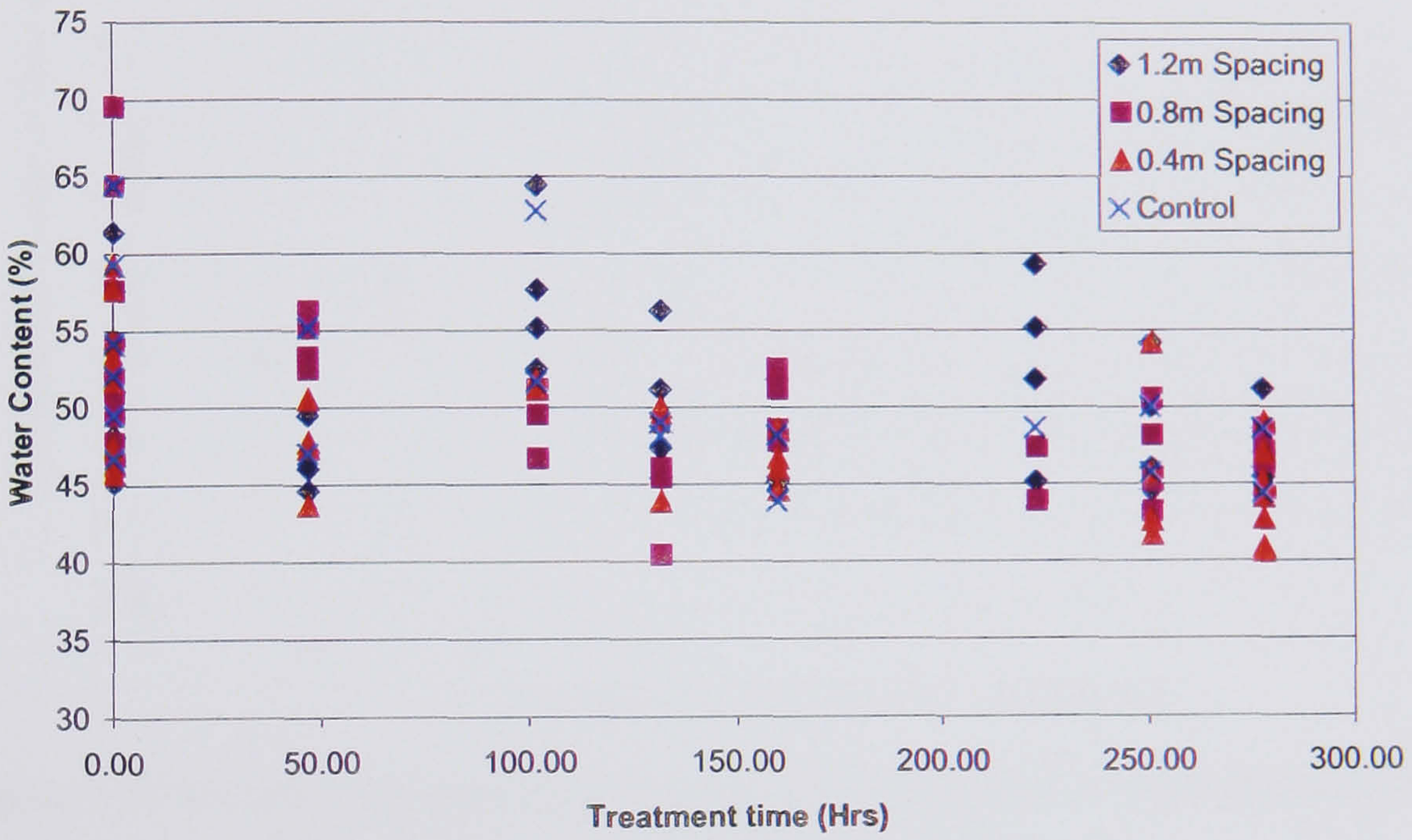

Figure 5.45 Water content against treatment time (0.25m depth)

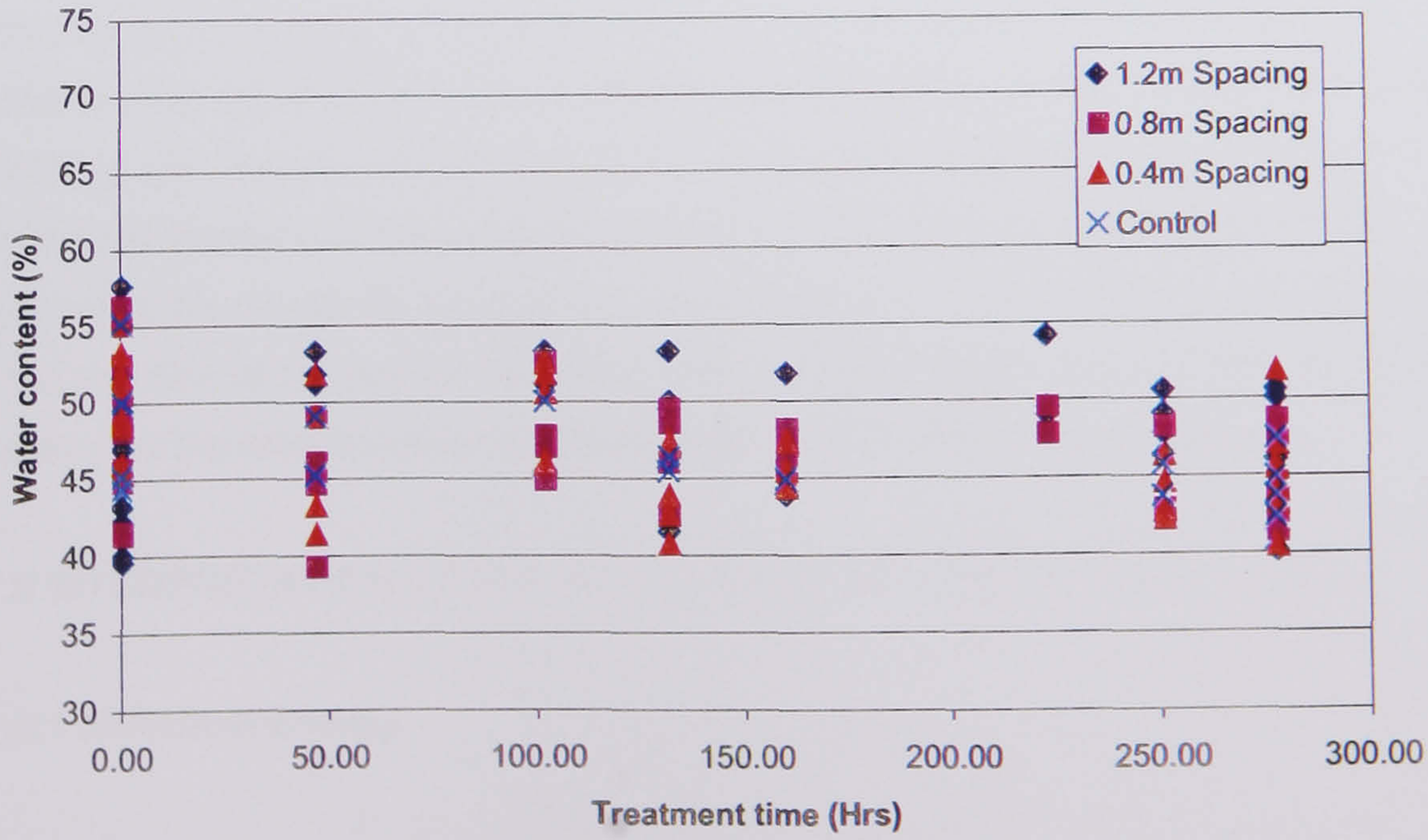

Figure 5.46 Water content against treatment time (0.5m depth)

5.7.8.5 Deformation Of The Wall

The results of the deformation monitoring of the front face of the wall measured using survey offsets, as discussed in §5.7.7, are presented in Figure 5.47 for the monitoring pegs located at mid-height of the first lift of the construction (i.e. 300mm above construction platform level).

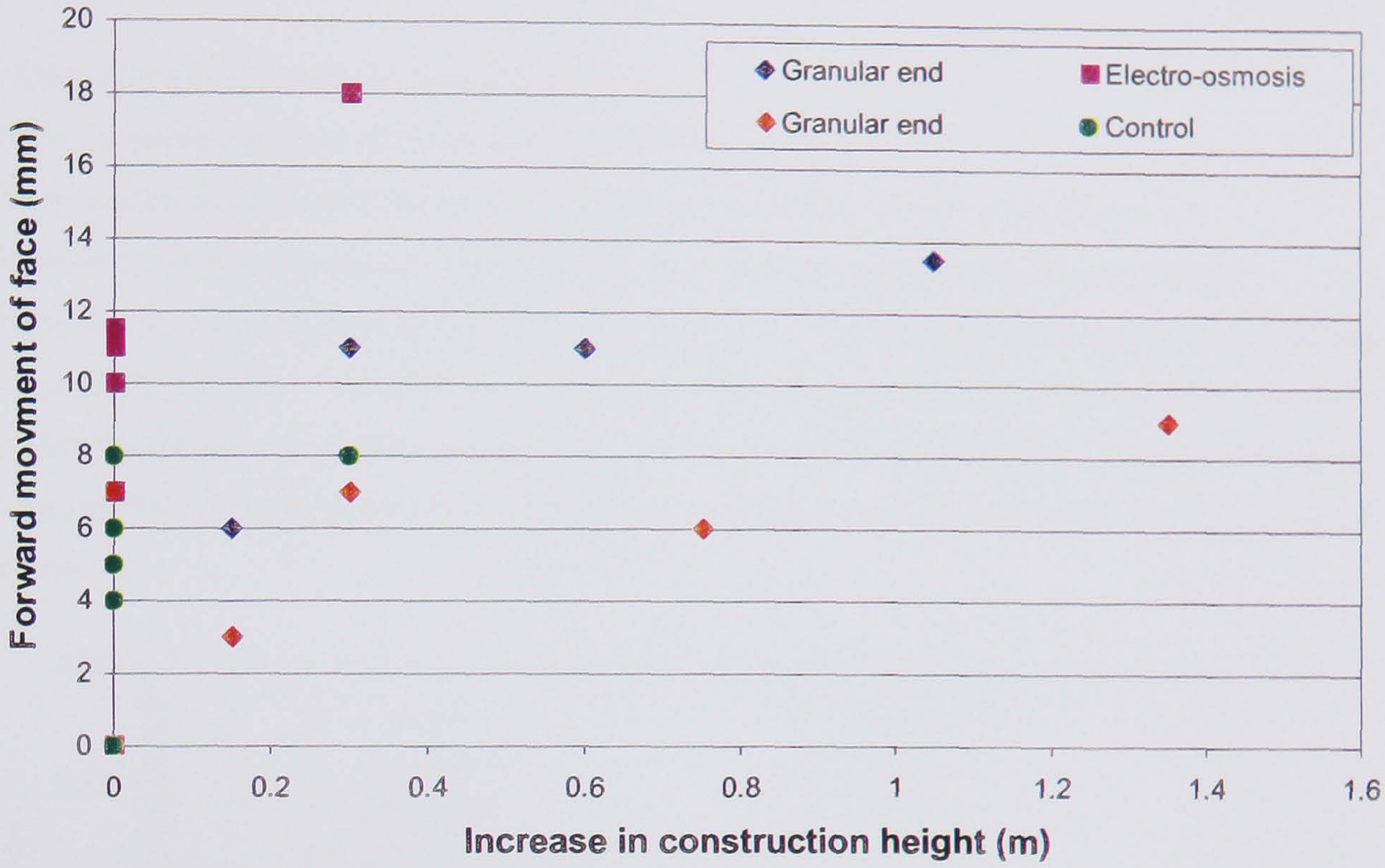

Figure 5.47 Results of monitoring of movement of front face of Joint Stocks wall

The results show a general trend of forward movement of the face of the wall as the height of the wall increases. This result is as would be expected as the lower lift of the wall becomes loaded by the construction of overlying layers it becomes compressed and due to a Poisson's ratio effect expands horizontally outwards as the reinforcement begins to take increasing load and the slack in the system is taken up. The taking up of the slack is reflected as flattening of the slope of the curve as the construction height increases, this is best seen in the results for the granular ends of the trial. The results are not complete for the full construction of the wall as the line of sight between the two survey points became obscured by the erection of the scaffolding at the front of the wall structure.

5.7.9 INTERPRETATION OF THE RESULTS OF THE JOINT STOCKS TRIAL

5.7.9.1 Electrical Energy

The field results obtained from the trial and presented in Figure 5.42 cannot be directly compared with those obtained from the laboratory testing (electro-osmosis cell) due to a difference of scale of the volume of soil being treated by electro-osmosis. To allow a direct

comparison of the results the current drawn at the set voltage (30V) may be converted into an overall electrical conductivity (σ) of the system by means of rearranging Equation 5.34:

$$\sigma = \frac{1}{R}\frac{L}{A} \qquad \text{Eqn. 5.34}$$

Where:

$$R = \frac{V}{I} = \frac{30V}{I} \qquad \text{Eqn. 5.35}$$

L= Distance between electrodes (0.3m)

A= Cross-sectional area of the trial ($24*3=72m^2$)

This is a simplification of the reality in that it assumes the system is acting in a 1-Dimensional (i.e. plate electrodes) manner, and that the voltage gradient and hence resistance is constant throughout the whole trial wall. This simplification is felt to be justified, as due to the complex variation of the voltage within the wall and the crudity of the current monitoring system, analogue gauges, further refinement is unjustifiable. Hence, the results of the electrical conductivity for the wall are presented in Figure 5.48 in terms of each lift of the wall.

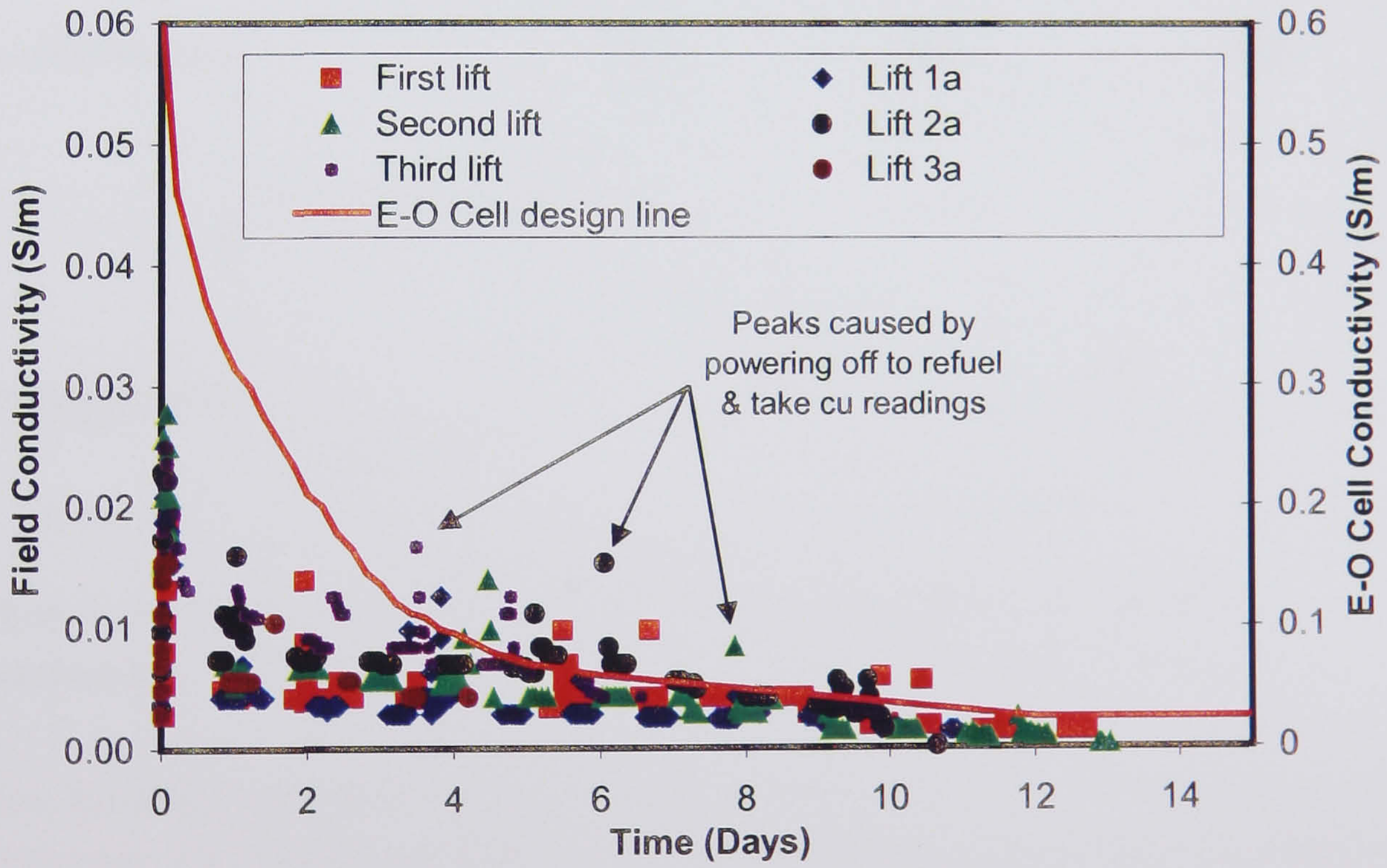

Figure 5.48 Variation of electrical conductivity, laboratory and field (*Note factor of 10 between vertical scales*)

Additionally, in Figure 5.48 is presented the design line derived from the results of the variation of electrical conductivity obtained from the electro-osmosis cell and presented previously in Figure 5.33.

The peaks that occur in the field results of conductivity are as a result of the temporary powering off of the installation for refuelling, measurement of shear strength/water content or during weekends when the installation was powered off to prevent the generator running out

of fuel and so as not to leave the trial unattended for in excess of 48 hours. The increase in conductivity associated with these periods of powering off are of the same origin as those observed by other researchers, and are a result of the redistribution of the chemical species that have been differentiated by the electro-osmosis process (Acar *et al* 1990, Grey & Somogyi 1977, Sprute & Kelsh 1975).

It will be seen from Figure 5.48 that the actual electrical conductivity measured in the field was approximately 10 times less that that obtained from the laboratory electro-osmosis cell. This result is logical when the configuration of the two different situations is considered. The electro-osmosis cell uses plate electrodes and hence the electrical field established is 1-Dimensional, and thus theoretically the voltage gradient that occurs within the cell is uniform, see Figure 5.49.

In the field trial the voltage is applied to the wall by means of EKGs which may be considered as point electrodes, thus generating an essentially 2-Dimensional electrical field, with the effect being more pronounced at greater spacings between electrodes of the same polarity, as demonstrated in the finite difference analysis undertaken in §5.7.4.2 and §7.6.2, and as shown schematically in Figure 5.49.

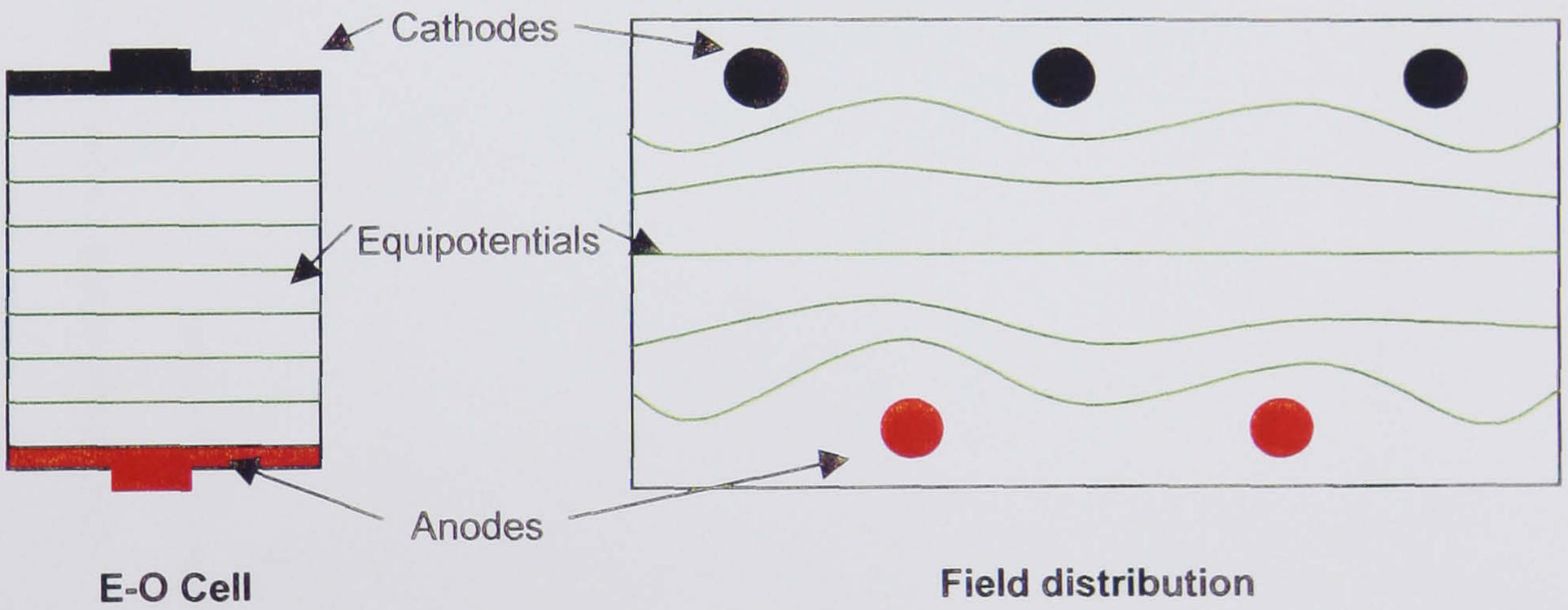

Figure 5.49 Electrical field characteristics of e-o cell and field trial electrode distributions

Thus, the power estimations made in §5.7.4.4 are on the high side by an order of magnitude. Additionally, it is interesting to note that the electrical conductivity presented by Casagrande (1983), presented in Figure 5.29 demonstrated a conductivity variation from 0.4S/m to 0.12S/m, which is also of the order of 10 times greater than that achieved in the field. Again, the explanation for this is thought to be the electrode configuration.

Additionally, from Figure 5.47 it will be seen that the electrical conductivity of the trial underwent a reduction with time of the order of 95% from an initial value of approximately 0.026S/m to 0.0013S/m. This compares with the values suggested in the two design methods of 66% (Wrigley 1999) and 95% by the Author (§5.7.4.4).

5.7.9.2 Relations Between Shear Strength - Water Content And Time

The interpretation of the field measurements of the undrained shear strength, obtained from the hand shear vane, and corrected for conversion to field shear strength, was undertaken by superimposing the theoretically calculated shear strength based upon an initial water content and voltage gradient calculated by the finite element analysis. These results are plotted in Figures 5.50 and 5.51 for the two test depths of 0.25m and 0.5m. Additionally, due to the large variation in the results obtained from the hand shear vane, even within the zones of the same electrode spacing a zonal average was calculated for each of the electrode spacings used; 0.4, 0.8 & 1.2m and the control zone. This allowed easier interpretation of the results by eliminating the large degree of scatter that was present in the unrefined field results, as shown in Figure 5.52 and 5.53. The differentiation between the 0.25m and the 0.5m depth readings was maintained to illustrate the difference in the strength changes with proximity to the anodes or cathodes.

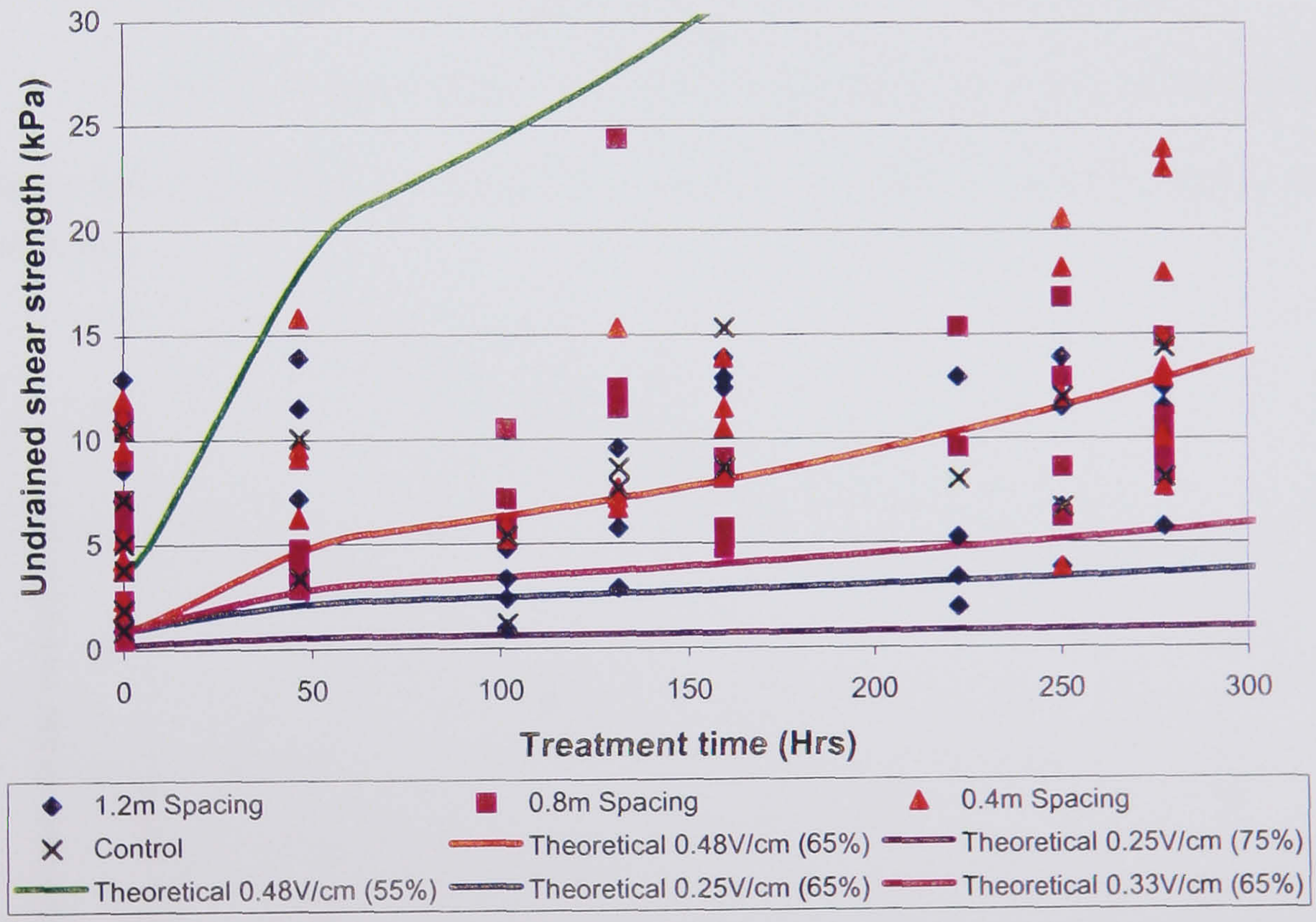

Figure 5.50 Theoretical and experimental results of c_u against treatment time, 0.25m test depth

Additionally, the results were normalised with respect to the undrained shear strength of the clay as initially placed, such that the percentage improvements were calculated. These are presented in Table 5.15 for all electrode spacings, control zone and the two test depths.

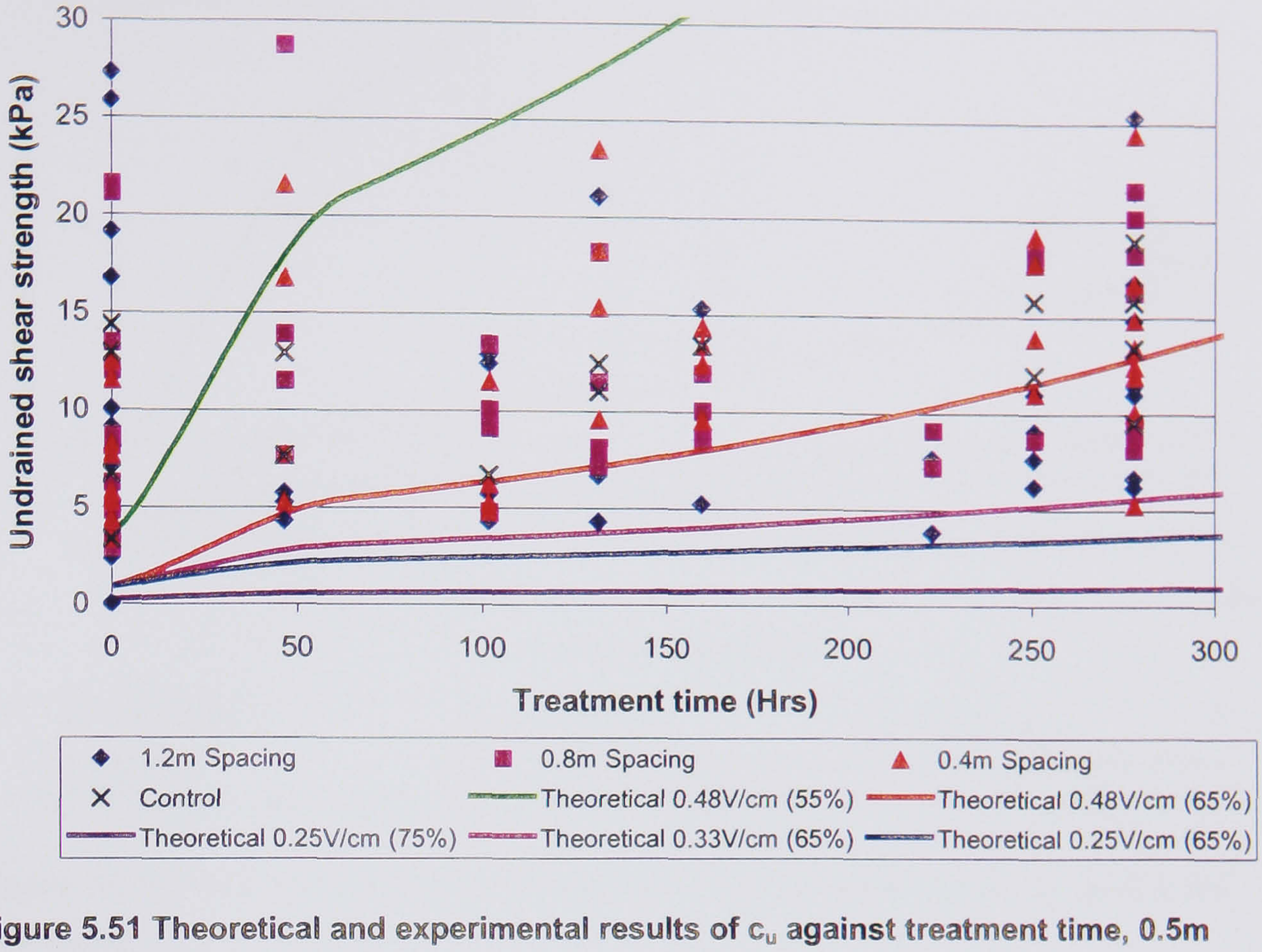

Figure 5.51 Theoretical and experimental results of c_u against treatment time, 0.5m test depth

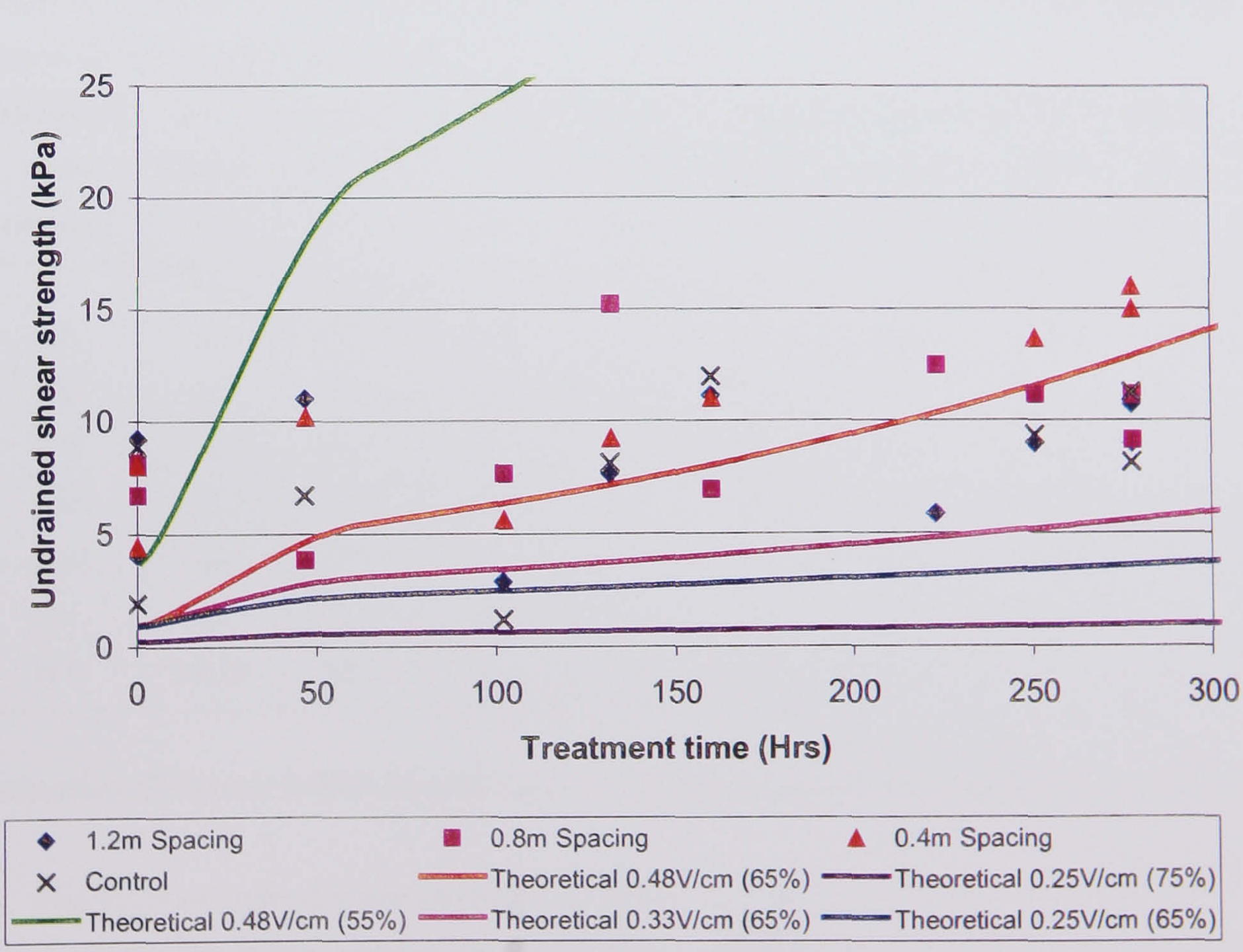

Figure 5.52 Theoretical and zonal average results of c_u against treatment time, 0.25m test depth

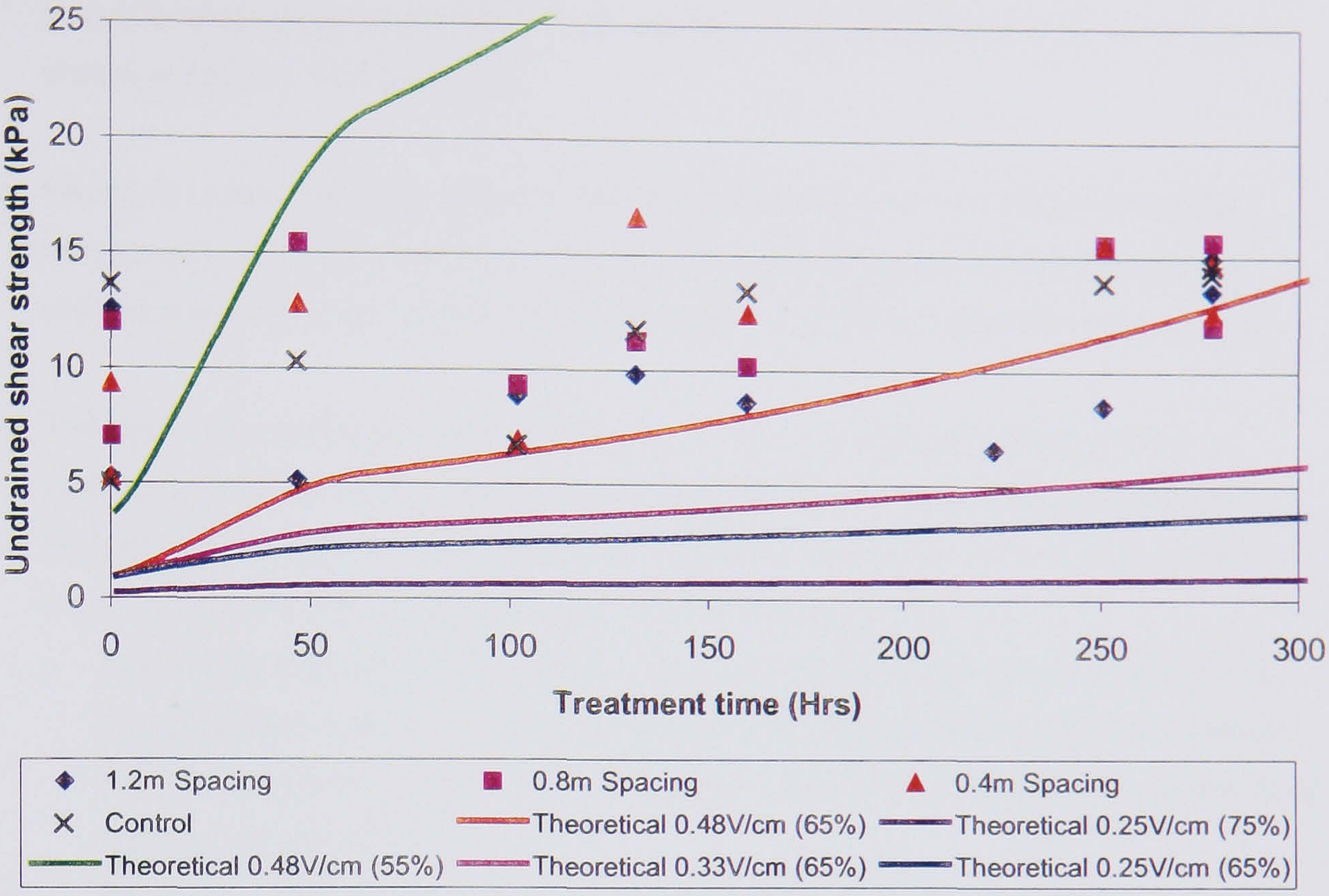

Figure 5.53 Theoretical and zonal average results of c_u against treatment time, 0.5m test depth

Table 5.15 Percentage improvement in c_u with treatment time for different electrode spacings and test depths

Treatment time (hours)	Electrode spacing (0.25m depth)				Electrode spacing (0.5m depth)			
	0.4m (%)	0.8m (%)	1.2m (%)	Cont. (%)	0.4m (%)	0.8m (%)	1.2m (%)	Cont. (%)
0	0	0	0	0	0	0	0	0
47	26.9	-52.9	19.5	-24.3	37.2	29.0	-59.1	-24.6
102	27.0	14.3	-29.4	-37.5	31.8	32.2	68.2	33.3
132	15.0	86.7	9.2	-8.1	78.2	-6.0	-21.9	-14.0
160	37.3	-14.7	20.8	35.1	33.3	-15.0	-31.4	-1.75
223	n/a	85.7	44.1	n/a	n/a	n/a	25.0	n/a
251	70.1	36.7	-2.6	5.4	65.4	30.0	-32.4	1.8
278	99.25	36.7	16.2	27	57.7	31.0	7.6	4.4

Inspection of Figures 5.50-5.53 and Table 5.15 yields several observations:

a) The initial undrained shear strength (c_u) demonstrated a large degree of scatter but generally was in the range of ≈3-15kPa, this is shown in Figures 5.50 to 5.53. The higher values being attributable to lumps of harder clay in the slurry.

b) The design line for an initial water content of 65% at a voltage gradient of 0.48V/cm shows a relatively good correlation with the field measurements of shear strength as shown in Figures 5.52 and 5.53.

c) Nearly all undrained shear strength results measured in the field fall within realistic ranges defined by the theoretical curves. The exceptions are the undrained shear strengths obtained before treatment began which shows an extremely large scatter.

d) The field measurements of zonal averages show an obvious improvement with increasing treatment time. This is shown graphically in Figures 5.52 and 5.53 and additionally tabulated in Table 5.15. The results in Table 5.15 show a wide variation in the percentage improvement achieved. This was caused by:

- Difficulty in successfully undertaking the hand shear vane test in the field due to accessibility problems and the presence of the reinforcement / EKG that hindered the insertion of the shear vane in to the clay. Additionally the poor reproducibility of test results with this apparatus.
- The initial measurement of zonal average, which demonstrated a large degree of scatter, strongly influences the subsequent results of percentage improvement, reflected in some of the negative values presented in Table 5.15.

However, it is noteworthy that the results for the 0.4m electrode spacing zone consistently show an increase in shear strength. Whereas, the results for the 1.2m electrode spacing zone and the control zone demonstrate a much larger fluctuation. The results for the 0.8m electrode spacing zone are generally intermediate.

e) The results obtained at a test depth of 0.25m are generally greater than those obtained at a test depth of 0.5m. Consideration of the electrode depths, anode at 0.45m and cathode at 0.15m, explains these results. The results at a depth of 0.5m are located below the anode in a zone of weaker electrical potential field; see Figure 7.25. Whereas, the results obtained at a depth of 0.25m are located between the anode and cathode in a zone of greater electric field intensity. Hence, the results at 0.25m depth would be anticipated to be greater than those at 0.5m depth, due to the greater value of V/L, subsequently used in Equation 5.32.

f) The control zone also shows an improvement in shear strength with time. This is as a result of the consolidation that occurs through self-weight and is aided by the inclusion of drainage paths through the electrodes and filter elements. However, due to the reduced nature of the improvement that took place within the control zone the continued construction of this zone became increasingly more difficult as the height of the construction increased.

g) The initial undrained shear strength assumed for the theoretical analysis is key in the theoretical prediction. This is attributable to two factors:

- The relationship between c_u and w_c is not linear, but approximately exponential, as shown in Figure 5.28, hence greater increases in c_u occur for a smaller reduction in w_c at lower water contents.
- The variation of the electro-osmotic permeability with time is not linear, as demonstrated in Figure 5.31, with a significant decrease in k_e taking place after a period of approximately 2 days (48 hours). This is reflected in Figures 5.50 to 5.53 by the significant change of slope in the predicted value of c_u that occurs after a treatment time of approximately 50 hours.

The combination of these two factors exaggerates the effect of electrokinetic treatment on soils with lower water contents, as shown by the curve for 55% initial water content in Figures 5.50 to 5.53 and also minimises the effect of treatment on soils with an initial high water content as shown by the curve for 75% initial water content in Figure 5.50 to 5.53.

h) The electrode spacing, and hence the voltage gradient, has a significant effect on the treatment process as demonstrated by the increased improvement of the 0.4m electrode spacing zone over the other zones. The theoretical analysis also predicted this as shown in Figures 5.50 to 5.53 by the three curves of 0.48V/cm, 0.33V/cm and 0.25V/cm corresponding to electrode spacings of 0.4, 0.8 and 1.2m respectively all at an initial water content of 65%.

5.7.9.3 Treatment Time

In the field trial the measurement of treatment time could only be measured indirectly by means of the shear strength and by means of the variation of current against generator time. Generally, as can be seen from Figure 5.48 the conductivity of the trial in the field had reached its residual value after a period of 10-12 days of generator operation. After this time the efficiency of the installation would be extremely low with the majority of the voltage being dropped across the high resistance zone adjacent to the anode as discussed in §2.7.5.5.

5.7.9.4 Economic Analysis

An economic analysis for a typical lift using approximate costs has been undertaken, assuming familiarity with the construction technique, i.e. there is no learning period when productivity is less. The construction considered involves only cohesive electro-osmotically enhanced reinforced soil, and not the standard granular reinforced soil construction.

Table 5.16 Economic analysis of electro-osmotically enhanced reinforced soil Costs per linear metre per 0.6m height, 3m deep, based upon Joint Stock trial experience.

Item	Whole unit	Units used	Cost	% Cost
Electrical distribution	£20 per 200m roll (reuse 8	4 @ 20m	£1-00	0.5
cables	times)	4 x 3m	£60-00	32.2
EKG	£5 per metre	7m x 2m	£73-50	39.5
Reinforcement + bodkin	£189 per 30m roll (1.2m wide)	10 days	£9-20	4.9
Fuel (Gas Oil)	46p per litre @ 2lit/hr	2x2wks	£33-33	17.9
Labour (Semi-skilled)	£200 per week per person	6hrs	£6-25	3.4
Plant	Occasional use 360° excav.	1x½ time	£20-83	11.2
Site Supervision	£500 per week (full time)	3.6T	-£18-00	-9.6
Soft cohesive fill	-£5 per tonne (no landfill tax)	**Total Cost**	**£186-11**	**100%**

The values presented in Table 5.16 assume that the overall length of the wall is 24m, hence, fuel, labour, plant and site supervision has been divided by a factor of 24.

5.7.10 CONCLUSIONS

5.7.10.1 Electrical Energy

The prediction of the electrical energy demand for the completed trial using the design methods suggested in §5.7.3 to 5.7.5 over predicts the actual electrical energy dawn by the field installation, with the method developed in this thesis giving a more accurate prediction than the method suggested by Wrigley (1999). The estimation of the reduction in electrical conductivity (σ) based upon the methodology suggested in this thesis gave the same percentage reduction (95%) as that measured in the field. The reduction factor suggested by Wrigley (1999) based upon Casagrande (1983) (66%) was found to over predict the energy demand.

On the basis of these results it is suggested that the design method developed in this thesis is employed but that a reduction factor is introduced into the analysis to account for the differences caused by the electrode layout between the electro-osmotic cell and the field installation.

$$\sigma_{Field} = F_{\sigma}\sigma_{E\text{-}OCell} \qquad \text{Eqn. 5.36}$$

On the basis of the Joint Stocks trial results F_{σ} is of the order of F_{σ}=0.1.

5.7.10.2 Shear Strength

The prediction of the increase in undrained shear strength of the soil with treatment time using the method suggested by this thesis was found to give curves that have a relatively good fit with the results obtained from the field. With the theoretical curve showing a very

good correlation with the results for the 0.4m electrode spacing zone within which the electrical field was most similar to that obtained in the laboratory for use in the theoretical model. However, its accuracy is greatly affected by the assumption of the initial water content and the voltage gradient.

5.7.10.3 Concluding Remarks

The theoretical prediction method suggested in §5.7.4 would appear to be a valuable predictive tool for estimating the change in undrained shear strength with time during an electro-osmotic treatment process. The accurate input of the initial soil and treatment parameters used in the analysis is, however, critical to its correct function. It is suggested that a sensitivity study is undertaken using the analysis method and an envelope of shear strength / treatment times established for a realistic range of conditions that may exist in the field and that appropriate laboratory testing is used to establish the variation of k_e to be used in the analysis.

5.7.11 RECOMMENDATIONS FOR FURTHER WORK

It is recommended that the value of F_σ=0.1 is refined and confirmed based upon further field trials/applications using the EKG system with a variety of electrode configurations.

It is suggested that the site of the Joint Stocks trial wall is revisited with a cable tool percussion drilling rig in order to undertake a series of continuously sampled boreholes through the control and electro-osmotically treated zones of the wall to ascertain the variations of undrained shear strength with depth through the wall. Additionally, plasticity indices testing could be undertaken to establish any change of plasticity that have occurred as a result of the electro-osmotic treatment process.

5.8 SYNOPSIS OF CHAPTER 5

This chapter has introduced the fundamental mechanism of reinforced soil from first principles, covering the aspects of reinforcement orientation, soil/reinforcement interaction and the concept of strain compatibility both in granular and cohesive soils. The conventional methods of reinforced soil analysis have been described.

The focus was then shifted purely to the application of cohesive materials to reinforced soil. A historical review of both experimentation and experience in cohesive reinforced soil, as well as two commercially available techniques for the utilisation of cohesive fill in reinforced

soil, was given. This was followed by a review of previous work undertaken in the application of electro-osmosis to reinforced soil.

The Joint Stocks wall, built as a full-scale trial of electro-kinetically enhanced reinforced soil was described. Initially the laboratory testing of fill materials to be used in the wall was discussed, followed by the design of the wall. The design was initially undertaken using long-term soil parameters and the tie-back wedge analysis method to establish the reinforcement layout. The short-term analysis was then undertaken using four different analysis methods considering and not considering the presence of the reinforcement to ascertain the undrained shear strength that electro-osmosis was required to produce.

This was followed by the electro-osmotic design for the wall. Initially a simplistic design was undertaken to establish the estimated treatment times for the different electrode spacings considering two different initial water contents. The simplistic design was enhanced by using the laboratory distribution for the variation in k_e, and additionally by refining the voltage gradient parameter (V/L) using finite difference and resistance path analyses. These results were used to produce a predicted envelope of undrained shear strength of the fill against treatment time.

The anticipated power demand of the installation was calculated using two methods; using the variation of electrical conductivity of the soil obtained from laboratory testing and by applying a global reduction factor to the initial electrical conductivity of the soil.

The construction processes for the wall were discussed for both the granular and cohesive sections of the Joint Stocks wall, additionally the monitoring regime adopted in the field was described.

The results of the trial were presented in terms of fuel consumption, electric current drawn, undrained shear strength variation with treatment time and water content variation with treatment time. The interpretation of the results was undertaken by comparing the measured with the predicted behaviour for the electrical conductivity and the undrained shear strength for both the electro-osmotically treated zones and the control zone. A discussion regarding the treatment time and the economics of the trial was also undertaken.

A series of conclusions were drawn from the interpretation of the results with respect to electrical energy and shear strength prediction with regard to the design method developed earlier in the chapter. It was generally found that the design method developed was suitable for use. Recommendations for further improvement to the design method were given together with further investigation of the Joint Stocks trial.

5.9 CHAPTER 5 REFERENCES

1. Acar, Y.B., Gale, R.J., Hamed, J. & Putnam, G. (1990) *Acid / base distributions in electrokinetic soil processing.* Transportation Research Record 288, Transportation Research Board, National Research Council, Washington DC, pp 23-34.
2. Bergado, D.T., Chai, J.C., Alfaro, M.C. & Balasubramaniam, A.S. (1994) *Improvement techniques of soft ground in subsiding and lowland environments.* A.A. Balkema, Rotterdam, p 222.
3. Bishop, A.W. & Bjerrum, L. (1960) *The relevance of the triaxial test to the solution of stability problems.* Proceedings of the research conference on shear strength of cohesive soils, Boulder, Colorado, ASCE, New York, pp 437-501.
4. Bjerrum, L., Moum, J. & Eide, G. (1967) *Application of Electro-Osmosis to a foundation problem in a Norwegian quick clay.* Géotechnique, 17, pp 214-235.
5. Bjerrum, L. (1972) *Embankments on soft ground.* Proceedings of the ASCE, Speciality Conference on Performance of Earth and Earth Supported Structures. Purdue University, Vol. 2, pp 1-54.
6. Boden, J.B., Irwin, M.J., & Pocock, R.G. (1978) *Construction of experimental reinforced earth walls at the TRRL.* Ground Engineering, Oct., Vol. 11, No. 7.
7. Bolton, M.D. (1991) *Reinforced soil: laboratory testing and modelling.* In: Performance of reinforced soil. Eds. McGown, Yeo and Andrawes, Thomas Telford, London, pp 287-298.
8. British Standards Institution (1990a) *British Standard Methods of Test for Soils for Civil Engineering Purposes, Part 2. Classification Tests; BS 1377.* BSI, 2 Park Street, London, WA1 2BS.
9. British Standards Institution (1990b) *British Standard Methods Of Test For Soils For Civil Engineering Purposes, Part 3. Chemical And Electro-Chemical Tests; BS 1377.* BSI, 2 Park Street, London, WA1 2BS.
10. British Standards Institution (1990c) *British Standard Methods Of Test For Soils For Civil Engineering Purposes, Part 7. Shear strength tests (total stress) BS 1377.* BSI, 2 Park Street, London, WA1 2BS.
11. British Standards Institution (1990d) *British Standard Methods Of Test For Soils For Civil Engineering Purposes, Part 8. Shear strength tests (effective stress) BS 1377.* BSI, 2 Park Street, London, WA1 2BS.
12. BSI (1991) *British Standard methods of test for Geotextiles, Part 8, Determination of sand - geotextile behaviour by direct shear, BS 6906.* British Standards Institution, London.
13. BSI (1995) BS *8006: Code of Practice for Strengthened/Reinforced Soil and other fills.* British Standards Institution, London.

14. Bush, D.I. (1988) *Evaluation of the effects of construction activities on the physical properties of polymeric reinforcing elements.* In Ochiai, Hayashi & Otami (Eds.) Theory and Practice of Earth Reinforcement, IS-Kyushu, Japan, Balkema, pp 63-68.
15. Carter, M. & Bentley S.P. (1991) *Correlations of Soil Properties.* Pentec Press, London. p 130.
16. Casagrande, L. (1983) *Stabilisation of soils by means of electro-osmosis, state-of-the-art.* Journal of the Boston Society of Civil Engineers Section, ASCE, winter, Vol. 69, No. 2, pp 255-302.
17. CIRIA (1996) *Soil Reinforcement with Geotextiles.* Construction Industry Research and Information Association (CIRIA) Special Publication 123. p 332.
18. Coulomb, C.A. (1776) *Essai sur une application des régeles des maximus et minimus a quelque problèmes de statique re'latif à l'architecture.* Memoirs Divers Savants 7, Académie Sciences, Paris.
19. Craig, R.F. (1992) *Soil Mechanics*. Fifth Edition, Chapman & Hall, London. p 427.
20. Department of Transport (1978) *Reinforced earth retaining walls and bridge abutments.* Tech. Memo BE 3/78.
21. Department of Transport (1993) Manual *of Contract Documents for Highway Works, Specification for Highway Works.* Department of Transport, London, HMSO.
22. Dyer, M.R. (1985) *Observation of the stress distribution in crushed glass with application to soil reinforcement.* Doctor of Philosophy Thesis, University of Oxford, U.K.
23. Grey, D.H. & Somogyi, F. (1977) *Electro-osmotic dewatering with polarity reversals.* Journal of the Geotechnical Engineering Division, ASCE, Vol. 103, No. GT1, pp 51-54.
24. Hamir, R., Jones, C.J.F.P. & Clarke, B.G. (2001) *Electrically conductive geosynthetics for consolidation and reinforcement.* Geotextiles and Geomembranes, Vol. 19, No. 8, Elsevier, pp 455-483.
25. Hamir, R. (1997) *Some aspects and applications of electrically conductive geosynthetic materials.* Doctor of Philosophy Thesis, University of Newcastle upon Tyne, U.K. p 225.
26. Heshmati, S. (1993) *The action of geotextiles in providing combined drainage and reinforcement to cohesive soil.* Doctor of Philosophy Thesis, University of Newcastle upon Tyne, U.K. p 225.
27. Heyman, J. (1972) *Coulomb's memoir on statics: an essay in the history of civil engineering.* Cambridge University Press, Cambridge, U.K.
28. Ingold, T.S. (1980) *Reinforced Clay.* Doctor of Philosophy Thesis, University of Surrey, U.K.
29. Ingold, T.S. (1981) *A laboratory simulation of reinforced clay walls.* Géotechnique, Vol. 31, No. 3, pp 399-412.
30. Jewell, R.A. (1980) *Some effects of reinforcement on the mechanical behaviour of soils.* Doctor of Philosophy Thesis, University of Cambridge, U.K.
31. Jewell, R.A. (1985) *Material properties for the design of geotextile reinforced slopes.* Geotextiles and Geomembranes, Vol. 2, pp 83-109.

32. Jewell, R.A. (1990) *Reinforcement bond capacity.* Géotechnique, Vol. 40, No. 3, pp 513-518.
33. Jewell, R.A. & Jones, C.J.F.P. (1981) *The reinforcement of clay soil and waste materials using grids.* Proceedings of the 10th International Conference on Soil Mechanics and Foundation Engineering, Stockholm, Sweden, Vol. 3, Balkema, pp 701-706.
34. Jewell, R.A., Milligan, G.W.E., Sarsly, R.W. & DuBois, D.D. (1984) *Interaction between soils and grids.* In Polyester Grid Reinforcement in Civil Engineering, Thomas Telford, London, pp 18-20.
35. Jewell, R.A. & Wroth, C.P. (1987) *Direct shear tests on reinforced sand.* Géotechnique, Vol. 37, No. 1 pp 53-68.
36. Jones, C.J.F.P. (1990) *Construction Influences on the performance of reinforced soil structures, State-of-the-art review.* Proceedings of the International Conference on Reinforced Soil, Glasgow, pp 97-116.
37. Jones, C.J.F.P. (1996) *Earth Reinforcement and Soil Structures.* Thomas Telford Publishing, London. p 379.
38. Jones, C.J.F.P., Fakher, A., Hamir, R. & Nettleton, I.M. (1996) *Geosynthetic materials with improved reinforcement capabilities.* Proceedings of the International Symposium on Earth Reinforcement, Fukuoka, Kyushu, Japan, 12-14 November, Vol. 2, pp 865-883.
39. Keller Comtec (2000) *Retaining Solutions.* Brochure, Keller Comtec, Barham Court Business Centre, Teston, Maidstone, Kent, ME18 5BZ, U.K.
40. Kempton, G.T., Jones, C.J.F.P., Jewell, R.A. & Naughton, P.J. (2000) *Construction of slopes using cohesive fills and a new innovative geosynthetic.* Proceedings of the 2nd European Conference on Geosynthetics, Bologna Italy. Paper No. 97. pp 825-828.
41. Kerisel, J. (1972) *The language of models in soil mechanics.* 5th European Conference on Soil Mechanics and Foundation Engineering, Madrid, Spain. Vol. 2, Balkema, pp 9-30.
42. Kishida, H. & Uesugi, M. (1987) *Tests on the interface between sand and steel in the simple shear apparatus.* Géotechnique, Vol. 37, No. 1, pp 45-52.
43. Kvaerner (1999) *Resistance Path Spreadsheet.* Produced by NEW Associates.
44. Laidler, P.J. (1999) *The dewatering of bentonite slurry using electro-osmosis and electrophoresis.* Master of Engineering dissertation, Department of Civil Engineering, University of Newcastle upon Tyne, U.K.
45. Lo, K.Y., Ho, K.S. & Inculet, I.I. (1991a) *Field test of electroosmotic strengthening of soft sensitive clay.* Canadian Geotechnical Journal, Vol. 28, pp 74-83.
46. Lo, K.Y., Inculet, I.I. & Ho, K.S. (1991b) *Electroosmotic strengthening of soft sensitive clay.* Canadian Geotechnical Journal, Vol. 28, pp 62-73.
47. McGown, A. (1979) *Discussion on session 8: design parameters for artificially improved soils.* Proceedings of the 7th European Conference on Soil Mechanics, Brighton, U.K., Vol. 4, pp 284-287.

48. McGown, A., Andrawes, K.Z. & Al-hasani, M.M. (1978) *Effect of inclusion properties on the behaviour of sand.* Géotechnique, Vol. 28, No. 3, pp 327-346.
49. Met Office (2000) weather data for April 2000 available at http://www.met-office.gov.uk/
50. Microsoft (1997) *Microsoft Excel 97.* Microsoft Corporation Ltd.
51. Ministères des Transports (1979) *Direction générales des transports intérieurs - les ouvrages en Terre Armée - recommandations et règles de l'art.* Paris.
52. Mitchell, J.K. (1993) *Fundamental of Soil Behaviour.* 2nd Edition, John Wiley & Sons. p 437.
53. Mitchell, J.K. & Villett, W.B.C. (1987) *Reinforcement of earth slopes and embankments.* National Co-operative Highway Research Program Report 290, Transportation Research Board, National Research Council, Washington D.C.
54. Mitchell, J.K. & Wan T.Y. (1977) *Electro-Osmotic consolidation - Its effects on soft soils.* Proceedings of the 9th International Conference on Soil Mechanics and Foundation Engineering, Tokyo, Japan, Vol. 1, Balkema. pp 219-224.
55. Murray, R.T. & Boden, J.B. (1979) *Reinforced earth wall constructed with cohesive fill* Colloque International sur le renforcement des sols: terre armée et autres techniques, Paris Association amicale des ingénieurs anciens eleleves de L'Ecole nationale des ponts et chaussées.
56. Netlon Ltd. (1986) *Guidelines for the design and construction of reinforced soil retaining walls using "Tensar" geogrids.* Technical report, Netlon Ltd., Kelly St., Blackburn, U.K. March.
57. Netlon Ltd (1990) *Long term performance of "Tensar" geogrids.* Technical report, Netlon Ltd., Kelly Street, Blackburn, U.K.
58. Netlon Ltd (1998) *Winwall Version 6.14.* Reinforced Soil Design Package, Tensar International, New Wellington St., Blackburn, BB2 4PJ.
59. Nettleton, I.M., Jones, C.J.F.P., Clarke, B.G. & Hamir, R (1998) *Electrokinetic geosynthetics and their applications.* Proceedings of the 6th International Conference on Geosynthetics, Atlanta, Georgia, USA. 25-29 March, Vol. 2, pp 871-876.
60. Palmeira, E.M. & Milligan, G.W.E. (1989) *Scale and other factors affecting the results of pullout tests on geogrids buried in sand.* Géotechnique, Vol. 39, No. 3, pp 511 - 524.
61. Piaskowski, A. (1957) *Investigations on osmotic flow in soils in relation to different characteristics.* Proceedings of the 4th International Conference on Soil Mechanics and Foundation Engineering, London, U.K., pp 89-92.
62. Potyondy, J.G. (1961) *Skin friction between various soils and construction materials.* Géotechnique, Vol. 11, No. 4, pp 339-359.
63. Schlosser, F. & Long, N.T. (1974) *Recent results in French research in reinforced soil* Journal of the Construction Division, Proceedings of the American Society of Civil Engineers, Vol. 100, No. CO3, Sept., pp 223-237.

64. Skempton, A.W. (1948) *The ϕ'=0 analysis of stability and its theoretical basis.* Proceedings of the 2nd International Conference on Soil Mechanics, Rotterdam, Vol. 1, pp 72-77.
65. Sprute, R.H. & Kelsh, D.J. (1975) *Limited field tests in electrokinetic densification of mine tailings.* R1 8034, U.S. Bureau of Mines.
66. Sridharan, R., Srinivasa Murthy, B.R., Bindumadhava & Revanasiddappa, K. (1991) *Technique for using fine grained soil in reinforced earth.* Journal of Geotechnical Engineering, ASCE, Vol. 117, No. 8, August, pp 1174-1190.
67. Stroud, K.A. (1990) *Further Engineering Mathematics - programmes and problems.* 2nd Edition, Macmillan Education, London. p 1063.
68. Tatsuoka, F. (1992) *Roles of facing rigidity in soil reinforcing.* In Earth Reinforcement Practice, Eds. Ochiai, Hayashi & Otani, Balkema, pp. 831-870.
69. Tatsuoka, F., Murata, O. & Tateyama, M. (1992) *Permanent geosynthetic-reinforced soil retaining walls used for railway embankments in Japan.* Geosynthetic-reinforced soil retaining walls, Ed. Wu, Balkema, pp. 101-130.
70. Tatsuoka, F., Tateyama, M. & Koseki, J. (1995) *Performance of geogrid-reinforced soil retaining walls during the great Hanshin - Awaji earthquake, January 17 1995.* 1st International Conference on Earthquake Geotechnical Engineering, IS-Tokyo, November.
71. Terram Ltd (2000) Paradrain website: www.paradrain.com
72. Terzaghi, K. (1936) *The shearing resistance of saturated soils and the angle between the planes of shear.* Proceedings of the 1st International Conference on Soil Mechanics, Cambridge, Mass., USA, Vol. 1, pp. 54-56.
73. Terzaghi, K. & Peck, R.B. (1967) *Soil Mechanics in Engineering Practice.* 2nd Edition, John Wiley, New York. p 566.
74. Vidal, H. (1963) *Diffusion restpeinte de la terre armée*, Patent No. 1 069 361. Patent Office, London.
75. Vidal, H. (1966) *La terre armée.* Annales de L'Institut Technique du Bâtiment et des Travaux Publics, 19, nos. 223-4, July -August, France.
76. Vidal, H. (1969a) *La terre armée (réalisations récentes).* Annales de L'Institut Technique du Bâtiment et des Travaux Publics, nos. 259-60, July -August, France.
77. Vidal, H. (1969b) *The principle of reinforced earth.* Highway Research Record 282, Highway Research Board, National Research Council, Washington D.C., 1-16.
78. Westergaard, H.M. (1938) *A problem of elasticity suggested by a problem in soil mechanics, soft material reinforced by numerous strong horizontal sheers.* Mechanics of solids, Timoshenko 60th Anniversary Volume, Macmillan, New York. pp 268-277.
79. Williams, B.P, Smyrell, A.G. & Lewis P.J. (1993) *Flownet diagrams - the use of finite differences and a spreadsheet to determine potential heads.* Ground Engineering, June, pp 32-38.

80. Williams, N.D. & Houlihan, M.F. (1987) *Evaluation of interface friction properties between geosynthetics and soils.* Geosynthetics '87 Conference, New Orleans, pp 617-627.
81. Wrigley, N.E. (1999) *The practical use of electro-osmosis.* Personal communication.
82. Young, H.D. & Freedman, R.A. (1996) *University Physics* 9th Edition, Addison Wesley Publishing Co. Inc. Massachusetts, USA. p 1259.

5.10 CHAPTER 5 PLATES

Plate 5.1 - Upper electrodes & filters ready for placing of clay slurry (granular ends also visible)

Plate 5.2 - Placing of clay slurry by 360° excavator (lake in which clay was placed also visible)

Plate 5.3 - Levelling of clay slurry and removal of air voids

Plate 5.4 - Levelling of slurry, demonstrating very fluid state of slurry as placed (reinforcement of underlying layer also visible)

Plate 5.5 - Detail of front face clearly showing migration of water to cathode locations

Plate 5.6 - Close up of clay surface above a cathode showing ponding of water and migration of fines to the surface

Plate 5.7 - **Detail of upper clay surface at cathode location showing ponding of water at surface and escape of H_2 gas bubbles**

CHAPTER 6

VOLUMETRIC CONTROL OF SOILS

6.1 VOLUMETRIC CONTROL - INTRODUCTION

Electro-osmosis removes water from a soil mass and can produce an effect equivalent to an effective overburden pressure of approximately 100kPa (see § 4.2.2.1), thus effectively overconsolidating the soil mass. It may also be used to reduce volume changes due to wetting and drying. Additionally, to a minor extent electro-osmosis can also change the properites of the clay minerals present in a soil mass bringing about a reduction in both the liquid and plastic limits, as demonstrated by Gwede (1998) and Bjerrum *et al* (1967), and as a consequence generally reducing the susceptibility to volume change as a result of changes in water content. This is shown in Figure 6.1 by the correlations between the percentage volume change and the swell index for liquid limit and plasticity index.

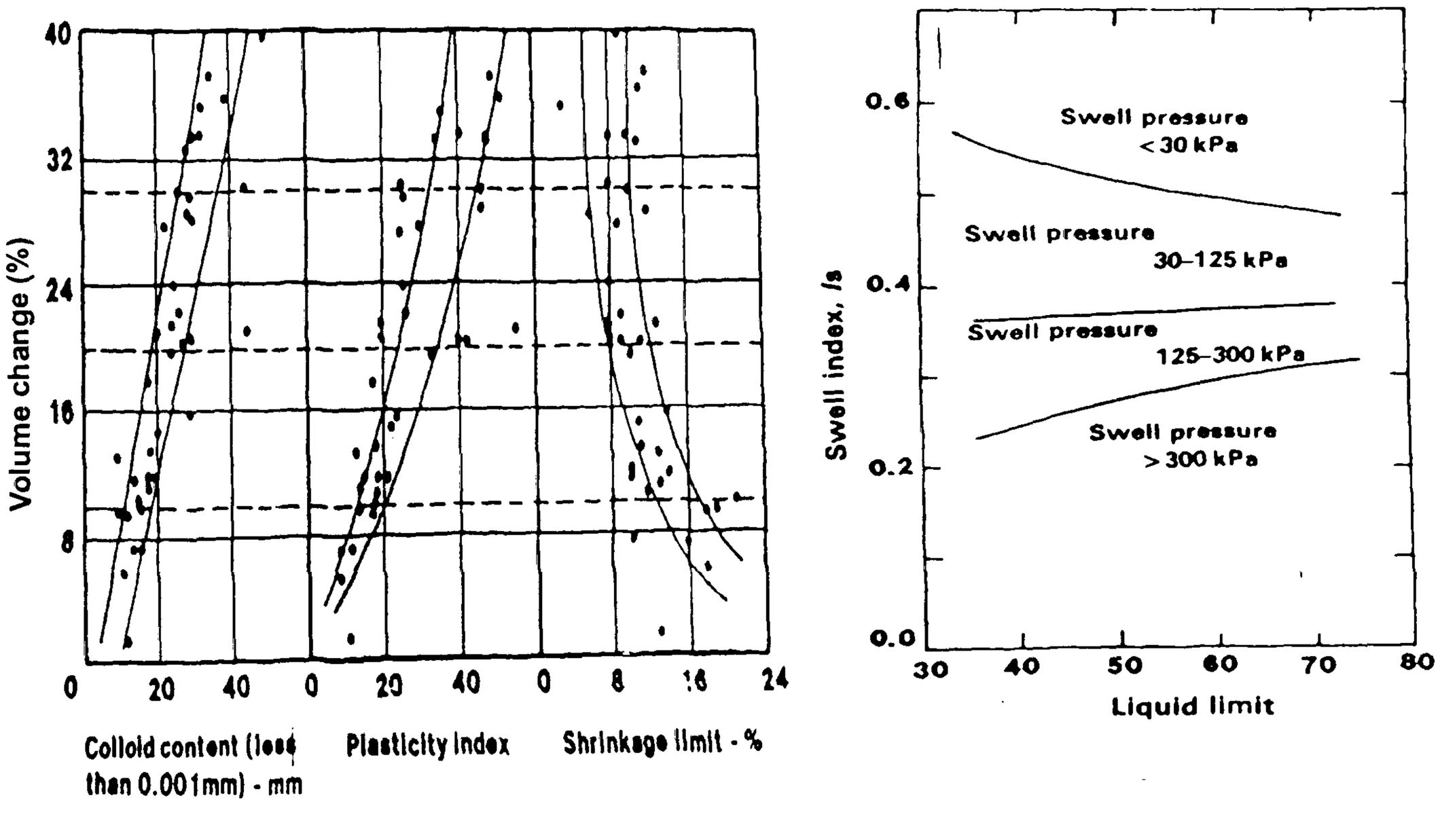

Figure 6.1 Relationship between volume change and plasticity index and swell index and liquid limit (Holtz & Gibbs 1956 & Vijayvergiya & Ghazzaley 1973)

The effect of the overconsolidation produced by electro-osmosis has been discussed previously in § 4.2.3.

6.2 WIMBLEDON PARK - SOUTHFIELDS TRIAL

The purpose of this trial was to demonstrate, in the field, the application of electro-osmosis to reduce the potential for volume change of a London Clay embankment that was experiencing significant volume changes as a result of seasonal variations in water content.

6.2.1 SITE LOCATION AND TOPOGRAPHY

The site is located in southwest London approximately 3km south of Putney Bridge on the River Thames. The Embankment supports the London Underground District Line between Wimbledon Park and Southfields Stations, at the end of Revelstoke Road, between chainages Ch D/166 DEB 0200m and D/166 DEB 0900m. Ordnance Survey Sheet 176 Grid Reference 248727 (Ordnance Survey 1995).

The topography of the location is generally flat with a level of between 15m and 20m Above Ordnance Datum (AOD), or 115m to 120m Above Track Datum (ATD). Track datum is taken as zero at an ordnance datum of -100m to keep all track elevations positive.

6.2.2 GEOLOGY

The 1:50,000 Geological map of the site (BGS 1981) indicates the site to be underlain by Clay Head Deposits over London Clay. This stratigraphy has been confirmed on site by a site investigation undertaken by Soil Mechanics Ltd (Soil Mechanics Ltd 1996).

The Clay Head Deposits are probably derived by periglacial solifluction or hillwash from solid or drift deposits during the Quaternary Epoch.

The London Clay deposits are of marine origin deposited during the Paleogene Period (Curry 1965). The London Clay in its unweatherd state is a dark brownish or blue grey clay, which weathers to a brown or yellowish brown. It is not a pure clay, but contains varying and sometimes large quantities of silt or fine sand; materials coarser than fine sand grade are typically absent (Curry 1965). The mineralogy of the clay fraction as analysed by Grim (1953) for a sample from Chingford gave; Illite 70%, Kaolinite 20% and Montmorillonite 10%. The sand fraction is mostly quartz with a little feldspar and the silt fraction consists of the same minerals with a little mica. The London Clay in its undisturbed state is overconsolidated.

The embankment itself generally consists of cohesive fill material comprising soft to very stiff clay with some sand and occasional fine to coarse gravel overlain by a granular fill generally comprising loose to dense fine to coarse gravel of ash, slag, burnt clay, flint and limestone

(Howard Humphreys 1997). The thickness of this ash layer is variable but is generally of the order of 1m. In certain locations, under the embankment, above the Clay Head Deposits a thin layer of relict topsoil exists which is typically darker and more organic in nature than either the embankment fill or the Clay Head Deposits.

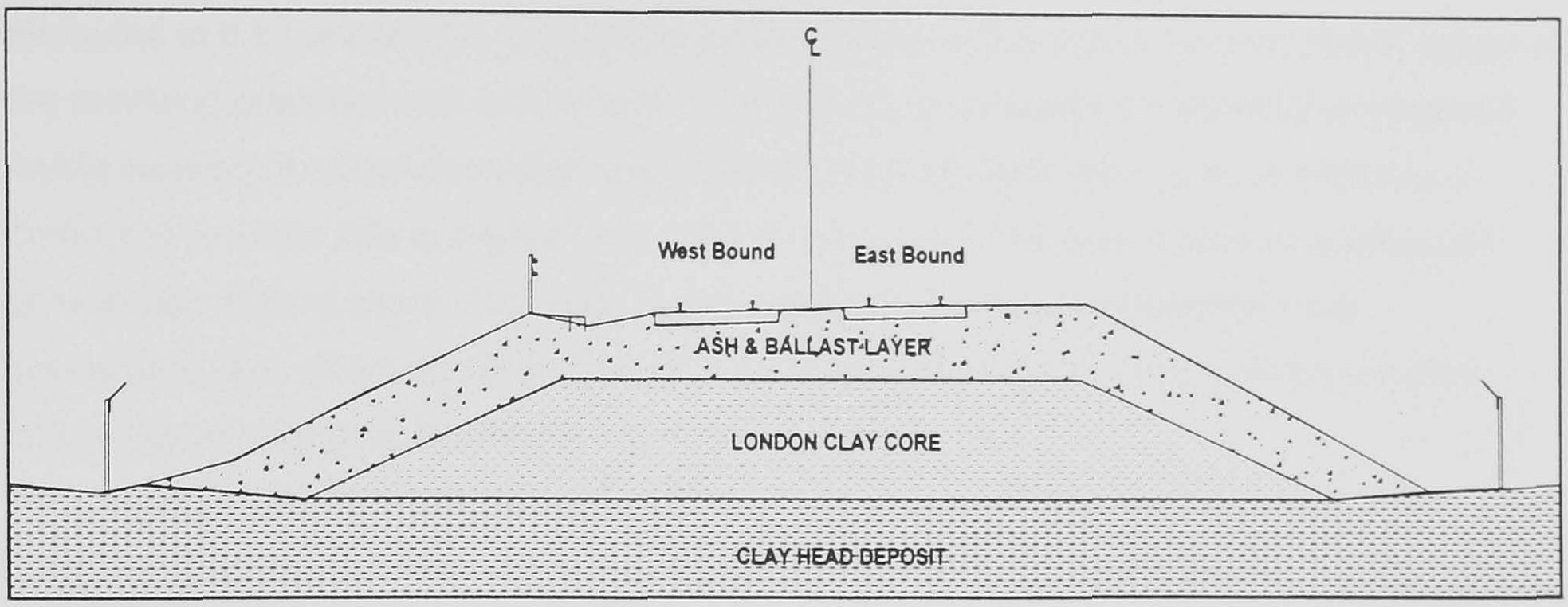

Figure 6.2 Cross-section through Wimbledon Park - Southfields embankment

6.2.3 HISTORY AND DESCRIPTION OF THE SITE

The Metropolitan District Line was extended from West Brompton to Putney Bridge in 1880. In 1889, the line between Wimbledon and Putney Bridge was opened. It was a joint venture between the London and South Western Railway (LSWR) and the District Line as a four track section from Wimbledon over which the LSWR had running rights. The four tracks separate into two sets of two tracks south of Wimbledon Park. The eastern two tracks serve as an LSWR link between Wimbledon and the LSWR Reading and Windsor line with a spur being constructed to East Putney. The western two tracks continuing to East Putney. Island stations were constructed between the tracks at Southfields and Wimbledon Park to be served by District Line trains. LSWR never took up their running rights over this section of track between Wimbledon Park and East Putney. This dates the embankment at over 120 years old.

The section between Southfields and Wimbledon Park stations was constructed predominantly on embankment along the eastern edge of Wimbledon Park and due to the antiquity of the embankment it is most likely that it was constructed by means of end tipping. The 1902 Ordnance Survey map of the area shows a housing development to the east of the line immediately to the south of Southfields station. The remaining housing which now infills the eastern side of the line was constructed in the 1920's. The western side of the line is occupied by Wimbledon Park and has remained undeveloped since the construction of the railway (Howard Humphreys 1997).

6.2.4 DEFINITION OF THE PROBLEM

The problem encountered on the Wimbledon Park-Southfield embankment is that the ride quality of the trains passing over this section of track is being significantly affected by the differential movement of the tracks. The origin of this differential movement has been attributed to the London Clay core of the embankment, which due to the permeable nature of the overlying granular track ballast and the ash layer, is subjected to seasonal wetting and drying causing resultant shrinkage and swelling of the embankment core, reflected as a deterioration in the ride quality of the underground trains. The poor quality or absence of compaction of the London Clay core during construction of the embankment has exacerbated this effect as the clay in not in a uniform state of dry density which results in differential shrinkage and swelling within the core itself.

As a result of this problem the University of Newcastle upon Tyne was approached by Kvaerner Cementation Foundations, a member of the EPSRC steering group, if they would like to undertake a small-scale trial of electro-osmotic volume control on this stretch of embankment. Adjacent to a section where they were undertaking hard engineering solutions to overcome the volume change problems. The engineering solution adopted adjacent to the trial was the construction of small diameter bored piles at the crest of the embankment to constrain the core of the embankment. The problem with this solution was the high cost of construction.

6.2.5 LABORATORY TESTING

Undisturbed U100 and bulk disturbed samples were made available to the Author of both the London Clay core and ash materials, as well as a water sample obtained from a standpipe within the embankment. These samples were tested in the soil mechanics laboratory of the University of Newcastle upon Tyne for their suitability to treatment by electro-osmosis. A summary of the classification testing undertaken is given in Table 6.1.

Table 6.1 Summary of classification testing on Wimbledon Park-Southfields materials

TEST	Test Method	London Clay core	Ash
Liquid limit	BS 1377: Part 2	66%-73%	N/A
Plastic limit	BS 1377: Part 2	23%	N/A
As received w	BS 1377: Part 2	24%	18%
As received conductivity	BS 1377: Part 3	0.0548S/m	0.0383S/m
Free swell	ASTM D4546-96	70%	N/A
Linear shrinkage	BS 1377: Part 2	13%	N/A
Undrained shear strength	BS 1377: Part 7	12-20kPa	N/A
Coeff. Vol. Compressibility	BS 1377: Part 5	0.04-0.14m^2/MN	N/A

In addition to the standard classification tests summarised in Table 6.1 electro-osmosis tests were also undertaken on the London Clay to assess the applicability of electro-osmosis to the core of the Wimbledon Park - Southfields embankment. Due to the fact that the clay in the embankment core would be treated in its in situ state (i.e. without remoulding), it was decided that the most realistic results would be obtained by testing an undisturbed block sample. Thus, an undisturbed block sample was obtained from the site and tested in the laboratory using an "electro-osmosis box". This apparatus is described in detail by Nettleton (1996) and Adali (1999), and its general characteristics summarised here in Figure 6.3.

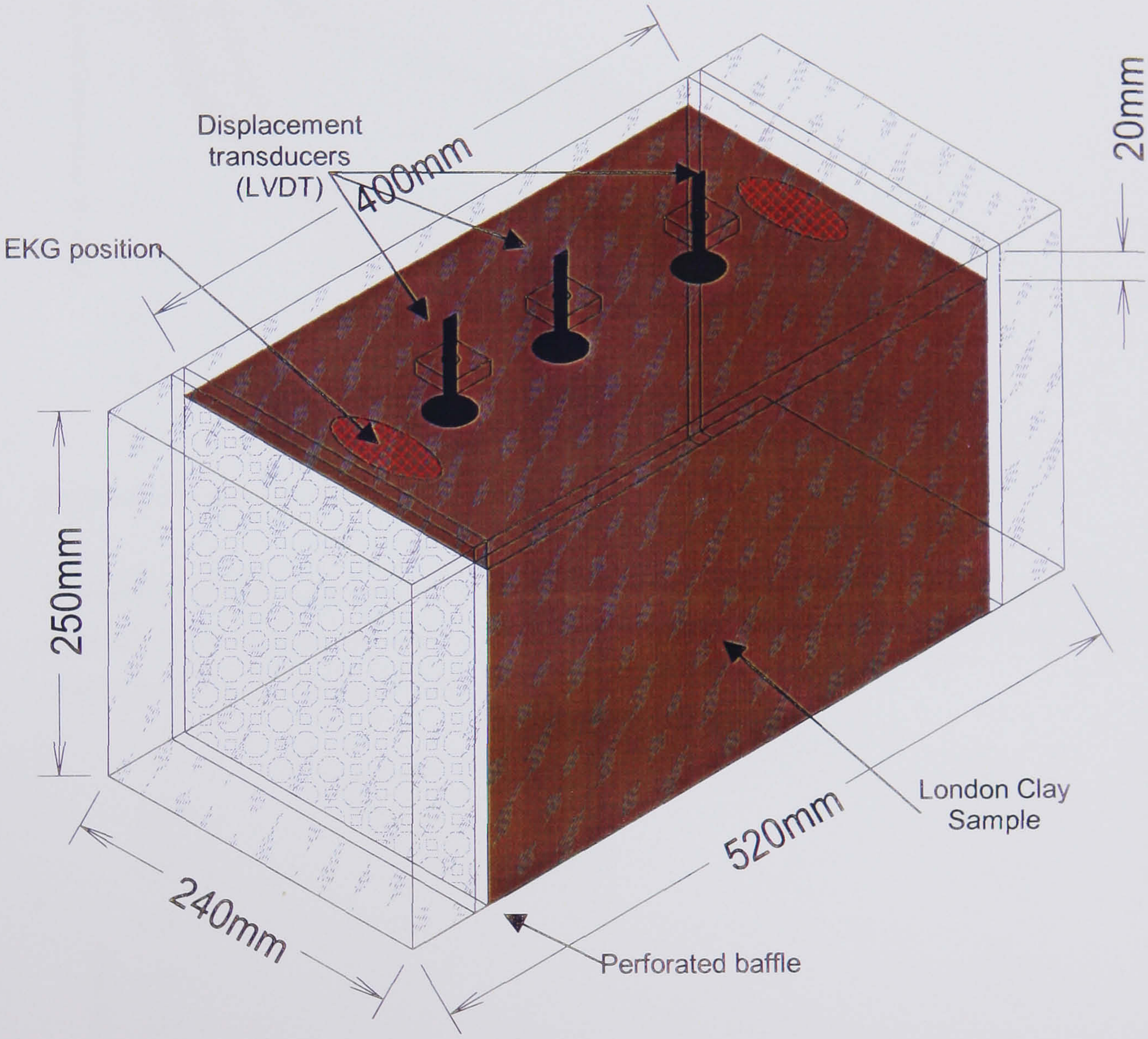

Figure 6.3 Electro-osmosis box used for testing in situ block sample

The block sample of London Clay was cut to the correct size and placed inside the electro-osmosis box. Two holes were then bored in the block sample at the desired electrode positions using a U38 sample cutter. The EKG electrodes were then inserted in to the holes and the holes backfilled with bentonite slurry. The purpose of the bentonite slurry was to ensure good electrical contact between the EKG and the London Clay. Additionally, it was envisaged that bentonite would be used in the field trial both to ensure the stability of the electrode bore and also to ensure electrical continuity between the EKG and the London Clay embankment core, see §6.2.8. The voltage applied across the soil sample was

0.2V/cm. The movement of the upper clay surface in the electro-osmosis box as a result of the electro-osmosis treatment as registered by the LVDT is presented in Figure 6.4.

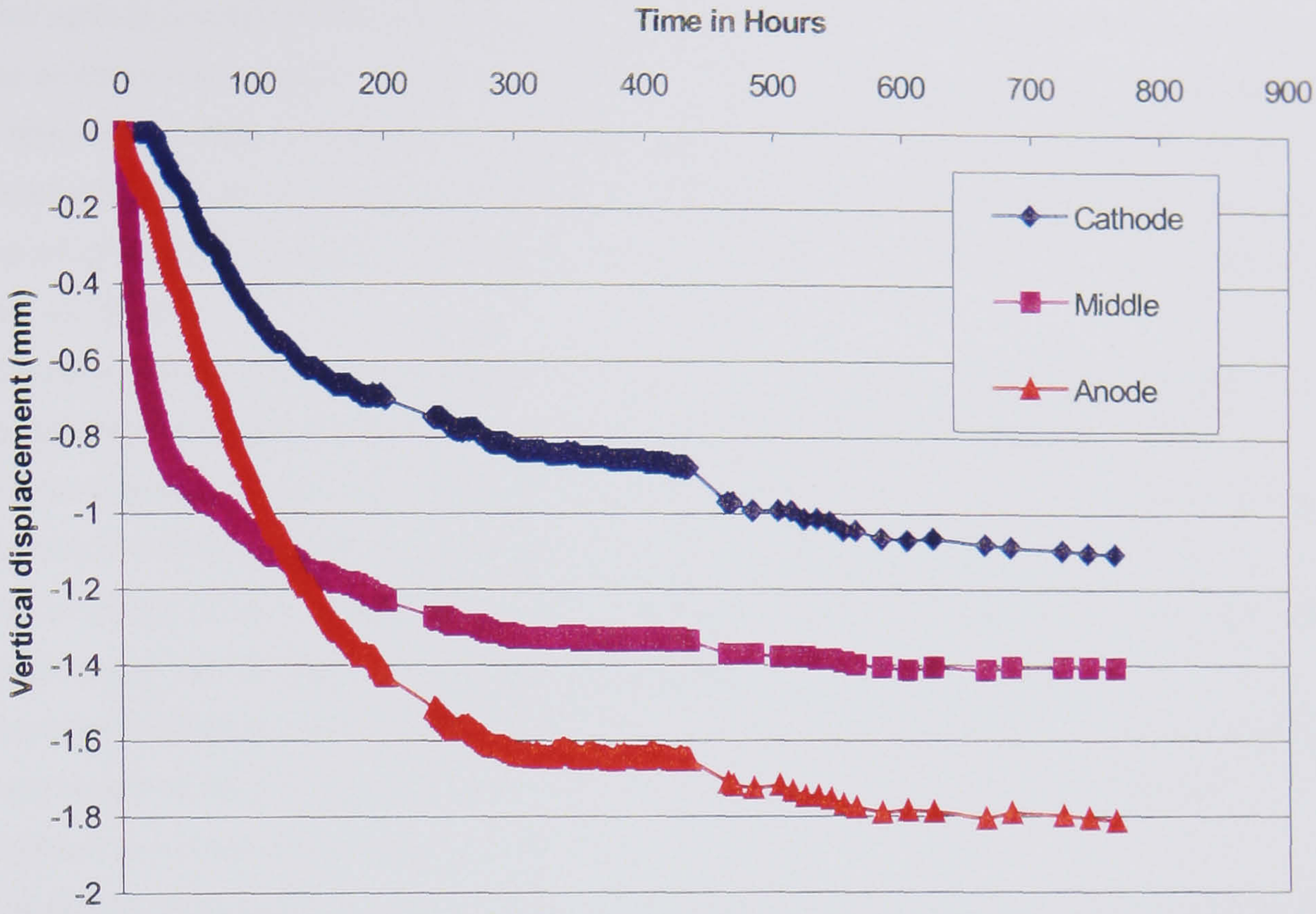

Figure 6.4 Vertical displacement of the clay surface in the electro-osmosis box

Transforming these absolute displacements into percentage strains based upon the block height of 23cm gives the results as shown in Figure 6.5. This figure allows the extrapolation of the laboratory results to the trial embankment, see §6.2.7.1.

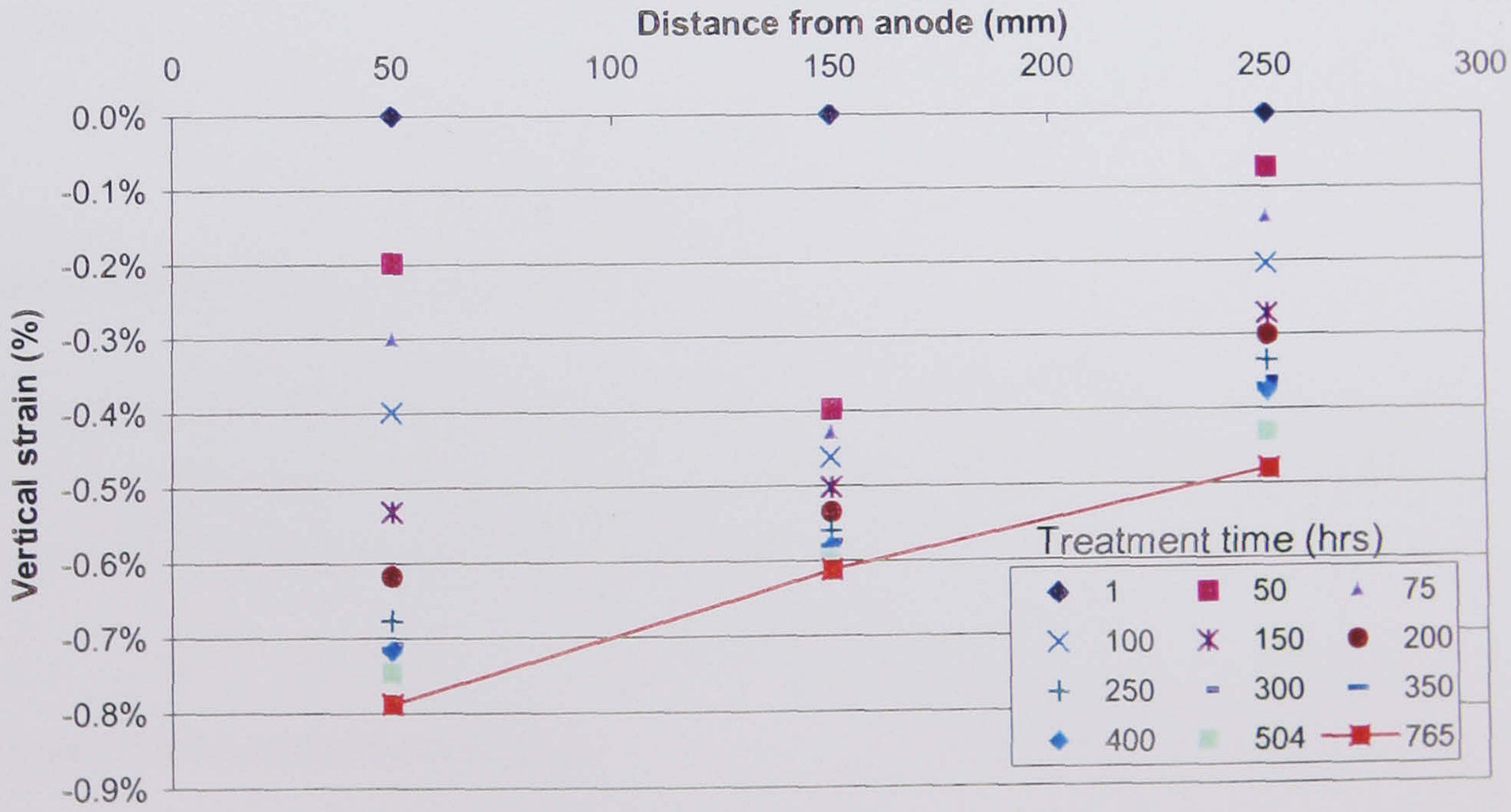

Figure 6.5 Vertical displacement strains in electro-osmosis box at different treatment times

6.2.6 DESIGN OF THE TRIAL

The vertical geometry of the trial was essentially controlled by the accessibility to the side of the embankment and the movement limitations of the crawler drill that was used to install the electrodes. In order to treat as much of the core as possible one row of electrodes was located as high up the embankment as was possible, without been located in the ash, and the other row was located as low down as possible without penetrating the natural ground with the bore.

The bore produced by the drill was required to be subhorizontal due to the requirement to backfill the bore with bentonite slurry once the EKG was installed, see §6.2.8. The manoeuvrability of the Casagrande C6 hydraulic crawler drill used for the installation placed a restriction on the installation in that the minimum inclination for the bores was 5° subhorizontal. These restrictions essentially governed the vertical geometry of the trial, with a spacing of ≈2.75m between anodes and cathodes.

The horizontal geometry of the trial was also partly governed by access problems in that the mast length of the C6 drill rig was 4m and it had to be located between trees located adjacent to the embankment, see Plate 6.1.

The extent of the trial was 17m in length with a total of 8 anodes and 9 cathodes located in a staggered pattern, with an average spacing between electrodes of approximately 2.1m, as shown in Figure 6.6.

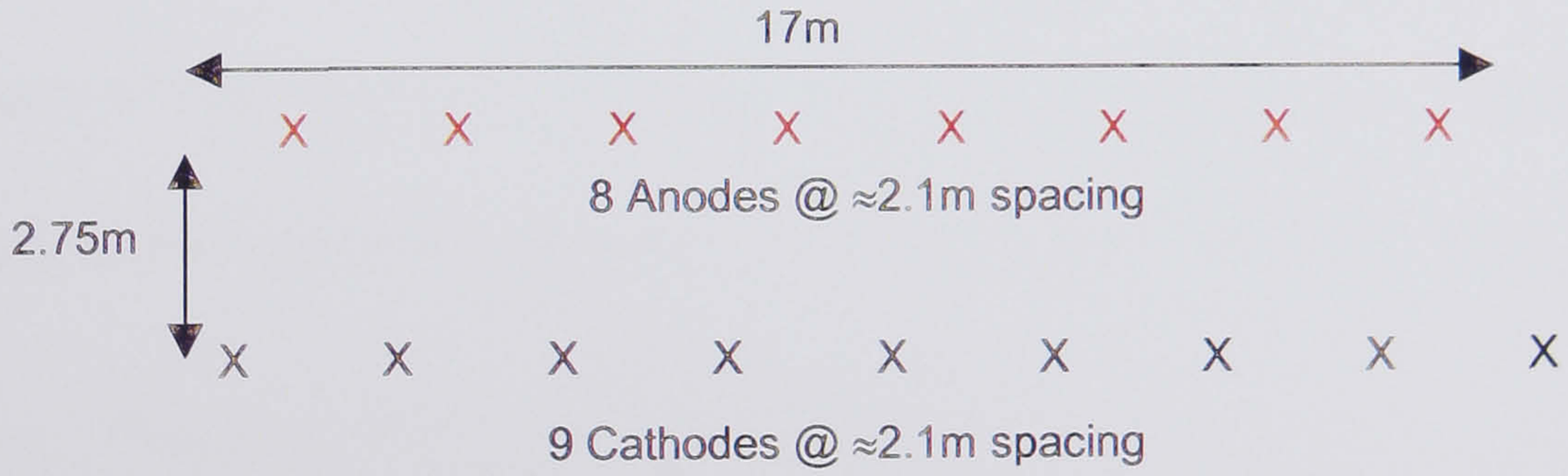

Figure 6.6 Electrode installation geometry

A finite difference analysis of the installation was not considered necessary by the Author as the anode-anode spacing was less that the anode-cathode spacing and, thus, the electrical field produced should be essentially 1-dimensional (Alshawabkeh *et al* 1999).

6.2.7 ANTICIPATED PERFORMANCE

The anticipated performance of the trial was composed of three elements, induced settlement, power requirements and volume change.

6.2.7.1 Induced Settlement

The settlement induced by the application of electro-osmosis was estimated in two ways, using the equivalent surcharge method described in §4.2.2 and additionally by extrapolation of the settlement results obtained from the electro-osmosis box. The equivalent surcharge method uses the coefficient of volume compressibility (m_v) obtained from the laboratory testing, Table 6.1, and assumes that electro-osmosis is equivalent to applying a surcharge of 100kPa at the anode varying linearly to 0kPa at the cathode. In the Wimbledon Park - Southfields embankment the only significant difference was the horizontal inclination of the electrodes, as opposed to the vertical inclination associated with a conventional consolidation application.

For the purposes of calculation, m_v, was assumed to have a linear variation over the stress range of 0-100kPa. Thus, an average increase in effective stress associated with the application of electro-osmosis of 50kPa was assumed to apply over the distance between the anodes and cathodes (≈2.75m), as shown in Figure 6.7.

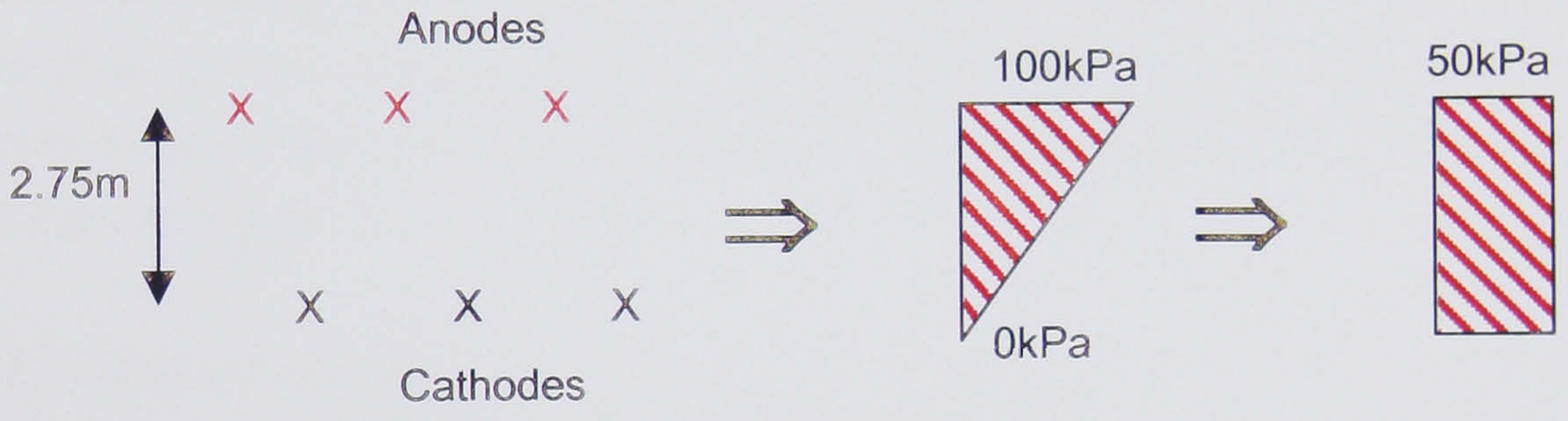

Figure 6.7 Equivalent surcharge produced by horizontally inclined electrodes

Thus, for the range of m_v established from the laboratory testing:

$$\rho_{\min} = m_{v\min}\Delta\sigma_v h = 0.04\mathrm{m}^2/MN * 50kPa * 2.75m = 6mm$$

$$\rho_{\max} = m_{v\max}\Delta\sigma_v h = 0.14\mathrm{m}^2/MN * 50kPa * 2.75m = 20mm$$

Hence, an anticipated settlement in the range of 6-20mm would be expected.

Using the results of the settlement strains obtained from the electro-osmosis box, Figure 6.5, it will be seen that the average settlement strain, i.e. the strain at the central position is of the order of 0.6%, thus extrapolation this result to the 2.75m height of the London Clay core located between the anodes and cathodes in the embankment gives:

$$\rho_{strain} = 0.6\% * 2.75m = 16.5mm$$

This is in excellent agreement with the anticipated results using the equivalent surcharge method and the coefficient of volume compressibility.

6.2.7.2 Estimation Of Electrical Power

From the laboratory measurements of conductivity of the London Clay and the ash it is apparent that the London Clay is more conductive than the ash material, and in the field the majority of the electrode length was installed in the London Clay core as shown in Figure 6.8. Hence, the probability of short-circuiting the system through the ash layer was minimal. Due to the relatively high electrical conductivity of the soil to be treated in comparison with the range suggested as suitable electrical conductivity, see §7.2.2.2, simple resistance calculations were undertaken. These calculations indicated that the overall resistance of the system would be approximately 0.25Ω. Thus, an applied voltage of in excess of approximately 40V would lead to a current of 10Amps per electrode, i.e. the maximum permissible current rating per electrode. It was, therefore, suggested that the trial was configured to act as constant current and then constant voltage to prevent overloading of the electrodes and accelerated degradation, see §3.5.4.

The electrical power results of the electro-osmosis box were lost due to a failure of the Automated Data Acquisition Unit (ADU). Hence, a prediction of the increase in resistance with time cannot be made based upon the laboratory results. However, previous experience would indicate a decrease in the current drawn of the order of 66-95% with time, see §5.7.9.1 and §4.3.4.3.

6.2.7.3 Volume Change

The beneficial effects of electro-osmosis to improve the volume change characteristics of the London Clay core may be though of as comprising of two elements:

- ***Overconsolidation*** of the London Clay such that the subsequent shrinkage and swelling occurs over a different portion of the *e* - log *p* graph and has a less pronounced effect upon the core, as shown in Figure 4.16.
- ***Electro-chemical changes*** to the clay mineralogy, i.e. changes in the particle size to a more coarse grain size and changes in the plasticity index which make the soil less prone to volume change, see Figure 6.1.

6.2.8 ELECTRODE INSTALLATION

The installation procedure for the EKGs consisted of the following steps:

- Positioning of the Casagrande C6 hydraulic drill over the proposed electrode position with the drill string inclined as close to the horizontal as possible (5° subhorizontal). For the upper electrodes (anodes) a small platform was constructed,

and for the lower cathode electrodes a small temporary cut was made in the shoulder of the embankment as shown in Plate 6.1.

- 100mm diameter bore was drilled, cased to the mid-length of the bore, i.e. approximately to the centre-line of the embankment, as shown in Figure 6.8, to prevent any movement of the tracks as a result of the bore.
- Reinforcing bars (approx. 16mmØ) were coupled together using screw couplers to the same length as the bore. Lantern spacers were placed along the length of the bar, approximately every 2m, to ensure that the bar was located in the centre of the bore. The EKG, with or without filter, cathode and anode respectively, was then cable tied to the re-bar as shown in Plate 6.2. The temporary casing from the bore was then extracted and the EKG/re-bar was then manually pushed into the bore up to its full length. The EKG was left over length by approximately 1-2m to allow for subsequent connection.

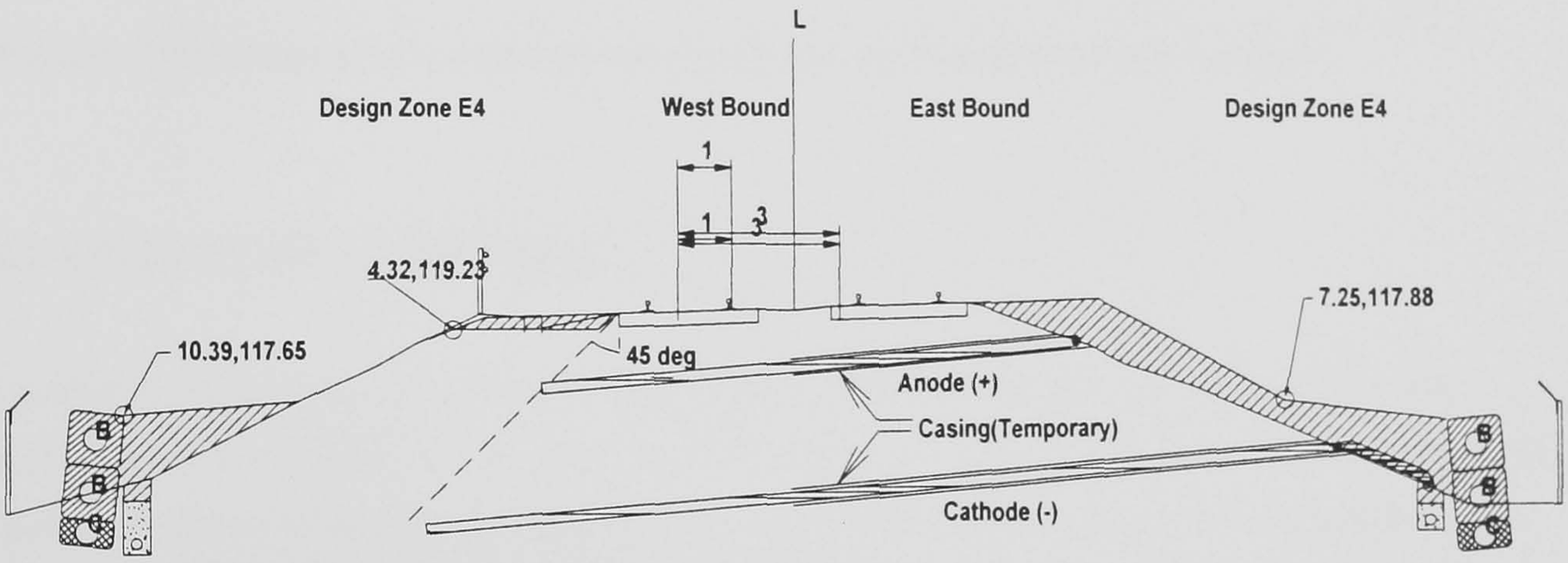

Figure 6.8 Schematic of electrode installation at Wimbledon Park - Southfields

- Bentonite slurry with the lowest water content possible that permitted pumping was then tremmied into the bore to prevent collapse and to ensure electrical contact of the EKG with the London Clay core of the embankment, as shown in Plate 6.3. Once the bore was full the tremmie pipe was extracted.
- The EKG was then passed through a drain/drainage pipe to allow its passage through the embankment shoulder fill that was subsequently replaced. For the cathodes the pipe also allowed connection to the granular toe drain constructed in the slope, thus facilitating the drainage of any fluid collected by the cathode. This detail is presented in Figure 6.9 together with a system developed to measure the fluid produced at the cathode by means of a dip-meter.
- The embankment works were terminated with the electrical connections being left until the last moment to prevent any possible damage to the cabling and for the safety of the workers connecting the electrodes.

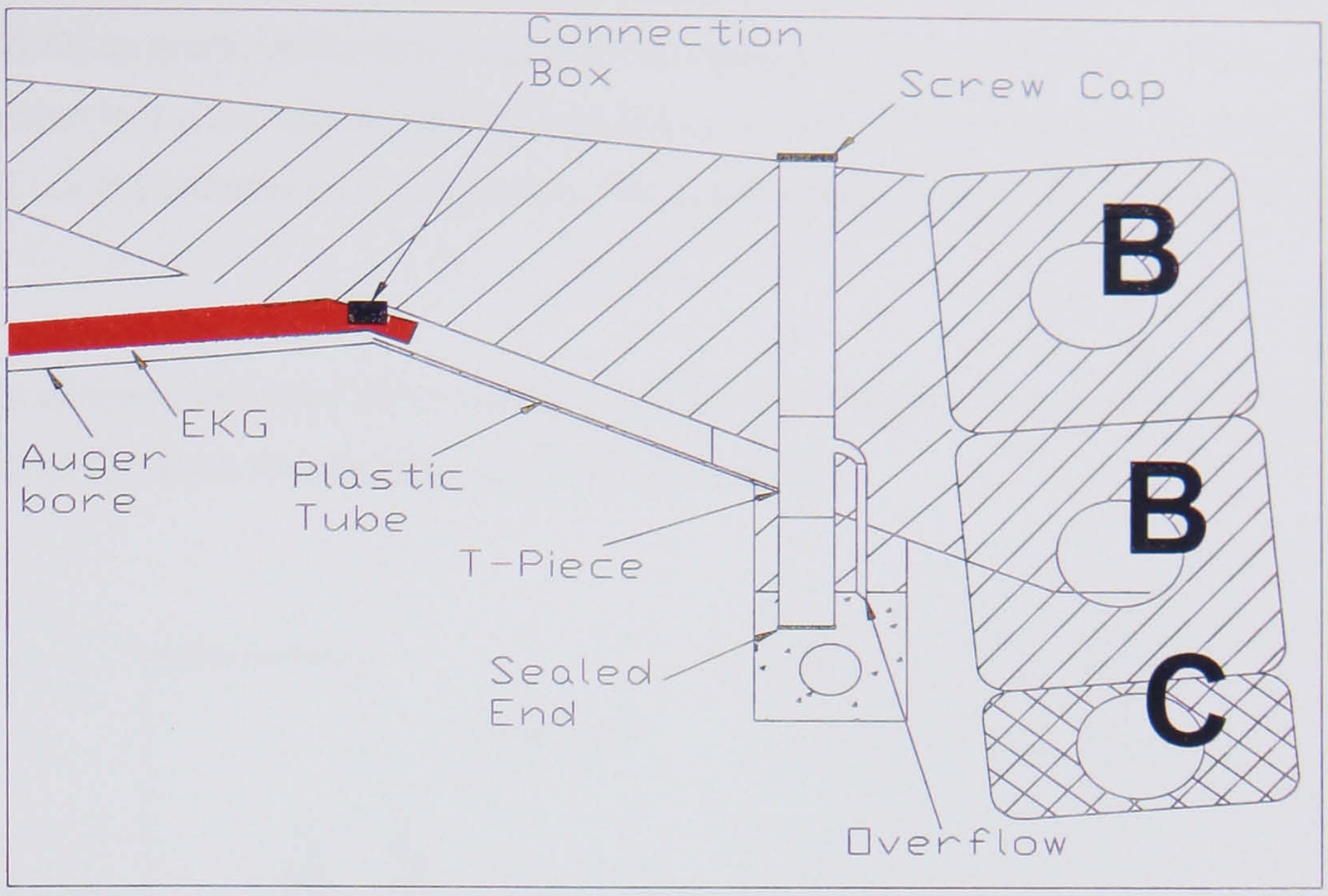

Figure 6.9 Plumbing of cathodes into toe drain and measurement system

6.2.9 ELECTRODE CONNECTION

London Underground Ltd. placed a requirement upon the trial that all cabling had to be armoured with an earth return. The reason for this was so that if anyone were digging in the trial area when the electro-osmosis trail was powered up they would not be subjected to an electrical shock if their digging implement severed the power distribution cables. Details of the armoured earth return connection may be found in §3.5.6.

6.2.10 ELECTRICAL INTERFERENCE AND SIGNALLING

After the installation of the electrodes into the embankment was complete AMEC Rail, who were responsible for maintaining this section of track, raised serious concerns relating to the effect of the electro-osmosis trial on the signalling/traction systems of this stretch of track. These concerns eventually lead to the trial being postponed.

The signalling system used by London Underground over the stretch of track in question consisted of an unusual old design British Rail system. This Westinghouse track signalling system involves sending a low voltage alternating current (AC), with a frequency of 50Hz, through the running rails to detect the presence of a train by its short-circuiting effect between the running rails. This signalling system is used by both London Underground and South West Trains rolling stock, although the traction supply system used by each is different.

For safety reasons concerns were raised that, as the trial was to use full wave rectified and smoothed AC to produce the direct current (DC) necessary for the trial, the 50Hz harmonics would remain in the DC supply with the result that the weak alternating electrical field produced could generate an AC current in the running rails and cause a potential signalling fault.

The origin of these potential 50Hz harmonics is demonstrated in Figure 6.10 that shows a conventional full wave rectification circuit with smoothing.

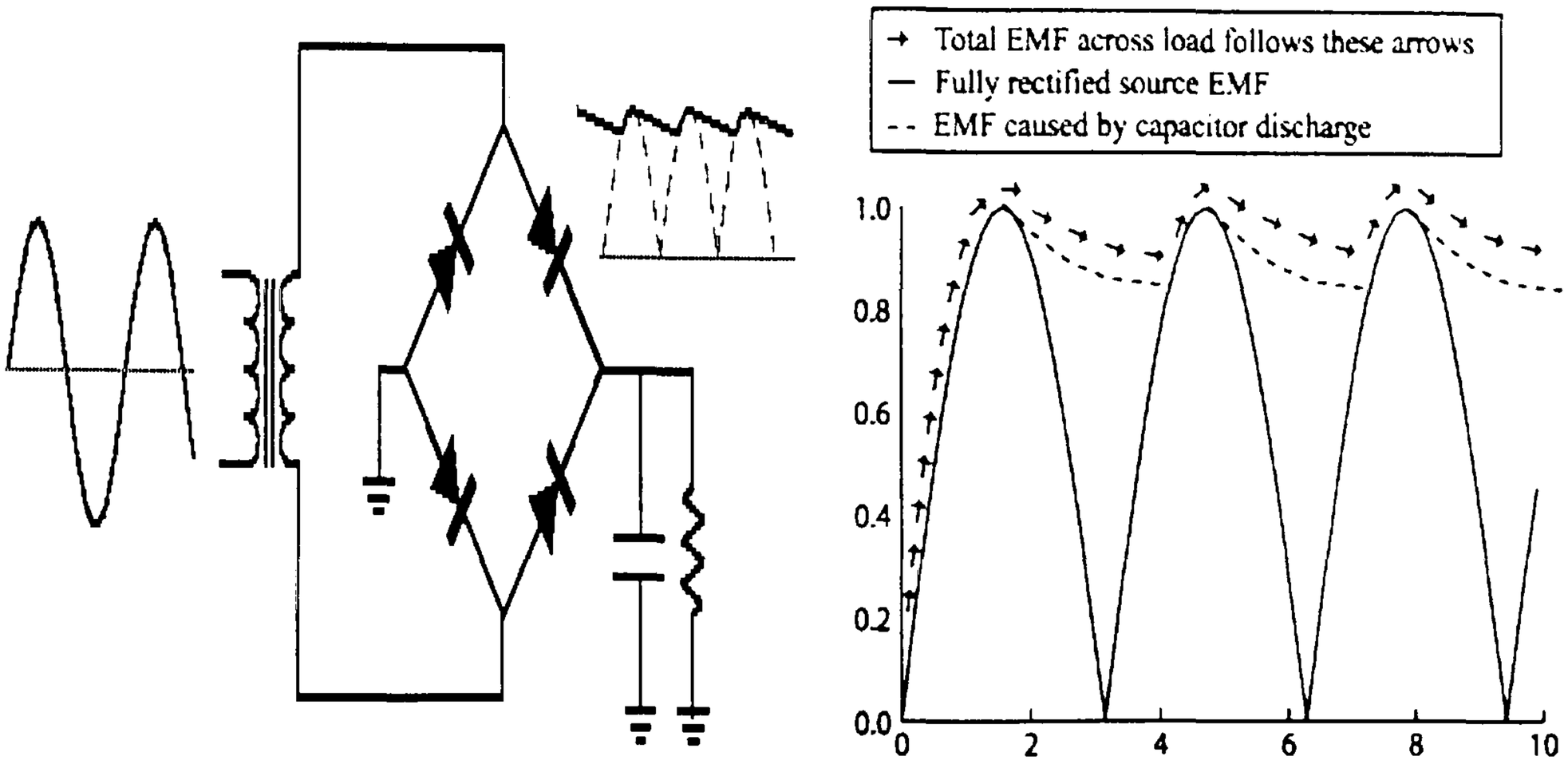

Figure 6.10 Full wave rectification with smoothing and the development of harmonics

Due to the possible presence of these 50Hz harmonics in the power supply, as a result of rectifying conventional three phase AC supply, it was decided that a full night-time possession of the track with a live train present, the trial powered up and all signalling in operation would be appropriate to answer any safety problems associated with the signalling system. The approximate cost of such a possession was stated as being of the order of £10,000 and an associated Hazardous Operation (Haz. Op.) analysis in the range of £10,000 - £15,000 (Pedley 2000). London Underground agreed to cover the costs of the possession, but to date this has not been arranged.

6.2.11 CONCLUSIONS

No definitive conclusions can be made with regard to the application of electro-osmosis to volume control in the field due to the fact that the trial was never powered up. However, the laboratory results suggested that the treatment would have been effective. The trial did provide the opportunity to develop installation and connection protocols for EKG electrodes.

6.2.12 RECOMMENDATIONS FOR FURTHER WORK

- The most obvious recommendation that may be made is that the Wimbledon Park-Southfields trial is powered up, albeit by conducting the required night-time possession and associated Hazardous Operations analysis in full, or at a later date when the signalling system over this stretch of track is modernized and is not susceptible to interference from the possible harmonics generated by the electro-osmosis trial.
- Further laboratory investigations in to how the application of electro-osmosis to a soil alters the volume change properties are required. This should be undertaken for a range of soil types with a range of different mineralogies. The effects that should be analysed are the change in particle size distribution and the alteration of plasticity indices, as well as the effect of overconsolidation. The effect of cycles of wetting and drying on the electro-osmotically treated soil should also be investigated.

6.3 SYNOPSIS OF CHAPTER 6

The laboratory testing undertaken on the London Clay and ash samples obtained from the Wimbledon Park-Southfields trial indicated that the embankment core should be amenable to treatment by electro-osmosis. Particular credence may be given to the electro-osmosis box experiment undertaken which gave settlement strains of the order of 0.6%, which when extrapolated to the full-scale embankment gave settlement values of the same order of magnitude as those calculated by the equivalent surcharge method using a linearly varying surcharge.

The field trial was successfully installed using a novel installation technique using a Casagrande C6 hydraulic drill and the connections undertaken using armoured cable with earth return.

Due to safety fears highlighted after the installation of the trial was complete the trial is in abeyance waiting for a night-time possession to confirm that the treatment would not affect the antiquated signalling system used over this stretch of track.

6.4 CHAPTER 6 REFERENCES

1. Adali, E. (1999) *Study of electro-osmosis in multi-layered soils.* Master of Science dissertation, Geotechnical Group, University of Newcastle upon Tyne, U.K.
2. Alshawabkeh, A.N., Gale, R.J., Ozsu-Acar, E. & Bricka, R.M. (1999) *Optimization of 2-D electrode configuration for electrokinetic remediation.* Journal of Soil Contamination, Vol. 8 (6), pp 617-635.
3. ASTM (1996) *Standard test method for one-dimensional swell or settlement potential of cohesive soils.* Test Method D4546-96.
4. Bjerrum, L., Moum, J. & Eide, O. (1967) *Application of electro-osmosis to a foundation problem in Norwegian quick clay*. Géotechnique 17, pp 214-235.
5. British Geological Survey (1981) 1:50,000 Geological Map *South London* Sheet No. 270.
6. BSI (1990a) *BS 1377: Part 2: 1990: British Standards of test for Soils for civil engineering purposes, Part 2. Classification tests.*
7. BSI (1990b) *BS 1377: Part 3: 1990: British Standards of test for Soils for civil engineering purposes, Part 3. Chemical and electro-chemical tests.*
8. BSI (1990c) *BS 1377: Part 5: 1990: British Standards of test for Soils for civil engineering purposes, Part 5. Compressibility, Permeability and Durability Tests.*
9. BSI (1990d) *BS 1377: Part 7: 1990: British Standards of test for Soils for civil engineering purposes, Part 7. Shear Strength tests (total stress).*
10. Curry, D. (1965) *The Palaeogene Beds of South-East England* Proc. of the Geologists Association No. 76, pp 151-173.
11. Grim, E.R. (1953) *Clay Mineralogy.* International Series in the earth and planetary sciences. McGraw Hill Book Company, New York, p 384.
12. Gwede, D. (1998) *Further electro-osmotic testing of London Clay*. Report GR/L66090/SC8, Internal Report, Geotechnical Group, University of Newcastle upon Tyne, U.K.
13. Holtz, W.G. & Gibbs, H.J. (1956) *Engineering properties of expansive clays.* Transactions ASCE, Vol. 121. pp 641-677.
14. Howard Humphreys (1997) *Wimbledon Park to Southfields embankment, Ground Investigation, Interpretative Report* Ref. 84.530.7/WP/3151/IRWP-A02.
15. Nettleton, I.M. (1996) *Electro-bioremediation.* Internal Report, Geotechnical Group, University of Newcastle upon Tyne, U.K.
16. Ordnance Survey (1995) 1:50,000 Topographical Landranger Map *West London* Sheet No.176.
17. Pedley, M.J. (2000) *Personal communication.*
18. Soil Mechanics Ltd (1996) *Wimbledon Park to Southfields, Factual Report on Ground Investigation, Earth Structures Project* Report No. 8023/1 Revision 3, September.

19. Vijayvergiya, V.N. & Ghazzaley, O.I. (1973) *Prediction of the swelling potential for natural clays.* Proceedings of the 3rd International Conference on Expansive Soils, Haifi, Vol. 1, pp 227-236.

6.5 CHAPTER 6 PLATES

Plate 6.1 - Installation of EKG electrodes using Casagrande C6 hydraulic drill

Plate 6.2 - Connection of EKG to re-bar for insertion into the bore (lantern spacers also visible)

Plate 6.3 - Pumping of bentonite slurry into the bore by means of tremmie pipe (EKG cathode with filter in place also visible)

CHAPTER 7

ELECTRO-OSMOSIS - PHILOSOPHY AND DESIGN

7.1 INTRODUCTION

The purpose of this chapter is to bring together the philosophy that has been developed during the research with regard to electro-osmosis and EKG applications. Initially the criteria that have been developed for assessing the acceptability of soil for treatment by electro-osmosis are given. This is followed by the design philosophies developed by the Author for electro-osmotically enhanced reinforced cohesive soil, electro-osmotic consolidation, electro-osmotic volume control and the tools necessary for the analysis of electrode installations. A review of new and novel applications for electro-osmosis and EKG is also given.

7.2 SOIL ACCEPTABILITY CRITERIA FOR ELECTRO-OSMOSIS

As presented earlier in §2.7.5.1 to §2.7.5.3, the efficiency of electro-osmosis may be expressed in terms of k_i where:

$$k_i = \frac{k_e}{\sigma} \qquad \text{Eqn. 7.1}$$

The value of k_e has been shown to vary within relatively small limits and Casagrande (1952) has suggested that a value of $k_e = 5*10^{-5} cm^2/sec\text{-}V$ could be adopted for most soils. It will be seen from Equation 7.1 that the electro-osmotic efficiency is inversely proportional to the electrical conductivity, thus if the electrical conductivity of a soil is high then the electro-osmotic efficiency will be low.

In addition, as was shown in §4.2.2, the in situ hydraulic permeability of the soil is also important to the success of electro-osmosis. If the hydraulic permeability is excessively high then it is probable that gravitational forces will cause the re-circulation of pore fluid by conventional hydraulic flow and will negate any effect induced by electro-osmosis. However, if the hydraulic permeability is too low, then as demonstrated in §4.2.2.2 electro-osmosis will be inefficient due to the slow rate of consolidation.

From these considerations acceptability criteria for soils have been developed based upon standard and non-standard soil mechanics tests. The basis for advancing these criteria is to allow practicing engineers to make a relatively rapid assessment of the suitability of a soil on a site for treatment by electro-osmosis based upon standard soil mechanics laboratory tests that are routinely conducted as part of a traditional site investigation. This does not mean that electro-osmosis specific tests are not required in order to predict the performance of a particular site installation, but it should allow a more informed decision to be made at an

early stage as to whether to proceed with the more advanced, and expensive, specialised testing.

7.2.1 GENERAL CLASSIFICATION TESTS

The standard classification tests should be carried out in accordance with BS 1377: Part 2 (BSI 1990b) with the soil samples being taken and prepared in accordance with BS 1377: Part 1 (BSI 1990a). The macrofabric of the soil should also be identified and its repercussions upon the in situ permeability and conductivity assessed, guidance is given in McGown *et al* (1980)

7.2.1.1 Atterberg Limits

The liquid and plastic limits of the soil should be established in accordance with BS 1377: Part 2:1990 §4 and §5 (BSI 1990b) respectively. The Author recommends that the cone penetrometer method described in §4.3 of BS 1377: Part 2 (BSI 1990b) is used whenever possible for the determination of the liquid limit as the test is easier to carry out and the results are reproducible (BSI 1990b).

The liquid and plastic limits of a soil define the range within which a cohesive soil behaves in a plastic state as shown in Figure 7.1.

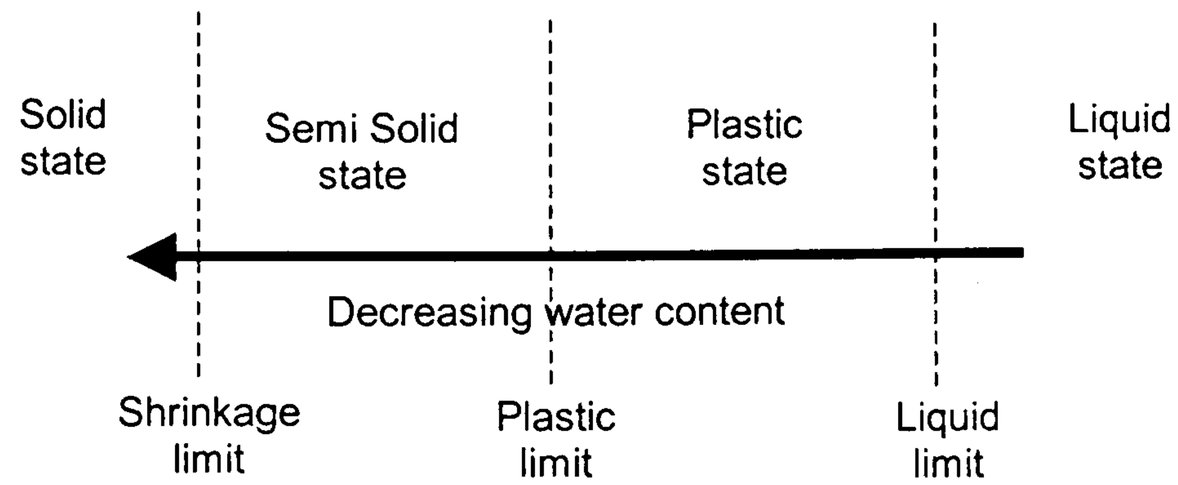

Figure 7.1 Consistency of cohesive soil with variation in water content (After Das 1997)

The value of the Atterberg limits of a cohesive soil depend upon several factors, including the quantity and type of clay mineral and type of absorbed cation (Mitchell 1993). Typical values for the Atterberg limits for different clay mineral types are given in Table 7.1.

It can be seen that the different clay mineralogies have a direct bearing upon the values of the Atterberg limits. It has also been shown that the electrical conductivity of a soil is influenced, to some extent, by the surface charge density (A_0) and is dependant upon the

clay mineralogy (see Table 2.2a & 2.2b). Hence, the relationship between the Atterberg limits and the electrical conductivity of the soil can be linked to soil mineralogy.

Table 7.1 Atterberg limits and associated parameters for different clay minerals (After Lambe & Whitman 1969 and Mitchell 1993)

Clay Mineral Type	Liquid limit (%)	Plastic limit (%)	Activity	Shrinkage limit (%)
Montmorillonite	100 - 900	50 - 100		8.5 - 1.5
Nontronite	37 - 72	19 - 27		
Illite	60 - 120	35 - 60	0.5 - 1.0	15 - 17
Kaolinite	30 - 110	25 - 40	0.5	25 - 29
Hydrated Halloysite	50 - 70	47 - 60		
Dehydrated Halloysite	33 - 55	30 - 45		
Attapulgite	160 - 230	100 - 120	0.5 - 1.2	7.6
Chlorite	44 - 47	36 - 40		
Allophane	200 - 250	130 - 140		

In addition to the mineralogy, the electrical conductivity of the soil in situ is partially governed by the electrical conductivity of the pore fluid and the water content. This has been demonstrated by the Author as shown in Figure 7.2.

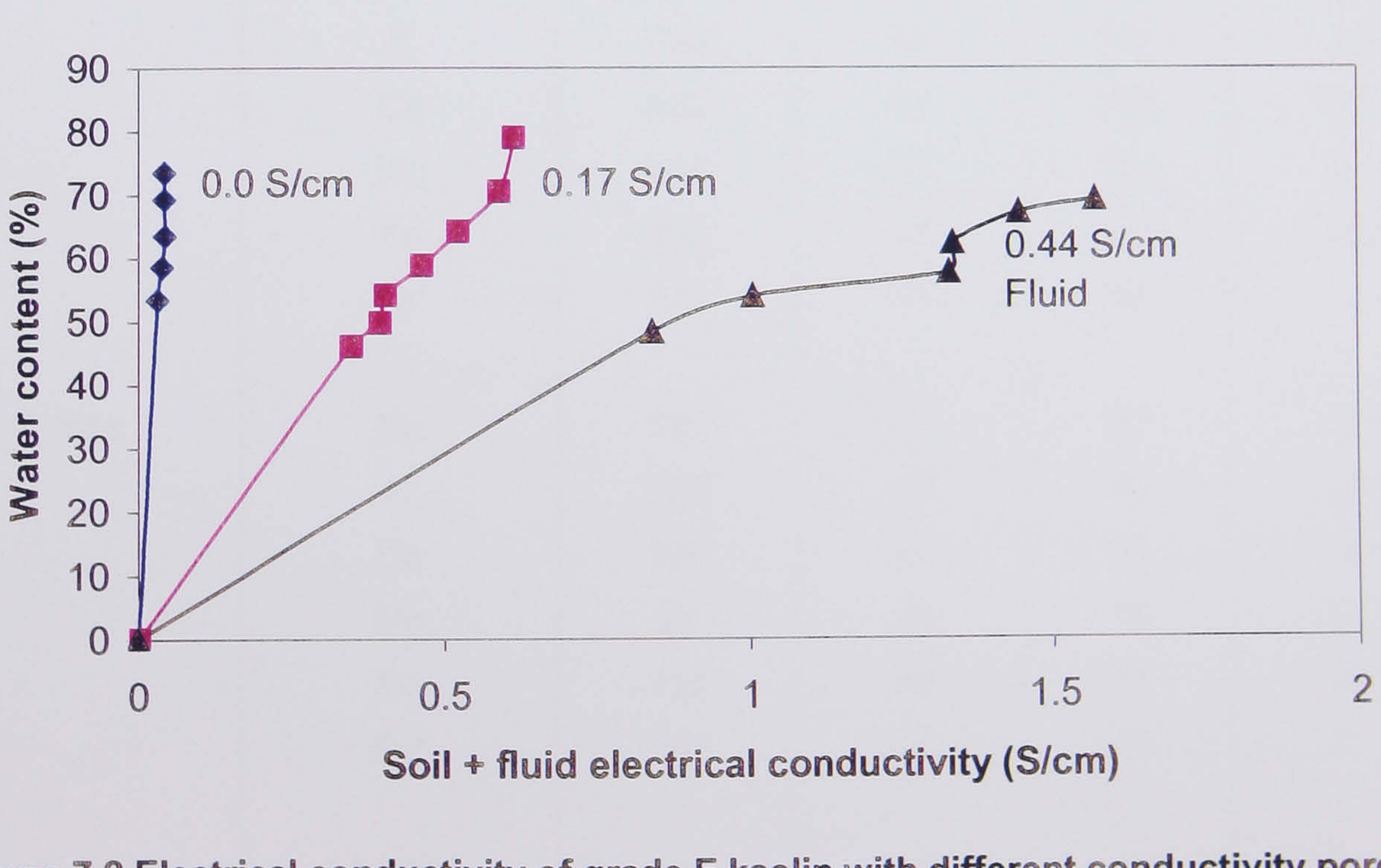

Figure 7.2 Electrical conductivity of grade E kaolin with different conductivity pore fluids

Figure 7.2 demonstrates that the effect of the conductivity of the pore water alone upon the overall conductivity of the fluid-soil mix is significant, as is the water content of the soil. The chemistry of the pore water, which is also reflected in the exchangeable cations present within the clay minerals, influences the range of results for the Atterberg limits presented in

Table 7.1. This influence may also be seen in Table 7.2, which presents the results of Atterberg limit tests for different clay minerals with different exchangeable cations. The monovalent cations (e.g. Na^+, K^+) give higher values of liquid and plastic limits whereas the presence of divalent and trivalent cations (e.g. Mg^{2+}, Fe^{2+}, Al^{3+}) give lower values. If the soil is tested repetitively the exchangeable cations can be flushed from the clay, as implied by the results given in Table 7.2 by Lambe & Whitman (1969), then a change in the Atterberg limits takes place. Thus, for samples which are to be tested with a view to utilising the results for prediction of the viability of electro-osmosis it is essential that the tests are undertaken in accordance with BS 1377: Part 2 (BSI 1990b) and not repetitively wetted and dried.

The validity of the correlation proposed for the acceptability of soils based upon the Atterberg limits and conductivity is demonstrated in Figure 7.3. The results presented in Figure 7.3 relate to a review of published electro-osmotic case studies where both the plasticity indices and electrical conductivities have been given (Bjerrum *et al* 1967, Casagrande 1952, Casagrande *et al* 1961, Fetzer 1967, Hamir 1997, Pugh 1999).

Table 7.2 Atterberg limits of clay minerals with different exchangeable cations (After Lambe & Whitman 1969). Key * = after five cycles of wetting and drying.

Mineral	Exchangeable cation	Liquid limit (%)	Plastic limit (%)	Plasticity index (%)	Shrinkage limit (%)
Montmorillonite	Na	710	54	656	9.9
	K	660	98	562	9.3
	Ca	510	81	429	10.5
	Mg	410	60	350	14.7
	Fe	290	75	215	10.3
	Fe*	140	73	67	
Illite	Na	120	53	67	15.4
	K	120	60	60	17.5
	Ca	100	45	55	16.8
	Mg	95	46	49	14.7
	Fe	110	49	61	15.3
	Fe*	79	46	33	
Kaolinite	Na	53	32	21	26.8
	K	49	29	20	
	Ca	38	27	11	24.5
	Mg	54	31	23	28.7
	Fe	59	37	22	29.2
	Fe*	56	35	21	7.6

The delineation of acceptable electrical conductivities (σ) and, hence, plasticity indices (PI) is based upon the limits proposed by Casagrande (1983) that an acceptable and economic range for the electrical conductivity is 0.05S/m - 0.005S/m. This range gives an associated acceptable range of plasticity index in the range of 5% to 30%. This criterion is adopted for the assessment of soils.

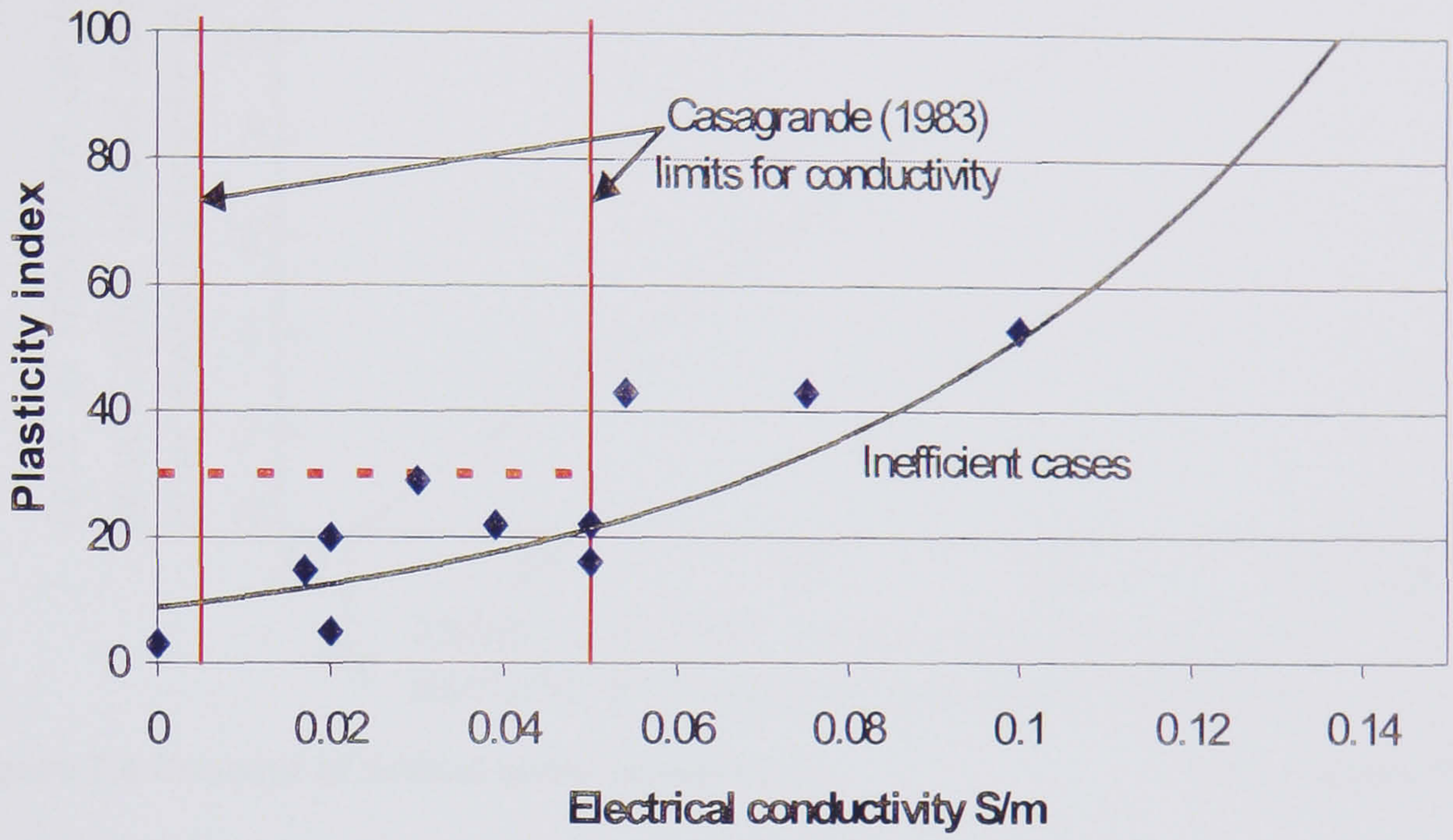

Figure 7.3 Conductivity against plasticity index for a range of natural soils

7.2.1.2 Water Content

The water content (w) or moisture content of the soil should be established in accordance with BS 1377: Part 2:1990 §3 (BSI 1990b). Once the water content has been established it can be related to the Atterberg limits by the liquidity index (*LI*) defined as:

$$LI = \frac{w - PL}{(LL - PL)} \qquad \text{Eqn. 7.2}$$

Where w is the water content, *LL* is the liquid limit and *PL* is the plastic limit.

As presented in §2.7.5.1, §2.7.5.2 and Figures 2.13, 2.14 and 2.15 the higher the water content of a soil the more electro-osmotically efficient it is, i.e. the value of k_i increases as w increases. In order to specify an acceptability criterion it is, therefore, necessary to define a lower limit for *w* below which the soil is too dry for electro-osmosis to have any effect on the soil.

Casagrande (1983) stated that the water content of cohesive soil can be reduced to, or slightly below, the plastic limit near the anode, and the degree of reduction will become less towards the cathode. This implies that there is little point in treating soils that have natural water contents at or near the plastic limit as the reduction in water content will be minimal.

Piaskowski (1953) introduced the concept of a critical moisture content (w_k) below which the loss of water through drainage by electro-osmosis tends towards zero, as demonstrated in Figure 7.4.

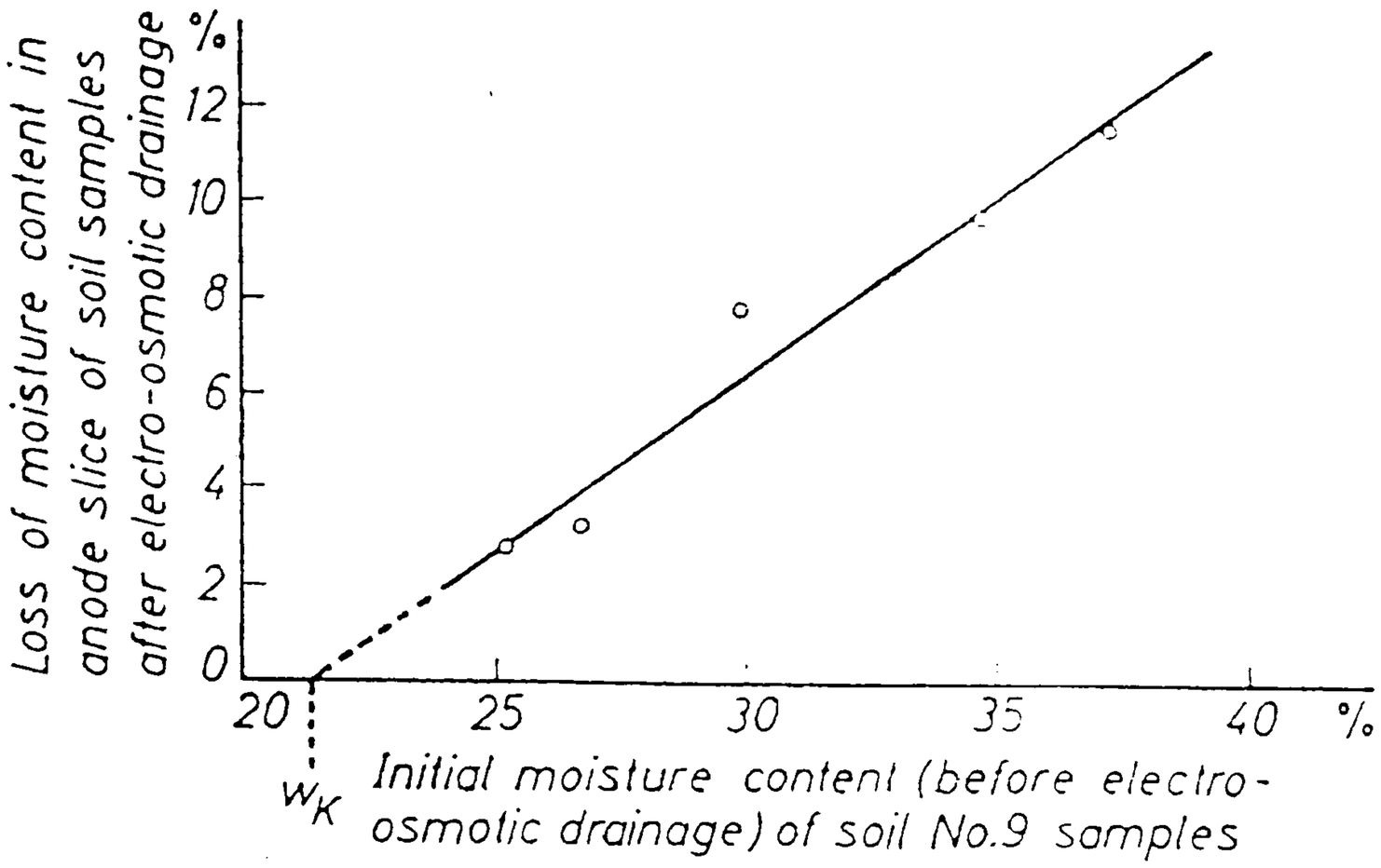

Figure 7.4 Concept of critical water content (w_k) (Piaskowski 1957)

Based upon the data given by Piaskowski (1953) the liquidity index at which w_k occurs for different soils may be calculated, i.e. a critical liquidity index (LI_k). It is important to note that it is not possible to state definitively a value for water content based upon w_k as it has to be related to the plastic limit for a soil, hence, the correlation to liquidity index. The data presented by Piaskowski (1953) for eight different soils is presented in Table 7.3 together with the values of LI_k calculated by the Author.

Table 7.3 Critical moisture content and critical liquidity index (After Piaskowski 1953)

Soil No.	Liquid limit (%)	Plastic limit (%)	w_k lower bound	w_k upper bound	LI_k lower bound	LI_k upper bound
10	36.4	15.2	13	15	-0.1	-0.01
9	44.3	15.6	19	21	0.12	0.19
19	48.6	16.2	19	21	0.09	0.15
4	68.9	27.2	25	29	-0.05	0.04
21	83.7	22.2	30	32	0.13	0.16
1	101	29.5	29	31	-0.01	0.02
26	104.6	31.4	38	40	0.09	0.12
25	103.8	26.4	39	41	0.16	0.19

From Table 7.3 the range of the critical liquidity index (LI_k) is -0.1 to 0.19. Therefore, a minimum liquidity index of 0.2 will be used in the acceptability criterion, the upper limit for the

liquidity index is open ended although natural soils are unlikely to be encountered at a liquidity index of much beyond 1.0. Simons & Menzies (1976) state that normally consolidated clays have a liquidity index in the range of 0.6 -1.0 and that overconsolidated clays have a liquidity index in the range 0 - 0.6. Hence, soils in the range 0.6 - 1.0 are preferable for treatment by electro-osmosis.

7.2.1.3 Particle Density

The particle density or specific gravity (ρ_s) of the soil particles should be established in accordance with BS 1377: Part 2:1990 §8 (BSI 1990b). The particle density of the soil particles gives little indication of the mineralogy present within the soil mass due to the large degree of overlap of the particle densities for the different clay minerals. This is shown in Table 7.4.

Table 7.4 Particle densities for different minerals (After Lambe & Whitman 1969)

Mineral	Particle Density (Mg/m^3)
Muscovite	2.7 - 3.1
Biotite	2.8 - 3.2
Chlorite	2.6 - 2.9
Pyrophyllite	2.84
Serpentine	2.2
Kaolinite	2.64 ± 0.02
Halloysite (2 H_2O)	2.55
Illite	2.60 - 2.86
Montmorillonite	2.75 - 2.78
Attapulgite	2.3

This parameter will not be used as an acceptability criterion although it is suggested that if this data is available it is compared to the values given in Table 7.4 together with the plasticity indices to give an indication of the soil mineralogy.

7.2.1.4 Particle Size Distribution

The particle size distribution of the soil should be carried out in accordance with BS 1377: Part 2:1990 §9 (BSI 1990b). A delineation of the particle size distribution chart to indicate the range of particle sizes suitable for treatment by electro-osmosis has been undertaken by Glossop & Skempton (1945) and is presented in BS 8004 (BSI 1986). This delineation is reproduced here as Figure 7.5

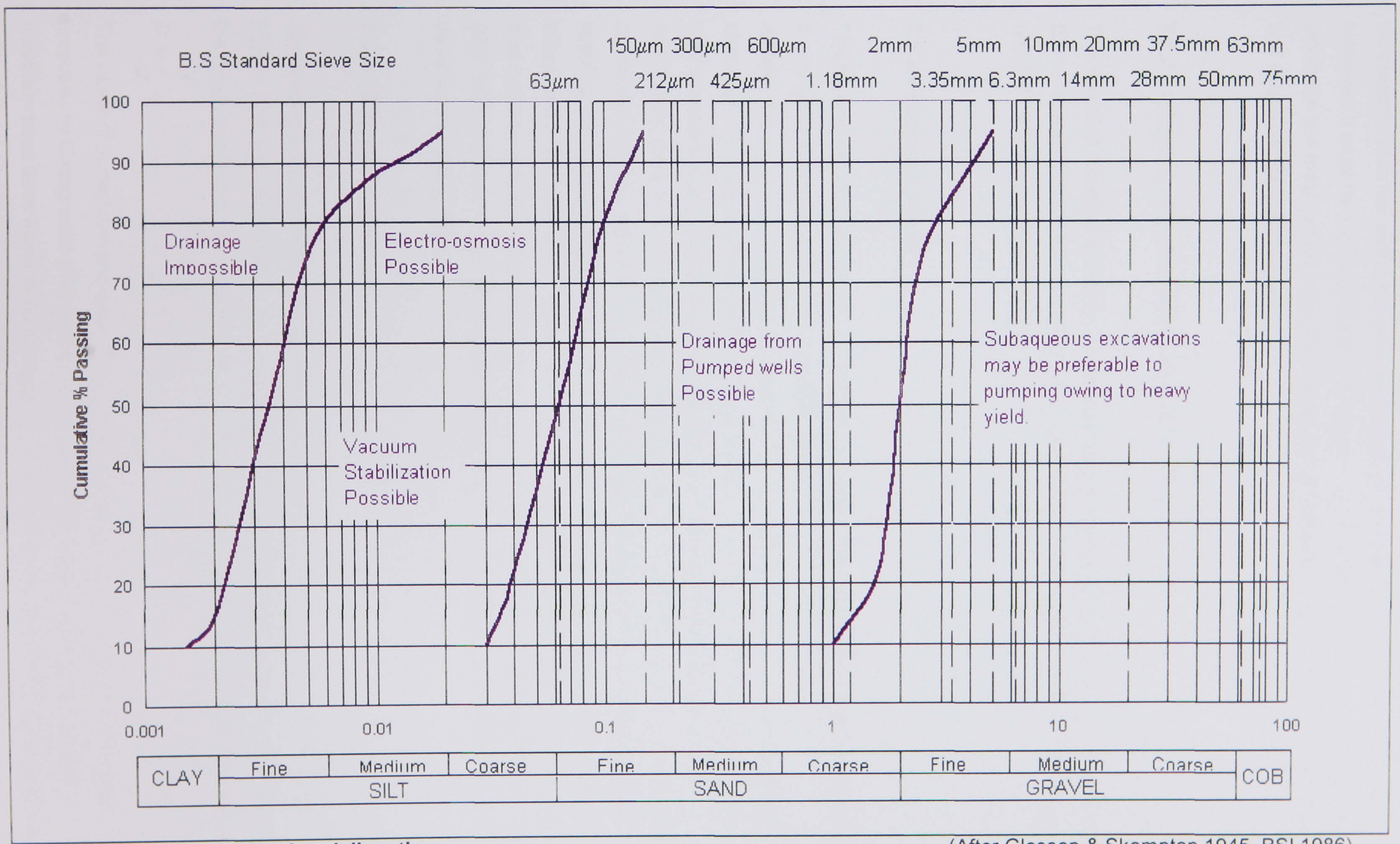

Figure 7.5 Particle size distribution delineation (After Glossop & Skempton 1945, BSI 1986)

The acceptability criterion for particle size distribution is that the majority of the particle size distribution curve lies within the delineated zone, i.e. a medium to fine SILT or silty CLAY. However, it must be appreciated that this criterion alone does not allow for any macrofabric within the soil mass, which may cause a significant increase in the hydraulic permeability and cause an application to fail.

7.2.2 CHEMICAL AND ELECTRO-CHEMICAL TESTS

The standard chemical and electro-chemical tests should be carried out in accordance with BS 1377: Part 3 (BSI 1990c) with the soil samples being taken and prepared in accordance with BS 1377: Part 1 (BSI 1990a).

7.2.2.1 Organic Content

The determination of the organic content through mass loss on ignition should be carried out in accordance with BS 1377: Part 3 §4 (BSI 1990c).
As was shown in Figure 2.8 the presence of organic matter in a soil can have a significant effect upon the cation exchange capacity, especially in high pH conditions, as may occur near the cathode and, therefore, have an effect upon the electro-osmotic efficiency. Additionally, there is no available published literature on the effects of organic matter content on electro-osmosis. However, the presence of organics in a soil are known to affect the hydraulic permeability and the compressibility of the soil mass, which is liable to have an effect on the susceptibility of the soil to treatment be electro-osmosis. Therefore, if the soil may be described as an organic CLAY or SILT in accordance with BS 5950: 1999 §41.4.6 (BSI 1999) then it is recommended that specific electro-osmotic testing is carried out to ascertain the soils suitability.

7.2.2.2 Electrical Resistivity

The electrical resistivity (ρ) of the soil should be determined in accordance with BS 1377: Part 3: 1990 §10 (BSI 1990c). The Author's experience is that the disk electrode method is the most appropriate. Electrical resistivity may be related to conductivity (σ) by Equation 7.3:

$$\sigma = \frac{1}{\rho} \qquad \text{Eqn. 7.3}$$

The range of acceptable and economic values of electrical conductivities (σ) has been proposed by Casagrande (1983) who stated that values within the range of 0.05S/m - 0.005S/m have been found to be acceptable. This criterion is adopted for the assessment of soils.

Values in excess of this range do not indicate that the soil is not susceptible to treatment by electro-osmosis, but that the electro-osmosis installation will draw a high current and is unlikely to be economic. The merits and economics of each site should be individually considered if necessary. It is essential that the site groundwater is used in any conductivity tests due to the significant effect it has upon the overall conductivity, as shown in Figure 7.2.

7.2.3 COMPRESSIBILITY AND PERMEABILITY TESTS

The standard compressibility and permeability tests should be carried out in accordance with BS 1377: Part 5 (BSI 1990d), with soil samples being taken and prepared in accordance with BS 1377: Part 1 (BSI 1990a). The falling head permeability test, which is the most appropriate for fine grained soils, is covered neither by the current British Standard, nor by the ASTM Standards on soil mechanics laboratory testing. The procedure given in Head (1982) §10.7.2 is recommended for undertaking the test.

7.2.3.1 One-dimensional Consolidation Parameters.

The one-dimensional consolidation parameters of the soil should be determined in accordance with BS 1377: Part 5:1990 §3 (BSI 1990d).
Electro-osmotic consolidation is normally two-dimensional, in that the electrical field and the flow of water / development of pore water pressures are in the same direction, whereas the surface settlements induced are in an orthogonal direction as shown in Figure 7.6a. However, the conventional oedometer, as described in BS 1377: Part 5 (BSI 1990d) applies an increase in effective stress and allows drainage of excess pore water pressures in the same plane, i.e. in the vertical direction, Figure 7.6 c&d. BS 1377: Part 5 (BSI 1990d) recommends that the soil specimen should be orientated such that in the laboratory test the soil will be loaded in the same direction relative to the stratum as the applied stress in situ. Electro-osmotic consolidation via vertical drains/electrodes is equivalent to consolidation using surcharging and vertical sand drains, in the sense that the applied pressure and drainage occur in two dimensions, Figure 7.6 a&b. Therefore, the coefficients of radial drainage are appropriate (Johnson 1970 and Das 1997). Johnson (1970) indicates that the coefficients of consolidation for radial drainage are best calculated from in situ field permeability tests and conventional one dimensional consolidation tests (Cedergren & Weber 1962 and Weber 1968). Johnson (1970) also states that the coefficient of consolidation for radial drainage will normally equal or exceed values obtained from laboratory consolidation tests with vertical drainage. The equations governing consolidation by radial drainage, which are applicable to electro-osmotic consolidation via vertical drains/electrodes, are (After Das 1997):

$$T_r = \frac{C_{vr} t}{AC^2}$$ Eqn. 7.4

$$C_{vr} = \frac{k_h}{m_v \gamma_w}$$ Eqn. 7.5

Where T_r is the time factor for radial flow, C_{vr} is the coefficient of consolidation in the radial direction, t is time, AC is anode-cathode spacing, k_h is the coefficient of horizontal hydraulic permeability, m_v is the coefficient of volume compressibility and γ_w is the bulk density of water.

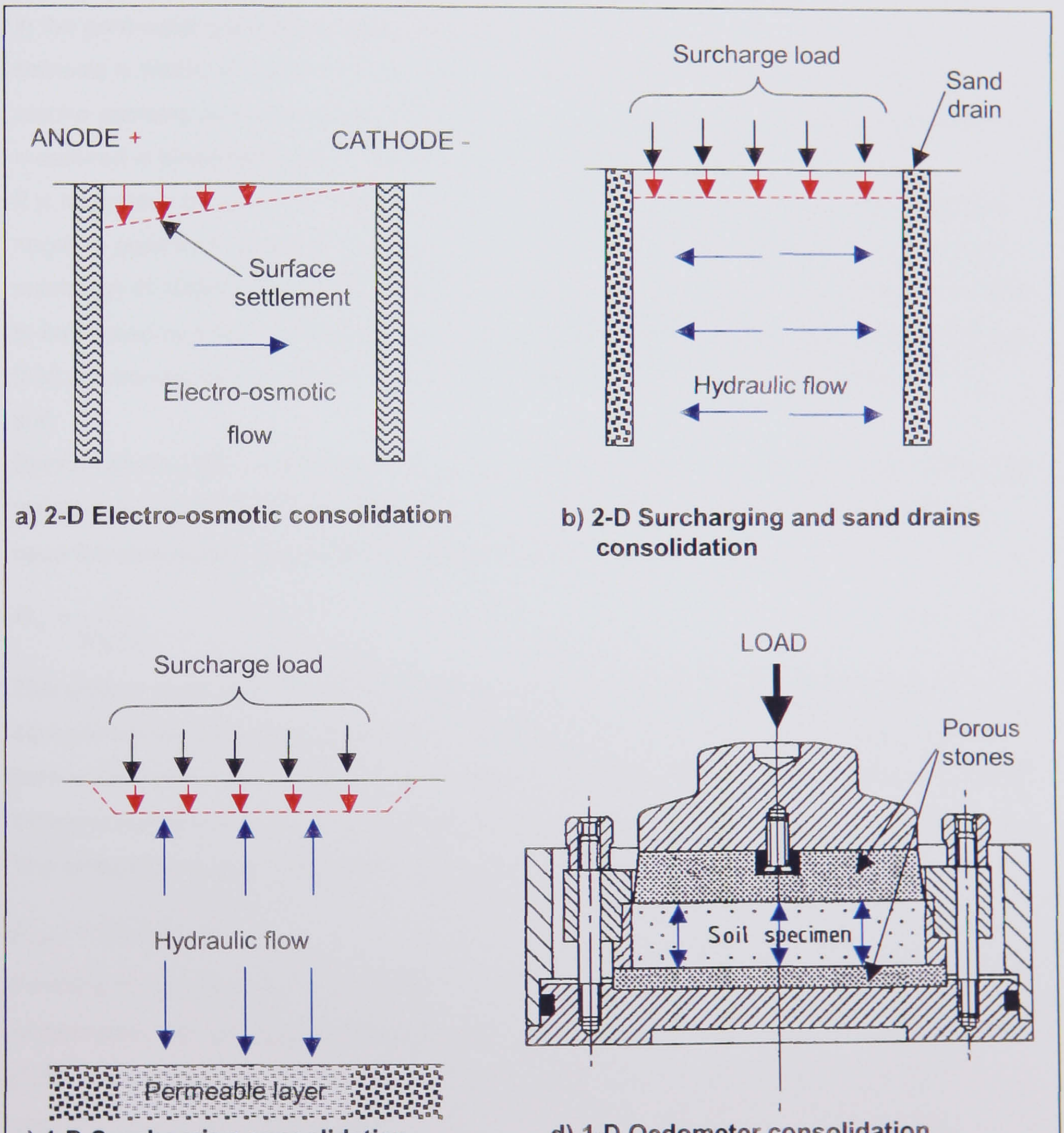

a) 2-D Electro-osmotic consolidation

b) 2-D Surcharging and sand drains consolidation

c) 1-D Surcharging consolidation

d) 1-D Oedometer consolidation

Figure 7.6 One and two dimensional consolidation configurations (After BSI 1990d)

Therefore, it is suggested that conventional oedometer tests are carried out in accordance with BS 1277: Part 5 (BSI 1990d) with the soil samples orientated such that the oedometric stress is applied in the vertical direction relative to the stratum in situ.

For instances where the application of the electrical potential difference and the associated settlement are in the same plane, i.e. a one dimensional case, such as those cited by Chen & Murdoch (1999), Chen *et al* (1999) and Pugh (2000) the vertical coefficient of hydraulic permeability is the appropriate one for use in Equation 7.5 and the situation is essentially identical to conventional surcharging without vertical sand drains, Figure 7.6c.

As stated in §2.7.5.6, Johnston (1978) demonstrated that due to the occurrence of cavitation in the pore water the minimum pore water pressure that can be generated by electro-osmosis is limited to approximately -100kPa. Bjerrum *et al*'s (1967) field application of electro-osmosis confirmed this by demonstrating that the minimum pore water pressures measured in piezometers were equivalent to -5m of hydraulic head.

It is suggested by the Author that this value of -100kPa be adopted as the minimum excess negative pore water pressure that may be generated in the field. Therefore, if an equivalent surcharge of 100kPa (i.e. approximately 5m of fill) causes little or no consolidation of the soil to be treated by electro-osmosis, as a result of overconsolidation or a high stiffness modulus, then electro-osmosis is unlikely to be a successful ground improvement technique for the soil.

Bjerrum *et al*'s (1967) paper may be used to qualify this assumption. Based upon the quoted values of $C_v = 0.5*10^{-7} m^2/sec$ and $k=2*10^{-10} m/s$ the value of m_v may be calculated based upon the assumption of $\gamma_w=10kN/m^3$ using Equation 7.6 (Carter 1983):

$$C_v = \frac{k}{m_v \gamma_w} \qquad \text{Eqn. 7.6}$$

This gives a value of m_v of 0.4 m^2/MN if the settlement caused by electro-osmosis is equivalent to an oedometric settlement. This is a reasonable assumption, as the negative pore water pressures are induced throughout the full depth of electrode embedment and the increase in effective stress ($\Delta\sigma_v'$) of 100kPa is applicable over the full depth of the electrode. The settlement is given by Equation 7.7 (Carter 1983):

$$\rho_{oed} = m_v \Delta\sigma_v' dz \qquad \text{Eqn. 7.7}$$

Inserting the values of m_v = 0.4 m^2/MN, $\Delta\sigma_v'$=100kPa and dz =10m (depth of electrode embedment) the calculated oedometric settlement (ρ_{oed}) is 400mm. Skempton and Bjerrum (1957) have shown that the actual consolidation settlement in the field varies from the calculated oedometric settlement by a geological factor (μ_g) as given in Equation 7.8:

$$\rho_c = \mu_g \rho_{oed} \qquad \text{Eqn. 7.8}$$

For most practical purposes the values of μ_g are as given in Table 7.5

Hence, for the sensitive clay at Ås (Bjerrum *et al* 1967) μ_g should be taken as 1.2 this gives a calculated consolidation settlement of 480mm this is in very good agreement with the

observed settlement on site of 500mm after 120 days of treatment (i.e. an error of less than 5%), validating the Author's assumption of electro-osmosis being equivalent to an increase in $\Delta\sigma_v'$ of 100kPa when the calculated value of u is less than -100kPa.

Table 7.5 Oedometric consolidation correction factor μ_g and clay type (Tomlinson 1995)

Type of clay	μ_g
Very Sensitive clays (soft alluvial, estuarine and marine clays)	1.0 - 1.2
Normally consolidated clays	0.7 - 1.0
Overconsolidated clays (London Clay, Weald, Kimmeridge, Oxford and Lias)	0.5 - 0.7
Heavily overconsolidated clays (glacial till, Keuper marl)	0.2 - 0.5

Based upon the postulation of an equivalent surcharge of 5m, the one-dimensional consolidation parameters may be defined as those that will undergo appreciable settlements under this load.

Typical values for the coefficient of volume compressibility (m_v) for a range of naturally occurring soils are given in Table 7.6. Based upon this table and a review of the available literature on successful case studies of electro-osmotic consolidation an acceptable range for m_v is shown to be 0.3 - 1.5 MN/m^2 i.e. a high compressibility clay/silt (Bjerrum *et al* 1967).

Table 7.6 Coefficients of volume compressibility for soils in their natural state (After Carter 1983 and Head 1982)

Type of Clay	**Descriptive term**	**Coefficient of volume compressibility (m_v) MN/m^2**
Heavily overconsolidated boulder clays, stiff weathered rocks (e.g. weathered Mudstone) & hard clay	Very low compressibility	<0.05
Boulder Clays, marls, very stiff or hard blue London Clay	Low Compressibility	0.05 - 0.1
Firm clays, fluvio-glacial clays, lacustrine deposits, weathered marls, firm boulder clays, London clay, normally consolidated clays at depth and firm tropical red clays	Medium Compressibility	0.1 - 0.3
Normally consolidated alluvial clays such as estuarine and delta deposits and sensitive clays	High Compressibility	0.3 - 1.5
Very organic alluvial clays and peats	Very High Compressibility	>0.15

The coefficient of volume compressibility (C_v) and its relationship to the hydraulic permeability and m_v is discussed in the following section.

7.2.3.2 Hydraulic Permeability

The hydraulic permeability of the soil to be treated by electro-osmosis should be ascertained by the falling head test in accordance with the procedure given in §10.7.2 of Head (1982). Initially reference should be made to the effective particle size representing 10% passing (D_{10}) of the soil obtained from the particle size distribution (§7.2.1.4). From the D_{10} particle size and Figure 7.7, it is possible to ascertain the type of permeability test most appropriate for the soil, i.e. falling head or constant head.

If Figure 7.7 indicates that the most appropriate test for the soil is the constant head test or computation then the soil is too coarse for treatment by electro-osmosis and recirculation of the pore fluid will take place under gravitational forces, rendering electro-osmosis unsuitable.

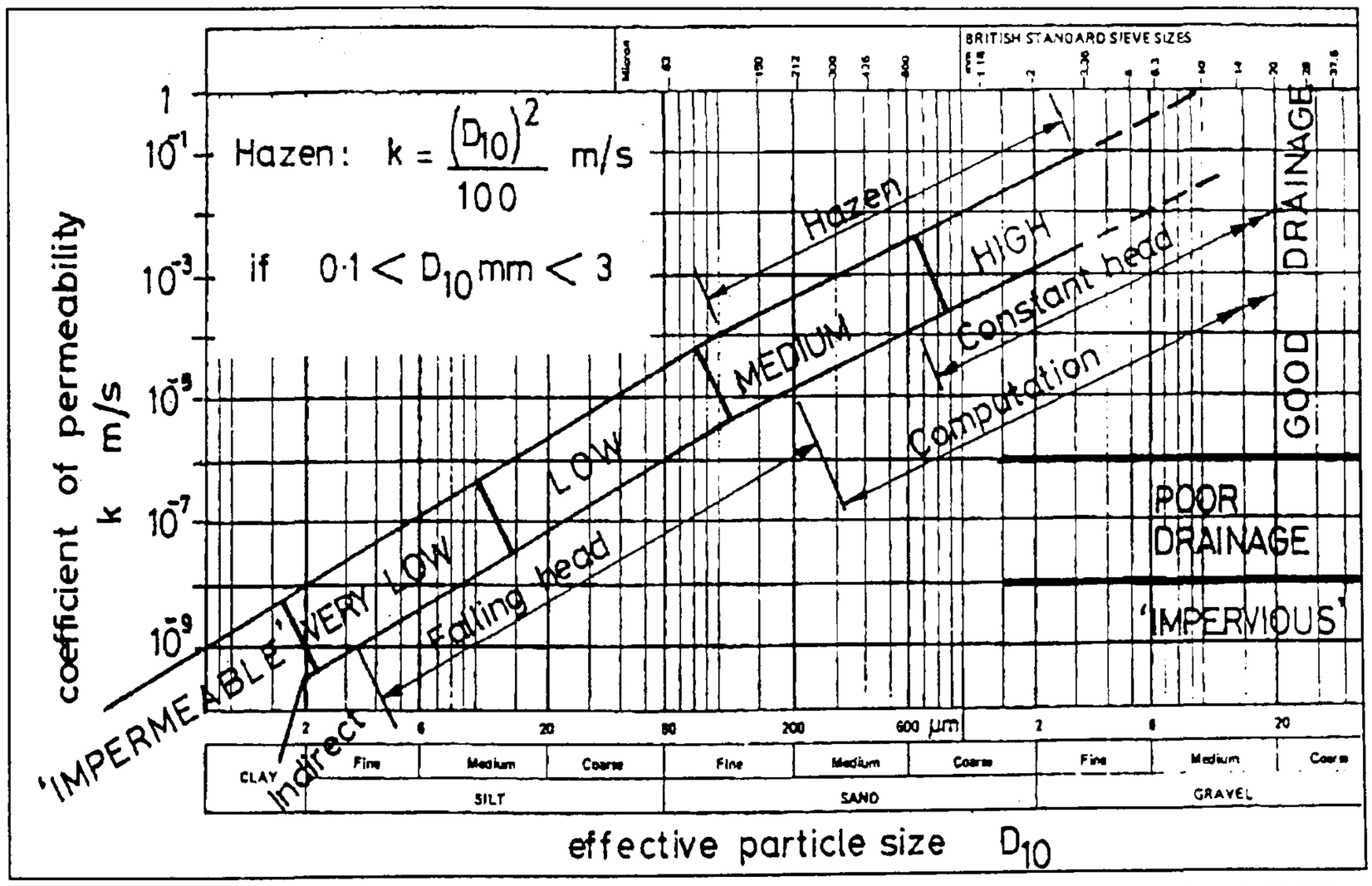

Figure 7.7 Permeability classification related to particle size (Head 1982)

This may be demonstrated by the equation that defines the porewater pressures at any point under an electrical potential gradient with a closed anode and open cathode (§2.7.5.6):

$$u = -\frac{k_e \gamma_w V}{k} \qquad \text{Eqn. 7.9}$$

Assuming a voltage of 100V (maximum safe voltage), γ_w=10 kN/m^3 and k_e=5*10^{-5}cm^2/sec-V (Casagrande 1983) the minimum theoretical negative pore water pressure that can be generated in different soil types is presented in Table 7.7.

From Table 7.7 it is apparent that any soil coarser than sand size will be unsuitable for treatment by electro-osmosis. This data is also presented graphically in Figure 7.8.

Table 7.7 Equivalent surcharge load for different soil types and permeabilities

Soil Type	Assumed permeability k (m/s) (After Das 1997)	-u (kPa) from Eqn. 7.9	Equivalent surcharge load (m of fill)
Gravel	10^{-2}	$5*10^{-5}$	$2.5*10^{-6}$
Sand	10^{-5}	0.05	$2.5*10^{-3}$
Silt	10^{-7}	5	0.25
Clay	10^{-9}	500	25

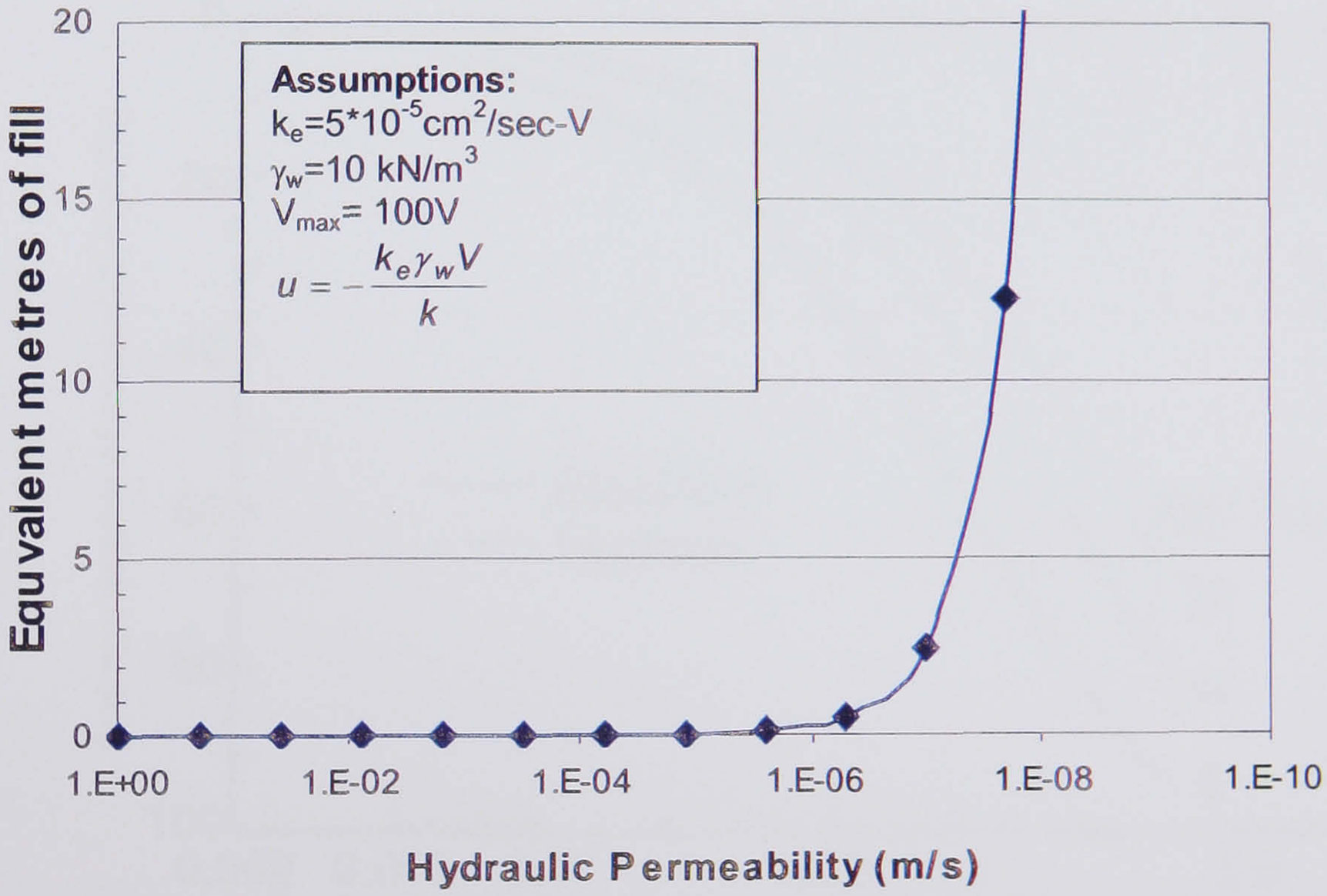

Figure 7.8 Theoretical equivalent fill height against hydraulic permeability

From §2.7.5.6 and Figure 7.8 it is apparent that for the generation of useful negative pore water pressures (i.e. equivalent to several metres of fill) the hydraulic permeability (k) needs to be less than 10^{-8}m/s, which from Table 7.7 indicates that fine SILT or silty CLAY type soils are the most appropriate.

The rate of electro-osmotic consolidation is governed by the hydraulic permeability of the soil as given in Equation 7.5. A low value of k will give a corresponding low value for the coefficient of consolidation (C_v). Using the chart presented by Esrig (1968) for the average degree of consolidation against time factor for radial drainage, as presented in Figure 7.9, it

is possible to calculate an acceptable range for C_v based upon the time available for consolidation. For most practical applications of electro-osmotic consolidation the ratio R_E/R_W (Anode-Cathode spacing / radius of electrode) will be in excess of 20, hence the curve for $R_E/R_W = 20$ should be used in Figure 7.9. From Figure 7.9 the time factor (T_r) for an average degree of consolidation of 90% is 0.05. Using Equation 7.4 a range of minimum acceptable C_v values has been established for three different electrode spacing (AC= 2m, 3m & 4m) and a range of possible consolidation times, these results are presented in Figure 7.10.

Table 7.8 presents a range of typical C_v values for a range of different plasticity clays and silt. From Figure 7.10 and Table 7.8 it will be seen that for slits and clays of low and medium plasticity the values of C_v will give reasonable coefficients of consolidation commensurate with realistic electrode spacings and project durations. The acceptability criteria for plasticity §7.2.1.1 proposed by the Author is also in good agreement with the values presented in Table 7.8.

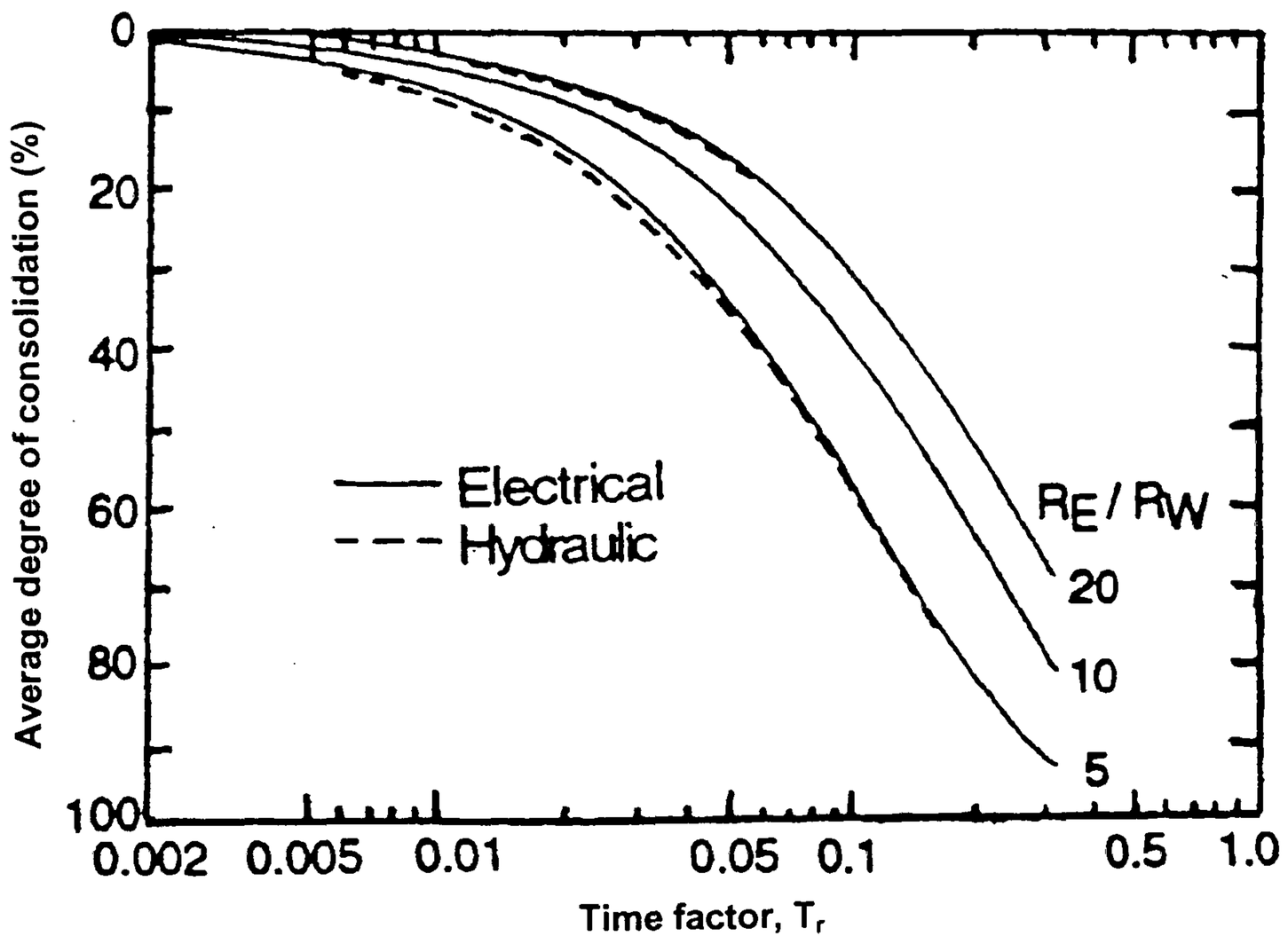

Figure 7.9 Average degree of consolidation against time factor for radial drainage (Esrig 1968)

The ideal soil for treatment by electro-osmosis is one in which the hydraulic permeability (k) is sufficiently low to generate negative porewater pressures of the order of -100 kPa and yet sufficiently permeable to give a realistic coefficient of consolidation (C_v) commensurate with the time-scale of the project.

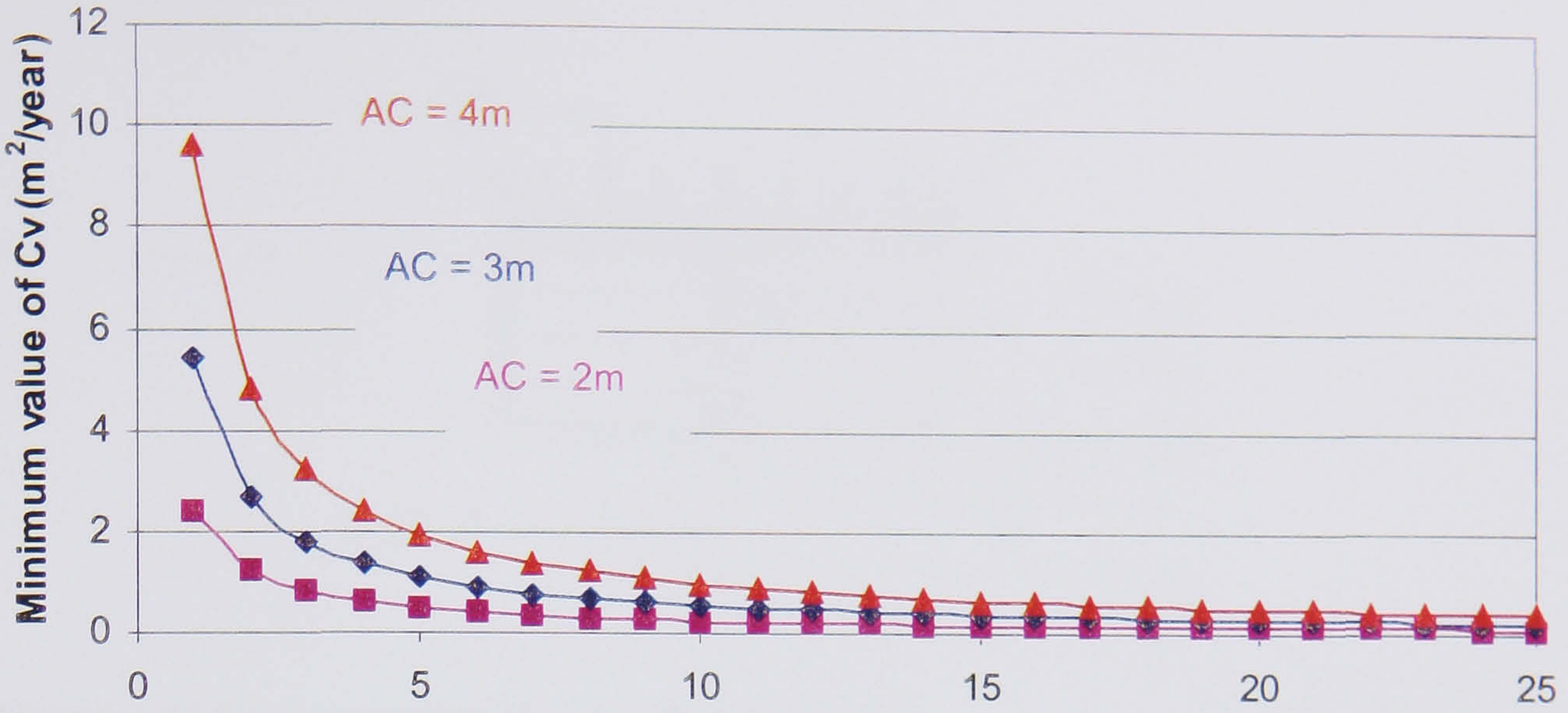

Figure 7.10 Minimum value of C_v against time available for consolidation

Table 7.8 Coefficient of consolidation for different soil types (Lambe & Whitman 1979)

Soil Type	Plasticity index range	Coefficient of consolidation C_v (m^2/year)	
		Undisturbed	Remoulded
Clays			
High Plasticity	Greater than 25	0.1 - 1	
Medium plasticity	25 - 15	1 - 10	About 25 to 50% of
Low plasticity	15 or less	10 - 100	undisturbed values
Silts	N/A	above 100	

7.2.4 CONSOLIDATION & PERMEABILITY IN HYDRAULIC CELLS

The standard consolidation and permeability tests in hydraulic cells and with pore pressure measurement should be carried out in accordance with BS 1377: Part 6 (BSI 1990e), with soil samples being taken and prepared in accordance with BS 1377: Part 1 (BSI 1990a). It is recommended by Head (1998) that consolidation with radial drainage to the centre of the cell is undertaken in accordance with BS 1377: Part 6 §3.8 (BSI 1990e) with equal strain loading and porewater pressure measurement at 0.55R from the centre of the base to simulate drainage wells as shown in Figure 7.11.

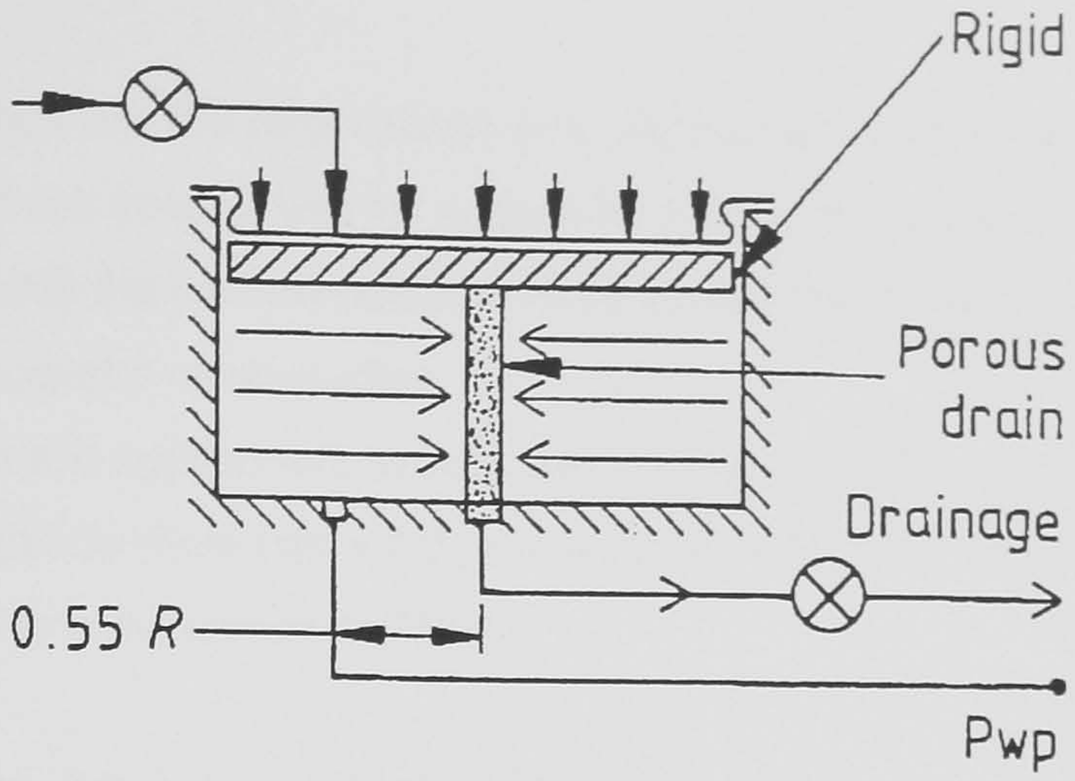

Figure 7.11 Recommended Rowe cell configuration (BSI 1990e)

As discussed in §7.2.3.1, the consolidation parameters that are most applicable to electro-osmosis installations with vertical electrodes/drains are the radial drainage consolidation parameter. The Rowe (Rowe & Barden 1966) cell is better suited than the oedometer for establishing these parameters as the loading and drainage regime are more akin to that which occurs in the field, additionally the sample size that may be tested is larger (75mm∅, 150mm∅ & 250mm∅). The influence of inclusions and laminations is, therefore, more likely to be reflected in the results obtained. The acceptability criteria for the consolidation parameters obtained from the Rowe cell are identical to those obtained from the oedometer, however, it must be appreciated that the quality of the results obtained is significantly better from the Rowe cell than from the oedometer. The measurement of the horizontal permeability in the field is to be preferred where this result is available for use in Equation 7.5.

Nicholls & Herbst (1967) reported on the construction and testing of an electro-osmotic type Rowe cell. The results given show a marked improvement in the consolidation of silty clay under electro-osmosis and surcharge loading, however, it is not possible to back analyse the results given due to a lack of test specifics and material parameters.

7.2.5 SHEAR STRENGTH - TOTAL STRESS

The standard total stress shear strength tests should be carried out in accordance with BS 1377: Part 7 (BSI 1990f), with soil samples being taken and prepared in accordance with BS 1377: Part 1 (BSI 1990a). The value of undrained shear strength (c_u) may be obtained by using one of the following tests described in BS 1377: Part 7 (BSI 1990f):

- Laboratory Vane §3.
- Direct Shear §4 & §5.

- Triaxial compression §8 & §9.

The preferred methods are the direct shear and the triaxial compression methods.
The values of c_u that are appropriate for soils to be treated by electro-osmosis are those that are commensurate with the parameters that have already been established and those that are published in successful case studies.
The values of c_u that are appropriate to soils with similar characteristics to those required for compressibility limitations (See Table 7.6) are ascertained from Table 7.9. This indicates that a value of c_u up to a maximum of 75kPa.

Table 7.9 Undrained shear strength for different soil types (Tomlinson 1998)

Type of Clay	Undrained shear strength (kN/m^2)
Heavily boulder clays, hard - fissured clays	>300
Very stiff boulder clays, very stiff blue London Clay	150 - 300
Stiff - fissured clays, stiff blue and brown London Clay, stiff weathered boulder clays	75 - 150
Firm normally consolidated clays (at depth), fluvio-glacial and lake clays. Upper weathered brown London Clay	40 - 75
Soft normally consolidated alluvial clays, marine, river and estuarine clays	20 - 40

Comparison of the liquidity index criteria with the undrained shear strength criteria using Figure 7.12 indicates that preferable soils (i.e. liquidity index of >0.6) will have a c_u of less than 20kPa where as soils that may still be acceptable (i.e. liquidity index >0.2) will have a c_u of less than 55kPa.

A review of the available literature for the range of c_u for soils that have been successfully treated indicates a range of 0.7kPa to 81kPa, which is in good agreement with the values obtained from Table 7.9 (Abiera *et al* 1999, Bjerrum *et al* 1967, Casagrande *et al* 1981, Chappell & Burton 1975, Eggestad & Føyn 1983, Esrig & Gemeinhardt 1967, Fetzer 1967, Lo *et al* 1991, Milligan 1994, Morris *et al* 1985, Wan & Mitchell 1975, Wan & Mitchell 1976).

A limit of 55kPa has been adopted as the acceptability criteria.

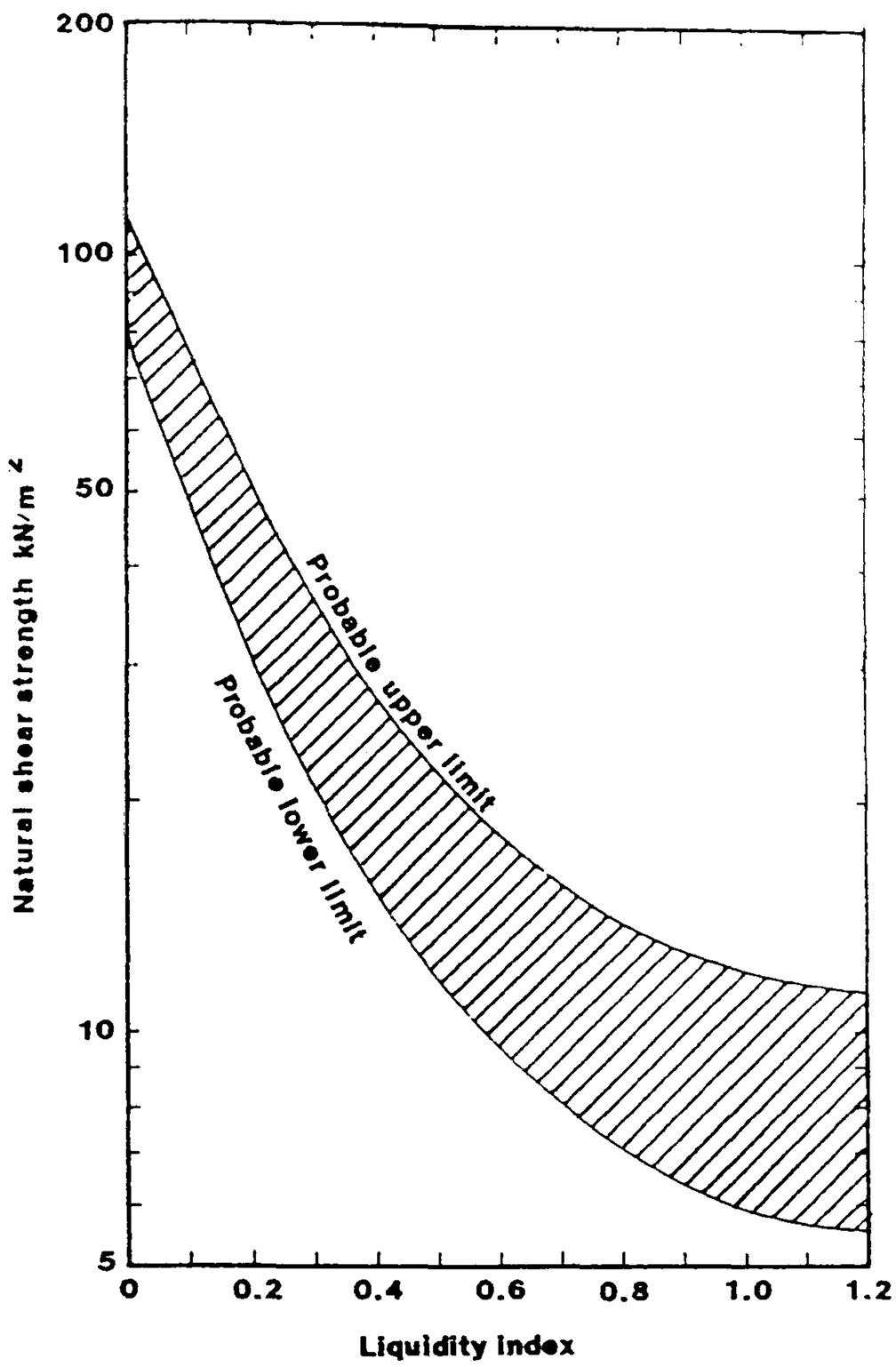

Figure 7.12 Undrained shear strength against liquidity index (Carter & Bentley 1991)

7.2.6 SHEAR STRENGTH - EFFECTIVE STRESS

The standard effective stress shear strength tests should be carried out in accordance with BS 1377: Part 8 (BSI 1990g), with soil samples being taken and prepared in accordance with BS 1377: Part 1 (BSI 1990a). The effective stress parameters of c' & ϕ' obtained from the testing, either consolidated undrained triaxial compression with measurement of porewater pressure or consolidated drained triaxial compression with measurement of volume change, are parameters that may be required for the long-term drained analysis of any future proposed building on a consolidation site or for the long term stability analysis of an electro-osmotically enhanced cohesive reinforced soil wall. As such, no specific values of c' & ϕ' can be specified that represent soils that are suitable for treatment by electro-osmosis. Table 7.10 presents typical values for the range of ϕ' for silts and clays, which are the soils that are amenable to treatment by electro-osmosis.

Table 7.10 Typical ϕ′ values for compacted clays (Carter & Bentley 1991)

Soil Type	Unified classification system designation	ϕ′ (degrees)
Silty Clays	SM	34
Silts and clayey silts	ML	32
Clays of low Plasticity	CL	28
Clayey silts, elastic silts	MH	25
Clays of high plasticity	CH	18

Electro-osmosis may be expected to increase the value of ϕ′ for treated soils as Pugh (1999) and Casagrande (1983) have demonstrated for London Clay and fine quartz sand respectively, in that the electro-osmotic process causes a shift in the particle size distribution to a coarser grain size. This shift being caused by cementation of particles due to high pH conditions and release of metal ions from the anode caused by corrosion (§ 2.7.5.5). The Author suggests that due to the difficulty in predicting the effects of electro-chemical cementing it is not relied upon in design and is seen as an additional factor of safety. Additionally, these gains may be lost during a reverse polarity stage.

Gibson (1953) has presented a correlation for the drained shear strength and the plasticity index for remoulded clays. These values should not deviate significantly from those for the normally consolidated clays and silts that are amenable to electro-osmosis. The correlation is presented here as Figure 7.13.

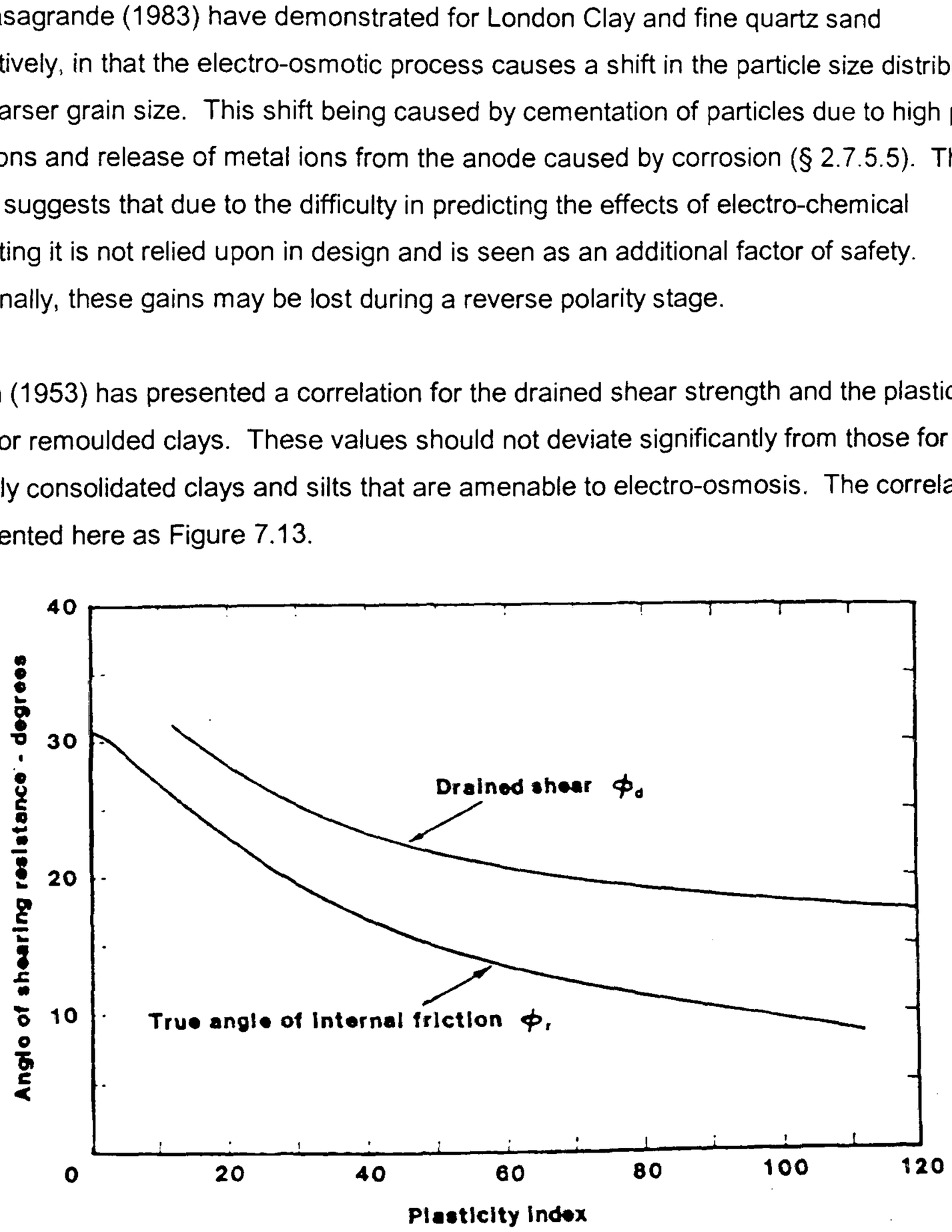

Figure 7.13 Drained shear strength against plasticity index (Gibson 1953)

As will be seen from Table 7.10 and Figure 7.13 the range of ϕ′ is large for soils that are amenable to electro-osmosis, but is generally less than 30°.

7.2.7 SPECIALIST ELECTRO-OSMOSIS TESTING

This suite of testing may be defined as the range of tests that currently are solely used for research. However, as the application of electro-osmosis becomes more widespread and as further literature becomes available in the public domain it is envisaged that these tests will become more commonplace.

7.2.7.1 Electro-Osmosis Cell

This cell was originally developed by Banerjee & Vitayasupakorn (1984), it was later modified by Hamir (1997) and has been used in several research projects since (Laidler 1999 and Gwede 2000). The cell is shown schematically in Figure 7.14, and its basic functions are described in the following text. The cell consists of a Perspex cylinder with a fixed base plate and an internal movable piston whose movement may be monitored by means of a displacement transducer (LVDT). Provision is made for the location of disk type electrodes both on the piston and on the fixed base plate by means of cable glands that permit the passage of an electrical cable into the cell, without the loss of pressure. Additionally, the cell incorporates side ports through which porewater pressure and voltage gradient may be measured if required by means of a hypodermic needle tipped with a piece of porous ceramic or plastic. The chamber behind the moveable piston may be pressurised to apply a consolidation pressure to the soil sample. Backpressure may also be applied to the soil sample through tubing which passes through the piston and the base plate, this tubing also acts as a drain for any excess porewater pressure. The interpretation of the results obtained from the cell is based upon comparison with a control cell. Further details of the cell may be found in Hamir (1997) and Laidler (1999).

7.2.7.2 Electro-Osmosis Box

The electro-osmosis box has been described previously in §6.2.5 and has been described by Nettleton (1996) and Adali (1999). The interpretation of the results is based upon the vertical strain produced a s a result of the application of an electrical potential difference. No further discussion will be given here regarding this apparatus.

7.2.8 CONCLUSIONS OF ACCEPTABILITY CRITERIA

The previous sections have summarised the range of standard classification and non-standard electro-osmosis tests that should be carried out on a soil in order to ascertain its suitability to treatment by electro-osmosis. However, it is appreciated that due to economic and time constraints it is not always possible to conduct the type or number of tests that is desirable in a project. As such, a guidance table has been produced by the Author to try and

assist in the selection of test types on the basis of cost and usefulness. This table is presented here as Table 7.11.

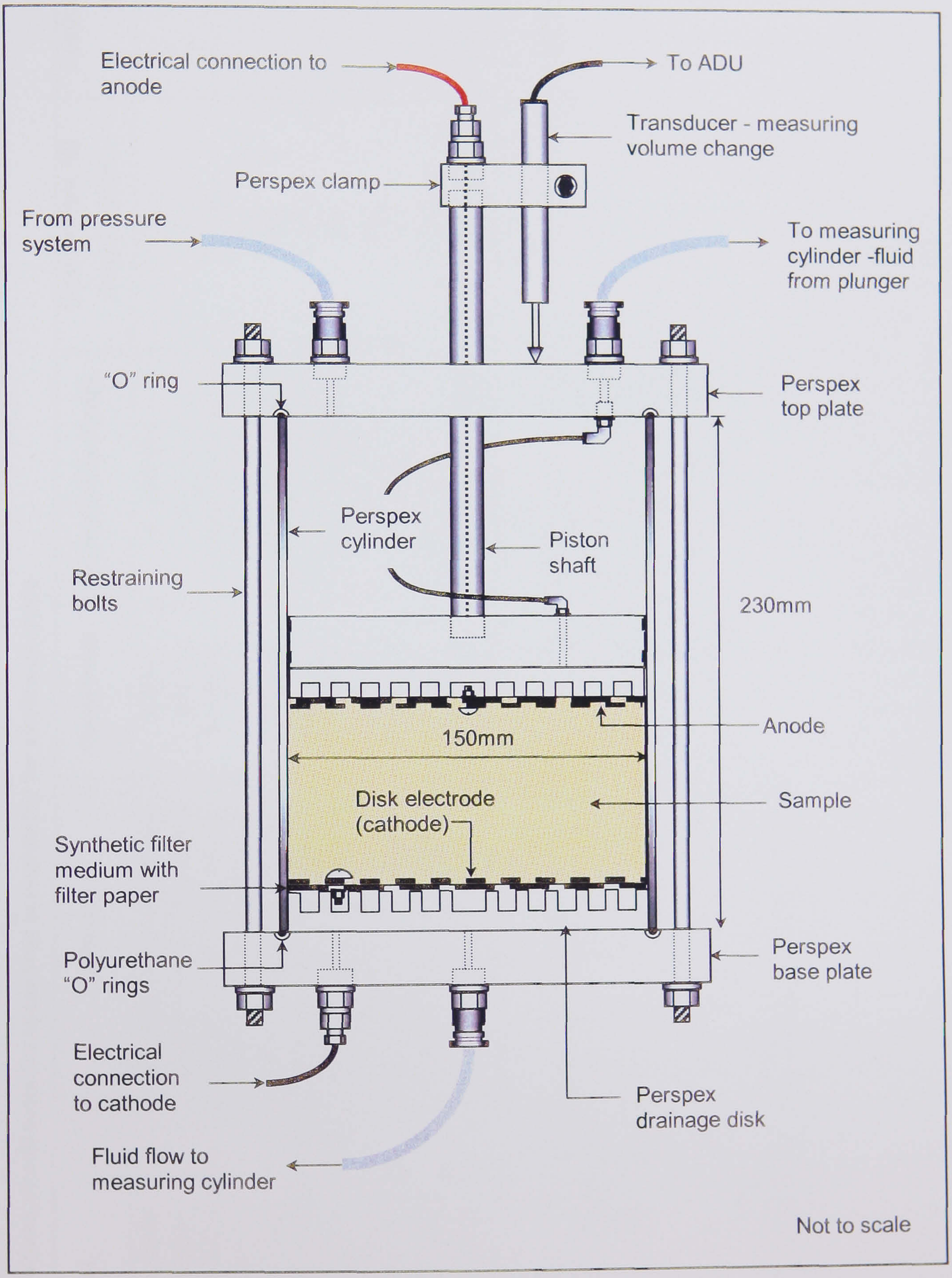

Figure 7.14 Schematic of electro-osmosis cell (After Laidler 1999)

Table 7.11 Usefulness of soil tests for assessing acceptability for electro-osmosis

Test	Reference	Usefulness	Acceptability Range	Cost per test (£) (Hughes 2001)	Cost/usefulness rank
Atterberg limits	BS 1377: Part 2 (BSI 1990b)	✕✕✕	5 - 30% P.I.	25	2
Water content	BS 1377: Part 2 (BSI 1990b)	✕✕✕	0.6 - 1.0 L.I.	5	1
PSD - sieve/ sedimentation	BS 1377: Part 2 (BSI 1990b)	✕✕✕✕	See Figure 7.5	25 / 40	2
Particle density	BS 1377: Part 2 (BSI 1990b)	✕	Not applicable	20	5
Organic content	BS 1377: Part 3 (BSI 1990c)	✕✕	Up to ORGANIC	≈30	4
1-D Consolidation Parameters	BS 1377: Part 5 (BSI 1990d)	✕✕✕	m_v = 0.3 - 1.5 MN/m^2	60	5
Disk Electrode	BS 1377: Part 3 (BSI 1990c)	✕✕✕	0.05 - 0.005 S/m	40	3
Hydraulic Permeability	Head (1982) §10.7.2	✕✕✕	<10^{-8} m/s	≈40	3
Undrained shear strength	BS 1377: Part 7 (BSI 1990f)	✕✕	<55 kPa	30	4
Drained shear strength	BS 1377: Part 8 (BSI 1990g)	✕	ϕ'<30°	≈120	6
Electro-osmosis cell	This thesis § 7.2.7.1	✕✕✕✕	Comparison with ctrl.	≈60$^{\cdot}$	4
Electro-osmosis box	This thesis § 6.2.5	✕✕✕✕	Comparison with ctrl.	≈60$^{\cdot}$	4

NOTES:

An assessment of the soils macrofabric should also be undertaken in accordance with McGown et al (1980) to assess the possibility of in situ short-circuiting and porewater recirculation.

$^{\cdot}$ *Estimation made by Author*

Legend

✕✕✕✕ Excellent, ✕✕✕ Good, ✕✕ Reasonable, ✕ Poor

7.3 DESIGN FOR ELECTRO-OSMOTIC CONSOLIDATION

The design procedure for electro-osmotic consolidation has been discussed in detail in Chapter 4, §4.2.2 and §4.3.3. The purpose of this section is to give an overview of the philosophy that has been developed for the design of electro-osmotic consolidation by the Author. The flow chart for of the design of electro-osmotic consolidation is given in Figure 7.17. The following sections elaborate upon the procedures involved in each step.

7.3.1 ESTABLISHMENT OF SOIL PARAMETERS

The soil parameters that are required to assess if a soil is suitable for treatment to electro-osmotic consolidation are similar to those used to assess the suitability of soil for use in reinforced electro-osmotically enhanced cohesive soil, except that greater emphasis is placed upon the volume change parameters and less upon the strength parameters. The soil parameters that should be established are given in Table 7.12, together with the reasons for obtaining them.

Table 7.12 Soil parameters required for electro-osmotic consolidation

Parameter	Reason
Soil acceptability criteria for treatment by electro-osmosis, see § 7.5	To assess if the soil is treatable by e-o and if it will be economically viable
Volume change parameters	To assess the amount of volume change that will take place
Undrained shear strength - undrained stiffness	To assess indirectly the effect of the electro-osmotic treatment
Macrofabric	To assess the probability of short-circuiting and porewater recirculation.

It is essential that these parameters are established for all strata that are present within the zone of influence of the trial, as layers of higher hydraulic permeability or of high electrical conductivity can cause the application to fail through recirculation of fluids or by short-circuiting if they are unforeseen and not designed out of the installation. Hence, establishing the stratigraphy and soil properties in the application zone are key issues.

7.3.2 PRELIMINARY ELECTRODE LAYOUT & ANALYSIS

There are no specific rules governing the electrode positions and each application should have an electrode layout specifically designed for it, and analysed using either finite

difference or resistance path techniques. However, points to be borne in mind when producing an initial trial layout are:

- The most efficient electrode array has generally been found to be staggered anodes and cathodes.
- The anode-anode/cathode-cathode spacing should be less than the anode-cathode spacing to produce an electrical field that is uniform and, thus, produce a uniform treatment of the ground.
- The closer the anodes and cathodes are together the more current the installation will draw for the same applied voltage.

7.3.3 SETTLEMENT, TREATMENT TIME AND POWER DEMAND

The estimation of the surface settlement, for an open cathode and closed anode that will be induced by the application of electro-osmosis is best estimated by the equivalent surcharge method, i.e. assuming that the negative porewater pressure generated is equivalent to an applied surcharge. It has generally been shown that the minimum negative porewater pressure that may be generated is -100 kPa, approximately equivalent to a surcharge of 5m of fill. Hence, for design purposes the application of electro-osmosis may be considered as the application of surface surcharge as presented in §4.2.2. Primarily, it is necessary to check using Equation 4.1 that a negative pressure of at least -100kPa is generated at the anode.

$$u = \frac{-k_e}{k} \gamma_w V_{max} \qquad \text{(Eqn. 4.1)}$$

Once, the minimum, negative pore water pressure has been confirmed as being equal to or less then -100 KPa. The surface settlement at the anode may be calculated using conventional consolidation theory.

$$\delta_{anode} = m_v \Delta\sigma_v' h \qquad \text{(Eqn. 4.11)}$$

Where, $\Delta\sigma_v' = 100kPa$, this settlement may then be assumed to vary linearly to 0mm at the cathode where no negative pore water pressure is generated. This procedure is a slight simplification in that a negative pore water pressure of less than -100 kPa may be calculated out to some distance from the anode, as shown in Figure 7.15. However, due to the complexity of the behaviour of the settlements in the field this simplification is considered to be valid. For example, Bjerrum *et al* (1967) reports greater settlements at the cathodes than at the anodes due to the strengthening of the ground at the anodes causing the metal re-bars used to hang-up, whereas the cathodes settled with the soil mass.

The treatment time, or rate of consolidation, for electro-osmosis may be calculated using a modification of conventional consolidation theory to take into account the open and closed nature of the cathode and anode respectively (see § 4.2.2.2 and § 4.3.3.1).

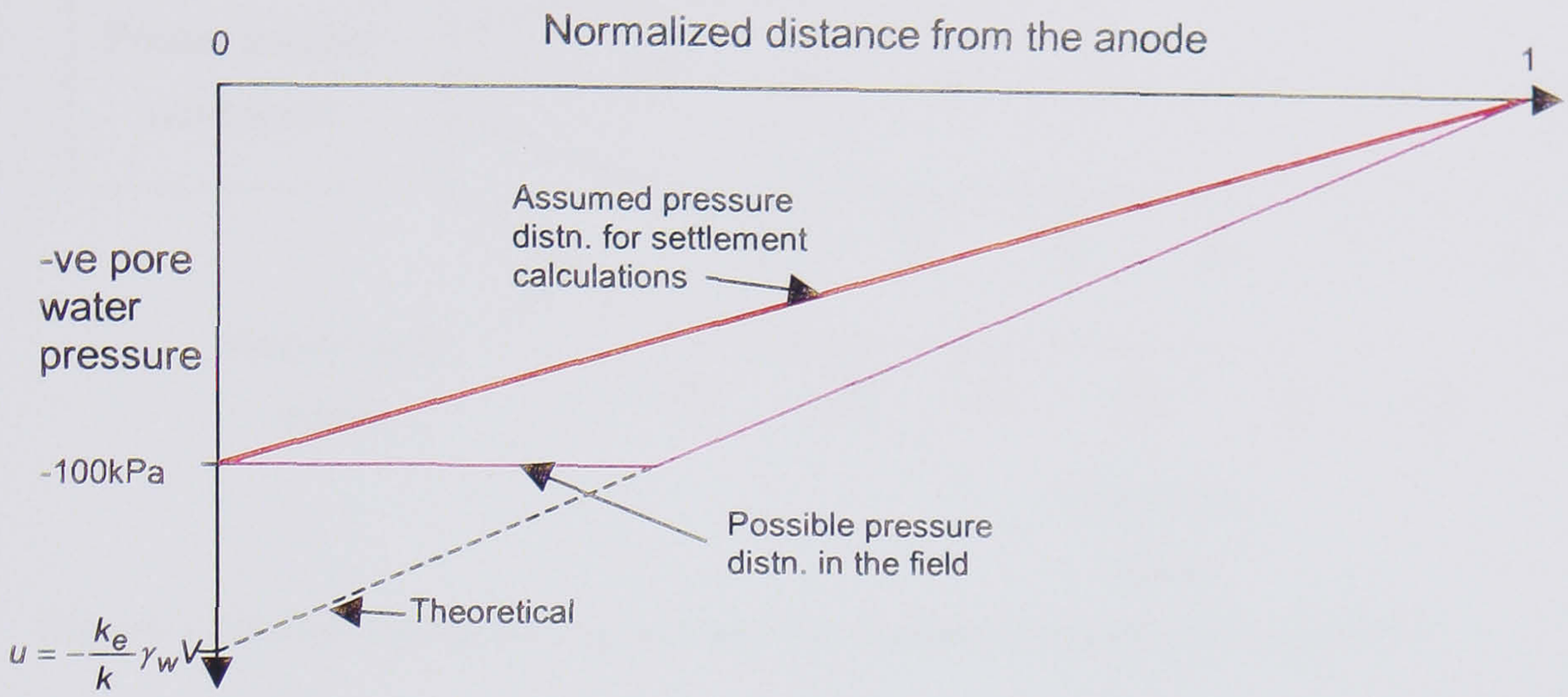

Figure 7.15 Negative porewater pressures

The estimation of the current demand of a consolidation trial may be estimated by the use of the equation suggested by Casagrande (1983) for consolidation applications, as presented in § 4.3.3.2:

$$I_t = ncs\sigma\frac{E}{L} \qquad \text{(Eqn. 4.13)}$$

A more realistic estimation may be undertaken by using a finite difference model and the laboratory variation of conductivity as measured in the electro-osmosis cell. The resistance path method may also be used, although it is suggested that the overall reduction factor for the electrical conductivity is increased to the order of 95%, based upon the observations made during this research.

7.3.4 INSTALLATION, CONNECTION & MONITORING

It is recommended that the EKG electrodes be installed by means of a wick drain lance. The electrical connection of the EKGs may be made using a double crimped-stripped connection, see §3.5.6.

The wiring of the EKGs may be made by individual cables; alternatively, heavier duty distribution cables may be used with disposable tails connecting to the electrodes as shown in Figure 7.16, the choice between these two methods should be based upon economic considerations.

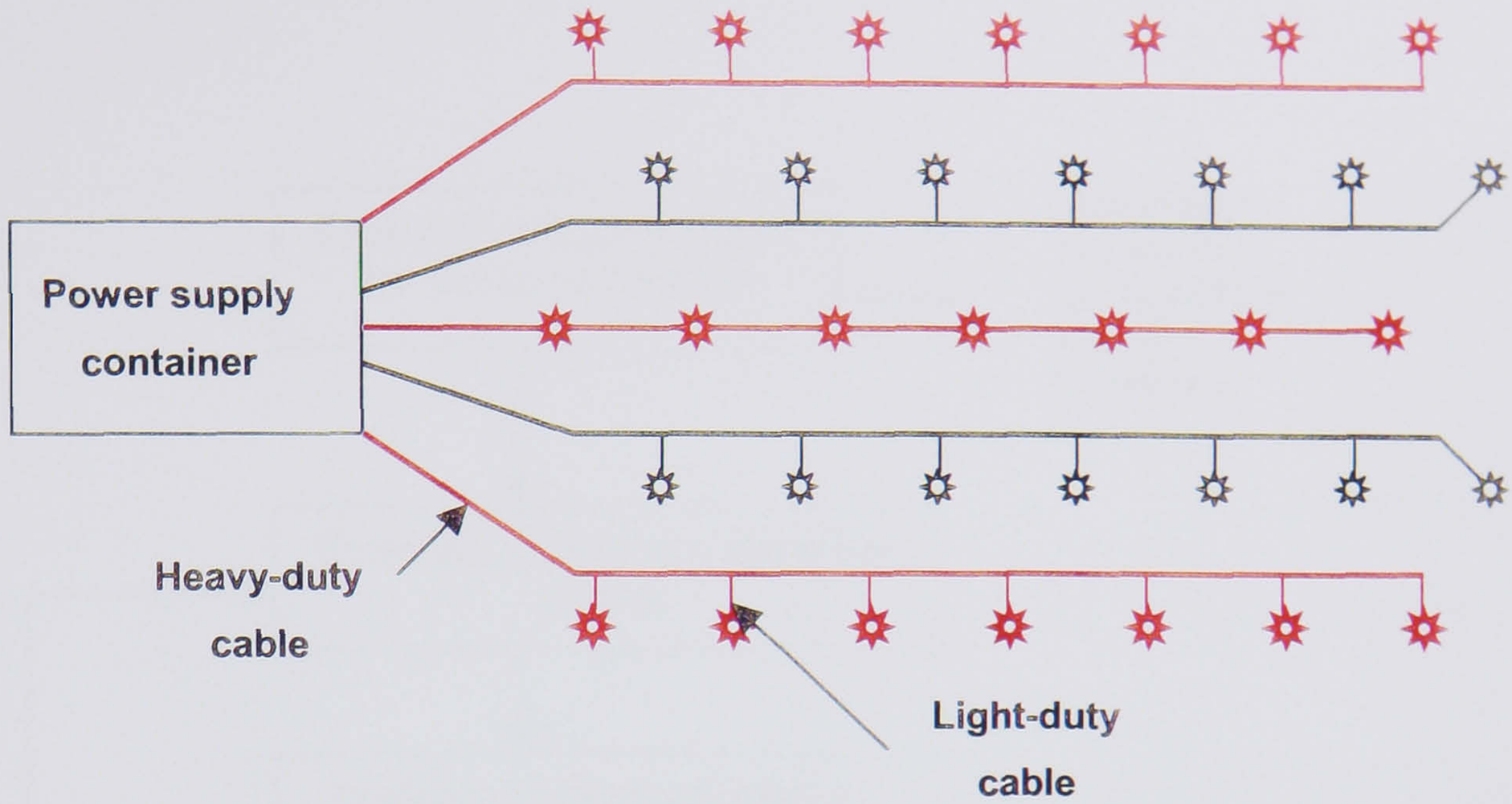

Figure 7.16 Alternative wiring system for electro-osmotic consolidation

A monitoring regime for a consolidation trial should contemplate the following variables.

- Surface settlements.
- Electrical power.
- Variation in undrained shear strength/stiffness.
- Variation in plasticity and water content.
- Water yield at cathodes.

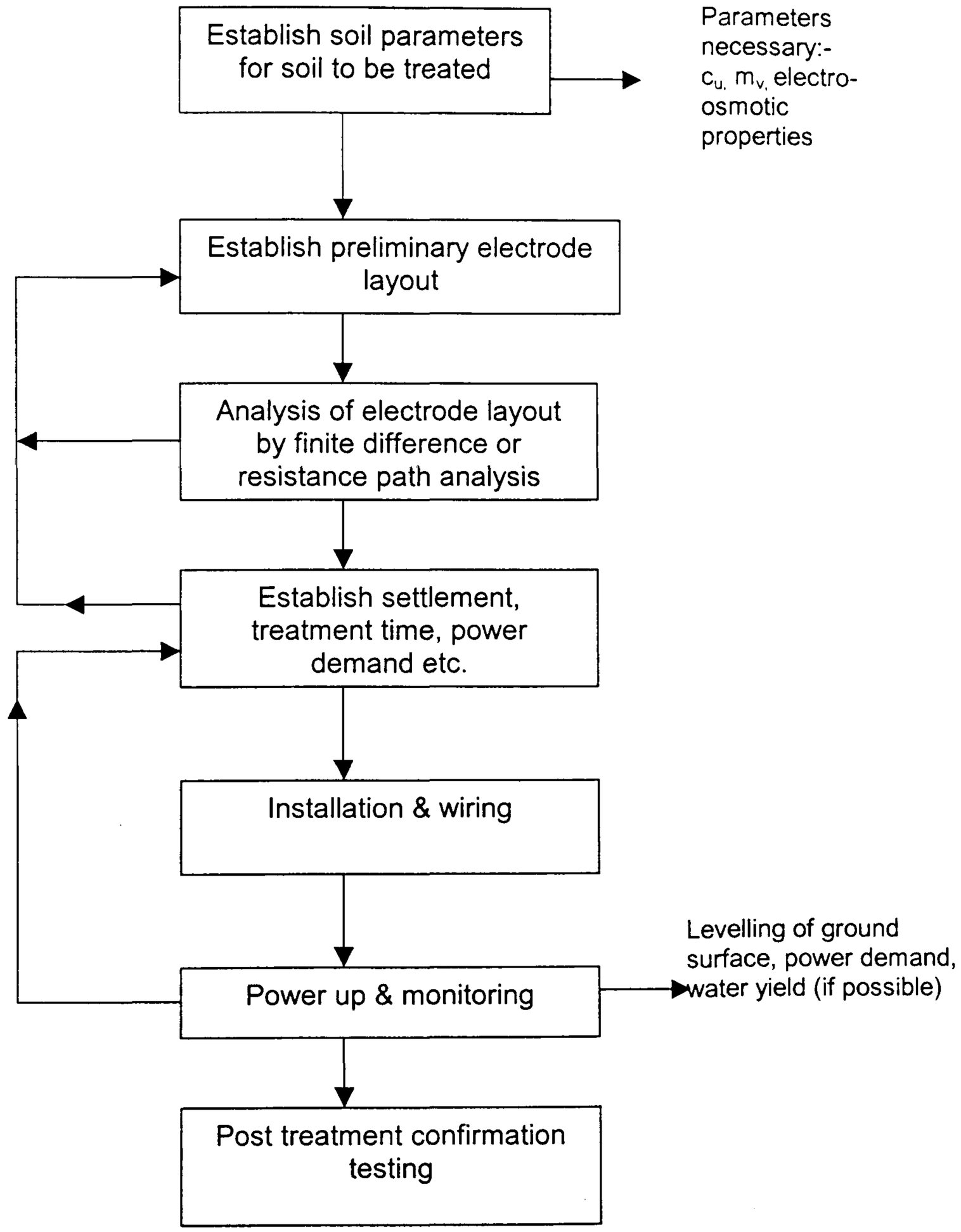

Figure 7.17 Flowchart of design and construction process for electro-osmotic consolidation

7.4 DESIGN FOR ELECTRO-OSMOTICALLY ENHANCED COHESIVE REINFORCED SOIL

The design procedure for electro-osmotically enhanced cohesive reinforced soil has been discussed in detail in § 5.7.3. The purpose of this section is to give an overview of the philosophy that has been developed for the design of an electro-osmotically enhanced cohesive reinforced soil by the Author. The chronology for the design of electro-osmotically enhanced reinforced soil is presented in Figure 7.19, which is a flow chart detailing the procedure to be undertaken for the design, construction and monitoring of an electrokinetically enhanced reinforced cohesive soil wall, the steps outlined in Figure 7.19 are elaborated upon in the following sections.

7.4.1 ESTABLISHMENT OF SOIL PARAMETERS

The soil parameters that have to be established for design are given in Table 7.13, along with the reasons for the establishment of these parameters.

Table 7.13 Soil parameters required for e-o enhanced reinforced soil

Parameter	Reason
Soil acceptably criteria for treatment by electro-osmosis - see § 7.2	To assess if the soil is treatable by e-o and if it will be economically viable
Undrained shear strength- water content relationship	To establish the water content reduction necessary to achieve short tem stability
Oedometer test on soil at the water content at which it is to be placed	Establish a prediction of the settlement that will occur during the electro-osmosis treatment process
Effective stress soil parameters c´& ϕ ´	Used for the long tem design of the reinforced soil wall

From the tests undertaken and using the criteria outlined in §7.2, it is possible to determine if the proposed fill material is amenable to treatment by electro-osmosis, and if the treatment will be economically viable. If the soil is found to be suitable to treatment by electro - osmosis the next stage is the design of the reinforcement layout using long-term design principles.

7.4.2 LONG-TERM DESIGN

The long term design of the wall, to establish the reinforcement layout, should be undertaken using critical state soil parameters due to the increased deformation required for strain compatibility when cohesive soil types are used, see §5.3. Additionally, careful consideration should be given to the value of effective cohesion (c´) used for long-term design, if the value of c´ is questionable a conservative assumption is to assume c´= 0.

Using the critical state soil parameters established from laboratory testing the long-term analysis should be undertaken using a tie-back wedge analysis (see Annex B). A coherent gravity type analysis is not considered suitable for the analysis of cohesive reinforced soil due to its empirical origins from field observations of high quality fill structures reinforced with high stiffness steel reinforcement. The complete opposite of cohesive reinforced soil where it is recommended that polymeric grid type reinforcement is used (Jewell 1980), see § 5.6.1. Using this methodology and analysis method the reinforcement layout is established for the structure.

7.4.3 SHORT-TERM DESIGN

The short-term design of the wall is undertaken using the reinforcement layout established from the long-term analysis, and is used to establish the required value of the undrained shear strength of the cohesive fill necessary to achieve short-term stability. The short-term stability analysis methods that are recommended to be undertaken are:

- Critical height - § 5.7.3.2.
- Coulomb - § 5.7.3.3.
- Discrete Theory - § 5.7.3.4.
- Composite Theory - § 5.7.3.5.

Using these analytical methods a range of values for the undrained shear strength of the cohesive fill is obtained based upon whether the presence of the reinforcement is considered or not. The higher values of undrained shear strength obtained from analysis are associated with the absence of reinforcement and the lower values considering its presence.
From the range of values established for the undrained shear strength a decision is made as to what value is required to ensure the short-term stability of the wall. The factors that need consideration to ascertain the value of undrained shear strength to be adopted include the rate of construction, accuracy of the monitoring techniques, accuracy of laboratory testing and the importance of the structure. Hence, the design value of undrained shear strength that electro-osmosis is required to achieve is obtained.

7.4.4 ELECTRO-OSMOTIC DESIGN

The required value of the undrained shear strength necessary for short-term stability has been ascertained using the short term stability analysis methods discussed in the previous section, §7.4.3, and a decision as to what value should be adopted taken. From laboratory and/or field testing it is possible to establish the initial undrained shear strength of the

cohesive fill material and its initial water content. Thus, the gain in undrained shear strength required for stability may be calculated as the difference between initial and required, and additionally the percentage reduction in water content from the laboratory relationship established between undrained shear strength and water content, as shown in Figure 7.18.

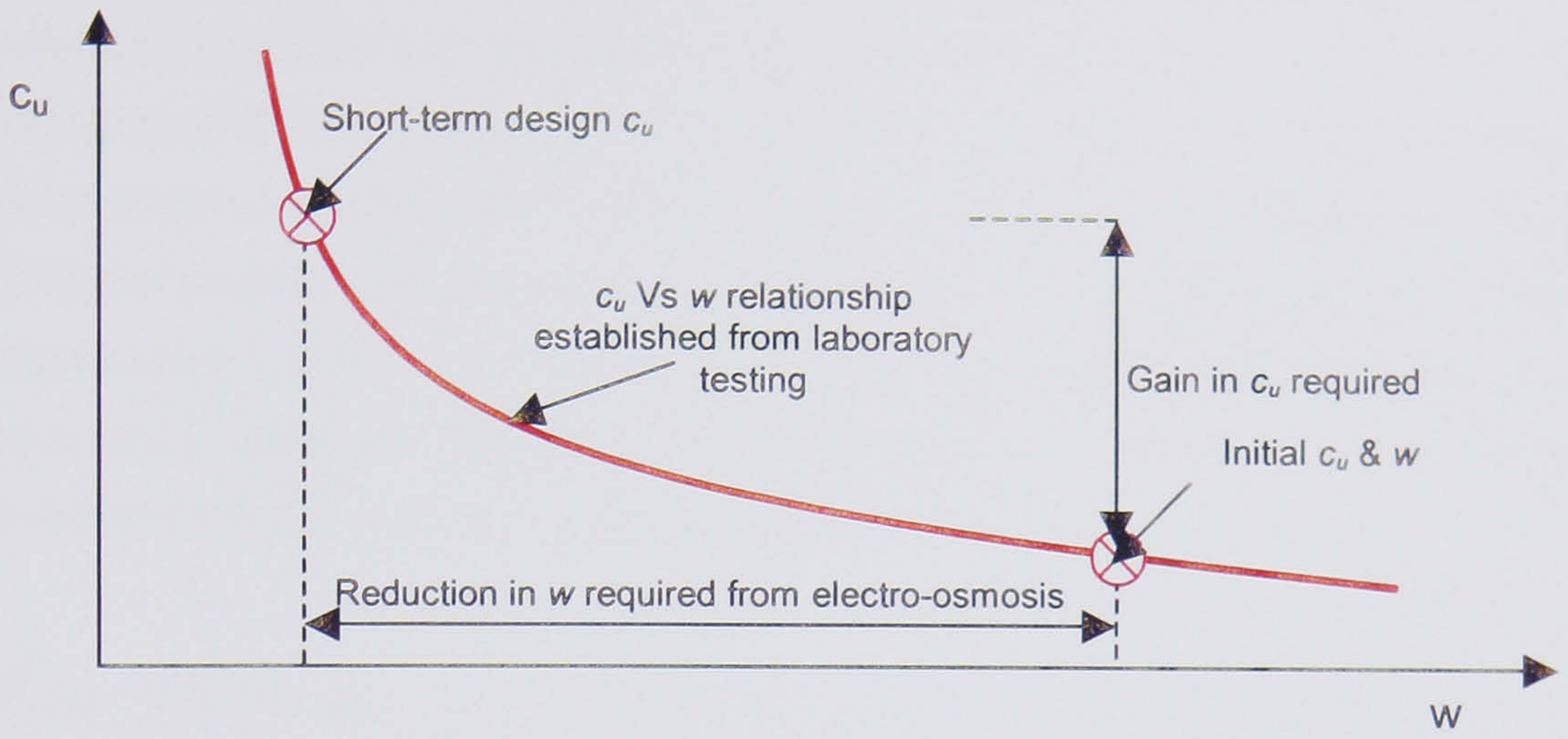

Figure 7.18 Calculation of reduction in w to achieve required increase in c_u

Knowing the required reduction of water content and the volume of fill to be treated, in any one lift, the volume of water that electro-osmosis is required to remove from the cohesive fill may be calculated, similar to the procedure undertaken for the Joint Stocks wall (see Annex D). The theory of electro-osmosis is then used to calculate the time required for the removal of the quantity of water (Q), as given in § 5.7.4.1.

$$\frac{Q}{t} = k_e \frac{V}{L} A \qquad \text{(Eqn. 5.32)}$$

The key variables in this equation are the values of k_e and V/L used for calculation, as the value of A is fixed by the geometry of the application.

The Author suggests that the best method of utilising Equation 5.32 is by means of a spread sheet where the volume of water removed over finite periods of time are calculated and from which the cumulative total volume of water removed may be calculated. In this way, it is possible to take into account the variation of k_e with time, which is obtained from laboratory tests on the fill material at the same water content and voltage gradient as will be used in the field. The other difficult parameter to asses for the calculation of the treatment time is the value of V/L. As a preliminary estimation, a simplistic linear variation may be assumed, i.e. dividing the applied voltage by the distance between the anodes and cathodes. This estimation will underestimate the treatment time as it over predicts the voltage gradient, as shown in Table 5.10, and assumes a fully 1-D electrical field. A more realistic estimation methods for the magnitude of the voltage gradient can be obtained by using the resistance path or preferably the finite difference method described in § 7.6.

An additional benefit of using the spreadsheet method for calculating in a step-wise manner the reduction in water content, is that an estimation of the variation of the undrained shear strength with time may also be obtained by using the relationship between water content and undrained shear strength obtained in the laboratory, see Figure 7.18.
The prediction of the electrical power that will be drawn by the field installation is difficult to estimate due to the variation of the electrical conductivity of the soil with time and the high variability of the electrode-soil interface resistance. The extrapolation of the soil conductivity determined using disk electrodes in the laboratory to the full-scale structure using discrete EKG electrodes could also lead to discrepancy. As a result the prediction of the current drawn using a simple 1-D resistive block model significantly overestimates the current drawn by a field installation. The experimental and fieldwork undertaken by the Author suggest that a reduction factor of up to 0.1 should be employed i.e.:

$$\sigma_{field} = 0.1\sigma_{e-o\,cell} \qquad \text{(Eqn. 5.36)}$$

The percentage reduction in the value of the electrical conductivity measured with time in the field was found to closely follow that measured in the electro-osmotic cell and it is suggested that this method is employed for design purposes.

7.4.5 CONSTRUCTION AND MONITORING

The construction of reinforced electro-osmotically enhanced cohesive soil has been described in detail in §5.7.6.3 and the reader is referred to this section for further information.
The monitoring regime for a reinforced electro-osmotically enhanced cohesive soil structure should cover the following elements:

- Fuel consumption.
- Variation of undrained shear strength/water content with time.
- Movement of the structure caused by the removal of water.
- Electrical power.

Additionally, an observational approach to construction should be adopted, comparing the design values and their development with time against those observed in the field, and the treatment modified as necessary.
It is also suggested that the monitoring is continued after the electrical power has been turned off to quantify any further movement/strength changes caused as a result of consolidation under loading by the construction of subsequent overlying layers.

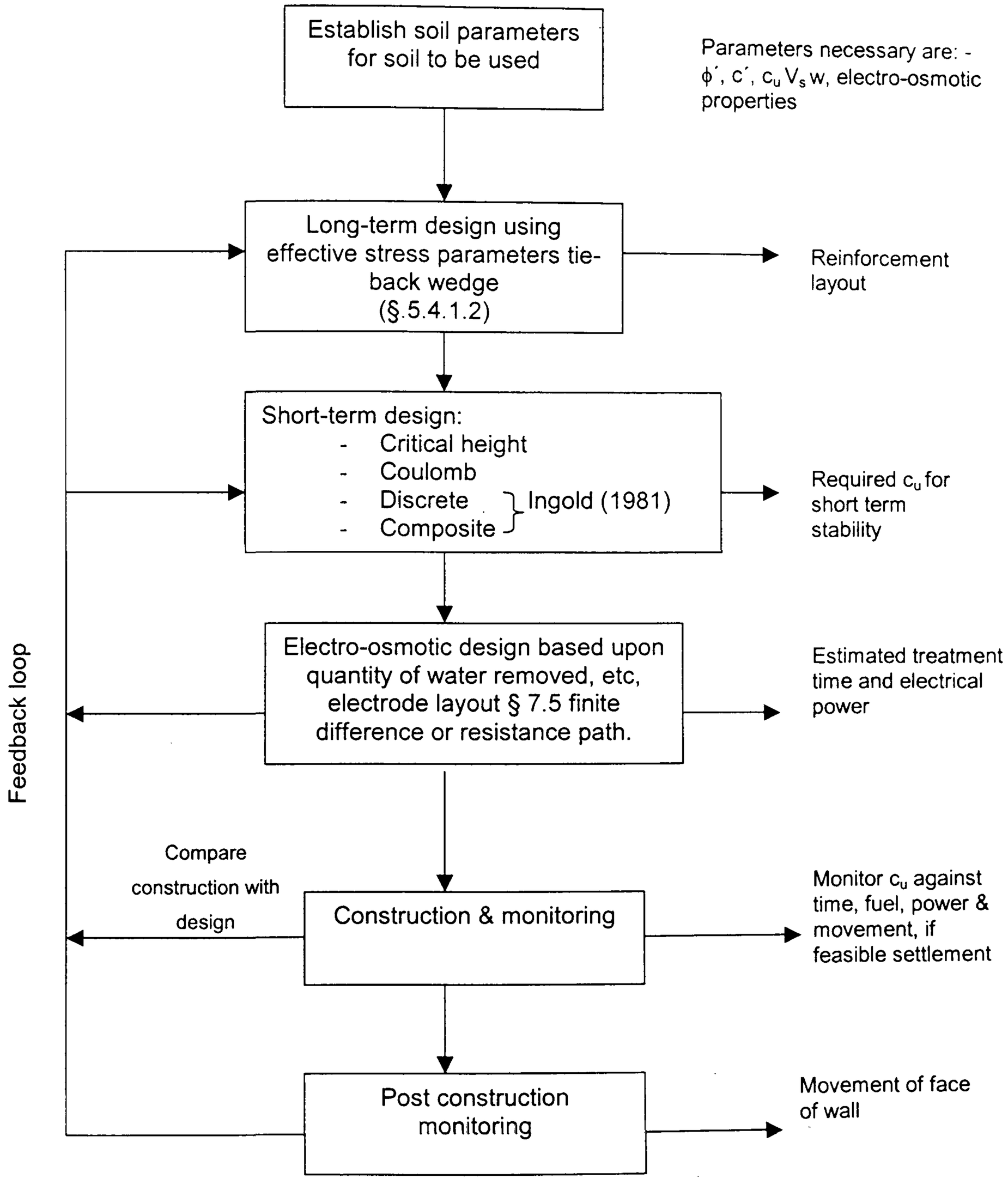

Figure 7.19 Flowchart of design and construction for electro-osmotically enhanced reinforced cohesive soil

7.5 DESIGN FOR ELECTRO-OSMOTIC VOLUME CONTROL

Although no field results have been obtained to confirm the validity of any design methods for volumetric control of soils by electro-osmosis, this section will provide suggestions as to how the Author would envisage any design method proceeding. The chronology for the design of electro-osmotic volume control application is presented in Figure 7.20.

Initially a suite of laboratory testing would be undertaken to assess the suitability of electro-osmosis to the soil type and fabric in question in a similar manner to those discussed in §7.3.1 & §7.4.1. Specific volumetric control testing may then be carried out on undisturbed samples of soil. This type of test would most likely be undertaken in the electro-osmosis cell or in some type of electro-osmotic oedometer of the type developed by Wan & Mitchell (1975) and Nicholls & Herbst (1967) in which the swelling pressure could be measured and the soil subjected to cycles of wetting and drying. Such work has been undertaken by Gwede (2000) although the results of this research are yet to be published.

Once the volumetric change and the consolidation settlement has been determined from the laboratory testing, the design of the electrode installation can proceed. This is best achieved using a finite difference analysis, although the resistance path method may also be applicable (see §7.6).

The installation method employed may be by means of a hydraulic crawler drill or similar, or some other means depending upon the required inclination of the electrodes and the accessibility to the site.

The monitoring for such an application should consider the following variables:

- Electrical power.
- Fuel consumption (if a generator is employed).
- Shear strength / stiffness.
- Water content - volume of water removed (if feasible).
- Settlement.

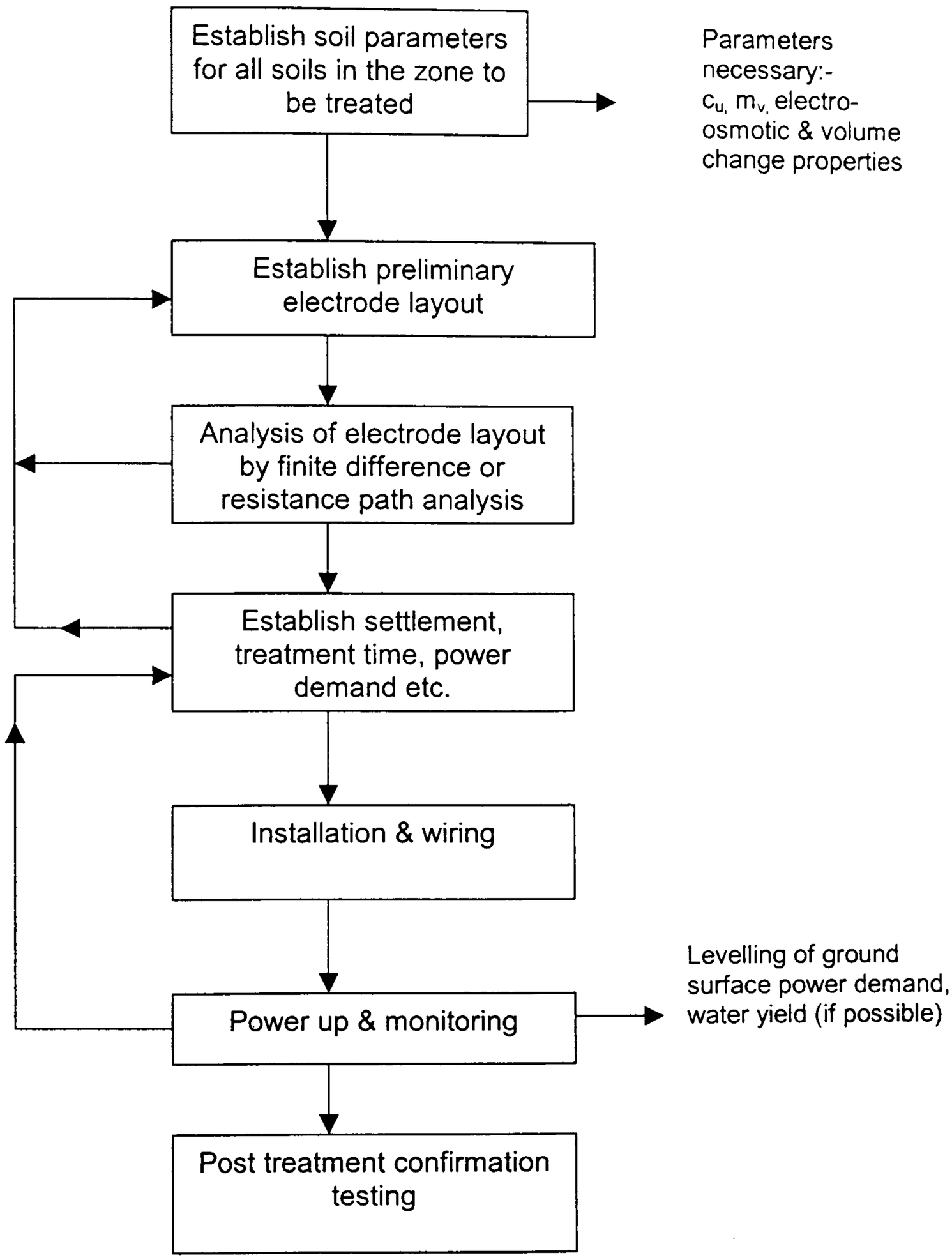

Figure 7.20 Design flowchart for electro-osmotic volume control

7.6 ANALYSIS OF ELECTRODE CONFIGURATIONS

There are three types of electrode configuration that may exist in practical electro-osmotic applications to geotechnical engineering. They may be classified depending upon the type of electrodes employed, and the equipotential field generated:

- **1-Dimensional**: - assumed to produce linear, equally spaced, equipotentials as a result of the generation of an electrical field by plate electrodes, or extremely closely spaced point electrodes.
- **Radial**: - circular equipotentials produced by discrete point electrodes unaffected by adjacent electrodes of like or unlike polarity.
- **Hybrid / complex**: - Non-linear or non-circular equipotentials produced as a result of the interaction of electrical fields produced by point electrodes that are within the zone of influence of one another.

These three forms of equipotential field are shown diagrammatically in Figure 7.21a, b & c respectively.

The ideal configuration for most electro-osmotic applications is one that makes the maximum use of the electrical potential available and produces as uniform an equipotential field as possible. The equipotential distribution that fulfils these requirements is the 1-dimensional field. However, for economic reasons it is seldom possible or feasible to install sufficient point electrodes or plate electrodes to produce a truly 1-dimensional field and in the majority of cases a hybrid / complex field is employed.

The problem that arises is how to measure quantitatively the equipotential field produced by a discrete electrode installation producing a complex / hybrid field in such a way that the analysis produces values for the potential gradient that may be used for electro-osmotic calculations. The available published literature on electrode configurations is meagre and unspecific and offers little, and sometimes conflicting, advice. Some of the more useful references include (see Figure 7.21c for spacing nomenclature):

i. Casagrande (1983) suggested spacings of 10 to 20ft (3.05 to 6.1m) between AC (Anode - Cathode) depending upon applied voltage and time available for treatment, but made no mention of AA (Anode - Anode) or CC (Cathode - Cathode) spacing.

ii. Schultz (1997) investigated the economics and calculation of optimum spacing, time and energy requirements for a 1-Dimensional sheet electrode configuration. The outcome of this investigation was that for minimal costs the longest possible

treatment time should be used together with a large AC spacing (≈5m), at a reduced potential difference.

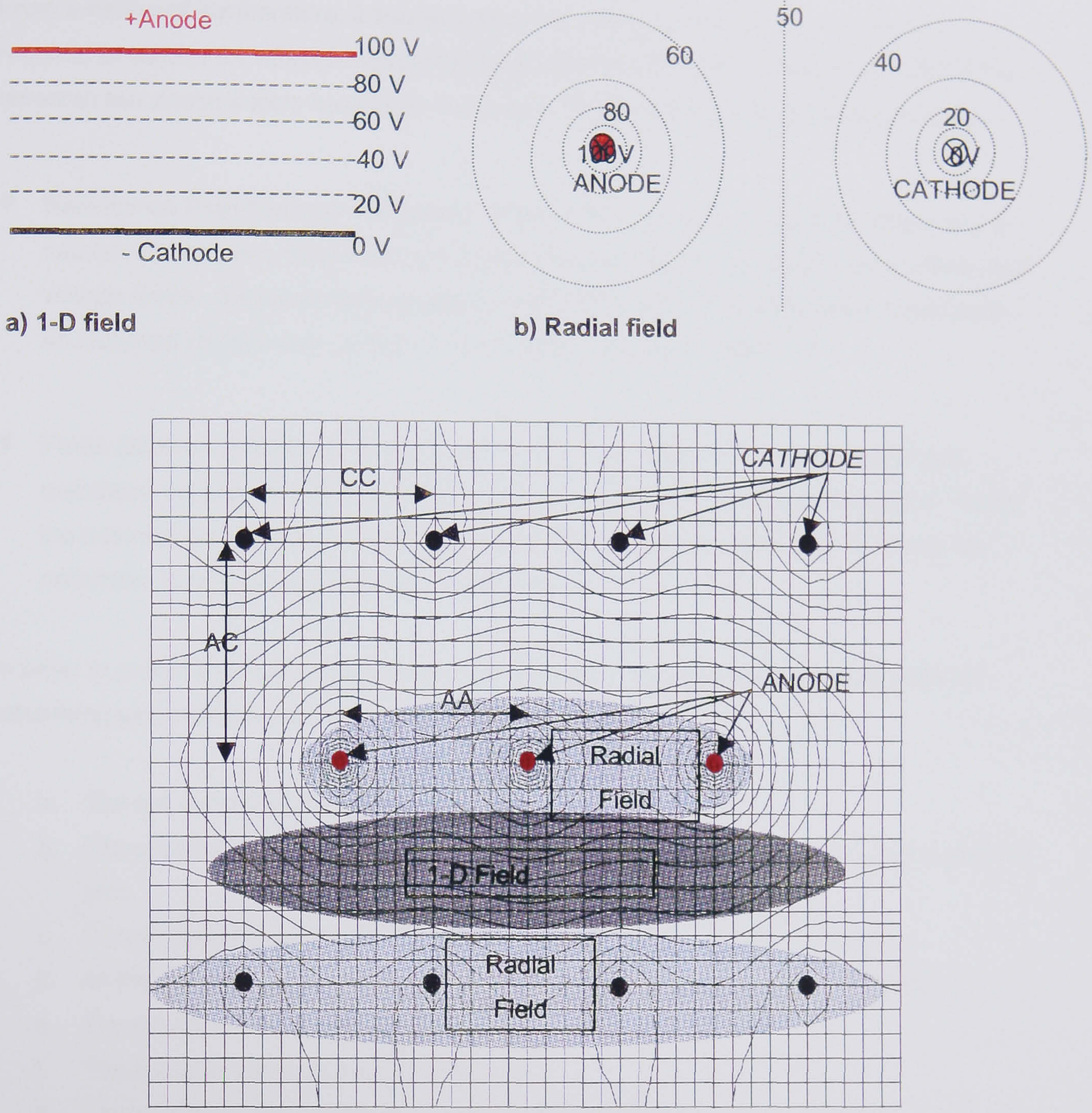

Figure 7.21 Equipotential field types

iii. Shang (1998) indicated that a uniform (1-D) electrical field may be assumed, provided that the depth of the electrodes exceeds the AC spacing and that the AC spacing is greater than the AA/CC spacing. No mention is made of the efficiency or economics of systems with regard to different AC and AA/CC spacings.

iv. Alshawabkeh *et al* (1999) undertook a study of 1-D and 2-D electrode configurations and looked into five different electrode configurations. The analytical method adopted was simplistic, using triangular zones of inefficiency based upon the electrode array geometry. This analytical method is considered by the Author to be

overly simplistic and qualitative for the analysis of realistic and large-scale electrode installations.

From a review of the literature, it was apparent that more rigorous analysis tools were required to assess the effectiveness of different electrode installation arrays. As part of this research two analysis tools have been developed for the investigation of electrode arrays.

- **Resistance Path Method**: Calculates 18 paths of resistance between an anode and a cathode based upon elemental cell resistances and, hence, calculates path currents and voltage drops. Simplified electro-osmotic flow calculations are undertaken based upon an idealised parallel zone portion of the paths of resistance, see § 7.6.1.

- **Finite Difference Method**: The finite difference approach uses a spreadsheet that calculates the electrical equipotential distribution based upon Laplace's equation. From the potential distribution, the average potential gradient along each flow path may be calculated in one or two directions, see § 7.6.2.

In order to proceed with these analytical methods it was necessary to make a number of simplifying assumptions that include (after Mitchell 1993):

a. The soil is homogenous and saturated.
b. The physical and physiochemical properties of the soil are uniform and constant with time.
c. No soil particles are moved by electrophoresis.
d. All the applied voltage is effective in moving water, i.e. no heat is generated.
e. The electrical field is constant with time.
f. There are no electrochemical reactions.
g. The Helmholtz-Smoluchowski equation is applicable.

The assumptions are incorrect due to the complexity of electrokinetic phenomena. However, to take these factors fully into account would greatly complicate any analysis and render it extremely non-user friendly. Some simplified assumptions may be made to increase the accuracy of the models developed and these are discussed further in §7.6.1.1.

7.6.1 RESISTANCE PATH METHOD

This concept was developed by Wrigley (1999) to determine the electrical power requirements of an electro-osmotic installation to aid the commercialisation of EPSRC research project GR/L66090. The principle adopted is as illustrated in Figure 7.22.

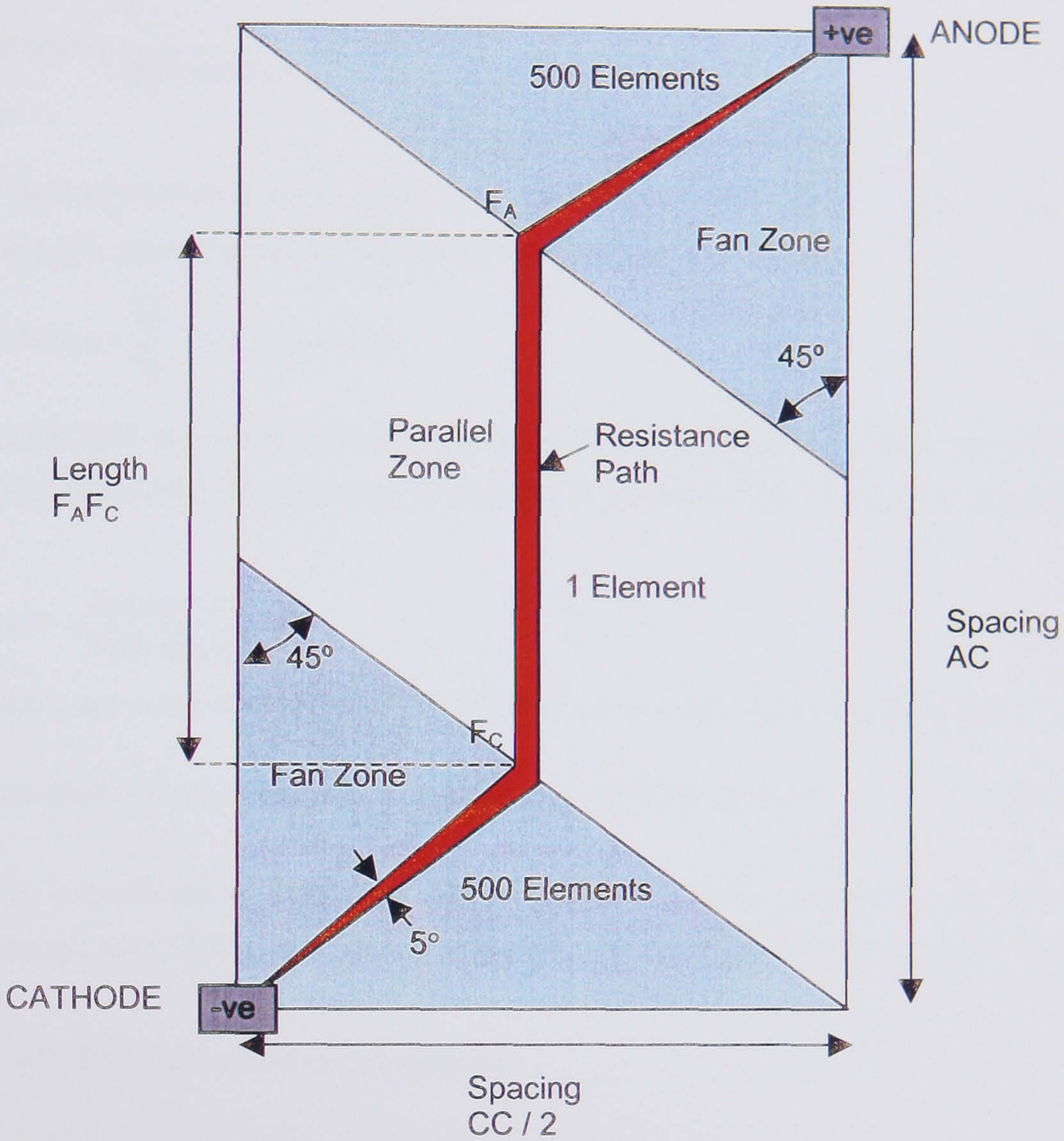

Figure 7.22 Resistance path concept (after Wrigley 1999)

The layout adopted for analysis assumes that the anodes and cathodes are arranged in a diamond pattern, i.e. the anodes are staggered relative to the cathodes. The unit of symmetry for analysis of the installation is thus a quadrant as shown in Figure 7.22. Each quadrant is subdivided into 18 resistance paths, with each resistance path consisting of 3 sections, fan-parallel-fan. At each end of each path there is a fan section that subtends an angle of 5°. The commercial EKG anodes/cathodes, for which the system was devised, have a circumference of 200mm. It was, therefore, assumed that each fan section has a width of 50/18 mm (2.8mm) adjacent to an anode/cathode. The "fan" zone of the resistance path is divided into 500 trapezoidal elements, with the width of each element being calculated by trigonometry. The average width of each trapezoidal element can thus be calculated and the length of each element obtained by geometry. As the depth of treatment is also known the average cross-sectional area of each trapezoidal element can be

calculated. The parallel zone of the resistance path is divided into one rectangular element, its width being calculated from the length of the fan-parallel boundary subtended by each 5° fan, and its length (F_AF_C) being calculated by geometry. The cross-sectional area of the element is then calculated from its width and depth.

Once the cross-sectional area and length are known for all elements the resistance of each element may be calculated from the conductivity of the soil. Thus:

$$\text{Cell resistance} = \frac{\text{Cell length}}{\text{Soil conductivity x Cell cross - sectional area}} \qquad \text{Eqn. 7.10}$$

The total path resistance is determined from the sum of all the cell resistances, trapezoidal and rectangular, along the particular resistance path under consideration:

$$\text{Path resistance} = \sum_{0}^{1001} \text{Cell resistances} \qquad \text{Eqn. 7.11}$$

Assuming the cells act as resistors in parallel and knowing the electrical potential difference between the anode and the cathode it is possible to determine the current per resistance path:

$$\text{Path current} = \frac{\text{Applied voltage}}{\text{Path resistance}} \qquad \text{Eqn. 7.12}$$

The quadrant current is determined from the path current and the total current is:

$$\text{Total electrode current} = 4 \text{ x Quadrant current} = 4 \text{ x} \sum_{0}^{18} \text{Path current} \qquad \text{Eqn. 7.13}$$

The voltage drop across each element can be calculated from its resistance and as the total current through each resistance path is known the voltage gradients can be determined:

$$\Delta V_{Element} = \text{Path current x Element resistance} \qquad \text{Eqn. 7.14}$$

7.6.1.1 Flow Calculation By The Resistance Path Method

The calculation of electro-osmotic flow by the resistance path method is based upon the average voltage drop across the 18 rectangular elements in the parallel zone of the analysed quadrant, see Figure 7.22. It is then assumed, by conservation of mass, that the rate of flow in this region must be equal to the rate of flow out of the cathode:

$$\text{E - O Flow} = k_e \text{ x} \left(\text{Average} \frac{\Delta V \text{ in parallel zone}}{\text{Length } F_AF_C} \right) \text{x A} \qquad \text{Eqn. 7.15}$$

This assumes that flow is entirely one-dimensional in the anode to cathode direction and that no orthogonal flow takes place (i.e. any interaction between horizontally adjacent cells is ignored).

The approximate time for dewatering a given volume of soil mass using the resistance path method is given by the following equation:

$$\frac{(\text{Vol. of Water to be removed per m}^3\text{ of soil}) \; x \; AC x \frac{CC}{2} \; x \; \text{Depth}}{\bar{k}_e \; x \; (\text{Average } \Delta V/L \text{ in parallel zone}) \; x \frac{CC}{2} \; x \; \text{Depth}} = \frac{(\text{Vol. per m}^3) \; x \; AC}{\bar{k}_e \; x \; (\frac{\Delta V}{L})} = \text{Treatment time}$$

Eqn. 7.16

It is possible to refine the resistance path analytical method to make the output more realistic using either or both of the following methods:

i. ***Reduction of electrical conductivity:*** a reduction factor for the value of the electrical conductivity of the soil may be included. The reduction factor can be applied directly to the input value of electrical conductivity and as such acts as an average value and does not take into account the large variation at the beginning of treatment, nor the significantly reduced conductivity value towards the end of treatment.

ii. ***Reduction of electro-osmotic permeability:*** Similar to that applied to electrical conductivity; a global reduction factor for the electro-osmotic permeability may be used. Again, this does not take into account the initial peak in the value of electro-osmotic permeability, or the reduced value after a period of treatment has passed.

7.6.1.2 Advantages And Disadvantages Of The Resistance Path Method

Advantages include:

- Easy to programme into a spreadsheet.
- Easy to incorporate into a "Black-box" type system.
- The mathematical inaccuracies in the method may be small in comparison to the variation in actual soil properties in a practical application.

Disadvantages include:

- The resistance paths have discontinuities at the electrode/soil interface and at the transition from the fan zone to the parallel zone.
- It is difficult to modify for non-diamond patterns of electrode installation and different electrode geometries.

- The reduction factors on electrical conductivity and electro-osmotic permeability do not take into account fully the true time dependant variation of these parameters. The result is an underprediction for short treatment times and an overprediction for long treatment times, both of the actual treatment time and the power drawn.
- Horizontal interaction between resistance paths is not considered.

7.6.2 FINITE DIFFERENCE METHOD

This analytical method was developed by the Author to analyse electro-osmotic installations as part of the EPSRC research programme GR/L66090 "Materials for Better Construction". The theory and method of analysis adopted by the finite difference method and its application to a conventional computer spreadsheet are discussed in the following sections.

7.6.2.1 Theoretical Background To The Finite Difference Analytical Method

The distribution of electrical potential over a plane area subject to certain boundary conditions is governed by Laplace's equation, Equation 7.17 (Stroud 1990).

$$\frac{\partial^2 \phi}{\partial x^2} + \frac{\partial^2 \phi}{\partial y^2} = 0 \quad \textit{Laplace's Equation} \qquad \text{Eqn. 7.17}$$

Where the potential function (ϕ) is a function of position (i.e. $V=\phi(x, y)$) and is independent of time. Das (1985 & 1997) demonstrated that seepage, which is also governed by Laplace's equation, may be represented approximately by finite difference equations. Smyrell (1991) showed how the finite difference solution for the related Poisson equation may be obtained by the use of a computer spreadsheet and developed examples for its application to torsional stiffness calculations of structural members. Williams *et al* (1993) illustrated that the use of a finite difference solution programmed into a computer spreadsheet could be used to obtain the solution of Laplace's equation for the calculation of hydraulic equipotentials based upon the equations developed by Das (1985). Thus, it is postulated that, electrical equipotentials which are also governed by Laplace's equation can be calculated using the same methodology as that developed by Williams *et* al (1993).

7.6.2.2 Philosophy Of Spreadsheet Finite Difference Analysis

The equipotential field generated by any array of electrodes can be modelled using a selection of standard nodes based upon a traditional 5-point element scheme. The nodes used in the spreadsheet and their associated functions are shown in Table 7.14.

The spreadsheet used for the analysis was Excel 97 (Microsoft 1997). Using the different node types given in Table 7.14 the complete electrode installation or a portion of the electrode installation may be meshed. The electrodes are modelled by using cells that contain assigned values of the maximum applied voltage at the anodes or zero volts (0V) at the cathodes.

Table 7.14 Spreadsheet - node types and function

Molecular Schematic of Node	Equation / Value	Usage
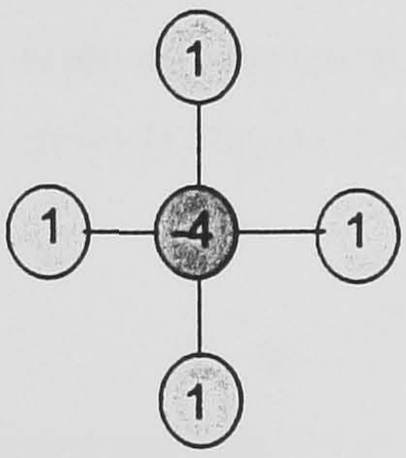	$h_0 = \frac{1}{4}\left(\sum_{x=1}^{4} h_x\right)$	General soil node
	Cathode X = 0 Anode X = Voltage applied	Anode/cathode nodes
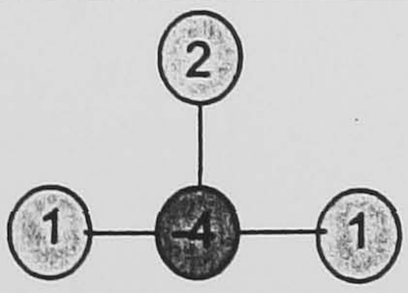	$h_0 = \frac{1}{4}\left(\sum_{x=1}^{2} h_x + 2h_2\right)$	Edge boundary node
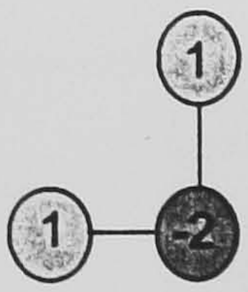	$h_0 = \frac{1}{2}\left(\sum_{x=1}^{2} h_x\right)$	Corner boundary node

Once the area had been meshed using the Finite difference elements the mesh was iterated to an accuracy of maximum change per iteration of 0.00001. Following this, the potential difference across each finite difference cell was calculated in the relevant direction, usually in the direction anode-cathode (dV/dx), and converted into a potential gradient, based upon the size represented by the finite difference cell (dx or dy). Subsequently the minimum, maximum and average cell potential gradients could be calculated for each column of cells. This method is shown in Figure 7.23.

An alternative method to calculate the average potential gradient was also used in subsequent calculations. This method consisted of producing a graph of the absolute values of the potential difference in each cell for the particular column of cells to be analysed. A best-fit line was then fitted over the portion of the graph of interest, usually the portion between anodes and cathodes, vertically along the cathode axis, anode axis and at a point midway between the two, these axes are shown in Figure 7.24. The gradient of the best-fit line gives the average potential gradient over the vertical column selected.

The results of calculating the potential gradients in these two different ways are presented in Figure 7.25. Figure 7.25 relates to the analysis employed in the Joint Stocks reinforced soil trial for an electrode spacing of 0.8m over an overall depth of clay of 600mm, see §5.7.4.2 and Table 5.10. Using these graphical methods the variation in the potential field may be deduced and a representative value of dV/dx selected for use in electro-osmotic calculations. In addition, if horizontal columns are used instead of vertical columns the values of dV/dy may also be obtained for use in orthogonal flow calculations. A screen extract of the Joint Stocks finite difference mesh with the columns used to obtain the graphs presented in Figure 7.25 is given in Figure 7.24.

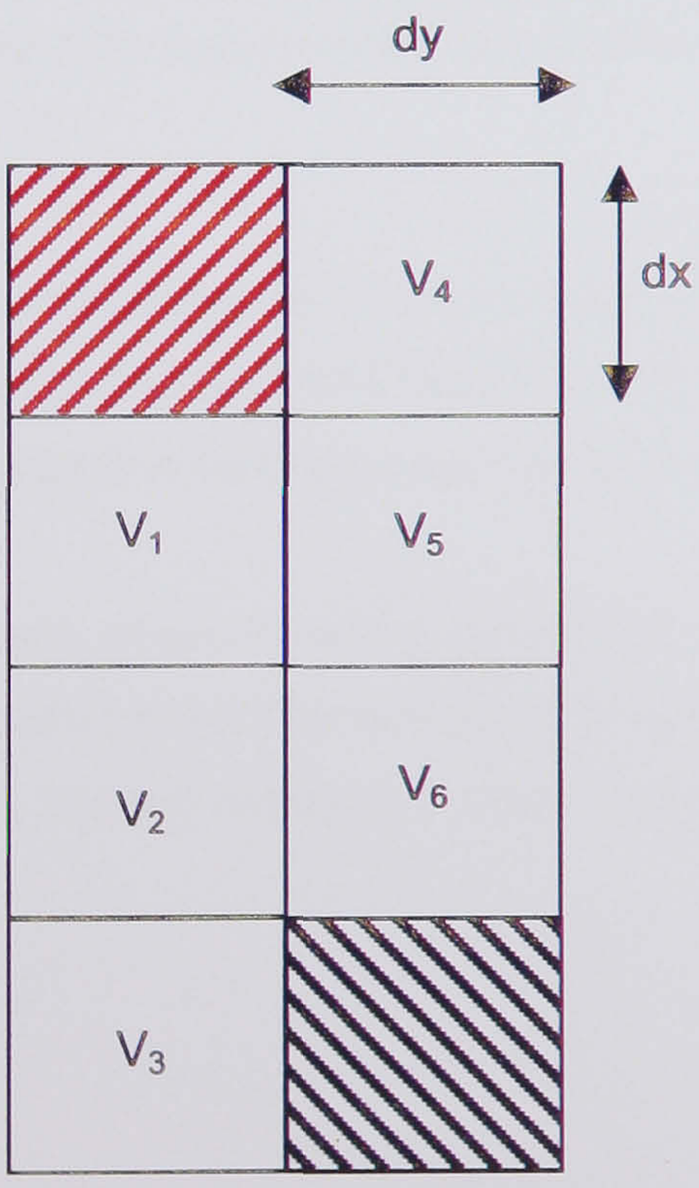

$$\frac{dV}{dx} = \sqrt{\left(\frac{v_1 - v_2}{dx}\right)^2}$$

$$\frac{dV}{dy} = \sqrt{\left(\frac{v_1 - v_5}{dy}\right)^2}$$

Figure 7.23 Calculation of potential gradients across finite difference cells

The geometry of the finite difference mesh used in the analysis is key to the accuracy of the output obtained. The Author has found that, as a general rule, the maximum cell size should be the same size as the electrode, although if the cells are smaller then accuracy is improved but calculation time is increased. Additionally, most spreadsheets have a limit to the width of the model that may be analysed, which limits the minimum cell size. For the Joint Stocks analysis 10mm x 10mm finite difference cells were employed with the

electrodes being represented by a rectangular block of cells 10mm x 100mm, i.e. 1 cell by 10 cells, Figure 7.24. A copy of the spreadsheet used for the calculation of the Joint Stocks wall voltage distributions is given on the CD accompanying this thesis (D:\Analysis\Finite difference.xls).

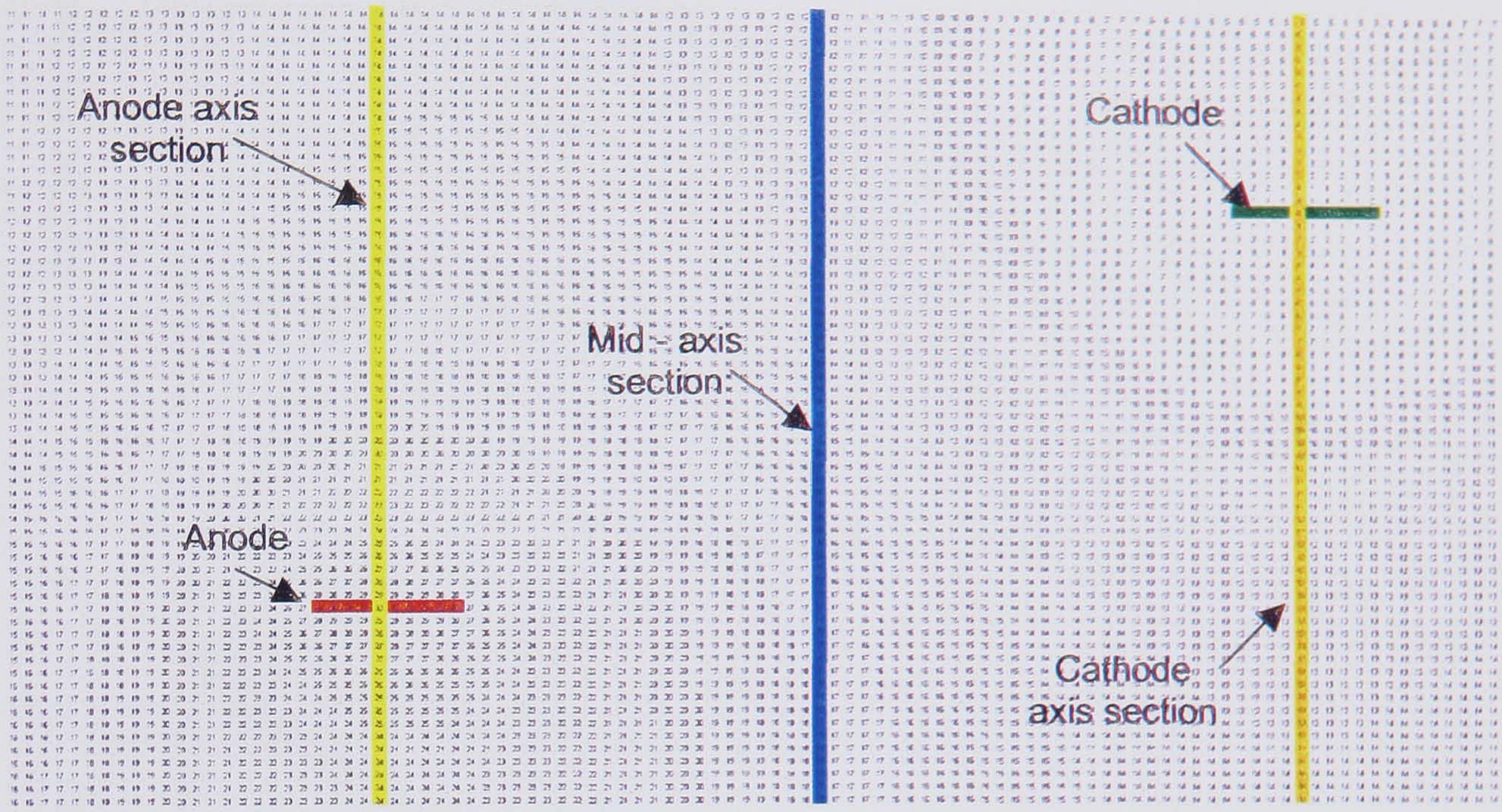

Figure 7.24 Screen print of finite difference mesh used for the Joint Stocks trial

When modelling the effects of electro-osmosis on reinforced soil the depth of the entire lift should be included and the extent of the analysis should include several electrode pairs. Analysing the central portion of the structure reduces the boundary condition effects.

Similarly, when modelling the effects of consolidation, a representative section of the installation should be taken with several electrodes on either side of the zone to be analysed. Again, this will reduce the effect of boundary conditions during analysis.

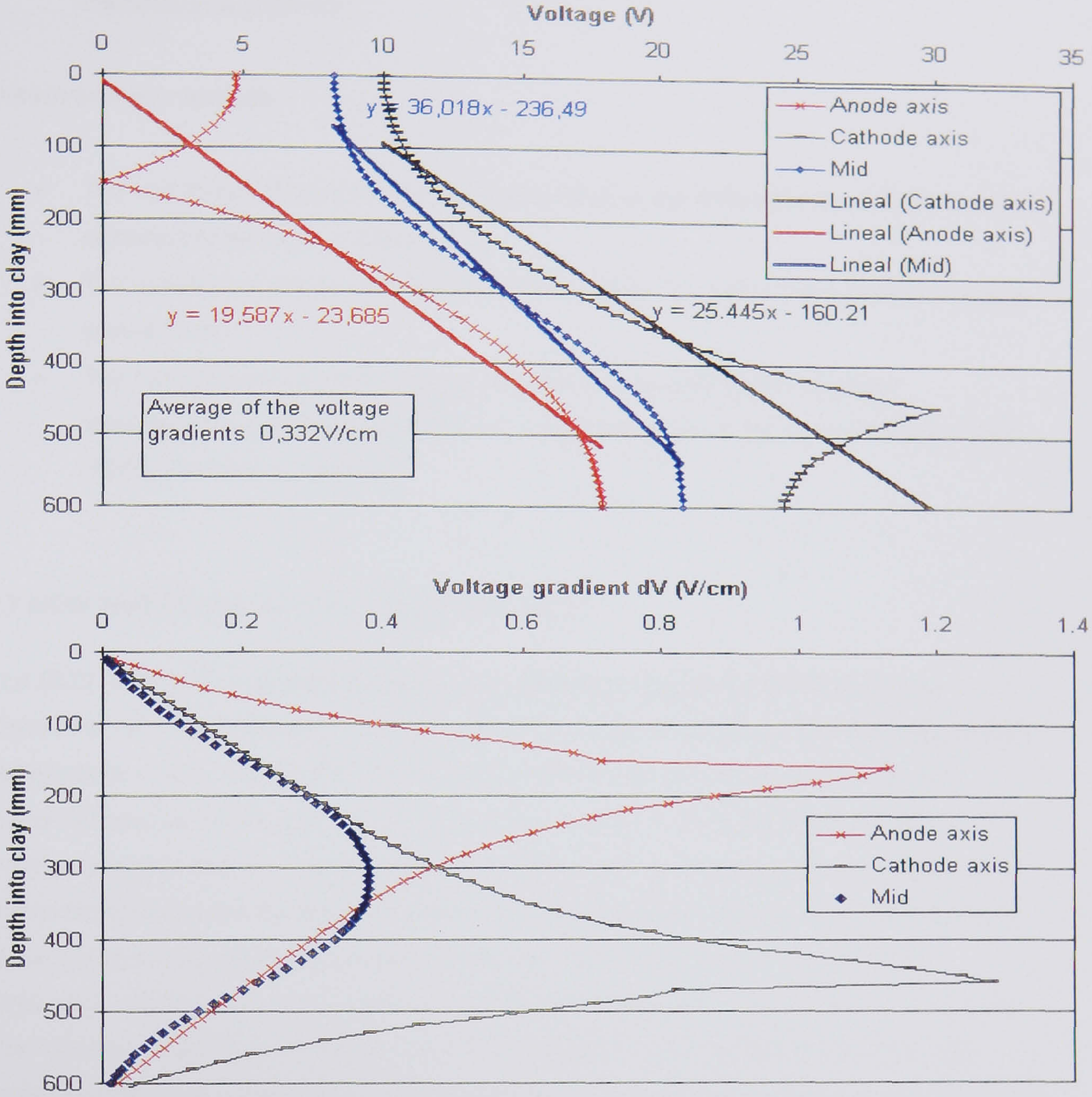

Figure 7.25 Examples of finite difference output for potential gradient calculations

7.6.2.3 Advantages & Disadvantages Of The Finite Difference Method

Advantages include:

- It is possible to model complete electrode installations, or a symmetrical section of an installation, regardless of the type of electrode array, i.e. standard / non-standard and the shape of the actual electrode.
- Voltage gradients, which may subsequently be used in an electro-osmotic spreadsheet calculation, can be determined. These can take into account the true variation in the electro-osmotic permeability with time obtained from laboratory testing.

- Cell errors in nodal calculations are easily detected as the complete voltage distribution is produced.

Disadvantages include:

- The calculation time is greater, both in setting up the finite difference mesh and in its subsequent iteration to solution.
- The variation of electrical power is not fully taken into account in subsequent power calculations.
- The finite difference method does not permit direct calculation of power requirements, and the assumption of a plate electrode or the use of Casagrande's (1983) equation is required.

7.7 NEW AND NOVEL APPLICATIONS FOR EKG

The EKG electrode developed by Netlon Ltd (1998) has limited durability, due to the electrochemical degradation of the conductive carbon black within the modified high-density polyethylene matrix, see §3.5.2. This results in the loss of electrical conductivity and increased porosity of the polymer covering to the metallic core of the EKG that would eventually lead to failure. The benefits of the EKG are that it is easy to install using conventional and currently available plant, it has a large surface area per unit length due to its net structure, it is easy to manhandle and it is more durable than normal metallic electrodes. Additionally, being formed from polymeric material it can be cut easily by hand. The following potential applications relate to the EKG in its current form with enhanced durability properties unless stated. The applications are assumed to take place in applicable soil types as discussed in §7.2.

7.7.1 TRENCHING & EXCAVATION

The EKG could be used in its existing form to produce localised lowering of the phreatic surface to allow trenching or other surface or sub-surface based excavation to take place. The operation could be single or multi-phase depending upon the circumstances. It would be possible to combine EKG dewatering with conventional well pointing technology in low permeability soils to achieve a more rapid drawdown of the phreatic surface, Figure 7.26.

An additional benefit of electro-osmotic dewatering is that the soil properties may be improved which will make excavation easier and more stable. A similar application has been suggested by Lomizé *et al* (1961).

PHASE 1	n/a	-	+	+	-	n/a
PHASE 2	-	+			+	-

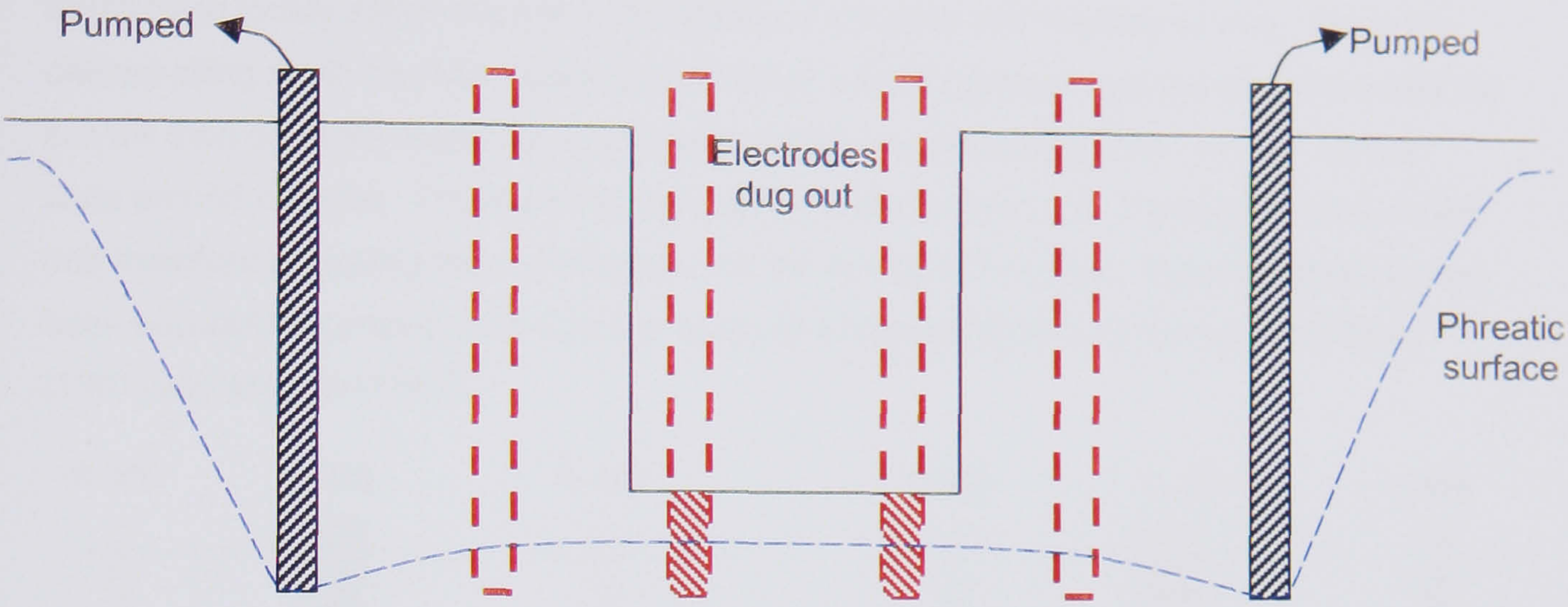

Figure 7.26 Multi-phase drawdown of the phreatic surface using EKG for excavation and trenching

7.7.2 TUNNELLING & PIPE-JACKING

Pipe-jacking or tunnelling in soft ground using a Tunnel Boring Machine (TBM), Earth Pressure Balance Machine (EPBM) or mining methods could be enhanced using EKG technology to improve the soil conditions in the vicinity of the tunnel or to reduce post construction settlements associated with the tunnel. If access to the surface was also available the EKG could be installed at the surface to assist the process. In addition, electro-kinetics could be used in very soft soils to reduce the possibility of chimney formation.

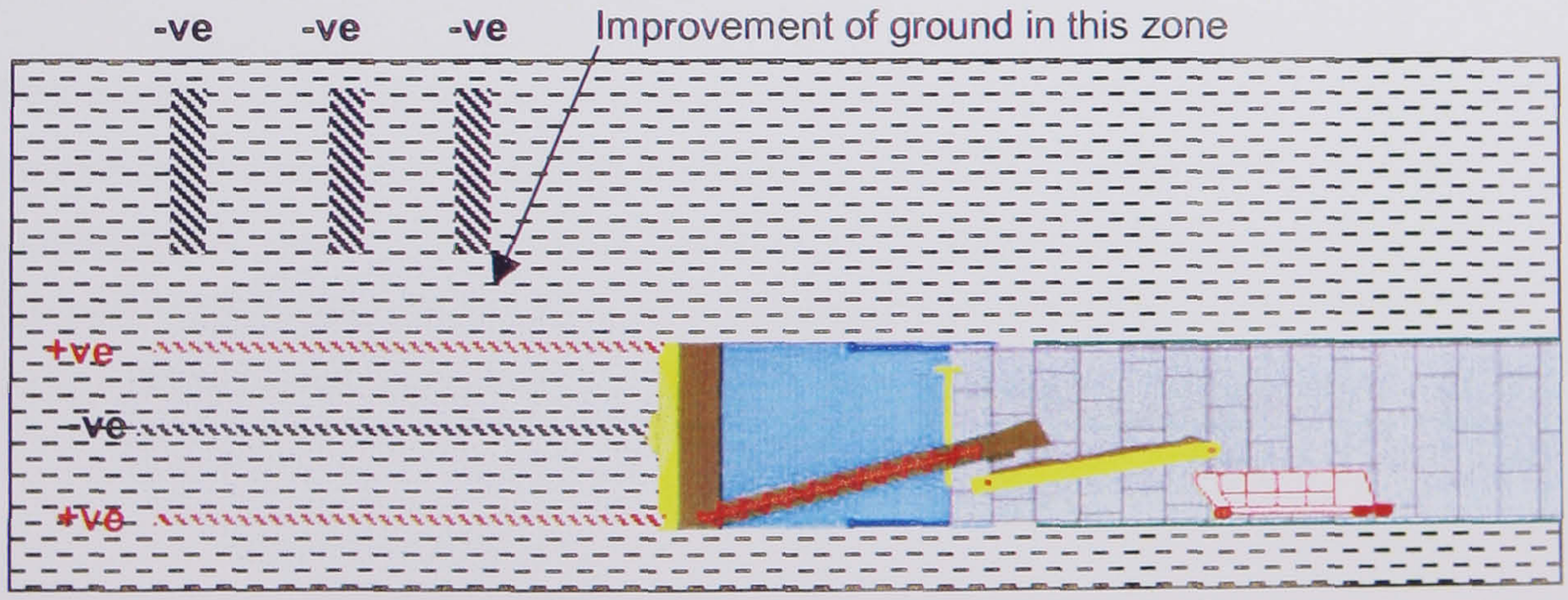

Figure 7.27 Application of EKG to tunnelling

7.7.3 PILING

Electrokinetic phenomena can assist with piling in two principal ways. If EKGs are installed in close proximity to the piling area and the steel piles are made into the cathodes the result would be to locally soften the soil in the vicinity of the piles and facilitate driving. Once the desired piling depth has been achieved the electro-kinetic process can be shut down and the soil will then gradually regain its equilibrium and the soil properties return to their former state around the piles. Preferentially the polarity could be reversed, making the piles anodic and therefore improving the soil properties in the vicinity of the piles. The latter process has been successfully employed in Canada using all metal electrodes, Soderman & Milligan (1961) and Milligan (1994).

Figure 7.28 EKG Applications to piling

7.7.4 SHRINKAGE AND SWELLING PREVENTION FOR SHALLOW FOUNDATIONS AND PIPELINES

EKG technology may be able to offer a remedy to the increasing problem associated with low-rise structures built with shallow foundations that are constructed on soils prone to shrinkage and swelling. In this case, the EKG would enable moisture control of the susceptible strata and either add or remove water as necessary to prevent the volume change of the founding stratum.

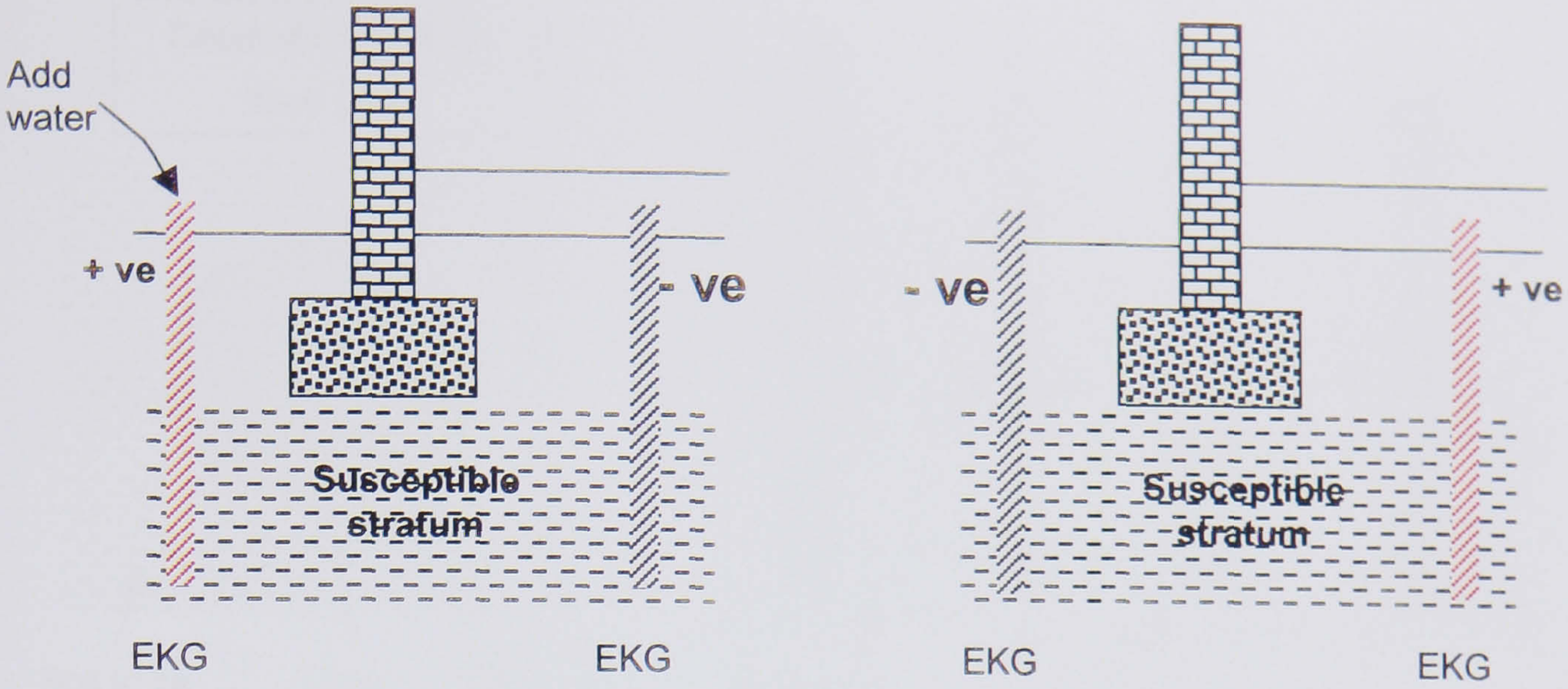

Figure 7.29 EKG used for stabilisation of shallow foundations

7.7.5 ELECTRO-REMEDIATION

The EKG has a potential application in the field of electro-remediation of a contaminated soil including the removal of heavy metal contamination and the introduction of biological and chemical species into strata. A full explanation of the potential applications in this relatively new and expanding field of application is beyond the scope of this thesis. The reader is referred to the following references for further information on potential applications in this field Pamuku (1996), DeFlaun & Condee (1997), Geokinetics (1996), Nettleton (1996) and Dawson & Gilman (2001).

7.7.6 ENHANCED LIME MIGRATION

EKG also has a potential application in improving existing lime pile techniques. In this case the EKG could be used as a conductive element to establish electro-osmotic flow to induce the migration of calcium ions through the soil thereby increasing the zone of influence of the pile by causing lime migration to a greater radius than occurs by conventional diffusion. A possible configuration for such an application is given in Figure 7.30.

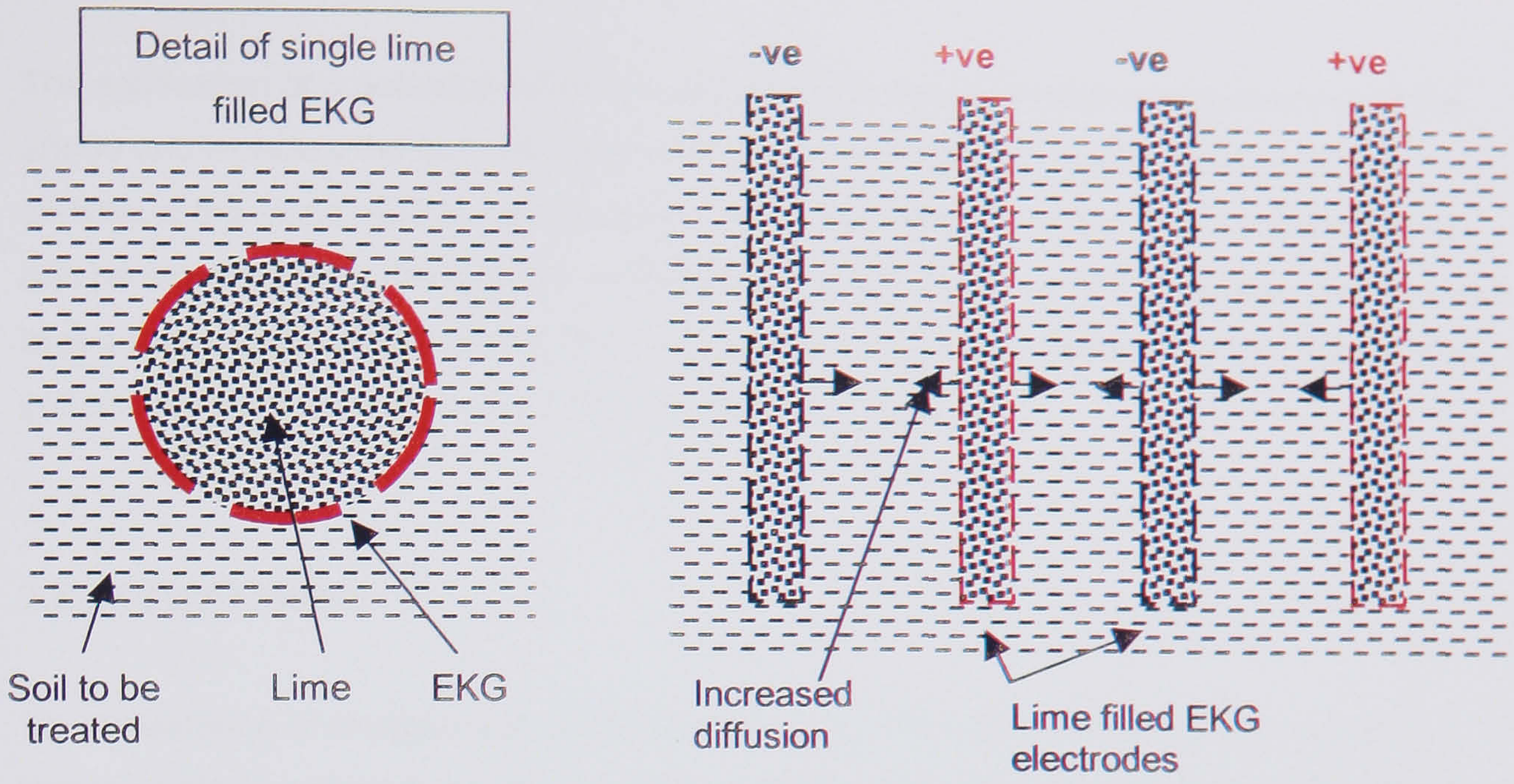

Figure 7.30 Enhancement of lime piles through the use of EKG

Polarity reversal may also be applied to this application to achieve a more uniform treatment of the soil.

7.7.7 SLOPE STABILITY

The stability of slopes may be improved through the use of EKG to achieve a more rapid dewatering of the soil and to act as drains to reduce porewater pressures within an unstable cohesive slope.

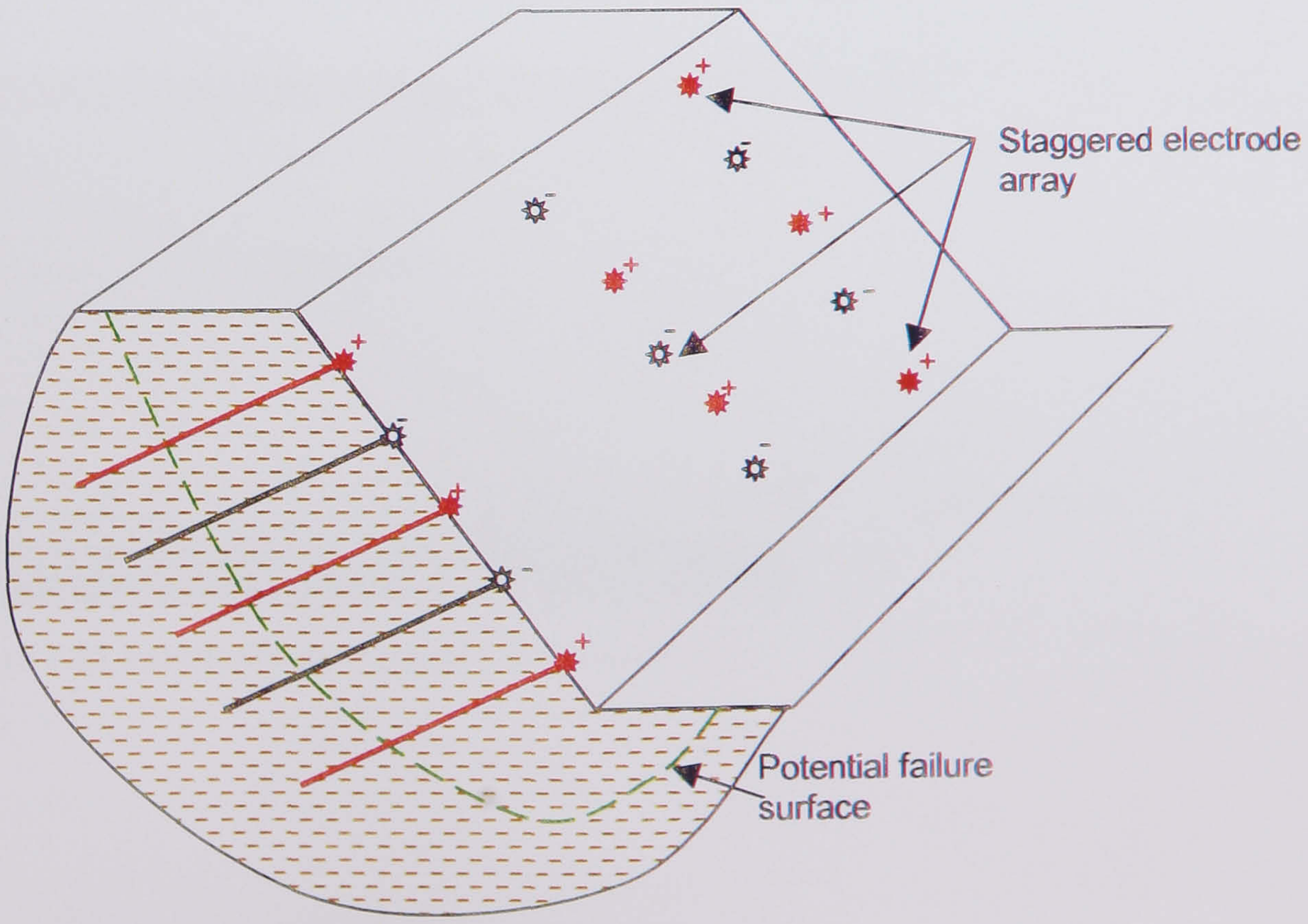

Figure 7.31 Application of EKG to slope stabilisation

The application of a potential difference will generate negative porewater pressures at the anode and increase the soil strength in this area resulting in an overall increase in the stability of the slope. EKGs can be formed as a drain and the water driven to the cathode can be removed from the slope in an efficient manner. Again, polarity reversal may be used to produce more uniform conditions. Electrokinetics could be used to increase the bond of soil nails or passive anchors by making them into anodes.

7.7.8 DEWATERING

The dewatering of sludges and slurries by means of electrokinetic technology has been demonstrated by several researchers (Colin 1986, Laidler 1999, Sunderland 1987a, b & c and Yukawa *et al* 1976) and EKG methods have potential applications in this field. The types of wastes that may be suited to dewatering using electro-osmosis and electrophoresis are:

- Mine tailings.
- Bentonite slurry from diaphragm walling / piling.
- Sewage sludges.

The EKG in its current form may not be sufficiently durable to act as a long-term anode (+) for these applications, see §3.5.4. However, it may be used as a cathode. A possible electrode configuration for use in dewatering is given in Figure 7.32.

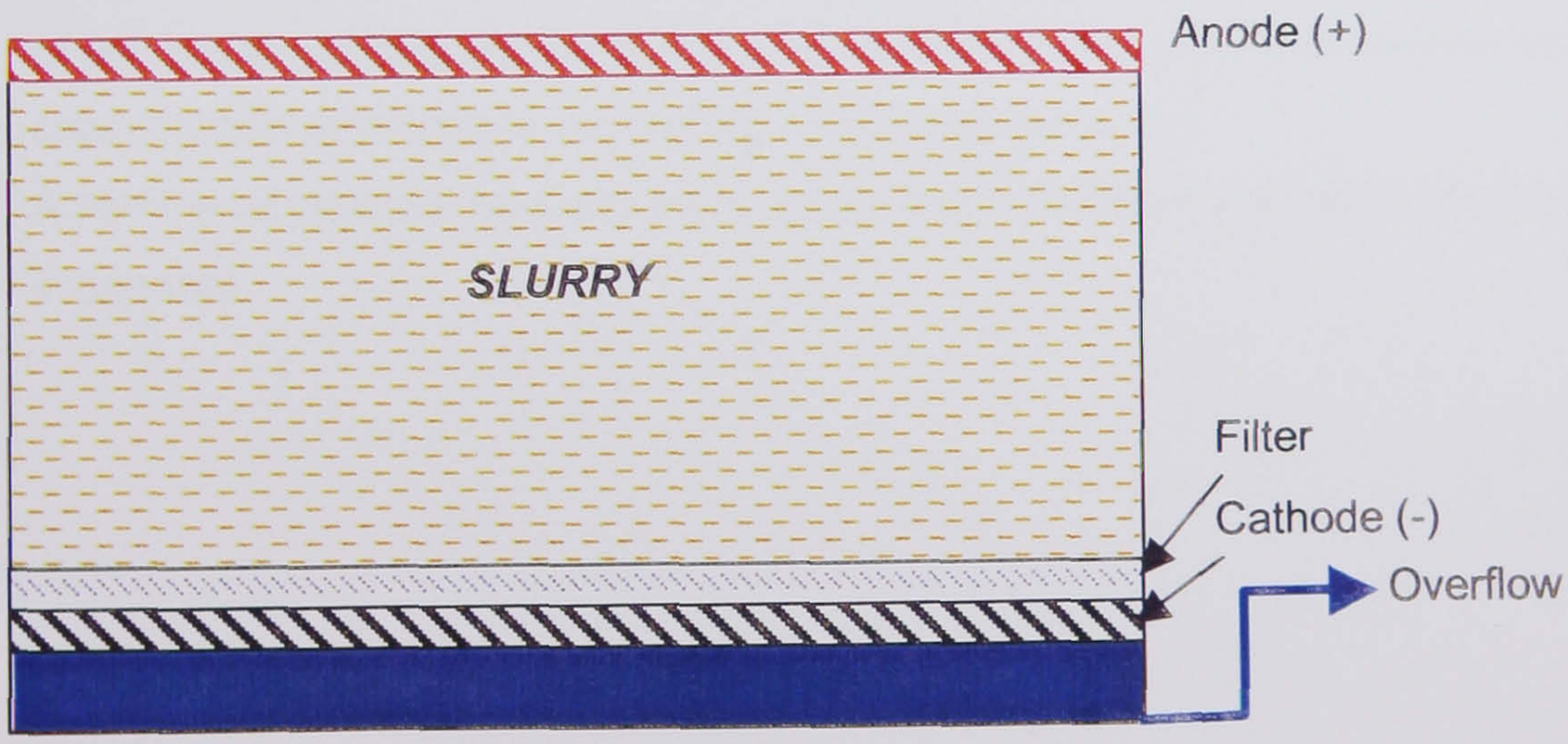

Figure 7.32 Electrode arrangement for dewatering

7.7.9 COMBINATION WITH EXISTING TECHNIQUES

Electro-osmosis may also be used in combination with existing ground improvement techniques to increase their efficiency or to allow their use after an initial treatment by electro-osmosis has been undertaken to create an initial improvement in the soil's characteristics. An example of such an application has been presented previously in §4.2.4 where electro-osmosis was combined with conventional surcharging. However, the sequence of the application may be varied to allow an initial improvement in the soil by electro-osmosis to allow a subsequent greater surcharge load to be placed and hence a shorter surcharging period may be achieved (see §4.1.2.1). Additionally, depending upon the electrode drainage characteristics they may subsequently serve as vertical drains during the surcharging phase of treatment.

Electro-osmosis may be combined with a wide range of both in situ and ex situ treatment methods wherever an initial reduction in water content, and subsequent increase in undrained shear strength, is beneficial to the performance of the conventional technique.

7.8 SYNOPSIS OF CHAPTER 7

This chapter has introduced a range of laboratory tests that may be used to ascertain the applicability of electro-osmosis to a particular soil type. The types of test that have been discussed are those commonly used in site investigation practice together with specific specialised electro-osmotic tests, using custom-made apparatus.
Other sections dealt with the analytical methods that the Author recommends for the design of electro-osmotically enhanced cohesive reinforced soil and for electro-osmotic consolidation applications, as well as volumetric control.
A number of potential new and novel applications for EKGs and electro-osmosis were then suggested.

7.9 CHAPTER 7 REFERENCES

1. Abiera, H.O., Miura, N., Bergado, D.T. & Nomura, T. (1999) *Effects of using electro-conductive PVD in the consolidation of reconstituted Ariake clay.* Geotechnical Engineering Journal of Southeast Asian Geotechnical Society, Vol. 30, No. 2, August, pp 67-83.
2. Adali, E. (1999) *Study of electro-osmosis in multi-layered soils.* Master of Science dissertation, Geotechnical Group, University of Newcastle upon Tyne, U.K.
3. Alshawabkeh, A.N., Gale, R.J., Ozsu-Acar, E. & Bricka, R.M. (1999) *Optimization of 2-D electrode configurations for electrokinetic remediation.* Journal of soil Contamination, vol. 8, No. 6, pp 617-635.
4. Banerjee, S. & Vitayasupakorn, V. (1984) *Oedometer tests.* Journal of Geotechnical Engineering, ASCE, Vol. 110, No. 8, August. pp 1007-1023.
5. Bjerrum, L., Moum, J., & Eide, O. (1967) *Application Of Electro-Osmosis To A Foundation Problem In A Norwegian Quick Clay.* Géotechnique, Vol. 17, pp 214-235.
6. British Standards Institution (1986) *British Standard Code of Practice for Foundations; BS 8004.* BSI, 2 Park Street, London, WA1 2BS.
7. British Standards Institution (1990a) *British Standard Methods Of Test For Soils For Civil Engineering Purposes, Part 1. General Requirements And Sample Preparation; BS 1377.* BSI, 2 Park Street, London, WA1 2BS.
8. British Standards Institution (1990b) *British Standard Methods of Test for Soils for Civil Engineering Purposes, Part 2. Classification Tests; BS 1377.* BSI, 2 Park Street, London, WA1 2BS.
9. British Standards Institution (1990c) *British Standard Methods Of Test For Soils For Civil Engineering Purposes, Part 3. Chemical And Electro-Chemical Tests; BS 1377.* BSI, 2 Park Street, London, WA1 2BS.
10. British Standards Institution (1990d) *British Standard Methods Of Test For Soils For Civil Engineering Purposes, Part 5. Compressibility, Permeability And Durability Tests BS 1377.* BSI, 2 Park Street, London, WA1 2BS.
11. British Standards Institution (1990e) *British Standard Methods Of Test For Soils For Civil Engineering Purposes, Part 6. Consolidation and permeability tests in hydraulic cells and with pore pressure measurement BS 1377.* BSI, 2 Park Street, London, WA1 2BS.
12. British Standards Institution (1990f) *British Standard Methods Of Test For Soils For Civil Engineering Purposes, Part 7. Shear strength tests (total stress) BS 1377.* BSI, 2 Park Street, London, WA1 2BS.
13. British Standards Institution (1990g) *British Standard Methods Of Test For Soils For Civil Engineering Purposes, Part 8. Shear strength tests (effective stress) BS 1377.* BSI, 2 Park Street, London, WA1 2BS.
14. British Standards Institution (1999) *Code of Practice for site investigations. BS 5950.* BSI, 389 Chiswick High Road, London, W4 4AL.

15. Carter, M. (1983) *Geotechnical Engineering Handbook.* Pentech press, London. p 226.
16. Carter, M. & Bentley, S.P. (1991) *Correlations of Soil Properties.* Pentech Press, London. p 130.
17. Casagrande, L. (1952) *Electro-Osmotic Stabilisation of Soils.* Jour. of the Boston Soc. of Civil Engineers section, ASCE, Vol. 39, pp 51-83.
18. Casagrande, L. (1983) *Stabilization Of Soils By Means Of Electro-Osmosis.* Jour. of the Boston Soc. of Civil Engineers section, ASCE, Vol. 69, No.2, pp 255-302.
19. Casagrande, L., Loughney, R. W., & Matich, M. A. J. (1961) *Electro-osmotic stabilization of a high slope in loose saturated silt.* Proc. 5th Int. Conf. on Soil Mech. and Found. Eng., Paris, Vol. 2, Balkema, pp 555-561.
20. Casagrande, L., Wade, N., Wakely, M. & Loughney, R. (1981) *Electro-osmosis projects, British Columbia, Canada.* Proceedings of the 10th European Conference on Soil Mechanics and Foundation Engineering, Rotterdam, Balkema, pp 607-610.
21. Cedergren, H.R. & Weber, W.G. (1962) *Subsidence of California Highways.* ASTM Special Technical Publication No. 322.
22. Chappell, B.A., & Burton, P.L. (1975) *Electro-Osmosis Applied To Unstable Embankment.* Journal of Geotechnical Engineering, ASCE, Vol. 101(GT8), pp 733-740.
23. Chen, J.L. & Murdoch, L. (1999) *Effects Of Electro-Osmosis On Natural Soils: Field Test.* Journal of Geotechnical and Geoenvironmental Engineering, ASCE, Vol. 125, No. 12, December, pp 1090-1098.
24. Chen, J.L., Al-Abed, S.R., Bryndzia, L.T. & Murdoch, L. (1999) *Cation transport and partitioning during a field test of electro-osmosis.* Water Resources Research, Vol. 35, No. 12, December, pp 3841-3851.
25. Colin, F. (1986) *Application Of Electrical fields To Thicken And Dewater Sewage Sludges.* New Developments in Processing Of Sludges & Slurries, Eds. Bruce, E.M. et al, Pub. Elsevier, London.
26. Das, B.M. (1985) *Advanced Soil Mechanics.* McGraw Hill, p 511.
27. Das, B.M. (1997) *Advanced Soil Mechanics.* 2nd Edition, Taylor & Frances Ltd, London, p 457.
28. Dawson, G.W. & Gilman, J. (2001) *Land reclamation technology - expanding the geotechnical engineering envelope.* Proc. Inst. Civil Engineers, Geotechnical Engineering, Vol. 149, No. 1, pp 49-61.
29. DeFlaun, M.F. & Condee, C.W. (1997) *Electrokinetic transport of bacteria.* Journal of Hazardous Materials, Vol. 55, Elsevier Science, pp 263-277.
30. Eggestad, Å. & Føyn, T. (1983) *Electro-osmotic improvement of a soft sensitive clay.* Proceedings of the 8th European Conference on Soil Mechanics and Foundation Engineering, Helsinki, Vol. 2, Balkema, pp 597-602.
31. Esrig, M.I. (1968) *Pore Pressures, Consolidation And Electrokinetics.* Journal of the Soil Mechanics And Foundation Division, ASCE, Vol. 94(SM4), pp 899-921.

32. Esrig, M.I. & Gemeinhardt, J.P. (1967) *Electrokinetic Stabilization Of An Illitic Clay.* Journal of the Soil Mechanics And Foundation Division, ASCE, Vol. 93(SM3), pp 109-128.
33. Fetzer, C.A. (1967) *Electro-Osmotic Stabilization Of West Branch Dam.* Journal of the Soil Mechanics And Foundation Division, ASCE, Vol. 93(SM4), pp 85-106.
34. Geokinetics (1996) *Electro-remediation, a clean up technology for the present and the future.* Brochure, Geokinetics, P.O Box 195,NL 3910 AD, Rhenen, The Netherlands.
35. Gibson, R.E. (1953) *Experimental determination of the true cohesion and true angle of internal friction in clays.* Proceedings of the 3rd International Conference on Soil Mechanics and Foundation Engineering, Zurich, Balkema, pp 126-130.
36. Glossop, R. & Skempton, A.W. (1945) *Particle size in silts and sands.* Journal of the Institution of Civil Engineers, Vol. 25, pp 85-105.
37. Greenwood, D.A. (1998) *Speculation on methods of stabilising slopes.* Ground Improvement, Vol. 2, Issue 3, Thomas Telford Ltd. pp 103-123.
38. Gwede, D. (2000) *Personal communication* regarding research undertaken during 1997 - 2000 at the Geotechnical Group, University of Newcastle upon Tyne, U.K.
39. Hamir, R. (1997) *Some aspects and applications of electrically conductive geosynthetic materials.* PhD Thesis, Geotechnical Group, Department of Civil Engineering, University of Newcastle upon Tyne, U.K.
40. Head, K.H. (1982) *Manual Of Soil Laboratory Testing, Vol. 2: Permeability, shear strength and compressibility tests.* Pentech Press, London. p 440.
41. Head, K.H. (1998) *Manual Of Soil Laboratory Testing, Vol. 3: Effective stress tests.* 2nd Edition, John Wiley & Sons Ltd, Chichester. p 428.
42. Hughes, D.B. (2001) *Personal communication* regarding laboratory testing prices at the Geotechnical Group, University of Newcastle upon Tyne, U.K.
43. Jewell, R.A. (1980) *Some effects of reinforcement on the mechanical behaviour of soils.* Doctor of Philosophy Thesis, University of Cambridge, U.K.
44. Johnson, S.J. (1970) *Foundation Precompression With Vertical Sand Drains.* Journal of the Soil Mechanics and Foundation Division, ASCE, SM1, Vol. 96, January, pp 145-175.
45. Johnston, I.W. (1978) *Electro-osmosis and its application to soil and foundation stabilisation.* In: Symposium on Soil Reinforcing and Stabilising Techniques in Engineering Practice. Sydney, Australia, University of New South Wales, pp 459-476.
46. Laidler, P.J. (1999) *The dewatering of bentonite slurry using electro-osmosis and electrophoresis.* 4th Year M.Eng. Dissertation, University of Newcastle upon Tyne, June.
47. Lambe, T.W. & Whitman, R.V. (1969) *Soil Mechanics.* John Wiley & Sons, Inc. New York, USA. p 565.
48. Lambe, T.W. & Whitman, R.V. (1979) *Soil Mechanics, SI Version.* John Wiley & Sons, Inc. New York, USA. p 553.
49. Lo, K.Y., Inculet, I.I., & Ho, K.S. (1991) *Electroosmotic strengthening of soft sensitive clays.* Canadian Geotechnical Journal, Vol. 28, pp 62-73.

50. Lomizé, G.M., Netushi, A.V. & Rzhanitzin, B.A. (1961) *Electro- osmosis processes in clayey soils and dewatering during excavations.* Proc. 5th ICSMFE, Paris, Vol. 2, Balkema, pp 62-67.
51. McGown, A., Marsland, A., Radwan, A.M. & Gabr, A.W.A. (1980) *Recording and interpreting soil macrofabric data.* Géotechnique, Vol. 30, No. 4, p 417-447.
52. Microsoft (1997) *Excel 97.* Microsoft Corporation.
53. Milligan, V. (1994) *First application Of Electro-Osmosis To improve Friction Pile Capacity-Three Decades Later.* In Proc. of the 13th Int. Conf. on Soil Mech. and Found. Eng., Jan. 5-10, Vol. 5, New Delhi, India, Balkema, pp 1-5.
54. Mitchell, J.K. (1993) *Fundamentals of Soil Behaviour.* 2nd Edition, John Wiley & Sons Inc. New York, USA. p 437.
55. Morris, D.V., Hillis, S.F., & Caldwell, J.A. (1985) *Improvement of sensitive silty clay by electroosmosis.* Canadian Geotechnical Journal, Vol. 22, pp 17-24.
56. Netlon Ltd (1998) *Electrically - Conducting Element,* U.K. Patent Application GB 2327686A.
57. Nettleton, I.M. (1996) *Electro-Bioremediation.* Internal Report, Geotechnical Group, University of Newcastle upon Tyne, Newcastle upon Tyne, U.K.
58. Nicholls, R.L. & Herbst, R.L. (1967) *Consolidation under electrical-pressure gradients.* Journal of the Soil Mechanics and Foundation Division, ASCE, SM5, Vol. 93, September, pp 139-150.
59. Pamuku, S. (1996) *Electro-chemical technologies for in situ restoration of contaminated subsurface soils.* Electronic Journal of Geotechnical Engineering, http:// 139.78.66.61/ejge/
60. Piaskowski, A. (1953) *Investigations on electro-osmotic flow in soils in relation to different characteristics.* Proceedings of the 4th International Conference on Soil Mechanics and Foundation Engineering, London. Balkema, pp 89 - 92.
61. Pugh, R.C. (1999) *Electrokinetic Geosynthetic Materials For Use In The Construction Industry - Mid Term Review Report.* Report No. GR/L66090/Mid-rev. Confidential report on EPSRC Research Project GR/L66090, Geotechnical Group, University of Newcastle upon Tyne, U.K.
62. Pugh R.C. (2000) A *full-scale field trial of electrokinetically enhances cohesive reinforced soil using electrokinetic geosynthetics.* Winning Paper in the IGS U.K. - Chapter Student papers competition, September.
63. Rowe, P.W. & Barden, L. (1966) *A new consolidation cell.* Géotechnique, Vol. 16, No. 2, p 162-170.
64. Schultz, D.S. (1997) *Electroosmosis technology for soil remediation: laboratory results, field trial and economic modelling.* Journal of Hazardous Materials, Vol. 55, pp 81-91.
65. Simons, N.E. & Menzies, B.K. (1976) *A Short Course In Foundation Engineering.* IPC Science and Technology Press. p 159.

66. Shang, J.Q. (1998) *Two-dimensional electro-osmotic consolidation.* Ground Improvement, Vol. 2, pp 17-25.
67. Skempton, A.W. & Bjerrum, L. (1957) *A contribution to the settlement analysis of foundations on clay.* Géotechnique, Vol. 7, pp 168-178.
68. Smyrell, A.G. (1991) *The derivation of torsional stiffness using a modern spreadsheet and an improved finite difference scheme.* Structural Engineer, Vol. 69, No. 24, pp 423-430.
69. Soderman, L.G. & Milligan, V. (1961) *Capacity of friction piles in Varved clay increased by electro-osmosis.* Proc. 5th Int. Conf. Soil Mech. & Found Eng, Paris, Vol. 2, Balkema, pp 143-148.
70. Stroud, K.A. (1990) *Further Engineering Mathematics - programmes and problems.* 2nd Edition, Macmillan Education, London. p 1063.
71. Sunderland, J.G. (1987a) *Electrokinetic dewatering & thickening: I Introduction and historical review of electrokinetic applications.* Journal of applied electrochemistry, No. 17, pp 889-898.
72. Sunderland, J.G. (1987b) *Electrokinetic dewatering & thickening: II Thickening of ball clay.* Journal of applied electrochemistry, No. 17, pp 1048-1056.
73. Sunderland, J.G. (1987c) *Electrokinetic dewatering & thickening: III Electrokinetic cells and their application to a range of materials.* Journal of applied electrochemistry, No. 17, pp 1171-1176.
74. Tomlinson, M.J. (1995) *Foundation design and construction.* 6th Edition, Longman Scientific and Technical, Harlow, U.K. p 536.
75. Wan, T.Y. & Mitchell, J.K. (1975) *New Apparatus For Consolidation By Electro-Osmosis.* Journal of Geotechnical Engineering, ASCE, Vol. 101(GT5), pp 503-507.
76. Wan, T.Y. & Mitchell, J.K. (1976) *Electro-Osmotic Consolidation Of Soils.* Journal of Geotechnical Engineering, ASCE, Vol. 102(GT5), pp 473-491.
77. Weber, W.G. (1968) *In situ permeabilities for determining rates of consolidation.* Highway Research Record No. 243.
78. Williams, B.P., Smyrell, A.G. & Lewis P.J. (1993) *Flownet diagrams - the use of finite differences and a spreadsheet to determine potential heads.* Ground Engineering, June, pp 32-38.
79. Wrigley, N.E. (1999) *The practical use of electro-osmosis.* Personal communication, October.
80. Yukawa, H., Yoshida, H., Kobayashi, K., & Hakoda, M. (1976) *Fundamental Study On Electroosmotic Dewatering Of Sludge At Constant Electric Current.* Jour. Chem. Eng. Japan, Vol. 9, No. 5, pp 402-407.

CHAPTER 8

SUMMARY AND MAIN CONCLUSIONS

8.1 SUMMARY

The research undertaken has covered the following aspects and applications of electro-osmosis and electrokinetic geosynthetics to the construction industry:

- A detailed review of the appropriate literature relating to electrokinetic phenomena in soils from the basic mechanisms through to field observations and applications.

- The development of a new electrically conductive geosynthetic that may be employed for electro-osmotic applications in construction uses, including studies relating to its durability and connection technology.

- An electro-osmotic consolidation trial using EKGs, together with the associated design and installation methods.

- The design and construction of an electro-osmotically enhanced cohesive reinforced soil wall.

- The design and installation of an electro-osmosis application to the volumetric control of a railway embankment.

- The identification of acceptability criteria to assess the potential of electro-osmosis and EKGs materials in treating a soil.

- A study of potential applications of EKGs to the construction industry.

8.2 MAIN CONCLUSIONS

A number of conclusions have been drawn from the research into EKG materials and technology. The purpose of the following sections is to bring together these conclusions under the relevant subject areas.

8.2.1 CONCLUSIONS REGARDING EKGs

- The electrically conductive band drain disclosed by Netlon Ltd (1998) based upon the idea of Nettleton (1996) has been used in the field for electro-osmotic consolidation, electro-osmotically enhanced cohesive reinforced soil, and for the volumetric control of a clay cored embankment. In the consolidation and reinforcement applications the EKG demonstrated adequate durability for the application. The Author has developed a means of estimating the field durability of the EKG under working field conditions (Annex A).

- The use of the filter elements on the EKG for consolidation applications should be exercised with caution and solely for cathode use.

- Technology has been developed for the connection of EKG to power distribution cables, it has been found that the most efficient connection is made by means of a stripped double crimped connection (§3.5.6).

8.2.2 CONCLUSIONS REGARDING ELECTRO-OSMOTIC CONSOLIDATION

- A theory for calculating the quantity of consolidation that can be achieved using EKG technology has been developed, based upon a review of the currently available literature, §4.2.2. The method is based upon a linearly varying equivalent surcharge, varying from 0kPa at the cathode to a maximum of 100kPa at the anode. The theory has been confirmed by laboratory testing on horizontal electrodes located in a London clay block sample, §6.2.7.1, and back analysis of published case studies, §7.2.3.1.

- A theory has also been suggested for the calculation of the rate of settlement of soil subjected to electro-osmotic treatment.

- An installation technique using a modified dynamic probe cone (DPH) has been developed for installing limited numbers of EKGs in soft ground conditions. For commercial applications the use of a wick drain lance is recommended.

- The Newburn Haugh field trial highlighted the importance of ascertaining soil parameters for all of the soils within the zone of influence of the consolidation application, if this is not done problems may arise from short-circuiting or recirculation of fluids.

- A design methodology for electro-osmotic consolidation has been developed and is presented in §7.3.

8.2.3 CONCLUSIONS REGARDING ELECTRO-OSMOTICALLY ENHANCED COHESIVE REINFORCED SOIL

- A new design methodology for electro-osmotically enhanced cohesive reinforced soil has been developed based upon; long-tern design, short-term design and electro-osmotic design, §7.4.
  - The long-term design is undertaken using conventional tie-back wedge analysis methods to ascertain the reinforcement layout required.
  - The short-term analysis is undertaken by four methods; critical height, Coulomb, discrete theory and composite theory. From these four methods, values for the undrained shear strength (c_u) are calculated considering and not considering the presence of the reinforcement. Based upon this procedure an engineering decision can be made as to what value of c_u is required in the field.
  - Electro-osmotic design is then used to ascertain the treatment time and power requirements to achieve the required value of c_u.

- The expected and measured field results, using the new design method, are in relatively good agreement, §5.7.9.2. The initial water content and the voltage gradient used in the design calculations are critical parameters in the design process.

- A new and novel construction technique has bee developed for the use of cohesive fill in reinforced soil, Figure 5.36.

- The typical cost for the construction of a single lift (0.6m high) of electro-osmotically enhanced reinforced cohesive soil has been calculated as approximately £180 per linear metre. This figure is based upon the costs involved in the Joint Stocks trial.

8.2.4 CONCLUSIONS REGARDING ELECTRO-OSMOTIC VOLUME CONTROL

- It has been shown that electro-osmosis can reduce the potential for volume change of a soil in two principal ways:

- ***Effective overconsolidation***, the application of the negative porewater pressure generated by electro-osmosis causes an overconsolidation of the soil such that subsequent wetting and drying cycles occur over a reduced swelling / reload portion of the *e* - log *p´* curve, §4.2.3.

- ***Electrochemical cementing,*** brought about by the electrokinetic process causes a change in the Atterberg limits of the soil making it less prone to volume change, Figure 6.1.

- A novel installation technique has been developed using a mobile hydraulic drill to install EKG electrodes at subhorizontal inclinations in limited access situations, see §6.2.8.

8.2.5 CONCLUSIONS REGARDING PHILOSOPHY

- Acceptability criteria have been developed for the assessment of the suitability of a soil for treatment by electro-osmosis. The acceptability criteria are based upon standard soil mechanics laboratory tests enhanced by the use of specialist electro-osmosis tests and an assessment of soil macrofabric, §7.2.

- Analysis methods for the quantification of the efficiency of electrode installation methods have been developed by means of finite difference and resistance path methods, §7.6.2 and §7.6.1.

- New and novel application areas for EKG and electro-osmosis have been suggested, §7.7.

8.3 FULFILMENT OF RESEARCH OBJECTIVES

The objectives for this research were stated in §1.2 at the beginning of this thesis. The principal objectives were the use of EKGs for the application areas of electro-osmotic consolidation and cohesive reinforced soil. These two objectives have been met by the undertaking of the Newburn Haugh and Joint Stocks trials respectively. During these trials experience has been gained in installation and connection technologies, reinforcing the future use of this technology for practical construction applications. Additionally, fundamental design methodologies have also been suggested for these two applications to

allow future work to be undertaken, and hopefully to further refine the methodologies as more experience is gained in their application, §7.3 and §7.4.

The application of electro-osmosis and EKG to the problem of volumetric control has also been considered. A successful installation and connection trial was undertaken at the Wimbledon Park - Southfield embankment trial. A more general design methodology for this type of application is also suggested, §7.5.

8.4 RECOMMENDATIONS FOR FUTURE RESEARCH

Several recommendations for further research have been made in the relevant chapters of this thesis as a result of the findings made during the present research work. The purpose of the following sections is to assemble these recommendations together and make additional recommendation relating to other areas associated with electrokinetic treatment of soils.

8.4.1 FUTURE EKG RESEARCH

As presented in Chapter 3 it is suggested that further research work into improving the durability of the Netlon EKG is undertaken. It is envisaged that this would primarily investigate variations in the geometry and structure of the existing EKG and look into the possibility of using more durable materials for its construction.

Additionally, completely new EKG configurations require investigation in order to combine more traditional geosynthetic functions with electrical conductivity, such as an EKG that combines the properties of reinforcement, drainage and electrical conductivity in a single element.

8.4.2 FUTURE RESEARCH INTO FIELD APPLICATIONS

The results of the Newburn Haugh field trial presented in Chapter 4 clearly illustrated the importance of assessing the soil's macrofabric for the successful application of electro-osmosis to in situ soils. This is an aspect that has received very little attention in the published literature and yet, as has been shown, can govern the success or failure of an electrokinetic application. This is an area that would be worthy of further research to determine the effects of a soil's macrofabric on electro-osmosis and additionally to attempt to define acceptability criteria for a soil's macrofabric.

The electrical conductivity of a soil measured in the laboratory and that subsequently obtained in a field application has shown a significant difference. This may be due to sample orientation during laboratory testing and the influence of macrofabric layering or other factors, such as the differences in the form of the electrical field between laboratory and field applications. The present research has suggested an electrical conductivity reduction factor of 0.1 between the laboratory measurement on remoulded samples and that used for field calculation. This area requires further work to establish the validity of this assumption for both undisturbed and remoulded soil samples.

The environmental repercussions as a result of undertaking electro-osmosis in the field have not been fully addressed. It is known that the application of electro-osmosis to a soil mass causes the formation of acid and base fronts at the electrodes and can cause changes in the soil mineralogy, but what is not known is what are the possible long-term implications to both the soil and groundwater caused by electro-osmotic soil treatment. These implications require investigation and assessment.

The effects of electro-osmosis on the volume change characteristics of a soil are not fully understood. It is known that as a result of the negative porewater pressures generated by electro-osmosis overconsolidation of the soil mass takes place, causing a reduction in the shrinkage and swelling potential. However, the electrochemical effects of electro-osmosis on a soil mass have not been fully quantified and the effectiveness of this element of the treatment, when the soil is subjected to cycles of wetting and drying, has not been fully investigated. This is an area that requires further fundamental research.

Finally, the suggested design and analysis methods presented in this thesis have been developed as a direct result of the field trials undertaken. These methods should be constantly revised and updated as more work is undertaken and published in this area.

8.5 CHAPTER 8 REFERENCES

1. Netlon Ltd (1998) *Electrically - Conducting Element,* U.K. Patent Application GB 2327686A.
2. Nettleton, I.M. (1996) *Electro-Bioremediation.* 1st year interim report for EPSRC Contract No. GR/K20590. Geotechnical Group, University of Newcastle upon Tyne, U.K.

ANNEX A

Theoretical EKG electrode durability calculations

Theoretical Durability of EKG Electrode.

Typical consumption rate for carbon ≈ 0.5 - 2.0 kg/A^{-1} year (Eastwood 1997)
Hence, adopt for calculation purposes a consumption rate of 1.0 kg/A^{-1} year

From geometry of an individual strand of the EKG:

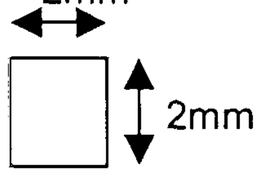

= 8 mm perimeter, 4 mm^2 x-sectional area.

Each EKG contains 20 strands (ignoring diagonal elements)
Thus, the exposed surface area per m length of EKG may be calculated:

$8 * 20 * 1000 = 160 * 10^3 mm^2$

Alternatively, as the volume per metre length of EKG.

$4 * 20 * 1000 = 80 * 10^3 mm^3$

Assuming EKG is only composed of polymer, i.e. no metal stringers are considered

$\rho = 1063 kg/m^3$ (Cablec 3892)
Hence, the mass of polymer per metre length of EKG is given by:

$80 * 10^3 mm^3 * 1063 kg/m^3 = 0.08504 kg/m$

Assuming that the conductive polymer has 30% (by mass) of free consumable carbon gives:

$0.08504 * 0.3 = 25.5g$ Carbon

Consequently, for a 3 m long electrode (Joint Stocks Trial) = 76.54 g consumable carbon
The consumption time is given by mass of consumable carbon/consumption rate.

$$\therefore \quad \frac{76.54g}{1\,kg/A^{-1}year} = 28 \text{ days/Amp.}$$

i.e. 14 days @ 2 Amps constant current.
2.8 days @ 10 Amps constant current.

From the Joint Stocks Trial:

35 electrode pairs and average current over 14 days ≈ 60 Amps.

$$\therefore \frac{60}{35} = 1.71 \text{ A/electrode} \Rightarrow \frac{28}{1.71} = 16.4 \text{ days}$$

Hence, the electrode is sufficiently durable for this application as the expected treatment time is less than the anticipated longevity of the EKGs.

Note: This calculation method over estimates the durability time as it does not consider the presence of the central core; required to distribute the current, which degrades at a more rapid rate.

However, the method gives a reasonable order of magnitude for the durability of the material.

Summary of assumptions:

- Carbon consumption only takes place at the anode.
- The current is equally distributed over the full length of the electrode by the copper core, i.e. there are no current "hot spots".
- EKG diagonal elements do not contribute to durability.
- Conductive polymer contains 30% free carbon in its matrix.

REFERENCES

Eastwood, B.J. (1997) *A fundamental study of the electrochemical failure mechanism of a novel impressed current cathodic protection system.* Doctor of Philosophy Thesis, Department of Chemistry, University of Newcastle upon Tyne, U.K., p.182.

ANNEX B

Tie back wedge theory used by the Tensar International "Winwall 6.14" design programme

Tensar
international

Theory used in the Tensar Tie-back Wedge walls design method

IB/WallTBW/16.4.98

1. Introduction

Tensar International have developed the Winwall computer program in order to produce designs in accordance with a traditional Tie-back Wedge method of analysis.

Sections 2 to 4 in this bulletin explain the design principles and theory used in the calculations undertaken by the program to consider the potential failure of the structure. Section 5 describes the calculations carried out to check that post-construction deformations do not exceed prescribed values.

2. Soil Properties and Grid Strengths

Due to the relatively large strains occurring within reinforced soil structures, critical state or constant volume values are used for the strength properties of the soils (i.e. f'_{cv}, c'_{cv}). It should be appreciated however that with the exception of some industrial fills (e.g. pulverised fuel ash), an effective cohesion value of zero is normally adopted.

The reinforcement is assumed to be placed in horizontal layers and its effect is to apply a series of restoring forces to the internal slip surface being considered in the analysis. The program considers a 1.0m wide section of the wall and the strength of the grid is included as a force per metre width. The strength of the reinforcement used in the calculations is the lowest strength expected in the grid over the design life of the structure. It will be either the design strength of the grid, or a lesser value if the anchorage length is insufficient to permit the full design strength to be mobilised.

The minimum installed long-term strength of the grid (MILTS) is calculated from:

$$MILTS = \frac{P_c}{f_m \times f_e \times f_d} \qquad \text{Equ 1}$$

where: P_c = creep limited strength of the grid for the specified design life and service temperature
f_m = partial factor to allow for material manufacturing variations and confidence in the extrapolated strength
f_e = partial factor for environmental conditions
f_d = partial factor for the effects of construction activities

An overall factor of safety (usually 1.35) is the applied to the MILTS to obtain the grid's design strength.

$$T_d = \frac{MILTS}{1.35} = \frac{P_C}{f_m \times f_c \times f_d \times 1.35} \qquad \text{Equ 2}$$

3. External Stability

Tensar International, New Wellington St, Blackburn BB2 4PJ, UK
Customer Services: Tel: 01254 262431 Fax: 01254 266868 E-mail: customerservices@tensar.co.uk
Design Support: Tel: 01254 262431 Fax: 01254 266873 E-mail design@tensar.co.uk

3.1 General

In order to ensure external stability of the structure, checks need to be undertaken for potential sliding failure, bearing failure and slip failure. Figure 1 defines the various soil properties within the structure and the principle loads acting for external stability calculations.

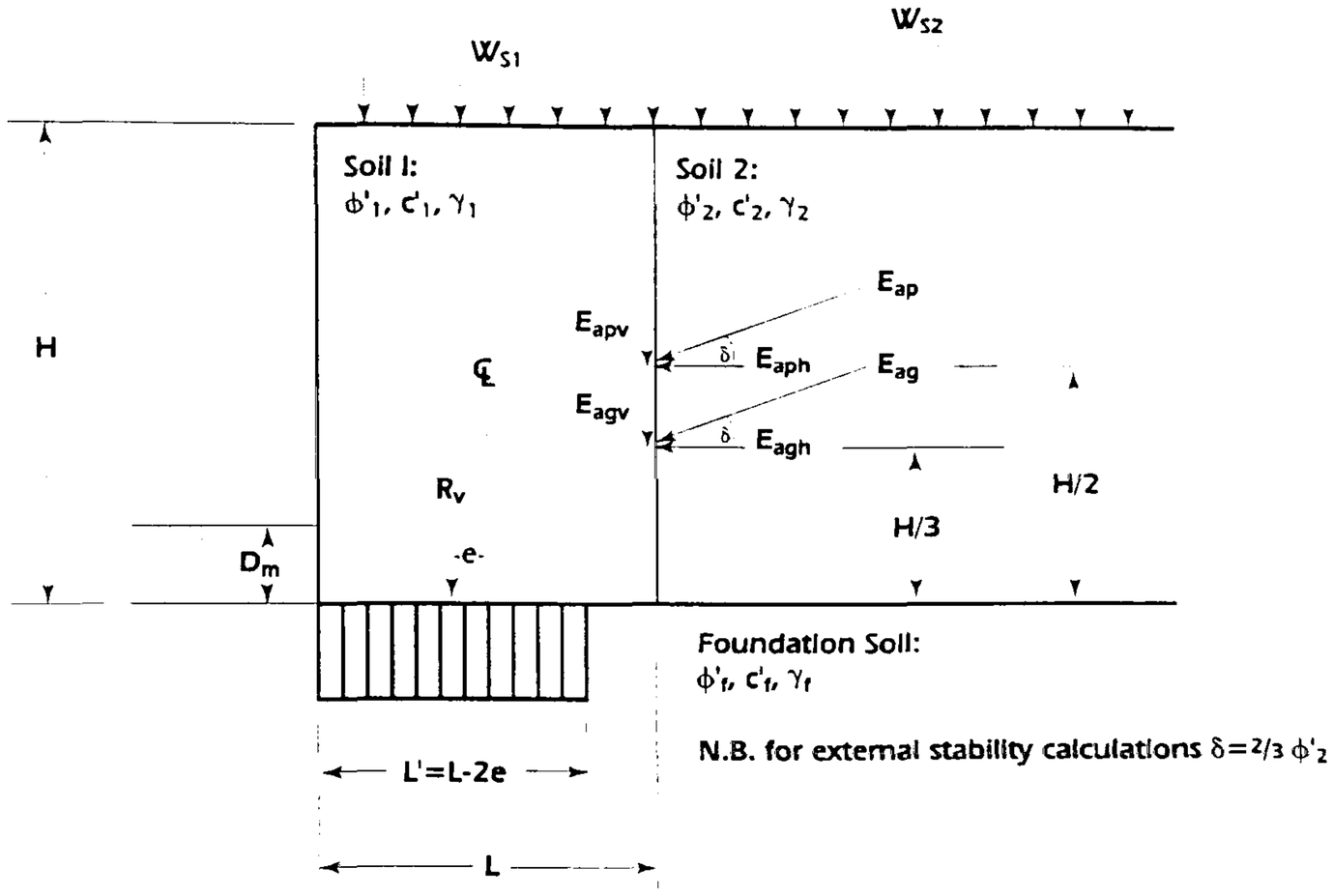

Figure 1

N.B.
L = base length of reinforced soil block
L' = effective base length assuming Meyerhof pressure distribution
H = height of structure
D_m = embedment depth
R_v = vertical component of resultant force
e = eccentricity of resultant force
f'_1, f'_2, f'_f = effective angle of friction for soils 1and 2 and the foundation soil
c'_1, c'_2, c'_f = effective cohesion for soils 1and 2 and the foundation soil
g_1, g_2, g_f = unit weight for soils soils 1and 2 and the foundation soil
w_{s1} = surcharge force on reinforced soil block
w_{s2} = surcharge force behind reinforced soil block
E_{ag} = active force due to soil
E_{ap} = active force due to surcharge w_{s2}
E_{agh} = horizontal component of active force from the soil
E_{agv} = vertical component of active force from the soil
E_{aph} = horizontal component of active force due to surcharge w_{s2}
E_{apv} = vertical component of active force due to surcharge w_{s2}

3.2 Active Earth Pressures

Winwall adopts a rigorous approach for the calculation of active earth pressures. The *Iterative Coulomb Wedge Check* examines the stability of a series of wedges emanating from the back of the reinforced soil block and by resolving the various forces acting on the wedge determines the maximum out of balance force due to the active earth pressure. For simple cases, engineers wishing to carry out independent checks of the Winwall calculations should obtain similar results using the conventional Coulomb formula for determining active earth pressures, otherwise a manual iterative check should be performed.

3.3 Sliding Failure

The factor of safety against sliding failure is given by the equation:

$$FoS = \frac{R_v \alpha_s \tan\phi' + \alpha_{bc}' c' L}{R_h} \qquad \text{Equ 3}$$

where:
R_v = vertical resultant force
R_h = horizontal disturbing force
a_s = coefficient of interaction relating soil/reinforcement bond angle with tanf'$_p$
a_{bc}' = adhesion coefficient relating soil/reinforcement bond with c'
f' = angle of internal friction (lower of f'$_1$ and f'$_f$)
L = base length of structure

It should be appreciated that Equation 2 is based on the assumption that there is a grid present at the base of the structure. In the event that this is not the case, a_s and a_{bc}' both become unity. Also, a_{bc}' is usually taken to equal a_s in the absence of specific test data.

A grid length is selected such that a factor of safety of 2.0 is achieved against sliding failure.

3.4 Bearing Failure

The bearing calculation in Winwall is carried out in accordance with the German DIN Standard 4017. The method has the advantage of taking account of the inclination of the resultant force by including inclination factors in the standard Terzaghi equations.

Where the eccentricity is positive, the bearing pressure exerted by the structure is taken to act over an effective base length, L' of L-2e i.e. a Meyerhof pressure distribution. If, however, the eccentricity is negative, a uniform pressure over the whole base is assumed.

The vertical component of the resultant force (R_v) is given by the equation:

$$R_v = \gamma_1 H + w_{s1} L + E_{apv} + E_{agv} \qquad \text{Equ 4}$$

where: E_{apv} and E_{agv} are the vertical components of the active pressure resulting from the surcharge (W_{s2}) and the backfill (Soil 2) behind the reinforced soil block respectively

The moment of the resultant force (M_{Rv}) is also determined and the eccentricity (e) of the resultant force is given by the equation:

$$e = \frac{M_{Rv}}{R_v} \qquad \text{Equ 5}$$

A check should be carried out to ensure that the resultant force acts within the middle third of the base length (L). This ensures that the back of the block does not begin to lift and also ensures safety against overturning.

The ultimate bearing pressure is given by the modified Terzaghi equation:

$$\sigma_f = c' N_c x_c + \gamma L' N_b x_b \qquad \text{Equ 6}$$

where:

$$x_b = \left(1 - \frac{h_b}{v_b + \frac{L'c'}{\tan\phi'_p}}\right)^3 \qquad \text{Equ 7}$$

$$x_c = x_d - \frac{1 - x_d}{N_d - 1} \qquad \text{Equ 8}$$

and

$$x_d = \left(1 - \frac{0.7h_b}{v_b + \frac{L'c'}{\tan\phi'_1}}\right)^3 \qquad \text{Equ 9}$$

where: h_b = horizontal failure load (i.e. $2E_{ah}$)
v_b = vertical failure load (i.e. $2R_v$)
N_b, N_c, N_d = bearing capacity factors as defined in DIN 4017

Note: the bearing capacity factors used in the program are obtained using the equations provided in the Standard and not the summary table

The factor of safety for bearing is then given by:

$$FoS = \frac{\sigma_f L'}{R_v} \qquad \text{Equ 10}$$

A grid length is selected such that a factor of safety of 2.0 is achieved against bearing failure.

In general, the worst case for bearing will be with full surcharge loading on the reinforced soil block (i.e. both the permanent and temporary parts of w_{s1} included in the calculation). However, in addition to checking this case, Winwall also examines the distribution of surcharge loads which results in the maximum overturning moment (i.e. only the permanent part of w_{s1} included). For walls with inclined faces this case can be critical due to a reduction in the effective base length (L').

3.5 Slip Failure

It is a requirement that the overall stability of the structure is considered by checking external slip surfaces; these include slip surfaces passing through the structure. The Winwall program cannot undertake this analysis but provides the user with the facility to export the otherwise completed design into Tensar's Winslope program so that this check can be carried out.

4. Internal Stability

4.1 Internal Sliding

Sliding along soil/soil and soil/reinforcement interfaces within the structure must be considered. Assuming base sliding is satisfactory, it is unlikely that internal sliding will be a problem. However, Winwall undertakes a sliding check at the top of any internal or external water surfaces. In each of these cases, it is assumed that a grid is present whether there is or not. An additional check is carried out at the bottom grid level if this is not at the base of the structure.

An exception to this procedure occurs when horizontal loads are introduced, for example in modelling bridge abutment conditions. In this event, in addition to the checks described above, the program also considers sliding at a level 1.0m below the horizontal load, again based on the assumption that a grid is present at this level.

4.2 Grid Rupture

The maximum tensile force (T_j) to be resisted by the j^{th} grid at a depth h_j below the top of the wall is determined from the summation of the various force components as follows:

$$T_j = T_{pj} + T_{sj} + T_{fj} - T_{cj} \qquad \text{Equ 11}$$

where: T_{pj} = component due to self weight of fill
T_{sj} = component due to vertical strip loading
T_{fj} = component due to horizontal shear force
T_{cj} = component due to soil cohesion (restoring force)

The component due to the self weight of the reinforced soil (T_{pj}) is given by:

$$T_{pj} = K_a s_{vj} S_{vj} \qquad \text{Equ 12}$$

where: K_a = coefficient of active earth pressure within Soil 1 (based on the Coulomb Equation)
s_{vj} = vertical stress acting on the j^{th} layer based on a Meyerhof pressure distribution
S_{vj} = the effective vertical spacing of the grids at the j^{th} layer

The component due to vertical strip loading (T_{sj}) is based on the pressure distribution shown in Figure 2. It should be appreciated that all vertical loads specified in Winwall are treated as vertical strip loads for the purposes of the analysis. When a vertical load acts over an entire area, the effect is identical to that of a uniform surcharge.

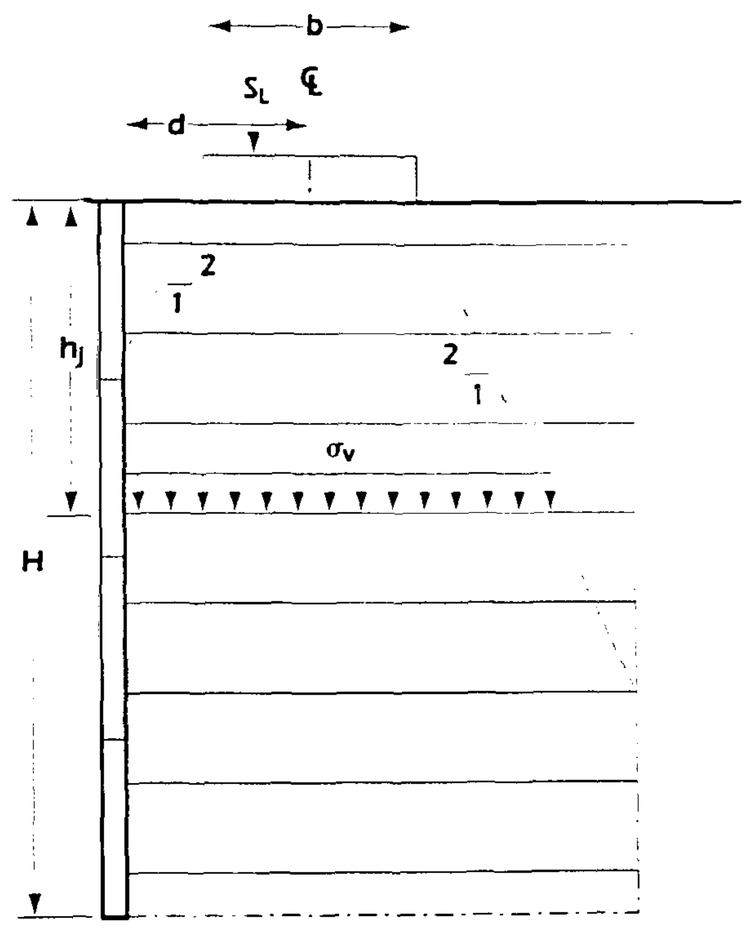

Figure 2

N.B. S_L = vertical loading applied to a strip contact area on top of the structure
b = width of strip contact area
d = length from front of wall to centreline of strip contact area
h_j = height above j^{th} layer to top of wall

For the purpose of determining the magnitude of the tensile force (T_{fj}) dispersal of the contact load (F_L) from the contact area is taken as shown in Figure 3.

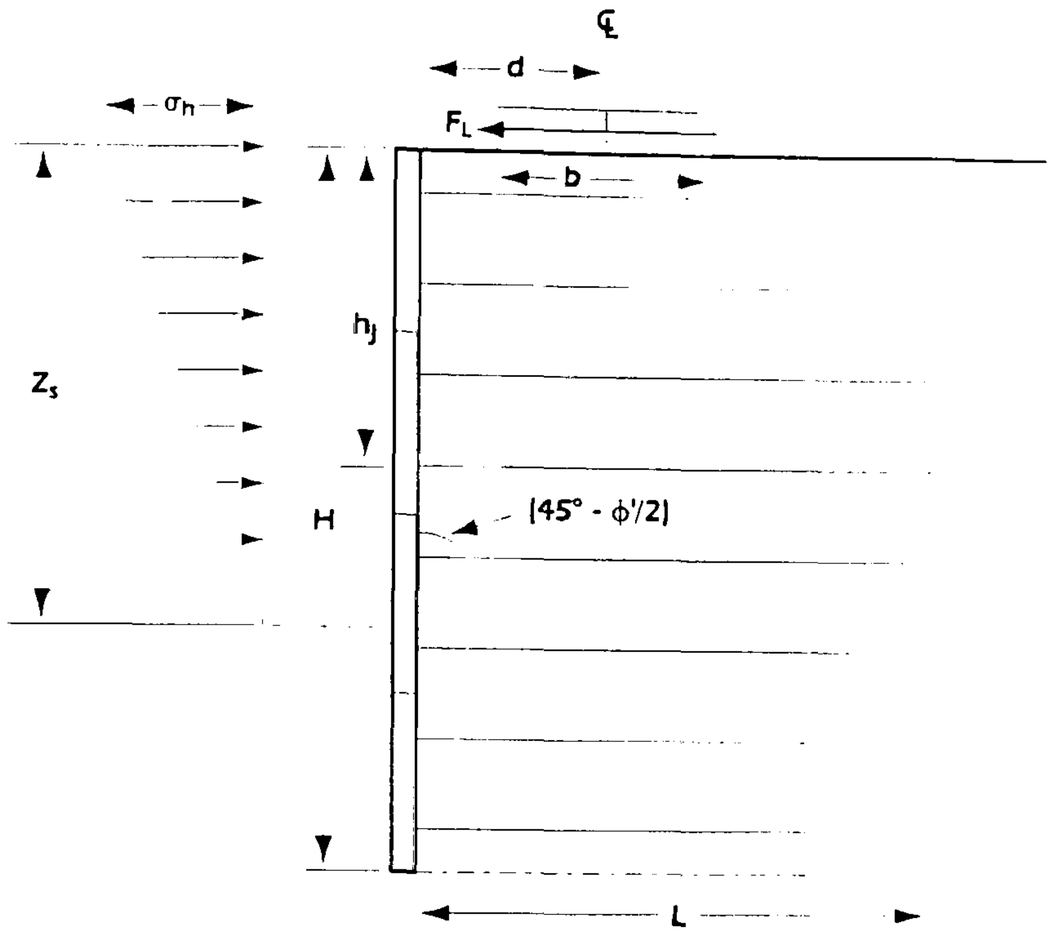

Length of zone over which horizontal stress acts (Z_s) = $\frac{d+b/2}{\tan(45° - \phi'/2)}$

Horizontal stress (σ_h) = $\frac{2F_L \tan(45° - \phi'/2)}{d+b/2}$

Figure 3

The restoring force due to cohesion (T_{cj}) is determined using the following equation:

$$T_{cj} = 2S_{vj}c'\sqrt{K_a} \qquad \text{Equ 13}$$

where: c' = effective cohesion of Soil 1

In order to ensure stability with regard to rupture failure, the following relationship must be satisfied for each grid:

$$T_D \geq T_j \qquad \text{Equ 14}$$

where: T_j = maximum tensile force (from Equation 10)
T_D = design strength of the grid (from Equation 2)

4.3 Wedge Stability

The resistance of the reinforced soil block to pull-out failure is determined by considering the stability of a series of one-part wedges. Analyses are undertaken at the base of the wall and, for walls up to 2.5m high, at five levels while for higher structures, checks are undertaken at ten levels. At each position, an Iterative Coulomb Wedge Check is undertaken to determine the wedge angle which produces the maximum out of balance force (T_{req}). This force is then compared with the sum of the restoring forces (T_{avail}) provided by each of the individual grids intersected by the wedge.

Where a grid is intersected beyond the minimum anchorage length required to mobilise its full design strength, a reduced restoring force for that particular grid must be included in the calculation. This value (T_{anch}) is given by the equation:

$$T_{anch} = \frac{P_j L_{ej}\left(\mu\gamma h_j + \mu w_s + \alpha_{bc}' c'\right)}{\text{factor of safety}} \qquad \text{Equ 15}$$

where: P_j = perimeter of grid j (=2.00m)

L_{ej} = anchorage length fo grid j
μ = $\alpha_p \tan\phi'_1$
h_j = height of fill above grid j
α_p = coefficient of interaction for grid pull-out

Notes: a_{bc}' is usually taken to equal a_p in the absence of specific test data
A factor of safety of 2.0 is usually adopted for the anchorage calculation

5. Post-construction Deformation Check

In order to ensure that the post-construction strains are acceptable, two checks are undertaken during the analysis.

5.1 The K_a x s_v Check

This check examines the post-construction strain occurring in the grids as a result of overburden pressure. It is assumed that wedges emanating from the toe at angles greater than 45-f'$_1$/2 mobilise the full active pressure given by K_a while wedges at angles less than f'$_1$ are subjected to zero active pressure (i.e. K_a is zero). The active pressure acting on wedges at angles between f'$_1$ and 45-f'$_1$/2 are obtained by linear interpolation as shown in Figure

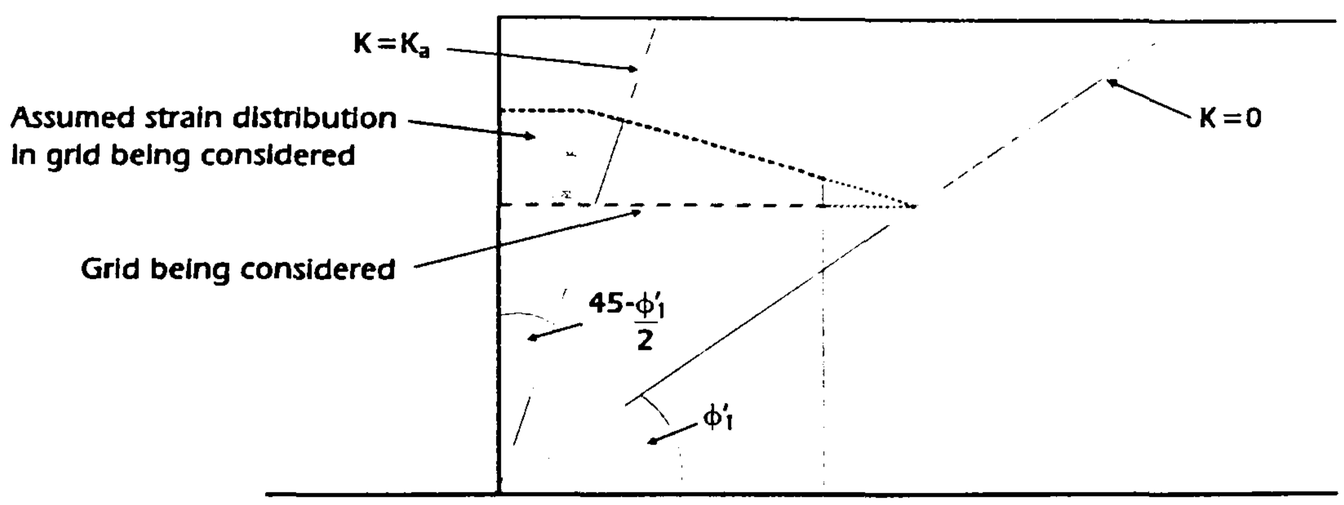

Figure 4

At any point, the force mobilised in the jth grid (s_j) is given by K_a x s_{vj}. The force required in order to mobilise 1% post-construction strain ($s_{1\%}$) (usually around two thirds of the creep limited strength) is determined for each grid type from isochronous curves. The actual post-construction strain (e_{pc}) in an individual grid is therefore approximated by the equation:

$$\varepsilon_{pc} = \frac{\sigma_{vj}}{\sigma_{1\%}} \qquad \text{Equ 16}$$

The program checks to ensure that the average post-construction strain in each grid does not exceed the prescribed 1% limit.

A similar approach is adopted for bridge abutments, but in this case the limit is reduced to 0.5% post-construction strain.

The greatest accuracy of the strain predicted by Equation 16 is obtained when the strain is close to the critical value. The calculation procedure used to determine the post-construction strain therefore changes depending on whether the structure is a normal wall or a bridge abutment.

5.2 The Wedge Check

The out of balance force (OBF) for a series of wedges are determined. The OBF for each wedge is then distributed amongst the grids cut by the wedge in proportion to the strength of the grids i.e. a grid with a design strength of 20kN/m would mobilise twice as much force as one with a design strength of 10kN/m as it is twice as stiff (Figure 5).

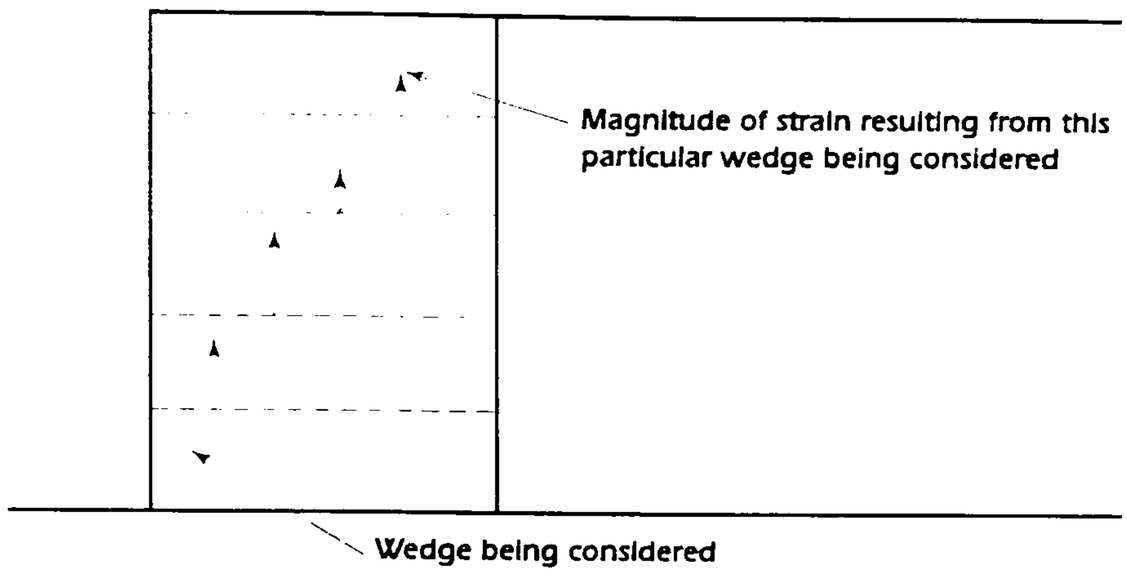

Figure 5

Groups of wedges at 2° intervals are analysed at the base of the wall and levels of one tenth of the height of the face (one fifth for walls up to 2.5m in height). The strain from each wedge in the individual grids is then determined in accordance with Equation 16 and a strain distribution curve is obtained (Figure 6). The area under the curve divided by the grid length defines the average post-construction strain for each grid and the program checks to ensure that this is less than the 1% or 0.5% limit appropriate for the type of structure.

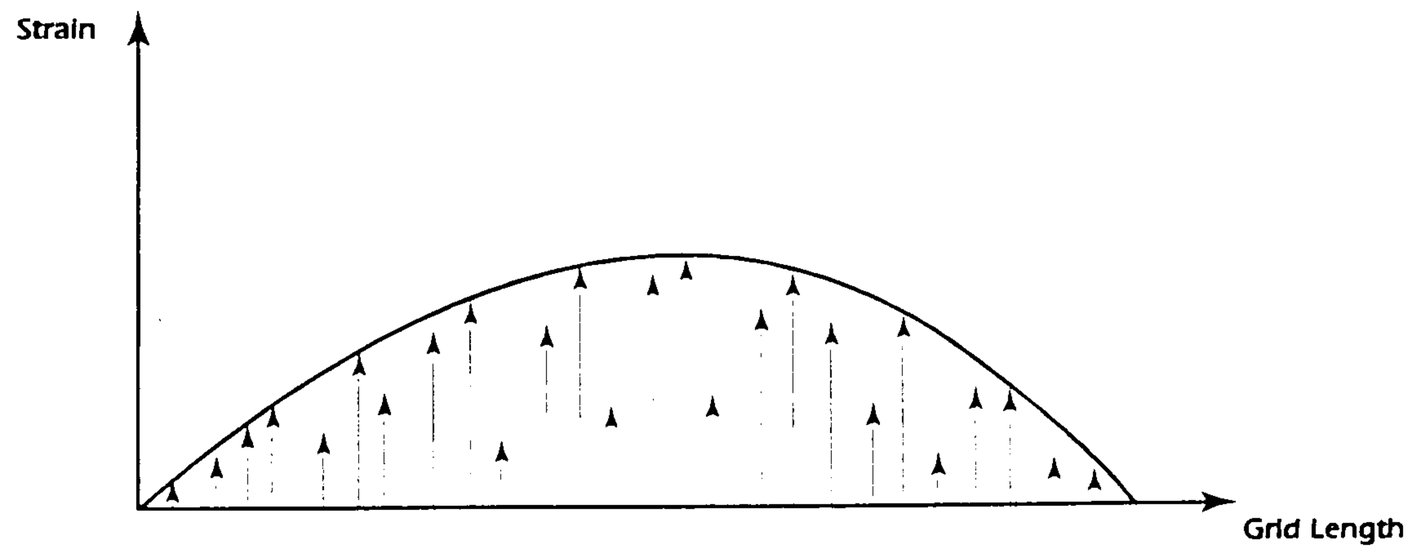

Figure 6

ANNEX C

Output from Winwall 6.14

Tensar International
New Wellington Street
Blackburn
BB2 4PJ United Kingdom
Tel: 01254 262431 Fax: 01254 696687; E-mail: design@tensar.co.uk

Tensar Grid Reinforced Soil Application Suggestion
Client: University of Newcastle Upon Tyne

Project:

EKG Trial Wall
Preliminary Geogrid layouts
c' = 0, phi'cv = 12.5deg

Objective:
Parametric study with assumed design parameters

Calculations in accordance with:
Tie-back Wedge Method and Tensar International Guidelines

Calculations carried out using Winwall Version 6.14
Details of the theory used in this program are available on request from:
Tensar International Limited, New Wellington Street, Blackburn, UK BB2 4PJ.
Telephone 01254 262431; Fax: 01254 696687; E-mail design@tensar.co.uk.

This document contains an Application Suggestion which has been prepared by Tensar International, on a confidential basis, to enable the application of **Tensar** geogrids to be evaluated. The Application Suggestion is merely illustrative and is not a detailed design.

This Application Suggestion is specific to the unique characteristics of the **Tensar** geogrids which are referenced within the calculations.

This Application Suggestion does not form the whole or any part of a contract. Its suitability for any project is the sole responsibility of the user and its professional advisors. The Netlon Group Limited is not responsible for any application of the Application Suggestion other than in conjunction with the sale of **Tensar.**

Input data

Geometry and facing details

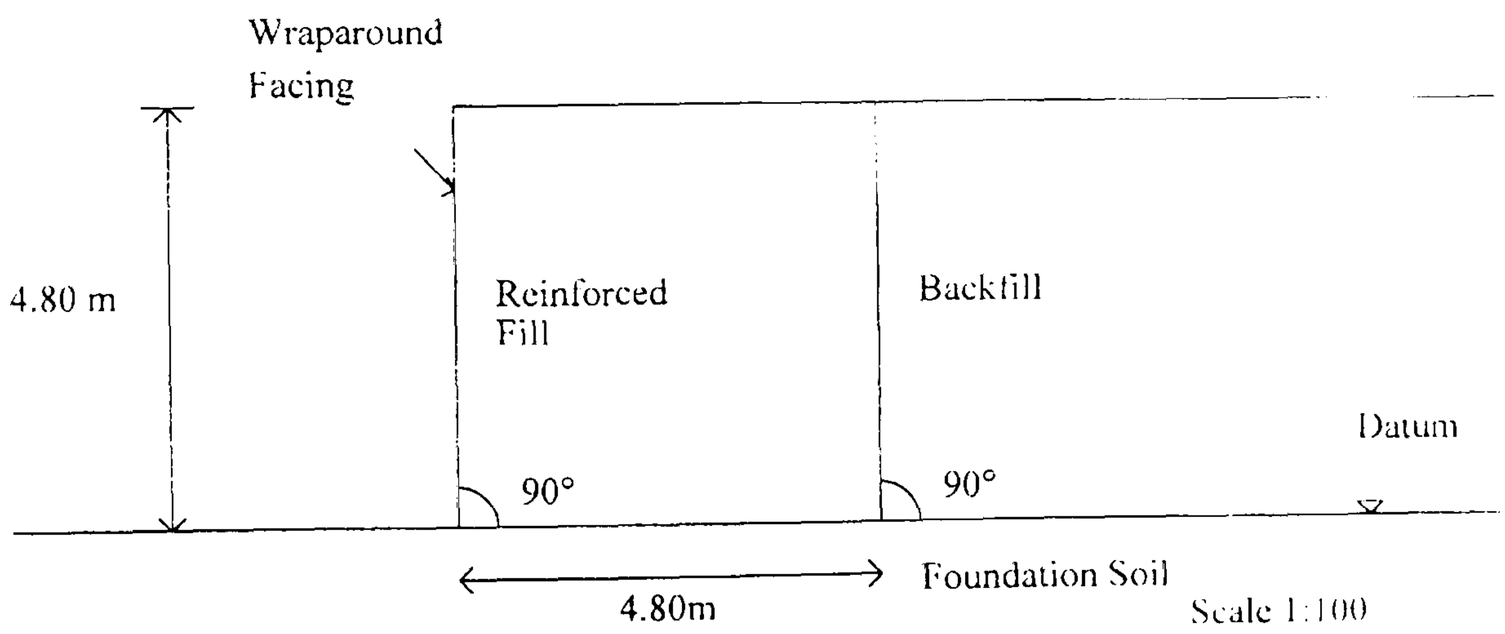

Soil properties

Soil type	c' (kN/m²)	ϕ'_{cv} (degrees)	Unit weight (kN/m³)
Reinforced fill	0.00	12.50	19.00
Backfill	0.00	42.50	1.00
Foundation	10.00	28.00	18.00

Reinforcement data

Grid type	P_c at 10°C kN/m	f_d	f_c	f_m	MILTS kN/m
40RE	23.00	1.00	1.0	1.0	23.00
80RE	38.50	1.00	1.0	1.0	38.50

Design strength is obtained by dividing Minimum Installed Long Term Strength (MILTS) by overall factor of safety = 1.350.

Coefficients of interaction:

Pullout	1.000
Sliding	0.800

Reinforcement layout

Base grid is Tensar 80RE at 0.000m above datum. Horizontal coverage of grids is 100%.

Tensar geogrid	Number of geogrids	Starting level above datum (m)	Vertical spacing (m)	Finishing level above datum (m)
80RE	2	0.450	0.450	0.900
80RE	3	1.500	0.600	2.700
40RE	3	3.300	0.600	4.500

There are a total of 9 layers of Tensar main reinforcement

Grid coordinates

Tensar Geogrid	Level above datum (m)	Left end (m)	Right end (m)	Length (m)
80RE	0.000	0.000	4.800	4.800
80RE	0.450	0.000	4.800	4.800
80RE	0.900	0.000	4.800	4.800
80RE	1.500	0.000	4.800	4.800
80RE	2.100	0.000	4.800	4.800
80RE	2.700	0.000	4.800	4.800
40RE	3.300	0.000	4.800	4.800
40RE	3.900	0.000	4.800	4.800
40RE	4.500	0.000	4.800	4.800

Secondary reinforcement

There are 8 intermediate grids of type Tensar SS20 of length 1.000m. placed at 0.300m intervals wherever spacing of main reinforcement exceeds 0.400m

RESULTS

External stability

External stability (using German DIN codes for bearing capacity)

Load case : A

All calculations are for 1m running length of structure with the width of the reinforced soil block = 4.800m at its base.

Calculation of forces and moments

The active forces on the back of the reinforced soil block are calculated by iterative Coulomb Wedge (DIN 4085) check to be:
Vertical load : 0.0kN/m. Horizontal load : 2.2kN/m.
These give an overturning moment about the centre of the base of 3.6kNm/m.
The total weight of the reinforced soil wall is 437.8kN; its overturning moment about the centre of its base is 0.0kNm

Sliding resistance check

There is a grid at the base of the wall, and therefore sliding on the grid must be considered: this allows for an alpha(sliding) of 0.800. The sliding resistance is 77.6kN. This gives a factor of safety against sliding of 34.810: this is >2.0 and is acceptable.

Bearing capacity check

The resultant acts at an eccentricity of 0.008m; this lies within the middle third and is acceptable.
The bearing capacity coefficients (DIN 4017) are as follows:

$N_c = 25.80$ $N_d = 14.72$ $N_b = 7.29$

x_b is 0.986; this gives an ultimate bearing pressure of 874.8kN/sq.m. over an effective length of 4.784m, giving an ultimate load of 4184.9kN. With a total vertical force of 437.8kN, this gives a factor of safety on bearing capacity of 9.560. This is >2.0 and acceptable.

Load case : B

All calculations are for 1m running length of structure with the width of the reinforced soil block = 4.800m at its base.

Calculation of forces and moments

The active forces on the back of the reinforced soil block are calculated by iterative Coulomb Wedge (DIN 4085) check to be:

Vertical load : 0.0kN/m. Horizontal load : 2.2kN/m.

These give an overturning moment about the centre of the base of 3.6kNm/m.
The total weight of the reinforced soil wall is 437.8kN; its overturning moment about the centre of its base is 0.0kNm

Sliding resistance check

There is a grid at the base of the wall, and therefore sliding on the grid must be considered: this allows for an alpha(sliding) of 0.800. The sliding resistance is 77.6kN. This gives a factor of safety against sliding of 34.810; this is >2.0 and is acceptable.

Bearing capacity check

The resultant acts at an eccentricity of 0.008m; this lies within the middle third and is acceptable.
The bearing capacity coefficients (DIN 4017) are as follows:

$N_c = 25.80$ $N_d = 14.72$ $N_b = 7.29$

x_b is 0.986; this gives an ultimate bearing pressure of 874.8kN/sq.m. over an effective length of 4.784m, giving an ultimate load of 4184.9kN. With a total vertical force of 437.8kN, this gives a factor of safety on bearing capacity of 9.560. This is >2.0 and acceptable.

Grid spacing check

Tensar geogrid	Level above datum (m)	Spacing (m)	Rupture Check			Post construction strain		
			Design strength T_D (kN/m)	Design load T_j (kN/m)	Layer OK?	Average strain based on T_j (%)	Average strain based on Wedge check (%)	Layer OK?
80RE	0.000	0.225	28.519	13.263	OK	0.000	0.000	OK
80RE	0.450	0.450	28.519	24.024	OK	0.253	0.248	OK
80RE	0.900	0.525	28.519	25.115	OK	0.508	0.534	OK
80RE	1.500	0.600	28.519	24.272	OK	0.729	0.728	OK
80RE	2.100	0.600	28.519	19.848	OK	0.679	0.703	OK
80RE	2.700	0.600	28.519	15.431	OK	0.561	0.599	OK
40RE	3.300	0.600	17.037	11.018	OK	0.693	0.628	OK
40RE	3.900	0.600	17.037	6.610	OK	0.423	0.433	OK
40RE	4.500	0.600	17.037	2.203	OK	0.143	0.130	OK

Wedge check

Wedges with highest T_{req}:

Front: x (m)	Front: y (m)	Back: x (m)	Back: y (m)	β worst	T_{req} (kN/m)	T_{avail} (kN/m)	OK or not?
0.000	0.000	3.852	4.800	38.75	141	187	OK
0.000	0.480	3.467	4.800	38.75	114	138	OK
0.000	0.960	3.082	4.800	38.75	90	114	OK
0.000	1.440	2.697	4.800	38.75	69	116	OK
0.000	1.920	2.311	4.800	38.75	51	90	OK
0.000	2.400	1.926	4.800	38.75	35	63	OK
0.000	2.880	1.541	4.800	38.75	23	37	OK
0.000	3.360	1.156	4.800	38.75	13	21	OK
0.000	3.840	0.770	4.800	38.75	6	22	OK
0.000	4.320	0.385	4.800	38.75	1	6	OK

Wedges with highest ratio of T_{req}/T_{avail}:

Note that the critical wedge when considering anchorage may not be the same as the one which requires the maximum reinforcement force.

Front: x (m)	Front: y (m)	Back: x (m)	Back: y (m)	β worst	T_{req} (kN/m)	T_{avail} (kN/m)	OK or not?
0.000	0.000	6.024	4.800	51.45	129	155	OK
0.000	0.480	7.352	4.800	59.56	87	89	OK
0.000	0.960	6.269	4.800	58.51	75	81	OK
0.000	1.440	5.270	4.800	57.48	61	97	OK
0.000	1.920	3.032	4.800	46.47	50	87	OK
0.000	2.400	2.615	4.800	47.46	34	61	OK
0.000	2.880	2.309	4.800	50.25	22	34	OK
0.000	3.360	1.736	4.800	50.33	12	20	OK
0.000	3.840	0.828	4.800	40.79	6	22	OK
0.000	4.320	0.416	4.800	40.89	1	6	OK

Tensar Reinforced Soil Application Suggestion

Tensar International
New Wellington Street
Blackburn
BB2 4PJ United Kingdom

Tel: 01254 26243
Fax: 01254 [illegible]
Email: design@tensar.co.uk

Soil Type	c' (kN/m²)	ϕ_{cv}' (deg)	γ (kN/m³)
Reinforced fill	0	13	19
Backfill	0	43	1
Foundation	10	28	18

Key / Material quantities

	Grid Type	Quantity in run
———	6 No. Tensar SR0RL	[illegible] m
- - - -	8 No. Tensar SS20	5 m
· · · ·	3 No. Tensar [illegible] RE	18 m

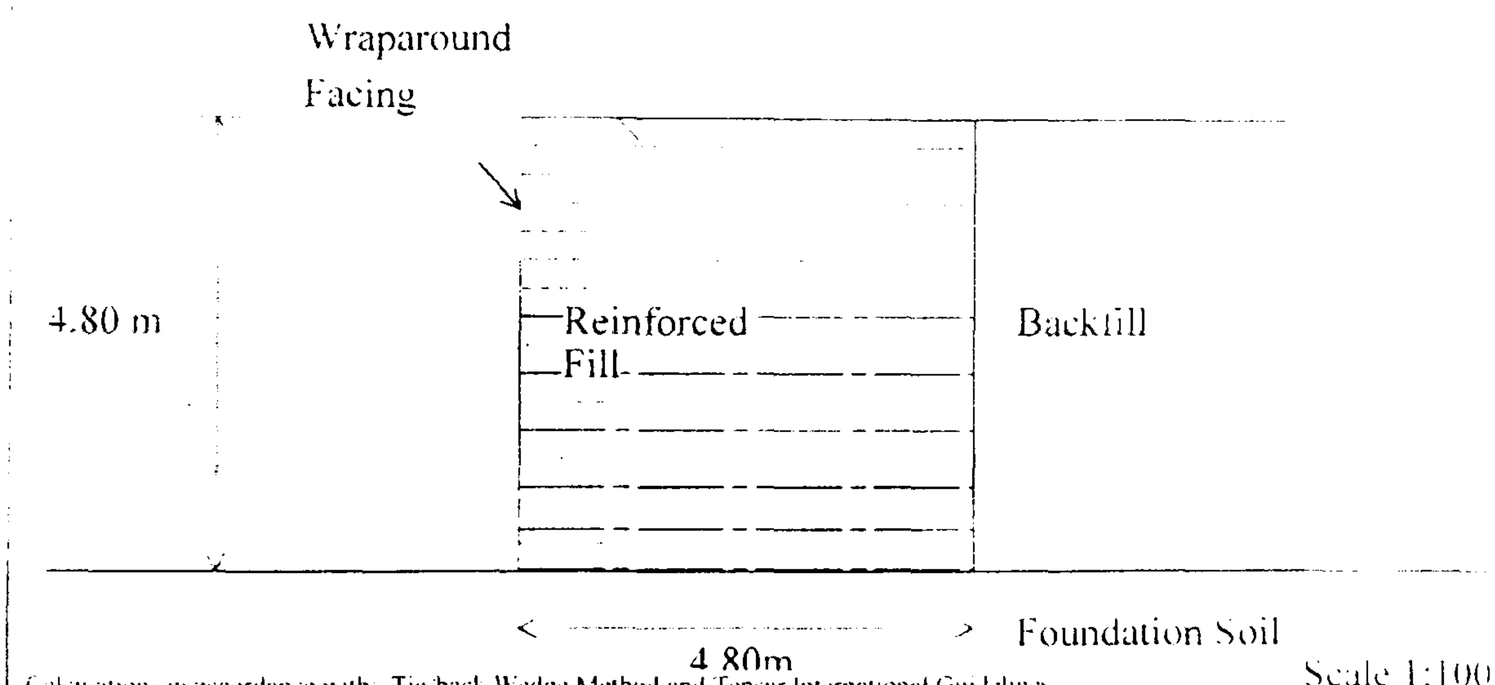

Calculations in accordance with: Tie-back Wedge Method and Tensar International Guidelines

Scale 1:100

Adequate consideration should be given by the designer to the provision of drainage in the above structure
For further details regarding this design please contact Tensar International

Client : **University of Newcastle Upon Tyne**

Project: **EKG Trial Wall**
Preliminary Geogrid layouts

c' = 0, phi'cv = 12.5deg

Objective:
Parametric study with assumed design parameters

Design prepared by : The Netlon Group Limited
Date : 12 Feb 1999 **Reference :** JP/99/046a

Tensar International
New Wellington Street
Blackburn
BB2 4PJ United Kingdom
Tel: 01254 262431 Fax: 01254 696687; E-mail: design@tensar.co.uk

Tensar Grid Reinforced Soil Application Suggestion
Client: University of Newcastle Upon Tyne

Project:

EKG Trial Wall
Preliminary Geogrid layouts
c' = 5kPa. phi'cv = 12.5deg

Objective:
Parametric study with assumed design parameters

Calculations in accordance with:
Tie-back Wedge Method and Tensar International Guidelines

Calculations carried out using Winwall Version 6.14
Details of the theory used in this program are available on request from:
Tensar International Limited, New Wellington Street, Blackburn, UK BB2 4PJ.
Telephone 01254 262431; Fax: 01254 696687; E-mail design@tensar.co.uk.

This document contains an Application Suggestion which has been prepared by Tensar International, on a confidential basis, to enable the application of **Tensar** geogrids to be evaluated. The Application Suggestion is merely illustrative and is not a detailed design.

This Application Suggestion is specific to the unique characteristics of the **Tensar** geogrids which are referenced within the calculations.

This Application Suggestion does not form the whole or any part of a contract. Its suitability for any project is the sole responsibility of the user and its professional advisors. The Netlon Group Limited is not responsible for any application of the Application Suggestion other than in conjunction with the sale of **Tensar.**

Input data

Geometry and facing details

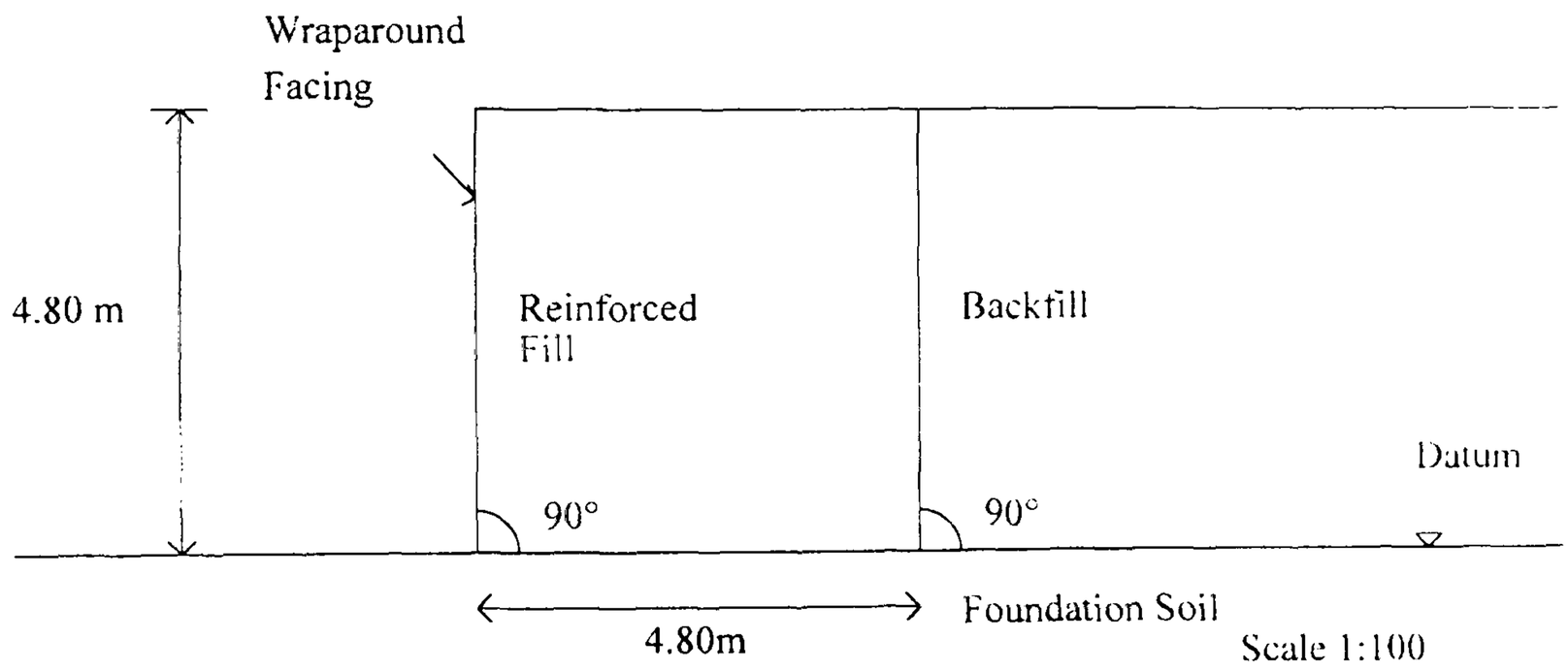

Soil properties

Soil type	c' (kN/m²)	ϕ'_{cv} (degrees)	Unit weight (kN/m³)
Reinforced fill	5.00	12.50	19.00
Backfill	0.00	42.50	1.00
Foundation	10.00	28.00	18.00

Reinforcement data

Grid type	P_c at 10°C kN/m	f_d	f_e	f_m	MILTS kN/m
40RE	23.00	1.00	1.0	1.0	23.00
80RE	38.50	1.00	1.0	1.0	38.50

Design strength is obtained by dividing Minimum Installed Long Term Strength (MILTS) by overall factor of safety = 1.350.

Coefficients of interaction:

Pullout	1.000
Sliding	0.800

Reinforcement layout

Base grid is Tensar 80RE at 0.000m above datum. Horizontal coverage of grids is 100%.

Tensar geogrid	Number of geogrids	Starting level above datum (m)	Vertical spacing (m)	Finishing level above datum (m)
80RE	3	0.600	0.600	1.800
40RE	4	2.400	0.600	4.200

There are a total of 8 layers of Tensar main reinforcement

Grid coordinates

Tensar Geogrid	Level above datum (m)	Left end (m)	Right end (m)	Length (m)
80RE	0.000	0.000	4.800	4.800
80RE	0.600	0.000	4.800	4.800
80RE	1.200	0.000	4.800	4.800
80RE	1.800	0.000	4.800	4.800
40RE	2.400	0.000	4.800	4.800
40RE	3.000	0.000	4.800	4.800
40RE	3.600	0.000	4.800	4.800
40RE	4.200	0.000	4.800	4.800

Secondary reinforcement

There are 8 intermediate grids of type Tensar SS20 of length 1.000m. placed at 0.300m intervals wherever spacing of main reinforcement exceeds 0.400m

RESULTS

External stability

External stability (using German DIN codes for bearing capacity)

Load case : A

All calculations are for 1m running length of structure with the width of the reinforced soil block = 4.800m at its base.

Calculation of forces and moments

The active forces on the back of the reinforced soil block are calculated by iterative Coulomb Wedge (DIN 4085) check to be:
Vertical load : 0.0kN/m. Horizontal load : 2.2kN/m.
These give an overturning moment about the centre of the base of 3.6kNm/m.
The total weight of the reinforced soil wall is 437.8kN; its overturning moment about the centre of its base is 0.0kNm

Sliding resistance check

There is a grid at the base of the wall. and therefore sliding on the grid must be considered: this allows for an alpha(sliding) of 0.800. The sliding resistance is 96.8kN. This gives a factor of safety against sliding of 43.418; this is >2.0 and is acceptable.

Bearing capacity check

The resultant acts at an eccentricity of 0.008m: this lies within the middle third and is acceptable.
The bearing capacity coefficients (DIN 4017) are as follows:

$N_c = 25.80$ $N_d = 14.72$ $N_b = 7.29$

x_b is 0.986: this gives an ultimate bearing pressure of 874.8kN/sq.m. over an effective length of 4.784m. giving an ultimate load of 4184.9kN. With a total vertical force of 437.8kN. this gives a factor of safety on bearing capacity of 9.560. This is >2.0 and acceptable.

Load case : B

All calculations are for 1m running length of structure with the width of the reinforced soil block = 4.800m at its base.

Calculation of forces and moments

The active forces on the back of the reinforced soil block are calculated by iterative Coulomb Wedge (DIN 4085) check to be:

Vertical load : 0.0kN/m. Horizontal load : 2.2kN/m.

These give an overturning moment about the centre of the base of 3.6kNm/m.
The total weight of the reinforced soil wall is 437.8kN; its overturning moment about the centre of its base is 0.0kNm

Sliding resistance check

There is a grid at the base of the wall, and therefore sliding on the grid must be considered: this allows for an alpha(sliding) of 0.800. The sliding resistance is 96.8kN. This gives a factor of safety against sliding of 43.418; this is >2.0 and is acceptable.

Bearing capacity check

The resultant acts at an eccentricity of 0.008m; this lies within the middle third and is acceptable.
The bearing capacity coefficients (DIN 4017) are as follows:

$N_c = 25.80$ $N_d = 14.72$ $N_b = 7.29$

x_b is 0.986; this gives an ultimate bearing pressure of 874.8kN/sq.m. over an effective length of 4.784m, giving an ultimate load of 4184.9kN. With a total vertical force of 437.8kN. this gives a factor of safety on bearing capacity of 9.560. This is >2.0 and acceptable.

Grid spacing check

Tensar geogrid	Level above datum (m)	Spacing (m)	Rupture Check			Post construction strain		
			Design strength T_D (kN/m)	Design load T_j (kN/m)	Layer OK?	Average strain based on		Layer OK?
						T_j (%)	Wedge check (%)	
80RE	0.000	0.300	28.519	15.276	OK	0.000	0.000	OK
80RE	0.600	0.600	28.519	26.106	OK	0.359	0.159	OK
80RE	1.200	0.600	28.519	21.671	OK	0.568	0.315	OK
80RE	1.800	0.600	28.519	17.243	OK	0.561	0.440	OK
40RE	2.400	0.600	17.037	12.823	OK	0.761	0.511	OK
40RE	3.000	0.600	17.037	8.409	OK	0.521	0.502	OK
40RE	3.600	0.600	17.037	3.998	OK	0.254	0.451	OK
40RE	4.200	0.900	17.037	0.000	OK	0.064	0.356	OK

Wedge check

Wedges with highest T_{req}:

Front: x (m)	Front: y (m)	Back: x (m)	Back: y (m)	β worst	T_{req} (kN/m)	T_{avail} (kN/m)	OK or not?
0.000	0.000	3.852	4.800	38.75	102	176	OK
0.000	0.480	3.467	4.800	38.75	80	150	OK
0.000	0.960	3.082	4.800	38.75	59	125	OK
0.000	1.440	2.697	4.800	38.75	42	97	OK
0.000	1.920	2.311	4.800	38.75	28	68	OK
0.000	2.400	1.926	4.800	38.75	16	68	OK
0.000	2.880	1.541	4.800	38.75	7	51	OK
0.000	3.360	1.156	4.800	38.75	1	34	OK
0.000	3.840	0.770	4.800	38.75	-2	17	OK

Wedges with highest ratio of T_{req}/T_{avail}:

Note that the critical wedge when considering anchorage may not be the same as the one which requires the maximum reinforcement force.

Front: x (m)	Front: y (m)	Back: x (m)	Back: y (m)	β worst	T_{req} (kN/m)	T_{avail} (kN/m)	OK or not?
0.000	0.000	5.129	4.800	46.90	98	160	OK
0.000	0.480	4.957	4.800	48.93	74	136	OK
0.000	0.960	3.644	4.800	43.50	58	121	OK
0.000	1.440	2.697	4.800	38.75	42	97	OK
0.000	1.920	2.311	4.800	38.75	28	68	OK
0.000	2.400	1.926	4.800	38.75	16	68	OK
0.000	2.880	1.541	4.800	38.75	7	51	OK
0.000	3.360	1.156	4.800	38.75	1	34	OK
0.000	3.840	0.770	4.800	38.75	-2	17	OK

Tensar Reinforced Soil Application Suggestion

Tensar International
New Wellington Street
Blackburn
BB2 4PJ United Kingdom

Tel : 01254 262431
Fax : 01254 [illegible]
Email : design@tensar.co.uk

Soil Type	c'	ϕ'_{cv}	γ
	(kN/m²)	(deg)	(kN/m³)
Reinforced fill	5	13	19
Backfill	0	43	1
Foundation	10	28	18

Key Material quantities

	Grid Type	Quantity in run
———	4 No. Tensar SR[illegible]	[illegible] m
— — —	8 No. Tensar SS2[illegible]	8 m
— — —	4 No. Tensar 4[illegible]	24 m

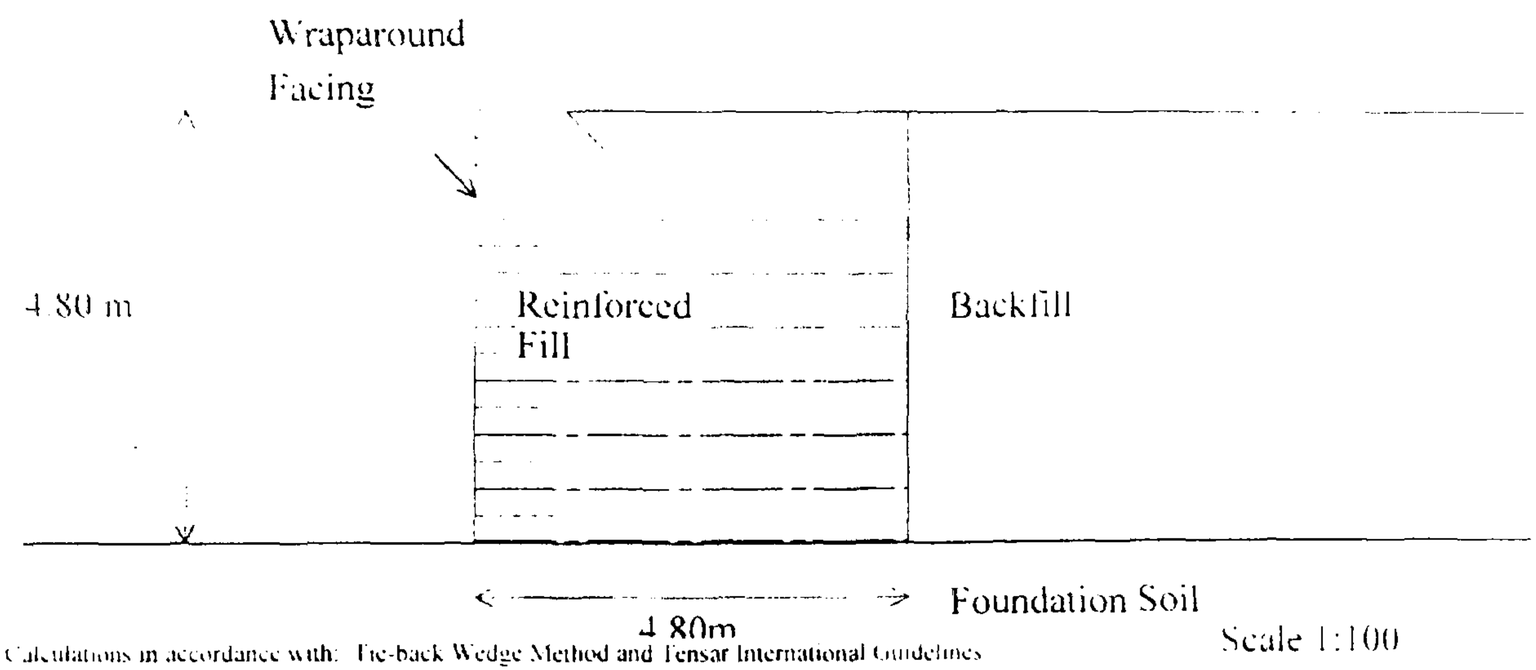

Calculations in accordance with: Tie-back Wedge Method and Tensar International Guidelines

Scale 1:100

Adequate consideration should be given by the designer to the provision of drainage in the above structure
For further details regarding this design please contact Tensar International

Client : **University of Newcastle Upon Tyne**
Project: **EKG Trial Wall**
Preliminary Geogrid layouts

c' = 5kPa, phi'cv = 12.5deg

Objective:
Parametric study with assumed design parameters

Design prepared by : The Netlon Group Limited
Date : 12 Feb 1999 **Reference :** JP/99/046d

Tensar International
New Wellington Street
Blackburn
BB2 4PJ United Kingdom
Tel: 01254 262431 Fax: 01254 696687; E-mail: design@tensar.co.uk

Tensar Grid Reinforced Soil Application Suggestion
Client: University of Newcastle Upon Tyne

Project:

EKG Trial Wall
Preliminary Geogrid layouts
c' = 0, phi'cv = 15deg

Objective:
Parametric study with assumed design parameters

Calculations in accordance with:
Tie-back Wedge Method and Tensar International Guidelines

Calculations carried out using Winwall Version 6.14
Details of the theory used in this program are available on request from:
Tensar International Limited, New Wellington Street, Blackburn, UK BB2 4PJ.
Telephone 01254 262431; Fax: 01254 696687; E-mail design@tensar.co.uk.

This document contains an Application Suggestion which has been prepared by Tensar International, on a confidential basis, to enable the application of **Tensar** geogrids to be evaluated. The Application Suggestion is merely illustrative and is not a detailed design.

This Application Suggestion is specific to the unique characteristics of the **Tensar** geogrids which are referenced within the calculations.

This Application Suggestion does not form the whole or any part of a contract. Its suitability for any project is the sole responsibility of the user and its professional advisors. The Netlon Group Limited is not responsible for any application of the Application Suggestion other than in conjunction with the sale of **Tensar.**

Input data

Geometry and facing details

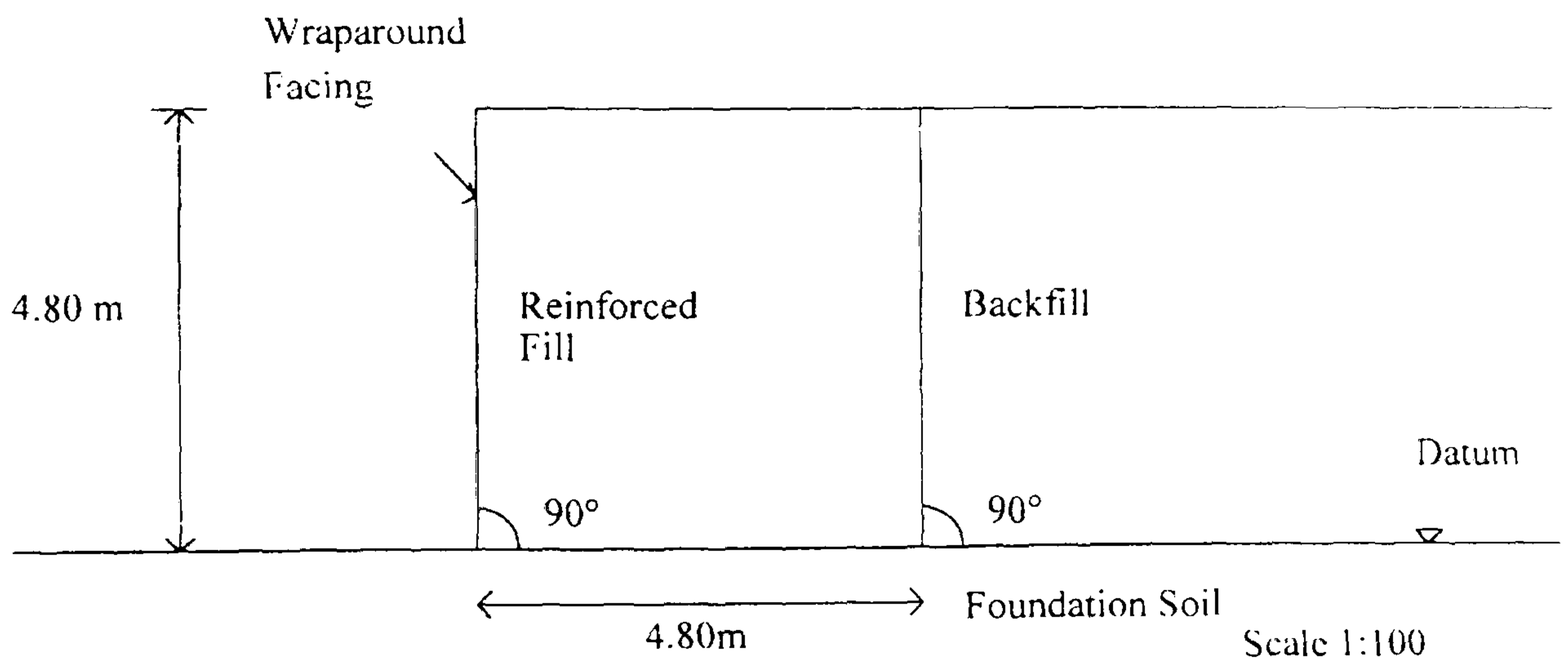

Scale 1:100

Soil properties

Soil type	c' (kN/m²)	ϕ'_{cv} (degrees)	Unit weight (kN/m³)
Reinforced fill	0.00	15.00	19.00
Backfill	0.00	42.50	1.00
Foundation	10.00	28.00	18.00

Reinforcement data

Grid type	P_c at 10°C kN/m	f_d	f_e	f_m	MILTS kN/m
40RE	23.00	1.00	1.0	1.0	23.00
80RE	38.50	1.00	1.0	1.0	38.50

Design strength is obtained by dividing Minimum Installed Long Term Strength (MILTS) by overall factor of safety = 1.350.

Coefficients of interaction:

Pullout	1.000
Sliding	0.800

Reinforcement layout

Base grid is Tensar 80RE at 0.000m above datum. Horizontal coverage of grids is 100%.

Tensar geogrid	Number of geogrids	Starting level above datum (m)	Vertical spacing (m)	Finishing level above datum (m)
80RE	3	0.600	0.600	1.800
40RE	4	2.400	0.600	4.200

There are a total of 8 layers of Tensar main reinforcement

Grid coordinates

Tensar Geogrid	Level above datum (m)	Left end (m)	Right end (m)	Length (m)
80RE	0.000	0.000	4.800	4.800
80RE	0.600	0.000	4.800	4.800
80RE	1.200	0.000	4.800	4.800
80RE	1.800	0.000	4.800	4.800
40RE	2.400	0.000	4.800	4.800
40RE	3.000	0.000	4.800	4.800
40RE	3.600	0.000	4.800	4.800
40RE	4.200	0.000	4.800	4.800

Secondary reinforcement

There are 8 intermediate grids of type Tensar SS20 of length 1.000m. placed at 0.300m intervals wherever spacing of main reinforcement exceeds 0.400m

RESULTS

External stability

External stability (using German DIN codes for bearing capacity)

Load case : A

All calculations are for 1m running length of structure with the width of the reinforced soil block = 4.800m at its base.

Calculation of forces and moments

The active forces on the back of the reinforced soil block are calculated by iterative Coulomb Wedge (DIN 4085) check to be:
Vertical load : 0.0kN/m. Horizontal load : 2.2kN/m.
These give an overturning moment about the centre of the base of 3.6kNm/m.
The total weight of the reinforced soil wall is 437.8kN; its overturning moment about the centre of its base is 0.0kNm

Sliding resistance check

There is a grid at the base of the wall, and therefore sliding on the grid must be considered: this allows for an alpha(sliding) of 0.800. The sliding resistance is 93.8kN. This gives a factor of safety against sliding of 42.073; this is >2.0 and is acceptable.

Bearing capacity check

The resultant acts at an eccentricity of 0.008m; this lies within the middle third and is acceptable.
The bearing capacity coefficients (DIN 4017) are as follows:

$N_c = 25.80$ $N_d = 14.72$ $N_b = 7.29$

x_b is 0.986; this gives an ultimate bearing pressure of 874.8kN/sq.m. over an effective length of 4.784m, giving an ultimate load of 4184.9kN. With a total vertical force of 437.8kN, this gives a factor of safety on bearing capacity of 9.560. This is >2.0 and acceptable.

Load case : B

All calculations are for 1m running length of structure with the width of the reinforced soil block = 4.800m at its base.

Calculation of forces and moments

The active forces on the back of the reinforced soil block are calculated by iterative Coulomb Wedge (DIN 4085) check to be:

Vertical load : 0.0kN/m. Horizontal load : 2.2kN/m.

These give an overturning moment about the centre of the base of 3.6kNm/m.
The total weight of the reinforced soil wall is 437.8kN; its overturning moment about the centre of its base is 0.0kNm

Sliding resistance check

There is a grid at the base of the wall, and therefore sliding on the grid must be considered: this allows for an alpha(sliding) of 0.800. The sliding resistance is 93.8kN. This gives a factor of safety against sliding of 42.073; this is >2.0 and is acceptable.

Bearing capacity check

The resultant acts at an eccentricity of 0.008m; this lies within the middle third and is acceptable.
The bearing capacity coefficients (DIN 4017) are as follows:

$N_c = 25.80$ $N_d = 14.72$ $N_b = 7.29$

x_b is 0.986; this gives an ultimate bearing pressure of 874.8kN/sq.m. over an effective length of 4.784m, giving an ultimate load of 4184.9kN. With a total vertical force of 437.8kN, this gives a factor of safety on bearing capacity of 9.560. This is >2.0 and acceptable.

Grid spacing check

Tensar geogrid	Level above datum (m)	Spacing (m)	Rupture Check			Post construction strain		
			Design strength T_D (kN/m)	Design load T_j (kN/m)	Layer OK?	Average strain based on		Layer OK?
						T_j (%)	Wedge check (%)	
80RE	0.000	0.300	28.519	16.164	OK	0.000	0.000	OK
80RE	0.600	0.600	28.519	28.265	OK	0.333	0.297	OK
80RE	1.200	0.600	28.519	24.210	OK	0.550	0.579	OK
80RE	1.800	0.600	28.519	20.163	OK	0.617	0.691	OK
40RE	2.400	0.600	17.037	16.123	OK	0.926	0.742	OK
40RE	3.000	0.600	17.037	12.088	OK	0.735	0.712	OK
40RE	3.600	0.600	17.037	8.056	OK	0.506	0.593	OK
40RE	4.200	0.900	17.037	6.041	OK	0.387	0.322	OK

Wedge check

Wedges with highest T_{req}:

Front: x (m)	Front: y (m)	Back: x (m)	Back: y (m)	β worst	T_{req} (kN/m)	T_{avail} (kN/m)	OK or not?
0.000	0.000	3.683	4.800	37.50	129	165	OK
0.000	0.480	3.315	4.800	37.50	104	140	OK
0.000	0.960	2.947	4.800	37.50	82	115	OK
0.000	1.440	2.578	4.800	37.50	63	88	OK
0.000	1.920	2.210	4.800	37.50	46	60	OK
0.000	2.400	1.842	4.800	37.50	32	62	OK
0.000	2.880	1.473	4.800	37.50	21	46	OK
0.000	3.360	1.105	4.800	37.50	12	30	OK
0.000	3.840	0.737	4.800	37.50	5	14	OK

Wedges with highest ratio of T_{req}/T_{avail}:

Note that the critical wedge when considering anchorage may not be the same as the one which requires the maximum reinforcement force.

Front: x (m)	Front: y (m)	Back: x (m)	Back: y (m)	β worst	T_{req} (kN/m)	T_{avail} (kN/m)	OK or not?
0.000	0.000	5.485	4.800	48.81	121	148	OK
0.000	0.480	5.496	4.800	51.83	95	122	OK
0.000	0.960	4.702	4.800	50.76	77	103	OK
0.000	1.440	4.321	4.800	52.13	58	79	OK
0.000	1.920	2.684	4.800	42.98	46	59	OK
0.000	2.400	2.130	4.800	41.59	32	61	OK
0.000	2.880	1.700	4.800	41.53	21	45	OK
0.000	3.360	1.271	4.800	41.43	12	29	OK
0.000	3.840	0.837	4.800	41.10	5	14	OK

Tensar Reinforced Soil Application Suggestion

Tensar International
New Wellington Street
Blackburn
BB2 4PJ United Kingdom

Tel : 01254 262431
Fax : 01254 696687
Email : design@tensar.co.uk

Soil Type	c' (kN/m²)	ϕ_{cv}' (deg)	γ (kN/m³)
Reinforced fill	0	15	19
Backfill	0	43	1
Foundation	10	28	18

Key / Material quantities

Grid Type	Quantity/m run
4 No. Tensar 80RE	23 m²
8 No. Tensar SS20	8 m²
4 No. Tensar 40RE	24 m²

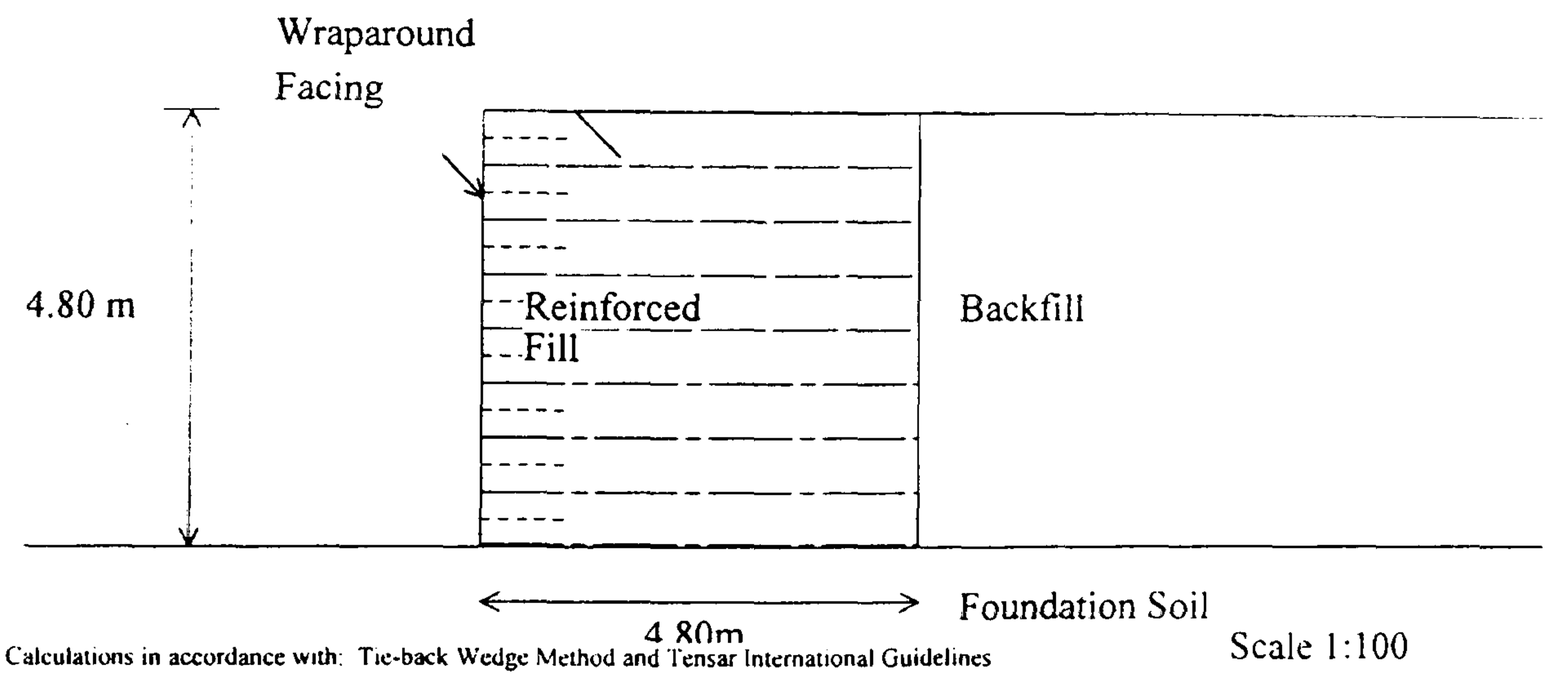

Calculations in accordance with: Tie-back Wedge Method and Tensar International Guidelines

Scale 1:100

Adequate consideration should be given by the designer to the provision of drainage in the above structure.
For further details regarding this design please contact Tensar International

Client : **University of Newcastle Upon Tyne**
Project: **EKG Trial Wall**
Preliminary Geogrid layouts
c' = 0, phi'cv = 15deg

Objective:
Parametric study with assumed design parameters

Design prepared by : The Netlon Group Limited
Date : 12 Feb 1999 **Reference :** JP/99/046b

Tensar International
New Wellington Street
Blackburn
BB2 4PJ United Kingdom
Tel: 01254 262431 Fax: 01254 696687: E-mail: design@tensar.co.uk

Tensar Grid Reinforced Soil Application Suggestion
Client: University of Newcastle Upon Tyne

Project:

EKG Trial Wall
Preliminary Geogrid layouts
c' = 0, phi'cv = 20deg

Objective:
Parametric study with assumed design parameters

Calculations in accordance with:
Tie-back Wedge Method and Tensar International Guidelines

Calculations carried out using Winwall Version 6.14
Details of the theory used in this program are available on request from:
Tensar International Limited, New Wellington Street, Blackburn, UK BB2 4PJ.
Telephone 01254 262431; Fax: 01254 696687; E-mail design@tensar.co.uk.

This document contains an Application Suggestion which has been prepared by Tensar International, on a confidential basis, to enable the application of **Tensar** geogrids to be evaluated. The Application Suggestion is merely illustrative and is not a detailed design.

This Application Suggestion is specific to the unique characteristics of the **Tensar** geogrids which are referenced within the calculations.

This Application Suggestion does not form the whole or any part of a contract. Its suitability for any project is the sole responsibility of the user and its professional advisors. The Netlon Group Limited is not responsible for any application of the Application Suggestion other than in conjunction with the sale of **Tensar.**

Input data

Geometry and facing details

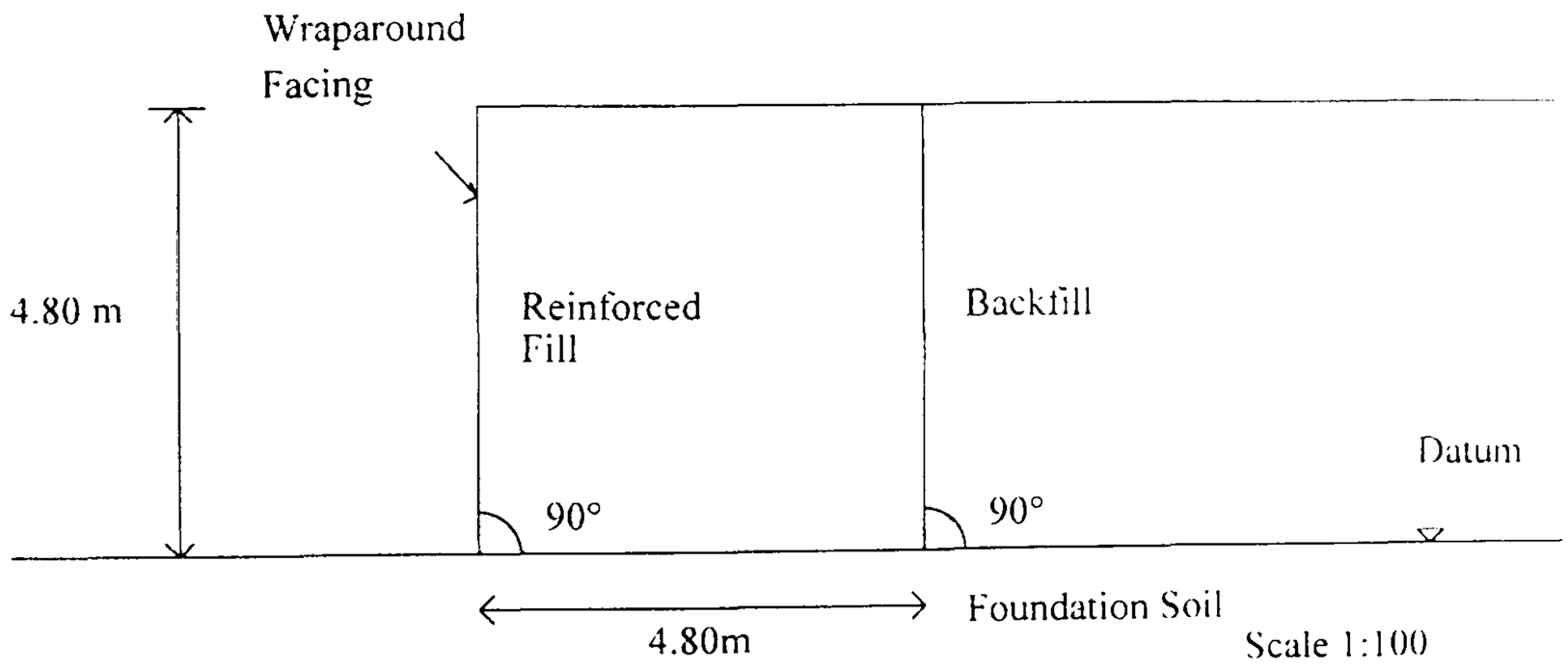

Soil properties

Soil type	c' (kN/m²)	ϕ'_{cv} (degrees)	Unit weight (kN/m³)
Reinforced fill	0.00	20.00	19.00
Backfill	0.00	42.50	1.00
Foundation	10.00	28.00	18.00

Reinforcement data

Grid type	P_c at 10°C kN/m	f_d	f_e	f_m	MILTS kN/m
40RE	23.00	1.00	1.0	1.0	23.00
80RE	38.50	1.00	1.0	1.0	38.50

Design strength is obtained by dividing Minimum Installed Long Term Strength (MILTS) by overall factor of safety = 1.350.

Coefficients of interaction:

Pullout	1.000
Sliding	0.800

Reinforcement layout

Base grid is Tensar 80RE at 0.000m above datum. Horizontal coverage of grids is 100%.

Tensar geogrid	Number of geogrids	Starting level above datum (m)	Vertical spacing (m)	Finishing level above datum (m)
80RE	2	0.600	0.600	1.200
40RE	5	1.800	0.600	4.200

There are a total of 8 layers of Tensar main reinforcement

Grid coordinates

Tensar Geogrid	Level above datum (m)	Left end (m)	Right end (m)	Length (m)
80RE	0.000	0.000	4.800	4.800
80RE	0.600	0.000	4.800	4.800
80RE	1.200	0.000	4.800	4.800
40RE	1.800	0.000	4.800	4.800
40RE	2.400	0.000	4.800	4.800
40RE	3.000	0.000	4.800	4.800
40RE	3.600	0.000	4.800	4.800
40RE	4.200	0.000	4.800	4.800

Secondary reinforcement

There are 8 intermediate grids of type Tensar SS20 of length 1.000m, placed at 0.300m intervals wherever spacing of main reinforcement exceeds 0.400m

RESULTS

External stability

External stability (using German DIN codes for bearing capacity)

Load case : A

All calculations are for 1m running length of structure with the width of the reinforced soil block = 4.800m at its base.

Calculation of forces and moments

The active forces on the back of the reinforced soil block are calculated by iterative Coulomb Wedge (DIN 4085) check to be:

Vertical load : 0.0kN/m. Horizontal load : 2.2kN/m.

These give an overturning moment about the centre of the base of 3.6kNm/m.
The total weight of the reinforced soil wall is 437.8kN; its overturning moment about the centre of its base is 0.0kNm

Sliding resistance check

There is a grid at the base of the wall, and therefore sliding on the grid must be considered: this allows for an alpha(sliding) of 0.800. The sliding resistance is 127.5kN. This gives a factor of safety against sliding of 57.150; this is >2.0 and is acceptable.

Bearing capacity check

The resultant acts at an eccentricity of 0.008m; this lies within the middle third and is acceptable.
The bearing capacity coefficients (DIN 4017) are as follows:

$N_c = 25.80$ $N_d = 14.72$ $N_b = 7.29$

x_b is 0.986: this gives an ultimate bearing pressure of 874.8kN/sq.m. over an effective length of 4.784m, giving an ultimate load of 4184.9kN. With a total vertical force of 437.8kN. this gives a factor of safety on bearing capacity of 9.560. This is >2.0 and acceptable.

Load case : B

All calculations are for 1m running length of structure with the width of the reinforced soil block = 4.800m at its base.

Calculation of forces and moments

The active forces on the back of the reinforced soil block are calculated by iterative Coulomb Wedge (DIN 4085) check to be:

Vertical load : 0.0kN/m. Horizontal load : 2.2kN/m.

These give an overturning moment about the centre of the base of 3.6kNm/m.
The total weight of the reinforced soil wall is 437.8kN; its overturning moment about the centre of its base is 0.0kNm

Sliding resistance check

There is a grid at the base of the wall, and therefore sliding on the grid must be considered: this allows for an alpha(sliding) of 0.800. The sliding resistance is 127.5kN. This gives a factor of safety against sliding of 57.150; this is >2.0 and is acceptable.

Bearing capacity check

The resultant acts at an eccentricity of 0.008m; this lies within the middle third and is acceptable.
The bearing capacity coefficients (DIN 4017) are as follows:

$N_c = 25.80$ $N_d = 14.72$ $N_b = 7.29$

x_b is 0.986; this gives an ultimate bearing pressure of 874.8kN/sq.m. over an effective length of 4.784m, giving an ultimate load of 4184.9kN. With a total vertical force of 437.8kN. this gives a factor of safety on bearing capacity of 9.560. This is >2.0 and acceptable.

Grid spacing check

Tensar geogrid	Level above datum (m)	Spacing (m)	Rupture Check			Post construction strain		
			Design strength T_D (kN/m)	Design load T_j (kN/m)	Layer OK?	Average strain based on		Layer OK?
						T_j (%)	Wedge check (%)	
80RE	0.000	0.300	28.519	13.460	OK	0.000	0.000	OK
80RE	0.600	0.600	28.519	23.536	OK	0.217	0.192	OK
80RE	1.200	0.600	28.519	20.160	OK	0.355	0.383	OK
40RE	1.800	0.600	17.037	16.790	OK	0.729	0.559	OK
40RE	2.400	0.600	17.037	13.426	OK	0.706	0.623	OK
40RE	3.000	0.600	17.037	10.066	OK	0.581	0.602	OK
40RE	3.600	0.600	17.037	6.709	OK	0.408	0.546	OK
40RE	4.200	0.900	17.037	5.031	OK	0.316	0.353	OK

Wedge check

Wedges with highest T_{req}:

Front: x (m)	Front: y (m)	Back: x (m)	Back: y (m)	β worst	T_{req} (kN/m)	T_{avail} (kN/m)	OK or not?
0.000	0.000	3.361	4.800	35.00	107	161	OK
0.000	0.480	3.025	4.800	35.00	87	134	OK
0.000	0.960	2.689	4.800	35.00	69	107	OK
0.000	1.440	2.353	4.800	35.00	53	80	OK
0.000	1.920	2.017	4.800	35.00	39	64	OK
0.000	2.400	1.680	4.800	35.00	27	66	OK
0.000	2.880	1.344	4.800	35.00	17	50	OK
0.000	3.360	1.008	4.800	35.00	10	34	OK
0.000	3.840	0.672	4.800	35.00	4	17	OK

Wedges with highest ratio of T_{req}/T_{avail}:

Note that the critical wedge when considering anchorage may not be the same as the one which requires the maximum reinforcement force.

Front: x (m)	Front: y (m)	Back: x (m)	Back: y (m)	β worst	T_{req} (kN/m)	T_{avail} (kN/m)	OK or not?
0.000	0.000	4.822	4.800	45.13	102	149	OK
0.000	0.480	4.455	4.800	45.88	82	125	OK
0.000	0.960	3.087	4.800	38.80	68	106	OK
0.000	1.440	2.762	4.800	39.42	52	79	OK
0.000	1.920	2.377	4.800	39.53	38	63	OK
0.000	2.400	1.902	4.800	38.40	27	65	OK
0.000	2.880	1.515	4.800	38.27	17	50	OK
0.000	3.360	1.008	4.800	35.00	10	34	OK
0.000	3.840	0.672	4.800	35.00	4	17	OK

ANNEX D

Water content reduction calculations

PHASE CALCULATIONS FOR ELECTRO-OSMOTIC TREATMENT

Initial Parameters for 65% Water content:

G_s = 2.65 (Typical value for an illitic clay)
V = 24m*3m*0.6m = 43.2m^3, Surface area = 24m*3m=72m^2
w = 0.65 as placed and w = 0.42 required after treatment by electro-osmosis

Assume soil is placed saturated

$$e = wG_s = 0.65 * 2.65 = 1.72$$

$$\rho_{bulk} = \frac{G_s(1+w)}{1+e}\rho_w = \frac{2.65(1+0.65)}{1+1.72} \bullet 10 = 1606.06 kg/m^3$$

$$\rho = \frac{M}{V} = \frac{M}{43.2} = 1606.06 \Rightarrow M = \rho V = 1606.06 * 43.2 = 69381.8 kg$$

$$n = \frac{V_v}{V} = \frac{e}{1+e} = \frac{1.72}{1+1.72} = 0.63$$

$$\frac{V_v}{V} = n = 0.63 \quad \Rightarrow \quad \frac{V_v}{43.2} = n \quad \Rightarrow \quad V_v = V_w = 27.35 m^3$$

$$e = \frac{V_v}{V_s} = 1.72 = \frac{27.35}{V_S} \quad \Rightarrow \quad V_S = 15.88 m^3$$

$$\frac{M_S}{V_s \rho_W} = G_S \quad \Rightarrow \quad 2.65 * V_S \rho_W = M_S \quad \Rightarrow \quad 2.65 * 15.88 * 1000 = 42070.15 kg$$

∴Check:

$$w = \frac{M_W}{M_s} \quad \Rightarrow \quad 0.65 = \frac{M_W}{42070.15} \quad \Rightarrow \quad M_W = 27345.6 kg$$

∴For w=0.42 as M_S remains constant:

$$0.42 = \frac{M_W}{M_S} \quad \Rightarrow \quad 0.42 = \frac{M_W}{42070.15} \quad \Rightarrow \quad M_W = 17669.4 kg$$

∴Reduction in water content:

$$27345.6 - 17669.4 = 9676.2 kg = 9.68 m^3$$

Reduction in overall height of the clay is given by volume loss/surface area:

$\frac{9.68m^3}{72m^2} = 0.13m$ i.e. a reduction of ≈13cm in the clay height (90% of a sandbag)

Initial Parameters for 75% water content:

G_s = 2.65 (Typical value for an illitic clay)
V = 24m*3m*0.6m = 43.2m^3, Surface area = 24m*3m=72m^2
w = 0.75 as placed and w = 0.42 required after treatment by electro-osmosis

Assume soil is placed saturated

$$e = wG_s = 0.75 * 2.65 = 1.99$$

$$\rho_{bulk} = \frac{G_s(1+w)}{1+e}\rho_w = \frac{2.65(1+0.75)}{1+1.99} \bullet 10 = 1552.3kg/m^3$$

$$\rho = \frac{M}{V} = \frac{M}{43.2} = 1552.3 \Rightarrow M = \rho V = 1552.3 * 43.2 = 67059.4kg$$

$$n = \frac{V_v}{V} = \frac{e}{1+e} = \frac{1.99}{1+1.99} = 0.67$$

$$\frac{V_v}{V} = n = 0.67 \quad \Rightarrow \quad \frac{V_v}{43.2} = n \quad \Rightarrow \quad V_v = V_w = 28.74m^3$$

$$e = \frac{V_v}{V_s} = 1.99 = \frac{28.74}{V_S} \quad \Rightarrow \quad V_S = 14.46m^3$$

$$\frac{M_S}{V_s\rho_W} = G_S \quad \Rightarrow \quad 2.65 * V_S\rho_W = M_S \quad \Rightarrow \quad 2.65 * 14.46 * 1000 = 38319kg$$

∴Check:

$$w = \frac{M_W}{M_s} \quad \Rightarrow \quad 0.75 = \frac{M_W}{38319} \quad \Rightarrow \quad M_W = 28739.25kg$$

∴For w=0.42 as M_S remains constant:

$$0.42 = \frac{M_W}{M_S} \quad \Rightarrow \quad 0.42 = \frac{M_W}{38319} \quad \Rightarrow \quad M_W = 16093.98kg$$

∴Reduction in water content:

$$28739.25 - 16093.98 = 12645.27 = 12.65m^3$$

Reduction in overall height of the clay is given by volume loss/surface area:

$$\frac{12.65m^3}{72m^2} = 0.176m$$ i.e. a reduction of ≈17.6cm in the clay height (15 cm = sandbag)